UNIVERSITÉ DE SHERBROOKE

Faculté de génie
Département de génie civil

DEVELOPPEMENT DE BETON A ULTRA-HAUTES PERFORMANCES (BFUP) A BASE DE VERRE – VERS UN BETON ECOLOGIQUE INNOVANT

DEVELOPMENT OF ULTRA-HIGH-PERFORMANCE CONCRETE (UHPC) USING WASTE GLASS MATERIALS – TOWARDS INNOVATIVE ECO-FRIENDLY CONCRETE

Thèse de doctorat
Spécialité génie civil

Nancy Ahmed SOLIMAN

A dissertation submitted in partial fulfillment
of the requirements for the degree of
Doctor of Philosophy
(Civil Engineering)

Jury : Arezki Tagnit-Hamou, directeur de thèse

Richard Gagné, rapporteur

Pierre-Claude Aïtcin, évaluateur

Thierry Sedran, évaluateur

Mohamed Lachemi, évaluateur

Sherbrooke (Québec), Canada **Juin 2016**

ABSTRACT

Conventional concrete (CC) may cause numerous problems on concrete structures such as corrosion of steel reinforcement and weaknesses of concrete construction. As a result, most of structures made with CC require maintenance. Ultra-high-performance concrete (UHPC) can be designed to eliminate some of the characteristic weaknesses of CC. UHPC is defined worldwide as concrete with superior mechanical, ductility, and durability properties. Conventional UHPC includes between 800 and 1000 kg/m^3 of cement particles, 25–35%wt of silica fume (SF), 0–40 wt% of quartz powder (QP), and 110–140 wt% quartz sand (QS) (the percentages are based on the total cement content of the mix by weight). UHPC contains steel fibers to improve its ductility and tension capacity.

The huge amount of cement used to produce UHPC not only affects production costs and consumes natural resources, limestone, clay, coal, and electric power, but it also negatively impacts the environment through carbon dioxide (CO_2) emissions, which can contribute to the greenhouse effect. Additionally, the particle-size distribution (PSD) of cement exhibits a gap at the micro scale that needs to be filled with more finer materials such as SF. Filling this gap solely with SF requires a high amount of SF (25% to 30% by cement weight) which is a limited resource and involves high cost. This significantly also decreases UHPC workability due to high Blaine surface area of SF. QS and QP use is also costly and consumes natural resources. As such, they are considered as impedances for wide use of UHPC in the concrete market and fail to satisfy sustainability requirements. Furthermore, based on an Environment Canada report, quartz causes immediate and long-term environmental harm because its biological effect makes it an environmental hazard. Furthermore, UHPC is generally sold on the market as a prepackaged product, which limits any design changes by the user. Moreover, it is normally transported over long distances, unlike CC components. This increases to the greenhouse-gas effect and leads to higher cost of the final product. Therefore, there is a vital need for other locally available materials with similar functions to partially or fully replace silica fume, quartz sand, or quartz powder, and thereby reduce the cement content in UHPC, while having comparable or better properties.

In some countries, and Canada in particular, large quantities of glass cannot be recycled because of the high breaking potential, color mixing, or high recycling costs. Most waste glass goes into landfill sites, which is undesirable since it is not biodegradable and less environmentally

friendly. In recent years, attempts have been made to use waste glass as an alternative supplementary cementitious material (ASCM) or ultra-fine aggregate in concrete, depending on its chemical composition and particle-size distribution (PSD).

This thesis is based on a new type of ecological ultra-high-performance glass concrete (UHPGC) developed at the Université de Sherbrooke. The concrete's design involved using waste glass of varying particle-size distributions obtained from cullets and optimizing the packing density of the entire material matrix. UHPGC can be designed with a reduced amount of cement (400–800 kg/m^3), silica fume (SF) (50–220 kg/m^3), quartz powder (QP)(0–400 kg/m^3), and quartz sand (QS) (0–1200 kg/m^3), while incorporating various waste-glass products: glass sand (GS) (0–1200 kg/m^3) with an average mean diameter (d_{50}) of 275 μm, a high amount of glass powder (GP) (200–700 kg/m^3) with average diameter (d_{50}) of 11 μm, a moderate content of fine glass powder (FGP) (50–200 kg/m^3) with d_{50} of 3.8 μm. UHPGC also contains steel fibers (to increase tensile strength and improve ductility) and superplasticizer (10–60 kg/m^3) as well as having a water-to-binder ratio (*w/b*) as low as that of UHPC.

Replacing cement and silica-fume particles with non-absorptive and smooth glass particles improves UHPGC rheology. Furthermore, using FGP as a SF replacement reduces the net total surface area of a SF and FGP blend. This decreases the net particle surface area, it reduces the water needed to lubricate particle surfaces and increases the slump flow at the same *w/b*. Moreover, the use of waste glass material in concrete leads to lower cumulative heat of hydration, which helps minimize potential shrinkage cracking.

Depending on UHPGC composition and curing temperature, this type of concrete yields compressive strength ranging from 130 up to 230 MPa, flexural strength above 20 MPa, tensile strength above 10 MPa, and elastic modulus above 40 GPa. The mechanical performance of UHPGC is enhanced by the reactivity of the amorphous waste glass and optimization of the packing density. The waste-glass products in UHPGC have pozzolanic behavior and react with the portlandite generated by cement hydration. This, however, is not the case with quartz sand and quartz powder in conventional UHPC, which react at high temperature of 400 ^{o}C. The waste-glass addition enhances clogging of the interface between particles. Waste-glass particles have high rigidity, which increases the concrete's elastic modulus. UHPGC also has extremely good durability. Its capillary porosity is very low, and the material is extremely resistant to chloride-

ion permeability (≈ 8 coulombs). Its abrasion resistance (volume loss index) is less than 1.3. UHPGC experiences virtually no freeze–thaw deterioration, even after 1000 freeze–thaw cycles. After laboratory assessment, the developed concrete was scaled up with a pilot plane and field validation with the construction of two footbridges as a case study. The higher mechanical properties allowed for the footbridges to be designed with about sections reduced by 60% compared to normal concrete.

UHPGC offers several economic and environmental advantages. It reduces the production cost of ultra-high-performance concrete (UHPC) by using locally available materials and delivers a smaller carbon footprint than conventional UHPC structures. It reduces the CO_2 emissions associated with the production of cement clinkers (50% replacement of cement) and efficiently uses natural resources. In addition, high amounts of waste glass cause environmental problems if stockpiled or sent to landfills. Moreover, the use of waste glass in UHPGC could save millions of dollars that would otherwise be spent for treatment and placing waste glass in landfills. Lastly, it provides an alternative solution to the construction companies in producing UHPC at lower cost.

Keywords: ultra-high-performance concrete, sustainability, ecofriendly, greenhouse gases, waste glass, packing density, mechanical properties, microstructure, and durability.

RÉSUMÉ

Le béton conventionnel (BC) a de nombreux problèmes tels que la corrosion de l'acier d'armature et les faibles résistances des constructions en béton. Par conséquent, la plupart des structures fabriquées avec du BC exigent une maintenance fréquent. Le béton fibré à ultra-hautes performances (BFUP) peut être conçu pour éliminer certaines des faiblesses caractéristiques du BC. Le BFUP est défini à travers le monde comme un béton ayant des propriétés mécaniques, de ductilité et de durabilité supérieures. Le BFUP classique comprend entre 800 kg/m³ et 1000 kg/m³ de ciment, de 25 à 35% massique (%m) de fumée de silice (FS), de 0 à 40%m de poudre de quartz (PQ) et 110-140%m de sable de quartz (SQ) (les pourcentages massiques sont basés sur la masse totale en ciment des mélanges). Le BFUP contient des fibres d'acier pour améliorer sa ductilité et sa résistance aux efforts de traction.

Les quantités importantes de ciment utilisées pour produire un BFUP affectent non seulement les coûts de production et la consommation de ressources naturelles comme le calcaire, l'argile, le charbon et l'énergie électrique, mais affectent également négativement les dommages sur l'environnement en raison de la production substantielle de gaz à effet de serre dont le gas carbonique (CO_2). Par ailleurs, la distribution granulométrique du ciment présente des vides microscopiques qui peuvent être remplis avec des matières plus fines telles que la FS. Par contre, une grande quantité de FS est nécessaire pour combler ces vides uniquement avec de la FS (25 à 30%m du ciment) ce qui engendre des coûts élevés puisqu'il s'agit d'une ressource limitée. Aussi, la FS diminue de manière significative l'ouvrabilité des BFUP en raison de sa surface spécifique Blaine élevée. L'utilisation du PQ et du SQ est également coûteuse et consomme des ressources naturelles importantes. D'ailleurs, les PQ et SQ sont considérés comme des obstacles pour l'utilisation des BFUP à grande échelle dans le marché du béton, car ils ne parviennent pas à satisfaire les exigences environnementales. D'ailleurs, un rapport d'Environnement Canada stipule que le quartz provoque des dommages environnementaux immédiats et à long terme en raison de son effet biologique. Le BFUP est généralement vendu sur le marché comme un produit préemballé, ce qui limite les modifications de conception par l'utilisateur. Il est normalement transporté sur de longues distances, contrairement aux composantes des BC. Ceci contribue également à la génération de gaz à effet de serre et conduit à un coût plus élevé du produit final. Par conséquent, il existe le besoin de développer d'autres matériaux disponibles localement ayant des fonctions similaires pour remplacer partiellement ou totalement la fumée de

silice, le sable de quartz ou la poudre de quartz, et donc de réduire la teneur en ciment dans BFUP, tout en ayant des propriétés comparables ou meilleures.

De grandes quantités de déchets verre ne peuvent pas être recyclées en raison de leur fragilité, de leur couleur, ou des coûts élevés de recyclage. La plupart des déchets de verre vont dans les sites d'enfouissement, ce qui est indésirable puisqu'il s'agit d'un matériau non biodégradable et donc moins respectueux de l'environnement. Au cours des dernières années, des études ont été réalisées afin d'utiliser des déchets de verre comme ajout cimentaire alternatif (ACA) ou comme granulats ultrafins dans le béton, en fonction de la distribution granulométrique et de la composition chimique de ceux-ci.

Cette thèse présente un nouveau type de béton écologique à base de déchets de verre à ultra-hautes performances (BEVUP) développé à l'Université de Sherbrooke. Les bétons ont été conçus à l'aide de déchets verre de particules de tailles variées et de l'optimisation granulaire de la des matrices granulaires et cimentaires. Les BEVUP peuvent être conçus avec une quantité réduite de ciment (400 à 800 kg/m³), de FS (50 à 220 kg/m³), de PQ (0 à 400 kg/m³), et de SQ (0-1200 kg/m³), tout en intégrant divers produits de déchets de verre: du sable de verre (SV) (0-1200 kg/m³) ayant un diamètre moyen (d_{50}) de 275 µm, une grande quantité de poudre de verre (PV) (200-700 kg/m³) ayant un d_{50} de 11 µm, une teneur modérée de poudre de verre fine (PVF) (50-200 kg/m³) avec d_{50} de 3,8 µm. Le BEVUP contient également des fibres d'acier (pour augmenter la résistance à la traction et améliorer la ductilité), du superplastifiants (10-60 kg/m³) ainsi qu'un rapport eau-liant (E/L) aussi bas que celui de BFUP.

Le remplacement du ciment et des particules de FS avec des particules de verre non-absorbantes et lisse améliore la rhéologie des BEVUP. De plus, l'utilisation de la PVF en remplacement de la FS réduit la surface spécifique totale nette d'un mélange de FS et de PVF. Puisque la surface spécifique nette des particules diminue, la quantité d'eau nécessaire pour lubrifier les surfaces des particules est moindre, ce qui permet d'obtenir un affaissement supérieur pour un même E/L. Aussi, l'utilisation de déchets de verre dans le béton abaisse la chaleur cumulative d'hydratation, ce qui contribue à minimiser le retrait de fissuration potentiel.

En fonction de la composition des BEVUP et de la température de cure, ce type de béton peut atteindre des résistances à la compression allant de 130 à 230 MPa, des résistances à la flexion supérieures à 20 MPa, des résistances à la traction supérieure à 10 MPa et un module d'élasticité supérieur à 40 GPa. Les performances mécaniques de BEVUP sont améliorées grâce à la

réactivité du verre amorphe, à l'optimisation granulométrique et la densification des mélanges. Les produits de déchets de verre dans les BEVUP ont un comportement pouzzolanique et réagissent avec la portlandite générée par l'hydratation du ciment. Cependant, ceci n'est pas le cas avec le sable de quartz ni la poudre de quartz dans le BFUP classique, qui réagissent à la température élevée de 400 ºC. L'addition des déchets de verre améliore la densification de l'interface entre les particules. Les particules de déchets de verre ont une grande rigidité, ce qui augmente le module d'élasticité du béton. Le BEVUP a également une très bonne durabilité. Sa porosité capillaire est très faible, et le matériau est extrêmement résistant à la pénétration d'ions chlorure (≈ 8 coulombs). Sa résistance à l'abrasion (indice de pertes volumiques) est inférieure à 1,3. Le BEVUP ne subit pratiquement aucune détérioration aux cycles de gel-dégel, même après 1000 cycles.

Après une évaluation des BEVUP en laboratoire, une mise à l'échelle a été réalisée avec un malaxeur de béton industriel et une validation en chantier avec de la construction de deux passerelles. Les propriétés mécaniques supérieures des BEVUP a permis de concevoir les passerelles avec des sections réduites d'environ de 60% par rapport aux sections faites de BC.

Le BEVUP offre plusieurs avantages économiques et environnementaux. Il réduit le coût de production et l'empreinte carbone des structures construites de béton fibré à ultra-hautes performances (BFUP) classique, en utilisant des matériaux disponibles localement. Il réduit les émissions de CO_2 associées à la production de clinkers de ciment (50% de remplacement du ciment) et utilise efficacement les ressources naturelles.De plus, la production de BEVUP permet de réduire les quantités de déchets de verre stockés ou mis en décharge qui causent des problèmes environnementaux et pourrait permettre de sauver des millions de dollars qui pourraient être dépensés dans le traitement de ces déchets. Enfin, il offre une solution alternative aux entreprises de construction dans la production de BFUP à moindre coût.

Mots-clés: béton ultra-haute performance, déchets de verre, développement, durabilité, gaz à effet de serre, matériaux verts, microstructure, optimisation granulaire et propriétés mécaniques

DEDICATION

To the researchers and engineers who appreciate the value of science and knowledge.

To my beloved parents who favored me over themselves and have given me all what they could? "My Mighty GOD! Bestow on them Your Mercy as they did bring me up when I was young."

To my husband supports me and understands my challenging and demanding circumstances as a researcher.

To my son Mustafa and my daughter Merriam came to life and have made a big difference in my life.

ACKNOWLEDGEMENT

First and foremost, praise and thanks go to my Creator and Provider (**The Mighty God**) for his uncounted grace undeservingly bestowed upon me. "Glory is to you, we have no knowledge except what you have taught us. Verily, it is you, the All-Knower, the All-Wise."

The author would like to express his greatest appreciation and thanks to her supervisor, **Prof. Arezki Tagnit-Hamou**, for his guidance, helpful advice, and encouragement during this research. The author had a lot of freedom in her work, which she has learned a lot from his thorough knowledge and experience as well as from his nice and decent personality. The author wishes to express her sincere gratitude to him for his patience and understanding during the course of this research. The author is proud to have worked with him and counts her lucky to be one of his PhD students. The Author can hardly find the right words to express the extent of his gratitude and thanks.

The author is greatly indebted to **Prof. Pierre-Claude Aïtcin** and **Dr**. **Ahmed Omran** for their cooperation, guidance, helpful advice, and encouragement during this research project. His unfailing guidance and continuous consulting efforts were valuable to this research. The Author can hardly find the right words to express the extent of his gratitude and thanks.

Appreciations are expressed to **Fahima Rousis** for her co-operations, assistances, and the fun we had during some difficult times of studies. The Author is greatly thanks to **all research assistants** and **all technicians** for their cooperation during the research. The author cannot forget to acknowledge many friends whom she has gained during her study; they made my stay int Sherbrooke enjoyable.

The Author also thanks the professors of Civil Engineering Department and all the faculty staff he has interacted with. Special thanks to **Prof. Ammar Yahia** for his cooperation**.**

The Author is thankful to the members of the dissertation committee; Prof. (**Thierry Sedran, Mohamed Lachemi, Pierre-Claude Aïtcin,** and **Richard Gagné**) for their valuable comments and advices.

This research was funded by the **Société des Alcools du Québec (SAQ) Industrial Chair** on "Valorization of Glass in Materials" and **The INNOV Grants from NSERC**, also had the support of a concrete producer **(Béton Génial)** The authors gratefully acknowledge these supports.

Finally, the author wishes to express her greatest and profound gratitude to her parents, brothers and sisters, for their support and encouragement. The author wishes to thank her husband for his love and the happiness he brought to her. The life here at Sherbrook would not have been so full without her husband and her two kids (***Mustafa and Mariam***).

The author,

Nancy Soliman

TABLE OF CONTENTS

LIST OF FIGURES

Chapter 1:

LIST OF TABLES

Chapter 2:

SYMBOLS AND NOTATIONS

UHPC	Ultra-high performance concrete
UHPC	Reactive powder concrete
Type HS cement	High-sulphate resistance cement
HPC	High performance concrete
NC	Normal concrete
SF	Silica fume
QP	Quartz powder
QS	Quartz sand
C	Cement
HRWRA	High-range water-reducing agent (superplasticizer)
GP	Glass powder
GA	Glass aggregate
WG	Waste glass
w/b	Water-to-binder ratio
w/cm	Water-to-cementitious material ratio
ρ	Density of a material (kg/m^3)
f_c'	Compressive strength
ITZ	Interfacial transition zone
PSD	Particle-size distribution
SEM	scanning electronic microscope
XRD	X-ray diffraction
C-S-H	calcium silicate hydrate
E_c	Young's modulus
ν	Poisson's ratio

1 Introduction

1.1 Ultra-High-Performance Concrete (UHPC)

Ultra-high-performance concrete (UHPC) is defined worldwide as concrete with a compressive strength (f'_c) of at least 150 MPa [Schmidt and Fehling 2005]. UHPC in the form of reactive-powder concrete (UHPC) regularly achieves compressive strengths of 180 to 210 MPa, flexural strength between 15 and 40 MPa, fracture energy up to 1200 J/m^2, elastic modulus of 50 GPa, and minimal long-term creep or shrinkage [Richard and Cheyrezy,1995, de Larrard and Sedran 1994]. It can also resist freeze–thaw and scaling conditions without visible damage, and it is nearly impermeable to chloride-ion penetration [Roux et al. 1996]. A typical UHPC is composed of cement, quartz powder (QP), silica fume (SF), quartz sand (QS), and steel fiber [Richard and Cheyrezy 1994]. UHPC can achieve such high strength because it is designed to eliminate some of the characteristic weaknesses of normal concrete through enhanced homogeneity produced by eliminating coarse aggregate, enhancing packing density by optimizing the granular mixture through a wide distribution of powder size classes, improving the matrix properties by adding pozzolanic admixtures, reducing the water-to-binder ratio (*w/b*), and enhancing the microstructure with post-set heat treatment [Richard and Cheyrezy 1994]. UHPC incorporates steel fibers to improve the material's ductility and tension capacity [Richard and Cheyrezy 1995].

Currently, UHPC is used in producing special prestressed and precast concrete members [Yazici, 2007]. Applications include the production of nuclear-waste storage facilities [Yazici et al., 2009], precast/prestressed concrete highway bridge girders [Garas et al., 2009], pedestrian footbridges [Soliman and Hamouh, 2015], inner wedges and outer barrels for nonmetallic anchorage systems [Reda et al., 1999], rehabilitation and retrofitting of concrete structures (e.g., waterproofing layer on bridge decks, protection layer on crash barrier walls, and strengthening of industrial floors) [Brühwiler and Denarié, 2008].

Although the production costs of UHPC are relatively high, significant economic advantages can be achieved from its unique applications, including (i) reducing or eliminating passive reinforcement in structural elements by using steel fiber, (ii) using its ultra-high mechanical properties to reduce the

thickness of concrete elements and reduce the dead weight of structure elements (<70% compared to normal and high-performance concrete), and (iii) achieving a longer service life and lower maintenance costs through superior durability properties [Garas et al., 2009].

While good mechanical and durability characteristics are needed when producing cement-based materials, such products must be environmentally friendly (ecological) and deliver socioeconomic benefits [Aïtcin, 2000]. UHPC is designed with a higher cement content ranging between 800 and 1000 kg/m^3 [Richard and Cheyrezy 1994; 1995; Long et al., 2002]. Furthermore, the final hydration percentage of cement in UHPC has been estimated between 31% and 60% [Cheyrezy et al., 1995; Habel et al., 2006] due to the very low water-to-cementitious material ratio (*w/cm*). Any unhydrated cement particles work as micro aggregates. The huge amount of cement involved not only affects production cost and consumes natural sources, it also has a negative impact on the environmental conditions through CO_2 emissions and greenhouse effect.

Based on an Environment Canada report, quartz—the main component in UHPC—causes immediate and long-term environmental harm because its biological acitivty makes it an environmental hazard. Additionally, the International Agency for Research on Cancer (IARC) has classified respirable quartz as a Group 1 carcinogen (carcinogenic to humans). The U.S. National Toxicology Program has classified crystalline silica of respirable size as a human carcinogen. The basis for these classifications is sufficient evidence from human studies indicating a causal relationship between exposure to respirable crystalline silica in the workplace and increased lung-cancer rates in workers. Moreover, the use of QS and QP in UHPC results in higher costs and fails to meet sustainability requirements.

Silica fume an extreme fineness and high amorphous-silica content is an essential constituent in UHPC because of its physical (filler, lubrication) and pozzolanic effects. The particle-size distribution (PSD) of cement exhibits a gap at the micro scale that needs to be filled with finer materials such as SF. Filling this gap solely with SF requires a high amount of SF (25% to 30% by cement weight). This significantly decreases UHPC workability and increases concrete cost. Finding a material with a PSD between that of cement and SF could help reduce SF content and enhance concrete performance. Moreover, the limited available resources and high cost of SF restrict its applications in today's construction industry, providing impetus to seek out materials with similar characteristics as replacement.

In order to produce "greener" concrete and achieve the "sustainable-concrete" concept, some of the cement, SF, QS, and QP in conventional UHPC should be replaced with other safe local materials.

1.2 Waste-Glass Materials

The glass is produced by melting a mixture of silica, soda ash, and calcium carbonates ($CaCO_3$) together at relatively high temperature (not so high when compared to Portland cement), followed by cooling during which solidification occurs without crystallization. The glass can be recycled so many times without significantly altering its physical and chemical properties [Shayan and Xu, 2004]. Large quantities of glass cannot be recycled because of high breaking potential, color mixing, or expensive recycling costs [Terro, 2006]. In Quebec in 2010, only 49% of the glass was recycled; the remainder went into landfills. According to the USEPA in 2011, Americans generated 11.5 million tons of glass in the municipal solid-waste stream of which only 28% was recycled. As for Europe, the latest glass-recycling industry information published by FEVE indicates that the average glass-recycling rate in 2011 rose above the 70% threshold (over 12 million tons) [Topgu and Canbaz, 2004]. The amount of waste glass has gradually increased over recent years due to an ever-growing use of glass products. Most of the waste glass has been dumped in landfill sites, which is undesirable as it is not biodegradable and not environmentally friendly.

The waste-glass material that can be obtained by grinding unrecycled glass is considered an innovative material that could be used in concrete. Glass has been successfully used in concrete mixtures as a partial aggregate replacement in asphalt concrete, as well as a fine aggregate in pipe bedding, landfill-gas venting systems, and gravel backfill for drains) [Kateb, M.L. 2009]. In addition, GP with a particle-size distribution (PSD) of 38 to 45 μm can be used as a pozzolanic material in concrete. It can be incorporated into concrete in quantities similar to by-product admixtures (25% and 50%) [Zidol et al., 2012]. It reduces porosity and pore size as well as changes to mineralogy of cement hydrates, which leads to enhanced durability. According to the Leadership in Energy and Environment Design (LEED) certification, the use of glass in concrete can double the points resulting from the use of by-products such as (RHA, SF, FA, and BFS). GP is regarded as a postconsumer material, while the others are considered postproduction materials.

1.3 Objectives and Originality

Currently, there is a critical need for advanced building materials for North America domestic infrastructure, not only for new high-performance construction, but also to repair and enhance the performance of existing structures. These needed materials should be highly energy efficient, environmentally friendly, sustainable, affordable, and resilient. They should also meet multi-hazard and performance design criteria and be easy to produce and incorporate into construction methods and practice. Furthermore, these materials must be cost effective.

Mixed colored glass, which cannot be recycled, is normally disposed of in landfills, causing obvious environmental problems. Therefore, valorizing waste-glass materials by using them in UHPC gives a second life to waste glass and removes it from going to landfills or storage, which is undesirable. Indeed, not finding applications for waste-glass unnecessarily expends of nonrenewable natural resources, generates costs, and occupies land that could be used for purposes other than for stockpiling or landfills.

The main goal of this research was to develop an innovative ***ecofriendly, durable, and sustainable UHPC using waste-glass materials of various particle-size distributions (PSDs)***. The detailed objectives are as follows:

1. Develop a new method for optimizing the mix proportioning of conventional UHPC using locally available materials based on packing-density theories.
2. Investigate the possibility of using the following materials in conventional UHPC:
   (a) Glass sand (GS) as a granular replacement of QS
   (b) Glass powder (GP) as mineral admixture to replace QP and cement
   (c) Fine glass power (FGP) to replace SF
3. Produce various UHP**G**C classes with different mechanical and rheological properties using waste-glass materials of various PSDs using an experimental design approach.
4. Carry out field applications on full-scale structural elements (architectural panels, bridges) using the new generation of UHPGCs.

1.4 Methodology

An experimental program divided into four main phases (Fig. 1.1) was used to achieve the research objectives.

Phase I (Mix-design optimization): Develop an innovative method to produce eco-efficient mixtures of UHPC with locally available materials based on optimization using the packing-density and statistical mixture-design approaches. The compatibility between cement and different superplasticizer types was studied using the mini-slump flow test (ASTM C 230 M-03). The optimum superplasticizer content for a given *w/b* was assessed with a full factorial design approach. UHPC mixtures were designed with wide ranges of water-to-binder ratio (*w/b*) between 0.150 and 0.250 and polycarboxylate (PCE) superplasticizer dosages between 1% and 3% (%wt. of solids to cement). The measured responses were mini-slump flow, air content, unit weight, and compressive strength at different ages and under two different curing regimes. The curing regimes included a temperature (*T*) of 20ºC ± 2ºC and *RH* > 100%, and *T* of 90ºC and *RH* > 100% for 48 h. A number of mixtures with low-cost local materials available locally and excellent overall performance were targeted for different application sectors. The mixture embodying specific rheological characteristics, excellent overall performance, and cost-effectiveness constitutes the reference UHPC mixture. The results of this phase are presented in paper 1.

Phase II (Parametric study): Different ecofriendly UHPCs were developed by replacing QS, QP, cement, and SF with waste-glass materials of a given PSD (QS with GS, QP and cement with GP, and SF with FGP). Each single ingredient was replaced separately, while other components were kept constant. The mixture properties were assessed with the fresh-state tests (mini-slump flow, air content, temperature, unit weight, and calorimetry). Compressive strength and microstructure analysis at different ages and under two different curing regimes were investigated. The curing regimes were a temperature (*T*) of 20°C ± 2°C and *RH* > 100%, and *T* of 90°C and *RH* > 100% for 48 h. Papers 2, 3, and 4 present the results of this phase.

Phase III (synergetic effect of interaction of different PSD): In this phase, the synergetic effect of different materials was studied as combinations of waste glass with various PSDs. Various UHPGC classes with different mechanical and rheological properties were then designed using an experimental approach. Prediction models for various rheological and mechanical properties of UHPGC as functions of mixture proportioning were also established. Paper 5 presents the results of this phase.

Phase IV (scale-up and field validation): In this phase, the scale-up of UHPGC was performed with an automated concrete pilot plant (pan mixer with a 0.5 m^3 capacity) at the Université de Sherbrooke. The scale effect on rheological, mechanical, and durability properties for selected UHPGCs were performed with different techniques (rheology: ConTec viscometer, V-funnel flow-time test, J-Ring test, and L-box test; mechanical: f'_c, modulus of elasticity, tensile strength, stress–strain behavior, flexural characteristics; and durability: freezing and thawing, alkali–silica reaction, mechanical abrasion, scaling, permeability, and shrinkage.

The concrete was field validated by producing and casting two footbridges in the Université de Sherbrooke's campus. This project, financed by NSERC's INNOV program and the Université de Sherbrooke, also had the support of a concrete producer (Béton Génial). The concrete was produced in the university's pilot plant. The full characterization of the optimized UHPGC mixture used in the footbridges was performed. Papers 6 and 7 present the results of this phase.

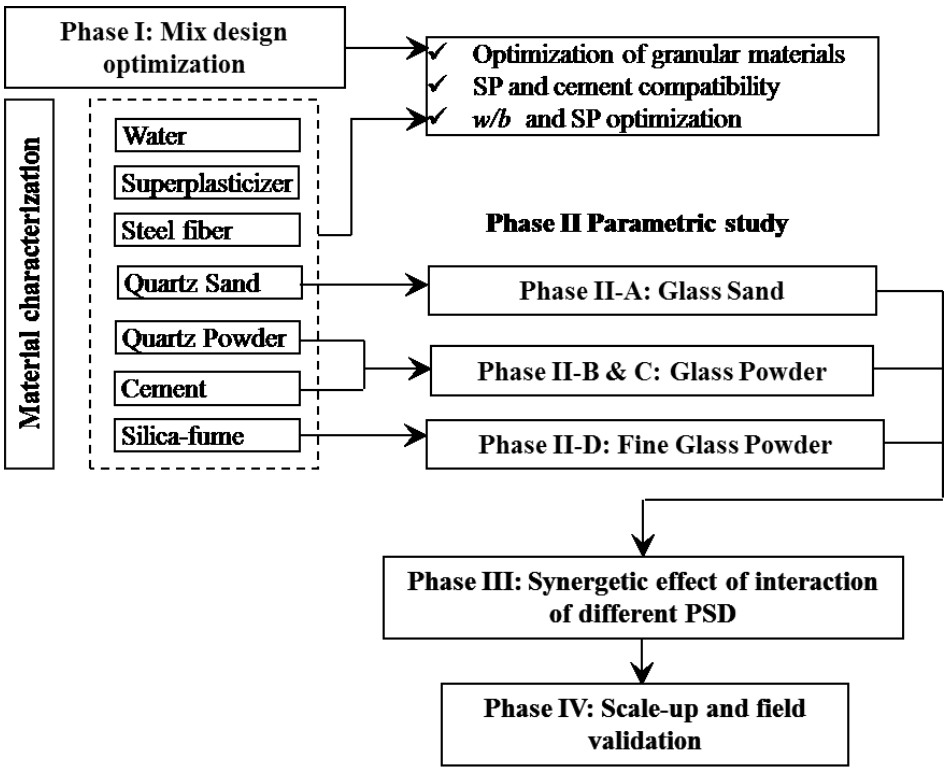

Fig. 1.1 Testing-program flow chart

1.5 Thesis Outline

A U.S. Patent: (Tagnit-Hamou, A. and Soliman, N., 2013. Ultra-High Performance Glass Concrete and Method for Producing Same," U.S. Patent Application No. 61/806,083, filed on March 28, 2013) resulted from this work. The whole doctoral thesis is divided into nine chapters and appendix (as shown in Fig 1.2), which are briefly described below.

Chapter 1 (Introduction): This chapter presents background on the research topic, the research project's objectives, and the methodology adopted.

Chapter 2 (Literature Review): This chapter breaks down into three parts. The first part gives an overview of the development and the basic principles underlying the development of UHPC. UHPC properties, including early-age properties, hydration and microstructure, dimensional stability, mechanical properties, durability, application, and sustainability are highlighted in this chapter. The second part provides also an overview of the significance of packing density, packing-density measurements, and the packing model in concrete. The third part is a comprehensive analysis of the literature on the use of glass in concrete. Its use as an aggregate and a supplementary cementing material is discussed in detail.

The subsequent six chapters correspond to seven technical papers that have either been accepted, submitted, or will be submitted for publication in scientific journals:

Chapter 3 (Mix-Design Optimization): This chapter presents an innovative method to produce eco-efficient mixtures of UHPC using locally available materials based on optimizing the packing density and a statistical mixture-design approach. Paper 1 presents the results of this chapter.

Paper 1: Soliman N.A., Tagnit-Hamou A. (2016) Using Particle Packing and Statistical Approach to Optimize Eco-Efficient Ultra-High-Performance Concrete. *ACI Materials Journal*. (Accepted and forthcoming).

Chapter 4 (Large-Particle Replacement in UHPC): This chapter introduces the feasibility of using ground GS to partially or totally replace QS in UHPC. Paper 2 presents the results of this chapter.

Paper 2: Soliman N.A., Tagnit-Hamou A. (2016) Utilization of Glass Sand as Alternative Silica Sand in UHPC. *Journal of Cement and Concrete Research*. (Accepted and forthcoming).

Chapter 5 (Fine-Powder Replacement in UHPC): This chapter presents the development of an innovative green UHPC with GP. In this chapter, cement and QP were replaced with different proportions of GP. Paper 3 presents the results of this chapter.

Paper 3: Soliman N.A., Tagnit-Hamou A. (2016) Development of Green Ultra-High-Performance Concrete Using Glass Powder. *Journal of Building and Construction Materials.* (Accepted and forthcoming).

Chapter 6 (Ultra-Fine Powder Replacement in UHPC): This chapter reports on a study to determine the possibility of producing and using fine glass powder (FGP) as a SF replacement in UHPC. Paper 4 presents the results of this chapter.

Paper 4: Soliman N.A., Tagnit-Hamou A. (12-16 March, 2016) Substituting Silica Fume with Fine Glass Powder in UHPC. Journal of Building and Construction Materials. (Accepted and forthcoming).

Chapter 7 (Synergetic Effect of Interaction of Different Particle-Size Distributions): This chapter presents the synergetic effect of interaction of waste glass with different PSDs on the rheological and mechanical properties of UHPGC. Paper 5 presents the results of this chapter.

Paper 5: Soliman N.A., Omran A.F., Tagnit-Hamou A. (2016) Statistical Design Approach for Producing Sustainable Ultra-High Performance Glass Concrete. *Journal of Cement and Concrete Research*. (To be submitted).

Chapter 8: (Scale-Up and Field Validation of UHPGC): This chapter presents laboratory characterization of various UHPGC mixtures in comparison to conventional UHPC mixtures in order to recommend an optimum UHPGC mixture for field validation. The possibility of producing

the optimized UHPGC, which was developed in laboratory in a small-scale mixer, on an industrial large scale with a pilot plant, and for casting two footbridges at the Université de Sherbrooke's campus is presented. Papers 6 and 7 present the results of this chapter.

Paper 6: Soliman N., Tagnit-Hamou A. (2015) Study of Rheological and Mechanical Performance of Ultra-High Performance Glass Concrete, *ACI Special Publication (ACI SP)*.

Paper 7: Soliman N., Omran A.F., Tagnit-Hamou A. (2015) Laboratory Characterization and Field Application of Novel Ultra-High Performance Glass Concrete. *ACI Materials Journal*. 41 (in press).

Chapter 9 (Conclusions and Future Work): This chapter summarizes the general conclusions about the results obtained from the experiments and analyses with respect to issues and observations discussed throughout the thesis. It also provides recommendations for future work.

Appendix: Contains three peer-reviewed conference papers and one non-peer-reviewed journal paper that have either been submitted or published:

Paper 8: Soliman N.A., Tagnit-Hamou A. (March 12–16, 2016) The study of Using Fine Glass Powder to Produce Ultra High Performance Concrete. 8th International Conference on Nano-Technology in Construction (NTC 2016), Sharm El-Sheikh, Egypt. (Awarded best paper).

Paper 9: Soliman N, Tagnit-Hamou A., Omran A. (July 18–20, 2016) Green Ultra-High-Performance Glass Concrete. First International Interactive Symposium on UHPC, Des Moines, Iowa, USA.

Paper 10: Soliman N., Aïtcin P.- C., and Tagnit-Hamou A. (May 12–16, 2014) New Generation of Ultra-High-Performance-Glass-Concrete. Advanced Concrete and Technologies. Lightweight and Foam Concretes. Education and Training. Publisher:

RILEM and CEB-fib, ISBN 978-5-7264-0809-5, Volume 5, Chapter 24, pp 218-227.

Paper 11: Tagnit-Hamou A., Soliman N., Omran A., Gauvreau N., and Provencher M. (2016) Novel Ultra-High Performance Glass Concrete. Concrete International, 37(3):41-47 (Awarded best invention).

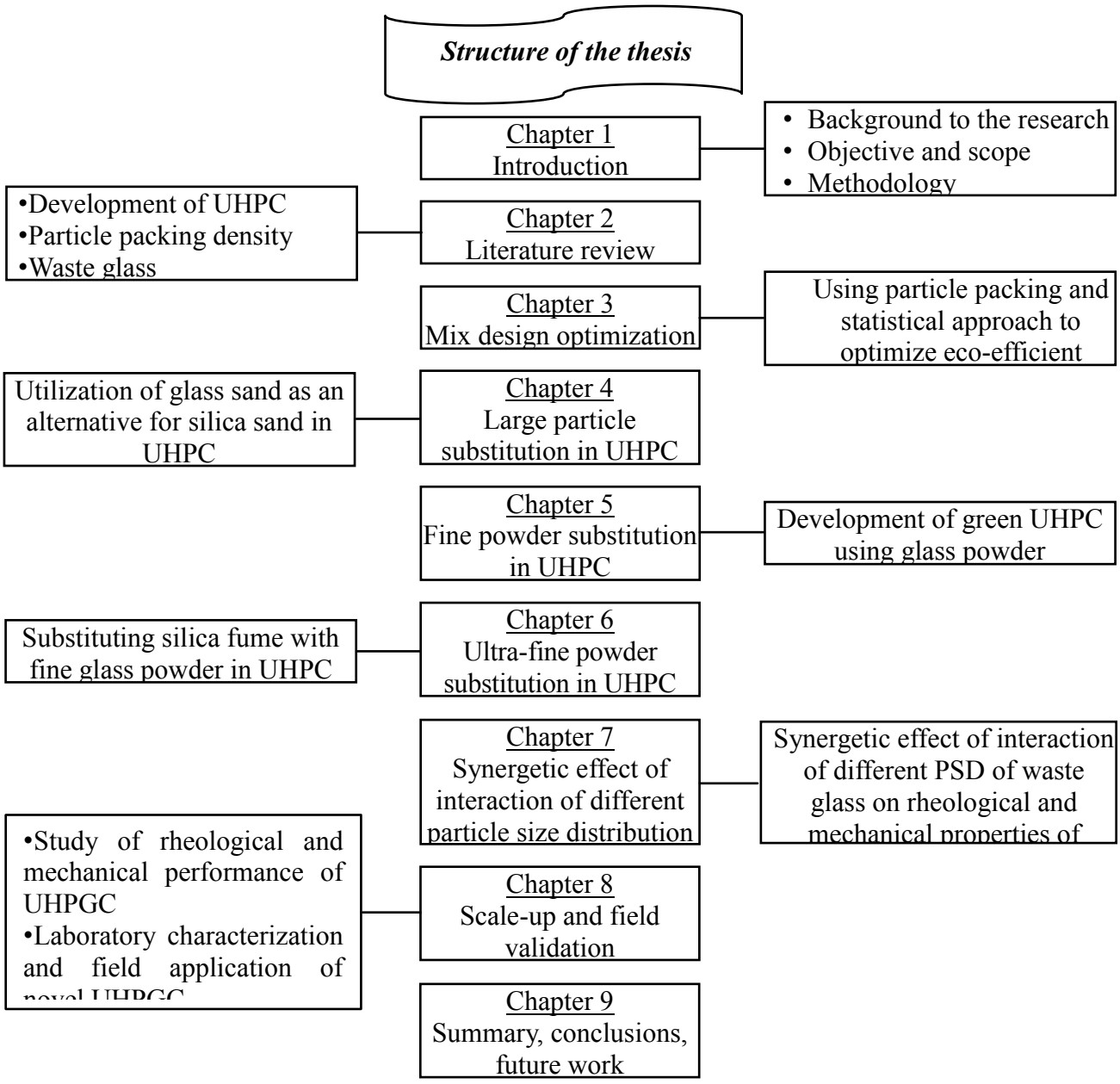

Fig. 1.2 Outline of this thesis

1.6 REFERENCES

- Aïtcin P-C (2000) Cements of yesterday and today – Concrete of tomorrow. Cement and Concrete Research, 30(9):1349-1359.
- Brühwiler, E. and Denarié, E., (2008) Rehabilitation of concrete structures using Ultra-High Performance Fiber-Reinforced Concrete, In: Proceeding of 2nd International Symposium on UHPC, Kassel, Germany, pp. 1-8.
- de Larrard, F.; and Sedran, T., (1994) Optimization of Ultra-High-Performance Concrete by the Use of a Packing Model," Cement and Concrete Research, V. 24, No. 6, pp. 997-1009
- Environment Canada, Health Canada. Screening assessment for the challenge. Report June 2013:7, Environment Canada, https://www.ec.gc.ca/default.asp?lang=en&n=FD9B0E51-1.
- FEVE (2013) Collection for Recycling Rate in Europe. The European Container Glass Federation. http://www.feve.org/FEVE-STATIS-2013/Recycling-2011-Glass-coll.html (Date accessed: September 11, 2013).
- Garas, V.Y., Kahn, L.F. and Kurtis, K.E., (2009) Short-term tensile creep and shrinkage of ultra-high performance concrete, *Cement and Concrete Composites*, Vol. 31, No. 3, pp. 147-152.
- Holschemacher, K. and Weiße, D., (2005) Economic mix design of ultra high strength concrete, *In: Proceedings of the 7th International Symposium on Utilization of High-Strength/ High-Performance Concrete*, Washington D.C., Vol. 2, pp.1133- 1144.
- Kateb, M.L. (2009) Utilisation des granulats de verre dans la fabrication des bétons architecturaux : cas des briques en bétons, mémoire de maîtrise, Dépt Génie Civil, Université de Sherbrooke.
- Recyc-Québec (2010) Le verre Fiches informatives.
- Reda, M.M., Shrive, N.G. and Gillott, J.E. (1999) Microstructural investigation of innovative UHPC," *Cement and Concrete Research*, Vol. 29, No. 3, 1999, pp. 323-329.
- Richard, P. and Cheyrezy, M. (1995) Composition of reactive powder concretes, Cement and Concrete Research 25 (7) 1501-1511.
- Schmidt, M.; Fehling, E. (2005) Ultra-high-performance concrete: research, development and application in Europe, ACI SP 225, 51-77.
- Shayan, A., & and Xu, A. (2004) Value-added utilisation of waste glass in concrete. Cement and Concrete Research, 34(1),81-89.

- Soliman N., Tagnit-Hamou A. (2015) Study of Rheological and Mechanical Performance of Ultra-High Performance Glass Concrete, ACI Special Publication (ACI SP).
- Terro, M. J. (2006) Properties of concrete made with recycled crushed glass at elevated temperatures. Building and Environment, 41(5),633-639.
- USEPA, (2013) Wastes - Resource Conservation - Common Wastes & Materials. Glass. updated. http://www.epa.gov/osw/conserve/materials/glass.htm. (Date accessed: 10-09-2013).
- Yazici, H., (2007) The effect of curing conditions on compressive strength of ultra high strength concrete with high volume mineral admixtures, Building and Environment, Vol. 42, No. 5, pp. 2083-2089.
- Yazici, H., Yardımcı, H.Y., Aydın, S. and Karabulut, A., (2009) Mechanical properties of reactive powder concrete containing mineral admixtures under different curing regimes," Construction and Building Materials, Vol. 23, No. 3, pp. 1223-1231.
- Zidol A, Tohoue Tognonvi M, Tagnit-Hamou A. (2012) Effect of glass powder on concrete sustainability. 1st International Conference on Concrete Sustainability (ICCS13), Ref # 0229.

2 Literature Review

2.1 Introduction

This chapter provides a brief overview of ultra-high-performance concrete (UHPC), including a review of the development of UHPC, the basic principles underlying its development, and its mechanical performance, durability, and applications. In addition, the chapter provides an overview of packing density in concrete: its significance in enhancing the mechanical performance and durability of concrete. An overview of packing measurements and a packing model are also presented. Finally, an overview of waste-glass materials is highlighted.

2.2 Development of ultra-high performance concrete

Over the last decades, large progress has been taking place in the field of development of cementitious materials. Intensive research efforts began in 1930th to improve f_c' of concrete. The development of concrete strength over 100 years is presented in Fig. 2.1. The f_c' has been roused from 60 MPa to 200 MPa Tang [2004]. This was possible by densification of the microstructure of the fresh cement paste with the use of efficient surface active agents (superplasticizer) and ultra-fine reactive particles. These resulted in creating a material with a minimum amount of defects, such as micro-cracks and interconnected pore spaces in order to satisfy the approaches of the potential ultimate strength of the components and enhanced durability.

Two main directions of research have been followed in developing the minimum defect materials; macro-defect free (MDF) and densified small PSD or densified system with ultra-fine particles [Rossi, 2005]. The MDF approach uses polymers to fill the pores in the concrete matrix. This process requires specific manufacturing conditions, including laminating the material by passing it through rollers. However, the MDF concrete can have tensile strength up to 150 MPa, it has some drawbacks such as susceptible to water, large creep, and brittleness [Rossi, 2005]. DSP concrete contains high amount of superplasticizer and silica fume (SF). Compared to MDF concrete, DSP concrete does not require the extreme manufacturing conditions, has much lower

tensile strength, and is brittle. Steel fibers have been used to improve the ductility of MDF and DSP concretes; however, MDF concrete maybe too viscous and unworkable. Conversely, DSP concrete can be supplemented with fibers resulting in UHPC. This relatively new material is characterized by an extremely dense microstructure, very high strength, superior durability, and high ductility.

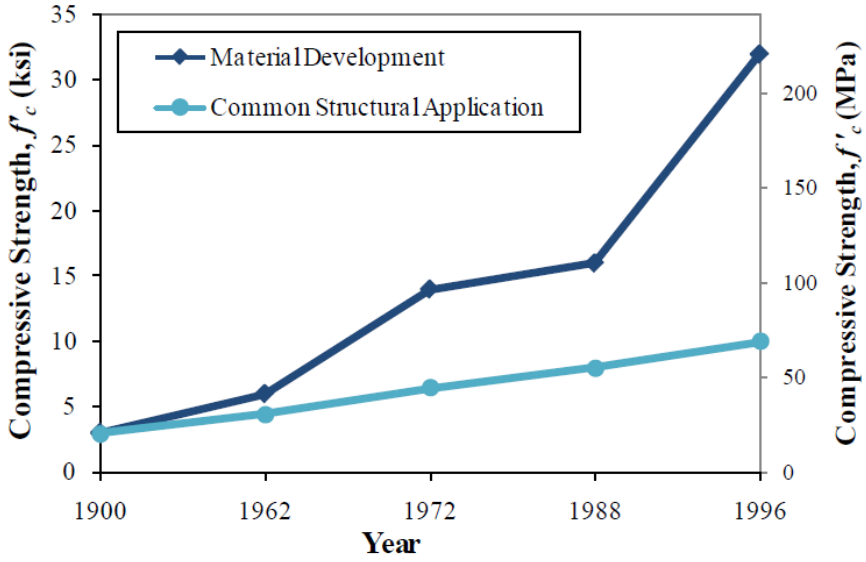

Fig. 2.1 Development of the compressive strength of concrete over 100 years

Several types of UHPC have been developed by different manufacturers in many countries. The main differences between the types of the UHPC are the type and amount of fibers used. The four main types of UHPC are slurry-infiltrated fiber concrete (SIFC), carbon-fiber-reinforced cement-based composites, compact reinforced composite (CRC), and reactive powder concrete (RPC). A brief summary for each type of the UHPC is given below.

Slurry-infiltrated fiber concrete – The SIFC is designed with high volume fraction of steel fiber; typically ranging between 8 and 25% of the total volume of mixture. Because of this high content of steel fiber, the mixture for a structural member is formulated by sprinkling the fiber into the formwork or over a substratum. Either the substratum is stacked with fibers to a prescribed height or the form is completely or partially filled with the fibers, depending on the design requirements. After the fibers placement, low-viscosity cement slurry is poured or

pumped into the fiber bed or into the formwork infiltrating into the spaces between the fibers. Typical cement/fly ash (FA)/sand proportions for the SIFC can vary from 90/10/0 to 30/20/50 by weight [Schneider, 1992]. The *w/cm* [i.e., water/(cement+FA), *w/ (c + FA)*] can range between 0.45 and 0.20 by weight, with a superplasticizer content of 0.625 to 2.5 kg per 100 kg of the total cementitious weight. Trial batches of the slurry mixture have to be carefully made with regard to the *w/cm* to achieve the required workability that can fully penetrate to the depth of the fibers.

Carbon-fiber-reinforced cement-based composites – Petroleum-pitch-based carbon fibers have recently been developed and used as reinforcement for cement based composites. The diameter of the carbon fibers varies from 10 to 18 μm and the length ranges between 3 and 12 mm. Typical tensile strength of carbon fibers ranges from 400 to 750 MPa. The carbon fibers are uniformly distributed and randomly oriented in the cement-based composites in the same manner as steel fibers. Because of the very small size of the carbon fibers, high fiber content can be obtained in the cementitious matrix at a typical volume fraction of 0.5 to 3% [Bayasi, 1992]. At a 3% fiber volume fraction, the spacing between the fibers is approximately 0.1 mm. The function of the carbon fibers is similar to that of the steel fibers in preventing the micro cracks from propagating and opening.

Compact reinforced composite (CRC) – CRC is the designation for a special type of Fiber Reinforced High Performance Concrete with high strength (150-400 MPa) developed by Aalborg Portland A/S and now marketed and sold by CRC Technology. Because of a large content of steel a fiber the matrix of CRC is very ductile and that makes it possible to utilize rebar's much more effectively without having large cracks under service conditions. CRC uses high amounts of fiber and uses different fiber sizes than those used in RPC (Rossi 2005)

Multi-scale cement composite – The MSCC has been developed by Laboratoire Central des Ponts et Chaussées (LCPC), which has a very high uniaxial tensile strength, more than 20 MPa. These materials are the direct implementation of the "Multi-Scale Concept" developed by Rossi [1997]. The idea is to mix short fibers with longer fibers in order to intervene at the same time on the material scale (increase of the tensile strength) and on the structure scale (bearing capacity and ductility). A Multi-Scale Cement Composite (MSCC) is then obtained.

Reactive powder concrete **–** The RPC developed by Pierre Richard at the scientific direction of Bouygues, France in early 1990th. It is characterized by extremely high physical properties, particularly strength and ductility [Richard and Cheyrezy, 1994]. The production theory of the RPC is built on previous research efforts such as the principle characteristics of the DSP [Bache, 1981] and those of the UHPC [de Larrard and Sedran, 1994]. The latter research efforts were based on the placement of different particles in a very dense arrangement. The RPC has a f_c' ranging from 200 to 800 MPa. The RPC is the most commonly available type of the UHPC and has been used in laboratory and field experiments.

RPC is the generic name for a class of cementitious composite materials of extremely high mechanical properties. An RPC can be designed using QS, QP, very large content of cement, extremely low *w/b*, highly reactive pozzolanic materials (typically SF), and fine steel fibers for increasing the tensile strength and improving the ductility. The very low *w/b* can be achieved by the incorporation of high dosage of superplasticizer. The RPC does not contain any coarse aggregate – the average size of the coarser particles QS is typically 250 μm [Richard and Cheyrezy, 1995].

The term of "reactive powder" used by Richard et al., [1995] within the first name of the UHPC reflects the fact that all the powder components in the RPC react chemically after the casting and curing of the sample. The cement reacts by conventional hydration; SF through pozzolanic reaction resulting in more calcium hydroxide; QS provides dissolved silica for the formation of further C-S-H gel; QP to alter the calcium oxide (CaO)/silicon dioxide (SiO_2) ratio and favour the formation of tobermorite and xonotlite when UHPC is subjected to heat treatment at a high temperature of 400 ^oCor setting pressure [Cheyrezy et al., 1995; Lee and Chisholm, 2005].

An RPC is designed using combination of quartz sand, quartz powder, SF, and cement to form a cementitious matrix supporting straight and smooth steel fiber reinforcements. These steel fibers are generally 12.5 mm in length and 180 μm in diameter [Richard and Cheyrezy, 1995]. Even through the *w/cm* is low because high amount of superplastizer is used, it can be mixed and vibrated in the same conditions as conventional concrete. The typical composition and mechanical properties of the RPC200 are presented in Table 2.1. The lower f_c' (170 MPa) corresponds to a 28 days curing at ambient temperature while the upper value (230 MPa) corresponds to a hot-curing at 90 ^oC after pre-curing at ambient temperature for 2 days [Richard and Cheyrezy, 1995]. The flexural strength and fracture energies vary depending on the

percentage of steel fibers added to the mixture. The strain at maximum stress encountered was approximately 10 times greater than the displacement at the opening of the first crack. This material can be used in pre-stressed member without passive reinforcement. RPC can be used without pre-stressing ten-meter-span beams. Pre-stressed, non-reinforced RPC200 with a ten-meter-span beams have been constructed and successfully tested [Richard and Cheyrezy, 1995].

RPC800 is restricted in its use to small or medium sized pre-fabricated structural elements such as bridge bearings, security vaults, and waste/transportation vessels. The components used in RPC800 are similar to those of RPC200 with the exception of steel fibers which are replaced by a stainless steel microfiber (with a length lower than 3 mm). The RPC800 is cured at 250 ^{o}C after demoulding. Improved properties are obtained through pressure applied in the moulds before and during setting [Richard and Cheyrezy, 1995]. Table 2.1 summarizes the typical composition and mechanical properties for pressurized sample cured at 400 ^{o}C for the RPC800. The f_c' can reach 680 MPa. When steel powder is used instead of quartz sand f_c' can reach 800 MPa. Fracture energy was in the range of 1200 to 2000 J/m^2. These values are more than ten times those obtained on conventional concrete. The RPC800 is a strong material that can be used as a substitute for steel [Richard and Cheyrezy, 1995].

Since RPC is the most commonly available types of UHPC and was used for the laboratory and field experiments in the current study, the term "UHPC" refers exclusively to RPC for the remainder of this report unless otherwise indicated. Also note that "heat treated" UHPC refers to the standard heat treatment at (90°C) for 48 hours unless otherwise indicated.

2.2.1 Principles underlying the development of UHPC

Several researchers [Richard and Cheyrezy, 1995; Schneider, 2002] have identified the basic principles used in the UHPC design, as follows:

a. Improvement of homogeneity by elimination of coarse aggregate.
b. Enhancement of compact density by optimization of granular mixture, and maintaining the fresh concrete under pressure at the placement stage and during setting;
c. Improvement in microstructure by post set hot curing for 2 days at 90°C to speed the activation of the pozzolanic reaction of the SF, resulting in a 30% gain in f_c'.

d. Increase in ductile behavior through the addition of an adequate volume fraction of steel microfibers.

Application of the first three principles without the fourth can lead to a concrete with a very high f_c' without any improvement in ductility. The addition of the steel fibers noted in the last principle helps to improve both tensile strength and ductility [Richard and Cheyrezy, 1995].

Table 2.1Typical composition and mechanical properties of RPC200 and RPC800 [Richard and Cheyrezy, 1995]

Constituents	RPC200	RPC800
Type V cement, kg/m^3	955	1000
Fine sand (150-400 μm), kg/m^3	1051	500
Ground quartz (4 μm), kg/m^3	--	390
Silica fume (18 m^2/g), kg/m^3	229	230
Precipitated silica (35 m^2/g), kg/m^3	10	--
Superplasticizer (Polyacrylate), kg/m^3	13	18
Steel fibers, kg/m^3	191	630
Total water, kg/m^3	153	180
Cylindrical compressive strength (f_c'), MPa	170 - 230	490 - 680
Flexural strength, MPa	25 - 60	45 - 102
Fracture energy, J/m^2	15000 - 40000	1200 - 2000
Young's modulus, GPa	54 - 60	56 - 75

2.2.1.1 Homogeneity enhancement

Conventional concrete and HPC are considered as heterogeneous materials, in which the aggregates (sand and gravel) form a skeleton of contiguous granular elements in the cementitious paste (cement, water, and additives). The hardness of the paste is less than that of the aggregate. For example, the Young's modulus for aggregate silica is 70 GPa, compared to 18 – 22 GPa for paste. Heterogeneity-related problems are significantly reduced with the UHPC for the following reasons; (a) elimination of coarse aggregates (replaced by fine sand with the mean PSD

approximately 250 μm, (b) improved mechanical properties of the paste, and (c) reduction in the aggregate/matrix ratio. The following sections illustrate these issues.

Both normal concrete and HPC suffer from a mismatch in the properties "crushing strength" and of their constituent materials; the aggregate and cement paste. They have significantly different elastic moduli. The mismatch in elastic moduli is eliminated in the UHPC by selecting constituent materials with similar elastic moduli [Gao et al., 2006]. The mechanical properties of paste are enhanced by addition of SF, crushed quartz, and active mineral materials, as well as the microstructure improvement. The UHPC have Young's modulus values exceeding 50 GPa, and can reach 75 GPa for those with highest densities. Thus the mismatch in elastic moduli has been totally eliminated by selecting constituent materials with similar elastic moduli. The increase in the Young's modulus for the UHPC paste, by comparison with that of conventional cementitious pastes, tends to attenuate the effects associated with disturbance of the mechanical stress field [Richard and Cheyrezy, 1995].

The principal characteristic of the UHPC is the use of powders in which aggregates and traditional sand are replaced by ground quartz less than 600 μm in size [Richard and Cheyrezy, 1995]. Consequently, a weak transition zone exists in the interface between the aggregate and paste in normal concrete and HPC do not present weak interfacial zone around aggregates like normal concrete. The aggregates in normal concrete become inclusions that form a rigid skeleton. When a compressive force is applied, shear and tensile stresses are developped at the interfaces between the aggregates, forming small cracks approximately proportional in size to the maximum aggregate diameter. In the UHPC, however, the aggregates are a set of inclusions in a continuous matrix, and the aggregate diameters are much smaller. Thus the compressive force can be transmitted by the matrix instead of a rigid skeleton of aggregates, which reduces the stresses developed at the aggregate-to-aggregate contact. The transmission of stresses by both the aggregates and the surrounding matrix in the UHPC leads to more uniform stress distribution, which can reduce potential for shear and tensile cracking at the interface [Richard and Cheyrezy, 1995]. Fig. 2.3 shows a representation of the force transfer through normal concrete compared to the UHPC [Walraven, 2002].

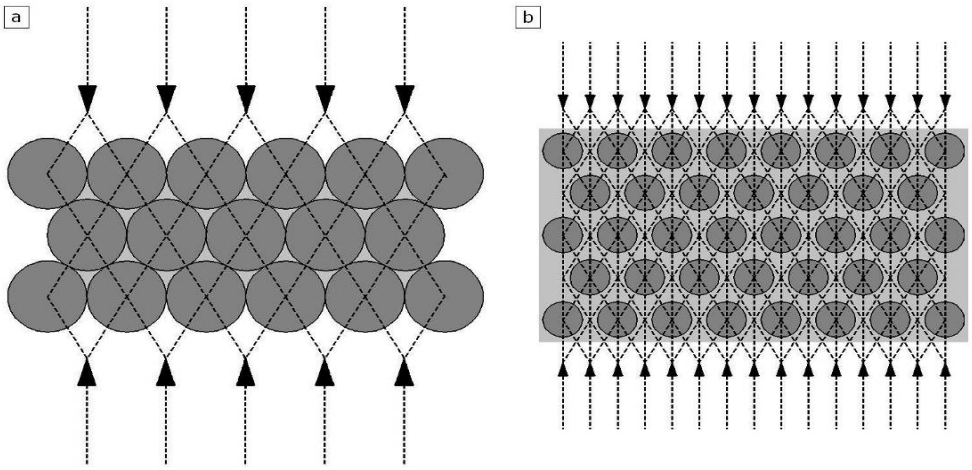

Fig. 2.2 Force transfer through (left) normal concrete and (right) UHPC [Walraven, 2002]

Richard and Cheyrezy [1994] reported that the effect of reduction in aggregate size, can be described as "meso-effect". Reduction of sand content represents a more global "macro-effect". In a conventional concrete, the aggregate (sand and gravel) are the most important components in terms of volume, and form a rigid skeleton of contiguous granular elements. This means that a major proportion of paste shrinkage is restricted by the granular skeleton, with increased porosity as a result. In UHPC, the paste volume is at least 20% greater than the voids index of non-compacted sand. Thus the aggregate used in the UHPC does not form a rigid skeleton, but a set of inclusions trapped in a continuous matrix [Richard and Cheyrezy, 1994]. Consequently, aggregate does not restrict paste shrinkage to a great extent), whereas global shrinkage is not restricted by the rigid skeleton.

According to the maximum paste thickness theory, however, completely eliminating both the fine and coarse aggregates is not entirely beneficial. Aggregates have a confining effect on cement paste. When the paste thickness between aggregates becomes large, the f_c' of the material actually decreases [de Larrard and Sedran, 1994]. Thus, fine aggregate is retained in the UHPC to maintain the highest possible f_c'.

2.2.1.2 Enhancement of compacted density

A. Optimization of granular matrix

UHPC mixtures are characterized by extremely high packing density [Richard and Cheyrezy, 1995; Ma and Schneider, 2002, and Schmidt and Fehling, 2005]. This higher density can be achieved by optimizing the proportioning of components to obtain a compact mixture. This optimization can be achieved by using packing density model (detailed in Section 2.4) [de Larrard and Sedran, 1994]. UHPC mixture is proportioned in such a way that the fine aggregate is a set of movable inclusions in the matrix, rather than a rigid skeleton. Use of smaller particles only to fill the voids between sand particles would lead to packing optimization, but a loose skeleton of sand particles would still remain.

In the UHPC, the PSD is also chosen so that, statistically, there is a wide distribution in granular class sizes, and each particle is surrounded by more than one layer of the next smaller particle size. For example, each sand particle would be surrounded by at least two layers of cement particles; each cement particle would be surrounded at least by two layers of SF particles, etc. This method is called spacing packing as shown in Fig. 2.4b [Richard and Cheyrezy, 1995]. This is very different from what is called an Apollonian packing, in which the grains of small size just fit into the holes left by the grains of large size as indicated in Fig. 2.2a. The expected result is the transmission of stress that should be much more diffuse and homogeneously distributed than in monodisperse packing as reported by Vernet [2004].

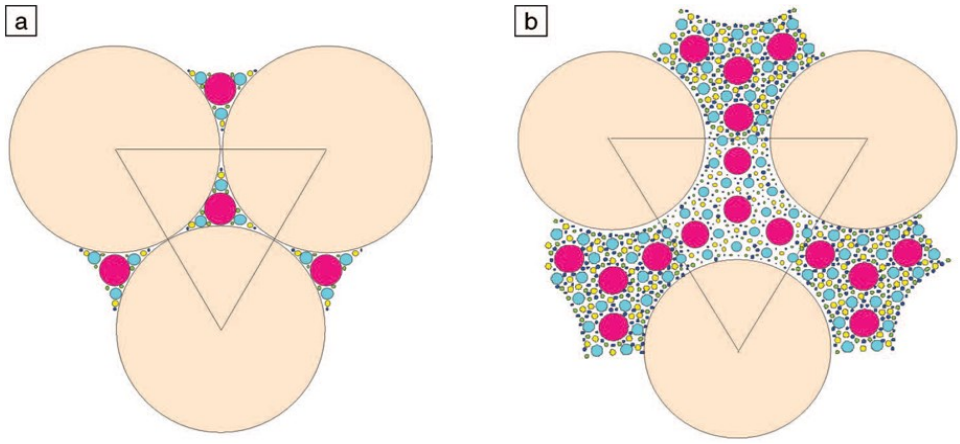

Fig. 2.3 Diagrams illustrating a) Apollonian packing and b) spacing packing [Vernet, 2004]

Richard and Cheyrezy [1995] found that maintaining a minimum ratio between the mean diameters of two consecutive granular class sizes of 13 gives the desired spacing packing. In other words, a fine aggregate with a mean diameter at least 13 times as large as cement and a SF

with a mean diameter at least 13 times as small as cement are chosen for the UHPC mix. Table 2.2 shows the mean diameters and diameter ranges for the solid particles in an UHPC mix. This approach helps to maximize density and create a more uniform stress distribution when the matrix is loaded as well as contributes for the enhancement of the mixture flowability [Richard and Cheyrezy, 1995].

Table 2.2 Granular class mean diameter and diameter ranges for UHPC mixtures [Richard and Cheyrezy 1995; Sobolev, 2004; Chan and Chu, 2004]

Component	Ratio to previous size class	Mean diameter	Typical diameter range
Steel fiber*	--	12.7 mm	--
Sand	51:1	250 µm	150 - 600 µm
Cement	19:1	13 µm	<100 µm
Crushed quartz (same class as cement)	1.3:1	10 µm	0.10 - 0.20 µm
Silica fume	67:1	0.15 µm	0.10 - 0.20 µm

*Note: Steel fiber mean diameter represents the largest dimension of fiber (length): the fiber diameter is 0.15 mm

B. Application of pressure

Another way to improve the density of the microstructure of the UHPC is to apply a pressure during setting. Richard and Cheyrezy [1995] reported that the application of pressure has favorable effects, according to the method and length of application. The application of pressure has three favorable affects: (a) eliminates or considerably reduces entrapped air in a few minutes, (b) removes excess water as long as formwork is not watertight, water is expelled via the formwork interstices, and (c) reduces some of the increases in porosity caused by self-desiccation, which is the drop in *RH* in concrete pores that leads to autogenous shrinkage [Bonneau et al., 1997]. In addition, if the applied confining pressure is maintained throughout the setting phase for the concrete (6 to 12 h after mixing), part of the porosity appearing in the sample as a result of chemical shrinkage can be eliminated [Richard and Cheyrezy, 1995]. Application of a pressure of 50 MPa to a test piece with a diameter of 7 cm for 30 min can

eliminate between 20% to 25% of the water initially introduced during mixing [Richard and Cheyrezy, 1995].

In reality, Roux et al. [1996] estimated from some of their tests that pressing the UHPC can reduce cumulative porosity by approximately 50%. The application of pre-setting and post setting pressure of 50 MPa for a period of 6 - 12 h increases the density by 5 to 6%, which further improve the microstructure, and eliminates entrapped air and excess water. Both features increase the f_c' of the UHPC. Table 2.3 summarizes the effect of pre-setting pressure on f_c' of the UHPC as demonstrated by Dallaire et al. [1998].

Table 2.3 Effect of pre-setting pressure on UHPC compressive strength [Dallaire et al., 1998]

Temperature (°C)	Pressure (MPa)	Compressive strength (MPa)
250	50	631
400	50	673
250	--	488
400	--	524

2.2.1.3 Selection of UHPC components

A. Typical UHPC components

A typical UHPC mixture contains sand, cement, SF, crushed quartz, fibers, superplasticizer, and water in the ranges shown in Table 2.1. The following sections describe in more details the role of each of these components.

Quartz Sand – Quartz sand particles are considered to be the largest PSD category in the granular mixture of the UHPC. Hence, a careful selection process is essential to avoid the formation of water pocket, air voids, and stress concentration points. The selection of sand is based on number of parameters reported by Richard and Cheyrezy [1995] such as maximum particle size of no more than 600 μm and minimum particle size not lower than 150 μm to prevent interference with the largest cement particles (80 - 100 μm).

Cement – A typical Portland cement or other similar cement can be used for preparing the UHPC. Aitcin [2000] suggested that the cement used for the UHPC should be coarse cement not rich in C_3S and C_3A. Low shrinkage cements may also be preferred since the high cement content in the UHPC tends to make it more susceptible to high shrinkage.

Interestingly, not all of the cement in the UHPC matrix hydrates due to the low water content of the mixture for the UHPC. While the hydrated cement acts as a bonding agent, the un-hydrated cement grains can act as hard inclusion reinforcing the matrix to have high elastic modulus of 120 GPa [Vernet, 2004].

Crushed quartz – Richard and Cheyrezy [1995] reported that a crushed crystalline quartz powder is an essential ingredient for heat-treated UHPC mixtures. The d_{50} of the crushed quartz used for the UHPC is 10 μm. This is found to be in the same granular class of cement.

Richard and Cheyrezy [1995] recommended that the ratio by weight adopted corresponds to the stoechiometric optimum for conversion of amorphous hydrates into tobermorite characterized by a C/S molar ratio of 0.83. This is achieved with a silica/cement ratio of 0.62. This ratio is obtained by adding SF and crushed quartz as a complement.

Since not all of the cement is hydrated, some of it can be replaced by quartz powder. Experiments by Ma and Schneider [2002] showed that up to 30% of cement volume can be replaced by crushed quartz with no reduction in the f_c'. Besides reducing the cement requirement, crushed quartz also improves the fluidity of the UHPC mixture. The improved flow characteristics may be due to the filling effect since the crushed quartz particles are slightly smaller than the cement particles. In addition, smaller amount of cement binding products are formed in first few minutes of the mixing that hinder the fluidity.

Silica fume – The SF can be defined as "very fine particle non crystalline silica produced in electrical arc furnaces as a byproduct of the production of silicon or alloys containing silicon" [ACI 116 R]. The average diameter of SF spheres is 0.1 μm, and its specific surface area is about 20000 m^2/kg measured by nitrogen absorption as compared to 250 to 450 m^2/kg for an ordinary Portland cement or fly ash [Ma and Schmider, 2002]. The SF contains from 85 to 95% SiO_2, and has a grey colour according to its carbon and iron content.

The SF can be used at low dosages (typically less than 4-6% by replacement of cement) to improve concrete rheology and enhance stability. However, it has a detrimental effect on rheology at higher dosages if it is not well dispersed. The use of SF causes a reduction in workability due to its high fineness, which is offset at least partially by its spherical particle shape. But at the same time, the SF can improve workability because the spherical particles displace water molecules from the vicinity of cement grains so that entrapped water molecules between flocculated cement particles are freed [Bache, 1981; Aitcin, 2000]. According to Park et al., [2005], the high reactivity of SF particles can increase adsorption to HRWRA, which reduces the amount available in solution and on cement particles and, thereby, decreases workability.

The SF used in the UHPC has both chemical and physical function in the plastic and hardened UHPC. The chemical contributions of SF are attributed to its very high amorphous silicon dioxide content. SF is a very reactive pozzolanic material in concrete. As Portland cement in concrete begins to react chemically, it releases calcium hydroxide (CH). The SF reacts with the produced CH to form additional calcium-silicate hydrate (C-S-H), which is very similar to C-S-H formed from the Portland cement hydration [Ma and Schneider, 2002]. This additional binder improves the hardened properties of the UHPC. In addition, SF enhances the rheological characteristics by lubrication of the mixture due to the perfect sphericity of the basic particles.

The physical effect of the SF addition to the UHPC is to bring millions of very small particles to the concrete mixture. In normal concrete, these very small particles lead to densify the transition zone between aggregate and paste and densify the matrix by filling the spaces between cement grains. This phenomenon is frequently referred to as particle packing or micro-filling even if SF not reacts chemically. The micro-filling effect would bring significant improvement of concrete mixture. In addition, the addition of SF leads to a reduction of bleeding by removal of water pockets below aggregate as well as reduction in permeability because coarse pores are replaced by fine discontinuous pores [Perry and Gillott, 2001].

SF used in UHPC should be pure with low carbon content, since carbon increases the water requirement and decreases flowability [Schmidt et al., 2003], SF slurry cannot be used because the quantity of water in the slurry often exceeds the total water required for the UHPC mixture [Richard and Cheyrezy 1995]. Zanni et al. [1996] found that SF consumption is highly dependent on heat treatment temperature and duration.

The amount of SF in concrete mixture is typically about 25% of the total binder material [Matte and Moranville, 1999]. The theoretical SF amount required for the reaction with products of cement hydration is 18%. The optimal SF can increase to about 25% to obtain densest mixture. Tests reveal the greatest f_c' could be achieved with incorporation of 30% of SF [Ma et al., 2003; Ma and Schneider, 2002]. In tests of UHPC with silica contents from 0% – 20%, Xing et al. [2006] found that the maximum flexural tensile strength occurred with a SF content of 20%, and the maximum f_c' occurred with a SF content of 5%. Bond strength between the fibers and the matrix of hardened UHPC also appears to be maximized with a SF content of 20% – 30% [Chan and Chu, 2004].

Water – The main parameter for assessing the quality of the granular mixture is water demand i.e. the minimum quantity of water which must be added to the powders to obtain fluidification [Richard and Cheyrezy 1995]. The voids index of the granular mixture corresponds to the sum of water demand and entrapped air. After selecting a granular mixture according to minimum water demand, optimum water content is analyzed using a more global parameter. This parameter is relative density d_o/d_s, where d_o designates the density of the concrete at demoulding, and d_s designates the solid density of the granular mixture assumed to be compacted (no water or air) [Richard and Cheyrezy, 1995]. The minimum *w/b* for a workable UHPC is 0.08. The term of the binder (*b*) is cement and silica fume. The relative density is not maximized at this *w/b*, as shown in Fig. 2.5. When the *w/b* is increased above the minimum value of 0.08, water replaces air without increasing the volume of the mixture up to a *w/b* of about 0.13. If the *w/b* is increased beyond this point, additional water increases the volume and thus decreases the density of the mixture. In Fig. 2.5, the mixtures represented by the descending branch of the graph have superior performance and workability to those represented by the ascending branch. Hence, the practical optimum *w/b* used is chosen slightly toward the higher values of *w/b* to ensure that the *w/b* of the actual mixture is slightly higher than the optimum theoretical value. Thus Richard and Cheyrezy [1995] identified 0.14 as the optimal *w/b* for the UHPC, which agrees exactly with the study of de Larrard and Sedran [1994] using a solid suspension model. Richard and Cheyrezy [1995] also agreed closely with Gao et al. [2006] and Lee and Chrisholm [2006], who reported an optimum *w/b* of 0.15 from experimental test samples. Wen-yu et al. [2004] reported an

optimum *w/b* of 0.16 through their tests. Table 2.4 summarizes the mean and range of *w/cm* and *w/b* used in the UHPC according to the study of [Voort et al., 2008].

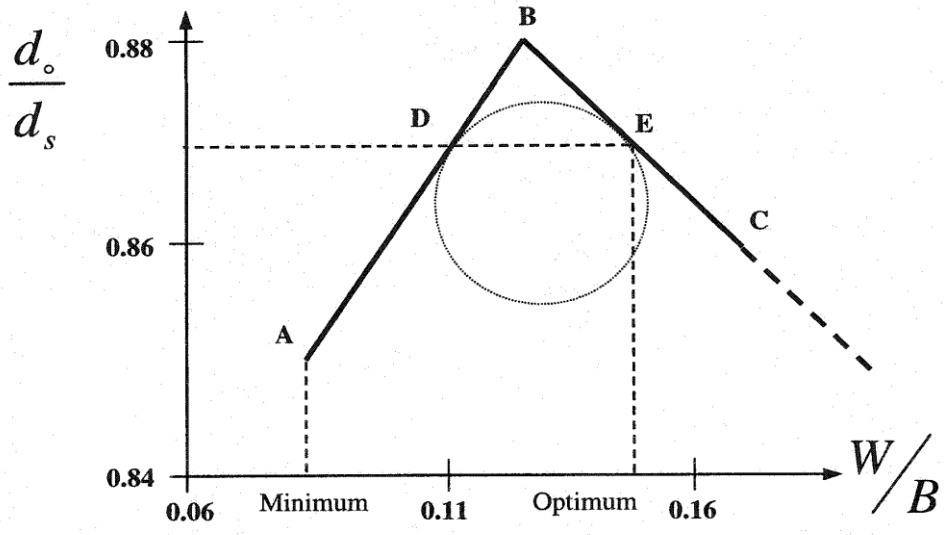

Fig. 2.4 Relative density versus water content [Richard and Cheyrezy, 1995]

Table 2.4 Low, mean, and high values of *w/b* and *w/cm* used for UHPC mixtures

Mix property	Low value	Mean value	High value
w/b	0.10 (Voo et al., 2001)	0.17	0.25 (Droll 2004)
w/cm	0.13 (Voo et al., 2001)	0.22	0.37 (Soutsos et al. 2005)

Superplasticizer – Superplasticizer used with the UHPC mixture is high-range water reducer composed of powerful organic polymers used to disperse cement particles and improving the flowability of mixes [Aïtcin et al., 2000]. Thus, superplasticizer can allow a lower *w/cm* and *w/b* to be used without sacrificing the workability of the mix. Currently, six different types of superplasticizer were used for the UHPC preparation [Rixom and Mailvaganam, 1999]. These types are superplasticizer based on polynaphathalene, polymelamine, lignosulphonates, polycarboxylate, polyacrylates, and polyphosphonate and different copolymers.

The superplasticizer plays an important role in the present development of the UHPC. The new cement-based materials (UHPC) have a very low porosity, which are obtained by the addition of very small reactive particles (diameter < 600 μm) whose role is to fill the interstitial spaces between larger particles. This addition can lead to very dense, high-strength, hardened materials.

Another positive point of this addition is that these new materials require a small amount of water because only a small quantity of hydrates is necessary to bind together the dense stack of solid particles. In fact, more hydrate formation that can be obtained when using larger water volume could lead to materials of considerably lower strength. When mixing such dry particles with small amount of water, the electric charges upon the solid particles tend to cause their aggregation and prevent a good distribution of water between solid particles, then preventing ultimately an optimal repartition of the hydrates formation between the particles. Consequently, the paste has a very low initial fluidity. Superplasticizer relatively helps to lower the surface tension of water. The addition of superplasticizer to the water is mandatory to allow the penetration of the fluid paste between the solid particles and to give to these dense mixes an adequate permeability to water. A high level of fluidity can be maintained in spite of the low water content by the use of only small amounts of superplasticizers. One can then obtain a better workability and high strength.

Since the UHPC uses such low *w/cm* and *w/b*, the optimum amount of superplasticizer is relatively high to ensure adequate workability [Vikan and Justnes, 2007]. The solid content of superplasticizer is approximately 1.6% of the cement content [Richard and Cheyrezy, 1995].

The relationship between superplasticizer effect and cement type, shows that cement with reduced amount of C_3A and low specific area adsorbs lower amount of superplasticizer. Therefore, larger amounts of superplasticizer should be available in aqueous phase to be responsible for greater dispersion of cement particles as well as for stronger retardation of C_2S and C_3S [Collepardi et al. 1999].

A study was conducted by Coppola et al. [1999] to test the effect of superplasticizer type on the f_c' of the UHPC. The results proved that, the acrylic-polymer admixture performed better than the naphthalene- or melamine-based superplasticizers in regard to lower water cement ratio and higher f_c' at 3-days age.

Schmiedmayer and Schachinger [1998] examined the effect of different dosage of superplasticizer with different mixing conditions (under atmospheric pressure or partial vacuum 15 kPa) on the bulk density, f_c', and flexural strength of the UHPC. The results showed that for each type of superplasticizer there is an optimum dosage (saturation dosage), which results in the highest flexural strength of UHPC. On the other hand, the flexural strength decreases

significantly in mixtures containing superplasticizer amount over that saturation point (optimum dosage for optimum mechanical properties). These were explained by Shirkavand and Baggott [1995], who showed that by increasing the superplasticizer dosage a more cohesive mixture was produced, with increased air content as a result. The amount of the obtained air voids had an average diameter of 0.1 - 1 mm, which increases with the increase of superplasticizer.

Plank et al. [2009] conducted methacrylate-ester- and allylether-based polycarboxylate on cement and SF paste having *w/cm* of 0.22. The results demonstrated that methacrylate-ester copolymers were found to disperse cement well, whereas allylether copolymers were more effective with SF. Mechanistic investigation in this study revealed that in cement pore solution, the surface charge of SF becomes positive by adsorption of Ca^{2+} onto negatively charged silanolate groups present on the silica surface. In such way, polycarboxylate copolymers adsorb to and disperse the SF grains. Hence, mixtures of both copolymers were tested in cement and SF paste [Plank et al., 2008]. These blends provide significantly better dispersion than using only one polymer.

B. Alternative UHPC components

Several authors have used cementitious material such as fly ash, slag, rice husk ash…etc. to replace the tradition UHPC components such as SF, quartz powder, and cement. The target when using these materials is to produce UHPC having a reduced price as well as to achieve the sustainability and green UHPC. The following paragraphs present the use of cementitious material to produce the UHPC.

Fly Ash (FA): Using FA is an alternative for the QP and cement. The FA has lubricating effect (similar to SF), helping make UHPC mixtures self-compacting [Walraven, 2002]. In addition, FA may have to be used instead of QP when the small diameter quartz particles cause respiratory health concerns.

Ground granulated blast furnace slag (GGBFS): Soutsos et al. [2005] found that up to 36% of cement can be replaced by blast furnace slag (BFS) without sacrificing f_c' or setting time. Yazici [2006] also found cement replacement of up to 40% with either FA or BFS slag had no

detrimental effects on f_c'. BFS can also be used in conjunction with crushed quartz as a cement replacement [Droll, 2004].

Yazici et al. [2008] reported that the UHPC containing high volume of binary SF–FA or binary SF–BFS or ternary SF–FA–BFS blends have satisfactory mechanical performance. In other words, utilization of FA and/or BFS in the UHPC production is very effective. According to test results, cement and SF content can be decreased by FA and/or BFS replacements. In other words, FA and BFS can be used as an alternative to SF in the UHPC. Moreover, reduction in SF content can reduce the superplasticizer demand considerably. Therefore, besides the reduced heat of hydration and shrinkage, the mixtures incorporating FA and BFS have also important environmental benefits [Yazici et al. 2008]. [Peng et al. 2010] studied the effect of using of the ultra-fine fly ash (UFFA) and steel slag powder (SS) as partially replacement of cement and SF content of UHPC. The experimental results indicate that the utilization of UFFA and SS in UHPC is feasible and has prominent mechanical performance. The microstructure analysis (SEM and TG-DTG-DSC) demonstrated that the excellent mechanical properties of UHPC containing SS and UFFA were mainly attributed to the sequential hydration filling effect of the compound system.

Rice husk ash (RHA): The RHA has been used as a cement alternative in the manufacturing of HPC. Van Tuan et al. [2011] found that the combination of SF and RHA can increase the total cement replacement up to 40% to produce UHPC. The addition of RHA does not. The RHA can be used as a mineral admixture to produce UHPC without significant decrease of the f_c' and the workability. A synergic effect between RHA and SF was also found to improve both the workability and the f_c' of the UHPC. This leads to a higher amount of the total cement replacement to make UHPC, which is very important for the sustainable development of the construction industry.

2.2.1.4 Post heat treatment and enhancement of microstructure

The primary function of heat treatment is to enhance the hydration reactions in concrete to further reduce porosity and enhance mechanical and durability properties of the mixture. Heat

treatment temperatures can vary between 90 and 400°C. The heat treatment may extend from 48 h to six days. The typical heat treatment used for the UHPC was a 48 h at 90°C.

The UHPC is formulated with high amount of SF and QP. The pozzolanic reaction of SF depends heavily on the temperature and duration of heat treatment. Consequently, heat treatment has the potential to greatly accelerate the reaction [Richard and Cheyrezy, 1995; Zanni et al., 1996]. The increased pozzolanic reactions of SF can lead to porosity decrease. Cheyrezy et al. [1995] reported that the overall porosity of UHPC is not changed with heat treatment but the intermediate porosity is converted into small diameter porosity. Roux et al. [1996] confirmed this finding and reported that the size of micropores can be reduced several orders of magnitude through heat treatment. Cheyrezy et al. [1995] also found that the heat treatment temperature for optimal porosity was 150 – 200°C. Heat treatment also improves ratio of bound water to free water in the UHPC. In fact, after heat treatment at 400°C, no free water remains in the UHPC [Cheyrezy et al., 1995]. Fig. 2.6 represents the percentage of bound water versus heat treatment temperature [Cheyrezy et al., 1995].

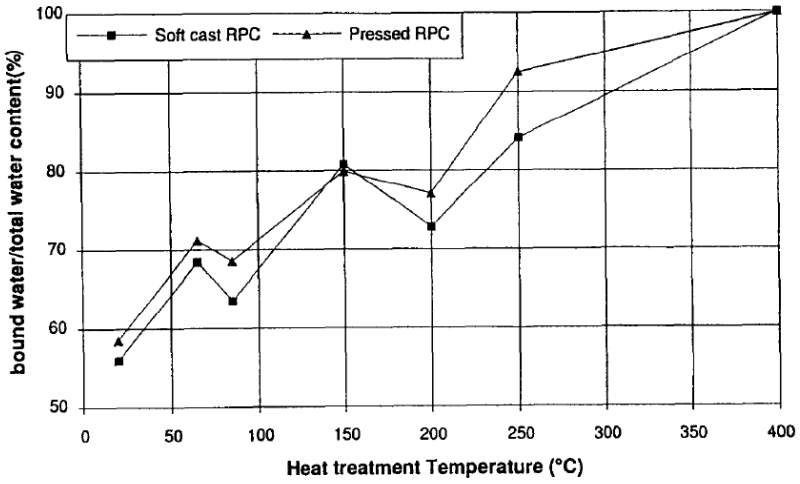

Fig. 2.5 Bound-water percentages versus heat treatment temperature in UHPC [Cheyrezy et al., 1995]

Based on the number of investigations carried out to investigate the effect of heat treatment on the microstructure of UHPC, the flowing conclusions can be drawn: [Richard and Cheyrezy, 1995; Cheyrezy et al., 1995; Zanni et al., 1996].

- Higher temperature leads to higher bound-water percentage. At 400 °C, no more excess free water remains in concrete.
- Heat-treatment temperature of UHPC leads to development of longer C–S–H chain. This phenomenon can be attributed to the progression of cement hydration and pozzolanic activities for both SF and crushed quartz.
- Heat treatment at 90°C modifying the microstructure of hydrates, however, these hydrates remain amorphous.
- Heat temperature in range of 150 - 200 ^{0}C can modify the chemical composition of the hydrated product by reducing CaO/SiO_2 and H_2O/CaO ratios and by the formation of Tobermorite [$Ca_5Si_6O_{16}\cdot(OH)_2\cdot 8H_2O$].
- For temperature ≥ 250 °C, almost all portlandite formed by cement hydration is consumed by pozzolanic reaction.
- High portion of cement remains unhydrated (degree of cement hydration varies in range of 40% to 60%).
- Ettringite was not observed by XRD. Due to the low amount of C_3A of the cement use.
- At high temperature (250 - 400°C), Truscottite [$Ca_{14}Si_{24}O_{58}\cdot(OH)_8\cdot 2H_2O$], Gyrolite [$NaCa_{16}\cdot(AlSi_{23}O_{60})\cdot(OH)_8\cdot 14H_2O$], Xonotlite [$Ca_6Si_6O_{17}(OH)_2$], and Hillebrandite [$Ca_6Si_3O_9(OH)_6$] are formed depending on CaO to H_2O (C/H) ratios.
- For temperature ≥ 300 °C, the decomposition of the superplasticizer takes place and continues as temperature increases.

2.2.1.5 Ductility enhancement

Designing UHPC without fibers gives a material very strong but brittle. A ductile behaviour can be obtained by the addition of steel fibers. The flexural strength can increase from 28 MPa to approximately 100 MPa and fracture energies from 50 to 40000 Jm^{-2} depending on the type of hot curing and amount of fibers added [Richard and Cheyrezy, 1994].

The fibers of 13-mm long and 0.15-mm diameter used in the UHPC should not exceed 4% the total volume according to Nielsen (1995) or 2.5% according to Rossi [2005]. The workability of the UHPC mixtures clearly decreases with increasing fiber size. A 2% fiber volume represents the most common content for the UHPC and corresponds to the most economic content identified by Richard and Cheyrezy [1995]. Fig. 2.7 shows an X-ray image of a 2% volumetric

fraction of steel fibers in a sample of UHPC. This figure shows the dense packing of fibers in the UHPC despite the low volumetric fraction [Acker and Behloul, 2004].

The orientation of fibers relative to the plane of cracking affects the ductile behavior of the UHPC, so care must be taken to properly mix and place the UHPC to avoid clustering of fibers and to ensure proper fiber dispersion within each UHPC element [Bayard and Plé, 2003].

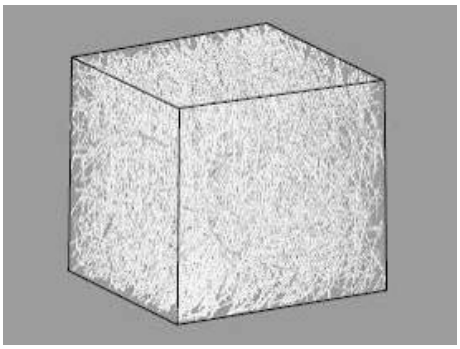

Fig. 2.6. X-ray image of fiber distribution 40-mm cube of UHPC [Acker and Behloul, 2004]

2.2.2 Fundamentals properties of UHPC

2.2.2.1 Early age properties

A. Density

Because UHPC has a very compact microstructure, its density is higher than that of HPC or normal concrete, and the weight per cubic foot is also slightly increased. Table 2.5 shows a comparison among the typical densities of UHPC, HPC, and normal concrete mixes. The density of UHPC is higher than that of normal concrete or HPC, but the slight increase in weight is easily offset by the much higher strength of UHPC. The average reported value for the density of UHPC mixes from 17 published mix descriptions was approximately 2510 kg/m^3 [Voort et al., 2008].

B. Workability

American Concrete Institute (ACI) Standard 116R-90 [ACI, 1990] defines workability as "that property of freshly mixed concrete which determines the ease and homogeneity with which it can be mixed, placed, consolidated, and finished. Workability is affected by every component of concrete and essentially every condition under which concrete is made. A list of factors includes the properties and the amount of the cement; grading, shape, angularity, C_3A content, and surface

texture of fine and coarse aggregates; proportion of aggregates; types and amounts of fiber added; Amount of air entrained; type and amount of pozzolan; types and amounts of chemical admixtures; temperature of the concrete; mixing time and method; and time since water and cement made contact. These factors interact so that changing the proportion of one component to produce a specific characteristic requires that other factors be adjusted to maintain workability [Neville and Brooks, 1987; Mindess and Young, 1981].

Table 2.5 Comparison between density of UHPC, HPC, and normal concrete

Concrete type	Typical density range
Normal concrete	(2290 – 2400 kg/m^3)
HPC	(2430 – 2480 kg/m^3)
UHPC	(2320 – 2760 kg/m^3)

(Compiled based on data presented by Kosmatka et al. [2002], Ma et al. [2003], and Teichmann and Schmidt [2004]

Shaheen and Shrive [2006] reported that UHPC is so thick and viscous materials as well as has zero slump flow at *w/cm* equal 0.13. Liu and Hung [2008] produced a highly flowable UHPC with the slump flow over 200mm. Ma and Schneider [2002] reported that the flowability of UHPC is improved when replacing 30% of cement by quartz powder. The result demonstrates that slump flow increases from 510 mm to 610 mm.

The workability of normal concrete is usually significantly reduced when fibers are included in the mix. Due to the fineness of the constituents of UHPC, however, interference issues between aggregates and fibers do not exist to the same degree as they do in concretes with coarse aggregates. Therefore, a reduction in workability is only expected for fiber contents greater than 2.5% to 4.0% by volume [Bonneau et al., 1997; Nielsen, 1998; Rossi 2005].

C. Setting time

Estimates of the setting time for UHPC vary widely. Richard and Cheyrezy [1995] identified the setting time as only six to 12 h, while other estimates of setting time were as high as 40 hours [Brown, 2006], it depends on the type of the superplasticizer. The large discrepancy in setting time is likely due to differences in researchers' definitions of setting time and/or to delays in

setting caused by the use of high amounts of plasticizer. Habel et al. (2006) identified the setting point as the point at which the stiffness of the mix reaches 1.0 GPa and autogenous shrinkage begins. From their study, they further determined the setting point of the UHPC mix to be 31.5 h, which corresponded to 16% of the final hydration. Graybeal [2006] defined the initial set and final set using the AASHTO T197 standard test method. He observed that initial set, defined as a penetration resistance of 3.4 MPa, occurred approximately 15 h after casting, and final set, defined as a penetration resistance of 27.6 MPa, occurred 18 to 20 h after casting.

2.2.2.2 Hydration and microstructure

A. Hydration

The heat of hydration is the heat generated when water and cement react. Strength development of concrete depends on the rate and hydration of cement. Composition (C_3S and C_3A) and fineness of cement, *w/cm*, type and contents of supplementary materials (fly ash, slag and SF), type and content ratio of chemical admixtures (superplasticizer, set accelerator, set retarder, etc.), and medium temperature have significant influence on cement hydration.

As stated previously, the UHPC is formulated with very low water content; consequently, not all of the cement grains are hydrated. Fig. 2.8 shows the maximum possible degree of hydration as a function of *w/cm*. The figure indicates that the maximum hydration percentage for a *w/cm* of 0.20 is approximately 50%. Habel et al. [2006] and Cheyrezy et al. [1995] estimate the final hydration percentage of the cement in UHPC range from 31% to 60%. These estimates agree with the chart from Bruegel and Guang. A slightly higher degree of hydration can be reached with water or steam curing compared to dry curing [Ay, 2004]. The unhydrated cement particles make UHPC potentially self-healing. Unhydrated cement particles have the ability to close up small cracks in the matrix when a small amount of additional water is introduced in the area of the crack [Granger et al., 2006; Sritharan et al., 2003]. Fig. 2.9 shows a self-healed micro-crack in a UHPC specimen.

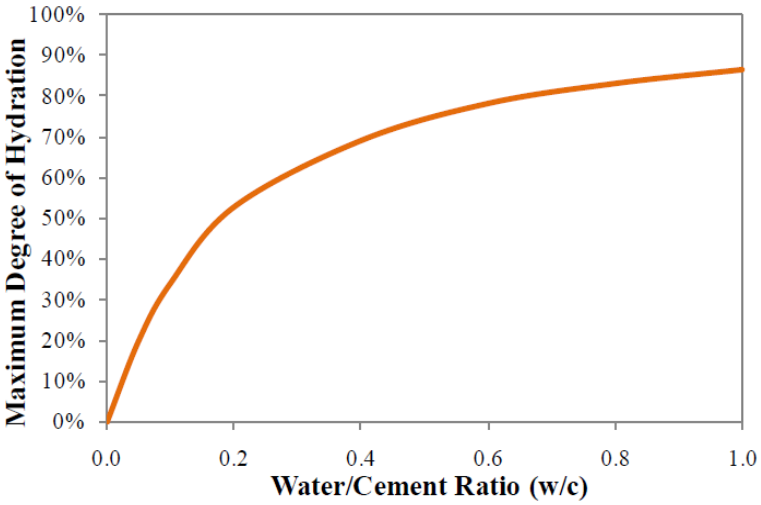

Fig. 2.7 Maximum degree of hydration versus *w/cm* [Breugel and Guang, 2004]

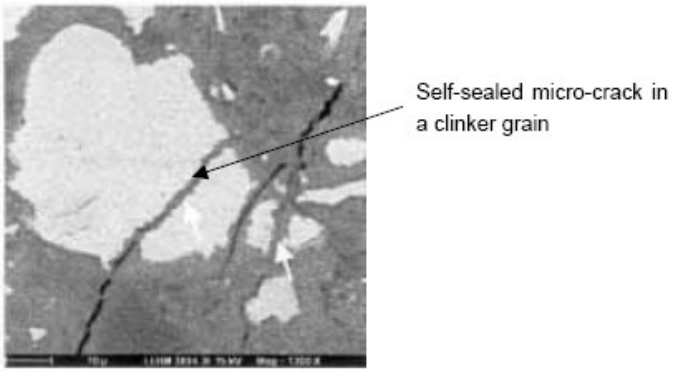

Fig. 2.8 Self-healing of UHPC micro-crack [Acker and Behloul, 2004]

Habel et al. [2006] investigated the hydration reaction of untreated UHPC. The results demonstrated that the hydration reaction initially develops very quickly and then slows down as almost all of the mixing water is consumed, as shown in the hydration model in Fig. 2.10. Approximately 96% of the final hydration is reached after 28 days after casting, and hydration has virtually stopped at 90 days. The fast development of the degree of reaction also led to a fast development of the mechanical properties. Thus, at 7 days, f_c' reached a value of 140 MPa, which was 81% of the final strength (for a degree of reaction = 1); the tensile strength, max was 5.8 MPa, corresponding to 60% of the final strength and the E_c was 43 GPa, corresponding to 84% of the final modulus. The high early strengths are advantageous to accelerate the construction process Habel et al. [2006].

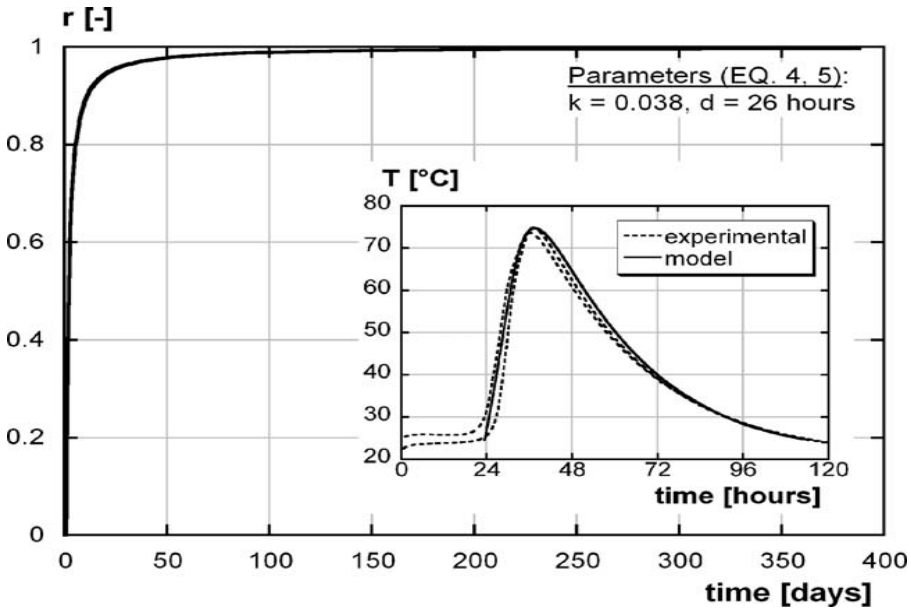

Fig. 2.9. Development of percentage of final hydration in untreated UHPC with time [Habel et al., 2006]

B. Microstructure development

UHPC with very low *w/b* and optimized granular mixtures shows a very dense microstructure [Reda et al., 1999; Schmidt and Fehling, 2005]. The extremely dense microstructures of UHPC can be observed by electron microscopy. Figure 2.11 shows the hydration process and the development of the UHPC microstructure observed by scanning electron microscope (SEM) [Möser and Pfeifer, 2008].

Up to a hydration time of eight hours and beyond, the microstructure of UHPC is dominated by spherical SF particles as shown in Fig. 2.11a. Isolated ettringite crystals with a short prismatic (length up to 400 nm) are visible between the SF spheres. The hydration of the clinker phase alite is retarded up to this point in time by the superplasticizer used, so that no C-S-H phases are observed. With the hydration process, after a time of 18 hours, C-S-H phases with a length of up to 200 nm are visible as seen in Fig. 2.6b. Fig. 2.6c presents hydration after a time of 4 days (heat-treated sample) the clinker grain shows only a marginal, heterogeneous dissolution structure of the alite phase). After 28 days of hydration the clinker grain shows a strongly dissolved area of the alite phase (reaction zone approximately 1 µm as shown under the white line in as shown in Fig. 2.11d [Möser and Pfeifer, 2008].

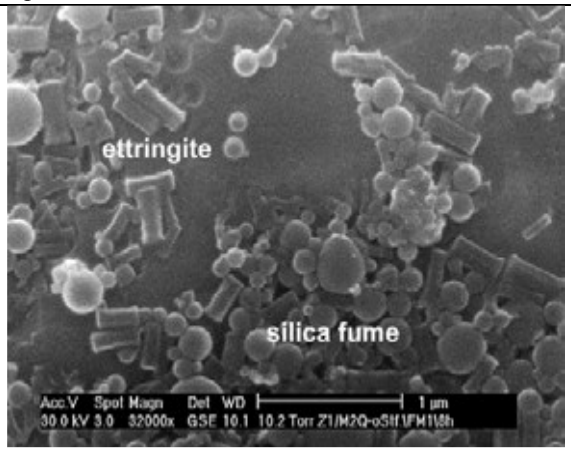

(a) Hydration at 8 hours: spherical SF particles and short prismatic (length up to 400 nm) ettringite crystals

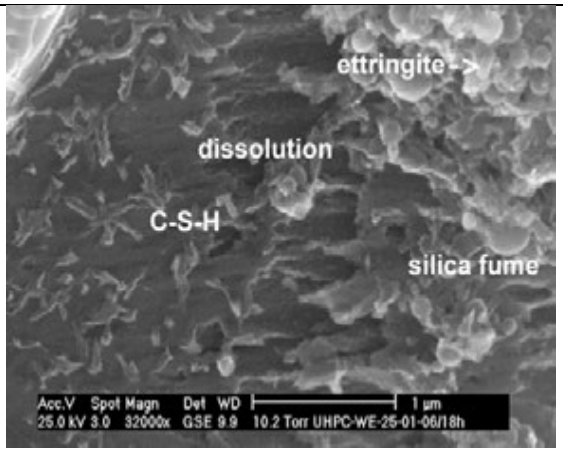

(b) Hydration at 18 hours: needle-like C-S-H phases (length up to 200 nm) and cavities on the surface of an alite grain

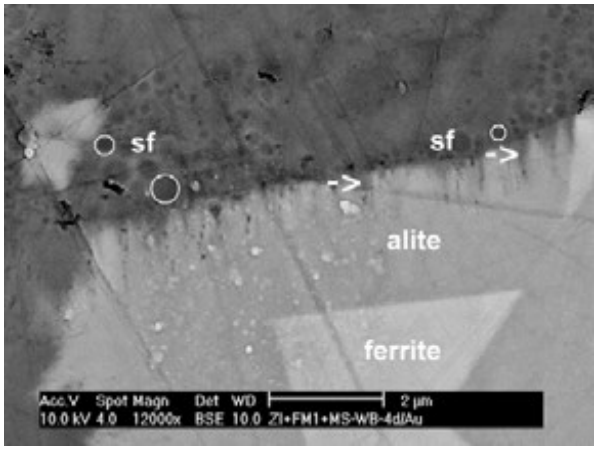

(c) Heat-treated sample after 4 days: marginal heterogeneous dissolution of alite (see arrows); SF- dark spheric

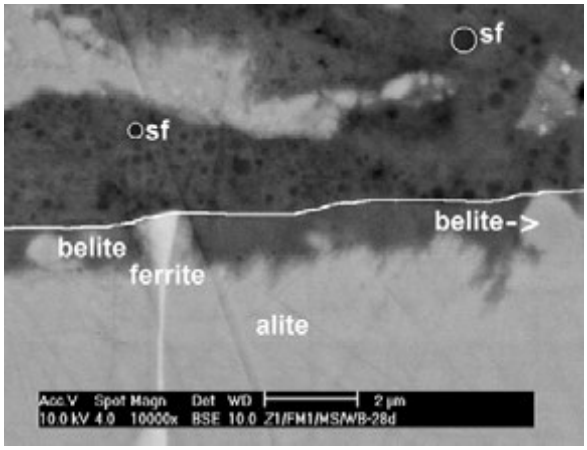

(d) Heat-treated sample after 28 days: phases of a clinker grain with different reactivity - the white line marks the former grain size

Fig. 2.10 Hydration of UHPC over time (a) 8 h, (b) 18 h, (c) 4 days, and (d) 28 days [Möser and Pfeifer, 2008]

Regarding to the interfacial transition zone (ITZ) between the cement paste and sand particles in UHPC, the thickness of this zone was found to be very small compared to that of conventional concrete [Reda et al., 1999]. This is due to the absence of coarse aggregate in UHPC resulting in a significant reduction of the wall effect normally occurring around the surface of larger size

particles. Fig. 2.12 represents a comparison between the transition zones of normal concrete and UHPC [Droll, 2004]. It can be seen that broad gaps between the cement matrix and aggregate grains up to 20 μm are clearly visible in normal concrete and a direct adhesion takes place only at a part of the complete contact surface, but is very small in the UHPC mixtures.

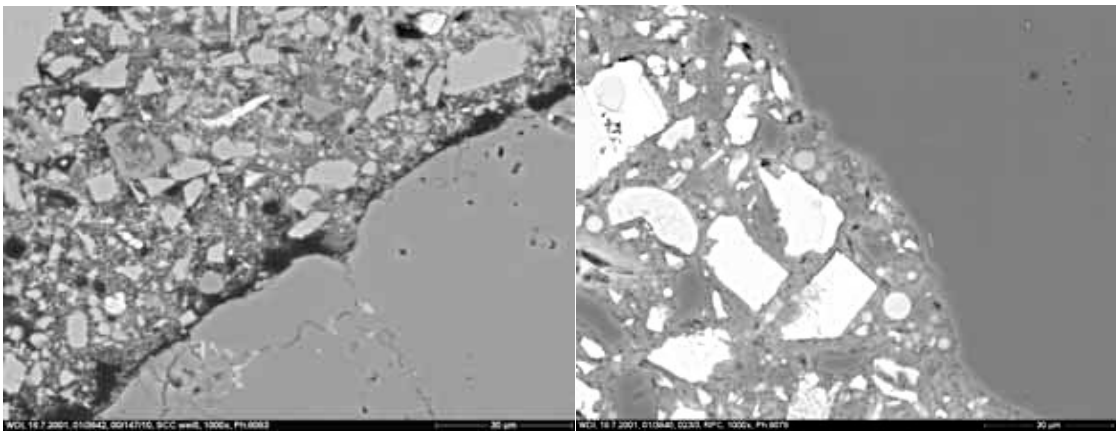

Fig. 2.11 Interfacial transition zone in a normal concrete and in UHPC with magnification of 1000X [Droll, 2004]

2.2.2.3 Dimensional stability

A. Shrinkage

Two types of shrinkage contribute to the total shrinkage in concrete – autogenous shrinkage and drying shrinkage. UHPC can experience large shrinkage values, but unlike normal concrete, autogenous shrinkage makes up a larger portion of the total shrinkage in UHPC than drying shrinkage according to tests by Schmidt et al. [2003] on untreated UHPC samples and on UHPC samples subjected to the standard heat treatment.

Autogenous shrinkage **–** Autogenous shrinkage of cement paste and concrete is defined as the macroscopic volume change occurring with no moisture transferred to the exterior surrounding environment. It is a result of chemical shrinkage linked to the hydration of cement particles. Autogenous shrinkage is driven by chemical shrinkage. The total volume of hydration products of cement and silica fume is approximately eight percent less than the total volume of the initial components. After mixing, chemical shrinkage proceeds uninhibited until the largest particles in the UHPC mix have no global degrees of freedom [Feylessoufi et al., 2001]. The solid skeleton

that forms restrains chemical shrinkage, causing air voids in the matrix [Habel et al., 2006a]. As a result, the RH in the pores of the concrete decreases rapidly in a process called self-desiccation [Loukili et al., 1999]. The self-desiccation causes increased capillary tension in the pores of the UHPC, and the capillary tension drives the shrinkage of the matrix. When the RH drops to 73% (point A) autogenous shrinkage stops at (point B). This nearly constant RH corresponds with a near stop in autogenous shrinkage in UHPC, as shown in Fig. 2.13 [Loukili et al., 1999].

Ma and Schneider [2002] reported that UHPC generally shows a higher autogenous shrinkage than HPC. They stated that high cement content and low *w/b* in UHPC may lead to autogenous shrinkage, which will induce micro cracks in early ages. The results of autogenous shrinkage of UHPC with different silica fume contents and *w/cm* is shown in Fig. 2.14.

With a high autogenous shrinkage possible, cracking is a concern in early-age UHPC behavior. A low *w/b* and associated high amount of cement make UHPC more susceptible to cracking from high shrinkage. Strategies used to control the restraint stresses developed in UHPC due to autogenous shrinkage include heat treatment with steam curing and application of pressure during setting.

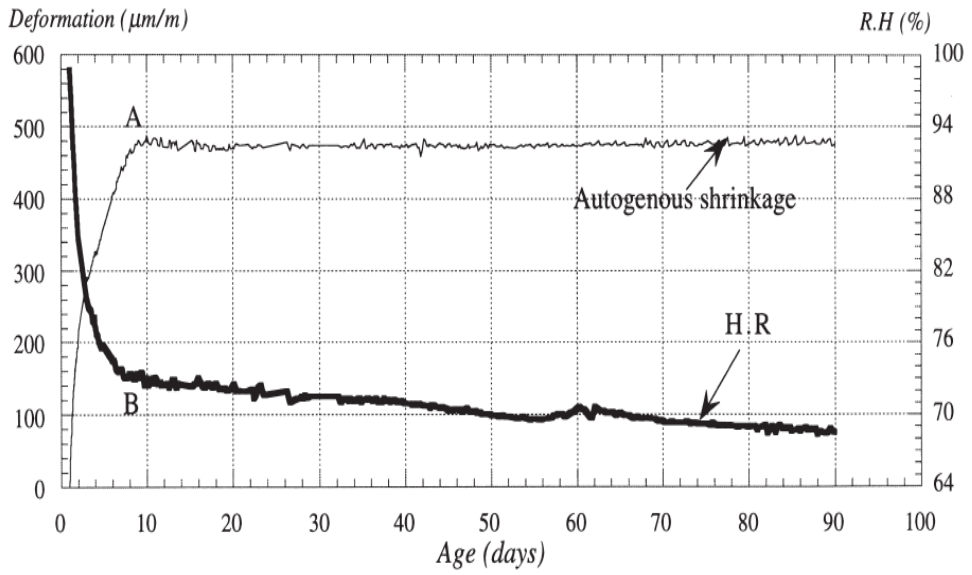

Fig. 2.12. Evolution of relative humidity (RH) and autogenous shrinkage with time [Loukili et al., 1999]

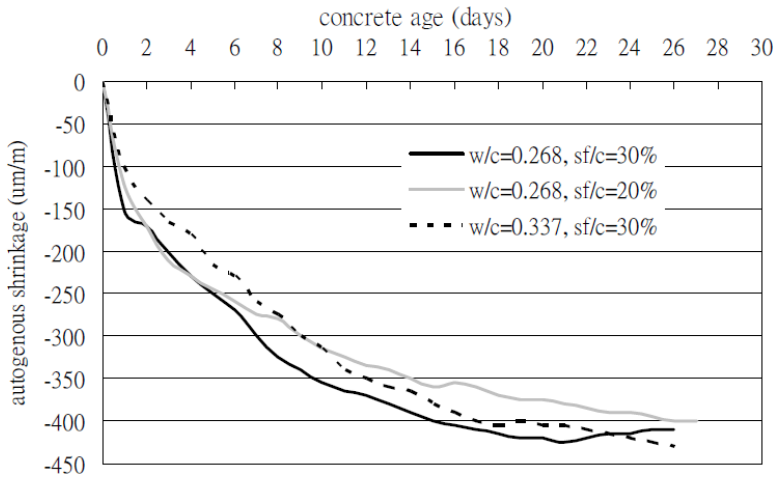

Fig. 2.13 Autogenous shrinkage of UHPC [Ma and Schneider, 2002]

Drying shrinkage – Drying shrinkage refers to the volume reduction in the cement matrix resulting from an overall loss of water to the environment through evaporation. As evaporating water is lost by capillary pores in the concrete, the vapor pressure drops and induces tensile stresses in the pores that cause the concrete to shrink (Cement and Concrete Association of Australia 2002). Habel et al. [2006] found that drying shrinkage in UHPC is most intense during the first 20 days, reaching a magnitude of 40×10^{-6} at day 20 and 80 $x10^{-6}$ by day 90. They also noted that the dense matrix of UHPC after 20 days largely prevents moisture exchange with the environment except in a localized zone at the surface. Cheyrezy and Behloul [2001] found a somewhat higher drying shrinkage of 170×10^{-6} at 90 days.

B. Creep

Creep is defined as the time-dependent increase in strain under constant load taking place after the initial strain at loading. The ultimate creep coefficient is 0.78 for untreated UHPC [Graybeal, 2006]. This is noticeably smaller than the creep coefficient expected for normal concrete, which is in the range of 2.0 to 4.0 [Jones and Cather, 2005; Acker and Behloul, 2004]. Similarly to normal concrete, the value of the creep coefficient for UHPC does appear to be greatly affected by the concrete age at loading [AFGC, 2002]. Table 2.6 represents how the magnitude of UHPC creep depends on loading age. Fig. 2.15 shows the reduction in creep achieved through heat

treatment. Graybeal [2006] measured a specific creep, defined as the ultimate creep per unit stress, of 21.2×10^{-6} MPa for untreated UHPC loaded at 28 days, confirming the accuracy of the Association Française de Génie Civil (AFGC) equation.

Table 2.6 Ultimate creep and creep coefficient for untreated UHPC with different loading ages [AFGC, 2002]

Concrete age at loading	Creep coefficient	Specific creep ($\times10^{-6}$ /MPa)
1 day	2.27	46.9
4 days	1.80	37.2
7 days	1.57	32.5
28 days	1.08	22.2

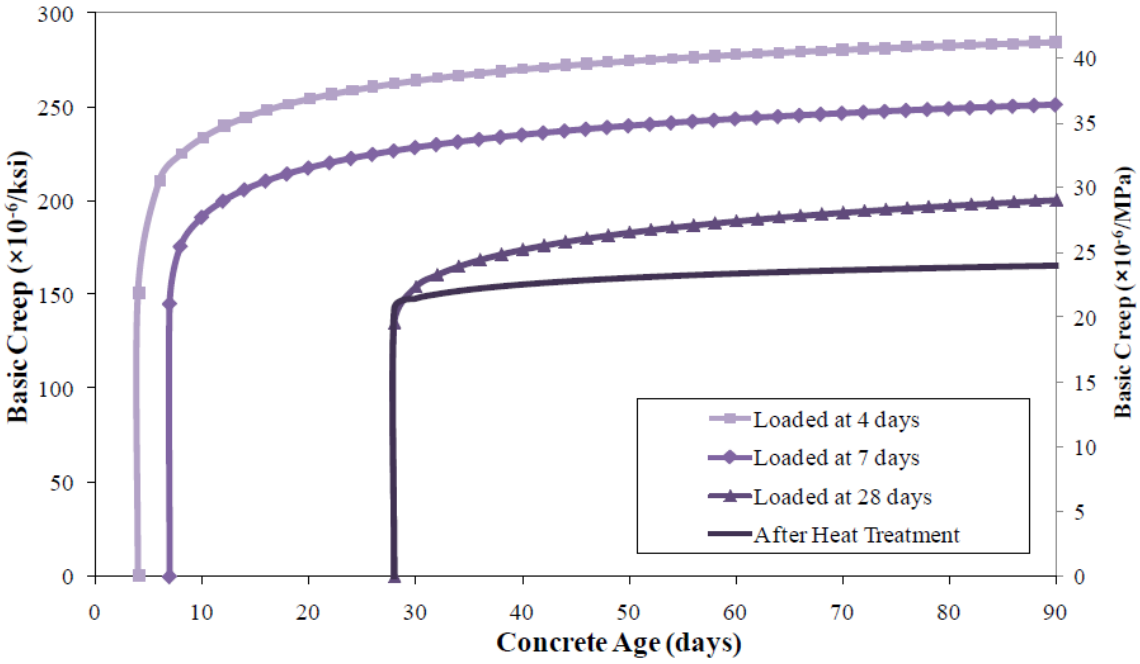

Fig. 2.14 Basic creep of UHPC for different loading ages [AFGC, 2002]

2.2.2.4 Mechanical properties

A. Compressive strength

One of the most noticeable characteristics of UHPC is its high f_c'. Richard and Cheyrezy [1995] demonstrated that UHPC is capable of reaching f_c' values of 200 - 800 MPa. The increase in f_c',

over NSC or HPC, can be attributed to the particle packing and selection of specific constituents, and thermal curing of UHPC. When undergoing a 48-hour thermal treatment of 90°C at 95% *RH*. Graybeal [2005] showed an increase of 53% over non-thermally cured specimens of the same age. This increase in f_c' may allow UHPC to get a foot hold in the long span and low span-to-depth ratio market segments which have been dominated by steel; creating choices for designers and owners.

The low *w/b* and use of a proper heat treatment to reduce the final porosity of UHPC increases f_c'. Shaheen and Shrive [2006] reported that f_c' increases rapidly with curing temperature between 23 and 150°C due to the acceleration of the hydration process as well as rises again between 200 and 300°C due to pozolanic reaction of quartz, which can be activated at this temperature. Table 2.7 summarizes f_c' values obtained for normal curing at 20°C for UHPC, UHPC with the standard heat treatment of 90°C for two days, and UHPC with higher temperature heat treatments of 160 – 250°C. It is important to note that some the UHPC samples subjected to the high temperature heat treatments were also subjected to a confining pressure while curing. The table allows comparison of results for different curing regimes obtained from the same samples sources that were produced and tested under similar conditions. The f_c' of UHPC generally appears to increase with increasing heat treatment temperature. The f_c' of UHPC was increased on average by 35 percent for the 90°C heat treatment samples with respect the strengths obtained for normal curing UHPC. This observation is made using the results reported for both heat treated and untreated UHPC in references in Table 2.7.

A maximum f_c' of 810 MPa has been achieved by Richard and Cheyrezy [1995] for a UHPC mix incorporating steel aggregates, heat treatment at (400 °C), and application of a 50 MPa confining pressure during setting. This type of extremely high strength UHPC has only been successfully produced in the laboratory and requires a demanding production process. Instead, applying pressure during setting and confining concrete in stainless steel tubes may be a more early way to achieve very high f_c' in UHPC members. A f_c' of 380 MPa was achieved by confining UHPC in 3 mm thick stainless steel tubes and applying the 50 MPa confining pressure for the design of the Sherbrooke Pedestrian Bikeway Bridge in Canada [Dallaire et al., 1998].

Table 2.7 Compressive strength for UHPC under different curing regimes

Author	Compressive strength, MPa		
	Normal curing [20°C]	Hot curing [90°C]	Hot curing [>150°C]
Richard and Cheyrezy, (1994)	170	230	630
Bonneau et al. (1997)	150	218	--
Colleparadi et al. (1997)	155	160	195
Ma and Schneider (2002)	150	200	--
Schmidt et al. (2003)	150	162	--
Heinz et al. (2004)	178	222	273
Soutsos et al. (2005)	135	185	--
Graybeal (2005)	130	193	--
Lee and Chisholm (2005)	160	205	230
Cwirzen (2007)	153	200	--
Tam and Tam (2012)	--	144 (24 h)	200 (24 h)

Regarding the effect of type and amount fiber added on f_c' of UHPC. Schmidt et al. (2003) remark f_c' "is practically not increased by the fibers," which occupied 2.5% of the volume of the UHPC mix in their tests. Reda et al. [1999] reported that the increase due to fibers is not as great as the increase that can be achieved through heat treatment, although the observed increase in strength is statistically significant with a fiber content of 2.0%. Bonneau et al. [1997], Herold and Müller [2004], Soutsos et al. [2005], and Lee and Chrisholm [2006] reported f_c' of the UHPC mixtures with both 0% and 2.0% to 2.5% fiber contents show an average increase in compressive strength of 30% with the increase in fiber content from 0 to 2.0 - 2.5%. Klemens [2004] compares the f_c' results for UHPC mixes utilizing different fiber types, including organic fibers and steel fiber contents. The results demonstrated that steel fibers increase the f_c' of UHPC when compared to the values obtained using organic fibers from approximately 150MPa to 200 MPa. Based on these investigations, it is concluded that the type and content of fibers do appear to influence the f_c' of UHPC.

B. Tensile strength

Normal concrete has a low tensile strength, typically between 2.1 to 4.8 MPa as calculated from equations by Kosmatka et al. [2002] for the range of f_c', so building codes and standards typically ignore concrete's contribution to tensile resistance for most structural applications. The tensile strength of HPC for the range of compression strengths can be estimated as 5.5 to 6.2 MPa based on equations by Yin et al. [2002]. When reinforced with steel fiber, UHPC develops a much more significant tensile strength; even beyond in the post-cracking regime due to the ability of steel fibers in the matrix to bridge micro-cracks [Voort et al., 2008].

Richard and Cheyrezy [1995], Bayard and Plé [2003], Cadoni et al. [2008], Habel et al. [2006b], and Rossi [2005] have found that UHPC can also experience some strain-hardening between its first tensile cracking strength and ultimate tensile strength. Graybeal reports a first cracking tensile strength of 9.7 to 11.0 MPa from direct tension tests on UHPC cylinders. Tests by Graybeal [2005] also demonstrate the tensile strength of untreated UHPC, at 5.5 to 6.9 MPa, is lower than that of heat-treated UHPC for the direct tension tests. Habel et al. [2006b] also developed a model for the development of the tensile strength of untreated UHPC. The direct tensile strength increases 46 percent from seven to 56 days. Therefore the rate of development of the tensile strength of UHPC is much slower than the rate of development of the f_c'.

***C.* Elastic modulus**

The E_c is a material dependent property which is often described as a mathematical relationship between stress and strain. Typically when the value is given for concrete, it is referencing the elastic portion of the compressive stress-strain curve up to 40% of the ultimate compressive strength as specified in ASTM C 469 standard test method for static E_c and Poisson's ratio (ν) of concrete in compression. The slope of the elastic portion of the stress-strain curve is the modulus of elasticity. The E_c is used in design calculations to predict deflection behavior of the element so the design can often satisfy the specified limit states.

The elastic modulus of normal concrete with f_c' values of 28 to 55 MPa is typically 25 to 35 GPa [ACI, 2005], and the elastic modulus of HPC with compression strengths of 83 to 124 MPa is approximately 33 to 44 MPa, according to the equations ACI Committee 363 [ACI, 1997] for HPC. UHPC has a high elastic modulus typically is range of 57 GPa to 70 GPa [Richard and

Cheyrezy, 1994]. Bonneau et al. [1996] show the elastic modulus of UHPC without fibers is 46 GPa compared to 49 GPa with a 2.0% steel fiber content, an increase of only about 6.5% due to the presence of fibers. Graybeal [2006] reported standard heat treatment increases the elastic modulus of UHPC 23% from 43 to 53 GPa. Ma and Schneider [2002] found that the elastic modulus increases is not proportioned to the increase of f_c' across different curing days as indicated in Fig. 2.16.

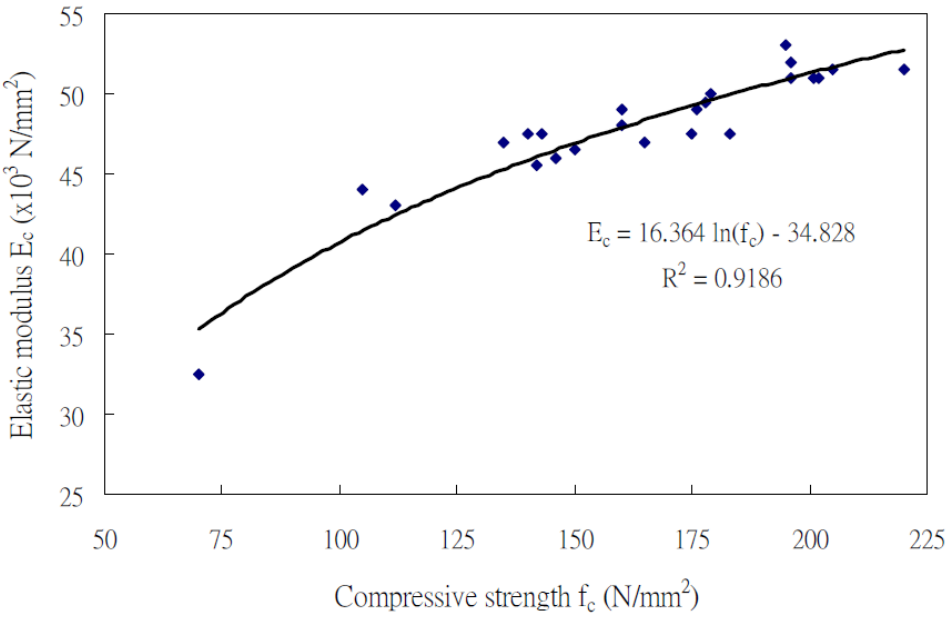

Fig. 2.15 Relationship between compressive strength (f_c') and elastic modulus of untreated UHPC [Ma and Schneider, 2002]

Many equations have been used to define the relationship between the elastic modulus and the f_c' of concrete. ACI Committee 318-5 [ACI, 2005] presents an equation which relates the 28 day f_c' of normal strength concrete to the E_c, The ACI 318-05 equation, is shown as Eq. (2.1). However, HPC has a much greater f_c' than normal strength concrete. ACI Committee 363-92 produced a relationship for higher strength concrete up to 83 MPa, as shown as Eq. (2.2).

According to ACI 318-05: $$E_c = 5700 \times \sqrt{f_c'} \quad (2.1)$$

According to ACI 363R-92: $$E_c = 4000 \times \sqrt{f_c'} + 1000 \quad (2.2)$$

The previous two equations do not apply as the high f_c' of UHPC lies above the range of applicable f_c'. Equations 2.3 to 2.5 have been developed specifically for UHPC, although the coefficient in the equation by Sritharan et al. [2003] is based on a single UHPC mix and is not intended for a broad range of f_c'.

According to Sritharan et al., 2003: $E_c = 5000 \times \sqrt{f_c'}$ (2.3)

According to Graybeal 2007: $E_c = 4620 \times \sqrt{f_c'}$ (2.4)

According to Ma et al. 2004: $E_c = 19000 \times \sqrt[3]{f_c'}/10$ (2.5)

where; E_c and f_c' are in (MPa).

D. Flexural strength

UHPC has superior flexural strength compared to normal and HPC. UHPC has a flexural strength around 30 - 60 MPa and had a toughness of 250 times that of normal strength concrete when reinforced with steel fibers [Richard and Cheyrezy, 1995]. Perry and Zakariasen [2003] showed that UHPC had flexural strengths ranging from 30 - 60 MPa which confirmed Cheyrezy's findings. Dugat et al. [1996] reported average modulus of rupture values of approximately 20 MPa and an ultimate flexural strength of 30 MPa. Graybeal and Hartmann [2003] attributed the increase in the flexural behavior of UHPC to the enhancement of particle packing and the addition of fibers which hold the cement matrix together after cracking has occurred. UHPC exhibits ductility because when the specimen begins to microcrack the small scale fibers reinforce the matrix causing less damaging cracks to form.

Typical UHPC behavior under flexure is characterized by linear elastic behavior up to the first cracking strength of the material, a strain-hardening phase up to the maximum load, and a strain softening phase after the maximum load is reached. Fig. 2.17 shows a typical load-deflection diagram for UHPC in bending with the typical phases labeled.

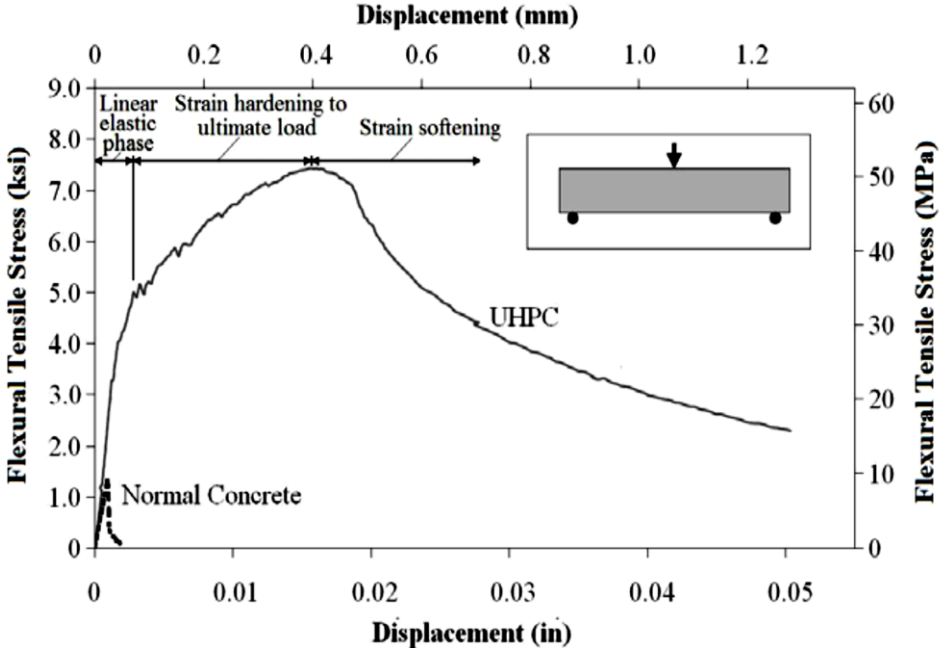

Fig. 2.16 Flexural tensile stress-deflection diagram of UHPC under single-point bending [Acker and Behloul, 2004]

E. Fracture energy

Fracture energy represents the total amount of work that must be done on a concrete beam to achieve complete failure. The large amount of energy required to fracture the steel fibers in the matrix gives UHPC much greater fracture energy than normal concrete. Fracture energy in UHPC subjected to standard heat treatment ranges from 20 000 J/m^2 to 47 300 J/m^2 [Gowripalan and Gilbert, 2000; Dugat et al., 1996]. For UHPC with short fibers and heat-treated 250°C the fracture energy is reduced to 1220 J/m^2 and 2200 J/m^2.

The rate of development of fracture energy is slower than the rates of development of the elastic modulus, f_c', and tensile strength [Voort et al., 2008]. This slow development is due to the fact that fracture energy depends largely on bond strength which is affected by the tensile strengths and elastic modulus of the UHPC mix [Dugat et al., 1996]. Fig. 2.18 represents the time rate of development of the fracture energy reported in untreated UHPC by Habel et al. [2006b]. The tensile and f_c' strengths, and elastic modulus rates of development are also included for comparison purposes. The increase in fracture energy is 93% from seven to 56 days for untreated UHPC.

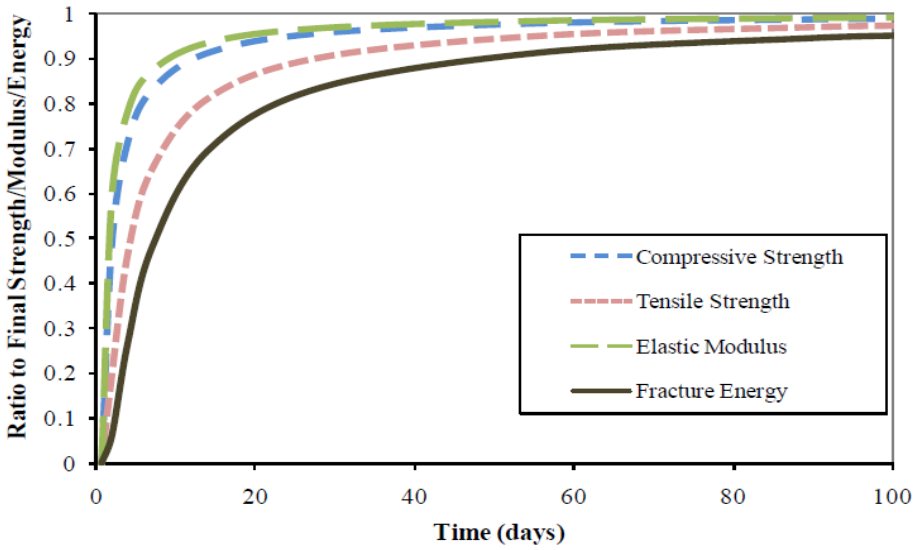

Fig. 2.17 Development of fracture energy and other properties of untreated UHPC without heat treatment [Habel et al., 2006b]

F. Stress-strain behavior

Typical compressive stress-strain behavior for a UHPC cylinder is shown in Fig. 2.19 according to [Acker and Behloul, 2004]. The stress-strain behavior of a normal concrete is also shown for comparison. The high strength and modulus and high ultimate compressive strain values can be clearly observed.

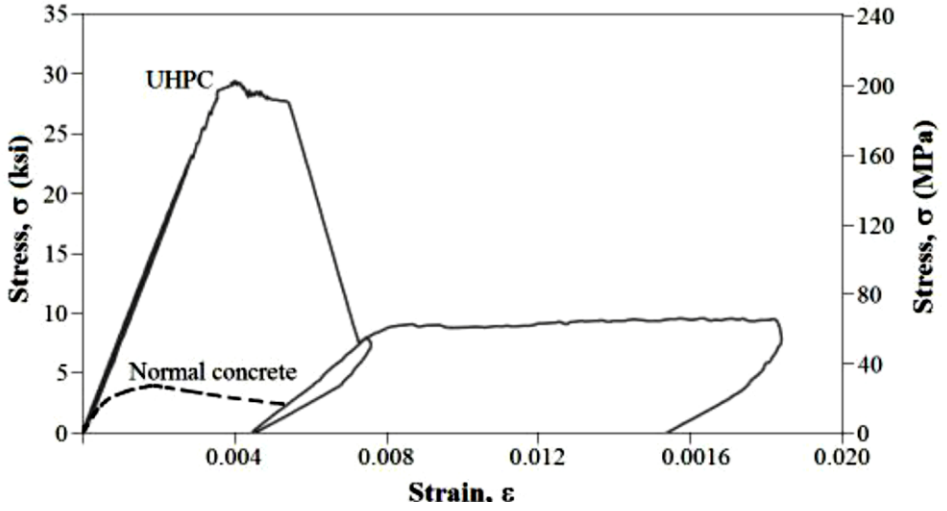

Fig. 2.18. UHPC compressive stress-strain behavior from tested cylinder [Acker and Behloul, 2004]

G. Poisson ratio (*ν*)

The ν is defined as the ratio of the transverse strain and the longitudinal strain. The value ν is an important parameter, particularly for plate, shell, and slab structures. The value of ν reported by various researchers range from 0.13 to 0.22 by Voo et al. [2001] and Dugat et al. [1996], respectively. The average reported ratio was approximately 0.18, which is in the 0.15 to 0.20 range of typical ν values for normal concrete.

2.2.3 Durability

The resistance of concrete to aggressive agents is governed by the nature and severity of the environment as well as by the concrete mix design and constitution. Deterioration mechanisms that typically occurr in concrete is carbonation and chloride attack. They are principally caused by an insufficient concrete impermeability and to high porosity. The decrease of the *w/cm* and addition of ultrafine particles contribute to improve the life of the concrete.

The very dense microstructure of UHPC not only results in higher f_c', but also leads to superior durability properties. This makes the UHPC both a high strength and a high performance material. The low porosity of the UHPC, particularly capillary porosity, leads to great improvements of the durability of the UHPC. The high durability of the UHPC may lead to reduced maintenance costs for the material and a possible reduction in the concrete cover required for resisting weather effects compared to normal concrete [Voort et al., 2008].

The porosity of the UHPC is discussed in the following section. The various durability properties reported for the UHPC are also presented and compared to HPC and normal concrete in the following sections.

2.2.3.1 Porosity

Porosity of concrete, including UHPC, is intrinsically related to its durability properties. Referring to UHPC, Perry [2001] noted that "The superior durability characteristics of UHPC are due to the low and disconnected pore structure, which is generated as a result of the use of a combination of fine powder materials". Both the total volume and size of pores in concrete matrix can be important for durability. Many durability parameters, such as the rate and depth of

ingress of contaminants and freeze-thaw damage, are principally caused by insufficient concrete impermeability and exaggerated porosity [Voort et al., 2008].

The porosity of the UHPC is minimized by an optimized granular distribution with particles of different diameters ranging between fractions of one micrometer and 500 μm. The total porosity of the UHPC appears to depend on the curing process applied to the material. In addition, the total porosity of the UHPC is also modified by a pressurization of the sample during setting, which removes air bubbles and expels excess water from the cement paste. Measurements of the total porosity range from 4.0% to 11.1% for the UHPC without heat treatment [Schmidt et al., 2003, Acker, 2001]. These values are ranging from 1.1% to 6.2% when the standard heat treatment is applied [Cwirzen, 2007; Herold and Müller, 2004]. Fig. 2.20 represents the cumulative porosity in UHPC sample [Cheyrezy et al., 1995]. The total porosity of the untreated UHPC was 8.4% approximately, with a reduction to 1.5% under heat treatment.

Dallaire et al. [1998] reported that the large capillary pores having a diameter greater than 50 nm may allow larger contaminant particles to penetrate into a matrix. Dowd and Dauriac [1996] reported that most pores in the UHPC have a diameter less than 5 nm. Schmidt et al. [2003] claimed that capillary porosity is nearly nonexistent in HPC. Other researchers have reported the capillary porosity in UHPC to be approximately 1.0 to 2.0%, by volume [Vernet, 2004; Teichmann and Schmidt, 2004]. Schmidt and Fehling [2005] reported that UHPC is characterized by the absence of capillary pores due to the very low *w/b* and the dense packing of the solids in the matrix. Fig. 2.21 represents the pore size distribution of a UHPC, HPC and normal strength concrete [Schmidt and Fehling, 2005].

The "percolation threshold" for a concrete is defined as the degree of hydration at which capillary pores become discontinuous. Bonneau et al. [2000] found the percolation threshold of the UHPC is 26%. Since the hydration of typical UHPC samples is at least 31% (Section 2.3.3), the UHPC can theoretically obtain zero capillary porosity. By comparison, the percolation threshold of HPC is approximately 54%. Using a SEM, Sritharan et al. [2003] found no interconnected pores on the surface of a cast UHPC. The porosity of UHPC is even more impressive when compared to normal concrete and HPC. Table 2.8 shows the total porosity, capillary porosity, and percolation threshold of normal concrete, HPC, and UHPC [Voort et al., 2008].

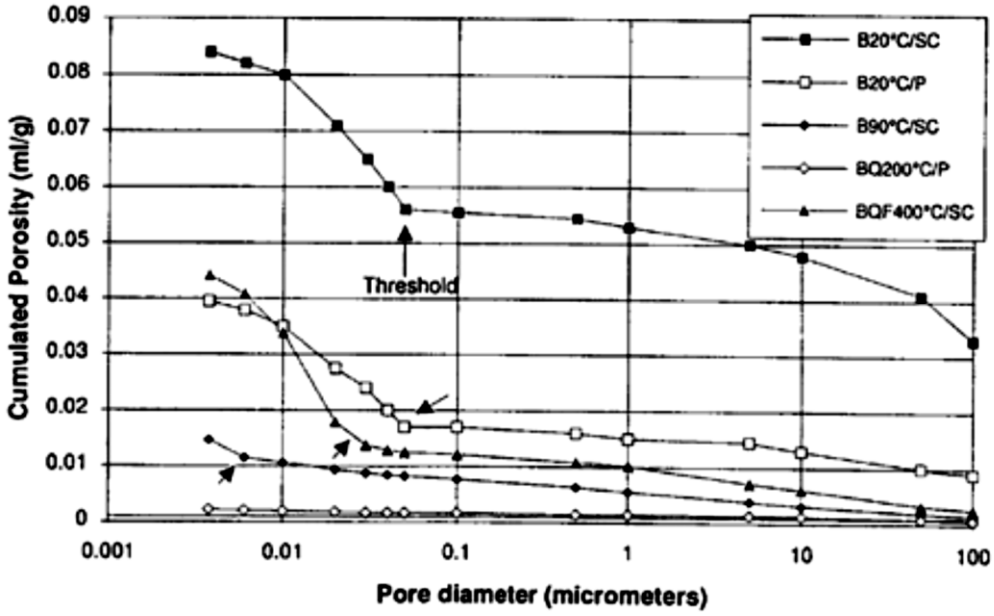

Fig. 2.19. Cumulative porosity of UHPC under different conditions [Cheyrezy et al., 1995]

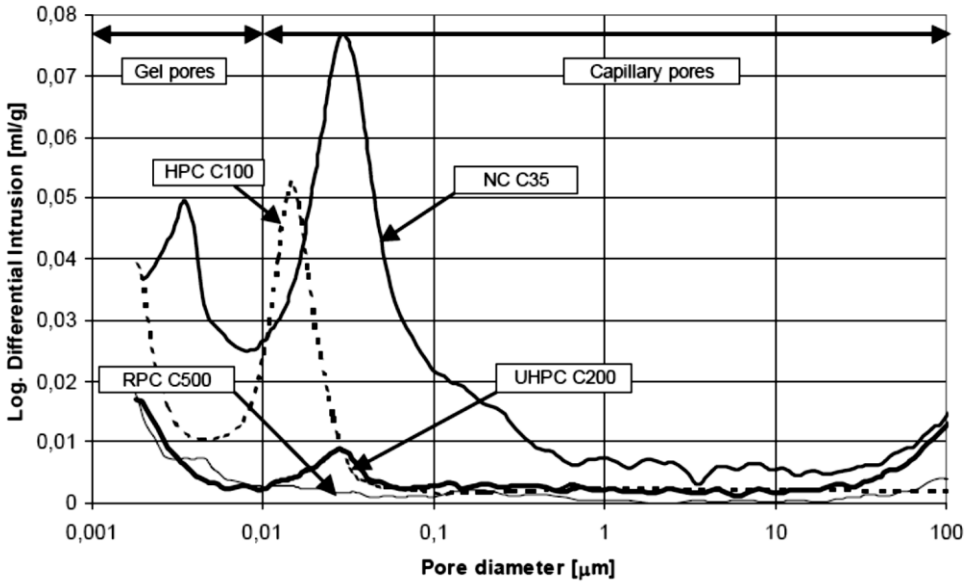

Fig. 2.20. Pore size distributions of UHPC, HPC, and normal strength concrete [Schmidt and Fehling, 2005]

The "percolation threshold" for a concrete is defined as the degree of hydration at which capillary pores become discontinuous. Bonneau et al. [2000] found the percolation threshold of the UHPC is 26%. Since the hydration of typical UHPC samples is at least 31% (Section 2.3.3),

the UHPC can theoretically obtain zero capillary porosity. By comparison, the percolation threshold of HPC is approximately 54%. Using a SEM, Sritharan et al. [2003] found no interconnected pores on the surface of a cast UHPC. The porosity of UHPC is even more impressive when compared to normal concrete and HPC. Table 2.8 shows the total porosity, capillary porosity, and percolation threshold of normal concrete, HPC, and UHPC [Voort et al., 2008].

Table 2.8. Total porosity, capillary porosity, and percolation threshold of normal concrete, HPC, and UHPC

Parameter	UHPC (with typical heat treatment)	HPC		Normal concrete	
		Value	Ratio to UHPC	Value	Ratio to UHPC
Total Porosity*	6%	8.3%	1.4	15%	2.5
Capillary Porosity*	1.5%	5.2%	3.5	8.3%	5.5
Percolation threshold (% hydration)#	26%	54%	2.1	>100%	Infinite

*[Teichmann and Schmidt, 2004] #[Bonneau et al., 2000]

2.2.3.2 Air permeability

The permeability of cement-based matrices depends mainly on the force system, chemical, and mineralogical compositions. Vernet [2004] measured the permeability of the UHPC to oxygen of less than 1×10^{-20} m^2. Compared to oxygen permeability of the UHPC, the permeability of HPC is 10 times greater (1×10^{-19} m^2), and that of normal concrete is 100 times greater (1×10^{-18} m^2) [Vernet, 2004]. This feature is crucial for building resistance to the penetration of aggressive agents. The low permeability presents opportunities for structures subjected to impermeability constraints (reservoirs, caissons, coatings, etc.) for longer life [Roux et al., 1996].

Since the main component of air is nitrogen, nitrogen permeability is sometimes investigated in addition to oxygen permeability. Since the air permeability of the UHPC is often near or lower than the sensitivity threshold of the testing apparatus, a wide range of permeabilities have been reported for the UHPC. Teichmann and Schmidt [2004] measured nitrogen permeability for the UHPC, HPC, and normal concrete. The results demonstrated that the nitrogen permeability of the UHPC was 1×10^{-19} m^2, for the HPC was 4.0×10^{-17} m^2, and for normal concrete was 6.7×10^{-17} m^2.

Comparing these results shows that the air permeability of HPC and normal concrete is 400 to 670 times greater than that of UHPC, respectively [Voort et al., 2008].

2.2.3.3 Freezing and thawing

If water can seep into concrete through capillary pores, it can freeze and expand when the ambient temperature drops, leading to crack or spall the concrete. One typical way to measure freeze-thaw resistance is to determine the ratio between the elastic modulus after a certain number of freeze-thaw cycles and the initial value, expressed as a percentage. Many tests have been performed on the UHPC that show that UHPC has excellent freeze-thaw resistance. Gowripalan and Gilbert [2000] and Bonneau et al. [1997] found the freeze-thaw resistance to be 100%. This can be attributed to the lack of interconnected pores in the UHPC. The Federal Highway Administration [2004] also found minimal degradation after 600 cycles. Shaheen and Shrive [2006] found 100% after 300 freeze-thaw cycles. Gao et al. [2006] even found 100% freeze-thaw resistance after 800 cycles. The UHPC samples at the Natural Weathering Exposure Station at Treat Island, Maine, showed also no significant degradation after over 500 freeze-thaw cycles and 4500 wet-dry cycles in saturated seawater [Vernet, 2004]. After subjecting the UHPC samples to 1000 freeze-thaw cycles, Lee et al. [2005] noted that the relative dynamic modulus reduces to 90%. Typical relative dynamic moduli after 1000 freeze-thaw cycles for both the HPC and normal concrete are 78% and 39% of the initial values, respectively [Voort et al., 2008].

2.2.3.4 Salt scaling

Another measure of durability is the mass lost due to salt scaling of the surface of concrete. Salt scaling can be an important parameter for structures exposed to saltwater and for concrete used as pavement or for bridge deck, due to the wide usage of deicing salts. Estimates of salt scaling of UHPC, reported in literature, vary from approximately 8 - 60 g/m^2 using 28 - 50 freeze-thaw cycles [Bonneau et al. 1997; Perry and Zakariasen, 2004]. The wide variation in the measured salt scaling may be due to the use of different testing methods and the level of precision obtained for each test method [Voort et al., 2008].

Since the total mass loss for UHPC is so low according to any of the sources (typical limits for concretes are 1000 - 1500 g/m^2, the actual mass loss is below the sensitivity threshold in some tests [Vernet 2004; Schmidt and Fehling, 2005]. The mass lost from salt scaling of HPC and

normal concrete are much higher than that of the UHPC at 150 g/m^2 for HPC and 1500 g/m^2 for normal concrete [Schmidt and Fehling, 2005].

2.2.3.5 Water absorption

An excessive absorption of water by concrete can cause certain structural disorders, notably the scaling of material through exposure to freezing/thawing and reinforcement corrosion, due to the penetration of chloride ions in tidal areas. Roux et al. [1996] reported that the water absorption of the UHPC is less than 0.20 kg/m^2. Fig. 2.22 represents the amount of water absorbed by non-pressurized UHPC200 and pressurized UHPC200c compared to normal concrete (C30) and HPC (C80). This very low level of absorption, coupled with the absence of an inflection point, is characteristic of a concrete with no capillary porosity [Roux et al., 1996]. Schmidt and Fehling [2005] listed water absorption factors for each type of concrete as 1.0 for UHPC, 11 for HPC, and 60 for normal concrete, however no further details concerning the basis of the factors were given [Voort et al., 2008].

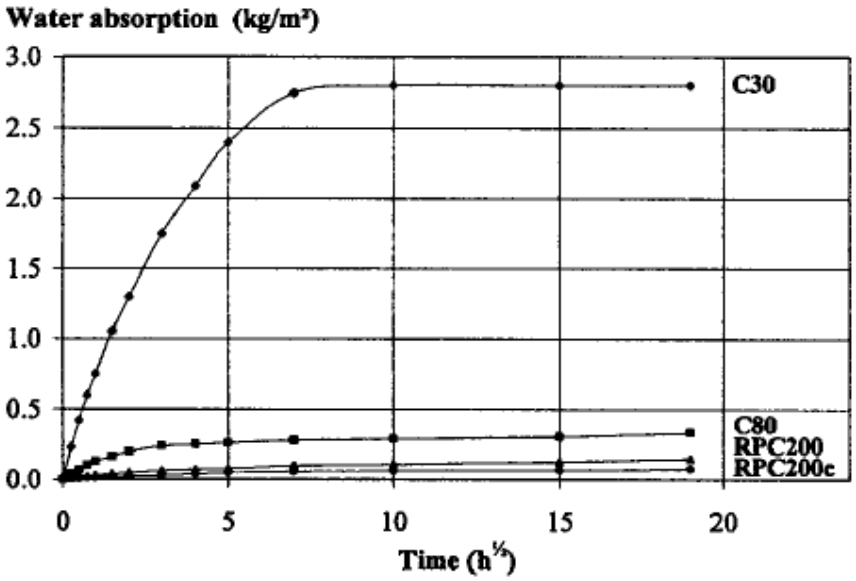

Fig. 2.21 Water absorbed by non-pressurized UHPC200 and pressurized UHPC200c compared to normal concrete (C80) and HPC (C30)

2.2.3.6 Diffusion and migration of chloride ions

The presence of chloride ions near metallic reinforcement is a major cause of corrosion. The passivating layer on the steel is attacked by chloride ions once their concentration exceeds a certain threshold level. Roux et al. [1996] estimated the diffusion coefficient for the UHPC to be 0.02 x 10^{-12} m^2/s compared to 0.6 x 10^{-12} m^2/s and 1.1 x 10^{-12} m^2 /s for HPC and normal concrete are, respectively.

In addition to the diffusion coefficient, the depth of penetration of chloride ions is also of interest to concrete durability. Gao et al. [2006] estimated the total depth of penetration for the UHPC in a 128-h long test with an increasing hydraulic pressure from 0.1 to 1.6 MPa by 2.7 mm. Schmidt et al. [2005] reported a total depth of penetration of 1 mm for a 6-h test with an applied 40 VDC voltage. In addition, the chloride ion penetration depth was 8 mm for HPC and 23 mm for normal concrete from the 6-h long test Schmidt et al. [2005].

The chloride ion permeability can be also evaluated is by measuring the total electric charge passed through a test sample. Bonneau et al. [1997] reported a total charge passed through a 51-mm thick heat-treated UHPC sample as 10 Coulombs, compared to 500 - 1000 Coulombs for a HPC, and 6000 Coulombs for a normal concrete. Schmidt et al. [2003] estimated the total charges passed by heat-treated UHPC sample of 3.5mm in thickness as approximately 20 Coulombs, compared to 200 Coulombs for the HPC, and 1700 Coulombs for normal concrete. Graybeal [2006] measured 18 Coulombs as the total charge passed through a 51-mm thick UHPC sample subjected to the standard heat treatment and 400 Coulombs for an untreated UHPC sample.

2.2.3.7 Carbonation

The resistance of concrete to carbon dioxide is measured by carbonation depth. Roux et al. [1996] conducted a natural carbonation test and two accelerated carbonation tests on UHPC sample. The results demonstrated that no carbonation depth after 90 days' exposure to a 100% carbon dioxide environment. Most researchers agreed that the typical carbonation depth for the UHPC after six months is approximately 0.5 mm [Perry and Zakariasen, 2004; Schmidt et al., 2003]. Schmidt and Fehling [2005] reported the typical carbonation depth after three years is approximately 1.5 mm for UHPC, compared to 4 mm for the HPC and 7 mm for the normal concrete.

2.2.3.8 Alkali silica reaction

This reaction can be defined as the chemical reaction in concrete between alkali hydroxides (hydroxyl ions associated with sodium and potassium from Portland cement and other constituents, such as admixtures and pozzolans and certain constituents of some aggregates. Under certain conditions, this reaction can result in deleterious expansion of the mortar or concrete resulting in cracking [Fares, 2008]. Pfeifer et al. [2009] examined an UHPC sample exposed to different temperature and moisture condition using electron microscopy. Results showed that products of alkali aggregate reaction are not locally developed and have no negative influence on durability. This behaviour is due to elimination of coarse aggregate in the UHPC, using pure crushed quartz sand particles, and the very low permeability of the UHPC that prevents the ingress of alkalis.

2.2.3.9 Reinforcement corrosion

The corrosion of metallic reinforcement in concrete results from electrochemical reactions with the interstitial water that acts as electrolyte. The reinforcement can behave either as cathode or anode. Initially, the cement-based matrix ensures the protection of the steel by promoting the formation of a passivating layer. The drop in pH caused by the carbonation of the matrix or the presence of chloride ions can activate the corrosion process. The electrolyte plays a pivotal role in assuming three distinct functions: (1) diffusion of aggressive agents, mainly CO_2 and chloride ions, (2) passage of electrical current of an ionic nature, and (3) passage of products formed during the corrosion of steel [Mehta and Monteiro, 1992].

Roux et al. [1996] found the corrosion rate for the UHPC to be less than 0.01 µm/yr. It has commonly been recognized that no corrosion risk in concrete for values less than 1.0 µm/yr. Visual inspection in the tests conducted by Roux et al. [1996] also showed no evidence of corrosion. The corrosion rates for the HPC and normal concrete are 25 to 120 times higher than the UHPC (0.25 and 1.2 µm/yr, respectively) [Roux et al., 1996].

2.2.3.10 Resistivity

Electrical resistivity is a measure of how strongly a material opposes the flow of electric current. A low resistivity indicates that the material allows the movement of electrical charge. The SI unit

of electrical resistivity is the ohm metre (Ω.m). Electrical resistivity is also defined as the inverse of the conductivity σ (sigma), of the material as indicated in Eq. (2.6).

$$\rho = \frac{1}{\sigma} \tag{2.6}$$

The low corrosion rate of UHPC is partially due to the high resistance of the material to conducting an electric current. The inclusion of steel fibers in the UHPC also reduces the resistivity of the material. Roux et al. [1996] showed through their tests that the resistivity of UHPC is still better than that of the HPC and normal concrete. The resistivity of a plain UHPC matrix without fibers is extremely high at 1.13 x 10^3 kΩ.cm. The presence of 2% of metallic fibers causes the material's resistivity to fall to 137 kΩ.cm. In comparison, the resistivity of the HPC is only 96 kΩ.cm, and that of normal concrete is 16 kΩ.cm [Roux et al., 1996].

2.2.3.11 Abrasion resistance

Abrasion resistance in concrete is usually measured as a relative mass loss index. Glass is used as a reference material that has a relative volume loss index of 1.0 [Dowd and Dauriac, 1996]. Perry and Zakariasen [2004] reported that the relative volume loss indices of UHPC range from 1.1 to 1.7. By comparison, the relative volume loss index is 2.8 for HPC and 4.0 for normal concrete [Roux et al., 1996].

2.2.4 Applications

2.2.4.1 Advantages of UHPC in construction

UHPC can lead to longer span structures with reduced member sizes compared to normal or HPC. A significant reduction in volume and self-weight can be expected with the UHPC members. Perry [2006] reported that the UHPC beam requires only half the section depth of the reinforced or prestressed concrete beams, which in turn reduced its weight by 70% or more. Fig. 2.23 shows ductile UHPC, steel, prestressed, and reinforced concrete beams with the same moment capacities [Perry, 2006]. The UHPC beam also has the same section depth as the steel beam, which is only slightly lighter than the UHPC member. As well as UHPC can also be used to reduce cross-sectional area compared to normal concrete in piping applications as shown in Fig. 2.24.

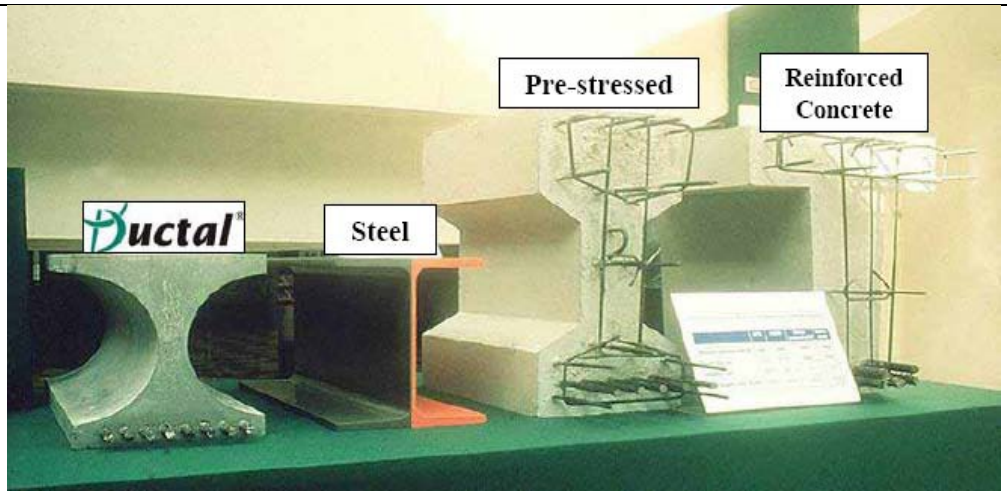

Fig. 2.22**.** Ductal, steel, prestressed, and reinforced concrete beams with equal moment capacities [Perry, 2006]

Fig. 2.23**.** Reduction in pipe wall thickness of UHPC (right) compared to an equivalent pipe with normal concrete (left) [Droll, 2004]

The superior durability properties of the UHPC are also advantageous in terms of service life and reduced maintenance costs. Many of the typical deterioration problems associated with concrete reinforcement can be alleviated in the UHPC due to its dense matrix and the reduction or elimination of steel reinforcement that is typically required in concrete members [Voort et al., 2008].

In addition, UHPC can be a very visually appealing building material. The smaller cross-sections can lead to a more stylish appearance for the structure. The high strengths even allow for previously impossible geometries to be constructed, some of which can be accomplished without the use of any steel reinforcement [Voort et al., 2008]. The UHPC can also be given a high-quality surface finish due to the fineness of the matrix. The UHPC can even be painted with a synthetic painting technique similar to that used by the auto industry [Dowd and Dauriac, 1996].

2.2.4.2 Cost-effective of UHPC

The UHPC is much more expensive than normal concrete. The cost of the materials used to make a UHPC can be split roughly in two equal parts, the cost of the powders, and the cost of the fibers. Bonneau et al. [1996] estimated the price of the UHPC with fibers as \$1400/m^3. Aïtcin [2000] reported a price of \$1000/m^3 of UHPC. Aïtcin [2000] reported the price had decreased to 750 \$/m^3, which agrees fairly with Blais and Couture [1999]. Aïtcin [2000] reported that the ability to use a lower volume of UHPC and the superior performance of the material warrant a comparison not volumetrically with normal concrete but by weight with steel. The UHPC can compete with structural steel that costs 1200-1500 \$/ton. Moreover, in some applications, UHPC should not compete not only with steel, but also with pig iron, aluminum, and even wood.

In addition, the use of UHPC reduces construction times and increases usable floor space or overhead clearance compared to the normal concrete. The use of longer-span bridge girders that can be fabricated using the UHPC could reduce the number of required piers and pier foundations. The predicted longer service life and lower maintenance costs of the UHPC could also lead to even more cost benefits. Increasing times required for steel structures may also lead to cost advantages for UHPC in addition to the possible reduction in cost per unit weight outlined above.

Aïtcin [2000] reports that the Quebec Ministry of Transportation (MTQ) determined that the initial cost of a 55 MPa bridge was 8% less than that of an identical 35 MPa bridge without taking increased service life into account. Therefore, it is reasonable to expect a cost saving when using ultra-high performance materials like UHPC.

2.2.4.3 Structure applications

As UHPC is being developed, the proper market has yet to be discovered to utilize its increased strength, durability, and flexural capacity. To date, this versatile material has been used in artwork, acoustical panels, precast elements, pedestrian bridges, and a few highway bridges [Voort et al., 2008]. A brief overview of UHPC applications in the world are presented in this section, however, more detailed investigations of these uses can be found in other references [Behloul and Cheyrezy 2002a and 2002b; Kollmorgen, 2004; Schmidt and Fehling, 2005].

The first structure in the world to be constructed using the UHPC was a pedestrian and bicycle bridge over the Magog River in Sherbrooke, Quebec, Canada in July 1997 (Fig. 2.25) [Blais and Couture 1999; Dowd and Dauriac, 1996]. Other transit applications include footbridges constructed in South Korea, Japan, France, and Germany. In Seoul, South Korea the Footbridge of Peace is shown in Fig. 2.26 [Brouwer, 2001]. In Japan, the Sakata-Mirai footbridge (Fig. 2.27) was completed in 2002 and demonstrated how a perforated webs in a UHPC superstructure can both reduce weight and be aesthetically pleasing [Tanaka et al., 2002].

Other applications in North America (United States and Canada), Europe, Asia, and Australia and Potential applications are are presented in [Federal Highway Administration, 2013] and The 2nd International Symposium on UHPC in Marseille, France.2013]

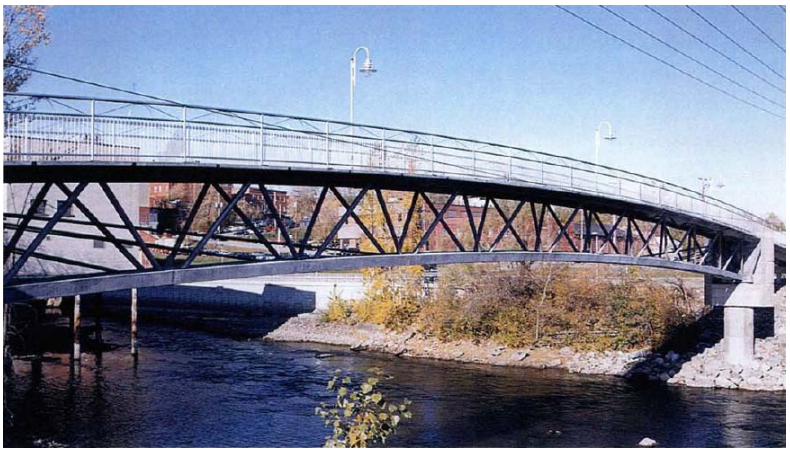

Fig. 2.24**.** Views of the completed Sherbrooke pedestrian bridge [Blais and Couture, 1999]

Fig. 2.25**.** Views of the completed footbridge of peace in South Korea [Brouwer, 2001]

Fig. 2.26**.** Views of the completed Sakata Mirai footbridge in Japan [Tanaka et al., 2002]

The UHPC has been used to manufacture acoustic panels for the Monaco underground train station [Lafarge North America, 2007]. The thin and light UHPC panels were cast with small holes to aid in their acoustic properties. The nonflammable panels are resistant to impact and create an aesthetically pleasing, bright environment for passengers. Acoustic panels have also been used along a roadway in Châtellerault, France, because of their resistance to car pollution and de-icing salts [Lafarge North America, 2007].

The UHPC can be used also in roofs and canopies. One of the most famous UHPC structures in the world is the Shawnessy LRT station in Calgary, Canada (Fig. 2.28). The design flexibility afforded by the UHPC allowed the architect to fulfill their desire for a free-flowing form design for this structure [Perry, 2006].

Fig. 2.27. Shawnessy LRT station with UHPC canopies [Perry, 2006]

2.2.4.4 Architecture applications

UHPC is a range of formulations which may be used for many different architectural applications. For architectural UHPC applications, Polyvinyl Alcohol (PVA) fibers are used in order to achieve ductile behavior under tension, which may eliminate the need for passive (non-prestressed) reinforcement. Architectural UHPC can achieve compressive strengths up to117 MPa and flexural strengths up to 10 MPa. Appropriate batching, casting, finishing and curing procedures are of the utmost importance in order to ensure the highest level of quality, appearance and performance.

One of the newest buildings where UHPC is used is the Fondation Louis Vuitton pour la Creation in Paris [Aubry et al., 2013]. This project is characterized by the high geometric complexity. The cladding is created from 19000 unique, prefabricated panels of UHPC. Each one is different from others, moulded individually and installed using a butt joint. The visualization of this building is shown in Figure 29. The construction will be finished in 2014. Another great example is the Museum of European and Mediterranean Civilizations (MUCEM) [Mazzacane et al. 2013] as shown in Figure 30, which is located in the port area of Marseille in France. It is the first building in the word to make such extensive use of UHPC. The tree-like facades, columns, brackets and bridges decks of the perimeter footbridges, facades and roof lattice, 115 and 69 meters long pedestrian footbridges and even the protective covers to the prestressing anchorage points are all made of UHPC. There are some other examples of similar applications, such as precast thin curved shells in a waste water treatment plant in France [Delplace et al. 2013]; roof

of the Jean Bouin stadium in Paris as shown in figure 31 [Mazzacane et al. 2013]; roof of the Olympic museum in Lausanne, Switzerland [Muttoni et al. 2013]; cladding for the Qatar National Museum [Menetrey, 2013]; and facades at Terminal 1 of Rabat airport in Morocco [Fabbri and Corvez 2013].

Fig. 2.28. Fondation Louis Vuitton pour la Creationin, Paris, France.

Fig. 2.29: MUSEUM, Marseille, France with UHPC lattice facade, roof and footbridge.

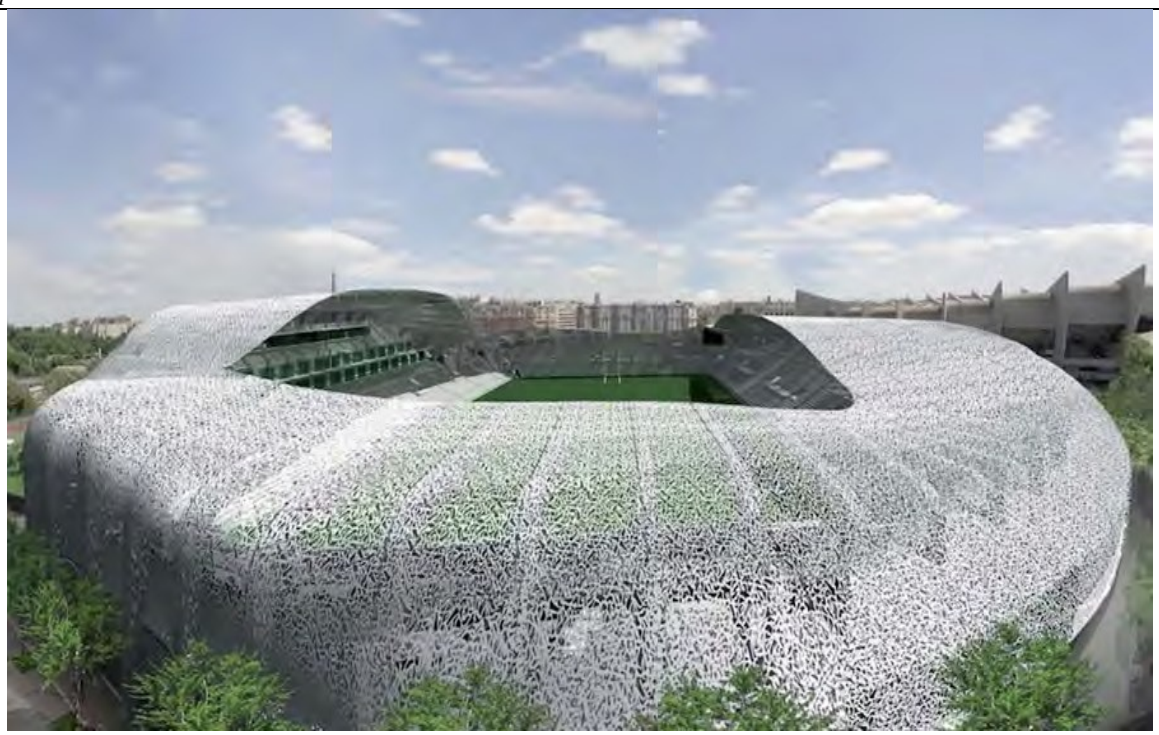

Fig. 2.30. Stade Jean Bouin, a 23,000 square meter UHPC lattice envelope and roof.

2.2.5 UHPC with sustainability

The term "sustain" means to support or to keep a process going. The goal of sustainability is to sustain life on the planet for the foreseeable future. There are three branches to secure sustainability: environment, economy, and society. To meet its goal, sustainable development must provide that these three components remain healthy and balanced. Furthermore, it must do so simultaneously and throughout the entire planet, both now and in the future. At the moment, the environment is probably the most important branch. Using sustainability by an engineer or architect means there is no negative impact on the environment. Thus the term sustainable has come to be synonymous with environmentally sound or friendly or "green".

The environmental branch has our attention now because deterioration of our environment is driving the current worldwide focus on sustainable development. We could cite countless examples of environmental deterioration, and all are important. Probably the most troubling for the long-term health of the planet and for the goal of sustainability are the climate changes resulting from the thinning of the ozone layer and the progressive decline in biodiversity resulting from loss of habitat. Both of these changes are a direct result of human development.

The economic component is given less attention in the developed countries, but is equally essential to the goal of sustainable development. There is poverty throughout the planet, and the global inequities in consumption of resources are staggering. Economic sustainability and environmental sustainability are closely linked. Much environmental degradation occurs when people are struggling to obtain the resources essential for life (food, water, shelter, etc.), and it is inevitable that the basic economic struggle may take precedence over environmental sustainability. Conversely, environmental deterioration exacerbates economic inequity. For example, diseases associated with lack of clean water are a significant cause of poverty.

The social component is also given less attention at the moment but will hopefully be brought into balance in the ensuing decades. The goal of sustainable development clearly requires stable social structures. Only with broad social commitment implemented by governmental policies we can progress towards sustainable development. War, probably inevitable in the absence of stable social structures, causes both economic disparity and environmental deterioration.

The use of UHPC can be translated to savings in the total materials required for the design of various structures. Walraven [2002] claimed, even though UHPC has higher cement content per cubic yard than normal concrete, structural members typically require fewer cubic yards of material, and as a result, the total quantity of cement used is about the same or perhaps even less for UHPC design solutions than those from normal concrete. Racky [2004] determined that while the cement content in the UHPC may be as much as twice that in normal concrete, the amount of the UHPC required for a large column application was only 44% of the normal concrete alternative, which supports Walraven's hypothesis. In addition, the total amount of aggregates, in which he includes both fine and coarse aggregates, used in structural members may be decreased by 30% with the use of the UHPC compared to the normal concrete [Walraven, 2002].

Despite of too few existing applications of the UHPC to allow a reliable comparison with normal concrete for average life-cycle durations and costs, most researchers agree that the excellent durability properties of the UHPC should increase the longevity of structures while minimizing maintenance costs [Racky, 2004; Blais and Couture, 1999]. Aïtcin [2000] noted that unlike normal concrete, UHPC can be recycled several times before being used as granular road base Sedran et al. [2009]. This recyclability is attributed to the fact that not all of the cement in the UHPC is hydrated during hardening, and unhydrated cement is therefore available for future reactions.

FA, slag, quartz powder and RHA used in the UHPC can also be obtained as by-products from the power industry. By employing materials that would otherwise be wasted, UHPC represents a step towards sustainability. The use of more mineral components and powders in place of cement for concrete applications is a step toward sustainability and helps to meet the sustainability mandates that may soon be implemented by some government agencies [Aïtcin, 2000].

2.3 Particle packing

2.3.1 Overview of particle packing density in concrete

In general, concrete is a particulate composite consisting of chemically reactive binders, fillers, and inert aggregate designed for specified strength. Nowadays, there is a demand for concrete to have not only strength but at the time high performance in term of workability, dimensional stability, and durability. Because of the conflicting requirements of these performance attributes, the mix design of such concrete is rather complicated and high dosage of chemical and minerals admixture may be added. Conventional mix design methods that are based on gradation of the materials (i.e., particle size) are not capable of managing such complexities. Therefore, refinements in mix design methods are necessary. One of the challenging methods for designing the concrete mixtures is particle packing density.

The field of particle packing deals with problem of selecting appropriate size and proportion of particulate materials to obtain compact mixture. Control of particle packing is very important to many branches of industry and science such as filter beds, ceramics, asphalts, and powder metallurgy. In considering packing, smaller particles should be selected to fill the voids between the large particles, leading to a smaller prosity within the entire skeleton. The concept of packing density is introduced to evaluate the arrangement of granular mixture. The packing density of granular mixtures can be defined as the volume of solids per total bulk volume. Fig. 2.29 illustrates how the concept of packing density can be applied with three granular systems, including single-, binary-, and ternary-systems [Stovall et al., 1986]. The single-sized aggregate can be packed together to occupy only a limited space, leading to a relatively low packing density. However, the multi-sized aggregates (binary and ternary systems) can be effectively packed to achieve higher packing density. The packing of all particles in the concrete mixture must be considered to avoid the interactions between particles. These interactions are recognized by the wall effect (when the fine particles are butting into the surfaces of very large size

particles) and the loosening effect (when the fine particles cannot fit themselves perfectly into the gaps of the larger size particles) [de Larrard, 1999].

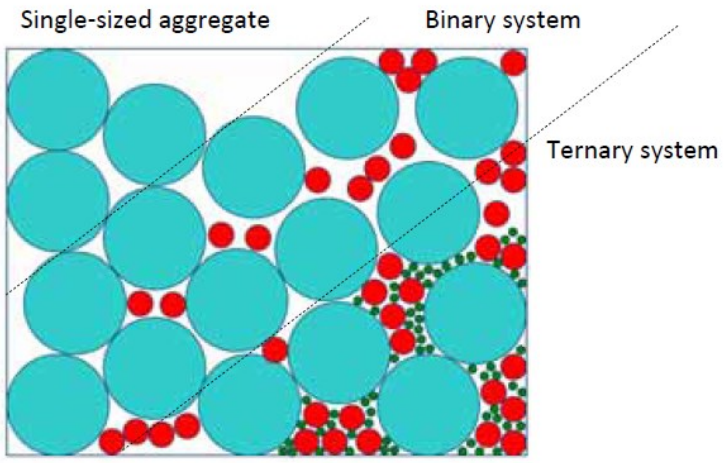

Fig. 2.31 Typical packing arrangements of binary and ternary mixtures [Stovall et al., 1986]

The concept of packing of aggregates has received attention form many researchers since the 19th century. In recent decades, particle-size optimization has gained new interest with the introduction of new concrete types, such as high-performance concrete (HPC), self-consolidating concrete (SCC), and UHPCSedran, de Larrard, [1999]. The packing density has proven to be one of the most important parameters influencing the performance of concrete (increasing strength, reducing permeability and bleeding, and reducing porosity in transition zone). For a fixed paste volume, the increase in packing density of aggregate can increase the workability of concrete at same *w/b*, or increase strength of concrete by reducing the *w/b* at a given workability. According to Goltermann et al., [1997], concrete mixtures should have more fine aggregate than what is required for the maximum packing density. It has to be noted that a small change in the sand content does not generally result in a large change in packing density. The use of higher volume fraction of aggregate, especially coarse aggregate, can improve strength, stiffness, creep, drying shrinkage, and permeability [Johansen and Andersen, 1991]. The use of higher packing density with continuous grading and a narrow grading span results in reduced segregation [de Larrard 1999].

The design of granular materials using the particle packing approach gives the advantages of taking into account the combined effect of shape, texture, and grading of the components as well

as method of compaction. Therefore, packing density can be used as an indirect indicator of aggregate geometrical characteristics. Packing density also provides an indication of the voids content, which must be filled with paste. Additional paste greater than the voids content is needed to mobilize aggregates and provide a certain level of flowability. Therefore, aggregates with higher packing density will generally allow a larger volume of aggregates and lower volume of paste to be used.

In general, higher packing density is preferred, although the maximum packing density may not be the optimal [Johansen and Andersen, 1991; Goltermann el al., 1997; Powers, 1932; Powers, 1968]. According to de Larrard [1999], selection of optimum course-to-fine aggregate ratio to achieve maximum packing density may be misleading because presence of cementitious materials provides a loosening effect. Based on the compressible packing model simulation [Sedran, de Larrard, 2000], the coarse-to-fine aggregate ratio should be increased when interaction from cementitious materials are included.

2.3.2 Measurements of particle packing density

Direct (or dry) and indirect methods are two methods for the measurements of particle packing density [Wong and Kwan, 2008]. The direct method determines directly the packing density from the bulk density of the packed particles. The indirect method calculates indirectly the packing density from consistence tests. There are two versions for the direct method: the first for coarse aggregate under compacted and uncompacted conditions, and the second for fillers under compacted condition. The British Standard, BS 812: Part 2, [1995] has specified the dry packing method for measuring the bulk density of aggregate, from which the voids content and packing density can be determined. For aggregate quantity of weight (w) and specific gravity (SG) filling a container of volume (V_c), the packing density (α) can be calculated from Eq. (2.7):

$$\alpha = \frac{V_s}{V_c} = \frac{w}{V_c \cdot SG} \tag{2.7}$$

One of the dry packing problems is that the bulk density of a powder is very much dependent on the state of compaction [Svarovsky, 1978]. It must be explicitly stated whether the measured bulk density is aerated, poured, tapped, or compacted bulk density. Moreover, the exact treatment to be applied to the powder sample has to be standardized as it could affect the test

results and their interpretation. Another major problem with the dry packing is that with decreasing particle size, the adhesion phenomena arising from Van der Waals and electrostatic forces between the particles can cause agglomeration leading to increased voids content [Yu AB, 1997]. According to Pietsch [1995], the critical size is approximately 100 μm. At a smaller particle size, the ratio of inter-particle force to gravity is greater than unity and agglomeration is likely to be significant. That is why the packing behaviour of fine particles is different than that of coarse particles. In general, the dry packing method overestimates the voids content and underestimates the packing density of fine particles.

The wet method measures the voids content in a cementitious material sample in terms of water demand. This water is taken as the minimum water content for the cementitious material to form a paste and achieve a certain consistence. Such practice is based on the fact that for any cementitious materials, there is minimum water content for the formation of a paste and at this minimum water content, the voids content is also minimal. In many cases, it is further assumed that there is no air entrapped in the paste. Hence, the volume occupied by the minimum water content may be taken as the minimum voids content of the cementitious materials. This voids content is used to evaluate the packing density.

There are several approaches to measure the packing density of powder. de Larrard [1999] determined the packing density by measuring the amount of water with or without admixtures that must be added to cement to transfer it from a humid powder to a thick paste. Alternatively, this determination can be made by using the Vicat test for measuring the water content to reach normal consistency defined in ASTM C 187, or by using the single drop test described by Bigas and Gallias [2002]. The single drop test is not influenced by the presence of superplasticizer. For each of these methods, the actual packing density (ϕ) is calculated as shown in Eq. (2.8):

$$\phi = \frac{1}{1 + \rho_c \cdot (w/s)} \tag{2.8}$$

where; ρ_c is the density of the solid materials, w is the mass of water, and s is the mass of solid.

2.3.3 Particle packing models

Packing models - are used to estimate the optimum packing density of the solid combination and minimise the voids ratio. Over the years, three distinct approaches for optimizing the particle packing density:

1. Optimization curves: In this approach, the various particle groups for the different materials are combined in such a way that the total particle size distribution of the entire mixture is closest to an 'ideal' grading curves to achieve the highest packing density. The 'ideal' curves were obtained from practical experiments and theoretical calculations.
2. Particle packing models: These are analytical models that can calculate the overall packing density of a mixture based on the geometry of the combined particle groups.
3. Discrete element models (DEM): These are computer-based models that can be used to generate 'virtual' particle structure for a given PSD and calculate the packing density from this virtual structure.

Continuous models - use groups of particles, each with a specific particle size distribution, that are combined to produce a total particle size distribution of the mixture closest to an optimal curve. Fuller and Thompson model, [1907], Andreasen and Andersen model, [1930], and Funk and Dinger model, [1994], are example of continuous models. These curves should lead to the mixture with the highest packing density, by combining optimal amounts of differently sized particles. According to the optimization curves a wider range of the particle size distribution results in a higher packing density. Also, adjusting mixture composition to a fixed optimization curve is relatively easy since it requires only a limited amount of input parameters. Only the particle size distributions of the available materials are necessary to optimize a concrete mixture. The output of the model is an optimized particle size distribution, which leads to a mixture with the highest packing density. The differences in particle shape and particle packing of different size groups are not taken into account when optimize a concrete mixture. However, the particle shape greatly influences the packing density, especially, when particles of several size classes, with varying particle characteristics, are used [Walker, 2003; Zheng et al., 1990].

Discrete element models - is generate a 'virtual' particle structure from a given particle size distribution. In the earliest models, once a particle was placed, its position would not change anymore. In these static simulations usually particles are randomly positioned in a defined space,

starting with the largest particles. The result is a three dimensional space filled with particles of different sizes distribution, which usually do not have contact with each other. An example of models using static simulations is Zheng and Stroeven [1999]. With increasing computational speed, the models developed to dynamic models in which all particles can move. Particles are generated and subsequently move because of forces acting on the particles. For example, particles can experience gravity and can collide or remain situated. In this way, the resulting packing corresponds to a random loose packing. Examples of models using dynamic simulations are Fu and Dekelbab, [2003], Stroeven and Stroeven, [1999], Kolonko et al., [2008]. To find the mixture composition with the highest packing density, several mixture compositions should be simulated, which is very time consuming. Especially with broader particle size distributions, computational time increases with hours, because of the high amount of small particles in the mixture. Some researchers solve this problem by making use of a stepwise approach in which small particles are packed and then serve as a matrix between larger particles [Kolonko et al., 2008]. However, this leads to an increase of input parameters, which already consist of particle size distribution, container size and/or the amount of particles, but should now include several model parameters such as gravity, density, damping, elasticity, shear, friction and particle contact.

Particle packing models - the purpose of analytical particle packing models is to calculate the theoretical packing density of a mixture. The calculation is based on the particle size distribution and the packing density of the different particle groups that are present in the mixture. The well-known model Furnas [1929], Aim and Goff [1964], Tufar [1976], Stovall [1786], Dewar [1886], compressible packing model de Larrard [1999], and the compaction – interaction packing model (CIPM) Fennis et al., [2010] is some common example of Particle packing models. Each of these models differs in how particle interaction such as wall effect, loosening effect and/or compaction energy is implemented in the mathematical equations of the models. The explaining the differences between the mathematical equations of these models, reference is made to overviews all model types by [Fennis, 2008; Funk and Dinger, 1994; Goltermann et al., 1997; Johansen and Andersen, 1991; Kumar and Santhanam, 2003]. The input parameters are the packing density and particle size distribution of the particle groups, possibly combined with the compaction

energy at which the packing density is measured. The output of an analytical packing model is the theoretical packing density of the mixture.

The continuous models did not consider the particle shape, however, particle shape greatly influences the packing density. Analytical particle packing models and discrete element models can calculate the maximum packing density of concrete mixtures with tacking into account a lot of parameters. However, due to limitations in computational speed discrete element models are not actually ideal for concrete mixture optimization, since numerous mixtures have to be evaluated to find the optimal composition. However, with the developing power of computers these models can be more efficient in the future. Consequently, at this moment analytical particle packing models provide the best solution for concrete mixture optimization based on particle packing density.

Between all the analytical models, the CPM and CIPM models are the best ones. The CIPM [Fennis-Huijben, 2010] is considered as an extension to the CPM [de Larrard, 1999]. The CIPM includes interactions due to the surface forces for very fine particles (≤ 125 μm). The values in the current model are based on limited data from experiments with cement and quartz powder. So the model is not validated with other materials. Especially with particles below micron range such as the silica fume the behavior can be quite different. Consequently, the CPM is choosing as it considers the mutual influence of compaction and interactions in the particle structure. The effects of particle shape and texture are indirectly taken into account in this model. This model has been found useful to optimize the packing density of granular mixtures of UHPC [de Larrard and Sedran 1994] and will be considered in this study.

Compressible packing model

The CPM [de Larrard 1999], which is based on a linear packing density model de Larrrad and Sedran [1994], enables the calculation of the packing density of polydisperse granular mixes with particle interaction, from the knowledge of three types of parameters: packing density of monosize classes, size distribution of the mix; and compaction energy for materials used (QS, QP, cement, and SF). The model takes into account the effect of compaction technique by making a distinction between the virtual packing density, which is the maximum theoretical packing density, and the actual packing density. de Larrard [1999] considered a mix of particles of any shape, divided into *n* classes of monosize particles (with respect to conventional sieving

process). In any mix, one may define the dominant class *i*, which forms itself a packing in the voids of the coarser particles where β_i is residual packing density, that the virtual packing density displayed when the class is isolated and fully packed. The packing density of the overall mixture is computed by noting that the bulk volume of the *i* class fills the space around the coarser grains; moreover, the volume of finer classes inserted in the voids of *i* class must be added. Two interaction effects must be accounted for in this calculation: the wall effect (b_{ij}), which describes an effect that larger particles cause the voids in the system, and the loosening effect (a_{ij}), which describes an effect where by the introduction of small particles, pushes the larger particles apart. In the model, it is assumed that those interactions are additive, which means that a possible intersection between the perturbed zones is neglected.

The overall virtual packing density (γ_i) for a mixture of one particle size class *i* with independent β_i values is defined by the Eq. 2.9, in which the loosening effect a_{ij} and the wall effect b_{ij} are taken into account. The wall effect (b_{ij}), which describes an effect that larger particles cause the voids in the system, and the loosening effect (a_{ij}), which describes an effect where by the introduction of small particles pushes the larger particles apart (Fig. 2.30). The loosening effect (a_{ij}) and wall effect (b_{ij}) can be estimated in from Eqs. 2.10 and 2.11, respectively

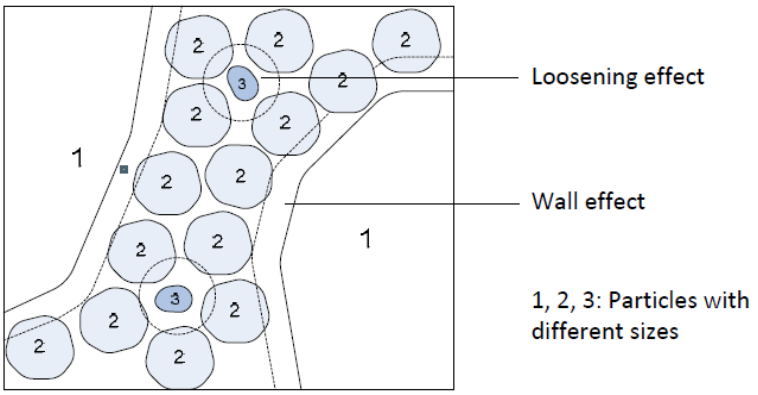

Fig. 2.32 Wall and loosening effects in a ternary system of granular mixture [de Larrard, 1999]

$$\gamma_i = \frac{\beta_i}{1 - \sum_{j-1}^{i-1}\left[1 - \beta_i + b_{ij}\beta_i\left(1 - \frac{1}{\beta_j}\right)\right] y_j - \sum_{j=i+1}^{n}\left[1 - a_{ij}\left(1 - \frac{\beta_i}{\beta_j}\right)\right]} \tag{2.9}$$

where; the y_i represents the volume fraction retained in each size class *i*.

$$a_{ij} = \sqrt{1-\left(1-\frac{d_j}{d_i}\right)^{1.02}} \tag{2.10}$$

$$b_{ij} = 1-\left(1-\frac{d_i}{d_j}\right)^{1.50} \tag{2.11}$$

where; d_i and d_j represent the average particle diameters of the i^{th} and j^{th} size class, respectively, in which d_i is larger than d_j ($d_i > d_j$)

The packing density can be defined in terms of the compaction index (K), which describes the packing process. For a given packing with a known K, the φ is defined implicitly in Eq. 2.12.

$$K = \sum_{i=1}^{n} K_i = \sum_{i=1}^{n} \frac{\frac{y_i}{\beta_i}}{\frac{1}{\varphi} - \frac{1}{\gamma_i}} \tag{2.12}$$

where; y_i is the volume fraction of class i, β_i is the residual (virtual) packing density of class i, γ_i is the virtual packing density when class i is dominant. The K value can be chosen for the packing process. The value of K depends on the compaction energy and should then be defined according to the compaction process. Table 2.9 presents the K values for different packing processes [de Larrard and Sederan, 1999]. The K values for the coarse aggregate combinations that provided the 'best-fit' value for the widest range of the particle combinations is equal 12.5 [Sedran, de Larrard, 2000].

Table 2.9 K values for various packing processes [de Larrard, 1999a]

Packing Process	Methods	K value
Dry	Pouring	4.1
	Rodding	4.5
	Vibration	4.75
	Vibration + compression of 10 kPa	9
Wet	Smooth thick paste [Sedran and de Larrard, 2000]	6.7
	Proctor test [Pouliot et al., 2001]	12
Virtual		∞

2.4 Waste glass

2.4.1 Overview of waste glass

Glass is relatively transparent material produced by melting a mixture silica, soda ash, and $CaCO_3$ at not so high temperature followed by cooling during which solidification occurs without crystallization. Glass is produced in many forms, including packaging of container glass (bottles and jars), flat glass (windows and windscreens), bulb glass (light globes), cathode ray tube glass (television screens and monitors) [Park et al., 2004]. Glass is an ideal material for recycling. The recycled glass in new container can be used in brick and ceramic manufacture. It conserves raw materials, reduces energy consumption, and the volume of waste that has to be sent to landfill. Glass can be recycled many times without significantly altering its physical and chemical properties [Shayan and Xu, 2004]. However, large quantities of glass are not recycled when broken, colours mixed, or recycling is expensive [Terro, 2006]. In United Kingdom, over three million tons of waste glass is produced annually, of which 71% comes from waste containers. In USA, the volume of yearly disposed waste glass is estimated as 14 million tons. In 2000th, about 90,000 ton of glass was considered as waste in Quebec/Canada. In Turkey, this amount reaches to 120,000 tons [Topgu and Canbaz, 2004]. The amount of waste glass gradually increased over recent years due to an ever-growing use of glass products. Most waste glasses have been dumped into landfill sites. The landfilling of waste glasses is undesirable because they are not biodegradable, which makes them environmentally less friendly.

There is a potential for using waste glass in the concrete construction. Waste glass can be used in concrete to replace a portion of the aggregate since it is a hard material with almost negligible water absorption. Another beneficial use for the waste glass is to use it as cement replacement. When glass is ground to a fine powder, it demonstrates pozzolanic properties. The use of glass in manufacturing of concrete has many benefits. Economically, it could save millions of dollars needed for the treatment and land filling of glass waste as well as reduce the price of concrete. Ecologically, it could reduce the CO_2 emissions associated with the production of cement clinkers as well as efficient use of natural resources.

2.4.2 Glass as aggregate replacement

Crushed glass or cullet, if properly sized and processed, can exhibit characteristics similar to that of gravel or sand. When used in construction applications, waste glass must be crushed and

screened to produce an appropriate gradation. Waste glass can be successfully used as aggregate in concrete given that the density of glass is similar to that of gravel and sand. However, the absorption of waste glass is much lower than that of sand. The waste glass adsorbs 14% less water than sand, which suggests that concrete made with glass aggregate would have a lower water absorption than concrete made with sand [Ismail and Lachmi, 2009]

The following sections present some remarks about the effect of glass aggregate (GA) on the performance of cement-based materials when used as a replacement of the natural aggregate.

2.4.2.1 Effect of glass aggregate on mechanical performance

Presence of GA in concrete can reduce the consistency of the concrete mix and adhesive bond of the ingredients inside the concrete mix [Taha and Nounu, 2008]. These authors observed severe bleeding and segregation when natural sand was replaced by waste recycled glass sand. They also noticed that the plastic properties of the concrete mix undergo notable changes. The smooth and plane surface of the large recycled glass particles can weaken the bond between the cement paste and the glass particles. The quality of a cube made with the same mix was significantly affected by the presence of the GA in the concrete.

The inherent cracks in the recycled GS particles, resulting from the crushing process of recycled glass in order to reduce the glass particle, can be considered as a source of weakness and can decrease concrete strength. Therefore, the strength of the concrete will be negatively affected. The presence of the GA in concrete reduces also its compaction compared to the control mix. Topcu and Canbaz [2004] used green waste soda glass with size between 4 and 16 mm to replace 15%, 30%, 45%, and 60% of the coarse aggregate. The results showed that incorporating large amount of GA resulted in a linear decrease in the f_c'. At 30% replacement, the f_c' was reduced by 15%. The poor geometry of the GA had the most influence on reducing the f_c'. Also, crushing of the glass caused weakness in the concrete because it produced cracks within the glass aggregate particles.

Park et al. [2004] tested the f_c' of concrete made with GA separated by colour and crushed finer than 5 mm. The fine aggregate was replaced by 30%, 50%, and 70% GA. The results demonstrated that the colour of GA did not affect the f_c'. When 30% of the fine aggregate was replaced by GA, the strength was only about 1% lower than that of the control. Even at higher

replacement levels, the strength was not significantly affected by GA. The authors suggested that the lower strength was due to lower adhesion between cement and glass than between sand and cement, which is probably due to the lower absorption of glass compared to sand.

The tensile and flexural strengths are adversely affected by the addition on GA to replace the aggregate in concrete. Park et al., [2004] reported that at a replacement level of 30% for the fine aggregate, the tensile strength decreased by 3%, in comparison to the control.

Turgut and Yahlizade [2009] studied the effect of fine and coarse waste glass on producing paving blocks. The test results showed that the replacement of fine aggregate by fine glass at level of 20% by weight has a significant effect on the f_c', flexural strength, splitting tensile strength, and abrasion resistance of the paving blocks as compared with the control sample due to the puzzolanic nature of fine glass. The f_c', flexural strength, splitting tensile strength, and abrasion resistance of the paving block samples with the fine glass replacement level of 20% were 69%, 90%, 47% and 15 % higher compared with the control sample, respectively.

2.4.2.2 Effect of glass aggregate on concrete durability

The recycled glass sand can reduce the permeability and enhance durability of the concrete mix as well as restrict the migration of the water and ions inside the concrete matrix. The texture properties of the glass particle can be improved by reducing the size of the particles to a very fine powder.

Taha and Nounu [2008] investigated the water absorption of concrete with waste glass replacing sand. It was found that, since glass is an impermeable material, the water absorption of the concrete was greatly reduced when glass was used as an aggregate, which could potentially improve the durability of concrete. Lam et al. [2007] reported also that low water absorption was also observed for the paving blocks made with waste glass aggregate.

Waste glass is used as aggregate for concrete. However, the applications are limited due to the damaging expansion in the concrete caused by ASR between high-alkali pore water in cement paste and reactive silica in the waste glass. The chemical reaction between the alkali in Portland cement and the silica in aggregate forms silica gel that not only causes crack upon expansion, but also weakens the concrete and shortens its life. Jin et al. [2000] reported that glass of particle size 1.18 to 2.36 mm produced the highest expansion whereas low expansion was observed at larger

and smaller particle sizes. Idir et al. [2010] reported that there is no any reactivity with ground waste glass when used as aggregate for mortars, thus indicating the feasibility of the waste glass reuse as fine aggregate in mortars and concrete.

Although the ASR remains always a concern when glass is used within concrete, studies were recently carried out to suppress the ASR expansion in concrete and find methods to recycle waste glasses. Some of the common methods to reduce deterioration associated with the ASR are to use low alkali cement, or use supplementary cementitious materials, or prevent water from entering concrete [Fournier and Bérubé, 2000], or treat the aggregates with admixtures [Topcu and Canbaz, 2008], use emerald green glass [Jin et aI., 2000]. A fly ash content of 20% of total binder content reduces greatly the ASR expansion resulted from glass aggregate in concrete [Polley et al., 1998]. Lam et al. [2007] reported that 10% FA used in the concrete can prevent ASR damage for paving blocks including GA. Shayan and Xu [2004] found that both 10% of SF and more than of 20% GP used as cement replacement were able to ensure no negative ASR expansion occurrence in mortar bars.

2.4.3 Glass as pozzolanic material

The high silica content, high surface area, and amorphous of glass powder (GP) suggests that it could perform well as a supplementary cementitious material. Therefore, the GP could be used to replace a portion of the cement in concrete. Table 2.10 compares the chemical composition of GP with ordinary Portland cement and two common pozzolans (SF and fly ash, FA) [Shayan and Xu, 2004; Shi and Zheng, 2007]. The SF has slightly higher silica content than the GP, however it is significantly finer. Particles of SF are less than 1.0 μm, with an average size of 0.1 μm [Kosmatka et al., 2002], while GP has particles between 38 and 45 μm. Because of its high silica content and fine particle size, SF is a very high pozzolan. The FA has less silica but is also finer than GP with particle size of approximately 20 μm [Kosmatka et al., 2002]. Based on silica content and fineness of glass, the GP is expected to perform well in cementitious materials. The GP could perform better than the FA; however, it cannot be expected to perform as SF [Saeed, 2013].

2.4.3.1 Mechanical properties and pozzolanic activity of glass powder

There is a few research works investigating GP blended cement behaviour. Nowadays, existing works investigated the behaviour of using different particle size of GP as a partial replacement of cement. Some of these works compared the pozzolanic behaviour of GP to that of other pozzolanic materials such as fly ash, slag and silica fume inside the concrete. Others investigated the f_c', durability, aggregate silica reaction and permeability of GP concrete.

Shao et al. [2000] investigated the pozzolanic activity and strength of concrete made with finely ground GP. 30% of the cement was replaced with GP, SF, and FA. The particle sizes of GP were 150, 75, and 38 µm. Fig. 2.32 shows that only the mix with 30% SF performed better than the control at 28 days; however, at 90 days the concrete with the 38 µm glass replacement of cement produced 8% higher strength compared to the reference mixture. The concrete with finer glass particles achieved higher strength than the concrete with coarser glass particles since finer glass is more reactive. The 75 and 38 µm glass satisfied the requirement of having a strength activity index of 75%, which is needed for a pozzolan to be beneficial to concrete [ASTM C 618-08]. The mixtures with 75 and 38 µm glass achieved strength results similar to FA [Shao et al., 2000]. [Tagnit-Hamou and Bengougam, 2012] concluded that finely ground GP exhibited very high pozzolanic activity.

Table 2.10 Comparison between chemical compositions of GP, cement, silica fume, and fly ash

Type	GP	cement	SF	FA
Silicon Dioxide (SiO_2), %	72.61	20.33	89.75	47.8
Calcium Oxide (CaO), %	11.42	61.78	0.38	3.36
Sodium Oxide (Na_2O), %	12.85	0.24	0.19	1.70
Potassium Oxide (K_2O), %	0.43	0.59	0. 34	1.70
Magnesium Oxide (MgO), %	0.79	3.29	0.05	0.81
Iron Oxide (Fe_2O_3), %	0.48	3.04	0.03	15.1
Aluminum Oxide (Al_2O_3), %	1.38	4.65	0.14	23.4
Sulfur trioxide (SO_3), %	0.09	3.63	0.04	1.33

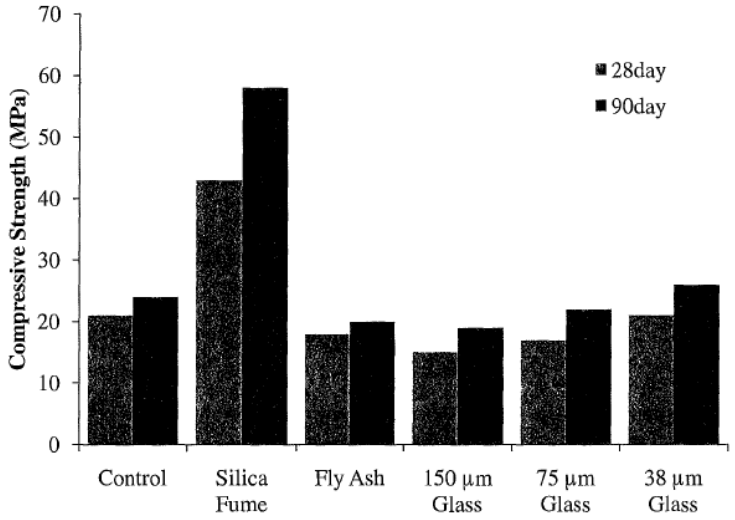

Fig. 2.33 Compressive strength of concrete with 30% of cement replacement with different pozzolanic materials [Shao et al., 2000]

An increase in curing temperature accelerates the activation of pozzolanic activity of both GP and coal FA. Mortar strength testing results indicated that the curing temperature has a greater influence on the pozzolanic activity of GP more than of fly ash [Saeed et al. 2011].

Shayan and Xu [2006] used GP with particle size smaller than 10 µm to replace 10%, 20%, and 30% of the cement. The results demonstrated lower f_c' at 28 days for mixtures made with GP compared to the reference mixture. However, as can be seen in Fig. 2.33, at 90 days' strength of the concrete containing different percentage of GP resulted in higher or approximately similar strength compared to the reference mixtures. This can be attributed to the pozzolanic reaction of the GP which is slower than the hydration of Portland cement [Shayan and Xu, 2006].

Chen et al. [2006] tested the f_c' of specimens with 40%, by weight, of electrical grade glass (E-glass). It was found that the f_c' of the specimens was 17%, 27% and 43% higher than that of control specimen at 28, 91, and 365 days, respectively. Taha and Nounu [2009] investigated the effect of substituting 20% of the cement with GP on the tensile strength of concrete. The results demonstrated that splitting tensile strength was adversely affected when both crushed glass and GP were used but there was no difference in the flexural strength [Taha and Nounu, 2008].

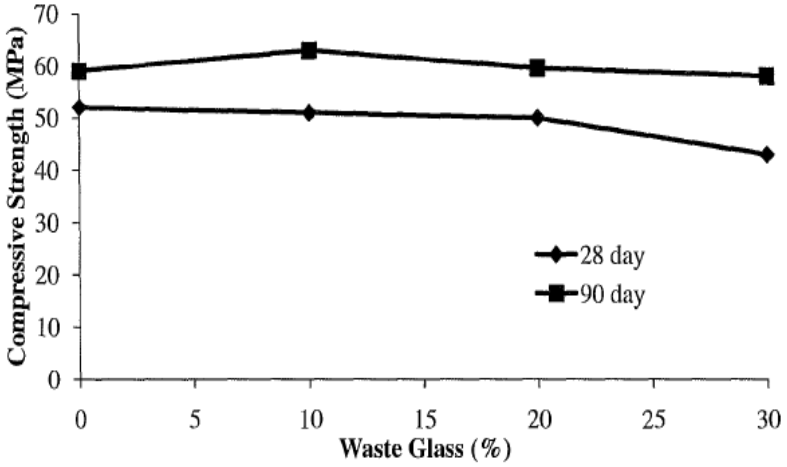

Fig. 2.34 Compressive strength of concrete with waste glass powder [Shayan and Xu, 2004]

2.4.3.2 Effect of glass powder on concrete durability

The use of milled waste glass as partial replacement of cement in concrete results in enhancement of durability characteristics such as adsorption, chloride permeability, and freeze–thaw resistance. This enhancement can be achieved through improvement of the pore system characteristics, filling effect of glass particles, and conversion of CH (available in the old mortar/cement paste attached to the surface of recycled aggregate) to C–S–H [Nassar and Soroushian, 2012; Zidol et al.2013].

Shayan and Xu [2006] used the GP manufactured from mixed colour waste packaging glass comprising soda-lime glass in order to investigate the performance of GP in concrete under field conditions. A field trial was conducted using a 40 MPa concrete mixture, incorporating various proportions of GP (0%, 20%, and 30%) as cement replacement. It was found that the GP reduced the chloride ion penetrability of the concrete, thereby reducing the risk of chloride-induced corrosion of the steel reinforcement in concrete.

Shao et al. [2000], Shayan and Xu [2004], Shayan and Xu [2006], and Schwarz et al. [2008], [Idir 2013] noted that there is no deleterious ASR expansion in concrete with particle less than 40 μm used to replace up to 30% of the cement. This may be because the pozzolanic reaction of GP with cement enhance the binding of alkali, making it unavailable for reaction with reactive aggregate.

Taha and Nounu [2008] studied the influence of two different mineral admixtures, lithium nitrate (is chemically classified as an alkali metal and can contribute to the total alkali content of

concrete.) and pozzolanic GP on the expansion induced by ASR. The presence of pozzolanic GP in concrete as cement replacement led to changes in the concentration of hydroxide ion OH^- in the pore solution, which is considered a direct reason in reducing the risk of ASR expansion. In their study, it was shown that lithium nitrate as a concrete chemical admixture can successfully reduce ASR expansion. Taha and Nounu [2008] reported that when 20% GP replaced the cement, the water absorption increased. The authors suggested that this was due to a change in the hydration products and the microstructure of the concrete when GP is used as a pozzolanic material.

2.5 Summary

In this chapter, a brief introduction to UHPC was presented including, the development of UHPC, the basic principles underlying the development of UHPC, mechanical performance, durability and applications of UHPC in this chapter. Conventional UHPC is composed of cement, quartz powder, silica fume, quartz sand and steel fiber. Depending on the type of material use and curing conditions the material can exhibit compressive strength (f_c') from 200 to 800 MPa, flexural strength between 30 and 141 MPa, fracture energy in the range of 1 200 to 40 000 J/m^2, elastic modulus of 50 to 75 MPa, and minimal long-term creep or shrinkage [Richard and Cheyrezy 1994]. It can also resist freeze-thaw and scaling conditions with virtually no damage, and it is nearly impermeable to chloride ions [Roux et al. 1996]. Currently, the UHPC is a promising material that is used for special pre-stressed and precast concrete elements. This material can also be used for industrial and nuclear waste storage facilities.

Although the cost of UHPC is generally high, some economic advantages exist in the UHPC applications. One of these advantages is possibility the reduction or elimination of the passive reinforcement in the structural elements by introducing steel fibers in UHPC. The thickness of the concrete elements can also be reduced due to the high mechanical performance and excellent durability when using the UHPC, which means materials and cost savings and decrease of the dead load. The superior durability properties of UHPC are also advantageous in terms of service life and lower maintenance costs.

While good mechanical and durability characteristics are needed when producing cement-based materials, such products are environmentally friendly (ecological) and deliver socioeconomic

benefits [Aïtcin, 2000]. UHPC is designed with a higher cement content ranging between 800 and 1000 kg/m^3 [Richard and Cheyrezy 1994; 1995; Long et al., 2002]. Furthermore, the final hydration percentage of the cement in UHPC has been estimated to range from 31% to 60% [Cheyrezy et al., 1995; Habel et al., 2006] due to the very low water-to-cementitious material ratio (*w/cm*). Any unhydrated cement particles work as micro aggregates. The huge amount of cement involved not only affects production cost and consumes natural sources, it also has a negative impact on the environmental conditions through CO_2 emissions and the greenhouse effect.

Based on an Environment Canada report, quartz—the main component in UHPC—causes immediate and long-term environmental harm because its biological diversity makes it an environmental hazard. Additionally, the International Agency for Research on Cancer (IARC) has classified respirable quartz due to occupational exposure as a Group 1 carcinogen (carcinogenic to humans). The U.S. National Toxicology Program has classified crystalline silica of respirable size as a human carcinogen. The basis for these classifications is sufficient evidence from human studies indicating a causal relationship between exposure to respirable crystalline silica in the workplace and increased lung-cancer rates in workers. Moreover, the use of QS and QP in UHPC results in higher costs and fails to meet sustainability requirements.

Silica fume of extreme fineness and high amorphous-silica content is an essential constituent in UHPC because of its physical (filler, lubrication) and pozzolanic effects. The particle-size distribution (PSD) of cement exhibits a gap at the micro scale that needs to be filled with finer materials such as SF. Filling this gap solely with SF requires a high amount of SF (25% to 30% by cement weight). This significantly decreases UHPC workability and increases concrete cost. Finding a material with a PSD between that of cement and SF could help reduce SF content and enhance concrete performance. Moreover, the limited available resources and high cost of SF restrict its applications in today's construction industry, providing impetus to seek out materials with similar characteristics as replacements.

In order to produce "greener" concrete and achieve the "sustainable-concrete" concept, some of the cement, SF, QS, and QP in conventional UHPC should be replaced with other safe local materials.

The ground glass material that can be obtained with different grain size distribution from non-recycled glass is considered as an innovative material that can be also used in concrete. The glass has been successfully used in concrete mixtures (as a partial aggregate replacement in asphalt

concrete, as well as a fine aggregate in pipe bedding, landfill gas venting systems, and gravel backfill for drains). In addition, the GP, with particle-size distribution (PSD) (38 - 45 μm), can be used as a pozzolanic material in concrete. It can be incorporated in concrete with similar quantity as of the by-product admixtures (25 and 50%). It reduces the porosity and size of pores as well as changes the mineralogy of the cement hydrates leading to enhancement of durability. According to the Leadership in Energy and Environment Design (LEED) certification, the uses of glass in concrete can double the points resulting from the usage of offer by-product materials such as (RHA, SF, FA, and BFS). The GP is regarded as a material of post-consumption while the others are regarded as materials of post-production. The use of glass in the manufacture of concrete has great benefits. Economically, it could save millions of dollars needed for the treatment and land filling of glass waste as well as reduce the price of concrete. Ecologically, it could reduce CO_2 emissions associated with the production of cement clinkers as well as efficient use of natural resources.

2.6 References

- ACI Committee 363, State-of-the-Art Report on High-Strength Concrete, ACI 363R-92, reapproved (1997) ACI Committee 363 Report, American Concrete Institute, Farmington Hills, Michigan, 1997, 55 pages
- Acker, P. (2001) Micromechanical analysis of creep and shrinkage mechanisms. Creep, Shrinkage and Durability Mechanics of Concrete and other Quasi-Brittle Materials. Ed. by Ulm, F.- J., Bažant, Z.P., and F.H. Wittmann. Elsevier: 15-25.
- Acker, P. (2004) Why Does Ultrahigh-Performance Concrete (RPC) Exhibit Such Low Shrinkage and Such Low Creep? Autogenous Deformation of Concrete: 141-153.
- Acker, P., and M. Behloul. (2004) Ductal® Technology: A Large Spectrum of Properties, Ultra High Performance Concrete, Kassel, Germany, Sept. 13-15: 11-23.
- Aïtcin P.-C., High Performance Concrete, E&FN Spon (1998).
- Aïtcin, P.-C. (2000) Cements of yesterday and today – Concrete of tomorrow. Cement and Concrete Research, Sept., Vol. 30, No. 9: 1349-1359.
- Aïtcin, P.-C., Lachemi, M., Adeline, R., Richard, P., (1998) The Sherbrooke reactive powder concrete footbridge. Structural Engineering International 8(2), pp. 140-144.

- Aitcin, P.-C., Richard, P., (1996) The pedestrian/bikeway bridge of Sherbrooke. In: Proceedings of the Fourth International Symposium on Utilization of High Strength/High-Performance Concrete, 29-31 May 1996, Paris, France, Eds. F. de Larrard, R. Lacroix, pp. 1399-1406.
- American Concrete Institute (ACI 318-05) (2005) Building Code Requirements for Structural Concrete and Commentary (ACI 318R-05). ACI, Farmington Hills, Michigan.
- American Concrete Institute (ACI) (1992) Report on High-Strength Concrete (ACI 363R-92), ACI, Farmington Hills, Michigan.
- American Concrete Institute ACI 116R (1990) Cement and concrete terminology. American Concrete Institute (ACI) manual of concrete practice, Part 1, Farmington Hills, MI.
- Andreasen, A.H.M. and Andersen, J. (1930) Über die Beziehung zwischen Kornabstufung und Zwischenraum in Produkten aus losen Körnern (mit einigen Experimenten). Colloid & Polymer Science, Vol. 50 (3), pp. 217-228.
- Association Française de Génie Civil (AFGC). 2002. Ultra High Performance Fibre-Reinforced Concretes - Interim Recommendations, Jan. AFGC.
- ASTM C 109 (2002) Standard Test Method for Compressive Strength of Hydraulic Cement Mortars (Using 2-in. or [50-mm] Cube Specimens). *American Society for Testing and Materials (ASTM International)*.
- ASTM C 1260, (2007) Standard Test Method for Potential Alkali Reactivity of Aggregates (Mortar-Bar Method). American Society for Testing and Materials: West Conshohocken.
- ASTM C 1314, (2007) Standard Test Method for Compressive Strength of Masonry Prisms. American Society for Testing and Materials: West Conshohocken.
- ASTM C 1437, (2007) Standard Test Method for Flow of Hydraulic Cement Mortar. American Society for Testing and Materials: West Conshohocken.
- Aubry S, Bompas P, Vaudeville B, (2013) A UHPFRC cladding challenge: the Fondation Louis Vuitton pour la Creation 'Iceberg'. In: Toutlemonde F, Resplendino J, eds. Proceedings of International Symposium on Ultra-High Performance Fiber-Reinforced Concrete. Marseille, France. 37–48.

- Ay, L. (Sept. 13-15 2004) Curing tests on ultra high strength plain and steel fibrous cement based composites, Proceedings of the International Symposium on Ultra High Performance Concrete, Kassel, Germany, 695-701.
- Bache, H. H. (1981) 'Densified cement-ultrafine particle-base materials,' in: Proc. 2nd Int. Conf. on Superplasticizers in Concrete, Ottawa, ON: pp. 185–213.
- Bayard, O., and O. Plé. (2003) Fracture mechanics of reactive powder concrete: material modeling and experimental investigations. Engineering Fracture Mechanics, May, Vol. 70, No. 7-8: 839-851.
- Bayasi, M.Z. (1992) Application of carbon fiber reinforced mortar in composite slab construction. In Proceedings of the International RILEM/ACI Workshop, Reinhardt, H.W. and Naaman, A.E., Eds., pp. 507–517. Chapman & Hall, New York
- Behloul, M. (1996) Les micro-bètons renforces de fibers. De l'éprouvevette aux structures, XIVèmes Journées de l'AUGC.
- Ben Aïm, R. and Le Goff, P. (1967) Effet de paroi dans les empilements désordonnés de sphères et application à la porosité de mélanges binaires Powder Technology, Vol. 1 (5), pp. 281-290.
- Bigas JP, Gallias JL (2002) Effect of fine mineral additions on granular packing of cement mixtures. Mag Concr Res 54(3):155–164
- Blais, P.Y., and M. Couture (1999) Precast, Prestressed Pedestrian Bridge – World's First, Reactive Powder Concrete Structure. PCI Journal, Sept., Vol. 44, No. 5: 60-71.
- Bonneau, O., Lachemi, M., Dallaire, E., Dugat, J., and P.-C. Aïtcin. (1997) Mechanical Properties and Durability of Two Industrial Reactive Powder Concretes. ACI Materials Journal, July-Aug., Vol. 94, No. 4: 286-290.
- Bonneau, O., Poulin, C., Dugat, J., Richard, P., and P.-C. Aïtcin. (1996) Reactive Powder Concretes: From Theory to Practice. Concrete International, Apr., Vol. 18, No. 4: 47-49.
- Bonneau, O., Vernet, C., Moranville, M., and P.-C. Aïtcin. (2000) Characterization of the granular packing and percolation threshold of reactive powder concrete. Cement and Concrete Research, Dec., Vol. 30, No. 12: 1861-1867.
- Breugel, K., and Y. Guang. (2004) Analyses of hydration processes and microstructural development of RPC through numerical simulation. Proceedings of the International Symposium on Ultra-High Performance Concrete, Kassel, Germany, Sept. 13-15: 253- 264.

- Bridge Engineering Center. (2007) News, 2006 Concrete Bridge Award, Iowa State University, Bulletin, May, Vol. 29, No. 5: 324-327.
- British Standards Institution (1995) BS 812 Testing of aggregates part 2: method of determination of density. BSI, London.
- Brown, J. (2006) Highway span features UHPC. Civil Engineering, 76(7), 24–26. Cement and Concrete Association of Australia, 2002.
- Cadoni, E., Caverzan, A., di Prisco, M. (2008) Dynamic behaviour of HPFR cementitious composites. In: Ultra High Performance Concrete (UHPC), Proceedings of the Second International Symposium on Ultra High Performance Concrete, 5-7 March 2008, Kassel, Germany, Eds. E. Fehling, M. Schmidt, S. Stürwald (Kassel, Germany: Kassel University Press, 2008), pp. 743-750. (in book pdf)
- Chan, Y.-W., and S.-H Chu. (2004) Chu. Effect of silica fume on steel fiber bond characteristics in reactive powder concrete. Cement and Concrete Research, July, Vol. 34, No. 7: 1167- 1172.
- Chen, C. H., Huang, R., Wu, J. K., & Yang, C. C. (2006) Waste E-glass particles used in cementitious mixtures. Cement and Concrete Research, 36(3), 449-456.
- Cheyrezy, M. 1999. Structural Applications of RPC. Concrete, Jan., Vol. 33, No. 1. London: 20- 23.
- Cheyrezy, M., and M. Behloul (2001) Creep and Shrinkage of Ultra-High Performance Concrete, Creep, Shrinkage and Durability Mechanisms of Concrete and other Quasi-Brittle Materials – Proceedings of the Sixth International Conference CONCREEP-6@MIT, Cambridge, MA, USA, 20-22 August. Ed. By Ulm, F.-J., Bažant, Z.P., and F.H. Wittmann. Elsevier: 527-538.
- Cheyrezy, M., Maret, V., and L. Frouin (1995) Microstructural Analysis of RPC (Reactive Powder Concrete). Cement and Concrete Research, Oct., Vol. 25, No. 7: 1491-1500.

  Cheyrezy, M., Roux, N., Behloul, M., Ressicaud, A, and A. Demonte (1998) Bond strength of reactive powder concrete. Proceedings of the 13th FIP Congress on Challenges for Concrete in the Next Millennium, Amsterdam, Netherlands, 23-29 May, Vol. 1: pp. 65- Civil Engineering Report (LACER), No. 7: 25-32.

- Collepardi, S., Coppola, L., Troli, R., and M. Collepardi (1997) Mechanical Properties of Modified Reactive Powder Concrete. Enco Journal. Concrete mixtures. Cement and Concrete Composites, Oct., Vol. 26, No. 7: 901-907.
- Collepardi, S., Coppola, L., Troli, R., Zaffaroni, P. (1999) Influence of the superplasticizer type on the compressive strength of reactive powder concrete for precast structures. In: Atti del 16 Congresso Internazionale BIBM'99, 25-28 Maggio 1999, Venezia, Italia, pp. 25-30.
- Corinaldesi V., Gnappi G., Moriconi G., and Montenero A., (Jan. 2005) "Reuse of ground waste glass as aggregate for mortars," Waste Management, vol. 2, pp. 197–201.
- Corinaldesi, V., Gnappi, G., Moriconi, G., & Montenero, A. (2005) Reuse of ground waste glass as aggregate for mortars. Waste Management, 25(2), 197-201.
- CSA A23.1, (2000) Concrete Materials and Methods of Concrete Construction/Methods of Test for Concrete. Canadian Standards Association: Mississauga.
- Cwirzen, A. (2007) The effect of the heat-treatment regime on the properties of reactive powder concrete. Advances in Cement Research, Jan., Vol. 19, No. 1: 25-33.
- Dallaire, E., Aïtcin, P.-C., and M. Lachemi (1998) High-Performance Powder. *Civil Engineering*, Jan., Vol. 68, No. 1: 48-51.
- de Larrard, F., (1999) Concrete Mixture Proportioning: a Scientific Approach, E&FN Spon, London.
- de Larrard, F., and T. Sedran. (1994) Optimization of Ultra-High-Performance Concrete by the Use of a Packing Model. Cement and Concrete Research, June, Vol. 24, No. 6: 997-1009.
- Delplace G, Hajar Z, Simon A, et al. Precast thin UHPFRC curved shells in a waste water treatment plant. In: Toutlemonde F, Resplendino J, eds. Proceedings of International Symposium on Ultra-High Performance Fiber-Reinforced Concrete. Marseille, France, 2013. 49–58.
- Dewar, J.D. (1999) Computer Modelling of Concrete Mixtures. London: E & FN Spon.
- Dowd, W.M., and C.E. Dauriac (Dec.1996) Reactive Powder Concrete. Construction Specifier, Vol. 49, No. 12: 47-52.
- Droll, K. (2004) Influence of additions on ultra-high performance concretes – grain size optimisation. Proceedings of the International Symposium on Ultra-High Performance Concrete, Kassel, Germany, Sept. 13-15: 285-301.

- Dugat, J., Roux, N., and G. Bernier (1996) Mechanical Properties of Reactive Powder Concretes. Materials and Structures, May, Vol. 29: 233-240.
- Edward GN (1996) Fiber-Reinforced Composites. *Concrete Construction Engineering Handbook, 2nd edition, Chapter 22.*
- Egosi N. G., (1992) Mixed broken glass processing solutions, in Proc. Utilization of Waste Materials in Civil Engineering Construction Conf. USA.
- *Engineering International*, Spring, Vol. 9, No. 1: 59-61.
- Fabbri R, Corvez D. (2013) Rationalisaztion of complex UHPFRC façade shapes. In: Toutlemonde F, Resplendino J, eds. Proceedings of International Symposium on Ultra-High Performance Fiber-Reinforced Concrete. Marseille, France, 27–36.
- Federal Highway Administration (2013) Ultra-High Performance Concrete: A State-of-the-Art Report for the Bridge Community, Publication No. FHWA-HRT-13-060, McLean, VA 22101-2296.
- Federal Highway Administration (FHWA) (2004) Achieving the Promise of Ultra-High-Performance Concrete. *Focus*, Nov. http://www.tfhrc.gove/focus/nov04/01.htm.
- Federico, L. M., & Chidiac, S. E. (2009) Waste glass as a supplementary cementitious material in concrete -critical review of treatment methods. Cement and Concrete Composites, 31(8), 606-610.
- Fennis S.A.A.M., Walraven J.C., Uijl J.A. den. (2006) Optimizing the particle packing for the design of ecological concrete. Proceedings of the 16. Internationale Baustofftagung, Weimar, Bunderepublik Deutschland. pp 1–1313 - 1–1320.
- Fennis, S.A.A.M., Walraven, J.C., Nijland, T. (2008) Measuring the packing density to lower the cement content in concrete. In J.C. Walraven & D. Stoelhorst (Eds.); Tailor made concrete structures: new solutions for our society. London UK: Taylor & Francis Group. pp. 419-424.
- Fennis-Huijben SAAM (2010) Design of Ecological Concrete by Particle Packing Optimization. Ph.D., Delft University of technology, The Netherlands: 277.
- Fennis-Huijben SAAM (2010) Design of Ecological Concrete by Particle Packing Optimization. *Ph.D., Delft University of technology, The Netherlands*: 277.

- Feylessoufi, A., Tenoudji, F.C., Morin, V., and P. Richard (2001) Early age shrinkage mechanisms of ultra-high-performance cement-based materials. Cement and Concrete Research, Nov., Vol. 31, No. 11: 1573-1579.
- Fournier, B. & Berube, M. (2000. Alkali-aggregate reaction in concrete: a review of basic concepts and engineering implications. Canadian Journal of Civil Engineering, 27(2),167-191.
- Fu, G. and Dekelbab, W. (2003) 3-D random packing of polydisperse particles and concrete aggregate grading. Powder Technology, Vol. 133, pp. 147-155.
- Fuller, W.B. and Thompson, S.E. (1907) The laws of proportioning concrete. ASCE J. Transport., Vol. 59, pp. 67-143.
- Funk, J.E. and Dinger, D.R. (1994) Predictive Process Control of Crowded Particulate Suspensions Applied to Ceramic Manufacturing. Boston: Kluwer Academic Publishers.
- Furnas, C.C. (1931) Grading Aggregates; Mathematical Relations for Beds of Broken Solids of Maximum Density. Industrial and Engineering Chemistry. Vol. 23 (9), pp. 1052-1058.
- Gao, R., Liu, Z.-M., Zhang, L.-Q., and P. Stroeven (2006) Static Properties of Reactive Powder Concrete Beams. Key Engineering Materials, Jan., Vol. 302-303: 521-527.
- Gilliland, S.K. (1996) Reactive Powder Concrete (RPC), A New Material for Prestressed Concrete Bridge Girders. Structures Congress - Proceedings, Vol. 1, Building an International Community of Structural Engineers: 125-132.
- Goltermann, P., Johansen, V. and Palbøl, L. (1997) Packing of Aggregates: An Alternative Tool to Determine the Optimal Aggregate Mix. ACI Materials Journal, Vol. 94 (5), pp. 435-443.
- Goltermann, P., Johansen, V. and Palbøl, L. (1997) Packing of Aggregates: An Alternative Tool to Determine the Optimal Aggregate Mix. ACI Materials Journal, Vol. 94 (5), pp. 435-443.
- Gowripalan, N. and R.I. Gilbert (2000) Design Guidelines for RPC Prestressed Concrete Beams. Sydney, Australia: School of Civil and Environmental Engineering, The University of New South Wales.
- Granger, S., Loukili, A., Pijaudier-Cabot, G., and G. Chanvillard (2006) Experimental characterization of the self-healing of cracks in an ultra-high performance cementitious material: Mechanical tests and acoustic emission analysis. Cement and Concrete.

- Graybeal B. A. and Hartmann J. L. (2003) Strength and durability of ultra-high performance concrete. In: Concrete Bridge Conference, Portland Cement Association.
- Graybeal, B. (2005) Characterization of the Behavior of Ultra-High Performance Concrete. PhD dissertation, University of Maryland.
- Graybeal, B. (2007) Compressive Behavior of Ultra-High-Performance Fiber-Reinforced Concrete. ACI Materials Journal, Mar.-Apr.: 146-152.
- Graybeal, B.A. (2006) Material Property Characterization of Ultra-High Performance Concrete. FHWA-HRT-06-103, Aug.
- Habel, K., Charron, J.-R., Denarié, E., and E. Brühwiler. (2006a) Autogenous Deformations and Viscoelasticity of UHPFRC in Structures. Magazine of Concrete Research, April, Vol. 58, No. 3: 135-145.
- Habel, K., Viviani, M., Denarié, E., and E. Brühwiler. (2006b) Development of the Mechanical Properties of an Ultra-High Performance Fiber Reinforced Concrete (UHPFRC). Cement and Concrete Research, July, Vol. 36, No. 7: 1362 – 1370.
- Heinz, D., and H.-M. Ludwig. (2004) Heat Treatment and the Risk of DEF Delayed Ettringite Formation in RPC. Proceedings of the International Symposium on Ultra-High Performance Concrete, Kassel, Germany, Sept. 13-15: 717-730.
- Herold, G., and H.S. Müller. (2004) Measurement of porosity of Ultra High Strength Fibre Reinforced Concrete. Proceedings of the International Symposium on Ultra-High Performance Concrete, Kassel, Germany, Sept. 13-15: 685-694.
- Idir, R. et al. (2010) Use of fine glass as ASR inhibitor in glass aggregate mortars. Construction and Building Materials 24, pp. 1309-1312
- Idir, R., Cyr, M., Tagnit-Hamou, A. (2013) Role of the nature of reaction products in the differing behaviours of fine glass powders and coarse glass aggregates used in concrete, Mater Struct, 46(1- 2), 233-243.
- Ismail, Z. Z. & AI-Rashmi, E. A. (2009) Recyclying of waste glass as a partial replacement for fine aggregate in concrete. Waste Management. 29 (2), 655-659.
- Ismail, Z. Z., & Al-Hashmi, E. A (2008) Use of waste plastic in concrete mixture as aggregate replacement. Waste Management, 28(11), 2041-2047.

- Jin, W., Meyer, C., & Baxter, S., (2000) "Glascrete" - Concrete with glass aggregate. ACI Materials Journal. 97(2),208-213. July 30. http://www.bec.iastate.edu/.
- Johansen, V. and Andersen, P.J. (1991) Particle Packing and Concrete Properties. In: Skalny, J. and Mindess, S. (eds). Materials science of concrete 2. Westerville: American Ceramic Society.
- Johansen, V. and Andersen, P.J. (1991) Particle Packing and Concrete Properties. In: Skalny, J. and Mindess, S. (eds). Materials science of concrete 2. Westerville: American Ceramic Society.
- Jones, T., and B. Cather. (2005) Ultra-High Performance Fibre-Reinforced Concrete, *Concrete*
- Kakizaki, M., Edahiro, H., Tochigi, T., and T. Niki. (1992) Fly Ash, Silica Fume, Slag, and Natural Pozzolans in Concrete: Proceedings, Fourth International Conference, Istanbul, Turkey, May. Ed. By V.M. Malhotra. American Concrete Institute, Detroit, MI: 997- 1016.
- Klemens, T., (2004) Flexible concrete offers new solutions. Concrete Construction – World of Concrete 49(12), pp. 72-74.
- Kolonko, M., Raschdorf, S. and Wäsch, D. (2008) A Hierarchical Approach to Estimate the Space Filling of Particle Mixtures with Broad Size Distributions. pp. 28.
- Kosmatka, S.H., Kerhoff, B., and W.C. Panarese (2002) Design and Control of Concrete Mixtures, 14th Ed. Portland Cement Association, Shokie, IL.
- Kozlova, S., Millrath, K., Meyer, c., & Shimanovich, S., (2004) A suggested screening test for ASR in cement-bound composites containing glass aggregate based on autoc1aving. Cement and Concrete Composites. 26(7), 827-835.
- Kumar, S.V. and Santhanam, M. (2003) Particle packing theories and their application in concrete mixture proportioning: A review. The Indian Concrete Journal, Vol. 77 (9), pp.1324-1331.
- Kurtis, K. E., & Monteiro, P. J. M. (2003) Chemical additives to control expansion of alkali-silica reactive gel: proposed mechanisms of control. Journal of Materials Science, 38(9), 2027-2036.
- Lafarge. (2007) Ductal® - Applications and References. http://www.ductal-lafarge.com /wps/portal/Ductal/ApplicationsAndReferences/.

- Lam, C. S., Poon, C. S., & Chan, D. (2007) Enhancing the performance of precast concrete blocks by incorporating waste glass - ASR consideration. Cement and Concrete Composites, 29(8),616-625.
- Lange F, Mo¨rtel H, Rudert V (1997) Dense packing of cement pastes and resulting consequences on mortar properties. Cem Concr Res 27(10):1481–1488.
- Lange F., Mörtel H., Rudert V. (1997) Dense packing of cement pastes and resulting consequences on mortar properties", Cement and Concrete Research, Vol. 27, No. 10, pp 1481-1488.
- Lee, M.-G., Chiu, C.-T., and Y.-C. Wang. (2005) The Study of Bond Strength and Bond Durability of Reactive Powder Concrete. Journal of ASTM International, July/Aug., Vol. 2, No. 7: 104-113.
- Lee, N.P., and D.H. Chisholm. (2006) Reactive Powder Concrete. Branz. http://www.branz.co.nz/branzltd/publications/pdfs/SR146.pdf.
- Liu, C.-T., Huang, J.-S., (2008) Highly flowable reactive powder mortar as a repair material. Construction and Building Materials 22, pp. 1043-1050.
- Loukili, A., Khelidj, A., and P. Richard. (1999) Hydration Kinetics, Change of Relative Humidity, and Autogenous Shrinkage of Ultra-High-Strength Concrete. *Cement and Concrete\BN Research*, Apr., Vol. 29, No. 4: 577-584.
- LRFD Bridge Design Manual, First Ed. Sept. 1. http://www.dotd.louisiana.gov/ highways/project_devel/design/bridge_design/documents/LRFD_Bridge_Design_Manual-version_2006.1.pdf.
- Ma, J., and H. Schneider (2002) Properties of Ultra-High-Performance Concrete. Leipzig Annual Civil Engineering Report (LACER), No. 7: 25-32.
- Ma, J., Dietz, J., and F. Dehn. (2003) Ultra High Performance Self Compacting Concrete. 3rd International Symposium on Self-Compacting Concrete, Reykjavik, Iceland, 17-20August: 136 142.
- Ma, J., Orgass, M., Dehn, F., Schmidt, D., and N.V. Tue. (2004) Comparative Investigations on on Ultra-High Performance Concrete with and without Coarse Aggregates, International Symposium on Ultra High Performance Concrete (UHPC), Kassel, Germany
- Matte, V., and M. Moranville (1998) Leaching of the Reactive Powder Concretes: Results on Transfer Properties. Nondestructive Characterization of Materials in Aging Systems:

Symposium Held November 30-December 4, 1997, Boston, Massachusetts, Vol. 503. Ed. by Crane, R.L., Achenbach, J.D., Shah, S.P., Matikas, T.E., Khuri-Yakub, P., and R.S. Gilmore. Materials Research Society: 145-150.

- Matte, V., and M. Moranville (1999) Durability of Reactive Powder Composites: influence of silica fume on the leaching properties of very low water/binder Pastes. Cement & Concrete Composites, Feb., Vol. 21, No. 1: 1-9.
- Mazzacane P, Ricciotti R, Lamoureux G, et al. Roofing of the Stade Jean Bouin in UHPFRC. In: Toutlemonde F, Resplendino J, eds. Proceedings of International Symposium on Ultra-High Performance Fiber-Reinforced Concrete. Marseille, France, 2013. 59–68.
- Mazzacane P, Ricciotti R, Teply F (2013) MUCEM: The builder's perspective. In: Toutlemonde F, Resplendino J, eds. Proceedings of Reinforced Concrete. Marseille, France. 3 16.
- Mehta PK, Monteiro PJM (1992) Concrete: Structure, Properties, and Materials, Book.
- Menetrey P. (2013) UHPFRC cladding for the Qatar National Museum. In: Toutlemonde F, Resplendino J, eds. Proceedings of International Symposium on Ultra-High Performance Fiber-Reinforced Concrete. Marseille, France. 351–360.
- Meyer, C. (2004) Concrete Materials and Sustainable Development in the USA. Structural Engineering International, Obtained: December 5, 2008 from http://www.civil.columbia.edu/meyer/publications/publ.html.
- Mihaljevic, S.N., Chidiac, S.E. (2009) Use of post-consumer waste in concrete and concrete block - literature review. In the proceedings of the Ji" Canadian Masonry Symposium, 3J May - 3 June 2009 (pp. 929-940). Toronto, Canada: Canada Masonry Centre.
- Mindess, S., and Young, J.F. (1981) Concrete. Prentice-Hall, Inc., Englewood Cliffs, NJ.
- Morin, V., Cohen-Tenoudji, F., Feylessoufi, A., and P. Richard (2002) Evolution of the capillary network in a reactive powder concrete during hydration process. Cement and Concrete Research, Dec., Vol. 32, No. 12: 1907-1914.
- Möser B., Pfeifer C., Stark J. (2009) Durability and microstructural development during hydration in ultra-high performance concrete. Concrete repair, rehabilitation and retrofitting II Taylor & Francis Group, London, p. 87–8.

- Muttoni A, Brauen U, Jaquier J L, et al. (2013) A new roof for the Olympic museum in Lausanne, Switzerland. In: Toutlemonde F, Resplendino J, eds. Proceedings of International Symposium on Ultra-High Performance Fiber-Reinforced Concrete. Marseille, France. 69–76.
- Nassar, Roz-Ud-Din, Soroushian, P. (2012) Srength and durability of recycled aggregate concrete containing milled glass aspartial replacement for cement. Construction and Building Materials. 29. 368-377.
- Neville AM (2000) Properties of concrete. 4th Ed., Prentice Hall, London.
- Neville AM, Brooks JJ (1987) Concrete technology. Longman Scientific & Technical, Harlow, Essex, UK, Wiley, New York.
- Neville, A.M. (1995) Properties of Concrete. Harlow: Longman.
- Nguyen V.T., Ye G., van Breugel K., Fraaij A.L.A, Bui D.D., (2011) The study of using rice husk ash to produce ultra high performance concrete, Construction and Building Materials 25(4) 2030-2035.
- Nielsen, C.V., (1995) Ultra high-strength steel fibre reinforced concrete, Part I: Basic strength properties of compresit matrix. Technical University of Denmark 323.
- Nielsen, C.V., (1995) Ultra high-strength steel fibre reinforced concrete, Part II. Department of Structural Engineering, Technical University of Denmark 324.
- Obla K.H., Hill R.L., Thomas M.D.A., Shashiprakash S.G., Perebatova O. (2003) Properties of concrete containing ultra-fine fly ash, ACI Materials Journal, Vol. 100, No. 5, pp 426-433.
- Park CK, Noh MH, Park TH (2005) Rheological properties of cementitious materials containing mineral admixtures. J. Cem. Concr. 35:842–849.
- Park S. B., Lee B. C and Kim J. H., (Dec. 2004) "Studies on mechanical properties of concrete containing waste glass aggregate," Cement and Concrete Research, vol. 34, pp. 2181–2189.
- Park, S.B., Lee, B.C., Kim, J.H. (2004) Studies on mechanical properties of concrete containing waste glass aggregate. Cement and Concrete Research, 34(12), 2181-2189.
- Peng, Y., Hu, S., Ding, Q., (2010) Preparation of reactive powder concrete using fly ash and steel slag powder. Journal Wuhan University of Technology, Materials Science Edition 25(2), pp. 349-354.

- Perry C and Gillott JE, (1995) The Influence of Silica Fume on the Strength of the Cement-Aggregate Bond, ACI Materials Journal, 156, 191-212.
- Perry, V. (2001) Reactive Powder Concrete. PCI Journal, July/Aug., Vol. 46, No. 4: 118.
- Perry, V. (2001) Reactive Powder Concrete. *PCI Journal*, July/Aug., Vol. 46, No. 4: 118.
- Perry, V. (2006) Ductal® - A Revolutionary New Material for New Solutions. Association of Professional Engineers and Geoscientists of the Province of Manitoba (APEGM). http://www.apegm.mb.ca/pdnet/papers/ductal.pdf.
- Perry, V., and D. Zakariasen. (12-15 Sept. 2004) First Use of Ultra-High Performance Concrete for an Innovative Train Station Canopy. Concrete Technology Today, Aug., Vol. 25, No. 2: 1-2, Perth, Australia.
- Pfeifer CG, Moeser B, Giebson C, Stark J (2009) Durability of ultra-high-performance concrete, 10th ACI International Conference on Recent Advances in Concrete Technology and Sustainability Issues. No. SP-261-1.
- Pietsch W (1997) Size enlargement by agglomeration. In: Fayed ME, Otten L (eds) Handbook of powder science and technology, 2nd edn. Chapman & Hall, New York.
- Plank J, Pöllmann K, Zouaoui N, Andres PR, Schaefer C. (2008) Synthesis and performance of methacrylic ester based polycarboxylate superplasticizers possessing hydroxy terminated poly (ethylene glycol) side chains. Cement and Concrete Research; 38(10) 1210-1216.
- Polley, C., Cramer, S. M., & de la Cruz, R. V. (1998) Potential for using waste glass in Portland cement concrete. Journal of Materials in Civil Engineering, 10(4), 210-219.
- Pouliot N., Sedran T., De Larrard F., Marchand J. (Juillet-Août 2001) Formulation des bétons compactés au rouleau à l'aide d'un modèle d'empilement granulaire, Bulletin des laboratoires des Ponts et Chaussées, N° 233, pp. 23-36.
- Powers TC (1968) the properties of fresh concrete. John Wiley & Sons, New York.
- Powers, T.C. (1968) The Properties of Fresh Concrete. New York: Wiley.
- Racky, P. (2004) Cost-effectiveness and Sustainability of RPC. Proceedings of the International Rebentrost, M., and B. Cavill. 2006. Reactive Powder Concrete Bridges. AustRoads Conference,
- Reda, M.M., Shrive, N.G., Gillott J.E. (1999) Microstructural Investigation of Innovative RPC. Cement and Concrete Research, Mar., Vol. 29, No. 3: 323-329.

- Richard, P., and M. Cheyrezy (1995) Composition of Reactive Powder Concretes. Cement and Concrete Research, Oct., Vol. 25, No. 7: 1501-1511.
- Richard, P., and M.H. Cheyrezy (1994) Reactive Powder Concretes with High Ductility and 200-800 MPa Compressive Strength. Concrete Technology: Past, Present, and Future – Proceedings of V. Mohan Malhotra Symposium. American Concrete Institute, Detroit, MI.
- Rixom R. and Mailvaganam N., Chemical Admixtures for concrete, E & FN Spon, London (1999).
- Rossi P., (1997) High performance multi-modal fiber reinforced cement composite (HPMFRCC): the LCPC experience, ACI Materials Journal 94 (6) 478–483.
- Rossi, P. (2005) Development of New Cement Composite Materials for Construction. Proceedings of the Institution of Mechanical Engineers, Part L: Journal of Materials: Design and Applications, Feb., Vol. 219, No. L1: 67-74.
- Roux, N., Andrade, C., M.A. Sanjuan (1996) Experimental Study of Durability of Reactive Powder Concretes. *Journal of Materials in Civil Engineering*, Feb., Vol. 8, No. 1: 1-6.
- Saeed H., Ebead, U., Tagnit-Hamou, A., Neal K. (2011) Stoichiometric study of activated glass powder hydration, Advances in Cement Research, 24(2), 91-101.
- Saeed, H., Tagnit-Hamou, A., Ebead, U., and Neale, K. (2012) Stoichiometric study of activated glass powder hydration." Advances in Cement Research, 91-101.
- Sangha, C. M., Alani, A. M., and Walden, P. J. (2004) Relative strength of green glass cullet concrete. Magazine of Concrete Research, 56(5), 293-297.
- Schmidt, M., and E. Fehling (2005) Ultra-High-Performance Concrete: Research, Development and Application in Europe. 7th International Symposium on Utilization of High Strength High Performance Concrete, Vol. 1: 51-77.
- Schmidt, M., Fehling, E., Teichmann, T., Bunje, K., and R. Bornemann (2003) Ultra-High Performance Concrete: Perspective for the Precast Concrete Industry. Concrete Precasting Plant and Technology, Vol. 69, No. 3: 16-29.
- Schmiedmayer, R., Schachinger, I. (August 1998) Influence of Superlasticizer Dosage and Mixing Procedure on the Density and Strength of Reactive Powder Concrete. International Symposium on High-Performance and Reactive Powder Concretes, Sherbrooke/Kanada, Band 3, S. 145-152.

- Schneider, B., (1992) Development of SIFCON through Applications', in High Performance Fiber Reinforced Cement Composites, H. W. Reinhardt and A. E. Naaman (eds.), RILEM Proc. no. 15, E & FN Spon, pp. 177–194.
- Schwarz, N., & Neithalath, N. (2008) Influence of a fine glass powder on cement hydration: Comparison to fly ash and modeling the degree of hydration. Cement and Concrete Research, 38(4), 429-436.
- Schwarz, N., Cam, H., and Neithalath, N. (2008) Influence of a fine glass powder on the durability characteristics of concrete and its comparison to fly ash. Cement and Concrete Composites, 30(6), 486-496.
- Sedran T., de Larrard, F. (1999) Optimization of self-compacting concrete thanks to packing model" Author(s): T. Sedran, F. de Larrard, 321-332.
- Sedran T., Durand C. and F. de Larrard (17-18 November 2009) An example of UHPFRC recycling, AFGC-FIB International workshop "Designing and Building with UHPFRC: State of the Art and Development", Marseille France.
- Sedran, T. and de Larrard, F., (2000) Manuel d'utilisation de RENE-LCPC, version 6.1d, logiciel d'optimisation granulaire, Laboratoire Centrale des Ponts et Chaussées.
- Shaheen, E., & Shrive, N. (2006) Optimization of mechanical properties and durability of reactive powder concrete. ACI Material Journal, 103(6), 444–451.
- Shao, Y., Lefort, T., Moras, S., & Rodriguez, D. (2000). Studies on concrete containing ground waste glass. Cement and Concrete Research, 30(1) 91-100.
- Shayan, A., & Xu, A. (2006) Performance of glass powder as a pozzolanic material in concrete: A field trial on concrete slabs. Cement and Concrete Research, 36(3),457-468.
- Shayan, A., and Xu, A. (2004) Value-added utilisation of waste glass in concrete. Cement and Concrete Research, 34(1) 81-89.
- Shi, C., & Zheng, K. (2007) A review on the use of waste glasses in the production of cement and concrete. Resources, Conservation and Recycling, 52(2), 234-247.
- Shirkavand, M., and Baggott, R., (1995) Effects of Superplasticizer on Workability and Flexural Strength of Autoclaved Calcium Silicates" Cement and Concrete Research, Vol.25, No.7, pp.1512-1522.
- Siddique, R. (2008) Waste Materials and By-Products in Concrete. Springer, 147-175.

- Sobolev, K. 2004. The development of a new method for the proportioning of high-performance concrete mixtures. *Cement and Concrete Composites*, Oct., Vol. 26, No. 7: 901-907.
- Soutsos, M.N., Millar, S.G., and K. Karaiskos. (2005) Mix Design, Mechanical Properties, and Impact Resistance of Reactive Powder Concrete (RPC). International RILEM Workshop on High Performance Fiber Reinforced Cementitious Composites in Structural Applications, Honolulu, HI, May.http://www.hpfrcc-workshop.org/HPFRCCworkshop/ Papers/F/Soutsos_ReactivePowderConcrete.pdf.
- Sritharan, S., Bristow, B., Perry, V. (2003). Characterizing an ultra-high performance material for bridge applications under extreme loads. In Proceedings of the 3rd International Symposium on High Performance Concrete, Orlando, FL.
- Stovall, T., Larrard, F. de and Buil, M. (1986) Lineair Packing Density Model of Grain Mixtures. Powder Technology, Vol. 48, 1-12.
- Stovall, T., Larrard, F. de and Buil, M. (1986) Lineair Packing Density Model of Grain Mixtures. Powder Technology, Vol. 48, pp. 1-12.
- Stroeven, P. and Stroeven, M. (1999) Assessment of packing characteristics by computer simulation. Cement and Concrete Research, Vol. 29, pp. 1201-1206.
- Svarovsky L (1987) Powder testing guide: methods of measuring the physical properties of bul powders. Elsevier Applied Science Publishers Ltd, England.
- Svarovsky L (Sept. 13-15 1987) Powder testing guide: methods of measuring the physical properties of bulk powders. Elsevier Applied Science Publishers Ltd, England, Symposium on Ultra High Performance Concrete, Kassel, Germany: 797- 805.
- Tagnit-Hamou, A., Bengougam, A. (2012) The use of glass powder as supplementary cementitious material, Concr Int, 34(3), 56-61.
- Taha, B & Nounu, G., (2009) Utilizing waste recycled glass as sand/cement replacement in concrete, J. Mater. Civil Eng. ASCE, vol. 21, no.12, 709–721.
- Taha, B., & Nounu, G. (2008) Properties of concrete contains mixed colour waste recycled glass as sand and cement replacement. Construction and Building Materials, 22(5), 713-720.
- Tanaka, Y., Musya, H., Ootake, A., Shimoyama, Y., Kaneko, O. (2002) Design and construction of Sakata-Mirai footbridge using reactive powder concrete. In: Proceedings of

the First fib Congress (FIB 2002), Osaka, Japan, Session 1 – Big projects and innovative structure, 417-424.

- Tang, M.-C. (Sept. 13-15 2004) High Performance Concrete – Past, Present, and Future. Ultra High Performance Concrete (UHPC). *Proceedings of the International Symposium on Ultra High Performance Concrete, Kassel, Germany*: 3-9.
- Teichmann, T., and M. Schmidt (2004) Influence of the packing density of fine particles on structure, strength and durability of RPC. Proceedings of the International Symposium on Ultra-High Performance Concrete, Kassel, Germany, Sept. 13-15: 313-323.
- Terro, M. J. (2006). Properties of concrete made with recycled crushed glass at elevated temperatures. Building and Environment, 41(5), 633-639.
- Topcu I. B. and Canbaz, M. (Feb. 2004) Properties of concrete containing waste glass. Cement and Concrete Research, vol. 34, 267–274.
- Topcu, i B., Boga, A. R, & Bilir, T. (2008) Alkali-silica reactions of mortars produced by using waste glass as fine aggregate and admixtures such as fly ash and LizC03. Waste Management, 28(5), 878-884.
- Topcu, I. B. and Canbaz, M. (2004) Properties of Concrete Containing Waste Glass. Cement and Concrete Research, 34(2), 267-274.
- Tue, N. V.; Ma, J.; and Orgass, M., (2008) Influence of Addition Method of Superplasticizer on the Properties of Fresh RPC. 2nd International Symposium on Ultra High Performance Concrete, Kassel, Germany, pp. 93-100.
- Van Tuan, N., Ye, G., Van Breugel, K., Fraaij, A.L.A., Bui, D.D., (2011) The study of using rice husk ash to produce ultra high performance concrete. Construction and Building Materials 25(4), pp. 2030-2035.
- Vernet, C.P. (2004) Ultra-Durable Concretes: Structure at the Micro- and Nanoscale. *MRS Bulletin*, May, Vol. 29, No. 5: 324-327.
- Vikan, H. and Justnes, H. (2007) Rheology of cementitious paste with silica fume or limestone. Cement and Concrete Research, 37(11), 1512-1517.
- Voo, J.Y., Foster, S.J., and R.I. Gilbert. (2003) Shear Strength of Fibre Reinforced Reactive Powder Concrete Girders without Stirrups. UNICIV Report No. R-421, Nov. The University

of New South Wales. http://www.civeng.unsw.edu.au/ research/publications/uniciv/R-421.pdf.

- Voo, J.Y., Foster, S.J., Gilbert, R.I., and N. Gowripalan. (2001) Design of Disturbed Regions in Reactive Powder Concrete Bridge Girders. *High Performance Materials in Bridges: Proceedings of the International Conference, Kona, Hawaii, July 29 – August 3*. Ed. By Azizinamini, A., Yakel, A., and M. Abdelrahman. American Society of Civil Engineers,Reston, VA: 117-127.
- Voort TLV, Suleiman MT, Sritharan S (2008) Design and Performance Verification of Ultra-High Performance Concrete Piles for Deep Foundations. Final Report, Sponsored by the Iowa Highway Research Board (IHRB Project TR-558):224.
- Walker, W.J. (2003) Persistence of Granular Structure during Compaction Processes. KONA, Vol. 21, pp. 133-142.
- Walraven, J.C. (2007) Futuro del hormigon con fibras. Applicaciones estructurales de hormigon con fibras, Oct. 9, Barcelona.
- Walraven, J.C. (9-11 Sept 2002) From Design of Structures to Design of Materials. Innovations and Developments in Concrete Materials and Construction: Proceedings of the International Conference Held at the University of Dundee, Scotland, UK. London: 805- 818.
- Walraven, J.C. (Sept. 13-15 2004) Designing with ultra high strength concrete: basics, potential and perspectives. Proceedings of the International Symposium on Ultra-High Performance Concrete, Kassel, Germany: 853-864.
- Walraven, J.C., and P. Schumacher (2005) Applications for Ultra-high Performance Concrete. TIEFBAU, No. 4: 230-234.
- Wen-yu, J., Ming-zhe, A., Gui-ping, Y., and W. Jun-min. (2004) Study on Reactive Powder Concrete Used in the Sidewalk System of the Qinghai-Tibet Railway Bridge. International Workshop on Sustainable Development and Concrete Technology, Beijing, China, May 20-21. http://www.cptechcenter.org/ publications/sustainable/jireactive.pdf.
- Wong, H.C. and Kwan, K.H. (2008) Packing density of cementitious materials: part 1- measurement using a wet packing method. Materials and structures, Vol. 41, pp. 689-701.

- Xing, F., Huang, L.-D., Cao, Z.-L., and L.-P. Deng. (2006) Study on Preparation Technique for Low-Cost Green Reactive Powder Concrete. Key Engineering Materials, Jan., Vol. 302-303: 405-410.
- Yan, Z.-G., and G.-P. Yan. (Jan. 2006) Experimental Study and Finite Element Analysis of RPC Footwalk Braces. Key Engineering Materials, Vol. 302-303: 713-719.
- Yazici H, Yiğiter H, Karabulut AŞ, Baradan B. (2008) Utilization of fly ash and ground granulated blast furnace slag as an alternative silica source in reactive powder concrete. *Fuel*;87(12):2401–2407.
- Yazici, H. (2006) The effect of curing conditions on compressive strength of ultra high strength concrete with high volume mineral admixtures. Building and Environment, May, Vol. 42, No. 5: 2083-2089.
- Yin, J., Zhou, S., Xie, Y., Chen, Y., and Q. Yan. (2002) Investigation on compounding and application of C80–C100 high-performance concrete. Cement and Concrete Research, Feb., Vol. 32, No. 2: 173-177.
- Yu, A.B., Zou, R.P. and Standish, N. (1996) Modifying the Linear Packing Model for Predicting the Porosity of Nonspherical Particle Mixtures. Ind. Eng. Chem. Res., Vol. 35 pp. 3730-3741.
- Zanni, H., Cheyrezy, M., Maret, V., Philippot, S., and P. Nieto. (1996) Investigation of Hydration and Autogenous Shrinkage of Ultra-High-Strength Concrete. Cement and Concrete Research, Apr., Vol. 29, No. 4: 577-584.
- Zheng, J. and Stroeven, P. (1999) Computer simulation of particle section patterns from sieve curve for spherical aggregate. In: Dhir, R.K. and Dyer, T.D. (eds). Modern concrete materials: binders, additions and admixtures: proceedings of the international Conference held at the University of Dundee, Scotland, UK on 8/10 September.
- Zheng, J. and Stroeven, P. (8-10 September 1999) Computer-simulation of particle section patterns from sieve curve for spherical aggregate. In: Dhir, R.K. and Dyer, T.D. (eds). Modern concrete materials: binders, additions and admixtures: proceedings of the international Conference held at the University of Dundee, Scotland, UK.

- Zheng, J., Johnson, P.F. and Reed, J.S. (1990) Improved Equation of the Continuous Particle Size Distribution for Dense Packing. Journal of the American Ceramic Society, Vol. 73 (5), pp. 1392-1398.
- Zidol, A. Tohoue Tognonvi, M., Tagnit-Hamou, A. (2013) Advances in durable concrete materials applied to the African context, International Conference on Advances in Cement and Concrete Technology in Africa

3 Mix Design Optimization

3.1 Introduction

This chapter presents an innovative method for producing ecoefficient mixtures of UHPC with locally available materials based on optimization of the packing density and a statistical mixture-design approach. The proportion of granular mixtures is predicted with the packing model developed by Sedran and de Larrard [2000], which has been successfully used to design UHPCde Larrard and Sedran [1994]. The study presents experimentally based models with high coefficients of correlation in predicting UHPC workability and strength as a function of mix-design parameters (*w/b* and superplasticizer dosage). Various UHPC mixtures were designed with wide ranges of water-to-binder ratios (*w/b*) between 0.150 and 0.250 and superplasticizer dosages between 1% and 3%, (%wt. solids to cement), using a full-factorial design approach highlighted in this chapter. Test results of the effect of packing density on fresh and compressive strength of UHPC are also presented. The chapter also includes descriptions of the materials, mix designs, and mixing sequences used in these experimental tests. The packing-density analysis, testing sequences, and methods used to examine the fresh properties and compressive strength test are also detailed. The UHPC mixture that gives specific rheological characteristics, excellent overall performance, and cost-effectiveness will be recommended as the reference mixture in this study.

In the following chapters, the waste-glass materials with different PSD were used to replace each individual component in this reference mixture, while keeping the content of other materials constant. For example, GP at different proportions was used to replace cement, while keeping QS, QP and SF quantities and superplasticizer dosages and w/b ratio constant in all mixtures.

3.2 Paper 1: Using Particle Packing and Statistical Approach to Optimize Eco-Efficient Ultra-High-Performance Concrete

Reference:

Soliman N.A., Tagnit-Hamou A. (2016) Using Particle Packing and Statistical Approach to Optimize Eco-Efficient Ultra-High-Performance Concrete. *ACI Materials Journal*. (Accepted and forthcoming).

Using Particle Packing and Statistical Approach to Optimize Eco-Efficient Ultra-High-Performance Concrete

Authors and Affiliation

Nancy A. Soliman is a member of the ACI international and Sherbrooke local chapters, and CRIB. She is a PhD candidate in the Department of Civil Engineering, University of Sherbrooke, QC, Canada. Her research interest includes NDT, UHPC, microstructure, and sustainable development.

Arezki Tagnit-Hamou, FACI, is a professor in the Department of Civil Engineering at the University of Sherbrooke, QC, Canada. He is also the Head of the cement and concrete group as well as holding an industrial chair on valorization of glass in materials. He is a member of ACI Committees 130 (Sustainability of Concrete) and 555 (Concrete with Recycled Materials), and RILEM TC DTA. His research interests include alternative supplementary cementitious materials, cement and concrete physicochemistry and microstructure, and sustainable development.

ABSTRACT

Ultra-high-performance concrete (UHPC) is characterized by a dense microstructure that yields ultra-high strength and durability properties. This paper presents an innovative method to produce eco-efficient mixtures of UHPC using locally available materials based on optimization using the packing-density (PD) and a statistical mixture-design approach. The results showed an optimal PD of 0.79% for a combination of all granular materials (quartz sand, quartz powder, cement, and silica fume). The study presents experimental-based models with high coefficients of correlation in predicting the workability, and strength of UHPC as a function of mix-design parameters (*w/b* and superplasticizer dosage). Contour diagrams to facilitate the use of the models were established. In this research, UHPC mixtures with a slump flow between 130 and 300 mm (5.1 and 11.8″) and compressive strength between 135 and 225 MPa (19.6 and 32.6 ksi) were produced; such concretes are required for different industrial applications.

Keywords: Concrete design, packing density, statistical-design approach, ultra-high-performance concrete (UHPC).

INTRODUCTION

Conventional vibrated concrete (CVC) has numerous problems, such as corrosion of steel reinforcement and fragility of concrete construction. As a result, most structures made with conventional concrete require annual maintenance.[1] Currently, there is a critical need for advanced high-performance building materials for infrastructure and repair.[2]

Ultra-high-performance concrete (UHPC) can be designed to eliminate some of the characteristic weaknesses of CVC.[3] UHPC is defined worldwide as concrete with superior mechanical, ductility, and durability properties. A typical UHPC contains a cement content (800 to 1000 kg/m^3 or 1350 to 1700 lb/yd^3), silica-fume (SF) content (25% to 35%, by cement weight), quartz powder (QP), quartz sand (QS), and steel fiber.[3] The steel fiber improves UHPC ductility. UHPC can achieve compressive strength (f_c) greater than 150 MPa (21.8 ksi), flexural strength (f_{fl}) of up to 15 MPa (2200 psi), elastic moduli (E_c) of 45 GPa (6500 ksi), and minimal long-term creep or shrinkage.[4,5] UHPC can also resist freeze–thaw cycles and scaling, and be nearly impermeable to chloride-ion penetration.[6,7]

UHPC is currently used for special prestressed and precast concrete elements, such as decks and abutments for lightweight bridges, marine platforms, precast walls, concrete repair, and urban furniture and other architectural applications.[2,8,9]

UHPC confers some economic advantages in overcoming this issue such as (1) reducing or eliminating the passive reinforcement in structural elements due to its steel-fiber content, (2) reducing the dimensions of concrete elements due to its ultra-high mechanical properties, (3) reducing the dead weight of structural elements by more than 70%, (4) extending the service life of structures, and (5) lowering maintenance costs due to superior durability properties.[10–12]

UHPC contains a large amount of cement, usually between 900 and 1,200 kg/m^3 (1500 to 2000 lb/yd^3).[4,13] This huge amount of cement not only affects production costs, it negatively impacts the environment as the result of CO_2 emissions and consumes natural sources.[12]

In recent years, several research projects have studied how to optimize UHPC mix proportioning. de Larrard and Sedran developed an UHPC by optimizing the granular mixture using the linear packing-density model (LPDM).[14] Later, de Larrrad modified the LPDM to take into account the effect of compaction technique by making a distinction between virtual PD(maximum theoretical packing density) and actual PD.[15] The modified model was called the compressible packing model (CPM). Implementing compaction energy in the CPM increases the accuracy of packing predictions compared to the LPDM. Teichmann and Schmidt proposed a method for maximizing the PD of cement and fillers in UHPC to obtain f'_c higher than 200 MPa (29 ksi).[16] Talebinejad *et al*. also designed a mix with a density of approximately 2400 kg/m^3 (4050 lb/yd^3) and f'_c of more than 250 MPa (36.3 ksi).[17] The final mixture contained more than 1500 kg/m^3 (2500 lb/yd^3) of cement: using such huge cement content release correspond to the high amount of CO_2 into the atmosphere during the fabrication of the cement, which has a negative effect on sustainability. Habel *et al.* [18] designed a UHPC based on the mix-design proportions proposed by Rossi *et al*.[19], but replacing their materials with those available locally in Quebec and Ontario without consideration to material packing. However, the final mixture contained 967 to 1087 kg/m^3 (1630 to 1830 lb/yd^3) of cement, the obtained f'_c was limited to 121-128 MPa (17.5-18.6 ksi). Park *et al.* performed a study in order to produce UHPC with f'_c of 180 MPa (26.1 ksi), by considering the effect of different variables, such as water-to-binder ratio (*w/b*), and the type and replacement proportion of the filling powder.[20] Wille *et al.* presented a design method for UHPC based on paste rheology. In this method, high spread values of paste (obtained using mini-slump measurement) imply high PD and thus high f'_c.[21] Wang *et al.* focused on the preparation of UHPC with ordinary raw materials by investigating the influence of binder content, *w/b*, and the replacement of cementitious materials on concrete fluidity and f'_c.[22] Ghafari *et al*. presented an analytical method based on the statistical mixture-design (SMD) approach for UHPC mixtures. [23] This method was developed to assess the influence of each parameter as well as their interaction on the various properties of UHPC.

Most of current mixture-design methods for UHPC involve an extensive series of tests and a large number of batches. None of these methods provides conclusive steps for UHPC design, especially when different materials are used. Furthermore, these methods do not mention which

UHPC constituents would perform optimally in producing certain rheological characteristics and meeting strength requirements. The current paper presents a design method for UHPC based on optimizing (1) the particle packing of granular materials and (2) *w/b* and HRWRA dosage using statistical models. This new method can yield various UHPC mixtures with a different range of rheological characteristics and strength requirements for different applications. This research also investigated the possibility of making UHPC with materials locally available.

RESEARCH SIGNIFICANCE

Advances in concrete technology and the demand for high-strength and green construction materials have given momentum to the development of UHPC. The UHPC currently available frequently comes as prepackaged dry materials without regular mix-design steps. The transportation of UHPC under such conditions greatly affects in carbon footprint and the final cost. This paper presents a review and methodology to produce different types of UHPC. This methodology is based on the particle packing and statistical-design approaches to optimize mix design. The statistical-design approach can be used to investigate the trade-off between different mix design parameters (*w/b* and HRWRA dosage) on concrete properties in order to minimize the number of experiments needed compared to using the traditional parametric study approach. The proposed UHPC design method yields several advantages: by using particle packing optimization techniques it is possible to optimize the particle packing in order to lower the cement content and optimum contents of materials in concrete without changing concrete properties in a negative way. The design method based on optimizing the particle packing of materials can reduce the energy consumption and CO_2 emissions of concrete by decreasing the cement content. Furthermore, the high density of the particle structure leaves less space for voids to be filled with water, which reduces the water demand and increases the strength of concrete. This mix-design approach for UHPC is also applicable when using locally available materials sought in different industrial sectors for environmental and economical purposes.

PROPOSED APPROACH FOR DESIGNING UHPC

Packing Density of Granular Materials

In recent decades, particle-size optimization has gained new interest with the introduction of new concrete types, such as high-performance concrete (HPC), self-consolidating concrete (SCC), and UHPC.[24] Optimizing system packing can reduce porosity and yield the strongest matrix. Optimizing the granular mixture requires more fine particles to fill system voids.[25] These fine particles expel water from the voids, help distribute water more homogenously in the system, and help improve mixture workability. The reduction in water demand due to a higher PD allows for using a lower *w/b* to achieve higher strength. Better packing would dramatically reduce the permeability of the hardened concrete, leading to higher concrete durability.[26-28]

Packing models are used to estimate the optimum PD of the solid combinations and minimize the void ratio. Over the years, three distinct approaches (continuous model [CM], discrete-element model [DEM], and particle-packing models [PPM]) have been used in proportioning solid ingredients.[24] The CM combines groups of particles having their own specific particle-size distributions (PSDs) to produce a final PSD of the mixture closest to an optimal curve. The models in references are examples of CM. [29, 30] The DEM generate a 'virtual' particle structure from a given PSD. Examples of the DEM can be found in references.[31, 32] The PPM calculates the theoretical PD of a mixture based on the PSD and PD of the various materials in the mixture, and possibly the compaction energy. Common examples of PPM are CPM[15], compaction–interaction packing model (CIPM)[33], and those in references.[34,35]

The CM does not consider particle shape, but it greatly influences packing density. The DEM can calculate the maximum PD of concrete mixtures while taking many parameters into account. Due to limitations in currently available computational speeds, the DEM is not an ideal method for concrete-mixture optimization, especially since many mixtures have to be assessed in order to find the optimal composition. The DEM could be more efficient, however, as computers become more powerful. Consequently, the analytical PPM provides the best solution for concrete mixture optimization. Of all the analytical models, the CPM and CIPM stand out as the best models. The CIPM is considered as an extension of the CPM. The CIPM includes interactions due to the

surface forces for very fine particles (≤125 μm or 0.0049″). The values in the current model are based on limited data from experiments with cement and quartz powder. So, the model has not been validated for other materials. Consequently, the CPM was considered in the current research as the mutual influence of compaction and interactions in particle structure.

Statistical Design Approach for Optimizing w/b and HRWRA Dosage

The statistical design of experiments is used to establish the trade-off between significant mix design parameters on targeted concrete properties for given set of constraints, while minimizing the number of trial batches.[36-38] Furthermore, using a statistical approach, prediction models describing the main influence and second-order interaction of various mix design parameters on a given concrete property. In this research, a full-factorial design approach was applied to optimize both the *w/b* and HRWRA dosage (represented as solids content to cement weight). The concrete properties investigated were the mini-slump flow diameter, air voids, f'_c after 2 days of hot curing (f'_c-2d-HC), and f'_c after 28 days of normal curing (f'_c-28d-NC). The normal curing (NC) consisted of a temperature (T) of 20±2ºC (68±4ºF) and a relative humidity (RH) of 100%, while the hot curing (HC) consisted of T = 90ºC (194ºF) and RH =100%. The prediction equations take into account only the most significant factors (variables) and their interactions. The equations can be linear or nonlinear (quadratic) based on the response behavior throughout the range of variables. Linear equations involve main variables and their interactions, while nonlinear formulas include higher-order variables (quadratic). Two-level statistical design of experiments for the two independent variables—*w/b* and *%solidHRWRA* (k = 2)—consists of four ($2^k = 4$) concrete mixtures in which each variable is set at two different coded levels of -1 (minimum) and +1 (maximum) within the modeled region. Four replicated central mixtures corresponding to a coded value of 0 were prepared to estimate the degree of experimental error for the anticipated models. Five additional UHPC mixtures were designed with variable *w/b* and *%solidHRWRA* to check the anticipated models, as shown in Table 1. The absolute values corresponding to the coded values of -1, 0, and +1 for the *w/b* parameter are 0.15, 0.20, and 0.25 and 1.0%, 2.0%, and 3.0%, respectively, for *%solidHRWRA*. The coded values can be calculated from Eqs. 1 and 2. The linear model associated with a two-level statistical design in the case of two independent variables (*w/b* and *%solidHRWRA*) can be expressed as indicated in Eq. 3.

Coded *w/b* value = (Absolute *w/b* value - 0.20)/0.05 (1)

Coded *%solidHRWRA* value = (Absolute *%solidHRWRA* value – 2.0%)/1.0% (2)

$y\ (response) = a_0 + a_1\ w/b + a_2\ \%solidHRWRA + a_3\ w/b \times \%solidHRWRA$ (3)

The model's coefficients (a_i) represent the contribution of the independent variables on the modeled response. During the derivation of the models, some of the single parameters or combination thereof may not have significant influence on the modeled response. Therefore, a backward elimination technique was used to remove the insignificant parameters. The accuracy of the established models was assessed by comparing the predicted-to-measured modeled responses using additional UHPC mixtures designed with given parameters included in the experimental domain of the established models. If the linear models did not accurately predict the modeled response, the modeled region could be expanded to take into account the quadratic effects and establish nonlinear models. [36,37]

EXPERIMENTAL PROGRAM

Mixture Compositions

Four UHPC mixtures (PD-0.75, PD-0.78, PD-0.79, and PD-0.81) with different packing densities (Table 1) were designed to investigate the influence of PD on workability and compressive strength. The number in the mixture name represents the PD of the granular materials used in the mixture. For example, the PD-0.76 mixture had PD of granular materials equals 0.76. These mixtures were designed with constant *w/b* of 0.20 and HRWRA of 2% of cement weight.

A total of other 10 UHPC mixtures were designed for the statistical design models; four mixtures for establishing the model (main matrix), four replicates of the mixture (0.2%-2.0%) to assess the experimental error in the model, and five mixtures for testing the model's capability for predicting the investigated responses. The 10 concrete mixtures were designed with various *w/b* (between 0.15 and 0.25) and different percentages of HRWRA solids relative to cement weight *(%SolidHRWRA*) (1% to 3%), as given in Table 1. The names of mixtures shown in Table 1 are a combination of two parts: *w/b* and *%SolidHRWRA*. For example, the 0.25%-3.00% mixture has a *w/b* of 0.25, and a *%SolidHRWRA* of 3.0%.

Material Properties

The rheology is strongly influenced by increasing cement fineness, C_3A and C_3S contents.[12] This is more pronounced in UHPC as the cement particles are very close to each other due to the very low *w/b* used. Therefore, it is important to select cement with the lowest C_3A and C_3S contents to enhance rheology. Consequently, high-sulfate-resistance cement (type HS-cem) with a low C_3A content, was selected. The HS cement had a specific gravity (*SG*) of 3.21, Blaine surface fineness of 370 m^2/kg (1806 $in.^2$/lb), and mean particle diameter (d_{50}) of 11 µm (0.0004″). The SF used in the mixture proportioning complied with CAN/CSA A3000 specifications and had an *SG* of 2.20, Blaine surface area of 20,000 m^2/kg (97648 $in.^2$/lb), and d_{50} of 0.15 µm (0.0006″). The UHPC was also designed with a QS of a *SG* of 2.70, maximum particle size (d_{max}) of 600 µm (0.024″), and d_{50} of 250 µm (0.01″). The QP with a *SG* of 2.73 and d_{50} of 13 µm (0.0005″) was used as a filler material. Table 2 shows the chemical composition of the materials used in this study. Figure 1 provides the PSD of the cement, QP, SF, and QS. A polycarboxylate (PCE)-based HRWRA with a *SG* of 1.09 and solid content of 40% (Sika Vicocrete 6200) was used as a superplasticizer.

Testing Procedures

The concrete batching was carried out with a high-energy shear mixer with a capacity of approximately 10 L (0.35 ft^3). To achieve a homogeneous mixture and avoid particle agglomeration, all powder materials were dry mixed for 10 min before the water and HRWRA additions. Approximately half of the HRWRA diluted in half of the mixing water was gradually added over 5 min of mixing time. The remaining water and HRWRA were gradually added between an additional 5 min of mixing. Upon the end of mixing, the UHPC fresh properties were measured, including fresh-concrete temperature, unit weight, and air content (ASTM C 185). The concrete flow was measured with the flow-table test (ASTM C 1437). ConTec 6 rheometer was employed to determine the rheological properties [yield stress (τ_0) and plastic viscosity (μ_{pl})]. The rheological test started 5 min after end of the mixing. The clylidrical molds for the compressive strength (100x200 mm) were then cast and stored at 23ºC (73ºF) and 50% RH for 24 hours. Two curing regimes were implemented after mold removal: NC and HC. In the NC, the samples were stored in a fog room at about 23ºC (73ºF) and 100% RH until testing. The

second mode of curing was HC at 90ºC (194ºF) and 100% RH for 2 days (48 hours). The f'_c at ages 1, 7, and 28 days for the NC and 2 days for the HC were measured on 50-mm (2″-) cubes measuring (ASTM C 109).

The PD was measured under two different conditions: dry packing for QS (PSD ≥ 125 µm or 0.005″) using the intensive-compaction-test (ICT) method and wet PD for cement, QP, and SF (PSD < 125 µm or 0.005″) using the Vicat test (ASTM C 187). The ICT machine consisted of a turntable and a cylinder exerting a pressure ranging between 20 and 1000 kPa (2.9 and 145 psi) during a certain number of cycles on the tested sample until the maximum density was reached. The applied pressure used was 20 kPa (2.9 psi) to avoid crushing of QS particles. If the sample of QS has a weight of (w) and a specific gravity (SG) fills a container with a volume (V_c), then the φ can be calculated as in Eq. 4, where V_s is the solids volume.

$$\phi = \frac{V_s}{V_c} = \frac{w}{V_c.SG} \tag{4}$$

Virtually all wet packing-density methods measure the voids content in samples of cementitious materials as the minimum water content needed to form a paste and achieve a certain consistency. [39] In the Vicat test, paste consistency is measured in terms of plunger penetration depth. The change in penetration depth with water content is not fully explored and only the water content at which the penetration depth is equal to 34±1 mm (1.34±0.04″) is arbitrarily taken to correspond to the water content for standard consistency. It is assumed that this water content for standard consistency is the same as the water demand of the fine materials.[40]. The amount of water from the test can be used to calculate the φ using Eq. 5.

$$\phi = \frac{1}{1 + \rho_s (w/s)} \tag{5}$$

where ρ_s is density of the solid materials, w is water mass, and s is mass of solid materials.

RESULTS AND DISCUSSION

Optimization of granular material using PD

Method of calculation

The packing densities of unitary, binary, ternary, and quaternary combinations were computed based on [Sedran, and de Larrard] approach.[15] Initially, the unitary PD of each individual material was determined. The results of the unitary PD measurements for each of the individual materials QS, cement, QP, and SF were 0.67, 0.58, 0.57, and 0.48, respectively. The unitary packing of the QS (0.67) was obtained by dry packing, and was slightly higher than those of the other ingredients. According to Sedran, and de Larrard [15], this could be attributed to the coarse friction being more amenable to compaction due to fewer contact points between grains than in the finer fraction. In addition, more rounded particles of the QS yielded greater PD than flaky particles. The SF had the lowest packing-density value among the four ingredients. This was due to the adhesion phenomena arising from the increase in the Van der Waals and electrostatic forces between the smaller particles, causing agglomeration, which generated higher voids content.[15] The packing index for QS was 9.0, while 6.7 for QP, cement, and SF.

The PD of the binary combination of QS and QP was then determined, as shown in Figure 2 (A). In general, the binary mixture showed higher PD than the unitary packing. This was obviously due to filling of the void spaces by the finer particles. The addition of the QP to the QS increased the packing up to 60%; after that point, the PD started to decrease. The combination of QS and QP yielded the highest PD of 0.74.

The ternary combinations were estimated by initially taking 11 binary mixtures of the QS and QP (with QS ranging from 100% to 0% and the corresponding QP ranging from 0% to 100%, both in increments of 10%) to which the cement was added from 0% to 100% in increments of 10% as a finer material Figure 2 (B). The highest PD of 0.76 was achieved for the ternary QS:QP:cement combination of 63%:7%:30%. Adding the cement to the binary packing of QS and QP slightly affected the PD due to the interaction between the particle size of the QP and cement. The improvement was rather marginal because the effects of particle interaction predominate in this case due to the closer size ratio.

From the results presented in Figure 2 (B), the 16 sets of ternary combinations of the QS, QP, and cement were selected to further study PD with the SF addition. In each of the 16 ternary combinations, the SF was added from 0% to 100% in increments of 10% as a finer material. The packing densities of the resulted quaternary mixtures were determined Figure 2 (C). The results showed that adding the SF increased the PD of the granular materials up to a certain level (about

20%) by filling the gaps between coarser materials in the ternary mixtures. Beyond that replacement ratio, the effect was noticed to decrease the packing.

The four quaternary combinations of QS:QP:cement:SF of 43.2%:10.8%:36%:10%, 32.6%:14%:46.5%:10.8%, 45.5%:0%:45.5%:9.1%, and 46.2%:12.3%:30.8%:10.7% had PD of granular materials of 0.75, 0.77, 0.79, and 0.81, respectively, were selected to study the effect of different PD on the fresh and hardening properties of UHPC. Obviously, the cement content was decreased with increasing PD while content of SF was increased as shown in Table 3. The cement content was (1006, 972, 792, and 687 kg/m^3) for the mixtures PD-0.75, PD-0.77, PD-0.79, and PD-0.81, respectively. While the SF content found to be (151, 195, 220, and 240 kg/m^3) for the mixtures PD-0.75, PD-0.77, PD-0.79, and PD-0.81%, respectively. It can be seen that the mixture PD-0.81 reaches a higher PD than Mixture PD-0.75, 0.81 compared to 0.75. This because the SF is composed of very small and glassy particles which are perfectly spherical which lead to fill the voids in the next larger granular class.

Packing Density and Rheology

The fresh properties, including, unit weight, air content, and concrete temperature of the four tested mixtures with various packing densities are presented in Table 3. The slump-flow diameters using flow table and mini-slump cone for the four mixtures, were measured immediately after mixing and the results are illustrated in Figure 3 right. The slump flow diameters were found to increase from 240 to 250, and then to 260 mm (9.4, 9.8, and 10.2″) for the mixtures with PDs of 0.75, 0.77, and 0.79, respectively, before a sudden drop to 170 mm (6.7″) for the mixture with the highest PD of 0.81. The shear stress (τ_0) vs. shear rate ($\dot{\gamma}$) curves for PD-0.75, PD-0.79, and PD-0.81 mixtures were found to follow the Bingham model ($\tau = \tau_0 + \mu_{pl} \cdot \dot{\gamma}$). The results of the τ_0 and μ_{pl} for these three mixtures are illustrated in Figure 3 left. The results showed a linear decrease of the viscosity with increasing the PD (from 140 to 50 Pa.s, or 0.020 to 0.007 psi, for the PD-0.75 to PD-81, respectively). The PD of the concrete between the 0.75 and 0.79 did not show significant influence on the τ_0 (163 and 167 Pa, or 0.023 and 0.024 psi). The mixture with the highest PD of 0.81 exhibited the highest τ_0 of 695 Pa (0.1 psi).

This can be explained primarily by the increase in maximum PD of the UHPC mixes made with finer additions (Table 3). Reducing the voids content by adding finer materials (SF and QP)

yields more available rheologically active water to coat the particle surfaces. However, on further increasing fineness by adding more SF of finer particles, it leads to a slump flow decrease. In this case, the positive effects of a higher maximum PD outweigh the negative effect of the larger specific surface. This means a very stiff consistency and unfavourable workability during concrete production in practice. Also, the SF uses hifger amount of HRWRA than Cement So HRWRA/(C+SF) decreases which lead to decreasethe slump flow. In addition, it is possible that the required mechanical properties cannot be achieved owing to insufficient de-aeration or an uneven distribution of fibres, if used.

In the UHPC mixtures of the higher PD values, the particles are highly compacted which increases the inherent internal forces between particles associated with higher yield stress. This explains the significant increase in the $\tau 0$ for PD-0.81 mixture. On the other side, incorporating higher contents (up to a given rate) of SF enhances the lubrication of particles, leading to viscosity decrease.

It worth noting that, the calculation of the theoretical PD values according CPM model does not take into account the effects of Van der Waal forces, friction between particles, the lubricant effect of superplasticizer, and mixing energy, which are considered as significant factors affecting the rheological parameters. Further studies are needed to cover these points.

Packing Density and Compressive strength

The compressive strength results at 28 days of normal curing and 2 days of hot curing for those four mixtures are presented in Table 3. The PD-0.81 mixture with the highest PD value of 0.81 had the highest compressive strength values under two curing regimes (169 and 217 MPa or 24.5 and 31.5 ksi for the normal and hot curing regimes) as shown in Figure 3 right.

The PD of the concrete between the 0.75 and 0.78 did not show significant influence on the compressive strength under two curing regimes. For example, the compressive strength for the mixtures PD-0.75 and PD-0.77 were 133.6 and 122.4 MPa or 19.29 and 17.69 ksi for the normal curing regimes and 161 and 158 or 158 MPa or or 23.35 and 22.9 ksi for hot curing regime, respectively. While the PD-0.79 mixture with the PD value of 0.79 had the compressive strength values under two curing regimes (150 and 196.5 MPa or 21.7 and 28.4 ksi for the normal and hot curing regimes. Based on the scatter of the results, the use of fine SF led to compressive

strengths which were somewhat higher. Furthermore, the use of a higher volume fraction of aggregate can result in improvements in strength, and stiffness, permeability.[41] In short, the mechanical properties of the concretes were roughly equivalent and therefore independent of the PD enhancement.

Selected Optimum Packing Density

While higher PD is preferred, the maximum PD may not be optimal.[41,42] When all the concrete particles are completely packed, the resultant concrete will have unlikely workability and placement. For the practical issues, fresh concrete needs to be placed and has to flow to at least a certain degree. Therefore, complete density packing is not suitable for concrete mixtures and, consequently, optimal packing is considered herein. On the other hand, the amount of QS should be slightly lower when selecting the optimum mix design. Reducing the sand content was found to be preferable for decreasing shrinkage and porosity.[3]

Packing theories indicate that the largest reduction in voids can be achieved with the aggregate phase. Nevertheless, strength is controlled by both the degree of packing and the degree of completion of the chemical reactions, such as hydration and pozzolanic reactions. Considering that the degree of pozzolanic reaction attains stoichiometric limits, SF+QP must be maintained at 0.63.[4] Hence, the finalized mix was chosen to satisfy all the conditions with regard to packing and reactivity in order to derive the maximum benefits of the UHPC.

Based on this information, the optimal PD was 0.79, which was obtained with the quaternary combination of QS: QP: cement: SF of 43.2%:10.8%:36%:10%. The final PSD for the combinations of the different materials (QS, QP, cement, and SF) used in the UHPC mixture shows a continuous particle distribution, as presented in Figure 1.

Statistical Models for Optimizing UHPC as Function of w/b and HRWRA Content

Table 3 provides the fresh and mechanical performances of the 10 UHPC mixtures tested to establish the statistical models. The different steps involved in generating and validating the models are described below.

Models Derivation

Four models for slump flow, air content, f'_c-2d-HC, and f'_c-28d-NC were derived as a function *w/b*, HRWRA solids, and combinations of both parameters. The R^2 and the estimates and Prob. >|t| values for each parameter were determined for each of the four derived models, as shown in Table 4. The estimates for each parameter refer to the coefficients determined using the least-squares approach. The Prob. >|t| term is the probability of getting an even greater t-statistic, in absolute values, that tests whether the true parameter is zero. Probabilities less than 0.10 are typically considered as significant evidence that the parameter is not zero, i.e., that the contribution of the proposed parameter has a significant influence on the measured response. Parameters with a probability greater than 0.10 were insignificant and not considered in the models. The proposed models had R^2 values between 0.80 and 0.99 (Table 4). The sign of the estimates (+/-) indicates the positive or negative effect of the parameter on the considered response. The established models using the coded are presented in Eqs. 6-9 and in Eqs. 10-13 using absolute values.

Slump flow (mm) = 207.8 + 71.63 *w/b* + 12.37 *solidHRWRA* + 7.63 *w/b***solidHRWRA* (6)

Air void (%) = 4.27 - 1.05 *w/b* + 0.61 *solidHRWRA* (7)

f'_c-2d-HC (MPa) = 189.69 - 25.5 *w/b* (8)

f'_c-28d-NC (MPa) = 151.74 - 23.25 *w/b* - 3.15 *solidHRWRA* (9)

Slump flow (mm) = -42.4 + 1127.5 *w/b* - 18.125 *solidHRWRA* + 152.5 *w/b***solidHRWRA* (10)

Air void (%) = 7.25 - 21 *w/b* + 0.61 *solidHRWRA* (11)

f'_c-2d-HC (MPa) = 291.7 - 510 *w/b* (12)

f'_c-28d-NC (MPa) = 251.2 - 465 *w/b* - 3.15 *solidHRWRA* (13)

The UHPC mixture (0.20%-2.0%) was tested four times to assess experimental errors for the developed models. Table 5 shows the mean ($\bar{x}$), standard deviation (σ), standard error corresponding to 95% confidence limit (*SE*), and relative error (*RE*) calculated according to a 95% confidence interval using the Student's distribution (Eq. 14), as follows;

$$RE = \frac{SE}{\bar{x}}.100\% = 3.1824\ \frac{\sigma}{\bar{x}\sqrt{n}}.100\% \quad (14)$$

where 3.1824 is a coefficient representing the 95% confidence interval for the Student's distribution for a number of observations (n) of 4.0. The *RE* values listed in Table 5 for the four responses were found to be lower than 6%. This means that there is less than a ±6% chance that

the contribution of a given parameter to the modeled response would exceed the value of the specified coefficient.

Effect of w/b and HRWRA on Model Responses

Slump flow: Based on Eq. 10, the *w/b* and HRWRA as well as their interaction positively affected the slump flow of the UHPC, as indicated by the + sign for each estimate. The *w/b* had about a six-times greater effect on slump flow than the HRWRA content (estimates of 71.63 for the *w/b* versus 12.37 for the HRWRA). This implies that water content played a greater role in the UHPC's flowability than the HRWRA dosage. Increasing the water content improved HRWRA diffusion in the matrix. Increasing the HRWRA dosage alone did not further improve flowability. For example, at a HRWRA dosage of 2%, increasing the *w/b* by only 0.01 (from 0.16 to 0.17) can result in about a 10% increase in slump-flow values (from 151 to 165 mm or 5.9 to 6.5″). At a *w/b* of 0.15, the slump flow could only be increased by 5% (from 134 to 141 mm or 5.3 to 5.6″) after significantly increasing the HRWRA dosage from 1.5% to 3.0%.

Air content: The air content was shown to be negatively influenced by an increase in *w/b* and positively by an increase in HRWRA dosage (Eq. 11). The increase in *w/b* decreased the air voids, while an increase in HRWRA resulted in higher air-void values. Polycarboxylate-based HRWRA on increasing the air content in concrete is well known.

Compressive strength: The model of compressive strength after 2 days of HC (Eq. 12) was greatly influenced by the *w/b*, while the HRWRA had no effect. In contrast, the model of compressive strength after 28 days of NC (Eq. 13) indicated that both the *w/b* and HRWRA dosage had an impact. Indeed, the established model (Eq. 13) indicates that the *w/b* had an impact about seven times greater than the HRWRA on the f'_c-28d-NC concrete. This can be seen in the parameter estimates (23.25 versus 3.15 for the *w/b* and HRWRA, respectively).

Validation of the Derived Models

Five UHPC mixtures were used to evaluate the accuracy of the established models by comparing the predicted to the measured responses. Table 3 provides the measured properties of these five mixtures. The measured properties were correlated to the predicted properties using the established models, as shown in Figure 4. The results indicated that the models for slump flow

and the f'_c-28d-NC concrete were able to predict the measured concrete properties with a 1:1 relationship. The f'_c-2d-HC model can yield prediction values 5% lower than the measured ones. A relatively high difference between the predicted and measured responses was obtained with air-content model (14%), although this difference was in the conservative direction.

Use of Established Models

Contour diagrams were established as a simple interpretation of the derived statistical models. The contour diagrams were used to compare the trade-off between the effects of the different parameters (*w/b* and HRWRA) on the considered responses. Two-dimensional contour charts were constructed to present how the responses (slump flow, air content, f'_c-2d-HC, and f'_c-28d-NC) changed with variations in the *w/b* and HRWRA (Figure 5). For example, the contour diagrams for slump flow show that *w/b* strongly improved the workability of the UHPC, while the effect of the HRWRA dosage was not significant. When *w/b* = 0.20, the change in the HRWRA content from 1.3% to 3% only changed the slump flow from 200 to 225 mm (7.9 to 8.9″).

Criteria of Multi-Parametric Optimization

After establishing the statistical models between mix design parameters and concrete properties as responses, all independent variables (mix design parameters) were varied simultaneously and independently to optimize the objective functions. The optimal solution tends to satisfy the requirements for each of the responses as much as possible without excessively compromising any of the requirements.

A specific criteria was proposed in selecting the optimum mix-design variables to obtain a UHPC mixture with maximum compressive strength and an acceptable range of slump based on the strategic marketing-decision (SMD) approach. A numerical optimization was used to optimize one or a combination of goals. From this perspective, the *w/b* was defined as “in range” while the HRWRA was defined as “minimum”. Since UHPC is defined as a composite cement material with a f'_c exceeding 150 MPa (21.8 ksi), the f'_c was defined as “in range” with a minimum value of 150 MPa (21.8 ksi); slump flow was also defined as “in range” with a minimum value of 200 mm (7.9″). At the end of the multi-objective optimization process, three different optimal solutions, with the desirability of the functions ranging from 0.76 to 0.85, were

obtained. Table 6 provides the predicted optimal compositions of the three UHPC mixtures and corresponding response values.

Based on the results presented in this research, three different UHPC mixture types using local materials can be proposed to respond to various construction demands (Table 7). The UHPC mixtures in Domain A are characterized by flowability lower than 200 mm but with f'_c-2d-HC greater than 200 MPa (29 ksi). Domain A can be obtained when designing the UHPC with low *w/b* between 0.15 and 0.18. On the other hand, highly flowable UHPC can be obtained, as in Domain C, using higher *w/b* between 0.225 and 0.25. The UHPC in Domain C is characterized by f'_c-2d-HC between 160 and 175 MPa (23.2 and 25.4 ksi).

CONCLUSIONS

Based on the results presented in this research, the following conclusions can be drawn:

- UHPC mixtures can be designed and produced with locally available materials using the particle packing and statistical-design approaches. Three different UHPC mixture types with slump flows between 130 and 300 mm and compressive strengths between 135 and 225 MPa (19.6 and 32.6 ksi) were produced to respond to various construction demands.
- The packing density definitely affects the rheological properties, and therefore fresh concrete workability. Higher packing density of UHPC yields a mixture with low viscosity due to the increased lubricant effect (with the addition of more fine materials) and increased yield stress (due to the increased compactness and friction between granular particles). Besides packing density, the flowability also depends on the fineness of the additions. The favourable effect of an increase in maximum packing density competes with the unfavourable effect of an increase in specific surface. Hence, the optimal packing density, not the maximum packing density, should be considered for UHPC design to allow proper workability and placement conditions.
- The water content has a much greater impact on flowability of the UHPC rather than the HRWRA dosage. Increasing the water content increases the dispersion of HRWRA molecules, thereby improves the matrix flowability. Increasing the HRWRA dosage alone does not further improve the workability.

- By decreasing the amounts of cement and HRWRA and by using local materials significantly decrease UHPC costs as well as reduce CO_2 emissions and energy consumption related to cement production.

ACKNOWLEDGMENT

The authors acknowledge Industrial Chair on Valorisation of Glass in Materials for the financial support. Also the authors express their appreciation and thanks to Dr. Ahmed Omran for his participation in the modelling analysis.

REFERENCES

1. Gupta, P. R.; and Shiu K. N. "Effective Repair and Maintenance Strategies for Parking Structures," Concrete Repair Bulletin, 2014, pp. 30-34.
2. U.S. Department of Homeland Security (DHS) Science and Technology (S&T). UHPC Ultra-High Performance Concrete. Technical report, pp. 23 (http://www.dhs.gov).
3. Richard, P.; and Cheyrezy, M., "Reactive Powder Concretes with High Ductility and 200-800 MPa Compressive Strength," ACI Special Publication, V. 144, 1994, pp. 507-518.
4. Richard, P.; and Cheyrezy, M., "Composition of Reactive Powder Concretes," Cement and Concrete Ressearch, V. 25, No. 7, 1995, pp. 1501-1511.
5. Dugat, J.; Roux, N.; and Bernier G "Mechanical Properties of Reactive Powder Concretes," Materials and Structures, V. 29, 1996, pp. 233-240.
6. Roux, N.; Andrade, C.; and Sanjuan, M., "Experimental Study of Durability of Reactive Powder Concretes," Journal of Materials in Civil Engineering, V. 8, No. 1, 1996, pp. 1-6.
7. Bonneau, O.; Lachemi, M.; Dallaire, E.; Dugat, J; and Aïtcin, P.-C., "Mechanical Properties and Durability of Two Industrial Reactive Powder Concretes," ACI Materials Journal, V. 94, No. 4, 1997, pp. 286-290.
8. Schmidt, M.; and Fehling, E., "Ultra-High-Performance Concrete: Research, Development and Application in Europe," ACI Special Publication, V. 225, 2005, pp. 51-77.
9. Aïtcin, P.-C.; Lachemi, M.; Adeline, R.; and Richard, P., "The Sherbrooke Reactive Powder Concrete Footbridge," Structure Engineering International, V. 8, No. 2, 1998, pp. 140–144.
10. Klemens, T., "Flexible Concrete Offers New Solutions," Concrete Construction, V. 49, No. 12, 2004, pp. 72.

11. Racky, P., "Cost-Effectiveness and Sustainability of UHPC," Proceedings of the Int. Sym. UHPC, Kassel, Germany, V. 13, No. 15, 2004, pp. 797-805.
12. Aïtcin, P.-C., "Cements of yesterday and Today-Concrete of Tomorrow," Cement and Concrete Research, V. 30, No. 9, 2000, pp. 1349-1359.
13. Graybeal, B. A., "Material Property Characterization of Ultra-High Performance Concrete," Publication no. FHWA-HRT-06-103, 2006.
14. de Larrard, F.; and Sedran, T., "Optimization of Ultra-High-Performance Concrete by the Use of a Packing Model," Cement and Concrete Research, V. 24, No. 6, 1994, pp. 997-1009.
15. (a) de Larrard, F., "Concrete Mixture Proportioning: a Scientific Approach," E&FN Spon, London, 1999.

    (b) T. Sedran, F. de Larrard, Manuel d'utilisation de RENE-LCPC, version 6.1d, logiciel d'optimisation granulaire, Laboratoire Centrale des Ponts et Chaussées, (2000).
16. Teichmann, T.; and Schmidt, M., "Influence of the PD of Fine Particles on Structure, Strength and Durability of UHPC," Int. Symp. on UHPC, Kassel, Germany, Sept. 13-15 2004.
17. Talebinejad, I.; Bassam, S. A.; Iranmanesh, A.; and Shekarchizadeh, M., "Optimizing Mix Proportions of Normal Weight Reactive Powder Concrete with Strengths of 200 – 350 MPa," Int. Symp. on UHPC, Kassel, Germany, Sept. 13-15 2004.
18. Habel, K.; Charron, J.-P.; Braike, S., Hooton, R. D.; Gauvreau, P.; and Massicotte, B., "Ultra-High Performance Fiber Reinforced Concrete Mix Design in Central Canada," Canadian Journal of Civil Engineering, V. 35, No. 2, 2008, pp. 217-224
19. Rossi, P.; Arca, A.; Parant, E.; and Fakhri, P., "Bending and Compressive Behaviors of New Cement Composite," Cement and Concrete Research V. 35, No. 1, 2005, pp. 27-33.
20. Park, J.; Kang, S. T.; Taek, K. K.; and Wook, K. S., "Influence of the Ingredients on the Compressive Strength of UHPC as a Fundamental Study to Optimize the Mixing Proportion," Int. Symp. on UHPC, Kassel, Germany, 2008, pp. 105–12.
21. Wille, K.; Naaman, A. E.; and Montesinos, G. J. P., "Ultra-High Performance Concrete with Compressive Strength Exceeding 150 MPa (22 Ksi):" ACI Mat. J, V. 108, No. 1, 2011.
22. Wang, C.; Yang, C.; Liu, F.; Wan, C.; and Pu, X., "Preparation of Ultra-High Performance Concrete with Common Technology and Materials," Cement and Concrete Composites, V. 34, No. 4, 2012, pp. 538-544.

23. Ghafari, E.; Costa, H.; and Julio, E., "Statistical Mixture Design Approach for Eco-Efficient UHPC," Cem. and Concr. Comp., V. 55, 2015, pp. 17-25.
24. Kumar, S. V.; and Santhanam, M., "Particle Packing Theories and Their Application in Concrete Mixture Proportioning," The Indian Concr. J., V. 77, No. 9, 2003, pp. 1324-1331.
25. Powers, T. C., "The properties of Fresh Concrete," John Wiley and Sons, New York, 1968.
26. Fennis, S. A. A. M.; Walraven, J. C.; and Nijland, T., "Measuring the PDto Lower the Cement Content in Concrete," In Walraven, J. C.; and Stoelhorst, D., (Eds.), Tailor Made Conc. Structures: New Solutions for our Society, London UK: Taylor and Francis Group, 2008, pp. 419-424.
27. Lange, F.; Mörtel, H.; and Rudert, V., "Dense Packing of Cement Pastes and Resulting Consequences on Mortar Properties," Cem. and Conc. Res., V. 27, No. 10, 1997, pp. 481-1488.
28. Neville, A. M., "Properties of Concrete," Harlow: Longman, 1995.
29. Fuller, W. B.; and Thompson, S. E., "The Laws of Proportioning Concrete," ASCE Journal Transport, V. 59, 1907, pp. 67-143.
30. Funk, J. E.; and Dinger, D. R., "Predictive Process Control of Crowded Particulate Suspensions Applied to Ceramic Manufacturing," Boston: Kluwer Academic Publishers, 1994.
31. Stroeven, P.; and Stroeven, M., "Assessment of Packing Characteristics by Computer Simulation," Cement and Concrete Research, V. 29, 1999, pp. 1201-1206.
32. Kolonko, M.; Raschdorf, S.; and Wasch, D., "A Hierarchical Approach to Estimate the Space Filling of Particle Mixtures with Broad Size Distributions," Bio-resourse., V. 9, No. 3, 2008. pp. 28.
33. Fennis-Huijben, S. A. A. M., "Design of Ecological Concrete by Particle Packing Optimization," Ph.D., Delft University of Technology, The Netherlands: 2010, pp. 277.
34. Stovall, T.; de Larrard, F.; and Buil, M., "Linear PDModel of Grain Mixtures," Powder Technology, 1986, pp. 48:1-12.
35. Dewar, J. D., "Computer Modelling of Concrete Mixtures," London: E & FN Spon, 1999.
36. Box, E. P.; Hunter, W. G.; and Hunter, J. S., "Statistics for Experimenters: an Introduction to Design, Data Analysis, and Model Building," Wiley Series in Probability and Mathematical Statistics, Wiley-inter science, 1978, pp. 653.
37. Montgomery, D. C., "Design and Analysis of Experiments," 6th Ed. John Wiley & Sons, 2005.

38. Omran, A. F.; Khayat, K. H.; and Elaguab, Y. M., "Effect of SCC Mixture Composition on Thixotropy and Formwork Pressure," J. of Mat. in Civil Eng., V. 24, No. 7, 2012, pp. 876-888.
39. Wong, H. C.; and Kwan, K. H., "PD of Cementitious Materials: Part 1- Measurement using a Wet Packing Method," Mat. and Structures V. 41, 2008, pp. 689-701.
40. Lange, F.; Mortel, H.; and Rudert, V., "Dense Packing of Cement Pastes and Resulting Consequences on Mortar Properties," Cem. and Conc. Res., V. 27, No. 10, 1997, pp. 1481–1488
41. Johansen, V.; and Andersen, P. J., "Particle Packing and Concrete Properties," In: Skalny, J.; and Mindess, S., (Eds.), Mat. Science of conc. 2, Westerville: American Ceramic Society, 1991
42. Goltermann, P.; Johansen, V., and Palbol, L., "Packing of Aggregates: an Alternative Tool to Determine the Optimal Aggregate Mix," ACI Mat. J., V. 94, No. 5, 1997, pp. 435-443.

LIST OF FIGURES

LIST OF TABLES

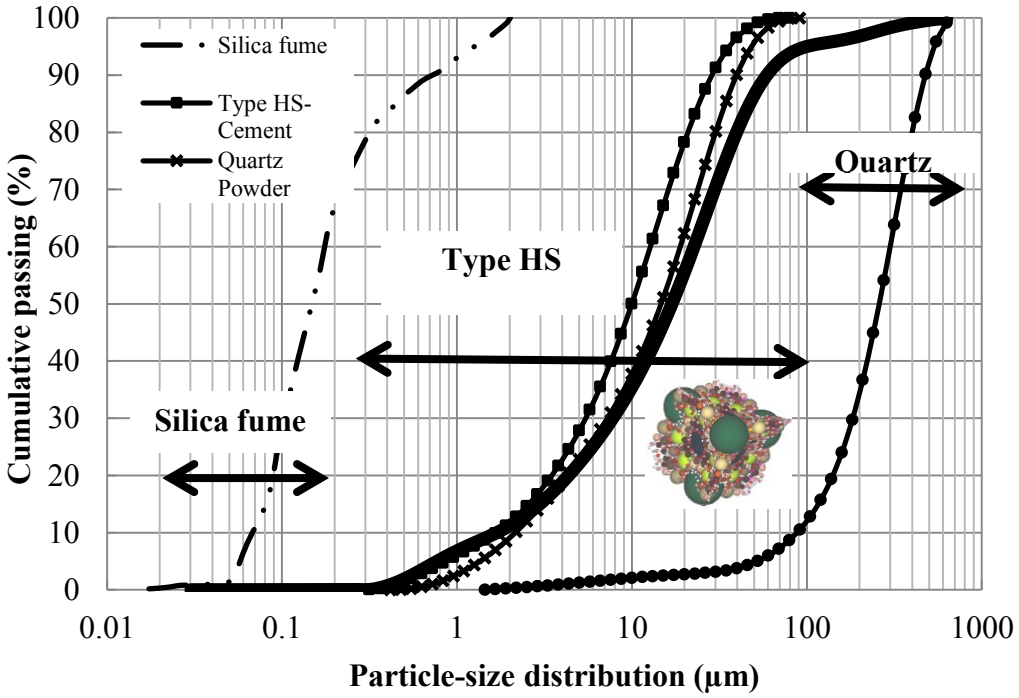

Figure 1 Particle-size distribution of cement, quartz powder, silica fume, quartz sand, and of UHPC (the combination of all granular materials) (1.0 µm = 0.0000394 in.)

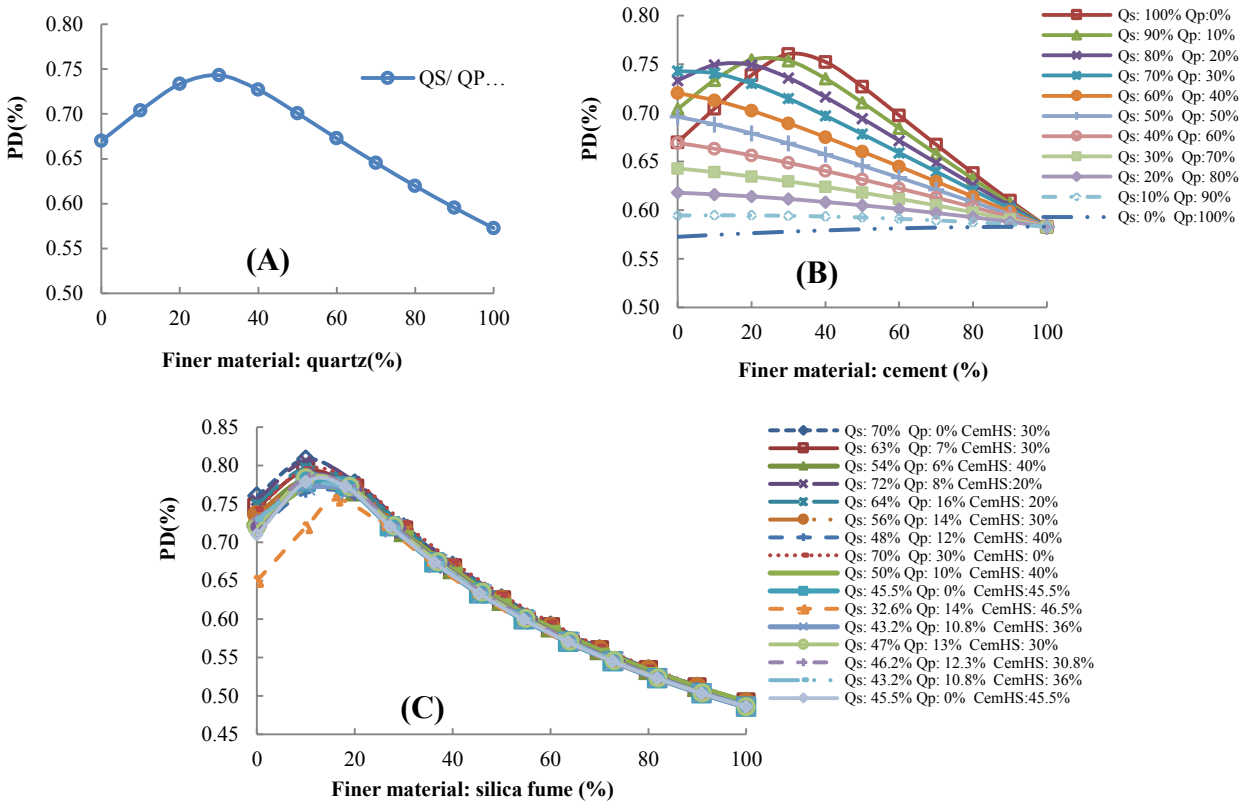

Figure 2 (A) Binary packing between quartz sand (QS) and quartz powder (QP), (B) ternary packing between QS, QP, and cement, and (C) quaternary packing of QS, QP, cement (CemHS), and silica fume

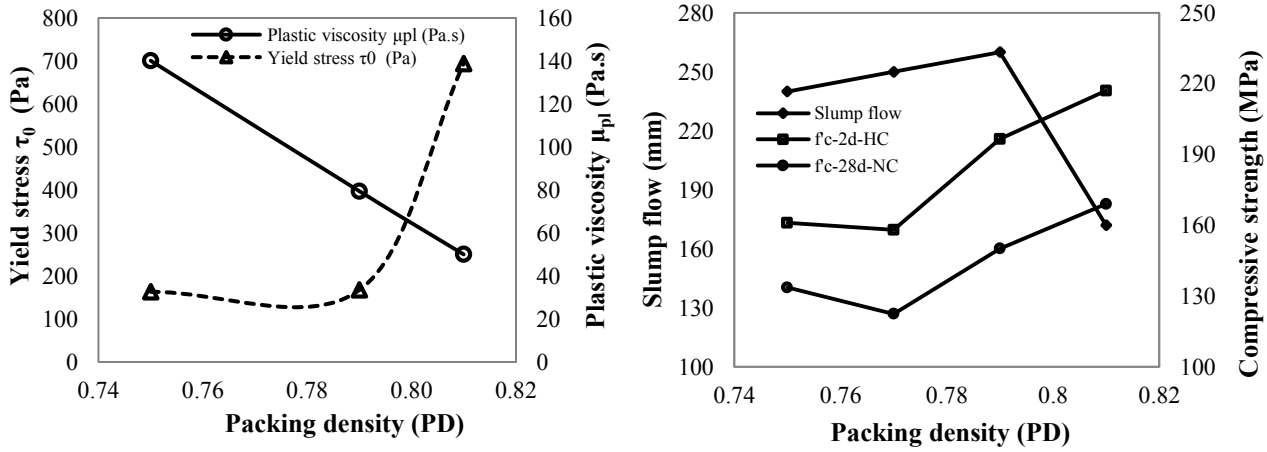

Figure 3 Solid PD related to (right) yield stress and plastic viscosity (left) slump flow and compressive strength

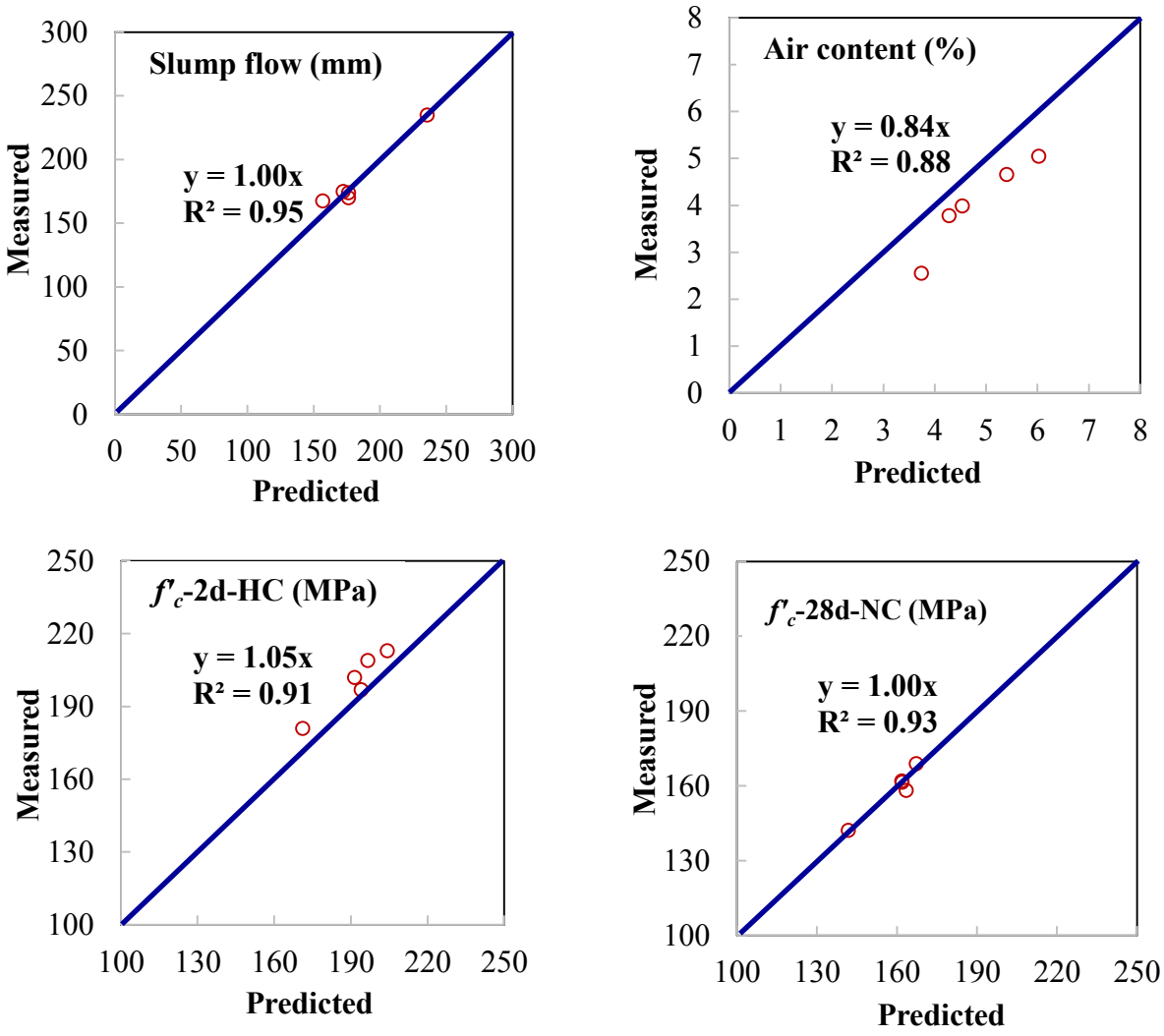

Figure 4 Measured versus predicted responses using derived models

(1.0 mm = 0.0394 in., 1.0 MPa = 145 psi)

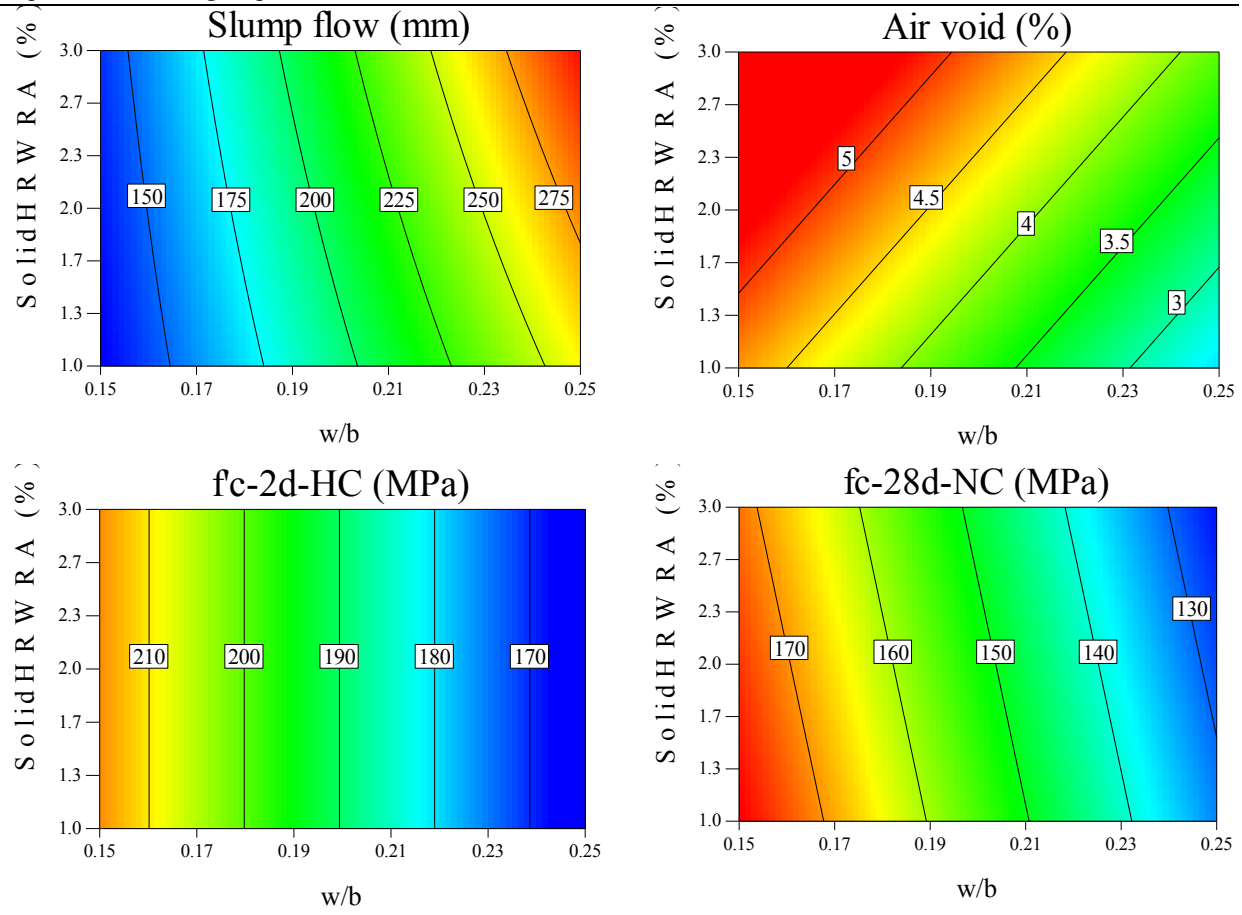

Figure 5 Trade-off of *w/b* and percentage of HRWRA solids on the slump flow, air content, f'_c-2d-HC, and f'_c-28d-NC (1.0 mm = 0.0394 in., 1.0 MPa = 145 psi)

Table 1 Mixture composition

UHPC Mixture			Mixture Composition (kg/m^3)						Coded Values		Absolute Values	
			Cement	Silica fume	Water	Quartz powder	Quartz sand	Solids in HRWRA	*w/b*	%solid HRWRA	*w/b*	%solid HRWRA
for optimizing PDof granular material		PD-0.75	1006	151	231	302	704	22				
		PD-0.77	972	195	233	--	975	21				
		PD-0.79	792	220	202	238	951	17				
		PD-0.81	687	240	185	275	1030	15				
Experimental design model	for establishing the models	0.15-1.0%	840	233	161	252	1008	9	-1	-1	0.15	1
		0.15-3.0%	828	230	159	248	994	27	-1	1	0.15	3
		0.25-1.0%	758	211	242	228	911	8	1	-1	0.25	1
		0.25-3.0%	749	211	239	225	899	24	1	1	0.25	3
	Central mixtures[#]	0.2-2.0%	792	220	202	237	951	17	0	0	0.20	2
	for models validation	0.175-2.5%	810	225	181	243	972	22	-0.5	0.5	0.175	2.5
		0.16-3.0%	820	228	168	246	984	26	-0.8	1	0.16	3
		0.185-1.0%	810	225	191	243	972	9	-0.3	-1	0.185	1
		0.18-1.25%	813	226	187	244	975	11	-0.4	-0.75	0.18	1.25
		0.225-1.5%	775	223	215	233	930	13	0.5	-0.5	0.225	1.5

[#] Repeated four times for testing model errors

1.0 kg/m^3 = 1.69 lb/yd^3

Table 2 Chemical compositions of HS cement, quartz sand, quartz powder, and silica fume

Identification	Quartz Sand	Quartz Powder	Type HS cement	Silica Fume
Silicon dioxide (SiO_2)	99.8	99.8	22	99.8
Iron oxide (Fe_2O_3)	0.04	0.09	4.3	0.09
Aluminum oxide (Al_2O_3)	0.14	0.11	3.5	0.11
Calcium oxide (CaO)	0.17	0.38	65.6	0.4
Titanium dioxide (TiO_2)	0.02	0.25	0.2	--
Sulfur trioxide (SO_3),	--	0.53	2.3	--
Magnesium oxide (MgO)	0.008	0.20	1.9	0.20
Sodium oxide (Na_2O)	--	0.25	0.07	0.20
Potassium oxide (K_2O)	0.05	3.5	0.8	0.50
Equivalent alkali (Na_2O_{eq})	--	--	0.9	--
Zinc oxide (ZnO)	--	--	0.09	0.25
Loss on ignition (LOI)	0.2	0.32	1.0	3.50
C_3S	--	--	50	--
C_2S	--	--	25	--
C_3A	--	--	2.0	--
C_4AF	--	--	14	--

Table 3 Fresh and mechanical performances of UHPC mixtures

Mixture name		Fresh Properties				Compressive Strength, MPa	
		Air void (%)	Unit weight, kg/m^3	Concrete temperature, ^{o}C (^{o}F)	Mini-slump flow diameter, mm	At 2 days of hot curing, f'_c-2d-HC	At 28 days of normal curing, f'_c-28d-NC
Mixtures for establishing the experimental design model	PD-0.75	4.5	2410	35 (95)	240	161	133.6
	PD-0.77	3.5	2393	32 (90)	250	158	122.4
	PD-0.79	2.7	2419	29 (84)	275	196.5	150.1
	PD-0.81	2.2	2432	29 (84)	172	217	169
Mixtures for establishing the experimental design model	0.15-1.0%	2.8	2389	32 (90)	132	226	179
	0.15-3.0%	4.2	2365	31 (88)	141.5	221	170
	0.25-1.0%	2.6	2295	29 (84)	260	169	131
	0.25-3.0%	3.7	2257	27 (81)	300	164	123
Central mixture	0.2-2.0%-A	3.8	2331	27 (81)	215	186.4	152
	0.2-2.0%-B	4.1	2336	28 (82)	216	187.1	151.9
	0.2-2.0%-C	3.7	2335	29 (84)	210	182.4	152.4
	0.2-2.0%-D	4.0	2331	29 (84)	212	188.9	155
Mixtures for validating the prediction model	0.175-2.5%	4.0	2338	30 (86)	170	209	167
	0.16-3.0%	5.0	2346	29 (84)	167	213	169
	0.185-1.0%	3.5	2357	30 (86)	175	205	168
	0.18-1.25%	4.0	2330	29 (84)	180	197	160
	0.225-1.5%	3.0	2236	26 (79)	230	182	142

1.0 kg/m^3 = 1.69 lb/yd^3, 1.0 MPa = 145 psi, 1.0 mm = 0.0394 in.

Table 4 Parameter estimates of derived models

	R^2	Term	C: Intercept	*w/b*	*solidHRWRA*	*w/b*solidHRWRA*
Slump flow	0.99	Estimate	207.8	71.63	12.37	7.63
		Prob>|t|	0.0001	<0.0001	0.0202	0.0829
Air void	0.80	Estimate	4.27	-1.05	0.61	N/A
		Prob>|t|	0.0188	0.0124	0.0771	N/A
f'_c-2d-HC	0.88	Estimate	189.69	-25.5	N/A	N/A
		Prob>|t|	0.0005	0.0005	N/A	N/A
f'_c-28d-NC	0.99	Estimate	151.74	-23.25	-3.15	N/A
		Prob>|t|	<0.0001	<0.0001	0.0184	N/A

Table 5 Repeatability of models (n = 4)

	Mean Value ($\bar{x}$)	Standard Deviation (σ)	Standard Error (*SE*)	Relative Error (*RE*)
Slump flow	207 mm (8.15″)	7.6 mm (0.3″)	12.1 mm (0.48″)	5.8%
Air void	4.6%	0.1%	0.2%	4.2%
f'_c-2d-HC	184 MPa (26.7 ksi)	4.5 MPa (0.65 ksi)	7.1 MPa (1.03 ksi)	3.9%
f'_c-28d-NC	153 MPa (22.2 ksi)	1.6 MPa (0.23 ksi)	2.6 MPa (0.38 ksi)	1.7%

Table 6 Criteria of multi-parametric optimization

Criteria	Target	Importance	Selected Mixture	Desirability
w/b	In range	+++	*w/b* = 0.17, SP = 2% *w/b* = 0.185, SP = 1% w/*b* = 0.20, SP = 1% w/*b* = 0.22, SP = 1%	0.73 0.85 0.76 0.83
HRWRA	Minimum	+++++		
Slump-flow	In range	+++++		
f'_c-2d-HC	In range	+++++		
f'_c-28d-NC	In range	+++		

Table 7 UHPC with local materials for various construction applications

Characteristics / Criteria	***Domain A***	***Domain B***	***Domain C***
Flowability of UHPC	stiff	flowable	highly flowable
Average flow diameter, mm (in.)	<200 (7.9)	200-250 (7.9-9.8)	> 250 (9.8)
w/b	0.15-0.18	0.19-0.225	0.225-0.25
% of solids in superplasticizer/cement weight	1-3	1-3	1-3
f'_c-2d-HC, MPa (ksi)	> 200 (29.0)	175-200 (25.4-29.0)	160-175 (23.2-25.4)
f'_c-28d-NC, MPa (ksi)	> 170 (24.7)	150-170 (21.8-24.7)	130-150 (18.9-21.8)

4 Large Particles Replacement in UHPC

4.1 Introduction

This chapter introduces the feasibility of using ground glass sand (GS) as partial or total replacement of quartz sand (QS) in UHPC. It is well known that the PSD of the QS used in UHPC mixtures ranges from 150 to 600 μm with a d_{50} value of 250 μm. The available GS on the market varies from 5000 to 80 μm. This required optimizing the grading PSD of the GS to be close to that of the QS as possible to arrive at a particular combination of granular materials, which can give the optimum packing density and optimum performance. After optimizing the GS's PSD, various replacement ratios varied between 0% and 100% for the QS were investigated. The effect replacing QS with GS was studied by measuring concrete packing density, fresh properties, compressive strength, ASR, and microstructure. The effect of normal and steam curing conditions on the compressive-strength properties was considered. This chapter also presents descriptions of the materials, mix designs, and mixing sequence used in these experimental tests. The testing sequences and methods used to examine the fresh properties, compressive strength, and ASR tests are also described.

4.2 Paper 2: Using Glass Sand as an Alternative for Silica Sand in UHPC

Reference:
Soliman N.A., Tagnit-Hamou A. (2016) Using Glass Sand as an Alternative for Silica Sand in UHPC. *Journal of Construction and Building Materials*. (Accepted and forthcoming).

Using Glass Sand as an Alternative for Silica Sand in UHPC

Nancy A. Soliman and Arezki Tagnit-Hamou*

* Corresponding author
Cement and Concrete Research Group, Dept. of Civil Eng., University of Sherbrooke
2500 Blvd. Université, Sherbrooke, Quebec, Canada J1K 2R1
Phone: 819-821-7993, E-mail: A.Tagnit@USherbrooke.ca

Biography:

Nancy A. Soliman is member of the ACI International and Sherbrooke Local Chapters, and CRIB. She is a doctoral candidate in the Department of Civil Engineering, University of Sherbrooke, QC, Canada. Her research interest includes NDT, ultra-high-performance concrete, microstructure, and sustainable development.

Arezki Tagnit-Hamou, FACI and professor in the Department of Civil Engineering at the University of Sherbrooke (QC, Canada) heads the cement-and-concrete group and holds an industrial chair on the valorization of glass in materials. He serves on ACI Committees 130 (Sustainability of Concrete) and 555 (Concrete with Recycled Materials), and RILEM TC DTA. His research interests include alternative cementitious materials, physical chemistry and microstructure of cement and concrete, and sustainable development.

ABSTRACT

Quartz sand (QS) with optimum grading, which represents the coarser particles (600 μm) in ultra-high-performance concrete (UHPC), can be obtained by crushing coarse sand or rocks using time-consuming, costly, and polluting processes. Mixed colored glass cannot be recycled and is normally disposed of in landfills, causing obvious environmental problems. This glass can be valorized, however, through grinding, and used in concrete. This paper investigates the

feasibility of using ground glass sand (GS) for partial or total replacement of QS in UHPC. The results demonstrate that compressive strength values of about 196 and 182 MPa after two days of hot curing can be achieved when replacing 50% and 100% of QS with GS, respectively, compared to 204 MPa measured for the reference UHPC containing 100% QS. Incorporating higher replacement rates of the GS was shown to produce UHPC of higher flowability and very dense microstructure that prohibited the alkali–silica reaction.

Keywords: alkali–silica reaction, glass sand, mechanical properties, microstructure, quartz sand, ultra-high-performance concrete.

1. INTRODUCTION

Large quantities of glass cannot be recycled because of high breaking potential, color mixing, or high recycling costs [1]. Most waste glass is routinely disposed of in landfill sites, which is undesirable as it is not biodegradable and not environmentally friendly [2]. As awareness has grown about the need to protect the environment, attention has increasingly focused on turning solid waste into concrete ingredients. Apart from the savings in terms of material and energy resources, reusing some solid wastes could result in better concrete performance in several areas. Fine glass particles (smaller than 75 μm) can exhibit pozzolanic reactivity, thereby improving the paste microstructure as well as the concrete's long-term strength and durability [3-4]. Studies have been conducted to determine the pozzolanicity of GP concrete, revealing that the GP's pozzolanic activity depends on its fineness. Moreover, the pozzolanic reaction takes place at a slower rate at early age, then accelerates at later age compared to cement hydration [5-16]. Furthermore, no alkali–silica reaction has been observed with finely ground glass powder (GP) [17]. Waste glass has been used as coarse and fine aggregates in concrete, because of its much lower absorption and similar density (2.60) to natural gravel and sand [18].

Better results were observed when replacing natural sand with GS (finer than 5 mm), since the texture properties of the glass particles can be improved by reducing the particle size. Park et al. [19] measured approximately similar f'_c (only 1% lower), and splitting-tensile (f_{st}) and flexural strength (f_{fl}) (only 3% lower) for concrete containing 30% GS as sand replacement compared to the control concrete. At higher replacement levels, they also noticed that the GS did not

significantly affect the strength. The authors suggested that this slightly lower strength was due to lower adhesion between the cement and glass than between the cement and natural sand, which is probably due to the lower absorption of the glass. In Turgut and Yahlizade's study [20] on producing paving blocks, the 20% replacement of sand with GS resulted in significant increases in the f'_c, f_{st}, f_{fl}, and abrasion resistance of 69%, 47%, 90%, and 15% compared to control, respectively. The authors attributed these increases to the GS's pozzolanic nature.

Since glass has very low absorption, the water absorption of the concrete containing GA can be greatly reduced, thereby potentially improving the concrete's durability [21]. Low water absorption was also observed for the paving blocks made with waste GA [20].

While the above investigations demonstrate that waste glass can be used as an aggregate in concrete, its applications are limited due to the damaging expansion in the concrete caused by alkali–silica reaction (ASR) between the high-alkali pore water in cement paste and the reactive silica in the waste glass. The chemical reaction between the alkali in portland cement and silica in the aggregate forms silica gel that not only causes cracks upon expansion, but also weakens the concrete and shortens its life. Jin et al. [17] reported that glass with particle sizes ranging from 1.18 to 2.36 mm produced the highest expansion, whereas low expansion was observed with larger and smaller particle sizes. Idir et al. [22] reported that glass particles larger than 1 mm produced ASR gel, but smaller particles produced C-S-H through pozzolanic reaction. Indeed, when the particles are slightly less than 1 mm, a nonexpansive local ASR gel forms around the particles, leading to better bonding between the particles and the cement paste [22]. Some of the common methods to reduce the deterioration associated with ASR are to use low-alkali cement, or use supplementary cementitious materials, or prevent water from entering the concrete [23], or treat the aggregates with admixtures [23,24]. A fly-ash content of 20% of the total binder content greatly reduces the ASR expansion resulting from glass aggregate in the concrete [25]. Lam et al. [26] reported that 10% fly ash used in the concrete can prevent ASR damage in paving blocks containing GA. Shayan and Xu [1] found that both 10% silica fume (SF) and more than 20% GP as a cement replacement were able to ensure no negative ASR expansion in mortar bars.

With recent developments in concrete technology, new generations of concrete have been produced, such as ultra-high-performance concrete (UHPC). The UHPC is defined worldwide as concrete with high mechanical, ductility, and durability properties [27]. Typical UHPC mix

designs consist of very high cement content, SF, quartz powder (QP), quartz sand (QS), and steel fiber [28]. The fiber inclusion in UHPC improves the material's ductility and flexural capacity. With UHPC, a f'_c greater than 150 MPa, a f_{fl} of up to 15 MPa, an elastic modulus (E_c) of 45 GPa, and minimal long-term creep can be achieved [28,29]. The UHPC can also resist freeze–thaw cycles and deicing-salt scaling without any visible damage, and it is nearly impermeable to chloride-ion penetration [30-32]. These excellent characteristics of UHPC are achieved by enhancing homogeneity, eliminating the coarse aggregate, enhancing packing density, improving microstructure, and including fiber [27,28]. Currently, UHPC is used in the construction of special prestressed and precast concrete elements, such as decks and abutments of lightweight bridges, marine platforms, precast walls, concrete repair, urban furniture, and other architectural applications [33-36].

Meeting the optimum grading requirement of QS (in the range of 150–600 μm), for homogeneity and optimum packing density of the UHPC matrix is one of the challenges in producing UHPC. In absence of the QS with the required optimum grading, it is common to obtain the grading by crushing coarse sand or rocks, which is time-consuming, costly, and polluting due to dust generation during crushing. Based on an Environment Canada report [37], QS dust causes immediate and long-term environmental harm because its biological diversity makes it an environmental hazard. Additionally, the International Agency for Research on Cancer (IARC) has classified respirable quartz due to occupational exposure as a Group 1 carcinogen (carcinogenic to humans). The U.S. National Toxicology Program has classified crystalline silica of respirable size as a human carcinogen. The basis for these classifications is sufficient evidence from human studies, indicating a causal relationship between exposure to respirable crystalline silica in the workplace and increased lung-cancer rates in workers [38]. Based on this information, an intensive effort to replace QS with other safe, harmless materials should be undertaken. Even though UHPC is an innovative durable material, it contains a large amount of natural QS. Replacing this sand with GS can significantly decrease its environmental impact.

The current research project aimed at producing UHPC with GS as a partial or total replacement of QS. The effect of QS replacement was studied by measuring the packing density of concrete, fresh properties, compressive strength, ASR, and microstructure. The effect of normal- and steam-curing conditions on the compressive-strength properties was considered.

2. RESEARCH SIGNIFICANCE

Sustainable development for construction involves using unconventional and innovative materials or reusing waste materials in order to compensate for the lack of natural resources and to find alternative ways for conserving the environment. Replacement of quartz sand (QS) in the UHPC mix design with glass sand (GS) derived from crushing waste-glass cullets could decrease the use of QS, whose sources are limited, costly, and environmentally hazardous. Replacing QS with GS can reduce dramatically the price of conventional UHPC by reducing the QS content or avoiding the transportation costs associated with QS when using locally available GS to produce UHPC. By incorporating GS as a replacement of QS in UHPC, environmental hazards and human carcinogenic risks associated with the use of QS could be avoided. Waste glass that is not biodegradable can be reused in concrete, so less material has to be stockpiled or placed in landfills.

3. EXPERIMENTAL PROGRAM

3.1 Testing Program

The key parameter for developing UHPC is to avoid using coarse aggregate and sand with large particle sizes that are normally used in the mix design of normal concrete (NC) and high-performance concrete (HPC), and replace them with ground quartz with particle sizes less than 600 μm [27]. Consequently, the weak transition zone at the interface between the aggregates and paste in NC can be attenuated, leading to maximum packing density and performance enhancement. Therefore, the coarser material used in conventional UHPC is QS with maximum particle sizes of less than 600 μm. Consequently, the main purpose of optimizing the grading (PSD) of the GS is to make it as close to that of QS as possible to arrive at a particular combination of granular materials, which can yield optimum packing density.

To obtain an optimum packing density for GS, the crushed GS was first separated into three grades similar to standard sand size fractions; grade 1 (320 μm < GS1 < 630 μm) course, grade 2 (160 μm < GS2 < 320 μm) medium, and grade 3 (80 μm < GS3 < 160 μm) fine. The packing densities of unitary, binary, and ternary combinations were computed based on the Sedran and de

Larrard approach [39,40] to obtain the optimum packing density of GS. Based on the packing density results, three sets of ternary combinations (the highest packing density) among GS1, GS2, and GS3 were selected. The three sets had PSDs with mean particle sizes (d_{50}) of 225, 275, and 350 µm, and were used to replace 100% of the QS in conventional UHPC. This was to select the optimum GS combination, not only based on the highest packing density, but also on producing optimum concrete properties (workability and compressive strength).

The best GS combination in terms of both packing density and concrete properties was then used with different QS replacements (0%, 50%, and 100%). The relevant effect of QS replacement in UHPC was studied in terms of concrete packing density, workability, mechanical properties, ASR, and microstructure.

The effect of two different curing conditions—normal curing (NC) at a temperature (T) of 20 ± 2°C and relative humidity (RH) of 100%, and standard steam hot curing (HC) at T = 90ºC and RH = 100% for 48 hours—was considered as a parameter affecting the compressive-strength properties of UHPC mixtures.

The mix-design optimization method, mixture composition, material properties, and test methods undertaken in this research are detailed in the following sections.

3.2 Materials

The C_3A and C_3S contents and fineness of cement are critical to control concrete rheology [41]. This is more pronounced with UHPCs designed with higher cement contents. Therefore, high sulfate-resistant cement (Type HS cement) with low C_3A and C_3S contents was selected for designing the UHPC mixtures. The SF used in the mixture proportioning complies with CAN/CSA A3000 specifications. The UHPC was also designed with QS with a specific gravity (SG) of 2.70 and a maximum particle diameter (d_{max}) of 600 µm. The QP with a SG of 2.73 and d_{50} of 13 µm was used as a filler material. The waste glass material with a d_{max} of 600 µm is referred as GS. The GS had a silica content of 73% and Na_2O content of 13%. Its SG was 2.60. Table 1 provides the chemical and physical properties of the type HS cement, SF, QS, QP, and GS materials. The physical properties included material SG, Blain surface fineness, d_{50}, and d_{max}. Figure 1 provides the single PSD for the Type HS cement, QP, SF, and QS as well as the PSD of the combined granular materials in the UHPC. The micrographs in Fig. 2 show the morphology

and size of particles for both QS and GS. The XRD analysis indicates that the QS is crystallized, while the GS is amorphous, as shown in Fig. 3.

A polycarboxylate (PCE)-based high-range water-reducing admixture (HRWRA) with a SG of 1.09 and solid content of 40% (Sika viscocrete 6200) was used in all the concrete mixtures.

3.3 Mix-Design Optimization and Mixture Composition

The granular structure strongly affects the balance between the rheological behavior and the mechanical performances of UHPC and the chemical reactivity of the constituents. The development of UHPC starts normally with a good design of the granular materials to obtain enhanced performance. This can be realized by optimizing the PSD and packing density of the granular materials. In this research, the design of the granular structure of the UHPC (reference mixture in Table 2) was made using the compressible packing model (CPM) developed by de Larrard and collaborators [39, 40]. Figure 1 shows the PSDs for all single materials and the combined materials to produce the reference UHPC mixture (Table 2). The water-to-binder ratio (*w/b*) of 0.19 and HRWRA dosage of 1.5% (% wt. of solids to cement weight) were used, which were obtained by optimizing the different UHPC mixtures carried out in a previous study [35]. In that study [35], various *w/b* and HRWRA concentrations were employed to yield different UHPC mixtures with certain rheological characteristics and strength properties.

The other five UHPGC mixtures in Table 2 were designed based on the reference UHPC mixture by taking into account the QS replacement with GS on a weight basis. The three mixtures (0QS/100GS-350, 0QS/100GS-275, and 0QS/100GS-225) in Series I contained GS with different PSDs (d_{50} of 350, 275, and 225 μm, respectively) as total QS replacement. Based in the results of the concretes in Series I, an optimum GS was selected to produce the concretes in Series II. In both mixtures in Series II, 50% and 100% of the QS content in the reference mixture were replaced with the optimum GS from Series I (d_{50} = 275 μm). The cement, SF, QP, *w/b*, and HRWRA contents were kept constant in all the concrete mixtures.

The names of the mixtures in Series I are combination of QS percentage and GS percentage. The number next to GS represents the d_{50} of the GS used in the mixture. For example, the 0QS/100GS-350 mixture had 0% of QS and 100% of GS with a d_{50} of 350 μm. In Series II, only

the replacement ratios of both the QS and GS were used, with adding a value for the d_{50} because the two mixtures in this series were made with same GS (d_{50} = 275 µm).

3.4 Test Methods and Concrete Preparation

The packing density was measured for different GS (PSD ≥ 125 µm) using the intensive-compaction-test (ICT) setup. The ICT machine consisted of a turntable and a cylinder exerting a pressure ranging between 20 and 1000 kPa over a certain number of cycles on the tested sample until the maximum density is reached. In our study, the applied pressure was 20 kPa to avoid crushing the GS particles. If the GS sample with a weight (w) and a specific gravity (SG) fills up the ICT container with a volume (V_c), then the packing density (φ) can be calculated, as in Eq. 1, where V_s is the solids volume:

$$\phi = \frac{V_s}{V_c} = \frac{w}{V_c.SG} \quad (1)$$

All the concrete mixtures were batched using high-energy shear mixer with a 10 l capacity. To achieve a homogeneous mixture and avoid particle agglomeration, all of the powdered materials were mixed for 10 min before water and HRWRA addition Approximately half of the HRWRA diluted in half of the mixing water was gradually added over 5 min of mixing time. The remaining water and HRWRA were gradually added over an additional 5 min of mixing time. Upon the end of mixing, the fresh properties of the UHPC mixtures were measured. The fresh tests included concrete temperature, unit weight, and air content (ASTM C 185 [42]). The concrete flow was also measured using the mini-slump cone and flow table (ASTM C 1437 [43]).

The compressive strength (f_c) measurements for the UHPC were determined using 50×50×50 mm cubes, according to ASTM C 109 [44]. The samples were tightly covered with plastic sheets and stored at 23°C and 50% RH for 24 hours before demolding. After demolding, the samples were cured under two different curing regimes: NC and HC. Under NC, the samples were stored in a fog room at a temperature of 23°C and 100% RH until the day of testing. The HC mode composed of curing the samples at 90ºC and 100% RH for 48 h before testing. Measurement of ASR expansion and mass variations over time were carried out for 50QS/50GS according to ASTM C1260 [45]. Standard mortar-bar molds (20×20×275 mm) were used to cast

the specimens for this series of tests. Because this UHPC contained no coarse aggregate, no special preparation of the batch ingredients was necessary before casting the bars. Four prisms were cast with the concrete mixture and remained tightly covered with plastic sheets in molds at 23°C and 50% RH for 24 h, before demolding. The first readings of length and mass changes were taken immediately after demolding. The specimens were immersed in a tap-water bath and then stored at 80°C for 24 h before measuring the "zero" readings of length and mass. The samples were then immersed in a NaOH solution and stored again at 80±2°C. The mass and length changes were subsequently measured daily for a total of 14 days of saturation in the NaOH solution.

Additional samples from the reference (after HC treatment) and 50QS/50GS concretes after finishing the ASR test were also prepared for microstructure analysis using scanning electron microscope (SEM).

4. RESULTS AND DISCUSSIONS

4.1 Optimizing Granulometry of Glass Sand in UHPC

4.1.1 According to Packing Density

The packing densities of unitary, binary, and ternary combinations were computed based on the approach presented in de Larrad [39]. Initially, the unitary packing density of each individual material was determined. The intensive-compaction-test (ICT) method was used for measuring the dry packing density of the GS with a PSD greater than 125 µm. The results of the unitary packing density for each of the three glass sands—GS1 (PSD = 320 – 630 µm), GS2 (PSD = 160 – 320 µm), and GS3 (PSD = 80 – 160 µm)—were 0.56, 0.55, and 0.50, respectively. The unitary packing of GS1 and GS2 were slightly higher than of GS3. According to [39, 40], this could be attributed to the coarse friction being more amenable to compaction due to fewer contact points between grains than in the finer fraction.

The packing density of the binary combination between the two finer GSs (GS1 and GS2) was then determined, as shown in Fig. 4 (left). In general, the binary mixture showed higher packing density than the unitary packing. This was obviously due to the filling of void spaces with the

finer particles. Adding GS2 to GS1 increased the packing up to 80% of GS2 and 20% of G1; after that point, the packing density started to decrease. The combination of 60% GS1 and 40% GS2 yielded the highest packing density of 0.60.

Ternary combinations among GS1, GS2, and GS3 were initially estimated by taking five binary mixtures between GS1 and GS2 (GS1 ranging from 80% to 40% and GS2 ranging from 20% to 60%, both in increments of 10%). For each ternary GS1-GS2, GS3 was added as a finer material in increments of 10% between 0% and 100% (see Fig. 4 [right]). The highest packing density value of 0.63 was achieved for two ternary GS1:GS2:GS3 combinations of 49%:21%:30% and 56%:24%:20%. The results show that adding GS3 at percentages between 10% and 50% increased the packing density of the granular materials by filling the gaps between the coarser materials in the binary mixtures.

Three sets of ternary combinations GS1:GS2:GS3 with packing-density values close to the maximum (0.63) were selected to study their effect on fresh properties and compressive strength in conventional UHPC. These three sets had percentages of 56%:24%:20%, 35%:35%:30%, and 36%:54%:10% with packing density values of 0.63, 0.62, and 0.60, respectively. Figure 5 gives the PSDs for these three GS combinations with d_{50} values of 350, 275, and 225 μm, respectively. According to their respective d_{50} values, they were designated as GS-350, GS-275, and GS-225, respectively.

4.1.2 According to Concrete Properties

Table 3 presents the fresh-concrete temperature, unit weight, air content, and mini-slump flow values of the UHPC mixtures in Series I compared to the reference mixture. Replacing the QS with GS-350 and GS-225 led to a decrease in workability. The slump flow decreased from 190 mm for the reference mixture to 175 and 170 mm in 0QS/100GS-350 and 0QS/100GS-225, respectively. The incorporation of GS-275 in the UHPC significantly increased the slump flow to 210 mm in 0QS/100GS-275, compared to 190 mm in the reference.

The particle packing density of the concrete decreased when GS-350 and GS-225 were incorporated, compared to the reference mixture. For example, the packing-density values obtained from the CPM for the reference, 0QS/100GS-350, and 0QS/100GS-225 mixtures were 0.79, 0.76, and 0.75, respectively. This was attributed to the increased content of finer particles

(80 to 160 µm) in GS-350 and GS-275, which decreased the concrete's workability. This resulted in an overlapping of the cement and QP particles, and the finer particles in GS3. In contrast to GS-350 and GS-225, including GS-275 in the UHPC—with a slightly lower particle packing density (0.78) due the decreased content of finer materials in GS3—resulted in slight improved concrete workability. In addition, the slight improvement in the flow characteristics reported for 0QS/100GS-275 compared to the reference mixture was due replacing QS with rough particles, in the latter mixture with GS with smooth surfaces. The unit weight of the reference mixture remained close to that of the concretes containing the three different GSs, given that the SG values of the QSs were not far from that of the GS (2.75 vs. 2.60, respectively), as seen in Table 1. Compared to the reference mixture made with only QS, the three mixtures containing GS in Series I showed relatively higher air contents. For example, 0QS/100GS-350 with GS-350 exhibited the highest air content of 5.5% (it is the major effect of using PCE HRWRA), which was found to be matched with the lowest particle packing density calculated for this mixture (0.74), while the mixture containing GS-275 showed a low air content of 4.6% that corresponded to a high particle packing density of 0.78. It should be noted that this air was entrapped air, and was generated by the PCE-based HRWRA used in the mix design. A defoaming agent was not used to reduce the entrapped air.

Figure 6 presents the compressive strength of the three mixtures in Series I compared to the reference mixture after different ages of NC and 2 days of HC. The figure also provides the corresponding packing-density values for the four mixtures. In general, the mixtures with GS exhibited lower f'_c compared to the reference mixture, regardless of age and curing conditions. For example, the 91-day f'_c of NC for the reference, 0QS/100GS-225, 0QS/100GS-275, and 0QS/100GS-350 mixtures were 182, 127, 157, and 128 MPa, respectively. The corresponding values after 2 days of HC were 204, 164, 182, and 153 MPa, respectively. The QS used in the present work performed well in producing the UHPC, mainly because of its very high silica content. On the other hand, the decrease in f'_c can be due to decreased packing densities in the mixtures incorporating GS (0.75, 0.78, and 0.76 for 0QS/100GS-225, 0QS/100GS-275, and 0QS/100GS-350, respectively) compared to the reference (0.79). In fact, when a compressive force is applied, the shear and tensile stresses develop at the interfaces between the aggregates and cement paste (transition zone), forming small cracks approximately proportional in size to the maximum aggregate diameter [28]. With regard to GS, the particles can measure 630 µm in

length according to the sieving test, but the actual length can be up to 1.0 mm (Fig. 2 right), which tends to have more cracking potential under same loading or lower strength capacity. Moreover, the lower strength can be related to the GS particle shapes, which are rough, elongated, and flattened compared to the rounded surfaces of the QS particles. The strength reduction related also to increase the air air contents when QS was replaced by GS.

The results for the three mixtures containing GS in Series I demonstrate that 0QS/100GS-275 had the highest packing density (0.78), which is very close to that of the reference (0.79). The workability properties of this concrete (mini-slump flow value = 210 mm) were better than that of the reference mixture (about 10% higher). The f'_c results measured for 0QS/100GS-275 were also the best among the three mixtures in Series I containing GS. This concrete exhibited f'_c values at 91 days of NC and 2 days of HC of 157 and 182 MPa, respectively (14% and 11% lower than the corresponding values reported for the reference mixture). Based on these results, the GS combination with a d_{50} of 275 μm (GS-275) will be discussed further in the following section as replacement for the various QS contents in the UHPC.

4.2 Replacement of Quartz Sand with Glass Sand with Optimum Granulometry

Different contents (0%, 50%, and 100%) of GS-275 (optimized in the previous section) were used to replace QS in the conventional UHPC, and their relevant effects on workability, mechanical microstructure, and durability (ASR) properties were investigated through the reference, 50QS/50GS, and 0QS/100GS mixtures, respectively.

4.2.1 Fresh Properties

Table 3 presents the fresh properties, including mini-slump flow, unit weight, air content, and concrete temperature, of 50QS/50GS and 0QS/100GS compared to the reference mixture. The mini-slump flow diameters were found to increase with higher GS contents: 190, 200, and 210 mm for the reference, 50QS/50GS, and 0QS/100GS mixtures, respectively, as illustrated in Fig. 7. This improvement was due replacing QS particles with the GS particles having low water absorption. Again, the use of PCE-based HRWRA without a defoaming agent resulted in higher

air content (3.8% to 4.6%). A slight increase (0.5% to 0.8%) in the air content was noticed with the addition of 50% and 100% GS compared to the reference concrete.

4.2.2 Compressive Strength

Figure 7 gives the compressive strength after 1, 7, 28, 56, and 91 days of NC and 2 days of HC for the reference, 50QS/50GS, and 0QS/100GS mixtures.

In general, the f'_c results obtained after 2 days of HC were higher (11% vs. 14%) than those obtained after 91 days of NC, regardless of the ratio of the QS replacement. This was due to the higher pozzolanic reaction of the SF in the UHPC mixture, which can be activated by high temperature. This pozzolanic reaction led to a denser microstructure of C-S-H, and therefore, faster strength development.

The f'_c values for 50QS/50GS were very close to that of the reference mixture. The f'_c values for the reference mixture at 91 days of NC and 2 days of HC were 182 and 204 MPa, respectively. The corresponding f'_c values of 50QS/50GS were 171 and 196 MPa, respectively (only 6% and 4% reductions, respectively). The f'_c of the UHPC containing 100% GS replacement showed a quite large reduction of 14% and 11% at 91 days of NC and 2 days of HC, respectively, compared to the reference mixture. Despite this reduction, it exhibited strength higher than the 150 MPa required for classification as UHPC. It reached 157 and 182 MPa after 91 days of NC and 2 days of HC, respectively. As explained earlier, the strength reduction related to GS replacement can be due to increase air content as well as the rough, elongated, flattened, and low absorbent nature of the GS particles.

4.2.3 Alkali– Silica Reaction

The limited use of GS in concrete is due to uncertainty about damaging expansion that might be caused by ASR between the high-alkali pore water in cement paste and the reactive silica in GS. For this reason, ASR expansion was assessed for 50QS/50GS. The accelerated ASR test was performed according to ASTM C1260 [44]. Figure 8 provides the variations of expansion due to accelerated ASR with time up to 16 days. The maximum expansion at 16 days was 0.03%, which was less than (about one-third) the limit specifying the “innocuous behavior” (0.10%). This low

expansion was obtained, however, the type HS cement used had higher alkali content [equivalent alkali (Na_2O_{eq}) = 0.9% (Table 1)]. The low ASR expansion for the UHPC containing GS can be attributed to the fact that the d_{max} of the GS particles used was smaller than 1 mm (630 μm). GS with such smaller particles produces C-S-H by pozzolanic reaction instead of ASR gel. Indeed, when the particles are slightly less than 1 mm a nonexpansive local ASR gel forms around the particles, which leads to better bonding between the particles and cement paste [22]. The low ASR expansion can also be explained by the very low *w/b* used for the UHPC (0.189), which does not provide enough moisture to initiate the reaction. This conclusion coincides with Vernet (2003), indicating that this UHPC is not susceptible to ASR due to its high silica-fume content and low permeability [46].

4.2.4 Microstructure Analysis

The samples from the reference mixture after HC treatment and 50QS/50GS concretes after completion of the ASR test were also prepared for microstructure analysis under scanning electron microscope (SEM). All of the samples were epoxy impregnated, polished, and carbon coated to facilitate SEM analysis. Figure 9 is a backscattering-scanning-electron (BSE) image of the reference mixture (A,B) and 50QS/50GS (C,D). Because of the low *w/b*, a large amount of unreacted cement, QP, and SF particles can be seen in the image. No visible capillary pores and cracks can be found, as well as portlandite ($Ca(OH)_2$) crystals. The UHPC was designed with close packing density and the use of pozzolanic mineral admixtures [47]. Therefore, it has very low porosity that is especially continuous. Entrained or entrapped spherical air pores were also observed in the UHPC matrix. Most of these pores were formed as a side effect of the superplasticizer used. Some of the black dots in Fig. 9 are probably the fingerprints of particles when the concrete was crushed. The figure clearly shows that the interfacial transition zone (ITZ) of the reference mixture was very thin or even nonexistent (Fig. 9).

Figure 9 (C, D) reveals no ASR gel or microcracking ring around the GS particles. These results indicate that there should be no concern about ASR problems with the concrete containing GS. Free water must be present in order for ASR to occur in any concrete. Given the low permeability of this UHPC, it is unlikely that ASR would be an issue when GS is used.

5. CONCLUSIONS

Based on the findings herein, the following conclusions can be drawn:

- The compressible packing model (CPM) in [39,40] can be applied on different glass sands of varying particle-size distributions to obtain a final glass sand with an ideal particle-size distribution curve and optimum packing density using unitary, binary, and ternary combinations.
- Glass sand with an ideal particle-size distribution curve [mean-particle diameter (d_{50}) of 275 μm (GS-275)] was obtained in this research project. The glass sand (as total replacement of QS) can increase workability (10% higher), but with compressive strength less than 13% compare to reference UHPC.
- An optimum UHPC mixture can be designed with 50% glass-sand replacement of quartz sand. This mixture can deliver approximately similar flowability and compressive-strength properties in comparison to the reference concrete.
- Incorporating 50% glass sand as quartz-sand replacement can yield a UHPC with a very dense microstructure and without any expansion from alkali–silica reaction. The results show that no alkali–aggregate reaction products are not developed locally and have no negative influence on durability. This behavior is due to the UHPC's very low permeability, which prevents alkali ingress.
- Glass sand can be efficiently used to produce UHPC and eliminate the need for quartz sand, yielding a cost-effective and environmentally friendly solution.

6. ACKNOWLEDGMENTS

This research was funded by Société des Alcools du Québec (SAQ). The authors gratefully acknowledge this support.

7. REFERENCES

1. Shayan A, Xu A. Value-added utilisation of waste glass in concrete. Cem Concr Res 2004;34(1):81–89.

2. FEVE. Collection for recycling rate in Europe. The European Container Glass Federation (http://www.feve.org/FEVE-STATIS-2013/Recycling-2011-Glass-coll.html date accessed: Sept. 11, 2013).
3. Du, H. and Tan, K. H., (2014). "Concrete with recycled glass as fine aggregates." ACI Materials Journal, 111(1), 47-58
4. Wright, J. R., Cartwright, C., Fura, D. and Rajabipour, F., (2014). "Fresh and hardened properties of concrete incorporating recycled glass as 100% sand replacement." Journal of Materials in Civil Engineering, 26(10), 04014073.
5. Shao Y, Lefort T, Moras S, Rodriguez D. Studies on concrete containing ground waste glass. Cem Concr Res 2000;30:91–100.
6. Dyer TD, Dhir RK. Chemical reactions of glass cullet used as cement component. J of Mat in Civil Eng 2001;13(6):412–417.
7. Shi C, Wu Y, Riefler C, Wang H. Characteristic and pozzolanic reactivity of glass powders. Cem Concr Res 2005;35:987–993.
8. Neithalath, N., (2008) "Quantifying the effects of hydration enhancement and dilution in cement pastes containing coarse glass powder." Advanced Concrete Technology, 6(3), 397-408.
9. Schwarz, N., Cam, H. and Neithalath, N., (2008). "Influence of a fine glass powder on the durability characteristics of concrete and its comparison to fly ash." Cement and Concrete Composites, 30(6), 486- 496.
10. Jain, J. A. and Neithalath, N., (2010). "Chloride transport in fly ash and glass powder modified concretes-influence of test methods on microstructure."Cement and Concrete Composites, 32(2),148-156.
11. Matos, A. M. and Sousa-Coutinho, J., (2012). "Durability of mortar using waste glass powder as cement replacement." Construction and Building Materials, 36, 205-215.
12. Khmiri A, Chaabouni M, Samet B. Chemical behavior of ground waste glass when used as partial cement replacement in mortars. Const and Build Mat 2013;44:74–80.
13. Carsana, M., Frassoni, M. and Bertolini, L., (2014). "Comparison of ground waste glass with other supplementary cementitious materials." Cement and Concrete Composites, 45, 39-45.
14. Kim, J., Moon, J. H., Shim, J.W., Sim, J., Lee, H.G. and Zi, G., (2014). "Durability properties of a concrete with waste glass sludge exposed to freeze-and-thaw condition and

de-icing salt." Construction and Building Materials, 66, 398-402.

15. Mirzahosseini M, Riding KA. Effect of curing temperature and glass type on the pozzolanic reactivity of glass powder. Cem Concr Res 2014;58:103–111.
16. Du, H. and Tan, K. H., (2014c). "Transport properties of concrete with glass powder as supplementary cementitious material." ACI Materials Journal, accepted for publication.
17. Jin, W., Meyer, C. and Baxter, S., (2000) "Glascrete concrete with glass aggregate." ACI Materials Journal, 97(2), 208-213.
18. Ismail, Z. Z. & AI-Rashmi, E. A. (2009). Recyclying of waste glass as a partial replacement for fine aggregate in concrete. Waste Management. 29 (2), 655-659.
19. Park, S. B., Lee, B. c., & Kim, J. H. (2004). Studies on mechanical properties of concrete containing waste glass aggregate. Cement and Concrete Research, 34(12),2181-2189.
20. P. Turgut, E. S. Yahlizade (2009) Research into Concrete Blocks with Waste Glass. World Academy of Science, Engineering and Technology, International Journal of Civil, Environmental, Structural, Construction and Architectural Engineering Vol:3, No:3, 2009.
21. Taha, B., & Nounu, G. (2008). Properties of concrete contains mixed colour waste recycled glass as sand and cement replacement. Construction and Building Materials, 22(5), 713-720.
22. Idir R, Cyr M, Tagnit-Hamou A. Use of waste glass as powder and aggregate in cement-based materials. SBEIDCO – 1st Int Conf on Sust built Env Infr in Developing Countries ENSET, Oran Algeria 12–14 October 2009:109–16.
23. Benoit Fournier, Marc-André Bérubé (2000) Alkali-aggregate reaction in concrete: a review of basic concepts and engineering implications. *Canadian Journal of Civil Engineering*, 27(2): 167-191, 10.1139/l99-072
24. Topcu, B., Boga, A. R, and Bilir, T. (2008). Alkali-silica reactions of mortars produced by using waste glass as fine aggregate and admixtures such as fly ash and LizC03. Waste Management, 28(5), 878-884.
25. Polley, C., Cramer, S. M., & de la Cruz, R. V. (1998). Potential for using waste glass in Portland cement concrete. Journal of Materials in Civil Engineering, 10(4),210-219.
26. Lam, C. S., Poon, C. S., & Chan, D. (2007). Enhancing the performance of precast concrete blocks by incorporating waste glass - ASR consideration. Cement and Concrete Composites, 29(8),616-625.
27. Richard P, Cheyrezy M. Composition of reactive powder concretes. Cem Concr Res

1995;25(7):1501–1511.

28. Richard P, Cheyrezy M. Reactive powder concretes with high ductility and 200-800 MPa compressive strength. ACI SP 144 1994:507–518.
29. Dugat J, Roux N, Bernier G. Mechanical properties of reactive powder concretes. Mat and Struc 1996;29:233–240.
30. Roux N, Andrade C, Sanjuan M. Experimental study of durability of reactive powder concretes. J of Mat in Civil Eng 1996;8(1):1–6.
31. Bonneau O, Lachemi M, Dallaire E, Dugat J, Aïtcin P-C. Mechanical properties and durability of two industrial reactive powder concretes. ACI Mat J 1997;94(4):286–290.
32. Soliman N, Tagnit-Hamou A. Study of rheological and mechanical performance of ultra-high-performance glass concrete. ACI SP-fib bulletin and FRC 2014 Joint ACI-fib Int Workshop. Fibre Reinforced Concrete: from Design to Structural Applications 2015:17.
33. Schmidt M, Fehling E. Ultra-high-performance concrete: research, development and application in Europe. ACI SP 225 2005:51–77.
34. Klemens T. Flexible concrete offers new solutions. Concr Const 2004;49(12):72.
35. Soliman N, Omran A, Tagnit-Hamou A. Laboratory characterization and field application of novel ultra-high performance glass concrete. ACI Mat J 2015: in press.
36. Racky P. Cost-effectiveness and Sustainability of UHPC. Proc. of the Int Symp on UHPC, Kassel, Germany 2004;13(15):797–805.
37. Environment Canada, https://www.ec.gc.ca/default.asp?lang=en&n=FD9B0E51-1
38. Environment Canada, Health Canada. Screening assessment for the challenge. Report June 2013:7.
39. de Larrard F. Concrete mixture proportioning: a scientific approach. London: Modern Concrete Technology Series, E&FN SPON, 1999.
40. Sedran, T., and de larrard, F., Manuel d'utilisation de RENE-LCPC, version 6.1d,logiciel d'optimisation granulaire, Laboratoire Centrale des Ponts et Chaussées, (2000).
41. Aïtcin P-C. Cements of yesterday and today–concrete of tomorrow. Cem Concr Res 2000;30(9):1349–1359.
42. ASTM C185. Standard Test Method for Air Content of Hydraulic Cement Mortar. ASTM International, West Conshohocken, PA. Developed by Subcommittee: C01.21, Book of ASTM Standards 2015; V 04.01: 4.

43. ASTM C1437. Flow of Hydraulic Cement Mortar. ASTM International, West Conshohocken, PA. Developed by Subcommittee: C01.22, Book of ASTM Standards 2007; V 04.01: 2.

44. ASTM C109. Standard test method for compressive strength of hydraulic cement mortars (using 2-in. or [50-mm] cube specimens). ASTM International, West Conshohocken, PA. Developed by Subcommittee: C01.27, Book of ASTM Standards 2016; V 04.01: 10.

45. ASTM C1260. Standard Test Method for Potential Alkali Reactivity of Aggregates (Mortar-Bar Method). ASTM International, West Conshohocken, PA. Developed by Subcommittee: C09.26, Book of ASTM Standards 2014; V 04.02: 5.

46. Vernet, C. (2003). "UHPC microstructure and related durability performance laboratory assessment and field experience examples." Proc., 2003 Int. Symp. on High Performance Concrete, Orlando, Fla.

47. Cheyrezy, M., Maret, V., and L. Frouin. 1995. Microstructural Analysis of RPC (Reactive Powder Concrete). Cement and Concrete Research, Oct., Vol. 25, No. 7: 1491-1500.

LIST OF TABLES

LIST OF FIGURES

Table 1 – Chemical composition (%) of Type HS cement, quartz sand, quartz powder, glass powder, and silica fume

	Identification	Quartz Sand	Quartz Powder	Glass Sand-0.60	HS Cement	Silica Fume
Chemical composition (%)	Silicon dioxide (SiO_2)	99.80	99.80	73.00	22.00	99.80
	Iron oxide (Fe_2O_3)	0.04	0.09	0.40	4.30	0.09
	Aluminum oxide (Al_2O_3)	0.14	0.11	1.50	3.50	0.11
	Calcium oxide (CaO)	0.17	0.38	11.30	65.6	0.40
	Titanium dioxide (TiO_2)	0.02	0.25	0.04	0.20	--
	Sulfur trioxide (SO_3),	--	0.53	--	2.30	--
	Magnesium oxide (MgO)	0.01	0.20	1.20	1.90	0.20
	Sodium oxide (Na_2O)	--	0.25	13.00	0.07	0.20
	Potassium oxide (K_2O)	0.05	3.50	0.50	0.80	0.50
	Equivalent alkali (Na_2O_{eq})	--	--	--	0.90	--
	Zinc oxide (ZnO)	--	--	--	0.09	0.25
	Loss on ignition (LOI)	0.20	0.32	0.60	1.00	3.50
Bogue components	C_3S	--	--	--	50.00	--
	C_2S	--	--	--	25.00	--
	C_3A	--	--	--	2.00	--
	C_4AF	--	--	--	14.00	--
Physical properties	Specific gravity	2.70	2.73	2.60	3.21	2.20
	Blaine surface area (m^2/kg)	--	--	--	430	20,000
	Mean particle diameter, d_{50}, (µm)	250	13	270	11	0.15
	Maximum particle diameter, d_{max}, (µm)	600	--	630	--	--

Table 2 – Concrete mix design (kg/m^3)

	Reference	Series I (100% replacement of QS with GS with different PSDs)			Series II (QS replacement with GS with optimum granulometry (d_{50} = 275 µm)	
Material		0QS/100 GS-350	0QS/100 GS-275	0QS/100 GS-225	50QS/50GS	0QS/100GS
Type HS cement	807	794	794	794	802	794
Silica fume	225	221	221	221	223	221
Water	196	192	192	192	194	192
Water-to-binder ratio *(w/b)*	0.189	0.189	0.189	0.189	0.189	0.189
Quartz sand	972	--	--	--	481	--
Glass sand (GS-350)	--	953	--	--	--	--
Glass sand (GS-275)	--	--	953	--	481	953
Glass sand (GS-225)	--	--	--	953	--	--
Quartz powder	243	238	238	238	241	238
Solid content in HRWRA	13	13	13	13	13	13

Table 3 – Fresh-concrete properties

Property	Reference	Series I (100% replacement of QS with GS with different PSDs)			Series II (QS replacement with GS with optimum granulometry (d_{50} = 275 µm)	
		0QS/100 GS-350	0QS/100 GS-275	0QS/100GS-225	50QS/50GS	0QS/100GS
Slump flow, mm	190	175	210	170	200	210
Air void, %	3.8	5.5	4.6	5.2	4.3	4.6
Unit weight, kg/m^3	2363	2292	2297	2300	2306	2297
Concrete temperature, °C	32	32	31	31	32	31

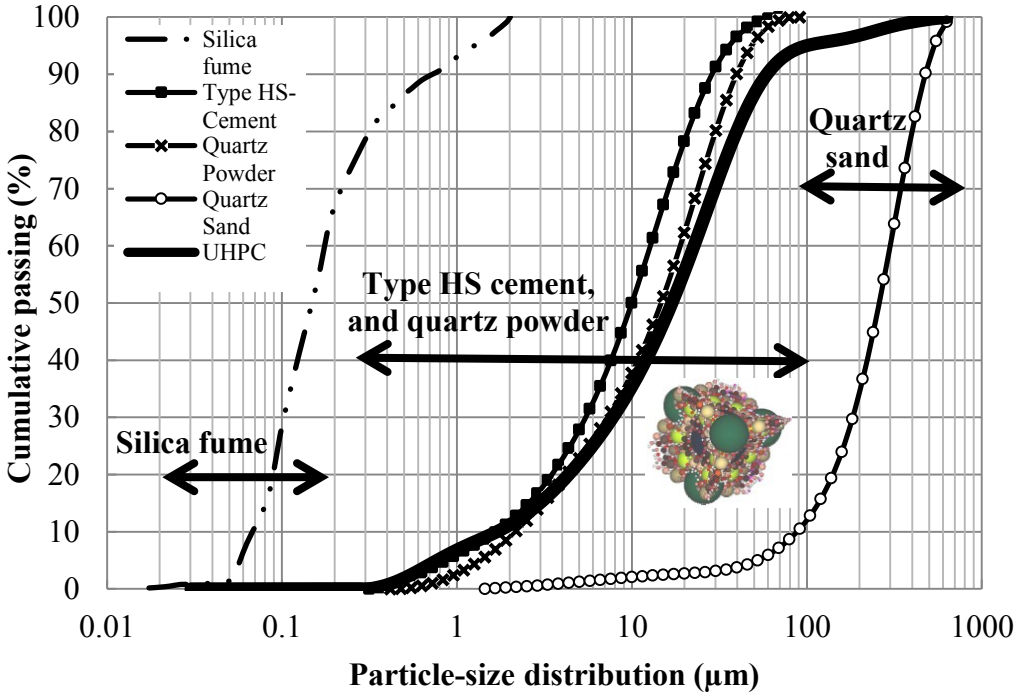

Fig. 1 – Particle-size distributions of individual and combined granular materials used in the UHPC reference-mix design

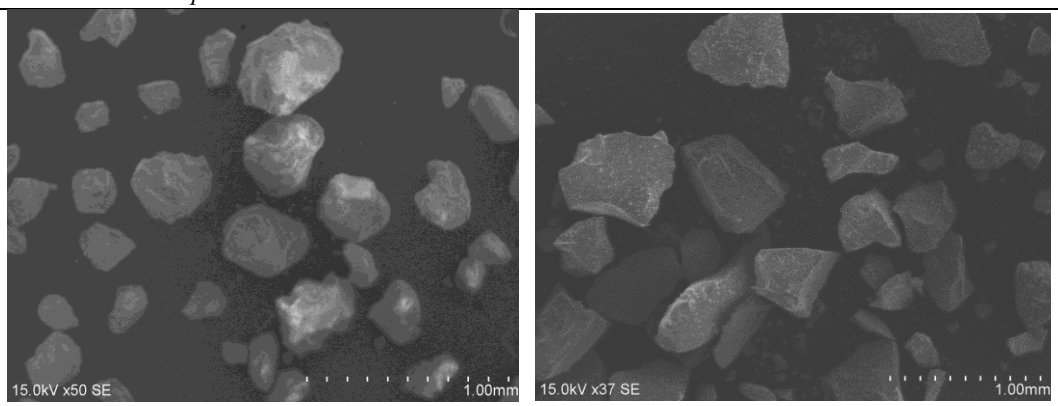

Fig. 2 – Photomicrograph of quartz sand (left) and glass sand (right)

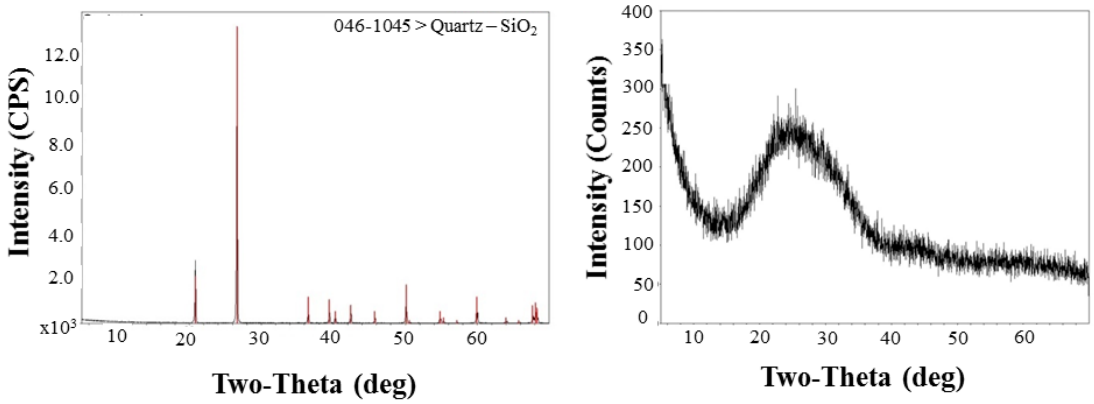

Fig. 3 – X-ray diffraction patterns for quartz sand (left) and glass sand (right)

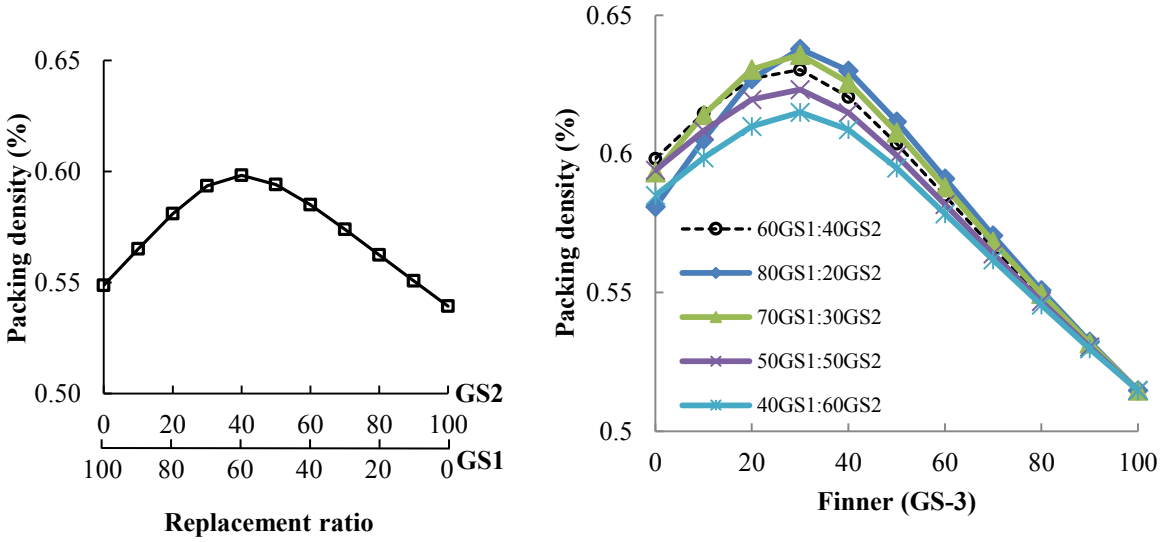

Fig. 4 – Binary packing between GS1 and GS2 (left), ternary packing between the optimum combination between GS1 and GS2 against GS3 (right)

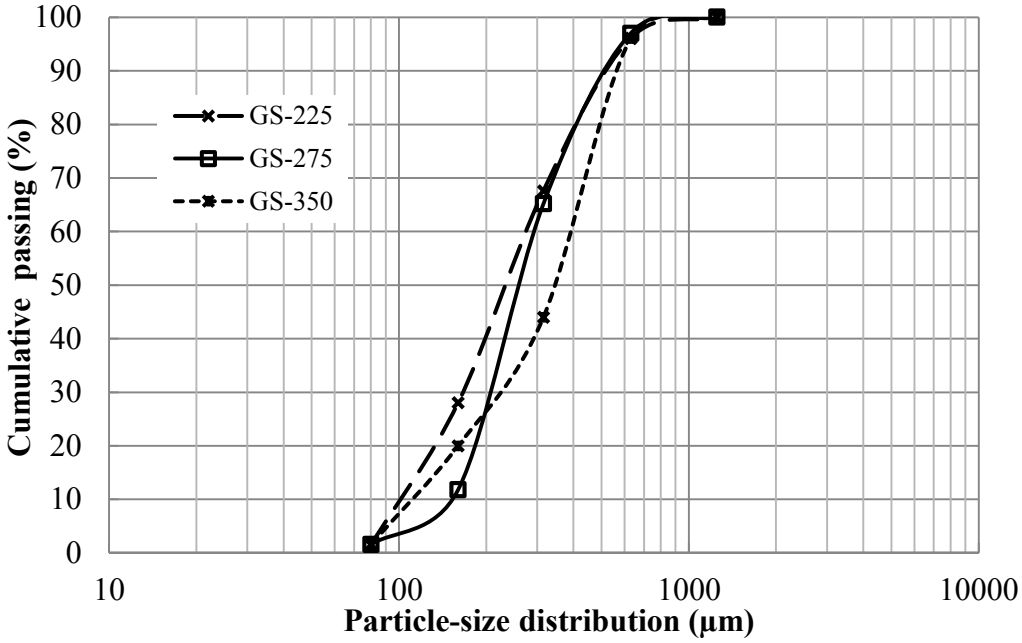

Fig. 5 – Particle-size distributions for the three combinations of glass sand

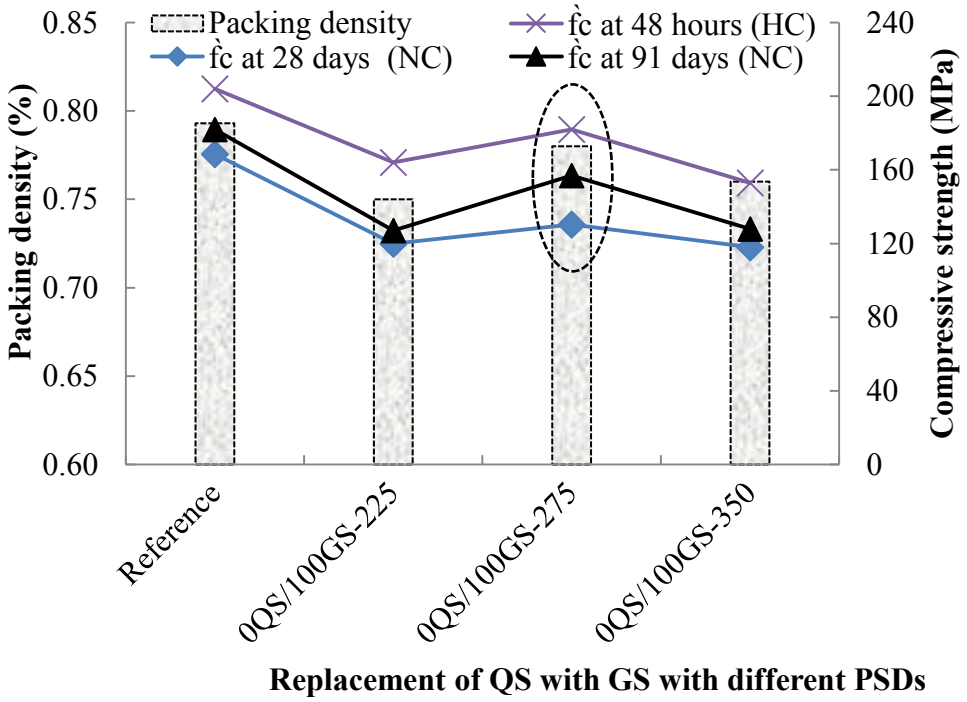

Fig. 6 – Particle-packing density and compressive strength for UHPC mixtures made with glass sand (GS) with different particle-size distributions (PSDs)

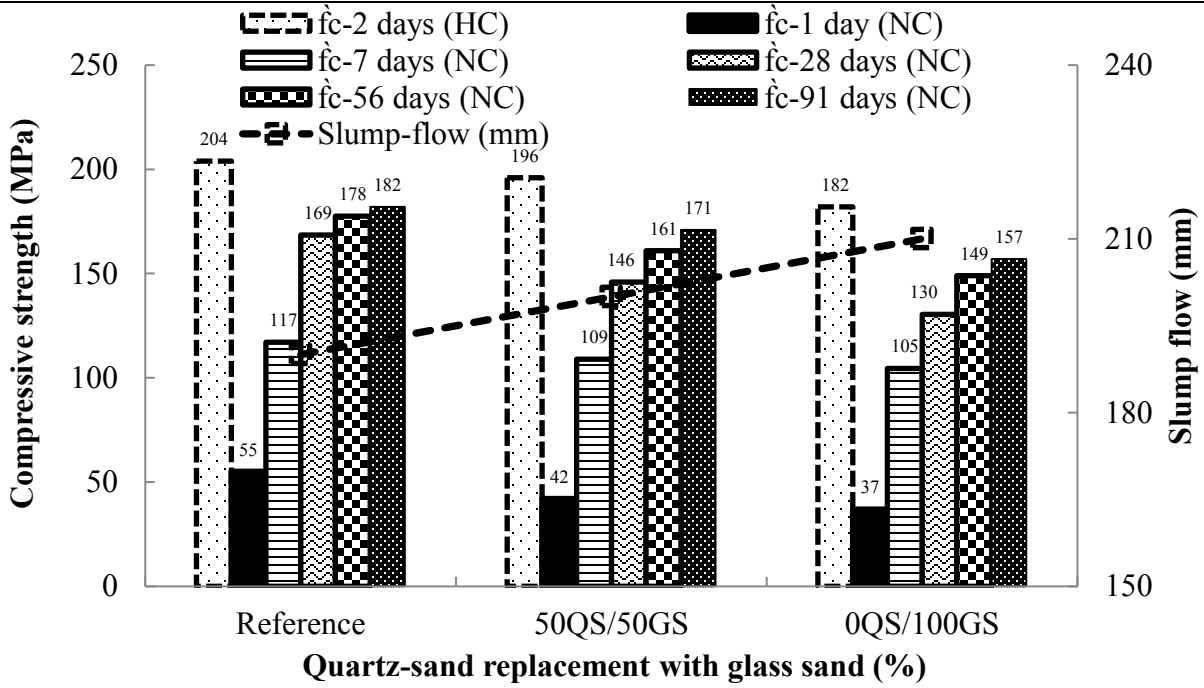

Fig. 7 – Effect of quartz-sand replacement with glass sand (d_{50} = 275 µm) on compressive strength after different ages of normal (NC) and hot-curing (HC) conditions

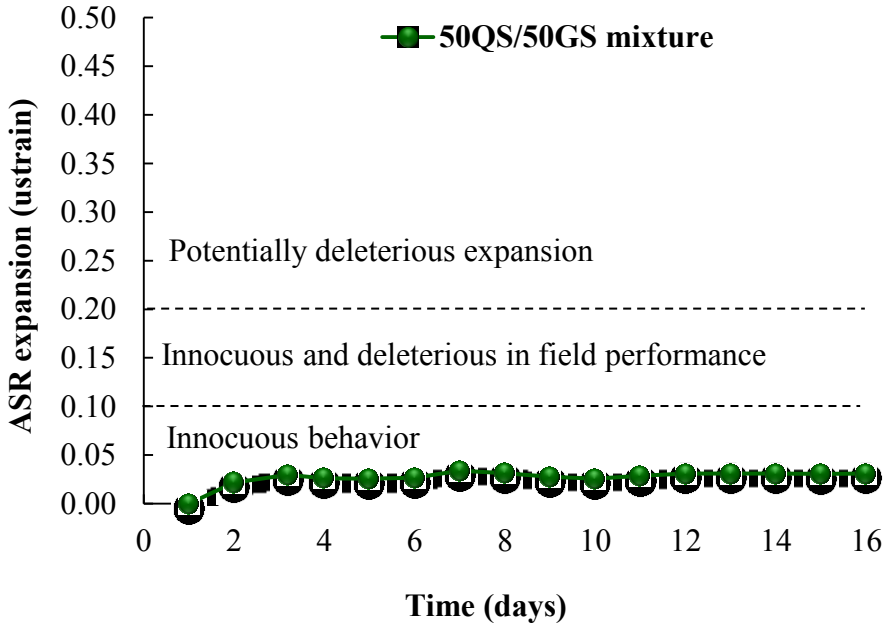

Fig. 8 – Variations in expansion due to accelerated alkali–silica reaction (ASR) with time for 50QS/50GS according to ASTM C 1260

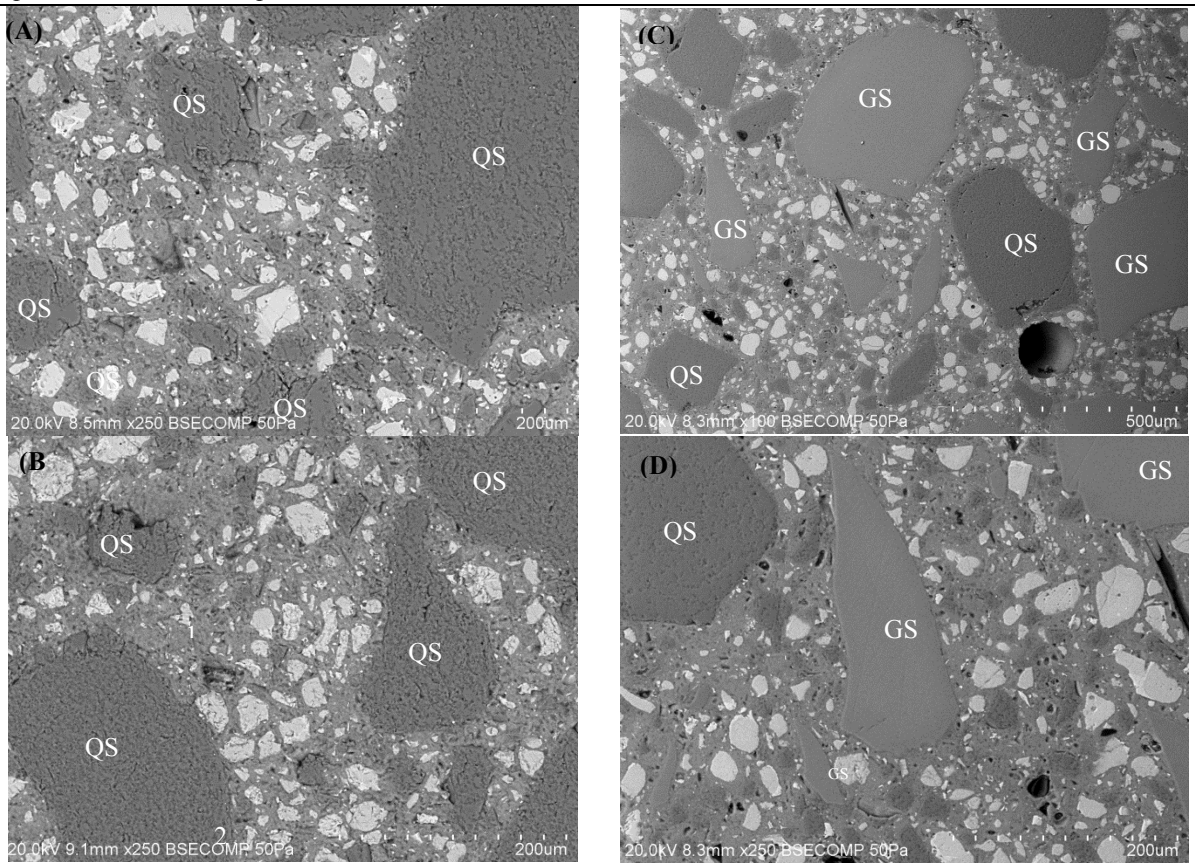

Fig. 9 – BSE/SEM images for reference mixture (A,B) and 50QS/50GS (C,D)

5 Fine Powder Replacement in UHPC

5.1 Introduction

In conventional UHPC production, portland cement is the component with the highest environmental impact because its production requires high amounts of energy and CO_2 is released when limestone is transformed into calcium oxide during the burning process. This chapter presents the development of an innovative sustainable and green UHPC with low CO_2 emissions. Moreover, based on an Environment Canada report, quartz powder (QP)—the main component in UHPC—causes immediate and long-term environmental harm because its biological diversity makes it an environmental hazard. The techniques for preparing low-cost, green, and sustainable UHPC concrete is investigated in this chapter, with the glass powder (GP) used to replace cement and QP. The possibility of replacing each single ingredient (i.e., QP and cement) with GP was investigated separately, while the other components were maintained constant. Based on the foregoing results, an optimum GP as partial replacement of cement and GP as a replacement of QP was conducted to obtain an optimal UHPC containing the maximum amount of GP. The following chapter presents the fresh and mechanical properties of an UHPGC with such a combination of GP as partial replacement of cement and QP. This mixture was batched with 2% steel fibers. The effect of GP on UHPC fresh properties, hydration kinetics, f_c, and microstructure was investigated. The effect of using two different curing conditions on the f_c and microstructural properties of the UHPC mixtures was also studied. Descriptions of the materials, mix designs, and mixing sequence used in these experimental tests are given in this chapter. More results on the production processing are provided in Paper number 8 (Appendix).

5.2 Paper 3: Development of Green Ultra-High-Performance Concrete Using Glass Powder

Reference:

Soliman N.A., Tagnit-Hamou A. (2016) Development of Green Ultra-High-Performance Concrete Using Glass Powder. *Journal of Building and Construction Materials*. (Accepted and in press).

Development of Green Ultra-High-Performance Concrete Using Glass Powder

Authors and Affiliation

Nancy A. Soliman, is a member of the ACI international and Sherbrooke local chapters, and CRIB. She is a PhD candidate in the Department of Civil Engineering, University of Sherbrooke, QC, Canada. Her research interest includes NDT, UHPC, microstructure, and sustainable development.

Arezki Tagnit-Hamou, FACI, is a professor in the Department of Civil Engineering at the University of Sherbrooke, QC, Canada. He is also the Head of the cement and concrete group as well as holding an industrial chair on valorization of glass in materials. He is a member of ACI Committees 130 (Sustainability of Concrete) and 555 (Concrete with Recycled Materials), and RILEM TC DTA. His research interests include alternative supplementary cementitious materials, cement and concrete physicochemistry and microstructure, and sustainable development.

ABSTRACT

A green ultra-high-performance glass concrete (UHPGC) with a compressive strength (f_c) of up to 220 MPa was prepared and its fresh, mechanical, and microstructural properties were investigated. The test results indicate that the fresh UHPGC properties were improved when the cement and quartz powder were replaced with nonabsorptive glass-powder (GP) particles. The strength improvement can be attributed to the GP's pozzolanicity and to its mechanical characteristics (very high strength and elastic modulus of glass). A microscopical investigation revealed the formation of a hydration rim around cement and GP particles. UHPGC provides technological, economical, and environmental advantages compared to traditional UHPC.

Keywords: Glass powder, green, heat of hydration, microstructure, sustainability, ultra-high-performance concrete.

1. INTRODUCTION

The recent developments in concrete technology are yielding new generations of concrete such as ultra-high-performance concrete (UHPC). UHPC has been defined worldwide as a concrete with high mechanical, ductility, and durability properties [1]. A typical UHPC mix design is composed of very high cement content, silica fume (SF), quartz powder (QP), quartz sand (QS), and steel fibers [2]. The fiber inclusion improves the UHPC's ductility and flexural capacity. UHPC can achieve compressive strength (f_c) higher than 150 MPa, flexural strength (f_{fl}) of up to 15 MPa, an elastic modulus (E_c) of 45 GPa, and minimal long-term creep [2,3]. UHPC can also resist freeze–thaw cycles and deicing-salt scaling with no visible damage, and it is nearly impermeable to chloride-ion penetration [4-6]. These outstanding characteristics of UHPC result from the enhancement of the homogeneity, the elimination of the coarse aggregate, the enhancement of the packing density, the improvement of the microstructure, and the incorporation of the fibers [1, 2]. Currently, UHPC is used in constructing special prestressed and precast concrete elements, such as decks and abutments for lightweight bridges, marine platforms, precast walls, concrete repairs, as well as urban furniture and other architectural applications [7-10].

Cement-based materials must not only have good mechanical and durability characteristics, but they must also be environmental friendly (ecological) and provide socioeconomic benefits [11]. UHPC is usually designed with a higher cement content ranging between 800 and 1000 kg/m^3 [1, 2]. The huge amount of cement not only affects production costs and consumes natural sources, but it also negatively affects the environment through the release of carbon dioxide (CO_2) emissions, which can contribute to the greenhouse effect. Furthermore, estimates put the final hydration percentage of the cement from 31% to 60% due to UHPC's very low water-to-cementitious material ratio (*w/cm*) [12, 13]. Unhydrated cement particles in UHPC act as microaggregates and lead rapid hydration reaction, high heat of hydration, and shrinkage cracking.

Based on an Environment Canada report [14], QP—the main component in UHPC—causes immediate and long-term environmental harm because its biological diversity makes it an environmental hazard . Additionally, the International Agency for Research on Cancer (IARC) has classified respirable quartz due to occupational exposure as a Group 1 carcinogen (carcinogenic to humans). The U.S. National Toxicology Program has classified crystalline silica

of respirable size as a human carcinogen. The basis for these classifications is sufficient evidence from human studies indicating a causal relationship between exposure to respirable crystalline silica in the workplace and increased lung-cancer rates in workers [15]. Based on this information, an intensive effort to replace QP with other safe, nonharmful materials should be undertaken.

In achieving the "sustainable" concrete concept, cement and QP can be replaced with mineral admixtures such as fly ash (FA), silica fume (SF), and ground granulated blast-furnace slag (GGBFS). Recently, various studies have been carried out to develop UHPC that is more ecologically and economically feasible. Soutsos et al. [16] found that up to 36% of cement could be replaced with GGBFS without decreasing f_c. Yazici [17] also reported that cement replacement of up to 40% with either FA or GGBFS had no detrimental effects on f_c. Van Tuan et al. [18] investigated the possibility of using rice-husk ash (RHA) to produce UHPC. They achieved f_c over 150 MPa by incorporating RHA in UHPC. The degree of cement replacement with FA and GGBFS in UHPC mixtures was also studied by Puntke [19] based on the concept of particle-packing density.

Recently, FA production has been reduced in North America because most of the coal-fired power plants are being refitted as gas-fired plants. In addition, shipping FA and GGBFS over long distances can increase the greenhouse-emission effect, as illustrated by the fact that transportation is responsible for more than 28% of Canada's total greenhouse-gas emissions [22]. So, using alternative materials available locally should be more beneficial for UHPC production.

Post-consumption glass can be recycled several times in many countries without significantly altering its physical and chemical properties. Large quantities of glass cannot be recycled because of the high breaking potential, color mixing, or high recycling costs [21]. Most of waste glass goes into landfill sites, which is undesirable since it is not biodegradable and less environmentally friendly [22]. In recent years, attempts have been made to use waste glass as an alternative supplementary cementitious material (ASCM) or ultra-fine filler in concrete, depending on its chemical composition and particle-size distribution (PSD) [23-24]. Glass ground to a particle size finer than 38 μm exhibits pozzolanic behavior, which contributes to concrete strength and durability [25-27]. The ground glass powder (GP) (with a particle size of 30 μm or smaller) can be used as an ASCM to partially replace cement in certain concrete types [28-31], thereby significantly decreasing the adverse effects caused by the alkali–silica

reaction [32]. This research indicates that incorporating waste GP in concrete holds high value and feasibility considering its economic and technical advantages.

According to Leadership in Energy and Environmental Design (LEED) certification, using glass in concrete can double the points earned from using other by-products such as SF, FA, and BFS. GP is regarded as a post-consumption material, while the others are considered post-production materials. Using GP as a cement replacement has very little environmental impact. The Recyc-Quebec analysis (2015) showed that valorizing glass bottles as GP in concrete can allow for its transportation within a radius of 9000 km without environmental impacts compared to landfilling.

The research program described herein aimed at developing an innovative low-cost, sustainable, and green UHPC by using GP. In this program, cement and QP were replaced with GP at different proportions, while keeping QS and SF quantities constant in all mixtures. The UHPC mixtures were optimized based on the packing-density theory. The effect of GP on fresh properties, hydration kinetics, f_c, and microstructure of UHPC was investigated. The effect of two different curing conditions on the f_c and microstructure properties of UHPC mixtures were also studied: normal curing (NC) at a temperature of 20 ºC ± 2ºC and relative humidity (RH) of 100%, and standard steam hot curing (HC) at a temperature of 90ºC and 100% RH for 48 h.

2. RESEARCH SIGNIFICANCE

In order to produce "greener" concrete than conventional UHPC, both the cement and QP were replaced with GP. This strategy reduces CO_2 emissions. Moreover, the glass is being reused, which cuts down on landfilled materials and saves more natural resources. This can reduce the carbon footprint of a typical UHPC. Replacing QP and cement with GP can also dramatically reduce the cost of conventional UHPC. For example, QP costs three times more than GP. Moreover, the transportation cost of materials can also be reduced by using locally available GP to produce UHPC.

In addition, UHPC has a very high cement content and very low *w/cm*, which results in rapid hydration, high heat of hydration, and shrinkage. Controlling this early-age shrinkage by replacing cement with GP is essential to ensure enhanced long-term performance and longer service life.

3. EXPERIMENTAL PROGRAM

The following section describes the material characteristics, mixture proportions, mix-design optimization, and specimen preparation.

3.1 Materials

In general, the cement C_3A and C_3S contents and cement fineness are critical for controlling concrete rheology [11]. This is more pronounced in case of UHPC, which is designed with higher cement content. Therefore, high sulfate-resistance cement (Type HS cement) with low C_3A and C_3S contents was selected for designing the UHPGC mixtures used herein. The SF complies with CAN/CSA A3000 specifications. The UHPC was also designed with QS with a specific gravity (*SG*) of 2.70 and a maximum particle size (d_{max}) of 600 µm. A QP with a *SG* of 2.73 and d_{50} of 13 µm was used as a filler material. A GP with a *SG* of 2.6 and d_{50} of 12 µm was used to replace cement and QP in traditional UHPC. Table 1 gives the chemical and physical properties of the Type HS cement, SF, QS, QP, and GP as well as the price of each material per ton. The physical properties include specific gravity, Blain surface fineness, mean particle-size diameter (d_{50}), and maximum particle diameter (d_{50}). Figure 1 provides the particle-size distribution (PSD) of the Type HS cement, QP, SF, and QS. The micrographs in Fig. 2 show the morphology and size of the cement, QP, and GP particles. Obviously, the cement powder consists of multi-size, multi-phase, irregularly shaped particles generally ranging in size from less than 1 µm to about 100 µm. The QP and GP have multi-size and irregular shaped particles. XRD analysis was performed to determine the nature of each material, as shown in Fig. 3. XRD analysis of the cement and QP indicate that they were crystallized, while the GP was amorphous.

A polycarboxylate (PCE) based high-range water-reducing admixture (HRWRA) with a specific gravity of 1.09 and solids content of 40% (SikaViscocrete 6200) was used in all the concrete mixtures. The price of HRWRA is 5$/liter.

Steel fibers measuring 13 mm in length and 0.2 mm in diameter were incorporated into the optimized mixtures.

3.2 Mix Design Optimization

UHPC development starts with designing the granular structure of all the granular components. The key factor for enhancing UHPC performance is optimizing the particle-size distribution and packing density. The granular structure strongly affects the balance between the UHPC rheological behavior and mechanical performances as well as the chemical reactivity of the constituents. The design of the granular structure of the UHPC used in our study was made according to the compressible packing model (CPM) developed by de Larrard et al. [33].

Figure 2 shows the PSD of all the materials and the optimized UHPC. The water-to-binder ratio (w/b) of 0.19 and the dosage of HRWRA (expressed as percentage of solids content in the HRWRA relative to cement weight, %SolidHRWRA) of 1.5% were obtained by optimizing the different mixtures designed with various w/b and HRWRA concentrations to yield concrete with certain rheological characteristics and strength requirements [31]. The GP, which had a PSD close to that of the cement and QP was used to replace the cement and QP by weight.

3.3 Mixture Proportioning

A total of 10 mixtures were designed to study the effect of GP on the fresh, hydration, mechanical, and microstructural properties of the UHPC: one traditional mixture without GP; five mixtures containing different percentages of GP as partial cement replacement (series I), two mixtures with 50% and 100% QP replacement with GP (series II), and two mixtures to study the synergetic effect of GP as replacement for both cement and QP (series III). The conventional UHPC prepared with cement, SF, QP, and, QS was considered as the reference. In series I, the cement was replaced by 10%, 20%, 30%, 40%, and 50% of GP by weight. In series III, the UHPC mixture was prepared with *GP* to replace 20% of cement and 100% of QP. A similar mixture was designed with 2% steel fiber addition. The SF, QS, *w/b*, and HRWRA were kept constant in all the mixtures. The 10 concrete mixtures were designed with a *w/b* of 0.189 and *%SolidHRWRA* of 1.5%, as given in Table 2. The mixture labels (Table 2) are a combination of two parts: cement or QP, and GP replacement ratios. For example, 90C/10GP contained 90% cement and 10% GP, while 50QP/50GP contained 50% GP and 50% GP.

The table 2 lists the mix proportions and associated costs (without fibers) for all of the mixes considered in this work. Cost is listed as a cost index in order to simplify the discussion later on. The cost index is simply the ratio of the mix's cost compared to the starting mixture published in [5], based on current prices in Canada. The index is a relative indicator of cost, since actual costs will vary in time and by location.

3.4 Specimen Preparation and Test Methods

All the concrete mixtures were batched using high-energy shear mixer with a capacity of 10 l. To achieve a homogeneous mixture and avoid particle agglomeration, all of the powder materials were mixed for 10 min before the water and HRWRA were added. Approximately half of the HRWRA diluted in half of the mixing water was gradually added over 5 min of mixing time. The remaining water and HRWRA were gradually added during an additional 5 min of mixing. At the end of mixing, the fresh properties of the UHPC mixtures were measured. The tests included concrete temperature, unit weight, and air content (ASTM C 185). Concrete flow was measured with the flow-table test (ASTM C 1437).

The heat flow was measured with a thermometric TAM air-conduction calorimeter, containing eight separate measuring cells. About 20 g of freshly mixed paste was weighed in a glass vial with a 24.5 mm inside diameter. The glass vial was sealed and placed in the calorimeter, and the heat flow was measured for about 52 h. During the test, isothermal conditions of 20 ºC ± 0.02ºC were maintained in the measuring cells. The initial heat peak, occurring right after the addition of the water to the cement, could not be measured because of the very low *w/b* needed to produce the UHPC required external mixing of the paste ingredients before placement in the calorimeter.

The f_c measurements for the UHPC were determined using 50×50×50 mm cubes, according to ASTM C 109. The flexural strength was determined on 100×100×400 mm prisms according to ASTM C 1018. The modulus of elasticity was measured on 100×200 mm cylinders according to ASTM C 469. The samples were tightly covered with plastic sheets and stored at 23°C and 50% RH for 24 h before the molds were removed. The samples were then cured under two different curing regimes: NC and HC. Under NC, the samples were stored in a fog room at a temperature of 23°C and 100% RH until the day of testing. The HC mode consisted of curing the samples at 90ºC and 100% RH for 48 h before testing.

The microstructure of the UHPC samples subjected to HC regime for 48 h. was observed with a scanning electron microscope (SEM: Hitachi S-3400N) coupled with energy dispersive spectroscopy (EDS: Oxford Inca). The SEM was operated at a pressure of 50 Pa, a voltage of 20 kV, and tungsten filament current of 80 μA. The SEM observations were performed on polished surfaces, from which a chunk of the concrete was removed and cast in resin. The cast samples was cut perpendicularly to its cross section and polished with a 1.0-μm roughness polishing pad. In this paper, each site of interest is presented with two SEM micrographs: a low-magnification micrograph shot 250 times and higher magnification micrographs shot 2.0k times, respectively.

4. RESULTS AND DISCUSSION

4.1 Cement Replacement with GP

Different GP contents (0%, 10%, 20%, 40%, and 50%) were used to replace cement in the conventional UHPC, and their relevant effects on workability, hydration kinetics, microstructure, and mechanical properties were investigated, as detailed below.

4.1.1 Fresh properties

Table 3 presents the fresh concrete properties. The flowability increased slightly when the GP content increased. This slight improvement was due to the replacement of cement particles by GP particles, which have low water absorption and smoother surfaces. Previous studies also indicate that cement paste and glass interaction was significantly decreased due to the surface smoothness of GP [34,35]. Another explanation for workability increasing with increasing GP content is cement dilution, which tends to reduce the formation of cement hydration products in the first few minutes of mixing. Therefore, there are less products to bridge various particles together.

In addition, the cement used in this study had a specific surface area of 430 m^2/kg, which is greater than that of the GP (380 m^2/kg). Therefore, the total surface area of the cement and GP blend decreased when using GP as cement replacement. Consequently, the water demand to lubricate particle surfaces decreased due to the drop in the net particle surface area, and hence the slump flow for the same *w/b*.

It is worth noting that the GP replacement of cement was by weight. As the specific gravity of GP is lower than that of cement, the solid particles-to-water ratio, by volume, is then higher in case of cement and GP blends compared to pure cement. This increases the friction between the solids in the paste in the case of the cement and GP blend, thereby resulting in a slight improvement in workability. This inverse effect of higher solid-to-water volume ratio was less effective on workability compared to the dilution of cement, smooth glass surface, and nonabsorptive nature of GP mentioned earlier. The higher GP content ended up yielding better workability.

As described in [36], superplasticizer efficiency largely depends on the zeta potential on the entire surface of the tested binder particles. In most cases, cement needs more superplasticizer to reach a certain slump flow compared to the common mineral admixtures. On the contrary, the mixture containing cement and GP required less superplasticizer than the mixture designed with cement alone.

Table 3 presents the air content and unit weight values for the UHPC containing various contents of GP. The greater the GP replacement of cement, the lower the unit weight due to the low specific gravity of the GP compared to the cement (2.6 vs. 3.2, respectively). All of the mixtures had air-content values in between 3.8 to 4.2% (high air content). The PCE-based HRWRA used in these concrete mixtures resulted in high amounts of entrapped air. A defoaming agent was not used to reduce entrapped air.

4.1.2 Hydration Kinetics

Isothermal calorimetry was performed to investigate the pozzolanic reaction of the GP on cement hydration at an early age. The rate of hydration heat emission and the cumulative hydration heat curves of the UHPC with 0%, 20%, 40%, and 50% GP replacements within the first 48 h after contact between the water and cementitious materials contact, normalized to the total binder (cement, SF, GP) weight in the mixture, are shown in Fig. 4. It is clear that the maximum heat flow and the total heat were reduced as the cement replacement with GP increased. Figures 5 A and B show that the maximum value of the second exothermic peak of 80C/20GP was 35% lower compared to the reference mixture. The maximum value of the second exothermic peak for 60C/40GP and 50C/50GP were 32% and 50% lower, respectively, compared to the reference

mixture. As shown in Fig. 5 B, at 12 hours, the heat emission was 34% lower after incorporating 20% of GP (80C/20GP mixture) compared to the reference mixture (from 30 to 20 J/g). Corresponding decreases of 55% (from 30 to 13.5 J/g) and 72% (from 30 to 9.5 J/g) were observed when the GP amount was 40% (60C/40GP mixture) and 50% (50C/50GP mixture), respectively. The 48-h heat emission showed decreases of 24% (from 125 to 95 J/g), 28% (from 125 to 95 J/g), and 37.5% (from 125 to 80 J/g) for 80C/20GP, 60C/40GP, and 50C/50GP, respectively, compared to the reference mixture. These reductions in the rate of heat evolution and the total heat generated were due to the dilution of the cement (reduction in overall volume of the cementitious materials) and, consequently, the hydration products. The results of this study are consistent with previous findings [37, 38]. The lower heat of hydration helps minimize the cracking resulting from increased temperature.

When the GP replacement of cement was 20%, the time of the end of the induction period (calculated as the time between the lower point of the heat flow curve and the first inflection point in the main peak) and the acceleration period (calculated as the time between the first and the second inflection points in the heat flow curve) relative to the main peak were shorter, as shown in Fig. 5 A,C. The ends of the induction period of the reference and 80C/20GP were 9.1 and 8.2 h, while the acceleration periods were about 7.1 and 6.8 hours, respectively. This can be attributed to the fact that fine glass powders can accelerate the cement hydration through the adsorption of calcium ions from the liquid phase and serve as nucleation and growth sites for C–S–H and other hydrates. At the same time, the high alkali (Na_2O) content in GP can act as catalyst in the formation of calcium silica hydrate at an early age [39, 40].

When the GP replacement of cement was higher than 20%, the ends of the induction and the acceleration periods relative to the main peak were delayed, as shown in Fig. 5A,C. For example, the end of the induction period for reference, 60C/40GP, and 50C/50GP mixtures are about 9.1, 9.7 and 11.2 hours, respectively. The acceleration period for the reference, 60C/40GP, and 50C/50GP mixtures are about 7.1, 7.3, and 7.5 hours, respectively. The increased level of cement replacement with GP (less cement content) increased both the *w/c* and superplasticizer solids content in the mix. This is more significant in UHPC production as a high superplasticizer dosage is used. This restricts Ca^{2+} diffusion and dilutes of the pozzolanic reaction of the GP. According to Jansen [41], complexation of Ca^{2+} ions from the pore solution by the superplasticizer can affect the polymer absorbed on the nuclei or the anhydrous grain surfaces,

which, in turn, might prevent nuclei growth or lead to dissolution of the anhydrous grains. This significantly retards early hydration of the cement and restricts $Ca(OH)_2$ generation. The pozzolanic reaction is delayed due to the inadequate amount of portlandite in the mixtures.

4.1.3 Microstructure

SEM was used to study the morphology and microstructure of the reference sample and the samples containing GP. Figure 6 shows the back-scattered electrons (BSE) images of the selected UHPC mixtures (reference and 80C/20GP) with HC. The figure clearly shows that the interfacial transition zone (ITZ) of the reference mixture without GP was very thin (Fig. 6 A); adding GP did not affect the ITZ (Fig. 6 C, E). The ITZ thickness in all the concrete mixtures was almost similar and very dense. Normally, ITZ microstructure is influenced by the "wall effect" in the vicinity of aggregate surfaces, and this region may extend by about 50 μm from the grain surface to the cement paste [42]. It is worth noting that all the granular materials were optimized using the CPM, which takes into account the influence of the wall effect. The QS used had particle sizes less than 600 μm, which also reduced the ITZ thickness. These interfacial characteristics are also attributed to the sequential hydration effects of the cement, SF, and GP, which improved the ITZ properties. Although the UHPC matrix was significantly more dense and homogeneous than the normal concrete, this indicates very low porosity [43]. Entrained or entrapped spherical air pores were also observed in the UHPC matrix. Most of these pores were formed as a side effect of the high amount of superplasticizer used. Some of the black points in (Fig. 6 A, B, C, D, E, D) are probably the fingerprints of QS or any each particles when the concrete is crushed.

In addition, no portlandite [$Ca(OH)_2$] was noticed in the matrix because it was consumed by the pozzolanic reaction of SF+GP.

The BSC images (Fig.6 B, D) of the reference and 80C/20GP subjected to heat treatment for 48 h showed a C–S–H hydration rim forming around cement and GP particles. The GP exhibited pozzolanic reaction and produced more C–S–H and enhanced the microstructure, as shown in Fig.6D. In addition, no ASR microcracking ring was found around the large glass-powder particle due to the adequate fineness of the glass powder and dense matrix, in accordance with the literature [44].

4.1.4 Compressive Strength

Figure 4 presents the compressive strengths of the mixtures at different ages and under different curing conditions (NC and HC). The replacement of cement with 10% and 20% GP yielded higher f_c values after NC (at different ages) and after HC (Fig. 4). The f_c values for the reference mixture at 91 days of NC and 2 days of HC were 179 and 204 MPa, respectively, while the f_c of 90C/10GP and 80C/20GP were 213 and 216 MPa at 2 days of HC and 198 and 201 MPa at 91 days of NC, respectively. The f_c of the UHPC with 30%, 40%, and 50% GP replacement (70C/30GP, 60C/40GP, and 50C/50GP, respectively) decreased by 10% to 20% at early ages (1, 7, and 28 days) of NC compared to the reference mixture. The results were different at later ages (56 and 91 days) of NC and also after HC. The f_c values at 2 days of HC and 56 and 91 days of NC for 70C/30GP, 60C/40GP, and 50C/50GP were close to the strength of the reference mixture (Fig. 4).

The concrete mixtures with GP exhibited higher mechanical properties at both 56 and 91 days of NC as well as at 2 days of HC due to the pozzolanic reaction of the GP with the hydrated cement product, which took place at a later age. Nevertheless, this pozzolanic reaction was slower than cement hydration [45-47]. A C–S–H gel can be generated, causing the microstructure of the concrete to densify. The newly generated C–S–H fills the pore structure in the concrete. Thus, the mechanical properties of the concrete are significantly improved at a later age of NC or with accelerated HC. Moreover, when the GP content increased in the concrete mixture, the *w/c* increased, which accelerated cement hydration. More portlandite can be generated, and more GP pozzolanic reaction developed, which yielded the successive strength improvement. Strength and rigidity were also improved by the glass particles acting as inclusions having very high strength and elastic modulus (70 GPa) [31].

Figure 4 compares the f_c obtained after NC at 91 days and HC. The results indicate that the f_c of UHPC specimens under HC were about 7% to 10% higher than that of those under NC, regardless of the cement replacement ratio. This was due to the higher pozzolanic reaction resulting from both SF and GP in the UHPC mixture that was activated by the high temperature. Such pozzolanic reaction led to a denser microstructure of C–S–H, resulting in faster strength development.

Based on our results, it can be summarized that the strength of the mixture with 20% GP replacement (80C/20GP) exhibited a greater increase in f_c of 8% and 13% at 56 and 91 days of NC, respectively, and 20% after 2 days of HC, compared to the reference mixture.

4.2 Effect of QP Replacement with GP

4.2.1 Fresh Properties

Table 3 presents fresh concrete temperature, unit weight, air content, and slump flow of the UHPC. The incorporation of the GP increased the slump flow. For example, the slump flow increased from 190 to 200 mm and to 210 mm when the GP replacement increased from 0% to 50% and 100% (reference, 50QP/50GP, 0QP/100GP, respectively). The particle packing density of concrete was observed to improve when more GP was incorporated in the mixture. For example, the packing density values obtained from the CPM for the reference (0% GP), 50QP/50GP, and 0QP/100GP were 0.79, 0.80, and 0.80, respectively. This was attributed to the GP have a smoother form than the QP, which also enhanced concrete workability. The unit-weight and air-content (high) values were similar for the reference (0% GP) and the concrete containing GP, as seen in Table 3.

4.2.2 Hydration Kinetics

Figure 8 presents the normalized rate of heat evolution and normalized cumulative amount of heat, relative to the total binder content, by weight, for the pastes with varying GP contents as QP replacement. The maximum rate of heat evolution and the total heat generated by the different pastes were similar, as shown in Figs. A and B, because of the slow rate of pozzolanic reaction of GP.

The presence of GP shortens the time to reach the peak hydration rate because fine glass powders can accelerate cement hydration via adsorption of calcium ions from the liquid phase and serve as nucleation and growth sites for C–S–H and other hydrates. At the same time, the high alkali content (Na_2O) in GP may act as a catalyst in the formation of calcium silica hydrate at an early age [39, 40]. The end of the induction period for the reference, 50QP/50GP, and 0QP/100GP was

about 9.1, 8.1 and 6.2 hours, respectively. The acceleration period of the reference, 50QP/50GP, and 0QP/100GP were about 7.1, 7.5, and 8.3 hours, respectively.

Consequently, according to the results obtained in this section, it can be concluded that the GP, as a QP replacement, accelerated the hydration kinetics of the UHPC at an early age.

4.2.3 Microstructure

Figures 6E and F show the microstructure of 0QP/100GP after HC, for example. The BSE of 0QP/100GP showed no separation between GP particles from the surrounding C–S–H phase, which could indicate the formation of a thin hydration rim due to the pozzolanic reactivity of the GP. In the reference mixture, partial separation of the QP particles from the surrounding C–S–H phase was observed, as shown in Fig. 6B. In this case, because the concrete was heated at a low temperature (90°C), the QP is considered as a filler material. The QP only reacts when subjected to heating at a temperature between 150 and 200 °C, by altering the calcium oxide (CaO)/silicon dioxide (SiO_2) ratios and favoring the formation of tobermorite and xonotlite. This takes place when UHPC is subjected to heat treatment and setting pressure [12]. The improvement in the f_c due to the QP replacement with GP was confirmed by microstructural observation in the following (section 4.2.4).

As mentioned in the case of cement replacement with GP (section 4.1.3), the figure reveals the existence of a dense microstructure and hydration rims around the cement particles.

4.2.4 Compressive Strength (f_c)

The inclusion of GP as a QP replacement increased the compressive strength of the UHPC mixtures compared to the reference, as shown in Fig. 7. For NC at 7 and 28 days, the f_c values of 50QP/50GP and 0QP/100GP were approximately similar to the reference mixture. At 56 and 91 days, the strength of the UHPC containing GP was higher than the reference. When the QP was totally replaced with GP (0QP/100GP), the concrete exhibited a higher increase in f_c of about 12% and 17% at 56 and 91 days under NC, respectively, compared to reference mixture. Furthermore, at all GP replacement levels, the f_c of 2-day HC specimens was greater than those

subjected to NC at all tested ages. After 2 days of HC, the f_c of the reference was 204 MPa, while the f_c values for 50QP/50GP and 0QP/100GP were 222 and 234 MPa, respectively.

It is worth noting that QP is considered as a microaggregate (an inert part when not heated) in UHPC design. It is characterized by the polymorphic modification of β-quartz, and it shows significant pozzolanic activity when its particle size is finer than 5 μm or it is subjected to hydrothermal treatment at temperatures above 150°C [12,48]. In contrast, ground GP with a particle size finer than 38 μm can exhibit pozzolanic activity at ambient temperature. Moreover, the GP increased cement solubility, which leads to increased portlandite. The amorphous silica in glass powder can react with CH and form C–S–H at a later stage of hydration [30]. Thus, concrete microstructure and compressive strength could be increased significantly and UHPC with superior mechanical properties prepared. In addition, the strength and rigidity improvements were also due to the fact that the glass particles served as inclusions with very high strength and elastic modulus (70 GPa).

It can be concluded that the total replacement of QP with GP gives the optimal composition of UHPC in terms of high strength and slump flow.

4.3 Synergetic Effect of Cement and QP Replacement with GP

Based on the foregoing results, the 20% GP as partial replacement of cement and 100% GP as a replacement of QP can be considered to be the optimal UHPC composition containing GP. Therefore, the following section presents the fresh and mechanical properties of an UHPGC with such a combination (80C20GP/0QP100GP). This mixture was batched with 2% steel fibers. The results of 80C20GP/0QP100GP (without steel fibers) and 80C20GP/0QP100GP-F (with fibers) is presented in comparison to the reference UHPC without GP.

4.3.1 Fresh Properties

Table 3 provides the fresh properties of the mixtures tested. The slump flow for the 80C20GP/0QP100GP was 220 mm compared to 190 mm for the reference. Incorporating steel fibers did not affect the fresh properties of the UHPGC. The corresponding value for

80C20GP/0QP100GP-F was 220 mm. The air contents for 80C20GP/0QP100GP and 80C20GP/0QP100GP-F were similar to that of the reference mixture.

4.3.2 Mechanical Properties

Figure 9 shows the compressive-strength results of the mixtures after NC for 1, 7, 28, 56, and 91 days and after HC for 2 days. As expected, the concrete samples with GP showed slightly higher f_c results compared to the reference. For example, the f_c values for reference and 80C20GP/0QP100GP were 176 and 190 MPa after 91 days of NC and 204 and 217 MPa after 2 days of HC, respectively. This increase in the f_c can be attributed to the pozzolanic reactivity and rigidity of GP particles. Based on this observation, it can be concluded that GP content significantly influences the f_c of UHPC.

Adding steel fibers (accounting for 2% of the UPHC by volume) only slightly increased the concrete's compressive strength. For example after HC, the f_c results for 80C20GP/0QP100GP and 80C20GP/0QP100GP-F were 221 and 217 MPa, respectively. After 28 days of NC, the f_c values were approximately similar (164 and 168 MPa, respectively). The respective values after 91 days of NC were 190 and 192 MPa. These results are consistent with those obtained by Schmidt et al. (2003) [48], who reported that their UHPC mixtures containing 2.5% of steel fiber (per volume) showed no compressive-strength increase compared to the reference.

Figure 9 compares the compressive-strength results obtained after NC and HC. The compressive strength of the UHPC generally appeared to increase with increasing heat treatment. The compressive strength of the UHPC under HC was an average of 30% higher than that of the samples under NC for 28 days. Its compressive strength after NC for 91 days was, however, slightly higher. HC only accelerated strength development. After HC and 91 days of NC, the strength-development values of the samples containing GP were 10% and 22% higher, respectively, than the reference concrete.

The inclusion of 2% fiber increased the flexural strength from 24 to 26 MPa after 91 days of NC and from 27 to 29 MPa after 2 days of HC. The hot curing showed no significant increase in flexural strength.

The modulus-of-elasticity results indicate that the concrete with GP or with 2% fiber revealed no significant differences between the NC and HC samples. The measured values for all of the concrete mixtures were about 50 + 5 GPa.

4.4 Evaluation of embedded CO2 emission and health impact of UHGC

To prove that the designed UHPGC is materials green and eco-friendly, its embedded $CO_{2\ eq}$ emission from cement and GP is evaluated in this study, focusing on the amount of cement and GP required for 1 m^3 of UHPC. The amount of $CO_{2\ eq}$ emission was estimated according to [50], which 1 ton of cement and GP produces 846 and 63 kg $CO_{2\ eq}$, respectively, including average transportation of raw materials with global US and Canadian data. Figure 10 presents the relationship between embodied $CO_{2\ eq}$ for the cement content and compressive strength at 28 days under NC regime for the concrete developed in this research as well as these references [5, 13, 16, 17, 45, 50-58]. Obviously, the enhancement of compressive strength of all the analyzed UHPCs corresponds to an increase of the embedded CO_2 emission and environmental impact. The UHPC mixtures designed with GGBS, FA and LP have a low embedded CO2 emission, with a comparable compressive strength at the same age. It can be notice that UHPGC developed in this study still have high compressive strength, and their embedded $CO_{2\ eq}$ emissions are still low. For example, The $CO_{2\ eq}$ and f_c values for the reference mixture were 700 kg/m^3 and 169 MPa at 28 days of NC, respectively, while the $CO_{2\ eq}$ of 70C/30GP and 50C/50GP were 482 and 410 kg/m^3 and f_c were 163 and 152 MPa at 28 days of NC, respectively. In sure the designed UHPGC has a lower environmental impact than the other UHPCs. Hence, In order to achieve "greener" concrete concept as well as with higher mechanical properties, cement was replaced by GP as well as the concrete design should be based on the optimized particle packing model. By this strategy, the CO_2 emission can be reduced and also the glass can be reused and therefore less material have to be landfilled and more natural resources could be saved.

4.5 Cost analysis and health impact of UHGC

Table 2 presents the *cost index* for all the tested UHPC mixtures. The cost presented refers to the price of the cementitious materials, excluding the cost of steel fibers. Figure 11 presents the *cost*

index for all UHPC mixtures normalized to the reference mixture (reference mixture). The 2-day compressive strength obtained under hot curing for those UHPC mixtures containing GP is also presented in Figure 11(left). The replacement of cement by GP led to a slight increase in the compressive strength upto the 20% replacement followed by slight decrease thereafter. However, a slight continuous decrease in the *cost index* can be observed with the augmentation of the replacement ratios. With the higher replacement ratios of QP by GP, a remarkable increase in the compressive strength and decrease of the *cost index* can be obtained as illustrated in Figure 11(right). In addition, the transportation cost of materials could also be reduced when using locally available GP in the production of UHPC.

An intensive effort to replace crystalized QP by other safe and healthy material, due its health problems, is demanded by the Environment Canada and the International Agency for Research on Cancer. The current research offers the amporphous GP as a safe and healthy material to replace QP [59].

5. CONCLUSIONS

Sustainable ultra-high-performance glass concrete (UHPGC) has been developed through the use of glass powder. The glass powder was obtained from recycled glass culets. The glass powder was used to replace cement and quartz powder in conventional UHPC. Typical UHPGC mixes were optimized using the compressible packing model. Based on the results obtained in our study, the following conclusions can be drawn:

- UHPGC can be designed with a ternary system of cement, glass powder, and silica fume.
- This UHGPC offers enhanced fresh behavior owing to its negligible water-absorption capability and smooth surface; the higher glass-powder content results in greater workability.
- Calorimetric analysis shows that replacing cement with GP reduces the maximum heat flow and total heat due to the dilution of cement in the concrete mixture. Replacing the quartz powder, however, didn't affect total heat. The replacement of cement of up to 20% with glass powder accelerated hydration kinetics. Beyond this level, hydration was delayed due to the dilution effect. Replacing the quartz powder accelerated hydration at every percentage of replacement.

- The BSC images of the reference, 80C/20GP, and 0QP/100GP subjected to hot curing for 48 h evidenced a C–S–H hydration rim forming around cement and GP particles. Partial separation of QP particles from the surrounding C–S–H phase was also observed.
- In terms of concrete compressive-strength development, the optimum replace of cement with glass powder was 20%, although 50% seems to be the optimum replacement with respect to flowability and sustainability. Compared to the reference, the mix with 50% glass powder exhibited 90% strength at 2 days under hot curing and 100% strength at 91 days under normal curing.
- Up to 100% of quartz powder can be replaced with glass powder and achieve compressive strengths up to 234 MPa after hot curing. Compared to the reference, the concrete with total quartz-powder replacement exhibited higher increases in compressive strength of about 12% and 17% at 56 and 91 days, respectively, under normal curing.
- More sustainable UHPGC can be produced when glass powder is used to replace both cement and quartz powder, such as in 80C20GP/0QP100GP, which recorded compressive strength, flexural strength, and modulus of elasticity of 220 MPa, 29 MPa, and 55 GPa, respectively. The total amount of glass powder used was about 400 kg/m^3.The replacement of quartz powder and cement with glass powder can significantly reduce the cost of UHPC and decrease the carbon footprint of a typical UHPC. The cost for transporting materials could be reduced when UHPC is produced with glass powder available locally.

6. ACKNOWLEDGEMENTS

This research was funded by Société des Alcools du Québec (SAQ) and the authors gratefully acknowledge this support.

7. REFERENCES

1. Richard P, Cheyrezy M. Composition of reactive powder concretes. Cem Concr Res 1995;25(7):1501–1511.
2. Richard P, Cheyrezy M. Reactive powder concretes with high ductility and 200-800 MPa compressive strength. ACI SP 144 1994:507–518.
3. Dugat J, Roux N, Bernier G. Mechanical properties of reactive powder concretes. Mat and Struc

1996;29:233–240.

4. Roux N, Andrade C, Sanjuan M. Experimental study of durability of reactive powder concretes. J of Mat in Civil Eng 1996;8(1):1–6.
5. Bonneau O, Lachemi M, Dallaire E, Dugat J, Aïtcin P-C. Mechanical properties and durability of two industrial reactive powder concretes. ACI Mat J 1997;94(4):286–290.
6. Soliman N, Tagnit-Hamou A. Study of rheological and mechanical performance of ultra-high-performance glass concrete. ACI SP-fib bulletin and FRC 2014 Joint ACI-fib Int Workshop. Fibre Reinforced Concrete: from Design to Structural Applications 2015:17.
7. Schmidt M, Fehling E. Ultra-high-performance concrete: research, development and application in Europe. ACI SP 225 2005:51–77.
8. Klemens T. Flexible concrete offers new solutions. Concr Const 2004;49(12):72.
9. Soliman N, Omran A, Tagnit-Hamou A. Laboratory characterization and field application of novel ultra-high performance glass concrete. ACI Mat J 2015:41.
10. Racky P. Cost-effectiveness and Sustainability of UHPC. Proc. of the Int Symp on UHPC, Kassel, Germany 2004;13(15):797–805.
11. Aïtcin P-C. Cements of yesterday and today–concrete of tomorrow. Cem Concr Res 2000;30(9):1349–1359.
12. Cheyrezy M, Maret V, Frouin L. Microstructural analysis of RPC (reactive powder concrete). Cem Concr Res 1995;25(7):1491–1500.
13. Habel K, Viviani M, Denarié E, Brühwiler E. Development of the mechanical properties of an ultra-high performance fiber reinforced concrete (UHPFRC). Cem Concr Res 2006;36(7):1362–1370.
14. Environment Canada, https://www.ec.gc.ca/default.asp?lang=en&n=FD9B0E51-1
15. Environment Canada, Health Canada. Screening assessment for the challenge. Report June 2013:7.
16. Soutsos MN, Barnett SJ, Bungey JH, Millard SG. Fast track construction with high-strength concrete mixes containing ground granulated blast furnace slag. ACI SP 228–19 2005:255–270.
17. Yazici H, Yigiter H, Karabulut AS, Baradan B. Utilization of fly ash and ground granulated blast furnace slag as an alternative silica source in reactive powder concrete. Fuel 2008; 87(12):2401–2407.
18. Tuan NV, Ye G, Breugel KV, Fraaij ALA, Bui DD. The study of using rice husk ash to

produce ultra-high performance concrete. Constr and Build Mat 2011;25(4):2030–2035.

19. Puntke W. Wasseranspruch von feinen kornhaufwerken. Beton Schriftenreih 2002:5.
20. Anderson K, Weis T, Thibault B, Khan F, Nanni B, Farber N. A costly diagnosis: subsidizing coal power with albertans' health. Report March 2013:78.
21. Shayan A, Xu A. Value-added utilisation of waste glass in concrete. Cem Concr Res 2004;34(1):81–89.
22. FEVE. Collection for recycling rate in Europe. The European Container Glass Federation (http://www.feve.org/FEVE-STATIS-2013/Recycling-2011-Glass-coll.html date accessed: Sept. 11, 2013).
23. Zidol A, Tognonvi TM, Tagnit-Hamou A. Effect of glass powder on concrete sustainability. 1st Int Conf on Concr Sust (ICCS13) 2012.
24. Terro MJ. Properties of concrete made with recycled crushed glass at elevated temperatures. Build and Env 2006;41(5):633–639.
25. Idir R, Cyr M, Tagnit-Hamou A. Use of waste glass as powder and aggregate in cement-based materials. SBEIDCO – 1st Int Conf on Sust built Env Infr in Developing Countries ENSET, Oran Algeria 12–14 October 2009:109–16.
26. Shi C, Wu Y, Riefler C, Wang H. Characteristic and pozzolanic reactivity of glass powders. Cem Concr Res 2005;35:987–993.
27. Shayan A, Xu A. Performance of glass powder as a pozzolanic material in concrete: a field trial on concrete slabs. Cem Concr Res 2006; 36:457–468.
28. Shao Y, Lefort T, Moras S, Rodriguez D. Studies on concrete containing ground waste glass. Cem Concr Res 2000;30:91–100.
29. Khmiri A, Samet B, Chaabouni M. A cross mixture design to optimise the formulation of a ground waste glass blended cement. Constr Build Mat 2012;28:680–686.
30. Vaitkevicius V, Serelis E, Hilbig H. The effect of glass powder on the microstructure of ultra-high performance concrete. Constr Build Mat 2014;68:102–109.
31. Soliman N, Aïtcin P-C, Tagnit-Hamou A. New generation of ultra-high performance glass concrete. Adv Concr Tech. Publisher: RILEM and CEB-fib, ISBN 978-5-7264-0809-5 Chapter 24, 12-16 May 2014;5:218–227.
32. Andrea S, Chiara BM. ASR expansion behavior of recycled glass fine aggregates in concrete. Cem Concr Res 2010;40:531–536.

33. de Larrard F. Concrete mixture proportioning: a scientific approach. London: Modern Concrete Technology Series, E&FN SPON, 1999.
34. Taha B, Nounu G. Utilizing waste recycled glass as sand/cement replacement in concrete. J of Mat in Civil Eng 2009; 21(12):709–721.
35. Ali EE, Al-Tersawy SH. Recycled glass as a partial replacement for fine aggregate in self-compacting concrete. Constr and Build Mat 2012 35:785–791.
36. Schmidt W. Design concepts for the robustness improvement of self-compacting concrete. Doctoral Thesis. Eindhoven University of Technology, Eindhoven Netherlands 2014.
37. Mirzahosseini M, Riding KA. Effect of curing temperature and glass type on the pozzolanic reactivity of glass powder. Cem Concr Res 2014;58:103–111.
38. Dyer TD, Dhir RK. Chemical reactions of glass cullet used as cement component. J of Mat in Civil Eng 2001;13(6):412–417.
39. Jawed, I. and Skalny, J. Alkalis in cement: a review II. effects of alkalis on hydration and performance of portland cement. Cem Concr Res 1978;8:37–51.
40. Khmiri A, Chaabouni M, Samet B. Chemical behavior of ground waste glass when used as partial cement replacement in mortars. Const and Build Mat 2013;44:74–80.
41. Jansen D, Neubauer J, Goetz-Neunhoeffer F, Haerzschel R, Hergeth WD. Change in reaction kinetics of a portland cement caused by a superplasticizer–calculation of heat flow curves from XRD data. Cem Concr Res 2012;42(2):327–32.
42. Maso JC. Interfacial transition zone in concrete. RILEM Reports, Taylor and Francis 1996:201.
43. Reda MM, Shrive NG, Gillott JE. Microstructural investigation of innovative UHPC. Cem Concr Res 1999; 29(3):323–329.
44. Liu SH, Xie GS, Li LH, Liu Y, Rao MJ. Effect of Glass powder on strength and microstructure of ultra-high performance. Cem-Based Mat 2012:1281-1284.
45. Du H, Tan KH. Waste glass powder as cement replacement in concrete. J of Adv Concr Tech 2014;12:468–477.
46. Tagnit-Hamou A, Bengougam A. Glass powder as a supplementary cementitious material. Concr Int 2012:56–61.
47. Mirzahosseini M, Riding KA. Effect of curing temperature and glass type on the pozzolanic reactivity of glass powder. Cem Concr Res 2014;58:103–111.

48. Zdeb T. Pozzolanic reactivity of ground quartz as a component of concrete with reactive powders. Cem Lime Concr 2007;(1):34–39.
49. Schmidt M, Fehling E, Teichmann T, Bunje K, Bornemann R. Ultra-high performance concrete: perspective for the precast concrete industry. Concr Precast Plant and Tech 2003;69(3):16–29.
50. Marland, G.; Boden, T.; Global CO2 Emissions from Fossil-Fuel Burning,Cement Manufacture, and Gas Flaring: 1751-2000. Carbon Dioxide Information Analysis Center, Oak Ridge National Laboratory Oak Ridge, TN, 2003.
51. Herold, G., and H.S. Müller. 2004. Measurement of porosity of Ultra High Strength Fibre Reinforced Concrete. Proceedings of the International Symposium on Ultra-High Performance Concrete, Kassel, Germany, Sept. 13-15: 685-694.
52. Ghafari E, Costa H, Júlio E, Portugal A, Durães L. The effect of nanosilica addition on flowability, strength and transport properties of ultra-high performance concrete. Mater Des 2014;59:1–9.
53. Soutsos, M.N., Millar, S.G., and K. Karaiskos. 2005. Mix Design, Mechanical Properties, and Impact Resistance of Reactive Powder Concrete (RPC). International RILEM Workshop on High Performance Fiber Reinforced Cementitious Composites in Structural Applications, Honolulu, HI, May.
54. Graybeal, B. 2005. Characterization of the Behavior of Ultra-High Performance Concrete. PhD dissertation, University of Maryland.
55. Habel K, Viviani M, Denarié E, Brühwiler E. Development of the mechanical properties of an Ultra-High Performance Fiber Reinforced Concrete (UHPFRC).Cem Concr Res 2006;36(7):1362–70.
56. Corinaldesi V, Moriconi G. Mechanical and thermal evaluation of Ultra High Performance Fiber Reinforced Concretes for engineering applications. Constr Build Mater 2012;26(1):289–94.
57. Yu R, Spiesz P., Brouwers H.J.H Development of an eco-friendly Ultra-High Performance Concrete (UHPC) with efficient cement and mineral admixtures uses. Cement & Concrete Composites 55 (2015) 383–394
58. Randl N, Steiner T, Ofner S, Baumgartner E, Mészöly T. Development of UHPC mixtures from an ecological point of view. Constr Build Mater 2014;67:373–8.
59. Recyc-Québec, 2015. Le verre Fiches informatives.

LIST OF TABLES

Table 1 – Chemical composition (%) of the type HS cement, quartz sand, quartz powder, glass powder, and silica fume

	Identification	Quartz Sand	Quartz Powder	Glass Powder	HS Cement	Silica Fume
Chemical Composition (%)	Silicon dioxide (SiO_2)	99.80	99.80	73.00	22.00	99.80
	Iron oxide (Fe_2O_3)	0.04	0.09	0.40	4.30	0.09
	Aluminum oxide (Al_2O_3)	0.14	0.11	1.50	3.50	0.11
	Calcium oxide (CaO)	0.17	0.38	11.30	65.6	0.40
	Titanium dioxide (TiO_2)	0.02	0.25	0.04	0.20	--
	Sulfur trioxide (SO_3),	--	0.53	--	2.30	--
	Magnesium oxide (MgO)	0.01	0.20	1.20	1.90	0.20
	Sodium oxide (Na_2O)	--	0.25	13.00	0.07	0.20
	Potassium Oxide (K_2O)	0.05	3.50	0.50	0.80	0.50
	Equivalent alkali (Na_2O_{eq})	--	--	--	0.90	--
	Zinc oxide (ZnO)	--	--	--	0.09	0.25
	Loss on ignition (LOI)	0.20	0.32	0.60	1.00	3.50
Bogue Components	C_3S	--	--	--	50.00	--
	C_2S	--	--	--	25.00	--
	C_3A	--	--	--	2.00	--
	C_4AF	--	--	--	14.00	--
Physical Properties	Specific gravity	2.70	2.73	2.60	3.21	2.20
	Blaine surface area (m^2/kg)	--	--	380	430	20,000
	Mean particle size, d_{50}, (μm)	250	13	12	11	0.15
	Maximum-particle size, d_{max}, (μm)	600	--	100	--	--
	Cost ($/ton)	235	560	150	220	450

Table 2 – Mixture proportioning (kg/m^3)

Material	Reference	Series I (cement replacement)					Series II (QP replacement)		Series III (synergetic effect)	
		90C/10GP	80C/20GP	70C/30GP	60C/40GP	50C/50GP	50QP/50 GP	0QP/100 GP	80C20GP/ 0QP100GP	80C20GP/ 0QP100GP-F
Type HS cement	807	724	639	556	473	392	807	807	636	623
Silica fume	225	224	222	221	219	217	224	224	221	216
Water	195	195	193	192	191	190	195	195	193	188
Water-to-binder ratio *(w/b)*	0.189	0.189	0.189	0.189	0.189	0.189	0.189	0.189	0.189	0.189
Quartz sand	972	966	960	953	947	941	967	967	955	935
Quartz powder	243	241	240	238	237	235	121	--	--	--
Glass powder	--	81	160	238	316	392	121	242	398	390
Solids content in PCE-based HRWRA	13	13	13	13	13	13	13	13	13	13
Steel fiber	--	--	--	--	--	--	--	--	--	158
Cost index ($/$ Referance	1	0.99	0.98	0.97	0.96	0.94	0.93	0.87	0.83	0.83

Table 3 – Fresh properties of UHPC mixtures containing glass powder as a replacement for cement and quartz powder

Property	Reference	Series I (cement replacement)					Series II (QP-replacement)		Series III (synergetic effect)	
		90C/10 GP	80C/20 GP	70C/30 GP	60C/40 GP	50C/50 GP	50QP/50 GP	0QP/100 GP	80C20GP/ 0QP100GP	80C20GP/ 0QP100GP-F
Slump-flow diameter, mm	190	195	205	210	215	220	200	210	220	217
Air void, %	3.8	3.8	4.2	4.1	4.2	4.7	4.1	4.0	4.0	4.3
Unit weight, kg/m^3	2458	2446	2426	2410	2394	2380	2450	2446	2414	2524
Concrete temperature, °C	34	31	28	26	25	23	31	29	28	27

LIST OF FIGURES

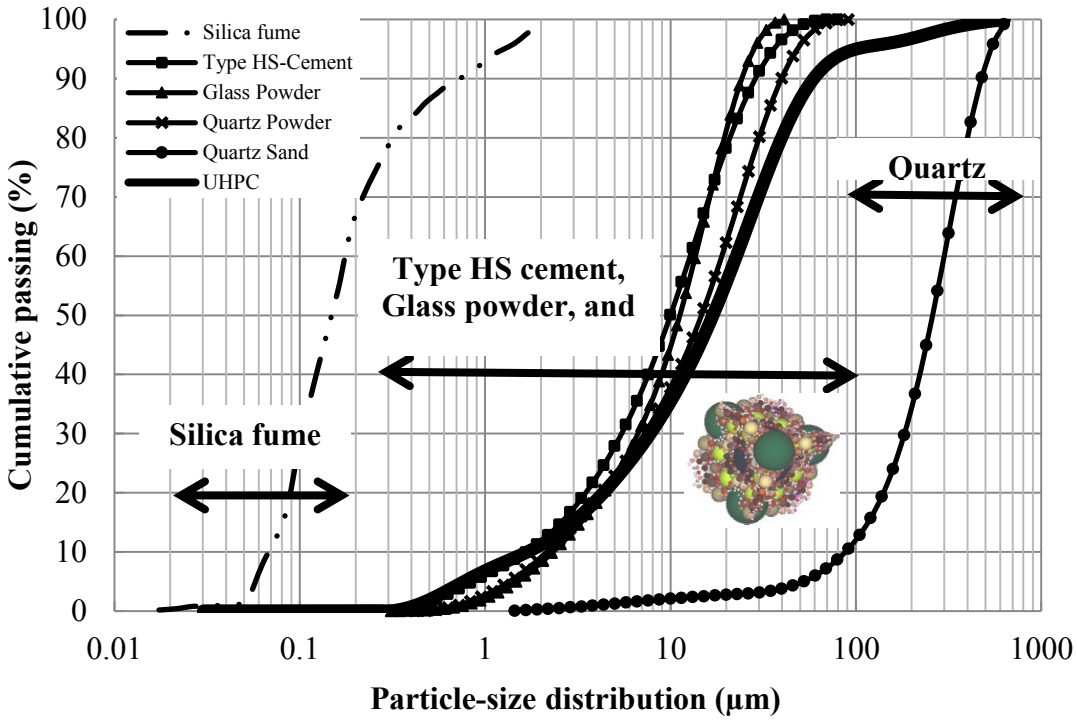

Fig. 1 – Particle-size distributions of individual and combined granular materials used in the UHPC mix design

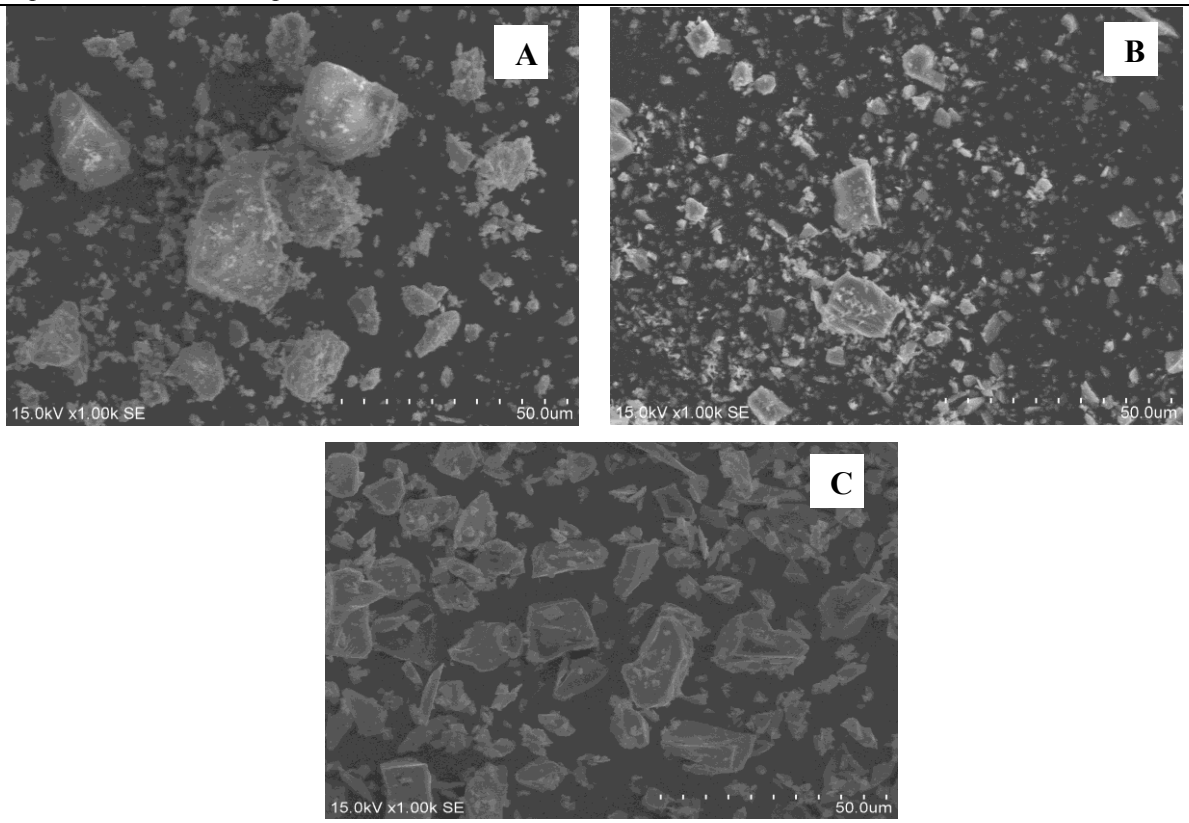

Fig. 2 – Photomicrographs of (A) type HS cement (B) quartz powder, and (C) glass powder

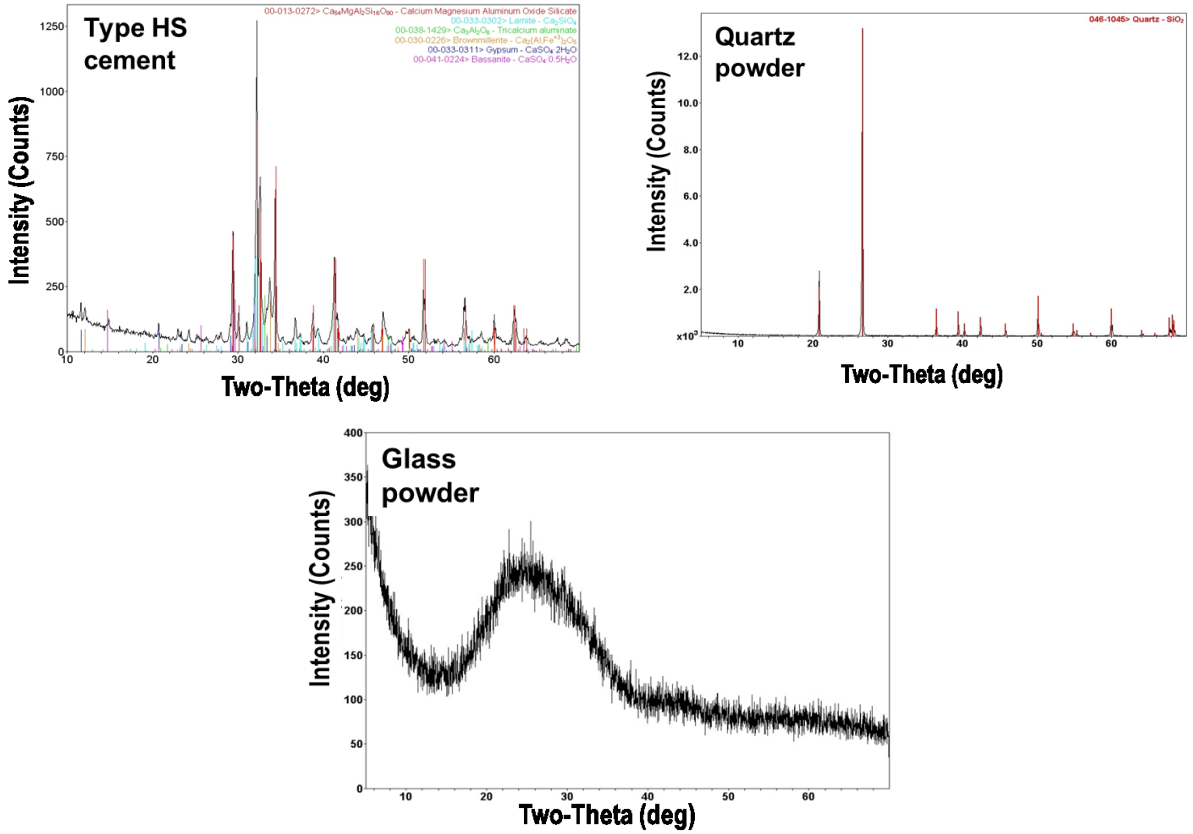

Fig. 3 – X-ray diffraction patterns for type HS cement, quartz powder, and glass powder

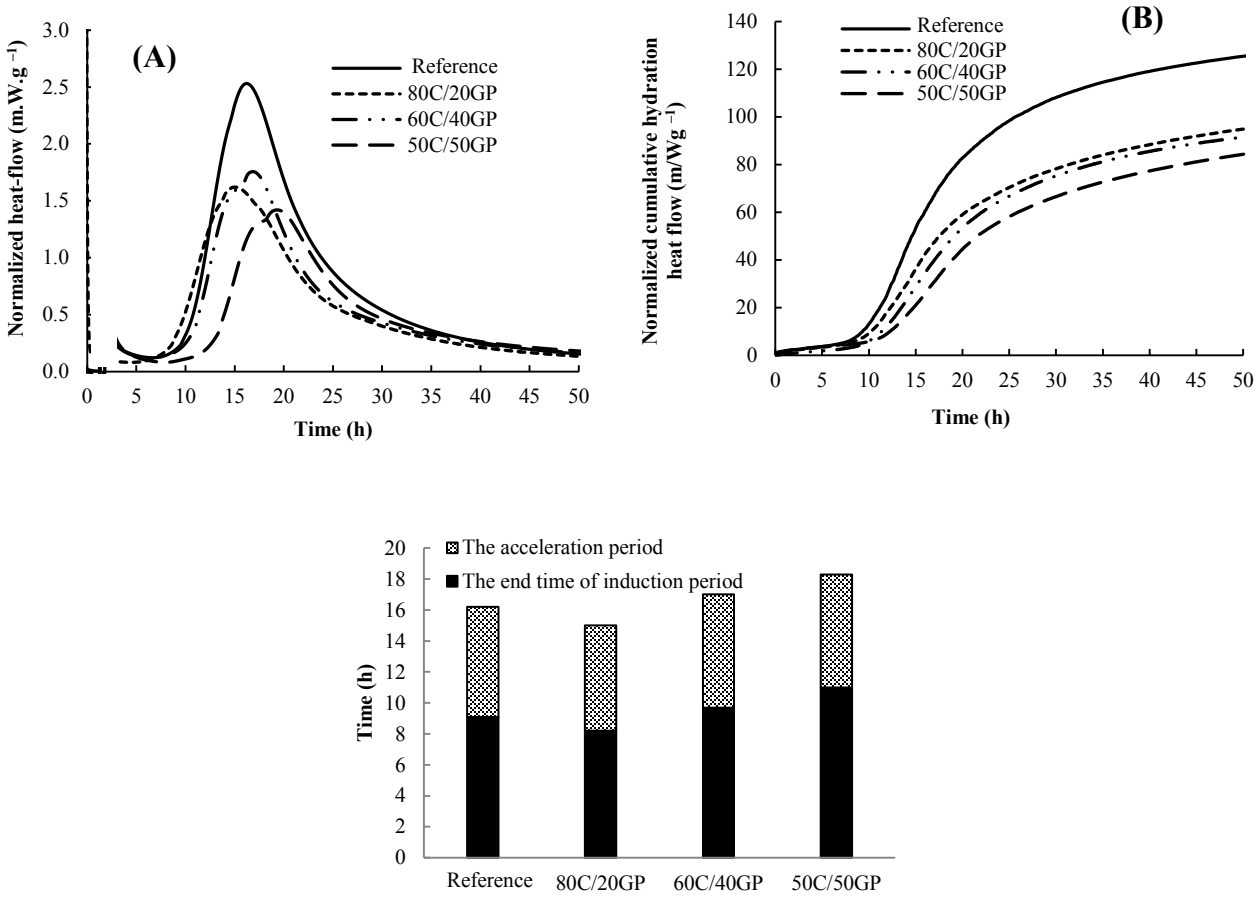

Fig. 4 – Hydration process of cement with various glass-powder replacement levels: (A) evolution of normalized hydration heat flow, (B) normalized cumulative hydration heat flow, and (C) acceleration and induction periods

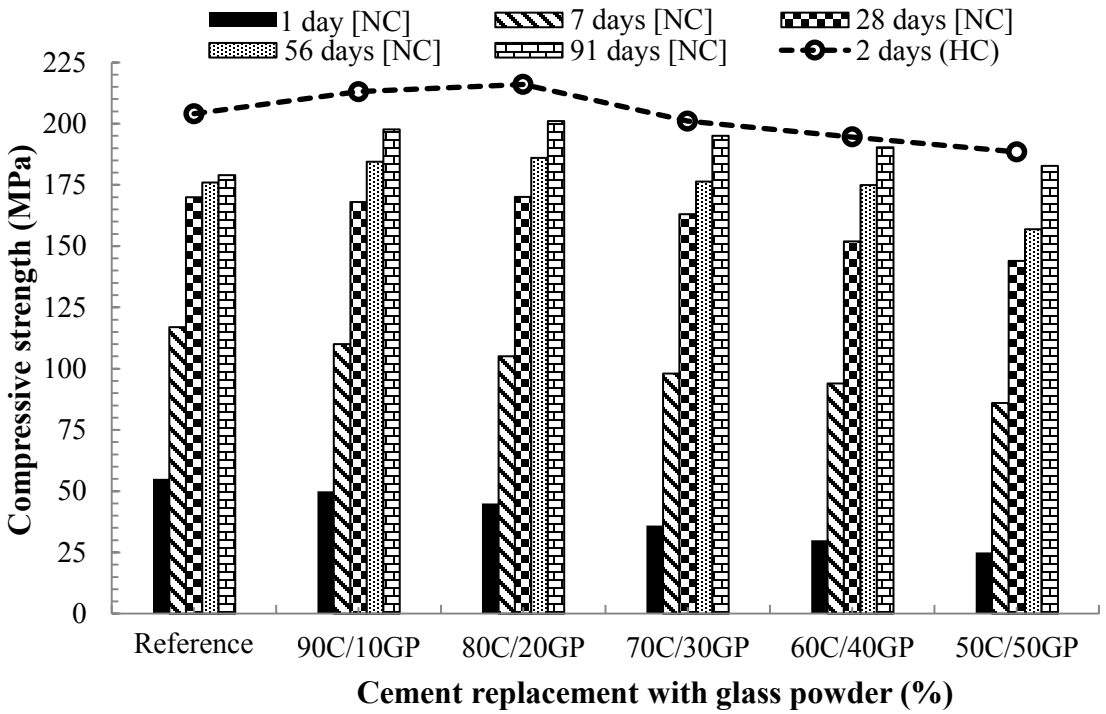

Fig. 5 – Effect of cement replacement with glass powder on compressive strength at different ages after normal curing (NC) and hot curing (HC)

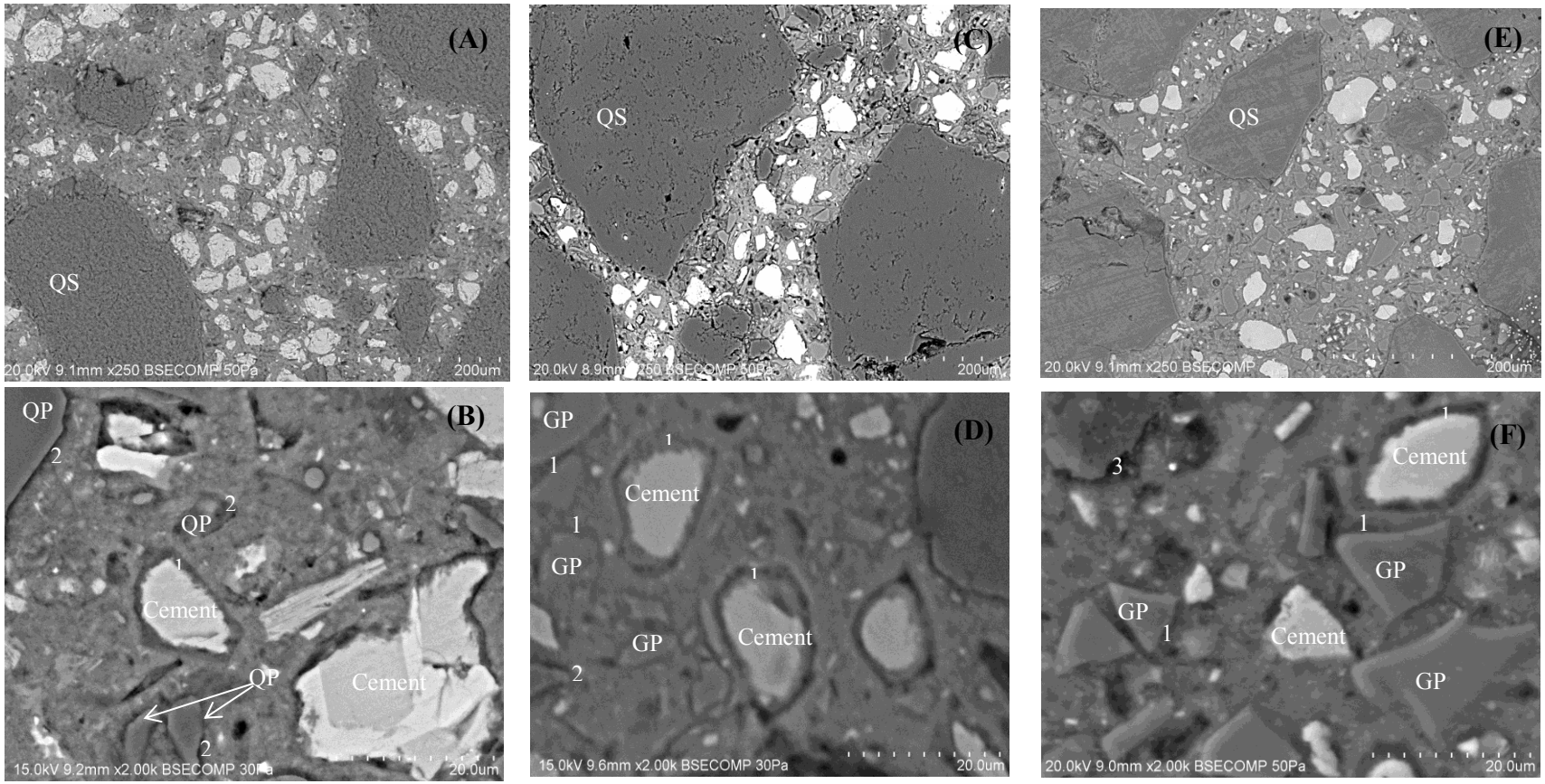

Fig. 6 – BSE/SEM image of specimens under 2 days hot curing (HC): (A,B) reference, (C,D) 80C/20GP, and (E,F) 0QP/100GP; (A,C,E) 250 times magnification (B,D,F) and 2.0K magnification, (1) hydration rim, (2) separation between unreacted QP particles and CSH phase

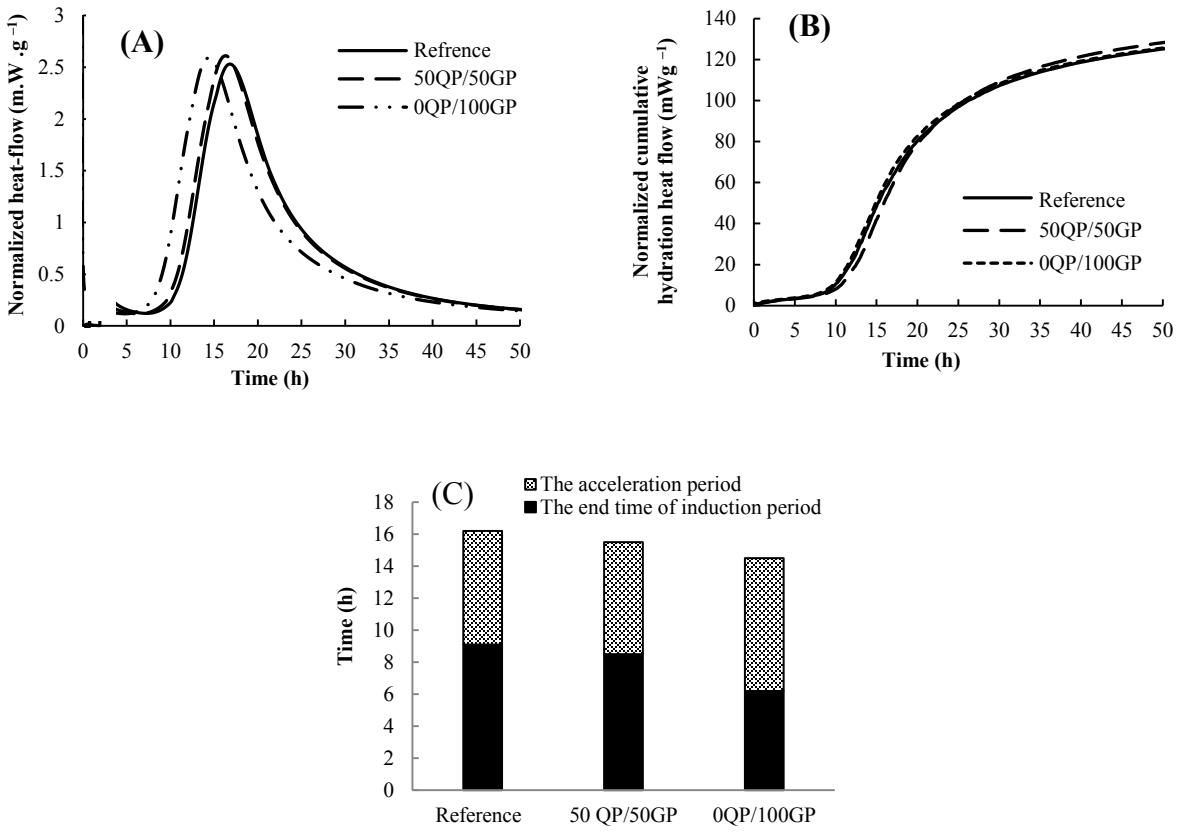

Fig. 7 – Hydration process of UHPC containing quartz powder with various replacement levels by glass powder: (A) evolution of normalized hydration heat flow, (B) normalized cumulative hydration heat flow, and (C) acceleration and induction periods

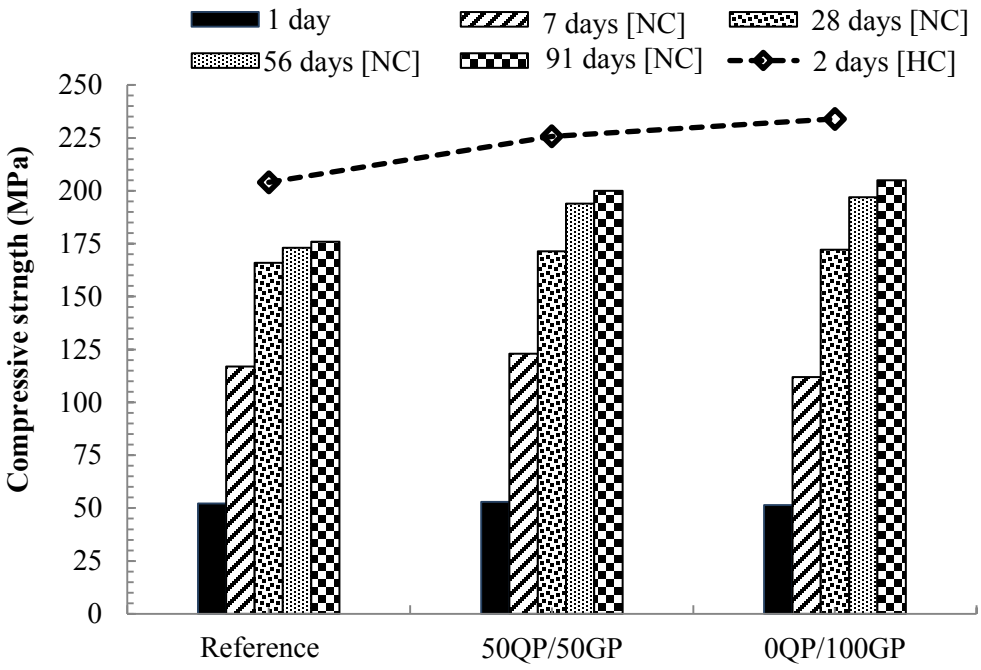

Fig. 8 – Effect of quartz-powder replacement with glass powder on compressive strength at different ages after normal curing (NC) and hot curing (HC)

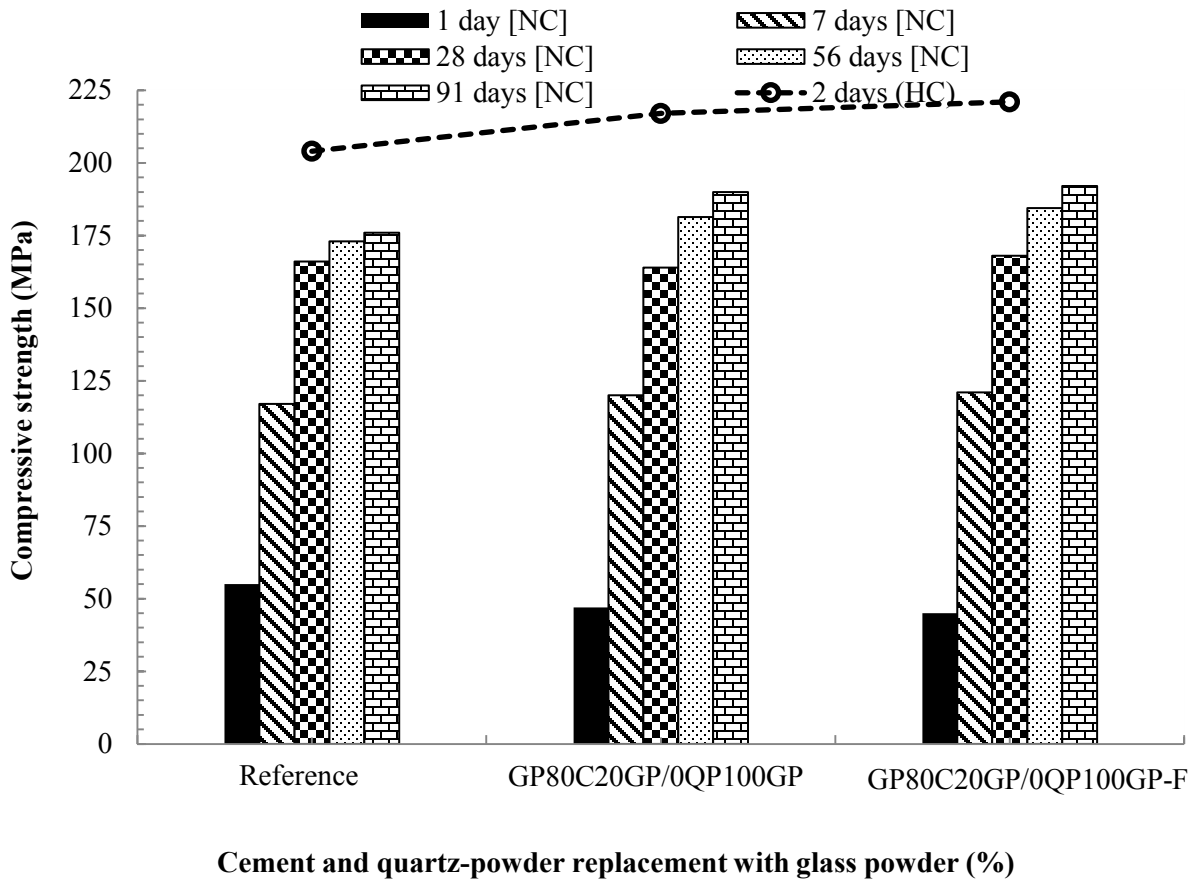

Fig. 9 – Synergetic effect of cement and quartz-powder replacements with glass powder on compressive strength at different ages after normal curing (NC) and hot curing (HC)

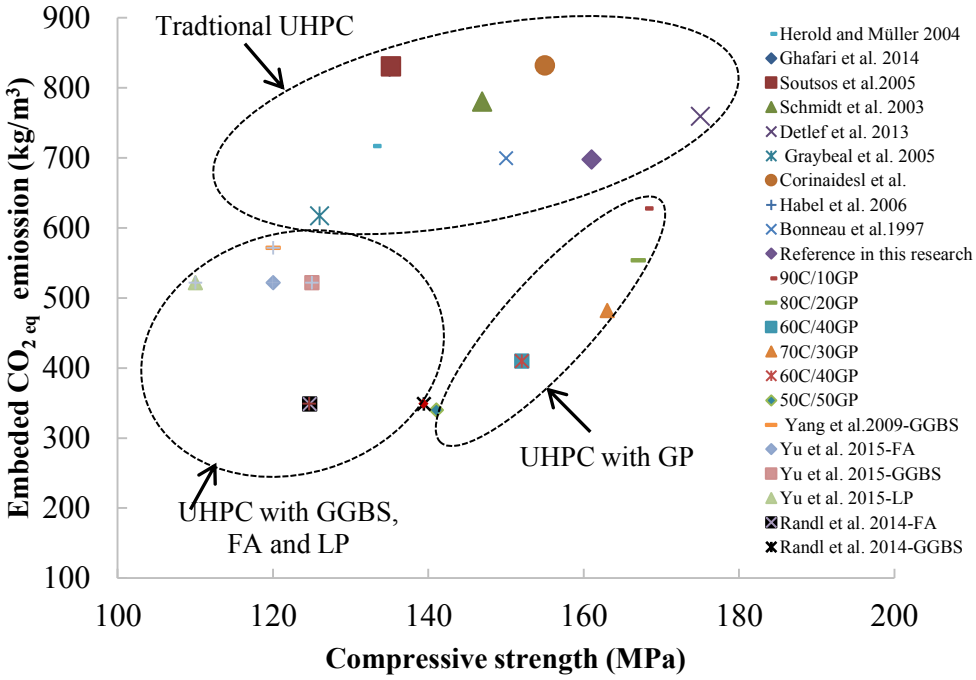

Fig. 10 – Relationship between embodied CO_2 eq for the cement content and compressive strength at 28 days obtained under normal curing

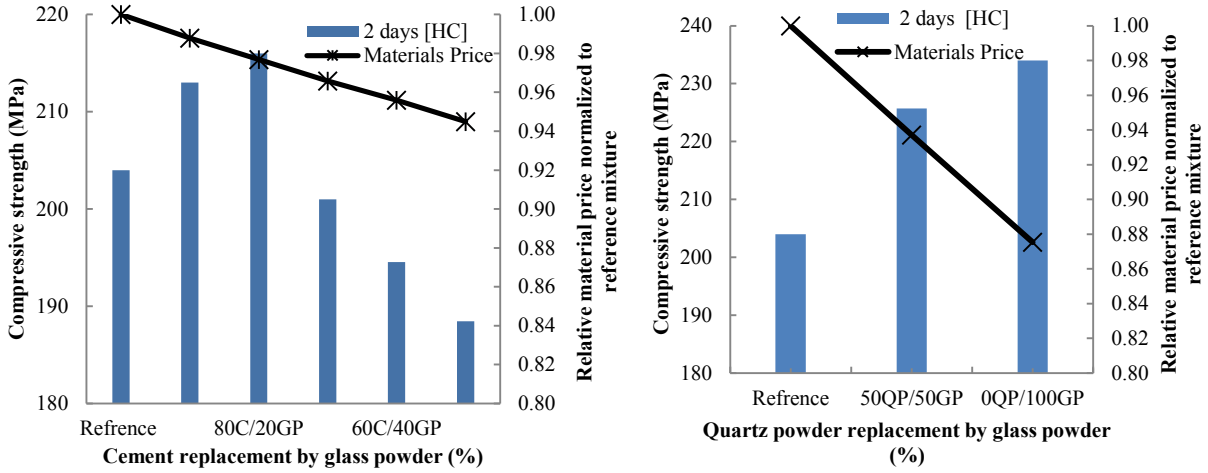

Fig. 11 – Relative material price normalized to reference mixture and the 2-day compressive strength obtained under hot curing for UHPC containing GP; cement replacement by GP (right) and QP replacement by GP (left)

6 Ultra-Fine Powder Replacement in UHPC

6.1 Introduction

This chapter reports on a study to determine the possibility of producing and using fine glass powder (FGP) as a silica fume (SF) replacement in UHPC. FGP with different levels of fineness were produced using an air classifier and jet mill as complete replacement of SF in UHPC mixtures. The workability, packing-density value, and compressive-strength properties of the resultant UHPC mixtures were used to select the optimum FGP fineness. The optimum FGP fineness was selected based on grinding efficiency and performance of the UHPC mixtures. After optimizing FGP fineness, SF replacement ratios varying from 0% to 100% were investigated. The effect of the optimum FGP on fresh properties, hydration kinetics, packing density and compressive strength in UHPC [quartz sand (QS), quartz powder (QP), and cement were kept constant] were investigated. The effects of two different curing conditions on compressive strength of the UHPC mixtures were studied. Descriptions of the materials, mix designs, and mixing sequence used in these experimental tests are given in this chapter.

6.2 Paper 4: Substituting Silica Fume with Fine Glass Powder in UHPC

Reference:
Soliman N.A., Tagnit-Hamou A. (12-16 March, 2016) Substituting Silica Fume with Fine Glass Powder in UHPC. *Journal of Building and Construction Materials.* (Accepted and in press).

Substituting Silica Fume with Fine Glass Powder in UHPC

N.A. Soliman, A. Tagnit-Hamou*

* Corresponding author

Cement and Concrete Research Group, Dept. of Civil Eng., University of Sherbrooke

2500 Blvd. Université, Sherbrooke, Quebec, Canada J1K 2R1

Phone: 819-821-7993, E-mail: A.Tagnit@USherbrooke.ca

Biography

Nancy A. Soliman is member of ACI International and Sherbrooke Local Chapters, and of the CRIB. She is a doctoral candidate in the Department of Civil Engineering, University of Sherbrooke, QC, Canada. Her research interest includes NDT, ultra-high-performance concrete, microstructure, and sustainable development.

FACI **Arezki Tagnit-Hamou** is professor in the Department of Civil Engineering at the University of Sherbrooke, QC, Canada. He also heads the Cement and Concrete Group and holds an industrial chair holder on the "valorization of glass in materials." He serves on ACI Committees 130 (Sustainability of Concrete) and 555 (Concrete with Recycled Materials), and RILEM TC DTA. His research interests include alternative cementitious materials, the physical chemistry and microstructure of cement and concrete, and sustainable development.

ABSTRACT

Given its extreme fineness and high amorphous silica content, silica fume (SF) is an essential and major constituent (25%–30% of cement content) of ultra-high-performance concrete (UHPC). At the same time, its limited resources and its high cost of SF impede the wide use of UHPC in the concrete market. This has motivated the search for other materials with similar functions to partially or fully replace SF in UHPC. This paper reports on a study to determine the possibility of producing and using fine glass powder (FGP) as a SF replacement in UHPC. The results show that FGP with a mean particle size (d_{50}) of 3.8 μm could be recommended as an optimal SF replacement. UHPC incorporating 50% FGP (d_{50} = 3.8 μm) as SF replacement can yield compressive-strength values of 200 MPa under 28-day normal curing and 235 MPa under 2-day steam curing. The use of FGP enhanced concrete workability (50% higher slump flow) compared to SF.

Keywords: Fine glass powder, heat of hydration, silica fume, sustainability, ultra-high-performance concrete.

1. INTRODUCTION

Recent developments in concrete technology have yielded new concrete types such as ultra-high-performance concrete (UHPC). UHPC is defined worldwide as concrete with superior mechanical [compressive strength (f_c) greater than 150 MPa], ductility, and durability properties [1]. Typical UHPC mix designs comprise a very high cement content, silica fume (SF), quartz powder (QP), quartz sand (QS), and steel fibers [2,3]. The fiber inclusion improves UHPC ductility and flexural capacity. UHPC can achieve a flexural strength (f_{fl}) of up to 15 MPa, an elastic modulus (E_c) of 45 GPa, and minimal long-term creep [2,3]. UHPC can also resist freeze–thaw cycles and deicing-salt scaling without any visible damage, and it is nearly impermeable to chloride-ion penetration [4-6]. These excellent characteristics are achieved by enhancing homogeneity, eliminating coarse aggregate, enhancing packing density, improving microstructure, and including fiber [1,2]. Currently, UHPC is used to fabricate special prestressed and precast concrete elements, such as decks and abutments for lightweight bridges, marine platforms, precast walls, concrete repair, and urban furniture and other architectural applications [7-10].

Ultrafine SF with high amorphous silica content has three main functions in UHPC: filling voids in the next larger granular class (cement), enhancing mix lubrication due to its perfectly spherical particles, and producing secondary hydrates through pozzolanic reactions with the primary hydration products [1]. Typically, SF represents about 25% of the total binder materials in UHPC [11]. The theoretical SF amount required to react with the products of cement hydration is 18% [11]. The optimal SF content increases to about 25% to obtain more dense mixtures. Tests revealed that the highest f_c can be achieved with a SF content of 30% [12]. The particle-size distribution (PSD) of cement exhibits a gap at the micro scale (Fig. 1A) that needs to be filled with more finer materials such as SF. Filling this gap solely with SF requires a high amount of SF (25% to 30% by cement weight), as shown in Fig. 1B. This significantly decreases UHPC workability and increases concrete cost. Finding a material with a PSD between that of cement and SF (Fig. 1C) could help reduce SF content and enhance concrete performance. Moreover, the limited available resources and high cost of SF restrict its applications in today's

construction industry, providing impetus to seek out materials with similar characteristics as replacements.

Post-consumer glass can be recycled in many countries several times without significantly altering its physical and chemical properties. Large quantities of glass cannot be recycled because of high breaking potential, color mixing, or expensive recycling costs [13]. Most waste glass goes into landfill sites, which is undesirable as it is not biodegradable and not environmentally friendly [12]. As awareness for protecting the environment has increased, the possibility of converting solid waste into concrete ingredients has drawn increasing attention. In addition to conserving materials and energy, reusing some solid wastes might improve the performance of concrete in several areas. In recent years, attempts have been made to use waste glass as alternative supplementary cementitious materials (ASCMs) or ultrafine fillers in concrete, depending on its chemical composition and PSD [14,15]. Using waste glass as fine aggregate provides concrete with higher chloride-penetration resistance [16-18]. Glass ground to a particle size finer than 38 μm exhibits pozzolanic behavior, which contributes to concrete strength and durability [19-21]. Depending on its fineness, glass powder (GP) exhibits slower pozzolanic reactivity than cement hydration. Thus, replacing cement with GP might decrease strength at an early age, but would increase it at later age. GP with a particle size of 30 μm or less has been used as ASCM to partially replace cement in various concrete types [22-25], significantly decreasing the adverse effects caused by alkali–silica reaction [26,27]. This research work indicates a high value and feasibility of incorporating waste-glass powder in concrete, considering its economic and technical advantages. While very little has been reported on how GP as an ASCM could affect cement paste hydration and microstructure [20], it appears that curing temperature might have a more obvious accelerating effect on the pozzolanic reactivity of GP than on that of FA.

According to Leadership in Energy and Environment Design (LEED) certification, using glass in concrete can double the points resulting from the use of other by-product materials such as SF, FA, and GGBFS. GP is regarded as a post-consumer material, while the others are considered post-production materials. Using GP as a cement substitute has very little environmental impact. The analysis carried out by Recyc-Quebec [28] showed that glass bottles valorized as GP in concrete can be transported within a radius of 8950 km without incurring environmental impacts as compared to landfilling.

The research program reported on herein aimed at developing an innovative low-cost, sustainable UHPC by using fine glass powder (FGP) to replace SF. The optimum FGP fineness was selected based on grinding efficiency and performance of the UHPC mixtures. For this program, FGP of different levels of fineness was produced using an air classifier and jet mill for use as complete replacement of SF in UHPC mixtures. The FGP with the optimum fineness was then used to substitute for different proportions of the SF in various UHPC mixtures (QS, QP, and cement were kept constant). The effect of FGP on fresh properties, hydration kinetics, and mechanical strength of UHPC were investigated. The UHPC mixtures were optimized based on the packing-density theory. The effects of two different curing conditions on compressive of UHPC mixtures were studied: normal curing (NC) at a temperature of 20ºC ± 2ºC and relative humidity (RH) of 100% and standard steam hot curing (HC) at a temperature of 90ºC and RH = 100% for 48 h.

2. RESEARCH SIGNIFICANCE

Replacing silica fume (SF) in UHPC mix designs with fine glass powder (FGP) could save the SF content, which is costly and in limited availability. Waste glass is not biodegradable but can be reused, which reduces the amount that has to be stockpiled or placed in landfills. Replacing SF with FGP can also reduce dramatically the price of conventional UHPC by reducing the SF content or avoiding transportation costs when using locally available FGP is used. Using FGP with medium particle sizes ranging between cement grains and SF particles as a partial SF replacement improves UHPC workability and enhances the concrete's microstructure.

3. EXPERIMENTAL PROGRAM

Fineness is one of the most important properties of materials relating to both physical and chemical effects (i.e., porous structure, filler effect, pozzolanic reaction, grinding energy, and mixture workability). In our study, glass powder was ground with an air classifier and jet mill to different degrees of Blaine fineness ranging between 12,000 and 380 m^2/kg by applying different grinding speeds. In order to determine the optimum fineness, the finely ground glass powder (FGP) was used in conventional UHPC mixtures to fully replace the SF content. The workability

and compressive strength properties of the resultant UHPC mixtures were used to select the optimum FGP fineness.

The FGP with a mean particle diameter (d_{50}) of 3.8 μm optimized in the first experiments was used to replace 0%, 30%, 50%, 70%, and 100% of the SF content in the conventional UHPC. The relevant effects on workability, hydration kinetics, microstructure, and mechanical properties were investigated.

The PSDs for all materials used in this study were determined by laser diffraction. The mix-design optimization method, mixture composition, material properties, and test methods undertaken in this research are detailed in the following sections.

3.1 Materials

In general, concrete rheology is greatly affected by C_3A and C_3S contents as well as cement fineness [11]. This is more pronounced in UHPCs designed with higher cement contents. Therefore, high sulfate-resistant cement (Type HS cement) with low C_3A and C_3S contents was selected for designing the UHPC mixtures. The SF used complied with CAN/CSA A3000 specifications. All of the UHPC mixtures were designed with QP as filler. The waste-glass material with a maximum particle size of 100 μm is referred as glass powder. The silica content of the powder was 73%, its Na_2O content 13%, and its specific gravity 2.60. Table 1 provides the chemical and physical properties of the Type HS cement, SF, QS, QP, and GP. The physical properties include specific gravity, Blain surface fineness, d_{50}, and maximum particle diameter (d_{max}). Fig. 2 gives the PSDs of the Type HS cement, QP, SF, QS, and GP at different levels of fineness. Micrographs Fig. 3A and C show the morphology of SF and FGP particles, respectively. The XRD analysis carried out on these two materials (Fig. 3B and D, respectively) revealed their amorphous nature. A polycarboxylate (PCE)-based high-range water-reducing admixture (HRWRA) with a specific gravity of 1.09 and solid contents of 40% (Sika Viscocrete 6200)) was used in all the concrete mixtures.

3.2 Mix-Design Optimization and Mixture Composition

UHPC development starts with the design of the granular structure of all constituent granular materials. The key factor for enhancing UHPC performance is optimizing its PSD and packing density. The granular structure strongly affects the balance between UHPC rheological behavior and mechanical performance well as the chemical reactivity of UHPC constituents. In our study, the granular structure of the reference UHPC mixture was designed according to the compressible packing model (CPM) developed by de Larrard et al. [29]. Fig. 2 shows the PSD curves for all of the constituent materials (cement, QP, SF, QS, and GP at different levels of fineness) and the optimized curve for the final reference UHPC mixture. The water-to-binder ratio (*w/b*) of 0.19 and HRWRA dosage (expressed as a percentage of solids weight in the HRWRA relative to cement weight) of 1.5% were obtained by optimizing the various mixtures designed with different *w/b* and HRWRA concentrations to yield concretes with certain rheological characteristics and strength requirements [25]. The UHPGC mixtures in Series I and II (Table 2) were designed based on the reference UHPC mixture by taking into account the SF substitution with FGP on a weight basis.

The four mixtures in Series I contained FGP with different PSDs (d_{50} from 2.8 to 12 μm) as total SF replacement. In the four mixtures in Series II, 30%, 50%, 70%, and 100% of the SF content in the reference mixture were replaced with the optimum FGP from Series II (d_{50} = 3.8 μm). The cement, QS, QP, *w/b*, and HRWRA contents were kept constant in all the concrete mixtures. In Series I, the number in the mixture name represents the d_{50} of FGP in the mixture. For example, the GP-5 mixture had FGP with a d_{50} = 5 μm. The mixture name in Series II has two parts: replacement ratios of SF and FGP. For example, the 50SF/50FGP mixture had 50% SF content and 50% FGP.

3.3 Specimen Preparation and Test Methods

All of the concrete mixtures were batched in a high-energy shear mixer with a 10 l capacity. To achieve a homogeneous mixture and avoid particle agglomeration, all of the powder materials were mixed for 10 min before the water and superplasticizer addition. Approximately half of the superplasticizer diluted in half of the mixing water was gradually added over 5 min of mixing time. The remaining water and superplasticizer were gradually added during an additional 5 min of mixing. At the end of mixing, the fresh properties of the UHPC mixtures were measured. The

tests included concrete temperature, unit weight, and air content (ASTM C185). The concrete workability was measured by taking the spread diameter of the mini-slump cone in the flow-table test (ASTM C1437).

The heat flow was measured with a thermometric TAM air-conduction calorimeter containing eight separate measuring cells. About 20 g of fresh mixed paste was weighed in a glass vial with an internal diameter of 24.5 mm. The glass vial was sealed and placed into the calorimeter and the heat flow was measured for about 72 h. During the test, isothermal condition of 20 °C ± 0.02°C was maintained in the measuring cells. The initial heat peak, occurring right after the addition of the water to the cement, could not be measured because the very low *w/b* in UHPC requires external mixing of the paste ingredients before placement in the calorimeter.

The f_c measurements for the UHPC were determined on 50×50×50 mm cubes according to ASTM C109. The samples were tightly covered with plastic sheets and stored at 23°C and 50% RH for 24 h before demolding. After demolding, the samples were cured under two different curing regimes: NC and HC.

4. RESULTS AND DISCUSSIONS

4.1 Production of Fine Glass Powder with Different Fineness

An air classifier and jet mill were used to grind the GP to a fine glass powder (FGP). Various classifier speeds between 2,000 and 22,000 rpm were used to produce different FGPs with different PSDs (d_{50} = 2.8–12 μm) (Table 3). After 15,000 rpm, the energy needed to produce finer particles is very high (3.0 and 7.5 kWh/kg d_{50} of 2.8 and 3.8 μm, respectively).

4.2 Optimizing Fineness of the Fine Glass Powder in UHPC

The FGPs produced (d_{50} of 12, 5, 3.8, and 2.8 μm) were used to completely replace the SF in GP-12, GP-5, GP-3.8, and GP-2.8 mixtures. The workability and mechanical-strength properties of these mixtures were used to select the optimum FGP fineness.

Fig. 4 shows the required superplasticizer (SP) dosages (expressed as a percentage of the SP solids weight to the total binder weight) and measured slump-flow diameters for the tested

mixtures made with FGP of different fineness for a target slump flow between 160 and 250 mm. The results show that FGP fineness strongly influences the concrete workability. When FGP with a small d_{50} was added, the SP dosage decreased. For example, FGP with d_{50} of 12.0, 5.0, 3.8, and 2.8 μm, required SP dosages of 2.5%, 2%, 1.5%, and 1.5%, respectively. GP-12, which contained large FGP particles (d_{50} = 12.0 μm) required the highest SP dosage (2.5%) yet yielded the lowest slump flow (160 mm). In fact, using the FGP particles with d_{50} = 12.0 μm led to a lower concrete packing density (0.69), resulting in poor workability and high SP dosage. Using FGP with this PSD increased concrete porosity, leading to the high SP demand. The SP dosage reduced significantly when the d_{50} of FGP decreased from 12 to 3.8 μm. Mixtures containing FGP with a d_{50} of 3.8 μm or less required similar SP dosages and were similar to that of the reference mixture. This is due to the fact that the finer FGP particles led to high particle packing density in the mixture and absorbed less mixing water than the coarse FGP particles. The respective particle packing-density values for GP-12, GP-5, GP-3.8, and GP-2.8 were 0.69, 0.71, 0.73, and 0.74 (Fig. 4). It can be concluded that FGP with a d_{50} of 3.8 μm can be used successfully to replace SF and leads to higher workability with the same SP dosage.

Table 4 provides the other fresh properties, including air void, unit weight, and concrete temperature. The mixtures containing FGP showed relatively higher air contents than the reference mixture made with SF alone. GP-12 with the coarser FGP particles evidenced the highest air content (6.5%), which matched the lowest particle packing density calculated for this mixture (0.69), while GP-2.8 showed the lowest air content (4.3%), corresponding to a particle packing density of 0.74. This high level of entrapped air was generated from the PCE-based HRWRA without defoaming agent.

Fig. 5 shows the effect of different FGPs as total replacement for SF on the compressive strength of UHPC over time and under the NC and HC curing conditions. It can be seen that the compressive strength increased as the FGP d_{50} decreased, not with standing, the development of GP-3.8's compressive strength was approximately similar to that of GP-2.8, with compressive-strength values over 150 MPa after 2 days of HC. This strength development was due to the enhanced packing density with the use of finer FGP particles, as shown in the particle-packing values in Fig. 5. The mixtures containing FGP developed lower compressive strengths than the corresponding values for the reference mixture. This is possibly due to the fact that SF having a better filler effect. Also, due to a lower pozzolanicity of the FGP which is coarser than SF

particles. It should be noted that the FGP totally replaced the SF. Performances might be improved with different replacement rates.

Based on the grinding energy as well as the workability and compressive strength results of the tested UHPGC mixtures, the FGP with a d_{50} of 3.8 μm can be recommended for partial SF replacement. The ratio between this diameter and the average diameter of cement particles is close to 12 to 13, which is the optimum ratio for particle packing.

4.3 Silica-fume replacement with optimum FGP

The FGP with a d_{50} of 3.8 μm optimized in the previous section was used to replace 0%, 30%, 50%, 70%, and 100% of the SF in the reference UHPC mixture (Series II). The relevant effects on workability, hydration kinetics, microstructure, and mechanical properties were investigated and are detailed below.

4.3.1 Fresh Properties

The fresh properties for the five concrete mixtures in Series II are shown in Table 4 (air content, unit weight, and concrete temperature) and Fig. 6 (slump flow). Comparing them to the reference mixture shows that adding more FGP replacement led to increased flowability because of the low water absorption and smooth surface of the FGP particles. The SF used in this study had a specific surface area of 22,000 m^2/kg, which is approximately, double that of the FGP (10,000 m^2/kg). Therefore, the net total surface area of the SF and FGP blend decreased when FGP was used as an SF replacement. Consequently, the water needed to lubricate particle surfaces decreased due to the decrease in the net particle surface area, increasing the slump flow at the same *w/b*. The particle packing density of all these mixtures also increased from 0.72 (0SF/100FGP mixture) to denser systems (0.75–0.78), which also enhanced the slump flow. All the mixtures with FGP had better slump than the reference.

Table 4 shows slight increases in the unit weight when replacing the SF with FGP due to the FGP having a higher specific gravity than the SF (2.6 vs. 2.2, respectively). All of the mixtures had air content values below 5%. The PCE-based HRWRA was responsible for this high level of entrapped air, given that a defoaming agent was not used. The FGP replacement significantly

decreased concrete temperature, which very positively affected concrete flowability and rheology.

4.3.2 Hydration Kinetics

Isothermal calorimetry was conducted to investigate the pozzolanic reaction of FGP on UHPC hydration at early age. Fig. 7 presents the rate of hydration-heat emission and the cumulative hydration-heat curves in the first 48 h after contact between the water and cementitious materials in the concrete mixtures with 0%, 30%, 50%, 70%, and 100% FGP replacement. These results have been normalized to the total binder weight in the mixture. Clearly, the maximum heat-flow values were a little bet higher at higher SF replacement levels. For example, the 50SF/50FGP and 30SF/70FGP mixtures had increases of 6% and 16%, respectively, in the second exothermic peaks compared to the reference mixture. In contrast, the 0SF/100FGP mixture had the lowest cumulative hydration heat of all the specimens compared to that of the reference mixture, exhibited the highest cumulative hydration heat (Fig. 7B).

Hydration was delayed as the FGP replacement level increased. In fact, the time of the end of induction period (calculated as the time between the lowest point in the heat-flow curve and the first inflection point in the main peak) and the acceleration period (calculated as the time between the first and the second inflection points in the heat-flow curve) relative to the main peak were delayed, as shown in Fig. 7C. To illustrate, the ends of the induction period for the reference, 50SF/50FGP, and 30SF/70FGP mixtures occurred at 9.1, 12, and 14.5 h, while the acceleration periods were about 7.1, 7.5, and 7.5 h, respectively. This delay in hydration is due to the decreased SF content, which decreased the number of different nucleation sites. The heat released at the second peak of hydration increased as a result of the increased FGP content contributing soluble alkalis.

The results herein are consistent with previous findings [30,31]. The delay in hydration with FGP concrete help to avoid strong temperature gradients.

4.3.3 Compressive Strength

Figure 6 presents the compressive strength of the concrete mixtures containing 0%, 30%, 50%, 70%, and 100% FGP after different curing ages and conditions (NC and HC). Replacing 30% and 50% of SF with FGP yielded higher f_c values under NC (at different ages) and HC regimes (Fig. 6). The f_c values for the reference mixture at 91 days of NC and 2 days of HC were 182 and 204 MPa, respectively. The corresponding f_c values were 196 and 234 MPa for the 70SF/30FGP and 185 and 220 MPa for the 50SF/50FGP mixtures, respectively. The 30SF/70FGP mixture exhibited strength similar to that of the reference mixture (Fig. 4). The mixture containing 100% FGP replacement had a 91-day f_c after NC 16% lower than the reference mixture. A decrease of 13% was also noted for the 2-day HC regime. To summarize, the compressive strength of the mixture with 30% FGP replacement (70SF/30FGP) was highest, with increases in f_c values of 4%, 8%, and 15% at 56 days of NC, 91 days of NC, and 2 days of HC, respectively, compared to the reference mixture.

Regardless of the SF replacement ratio, f_c increases of about 10% to 16% were observed in the specimens subjected to 2 days of HC (compared to 91 days of NC). This is attributed to the higher pozzolanic reaction resulting from both the SF and FGP in the mixture, which is activated by high curing temperatures. This pozzolanic reaction led to a denser microstructure of C-S-H in the cement paste, resulting in faster strength development.

5. CONCLUSIONS

Based on the obtained results from this study, the following conclusions can be drawn:

- The glass powder can be ground into finer particles with an air classifier and jet mill to produce fine glass powder with different levels of fineness or particle-size distributions.
- Based on the energy consumption of the air classifier and jet mill, as well as the workability and compressive strength properties of concrete containing the fine glass powder with different levels of fineness, fine glass powder with a mean particle size of 3.8 μm is recommended as a replacement for silica fume when producing UHPC.
- The particle-size distribution (PSD) of cement exhibits a gap at the micro scale that needs to be filled with more finer materials such as SF. Filling this gap solely with SF requires a high amount of SF (25% to 30% by cement weight). This significantly decreases UHPC workability and increases concrete cost. The optimum FGP has a PSD between that of cement

and SF help to reduce SF content and enhance concrete performance. This due the the SF used in this study had a specific surface area of 22,000 m^2/kg, which is approximately double that of the FGP (10,000 m^2/kg). Therefore, the net total surface area of the SF and FGP blend decreased when FGP was used as an SF replacement. Consequently, the water needed to lubricate particle surfaces decreased due to the decrease in the net particle surface area, increasing the slump flow at the same *w/b*. Moreover, the excess water enhances cement hydration, leading to enhancement in the compressive strength up to a given level.

- An optimum silica fume replacement ratio of 30% by fine glass powder can be recommended with respect to the compressive strength development. Compared to the concrete mix with silica fume, the mix with 30% fine glass powder exhibited 15% higher strength after 2 day of hot curing. The replacement ratio of 70% by fine glass powder gives approximately similar strength and enhances the workability by 50% compared to the mixture with only silica fume, but associated with setting time retardation. The 50% fine glass powder replacement can be considered as the optimum replacement ratio, as it enhanced the workability (20%) and strength (8%), while did not show any delay in the setting time.
- Replacing silica fume with fine glass powder can significantly reduce the cost of UHPC. Material transportation costs could also be reduced by using locally available fine glass powder in UHPC production.

6. ACKNOWLEDGEMENTS

This research was funded by the Société des Alcools du Québec (SAQ) and the authors gratefully acknowledge its support.

7. REFERENCES

1. P. Richard, M. Cheyrezy, Composition of reactive powder concretes, Cem. Concr. Res. 25(7) (1995) 1501–1511.
2. P. Richard, M. Cheyrezy, Reactive powder concretes with high ductility and 200-800 MPa compressive strength, ACI SP 144 (1994) 507–518.
3. J. Dugat, N. Roux, G. Bernier, Mechanical properties of reactive powder concretes, Mat. and Struc.

(29) (1996) 233–240.

4. N. Roux, C. Andrade, M. Sanjuan, Experimental study of durability of reactive powder concretes, J. of Mat. in Civil Eng. 8 (1) (1996) 1–6.
5. O. Bonneau, M. Lachemi, E. Dallaire, J. Dugat, P-C. Aïtcin, Mechanical properties and durability of two industrial reactive powder concretes, ACI Mat. J. 94 (4) (1997) 286–290.
6. N. Soliman, A. Tagnit-Hamou, Study of rheological and mechanical performance of ultra-high-performance glass concrete, ACI SP-fib bulletin and FRC 2014 Joint ACI-fib Int Workshop. Fibre Reinforced Concrete: from Design to Structural Applications (2015) 17.
7. M. Schmidt, E. Fehling, Ultra-high-performance concrete: research, development and application in Europe, ACI SP 225 (2005) 51–77.
8. T. Klemens, Flexible concrete offers new solutions, Concr. Const. 49 (12) (2004) 72.
9. N. Soliman, A. Omran, A. Tagnit-Hamou, Laboratory characterization and field application of novel ultra-high performance glass concrete, ACI Mat. J. (2015), in press.
10. P. Racky, Cost-effectiveness and Sustainability of UHPC, Proc. of the Int. Symp. on UHPC, Kassel, Germany 13 (15) (2004) 797–805.
11. V. Matte, M. Moranville, Durability of reactive powder composites: influence of silica fume on the leaching properties of very low water/binder pastes. Cem. Concr. Compo. 21 (1) (1999) 1–9.
12. J. Ma, H. Schneider, Properties of ultra-high-Performance concrete. Leipzig Annual Civil Engineering Report (LACER) (2002) 25–32.
13. A. Shayan, A. Xu, Value-added utilization of waste glass in concrete. Cem. Concr. Res. 34 (1) (2004) 81–89.
14. A. Zidol, T. M. Tognonvi, A. Tagnit-Hamou, Effect of glass powder on concrete sustainability. 1st Int. Conf. on Concr. Sust. (ICCS13) (2012).
15. M. J. Terro, Properties of concrete made with recycled crushed glass at elevated temperatures, Build. and Env. 41 (5) (2006) 633–639.
16. T. C. Ling, C. S. Poon, S. C. Kou, Feasibility of using recycled glass in architectural cement mortars, Cem. Concr. Compos. 33 (8) (2011) 848–854.
17. K. H. Tan, H. Du, Use of waste glass as sand in mortar: Part I – fresh, mechanical and durability properties. Cem. Conc. Compos. 35 (1) (2013) 109–117.

18. H. Du, K. H. Tan, Waste glass powder as cement replacement in concrete, J. of Adv. Concr. Tech. 12 (2014) 468–477.
19. R. Idir, M. Cyr, A. Tagnit-Hamou, Use of waste glass as powder and aggregate in cement-based materials. SBEIDCO – 1st Int Conf, on Sust, built, Env, Infr, in Developing Countries ENSET, Oran Algeria (12–14 October 2009) 109–16.
20. C. Shi, Y. Wu, C. Riefler, H. Wang. Characteristic and pozzolanic reactivity of glass powders, Cem. Concr. Res. 35 (2005) 987–993.
21. A. Shayan, A. Xu, Performance of glass powder as a pozzolanic material in concrete: a field trial on concrete slabs, Cem. Concr. Res. 36 (2006) 457–468.
22. Y. Shao, T. Lefort, S. Moras, D. Rodriguez, Studies on concrete containing ground waste glass, Cem. Concr. Res. 30 (2000) 91–100.
23. A. Khmiri, B. Samet, M. Chaabouni, A cross mixture design to optimize the formulation of a ground waste glass blended cement, Constr. Build. Mat. 28 (2012) 680–686.
24. V. Vaitkevicius, E. Serelis, H. Hilbig, The effect of glass powder on the microstructure of ultra-high performance concrete, Constr. Build. Mat. 68 (2014) 102–109.
25. N. Soliman, P.-C. Aïtcin, A. Tagnit-Hamou, New generation of ultra-high performance glass concrete, Adv. Concr. Tech. Publisher: RILEM and CEB-fib, ISBN 978-5-7264-0809-5, Chapter 24 (5) (12-16 May 2014) 218–227.
26. S. Andrea, B. M. Chiara, ASR expansion behavior of recycled glass fine aggregates in concrete, Cem. Concr. Res. 40 (2010) 531–536.
27. W. Jin, C. Meyer, Baxer, Glascrete-concrete with glass aggregate, ACI Mat. J. 97(2) (2000) 208–213.
28. Recyc-Quebec annual report 2014-2015. Des gestes porteurs d'avenir, In french, (2015) 52.
29. F. de Larrard, Concrete mixture proportioning: a scientific approach. London: Modern Concrete Technology Series, E&FN SPON (1999).
30. M. Mirzahosseini, K. A. Riding, Effect of curing temperature and glass type on the pozzolanic reactivity of glass powder, Cem. Concr. Res. 58 (2014) 103–111.
31. T. D. Dyer, R. K. Dhir, Chemical reactions of glass cullet used as cement component, J. of Mat. in Civil Eng. 13 (6) (2001) 412–417.

LIST OF TABLES

LIST OF FIGURES

Table 1 – Chemical compositions (%) of Type HS cement, quartz sand, quartz powder, glass powder, and silica fume

	Identification	Quartz sand	Quartz powder	Glass powder	HS cement	Silica fume
Chemical composition (%)	Silicon dioxide (SiO_2)	99.80	99.80	73.00	22.00	99.80
	Iron oxide (Fe_2O_3)	0.04	0.09	0.40	4.30	0.09
	Aluminum oxide (Al_2O_3)	0.14	0.11	1.50	3.50	0.11
	Calcium oxide (CaO)	0.17	0.38	11.30	65.6	0.40
	Titanium dioxide (TiO_2)	0.02	0.25	0.04	0.20	--
	Sulfur trioxide (SO_3),	--	0.53	--	2.30	--
	Magnesium oxide (MgO)	0.01	0.20	1.20	1.90	0.20
	Sodium oxide (Na_2O)	--	0.25	13.00	0.07	0.20
	Potassium oxide (K_2O)	0.05	3.50	0.50	0.80	0.50
	Equivalent alkali (Na_2O_{eq})	--	--	--	0.90	--
	Zinc oxide (ZnO)	--	--	--	0.09	0.25
	Loss on ignition (LOI)	0.20	0.32	0.60	1.00	3.50
Boge components	C_3S	--	--	--	50.00	--
	C_2S	--	--	--	25.00	--
	C_3A	--	--	--	2.00	--
	C_4AF	--	--	--	14.00	--
Physical properties	Unit weight	2.70	2.73	2.60	3.21	2.20
	Blaine surface area (m^2/kg)	--	--	380	430	20,000
	Mean particle size, d_{50}, (μm)	250	13	12	11	0.15
	Maximum particle size, d_{max}, (μm)	600	--	100	--	--

Table 2 – Mixture proportioning (kg/m^3)

Material		Reference	Series I (100% replacement SF with GP with different levels of fineness)				Series II (SF replacement with optimum FGP)			
			GP-12	GP-5	GP-3.8	GP-2.8	70SF/30 FGP	50SF/50 FGP	30SF/70 FGP	0SF/100 FGP
Type HS cement		810	823	823	823	823	813	816	819	823
Silica fume		225	--	--	--	--	163	113	68	--
Fine glass powder	Glass powder-12	--	229	--	--	--	--	--	--	--
	Glass powder-5.0	--	--	229	--	--	--	--	--	--
	Glass powder-3.8	--	--	--	229	--	63	113	159	229
	Glass powder-2.8	--	--	--	--	229	--	--	--	--
Water		196	199	199	199	199	198	197	198	199
Quartz sand		972	987	987	987	987	976	980	983	987
Quartz powder		243	247	247	247	247	244	245	246	247
Solid content in PCE-based HRWRA		13	13	13	13	13	13	13	13	13
Particle packing density		0.79	0.69	0.71	0.73	0.74	0.78	0.77	0.75	0.73

Table 3 – Optimization of fine-glass-powder granulometry with an air classifier and jet mill

Classifier speed (rpm)	0	2,000	5,000	10,000	15,000	22,000
Blaine surface (m^2/kg)	382	382	420	950	10,000	12,000
Maximum particle-size diameter, d_{max} (μm)	50	40	38	15	10	8
Mean particle-size diameter, d_{50} (μm)	12.0	12.0	12.0	5.0	3.8	2.8
Production rate of glass powder (g/h)	750	750	750	500	270	20

Table 4 – Fresh-concrete properties

	Reference	Series I (100% replacement of SF with FGP with different levels of fineness)				Series II (SF replacement with optimum FGP)			
Property		GP-12	GP-5	GP-3.8	GP-2.8	70SF/30FGP	50SF/50FGP	30SF/70FGP	0SF/100FGP
Air void, %	3.8	6.5	5.2	4.8	4.3	3.3	3.5	3.8	5.0
Unit weight, kg/m^3	2363	2337	2367	2378	2390	2386	2382	2402	2378
Concrete temperature, °C	34	28	28	29	31	31	29	28	28

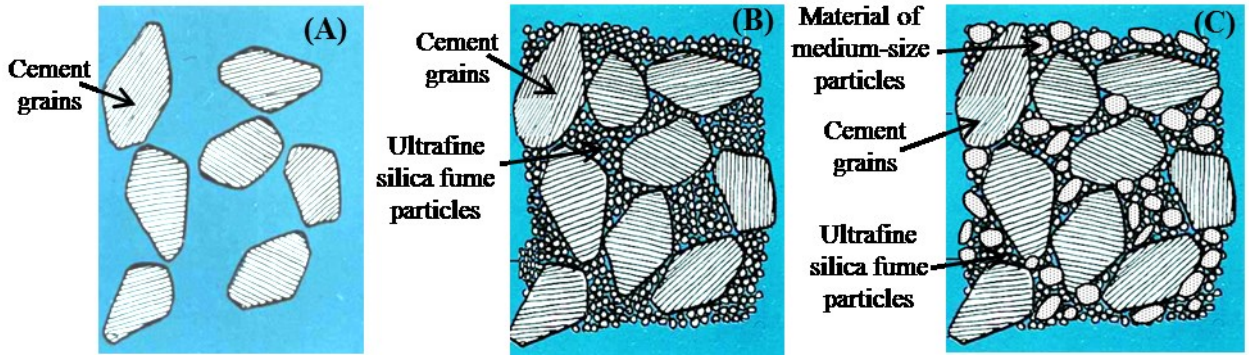

Fig. 1 – Sketch presents: (A) cement grains, (B) cement grains surrounded by many silica-fume particles, and (C) cement grains surrounded by silica-fume particles and a material with medium-size particles

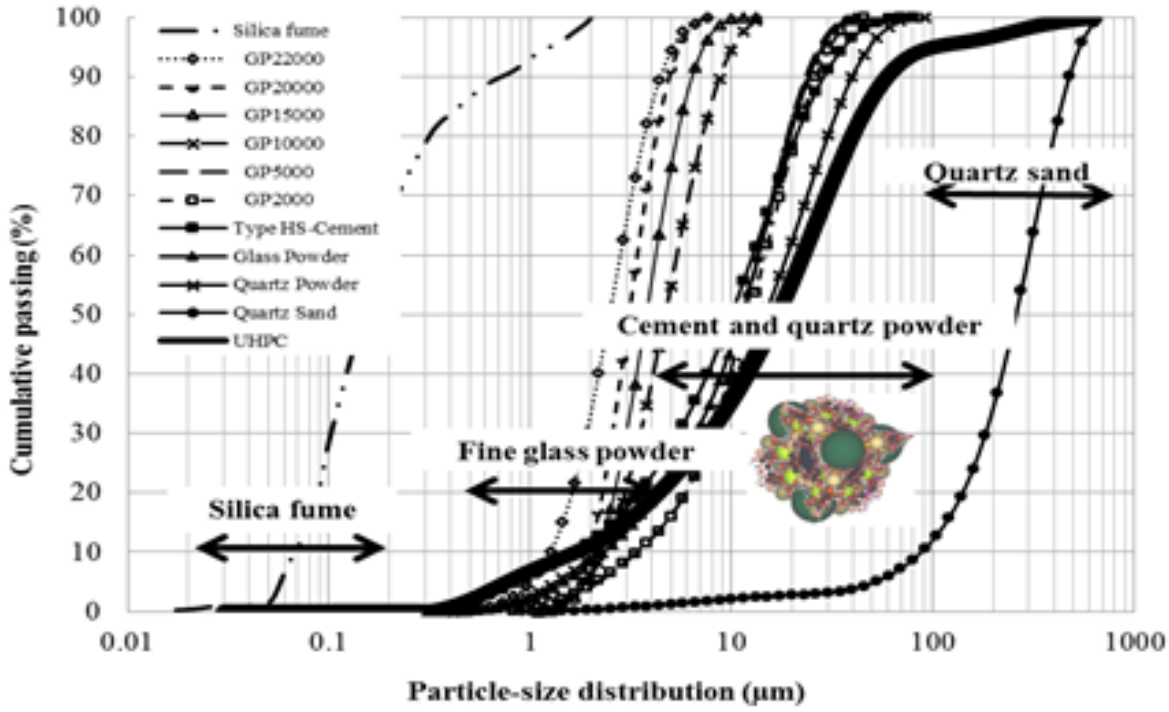

Fig. 2 – Particle-size distributions of individual and combined granular materials used in the UHPC mix design

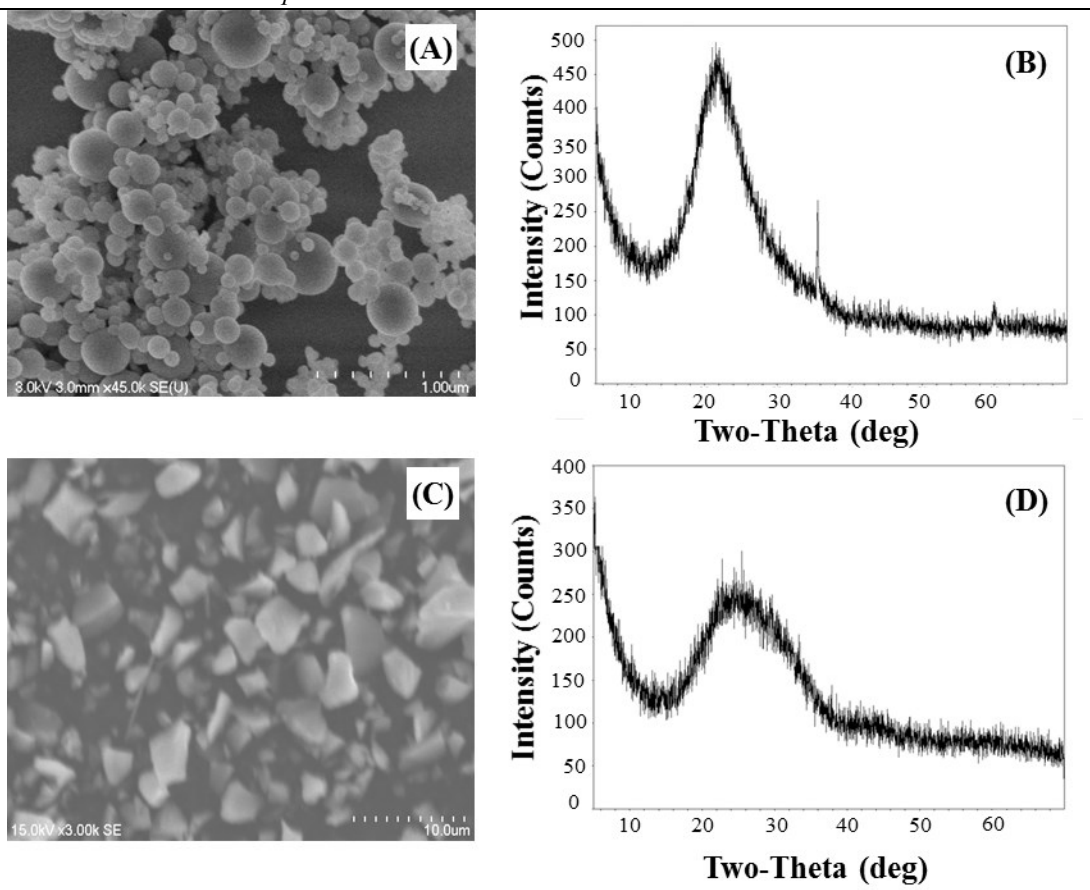

Fig. 3 – Silica fume: (A) photomicrograph and (B) X-ray diffraction patterns

Fine glass powder: (C) photomicrograph and (D) X-ray diffraction patterns

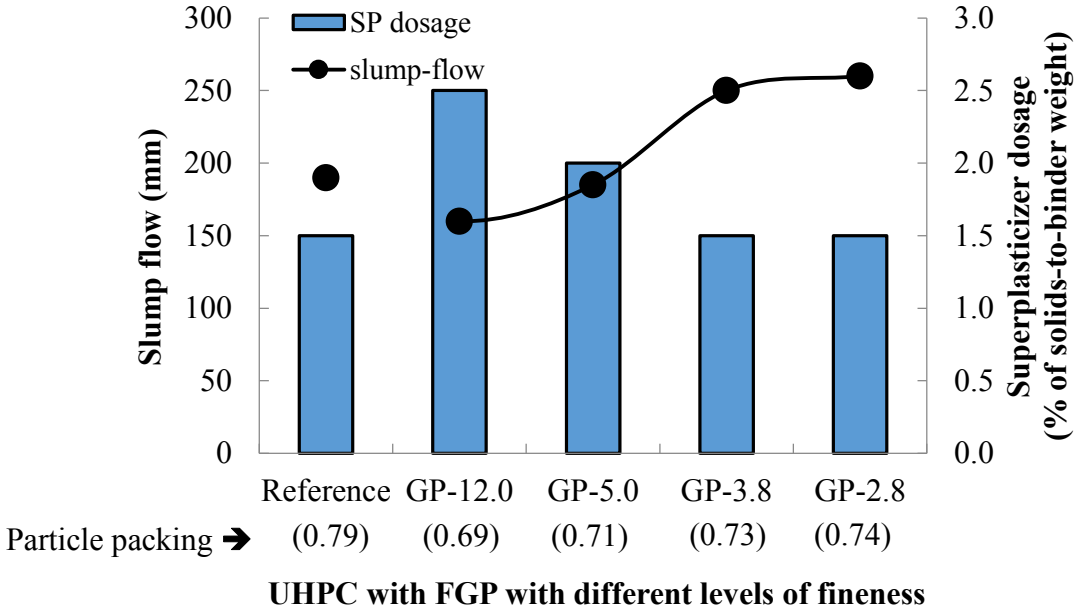

Fig. 4 – Slump-flow diameter and superplasticizer dosage for UHPGC mixtures made with fine glass powder (FGP) with different levels of fineness

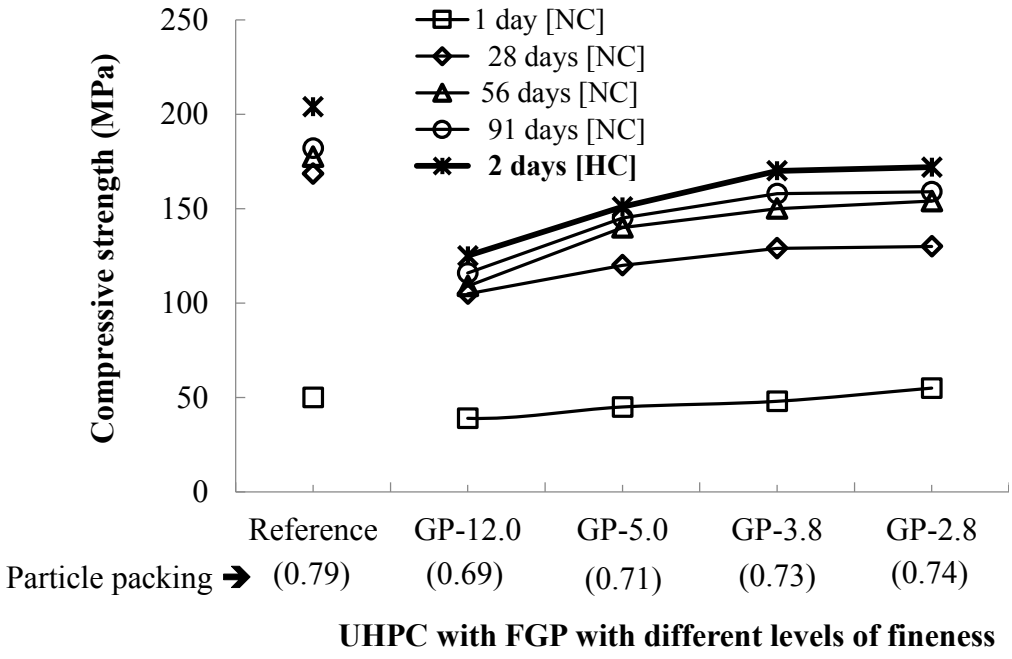

Fig. 5 – Compressive strength at different curing periods and under different conditions for UHPC mixtures made with fine glass powder (FGP) with different levels of fineness

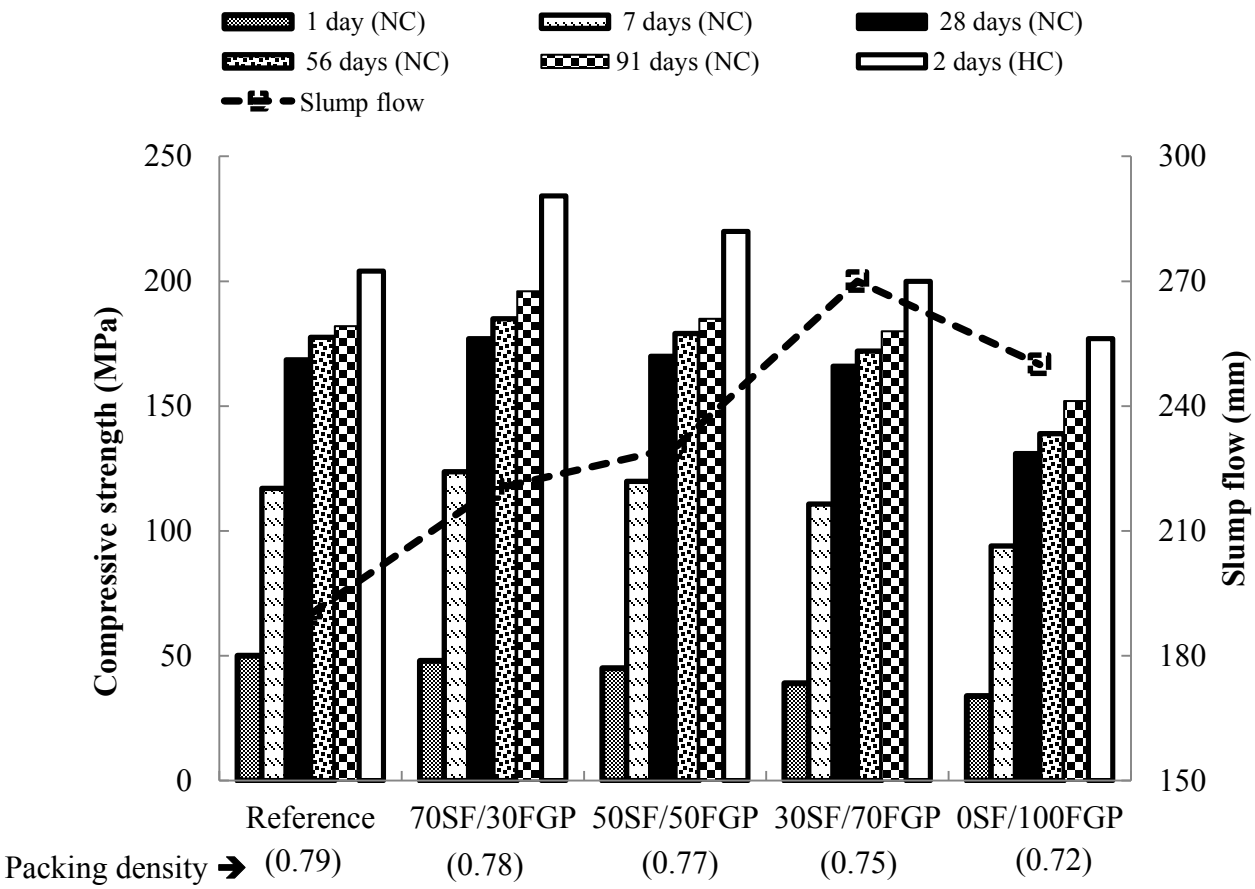

Fig. 6 – Effect of silica-fume replacement with fine glass powder on slump flow and compressive-strength development at different ages and under different curing conditions [normal (NC) and hot (HC) curing]

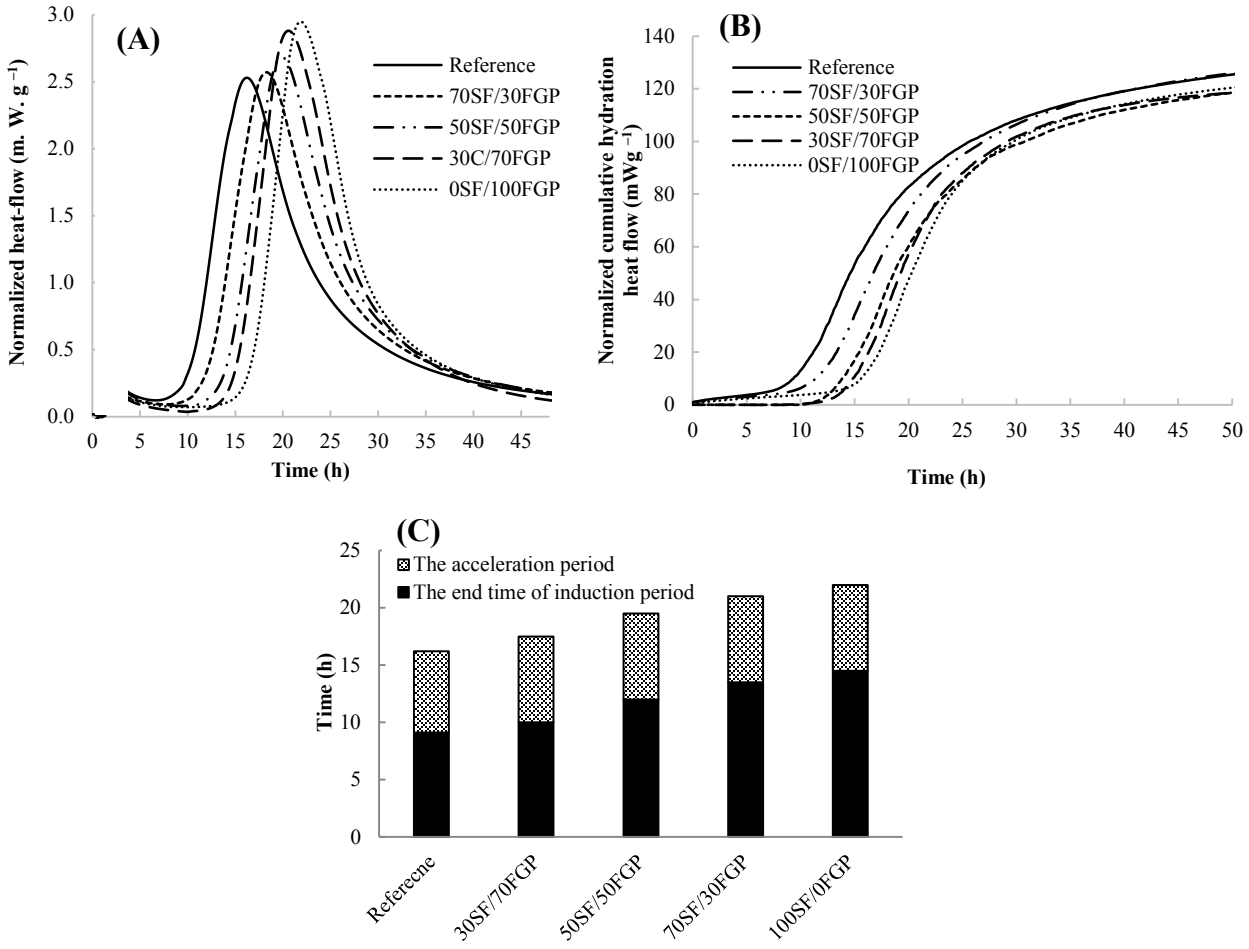

Fig. 7 – Hydration process of cement with different replacement levels of silica fume with fine glass powder: (A) evolution of normalized hydration-heat flow, (B) normalized cumulative hydration-heat flow, and (C) acceleration and induction periods

7 Synergetic Effect of Interaction of Different Particle-Size Distribution

7.1 Introduction

Chapter 7 presents the synergetic effect of interaction of different PSD of waste glass materials on fresh and mechanical properties of UHPGC. The cement was replaced by glass powder-1 (*GP1/C*) up to 40%, quartz powder was replaced by glass powder-2 (*GP1/QP*) up to 100%, silica fume was substituted by fine glass powder (*FGP/SF*) up to 50%, and glass sand replaced up to 50% of the quartz sand. An experimental design approach was applied to account for the water-to-binder ratio (*w/b*) and the four previous mixture parameters as well as their coupled interactions on the development of fresh and mechanical characteristics. Prediction statistical models were established, evaluated, and validated in this study. Contour diagrams to tradeoff between different UHPC ingredients to predict the various concrete performances are also presented in this paper. Finally, the derived models are used to optimize the concrete constituents' combination that gives the optimum performance. Descriptions of materials, mix designs, and mixing sequence used in these experimental tests are given in this chapter. More results in the production processing are details in the appendix in the paper 8.

7.2 Paper 5: Experimental design approach for producing eco-friendly ultra-high-performance-glass concrete

Reference:
Soliman N.A., Omran A.F., Tagnit-Hamou A. (2016) Experimental design approach for producing eco-friendly ultra-high-performance-glass concrete. *ACI materials Journal.* (to be submitted).

Experimental design approach for producing eco-friendly ultra-high-performance-glass concrete

Nancy Soliman[1] · Ahmed Omran[2] · Arezki Tagnit-Hamou[3]

Authors and Affiliation

Nancy A. Soliman, is a member of the ACI international and Sherbrooke local chapters, and CRIB. She is a PhD candidate in the Department of Civil Engineering, University of Sherbrooke, QC, Canada. Her research interest includes NDT, UHPC, microstructure, and sustainable development.

Ahmed F. Omran, is a postdoctoral fellow of Department of Civil Engineering, University of Sherbrooke and assistant professor of University of Minoufiya, Egypt. He holds BS and MS degrees in Civil Engineering from University of Minoufiya. He received Ph.D. degree from University of Sherbrooke. He is an active member of RILEM TC-233 FPC Committee. His research interests include durability of cement-based materials, development of new alternative supplementary cementitious materials (ASCM), sustainable development, concrete rheology, and formwork pressure.

Arezki Tagnit-Hamou, FACI, is a professor in the Department of Civil Engineering at the University of Sherbrooke, QC, Canada. He is also the Head of the cement and concrete group as well as holding an industrial chair on valorization of glass in materials. He is a member of ACI Committees 130 (Sustainability of Concrete) and 555 (Concrete with Recycled Materials), and RILEM TC DTA. His research interests include alternative supplementary cementitious materials, cement and concrete physicochemistry and microstructure, and sustainable development.

[1] PhD Candidate, Dept. of Civil Eng., Univ. of Sherbrooke. E-mail: Nancy.Soliman@USherbrooke.ca
[2] Research Associate in Cement and Concrete Research Group, Dept. of Civil Eng. University of Sherbrooke Canada, and Assistant Professor at University of Minoufiya, Egypt. Email: A.Omran@USherbrooke.ca
[3] (Corresponding author) Professor and head of Cement and Concrete Research Group, Dept. of Civil Eng., University of Sherbrooke. Address: 2500 Blvd. Université, Sherbrooke, Quebec, Canada J1K 2R1. Phone: (819) 821-7993, E-mail: A.Tagnit@USherbrooke.ca

Abstract:

Incorporating ground waste glass cullets in conventional ultra-high-performance concrete (UHPC) production can double the benefits of avoiding the stockpiling of waste glass in landfills, and replaces cement (C), quartz powder (QP), silica fume (SF), and quartz sand (QS) for the cost and environmental protection. This study presents the production of sustainable UHPC mixtures by incorporating ground waste glass cullets of different particle-size distributions (mean-particle diameter from 275 to 3.8 μm) to replace C (up to 40%), QP (up to 100%), SF (up to 50%), and QS (up to 50%) using an experimental design approach (the new concrete can recognized as ultra-high-performance-glass concrete UHPGC). The approach enables determining the influence of each individual investigated parameter (mixture ingredients) and their synergetic interactions on the measured responses (concrete characteristics) through establishing prediction statistical equations. The prediction models can be presented in form of contour diagrams to tradeoff between different UHPGC ingredients to find the various concrete performances. The coefficients of correlation (R^2: greater than 0.92) and experimental relative errors (less than 8%) showed the adequacy of the established statistical models to predict the required performance of the UHPGC. The validation of the models using extra 18 UHPGC mixtures confirmed the accuracy of the models for the prediction of concrete performances. The developed prediction models can be applied to optimize the proportions of the ingredients to achieve a given performance (desirability).

Keywords: Experimental design approach, Modeling, Sustainability, Ultra-high-performance concrete (UHPC), waste glass materials.

1. INTRODUCTION

Concrete is the most consumed material worldwide after water and thus plays a significant role in sustainability, which has the attention of all the scientific community. Concrete sustainability can be achieved by consuming (1) less concrete (by developing innovative architectural concepts and structural designs), (2) less clinker (by using higher volumes of alternative-supplementary

cementitious materials, ASCM), and (3) less cement in concrete mixtures (by using a smart concrete mixture proportioning approach) [1].

Ultra-high-performance concrete (UHPC) is a revolutionary concrete type, developed in the last decades, characterized by dense microstructure, ultra-high strength and durability characteristics [2,3,4]. Currently, UHPC is used in the construction of special pre-stressed and precast concrete elements, such as decks and abutments of lightweight bridges, marine platforms, precast walls, concrete repair, and urban furniture and other architectural applications [5,6,7,9]. Typical UHPC is composed of very high cement content (800 to 1000 kg/m^3), high content of silica fume (SF), quartz powder (QP) quartz sand (QS) and steel fiber [8]. The steel fiber in the UHPC improves the material's ductility and tensile capacity. The higher strength and superior durability characteristics of the UHPC help producing structural elements with smaller sizes, longer spans with same concrete dimensions, or structural elements with longer life span, which can fulfill the first issue of concrete sustainability mentioned earlier [1].

Although the numerous advantages were drawn when using UHPC, there are some concerns than can be reported about its ingredient materials. The composition of UHPC contains about three times cement content greater than that in normal concrete (typically 900 and 1100 kg/m^3) [10,11]. The huge amount of cement is not only affects the production cost and consumes the natural sources of C but also has a negative effect on the environment through the carbon dioxides (CO_2) emission, which can contribute to the greenhouse effect. Due to the very low water-to-cementitious material ratio (*w/b*), only 31% to 60% of this cement content hydrates [12,13], which opens door for possible replacement of large quantity of cement by alternative-like materials. This could be more soundness when knowing that the unhydrated cement particles are not desired as it can cause rapid hydration reaction, high heat of hydration, and shrinkage cracking. Recent studies revealed that UHPC could be developed using fly ash (FA), ground-granulated-blast-furnace slag (GGBFS), or rice-husk ash (RHA) to replace cement while maintaining similar strength [14,15,16]. Meeting the optimum grading requirement of QP (filler material in UHPC) and QS, for homogeneity and optimum packing density of the UHPC matrix is one of the challenges in producing UHPC. In absence of QP and QS with the required optimum grading, it is common to obtain the grading by crushing coarse sand or rocks, which is time-consuming, costly, and polluting due to dust generation during crushing. Based on environment Canada report, the crystalline silica in QP and QS have immediate and long-term

harmful effects on environment through their biological diversity that make them dangers to the environment [17]. Additionally, the International Agency for Research on Cancer (IARC) has classified respirable quartz from occupational exposure as Group 1 carcinogens (carcinogenic to humans). The U.S. National Toxicology Program classified crystalline silica of respirable size to be a human carcinogen. The basis for these classifications is sufficient evidence from human studies indicating a causal relationship between exposure to respirable crystalline silica in the workplace and increased lung cancer rates between workers [18]. Based on this information, an intensive effort to replace QP and QS by other safe and healthy materials should be realized. SF with extreme fine particles and high amorphous silica content improves concrete properties by enhancing "particle packing" or "micro filling" of cement particles [19], enhancing concrete mixture lubrication due to its perfect spherical particles, and producing secondary hydrates by pozzolanic reaction [20]. Due to the very high fineness of SF particles, the cement particles need higher SF content to fill the gaps within its particles. In case of UHPC with high cement content, this is more pronounced where the SF amount is about 25%-35% of cement weight. The higher SF quantity cause technical problems, given that it has limited resources and high production and transportation costs. SF may also contain trace amounts of crystalline quartz that may pose a health hazard [21].

Post consumption glass can be recycled in many countries several times without significant alteration of its physical and chemical properties. Large quantities of glass cannot be recycled because of high breaking potential, color mixing, or expensive recycling cost [22]. Most of the waste glass have been dumped into landfill sites, which is undesirable as it is not biodegradable and less eco-friendly [23]. Depending on its chemical composition and particle-size distribution (PSD), attempts have been made to use waste glass as ASCM to partially replace cement or ultra-fine fillers in concrete [24,25]. The ground glass (glass powder, GP) to a particle size finer than 38 μm exhibits pozzolanic behavior, which contributes to concrete's strength and durability [26,27,28]. The GP was successfully used as ASCM in normal strength concrete [29,30] and this significantly decrease the adverse effects caused by the alkali–silica reaction [31]. In recent years, the GP was incorporated in the UHPC mix design [32]. Soliman and co-workers designed new UHPC using waste glass materials ground to various PSDs and were successfully able to replace individually cement, QP, SF, QS by various GP of different fineness values [7,34,35,37,36,33]. According to the Leadership in Energy and Environment Design (LEED)

certification, the uses of glass in concrete can double the points compared to other by-product materials such as SF, FA, and GGBFS. The GP is regarded as a material of post-consumption while the others are regarded as materials of post-production. The use of GP as cement replacement has very little environmental impact. The analysis by [38], showed that the valorization of the glass bottles as GP in concrete can allow its transportation in a radius equals to 9000 km without environmental impacts compared to the landfilling. Based on these researches, there is a high value and feasibility of incorporating waste GP in concrete considering its economic and technical advantages.

The composition of UHPC results from the mixture of several constituents with a higher number of possible combinations and relative proportioning, makes the behavior of this type of concrete considerably more difficult to predict. This also requires an extensive series of tests with a large number of batches. Therefore, optimizing their contents is of great importance. The majority of researchers do not consider the specific effect of mixture parameter interactions on fresh and mechanical characteristics when designing UHPC. Design of experiments is a well-known approach based on statistical analysis of outcomes, which is used to ensure that valid results are efficiently obtained with minimum effort, time, and resources [39,40,41]. The experimental design approach can be considered as a mix design concept that considers the relative significance of primary mixture ingredients as well as their coupled interactions which govern the material performance.

This paper presents designing UHPC with waste glass materials ground to various PSDs (UHPGC). The cement was replaced by glass powder-1 (*GP1/C*) up to 40%, quartz powder was replaced by glass powder-2 (*GP1/QP*) up to 100%, silica fume was substituted by fine glass powder (*FGP/SF*) up to 50%, and glass sand replaced up to 50% of the quartz sand. An experimental design approach was applied to account for the water-to-binder ratio (*w/b*) and the four previous mixture parameters as well as their coupled interactions on the development of fresh and mechanical characteristics. Prediction statistical models were established, evaluated, and validated in this study. Contour diagrams to tradeoff between different UHPC ingredients to predict the various concrete performances are also presented in this paper. Finally, the derived models are used to optimize the concrete constituents' combination that gives the optimum performance.

2. EXPERIMENTAL PROGRAM

2.1. Testing program

Earlier UHPC mixtures were successfully designed using waste glass materials to replace individually cement, QP, SF, and GS [7,34,35,37,36,33]. The current study involves replacing all the ingredients at the same time. The glass powder (GP1) was used to partially replace cement (C) up to 40%. The SF was partially replaced by a fine glass powder (FGP) up to 50%. Glass powder-2 (GP2) was used replace the QP by up to 100%. The GS was also used to partially replace QS (from 0% to 50%). This four parameters (GP1/C, FGP/SF, GP2/QP, and GS/QS) and *w/b* were considered as parameters in the design of the UHPGC mixtures. The influence of these five parameters and their coupled effect on the superplasticizer (SP) dosage, air content, unit weight, and compressive strengths under different curing conditions and durations of UHPGC were evaluated using partial-factorial design approach (Table 1). The curing conditions included—normal curing (NC) at a temperature (T) of 20 ± 2°C and relative humidity (RH) of 100%, and standard steam hot curing (HC) at T = 90ºC and RH = 100%. The compressive strength under NC were measured at 1, 7, 28, 56, and 91 days ($f_{c1\text{-d-NC}}$, $f_{c7\text{-d-NC}}$, $f_{c28\text{-d-NC}}$, $f_{c56\text{-d-NC}}$, and $f_{c91\text{-d-NC}}$, respectively). The strength under HC was measured after 2 days ($f_{c2\text{-d-HC}}$). In some cases, the high SP dosage used in the concrete mix can cause a delay of the setting time. So, for these mixture the $f_{c1\text{-d-NC}}$ was measured after 2 or 3 days. For these reasons, the $f_{c1\text{-d-NC}}$ was not considered as a parameter in this study.

Three distinct ranges were considered for *w/b* (0.1850, 0.2175, and 0.2500), GP1/C (0%, 20%, and 40%), GP2/QP (0%, 50%, and 100%), FGP/SF (0%, 25%, and 50%), and GS/QS (0%, 25%, and 50%) to secure UHPGC mixtures of different performances (Table 1). These ranges corresponding to -1, 0, and +1 coded values. A 2^{5-1} experimental design necessitated testing 16 mixtures (UHPGC1 to UHPGC16). Three mixtures corresponding to the central points (UHPGC17) were also tested to estimate the experimental errors for each response. The compositions of the 17 UHPGC mixtures used in the factorial approach are given in Table 2. In total, eight responses were considered in the experimental design: SP dosage, air content, unit weight, $f_{c7\text{-d-NC}}$, $f_{c28\text{-d-NC}}$, $f_{c56\text{-d-NC}}$, and $f_{c91\text{-d-NC}}$, and $f_{c2\text{-d-HC}}$, as indicated in Table 1.

Extra 18 UHPGC mixtures were also designed with random ingredients (within the tested ranges of the ingredients used in the 16 mixtures involved in the prediction models) (Tables 1 and 2). The available fresh and mechanical properties of these 18 mixtures were employed to validate the prediction models.

The mixture composition, material properties, and test methods undertaken in this research are detailed in the following sections.

2.2. Mix design optimization and mixture proportioning

The development of UHPC starts with the design of the granular structure of the all granular materials. The key factor for enhancing UHPC performances is the optimization of particle size distribution and packing density. The granular structure strongly affects the balance between the rheological behavior and the mechanical performances of UHPC and the chemical reactivity of the constituents. In this research, the design of the granular structure of all UHPGC mixtures were made using the compressible packing model (CPM) developed by de Sedran and de Larrard [42].

The selected waste glass materials (GP1, GP2, and GS) with PSDs close to those of the conventional materials in the UHPC (C, QP, and QS, respectively). The FGP was the exceptional where it was selected to have intermediate PSD between that of SF and cement to fill the gap in between [36]. Figure 2 shows the PSDs of all materials. Various SP dosages (expressed as kg/m^3) were employed to secure certain rheological characteristics (target slump flow diameter of 240 ± 40 mm) (Table 2).

A total of 35 mixtures were designed in this research: 16 UHPGC mixtures (UHPGC1 to UHPGC17) for the main matrix, three repetitions of UHPGC17, and 18 UHPGC mixtures (UHPGC18 to UHPGC35) for the validation of the models. All the UHPGC mixtures were designed with 2% steel fiber addition.

2.3. Materials

In general, the contents of C_3A and C_3S in cement and cement fineness are critical for controlling concrete rheology [43]. This is more pronounced in case of the UHPC that is designed with

higher cement content. Therefore, high sulphate-resistant cement (Type HS cement) with low C_3A and C_3S contents was selected for designing the UHPGC mixtures. The SF used in the mixture proportioning complies with CAN/CSA A3000 specifications. The chemical and physical properties of Type HS cement, GP1, SF, FGP, QP, GP2, QS, and QS are shown in Table 3. The physical properties included materials specific gravity (SG), Blaine specific surface area, mean-particle size diameter (d_{50}), and maximum-particle diameter (d_{max}). The particle-size distributions (PSDs) of all materials are shown in Fig. 1.

The micrographs and XRD analysis were carried out to check the nature of each material, as shown in Fig. 2. The XRD analysis of cement, QP and QS indicated that they are crystallized, while the SF and GP are amorphous.

A polycarboxylate (PCE)-based high-range water-reducing admixture (HRWRA) with a specific gravity of 1.09 and solid content of 40% (Sika Viscocrete 6200) was used as superplasticizer (SP) in all concrete mixtures.

Steel fibers with 13 mm in length and 0.2 mm in diameter were incorporated in the finally optimized mixtures.

2.4. Mixing procedure, Specimen Preparation, and Test Methods

All the concrete mixtures were batched using high energy shear mixer with a capacity of 10 liters. To achieve a homogeneous mixture and avoid particles agglomeration, all powder materials were mixed for 10 min before water and HRWRA addition. Approximately half of the SP diluted in half of the mixing water was gradually added over 5 min of mixing time. The remaining water and SP were gradually added between an additional 5 min of mixing time. Upon the end of mixing, the fresh properties of the UHPGC mixtures were measured. The tests included concrete temperature, unit weight, and air content (ASTM C 185). The concrete flow was measured with the flow-table test (ASTM C 1437).

The compressive strength (f_c) measurements for the UHPGC were determined using 50×50×50 mm cubes, according to ASTM C 109. The samples were tightly covered with plastic sheets and stored at 23°C and 50% RH for 24 hours before demolding. After demolding, the samples were cured at two different curing regimes: NC and HC curing regimes. In the NC, the samples were

stored in a fog room at a temperature of 23°C and 100% RH until the day of testing. The HC mode composed of curing the samples at 90ºC and 100% RH for 48 hours before testing.

3. DEVELOPMENT OF STATISTICAL MODELS

3.1. Concrete properties

The various concrete properties in the fresh and hardened states are presented in Table 4. The fresh properties included slump flow diameters before and after 25 joltings, concrete temperature, air content, and unit weight of concrete. The SP dosages to secure slump flow values of 240 ± 40 before shocking and 265 ± 45 mm after shocking are also presented in Table 4. The compressive strength results ($f_{c7\text{-d-NC}}$, $f_{c28\text{-d-NC}}$, $f_{c56\text{-d-NC}}$, and $f_{c91\text{-d-NC}}$, and $f_{c2\text{-d-HC}}$) are also summarized in the same table.

3.2. Derivation of statistical models

The experimental design method provides an efficient tool for determining the predicted models as well as for optimizing the mixture proportion. The experimental region modelled is described in Table 1. In total, eight modeled responses (SP dosage, air content, unit weight, $f_{c7\text{-d-NC}}$, $f_{c28\text{-d-NC}}$, $f_{c56\text{-d-NC}}$, and $f_{c91\text{-d-NC}}$, and $f_{c2\text{-d-HC}}$) were derived as a function of the five mixture parameters (*w/b*, GP1/C, GP2/QP, FGP/SF, and GS/QS). The derived models are presented in Table 5 (Eqs. 1A to 8A) and Table 6 (Eqs. 1B to 8B).

The derived models are valid for mixture parameters corresponding to coded values between -1 and +1 given in Table 5 (Eqs. 1A to 8A). Three replicates of the central mixture (UHPGC17A, B, and C) at coded values of 0 were prepared to estimate the degree of experimental error for the modeled responses. The absolute values corresponding to the coded values of -1, 0 and +1 for the *w/b* parameter were 0.185, 0.2175 and 0.250. These values for GP1/C were 0%, 20%, and 40%, for GP2/QP were 0%, 50%, and 100%, for FGP/SF were 0%, 25%, and 50%, and that for the GS/QS were 0%, 25%, and 50%, respectively. The coded values can be calculated from the absolute values, as follows:

Coded w/b value = (Absolute w/b value - 0.2175)/0.0325 (9)

Coded GP1/C value = (Absolute GP1/C value - 20)/20 (10)

Coded GP2/QP value = (Absolute GP2/QP value - 50)/50 (11)

Coded FGP1/SF value = (Absolute FGP1/SF value - 25)/25 (12)

Coded GS/QS value = (Absolute GS/QS value - 25)/25 (13)

The estimate and Prob. >|t| values, as well as the coefficients of correlation (R^2) for the eight derived models were determined. The estimate for each parameter refers to the coefficients of the model found by the least square approach. The Prob. >|t| term is the probability of getting an even greater *t* statistic, in absolute value, that tests whether the true parameter is zero. Probabilities less than 0.10 are typically considered as significant evidence that the parameter is not zero, i.e. that the contribution of the proposed parameter has a significant influence on the measured response. The parameter of a probability greater than 0.10 was insignificant and was not considered in the models. The proposed models have high R^2 values ranged between 0.92 and 1.00 (Tables 5 and 6). Measured concrete mix parameters used in the derivation of the statistical models are correlated to the predicted responses using derived models in Fig. 3. The R^2 values for each correlation are indicated on the graphs.

The effects of the five considered mixture parameters and their interactions on the modeled responses (expressed in coded values) are compared in Table 5. The sign of the estimates (+/-) indicates the positive or the negative effect of the parameter on the considered response. The models expressed in coded values enable the comparison of the relative significance of the various parameters and their interactions on the modeled response through the value and the sign of the estimates. For example, the 91d-*f*c-NC response is affected mainly by the changes of the *w/b* and GP1/C (have the highest estimates of 9.45 and 9.44, respectively), followed by, FGP/SF (estimate of -3.39), GP2/QP (estimate of 3.27), and GS/QS (estimate of 2.86), with respective order. The *w/b*, GP1/C, FGP/SF, and GS/QS had negative signs indicating the negative effect of increasing those parameters on the 91d-*f*c-NC response. The positive sign of the GP2/QP indicate the positive direct effect of this parameter (GP2/QP) on the model response (91d-*f*c-NC).

The eight models expressed in the absolute values are given in Table 6 (Eqs. 1B to 8B). To use the model in absolute values, *w/b* is ranged between 0.185 and 0.250, GP1/C ranged between 0%

and 40%, GP2/QP ranged between were 0% and 100%, while both FGP/SF and GS/QS can be substituted with values from 0% to 50%.

3.3. Relative errors of derived statistical models

The central mixture (UHPC17) was tested three times to evaluate experimental errors for the developed models. Table 7 shows the mean ($\bar{x}$), standard deviation (σ), standard error corresponding to 90% confidence limit (*SE*), and relative error (*RE*) calculated according to a 90% confidence interval using the Student's distribution (Eq. 14), as follows;

$$RE = \frac{SE}{\bar{x}} 100\ (\%) = \frac{2.92 \times \sigma}{\bar{x}\sqrt{n}} 100\ (\%) \tag{14}$$

where, 2.92 corresponds to a coefficient representing 90% confidence interval for the Student's distribution for a number of observations (n) of 3. The *RE* values for the responses of HRWRA dosage, unit weight, and the five compressive strengths ($f_{c7\text{-d-NC}}$, $f_{c28\text{-d-NC}}$, $f_{c56\text{-d-NC}}$, $f_{c91\text{-d-NC}}$, and $f_{c2\text{-d-HC}}$) were lower than 2.4%. The *RE* was 8.1% for the air content response.

3.4. Validation of derived statistical models

Correlations between predicted eight responses using the derived statistical models and actual measurements obtained from the UHPGC18 to UHPGC35 mixtures are shown in Fig. 4. The trendline and the coefficient of correlation (R^2) for each relationship are calculated and presented in the figure. All prediction models produced excellent prediction values that ranged between -3% to +2%, except for the 7d-*f*c-NC model that presented 10% overestimation. The R^2 ranged between 0.81 and 0.99.

3.5. Contour diagrams for developed statistical models

Contour diagrams were established (Figs. 5 to 12) as a simple interpretation for the derived statistical models. The contour diagrams are used to compare the tradeoff between effects of the different parameters on the considered responses. Two-dimensional contour charts can be constructed to present how the response changes with a variation of the two parameters while the

other parameters remains constant. For example, eight contour diagrams for the 91d-*f*c-NC model (Fig. 11) were established to show the possible combinations of each two parameters, while maintaining the other three parameters constants. The top left graph in Fig. 11 was established by varying the w/b from 0.185 to 0.250 and GP1/C from 0% to 40%, while the GP2/QP, FGP/SF, and GS/QS were held fixed at 50%, 25%, and 25%, respectively. In this contour diagram, at a given *w/b*, the increase in the GP1/C leads to increasing the 91d-*f*c-NC strength. On the other side, decreasing the *w/b* (at a given GP1/C value) can increase the 91d-*f*c-NC strength.

3.6. Criteria of Multi-parametric Optimization

After establishing the statistical models between mix design parameters and concrete properties as responses, all independent variables (mix design parameters) were varied simultaneously and independently to optimize the concrete performance to satisfy various construction requirements. A specific criterion was proposed to select the optimum mix-design variables (containing maximum amounts of waste glass materials) to obtain a UHPGC mixture with maximum compressive strength and an acceptable range of superplasticizer based on the experimental design approach. A numerical optimization was used to optimize one or a combination of parameters. For example, the SP dosage can be defined as "minimum", the compressive strength can be defined as "maximum", while the replacement of concrete constituents by waste glass materials can be defined as "in the range". At the end of the multi-objective optimization process, different optimal solutions, with the desirability of the functions up to 0.96 (Fig. 13) was obtained. Table 6 provides the predicted optimal compositions of the three UHPC mixtures and corresponding response values.

Based on the research conducted to develop UHPGC using waste-glass materials, three different UHPGC mixture classes can be defined in responding to various construction demands (Table 8). The UHPGC mixtures in Class A are characterized by low flowability of about 200 mm but with 2d-fc-HC more than 200 MPa. Concrete mixes in Class A have a *w/b* between 0.185 and 0.200. Highly flowable UHPGC can be obtained, as in Class C, with higher *w/b* between 0.225 and 0.250. The UHPGC mixtures in Class C are characterized by 2d-fc-HC between 160 and 175 MPa. The concrete mixes in Class B blend the characteristics of those in Classes A and C. All

UHPGC mixtures in Classes A, B, and C are designed with steel fiber. Examples for UHPGC mixtures in each class, including the mix design and main characteristic performance, are presented in Table 9.

CONCLUSIONS

Based on the above results, the following conclusions can be drawn:

A statistical mixture design approach can be used to design UHPC when incorporating various waste glass materials ground to different particle size distributions as replacements of the main conventional materials (cement, quartz powder, silica fume, and quartz sand), in what can be defined as ultra-high-performance-glass concrete (UHPGC). The approach enables determining the influence of each individual investigated parameter (mixture ingredients) and their synergetic interactions on the measured responses (concrete characteristics) through establishing prediction statistical equations. The high values of coefficients of correlations (R^2: greater than 0.92) and experimental relative errors (less than 8%) proved the adequacy of the statistical models to predict the required performance of UHPGC. Contour diagrams to tradeoff between different UHPGC ingredients to predict the various concrete performances can be established using the prediction models. In addition, the models were successfully validated using 18 UHPC mixtures (of random compositions with the range of the tested parameters) confirmed the accuracy of the models for the prediction of concrete performances.

The developed prediction models can be applied to optimize the concrete ingredients to achieve given concrete performances with given desirability. Optimization of several responses was also efficiently accomplished, which revealed that it was possible to design a UHPGC mixture with maximum replacements of the conventional concrete ingredients with waste glass materials, minimum superplasticizer dosage, and simultaneously with various compressive strength values and an acceptable slump flow, to satisfy the various construction sectors.

ACKNOWLEDGMENTS

This research was funded by the Société des Alcools du Québec (SAQ) and the authors gratefully acknowledge its support.

REFERENCES

1.Mehta PK. Global concrete industry sustainability. ACI Mater J 2009;31(2):45–8.

2.First international symposium on ultra high performance concrete Kassel, Germany; September 2004.

3.Second international symposium on ultra high performance concrete Kassel, Germany; March 2008.

4.The third international symposium on ultra high performance concrete and nanotechnology for high performance construction materials. Kassel, Germany; 2012.

5.Schmidt M, Fehling E. Ultra-high-performance concrete: research, development and application in Europe. ACI SP 225 2005:51–77.

6.Klemens T. Flexible concrete offers new solutions. Concr Const 2004;49(12):72.

7.Soliman N, Omran A, Tagnit-Hamou A. Laboratory characterization and field application of novel ultra-high performance glass concrete. ACI Mat J 2015:41.

8. Richard, P., and Cheyrezy, M., "Reactive Powder Concretes with High Ductility and 200-800 MPa Compressive Strength", ACI SP 144, 1994, pp. 507-518.

9.Racky P. Cost-effectiveness and Sustainability of UHPC. Proc. of the Int Symp on UHPC, Kassel, Germany 2004;13(15):797–805.

10.Graybeal BA. Material property characterization of ultra-high performance concrete 2006.

11.Richard P, Cheyrezy M. Composition of reactive powder concrete. Cem Concr Res 1995;25(7):1501–11.

12.Cheyrezy M, Maret V, Frouin L. Microstructural analysis of RPC (reactive powder concrete). Cem Concr Res 1995;25(7):1491–1500.

13.Habel K, Viviani M, Denarié E, Brühwiler E. Development of the mechanical properties of an ultra-high performance fiber reinforced concrete (UHPFRC). Cem Concr Res 2006;36(7):1362–1370.

14.Soutsos MN, Barnett SJ, Bungey JH, Millard SG. Fast track construction with high-strength concrete mixes containing ground granulated blast furnace slag. ACI SP 228–19 2005:255–270.

15.Yazici H, Yigiter H, Karabulut AS, Baradan B. Utilization of fly ash and ground granulated

blast furnace slag as an alternative silica source in reactive powder concrete. Fuel 2008; 87(12):2401–2407.

16.Tuan NV, Ye G, Breugel KV, Fraaij ALA, Bui DD. The study of using rice husk ash to produce ultra-high performance concrete. Constr and Build Mat 2011;25(4):2030–2035.

17.Environment Canada, https://www.ec.gc.ca/default.asp?lang=en&n=FD9B0E51-1

18.Environment Canada, Health Canada. Screening assessment for the challenge. Report June 2013:7.

19. Detwiler RJ, Mehta PK. Chemical and physical effects of silica fume on the mechanical behavior of concrete. ACI Mat J 1989;86(6):609-614.

20. Richard P, Cheyrezy M. Composition of reactive powder concretes. Cem Concr Res 1995;25(7):1501–1511.

21. Jahr, J. "Possible Health Hazards from Different Types of Amorphous Silicas—Suggested Threshold Limit Values," Institute of Occupational Health, Oslo, Norway, 1980.

22.Shayan A, Xu A. Value-added utilisation of waste glass in concrete. Cem Concr Res 2004;34(1):81–89.

23.FEVE. Collection for recycling rate in Europe. The European Container Glass Federation (http://www.feve.org/FEVE-STATIS-2013/Recycling-2011-Glass-coll.html date accessed: Sept. 11, 2013).

24.Zidol A, Tognonvi TM, Tagnit-Hamou A. Effect of glass powder on concrete sustainability. 1st Int Conf on Concr Sust (ICCS13) 2012.

25.Terro MJ. Properties of concrete made with recycled crushed glass at elevated temperatures. Build and Env 2006;41(5):633–639.

26.Idir R, Cyr M, Tagnit-Hamou A. Use of waste glass as powder and aggregate in cement-based materials. SBEIDCO – 1st Int Conf on Sust built Env Infr in Developing Countries ENSET, Oran Algeria 12–14 October 2009:109–16.

27.Shi C, Wu Y, Riefler C, Wang H. Characteristic and pozzolanic reactivity of glass powders. Cem Concr Res 2005;35:987–993.

28.Shayan A, Xu A. Performance of glass powder as a pozzolanic material in concrete: a field trial on concrete slabs. Cem Concr Res 2006; 36:457–468.

29.Shao Y, Lefort T, Moras S, Rodriguez D. Studies on concrete containing ground waste glass. Cem Concr Res 2000;30:91–100.

30.Khmiri A, Samet B, Chaabouni M. A cross mixture design to optimise the formulation of a ground waste glass blended cement. Constr Build Mat 2012;28:680–686.

31.Andrea S, Chiara BM. ASR expansion behavior of recycled glass fine aggregates in concrete. Cem Concr Res 2010;40:531–536.

32.Vaitkevicius V, Serelis E, Hilbig H. The effect of glass powder on the microstructure of ultra-high performance concrete. Constr Build Mat 2014;68:102–109.

33. Tagnit-Hamou, A., and Soliman, N., "Ultra-High Performance Glass Concrete and Method for Producing same," U.S. Patent Application. No. 61/806,083, file March 28, 2013, Accepted March 2014.

34.Soliman N, Aïtcin P-C, Tagnit-Hamou A. New generation of ultra-high performance glass concrete. Adv Concr Tech. Publisher: RILEM and CEB-fib, ISBN 978-5-7264-0809-5 Chapter 24, 12-16 May 2014;5:218–227.

35. Soliman NA, Tagnit-Hamou A. Development of green ultra-high performance concrete using glass powder. Constr Build Mat. 2016(Submitted and pending decision):42.

36. Soliman N.A., Tagnit-Hamou A. (12-16 March, 2016) The study of Using Fine Glass Powder to Produce Ultra High Performance Concrete. 8th International Conference on Nano-Technology in Construction (NTC 2016), Sharm El-Sheikh, Egypt.

37. Soliman N.A., Tagnit-Hamou A. (2016) Using glass sand as an alternative for silica sand in UHPC. Journal of Construction and Building Materials. (submitted and pending decision).

38. Recyc-Quebec (2015)

39. Piepel GF, Cornell JA. Mixture experiment approaches: examples, discussion, and recommendations. J Qual Technol 1994;26(3):177–96.

40. Montgomery DC. Design and analysis of experiments: response surface method and designs. New Jersey; 2005.

41. Ghafari E, Hugo C, Júlio E. RSM-based model to predict the performance of selfcompacting UHPC reinforced with hybrid steel micro-fibers. Constr Build Mater 2014;66:375–83.

42. Sedran T. and de Larrard F. Manuel d'utilisation de RENE-LCPC, version 6.1d, logiciel d'optimisation granulaire, Laboratoire Centrale des Ponts et Chaussées, (2000).

43. Aïtcin P-C. Cements of yesterday and today–concrete of tomorrow. Cem Concr Res 2000;30(9):1349–1359.

LIST OF TABLES

LIST OF FIGURES

Table 1 – Partial-factorial experimental design to simulate effect of *w/b*, replacements of cement by glass powder 1 (*GP1*), quartz powder by glass powder 2 (*GP2*), silica fume by fine glass powder (*FGP*), and quartz sand by glass sand (*GS*) on UHPGC characteristics

Mixture	Coded values					Absolute values					Note
	w/b	*GP1/C*	*GP2/QP*	*FGP/SF*	*GS/QS*	*w/b* (ratio)	*GP1/C* (%)	*GP2/QP* (%)	*FGP/SF* (%)	*GS/QS* (%)	
UHPGC1	-1	-1	-1	-1	+1	0.1850	0	0	0	50	Main matrix
UHPGC2	-1	-1	-1	+1	-1	0.1850	0	0	50	0	
UHPGC3	-1	-1	+1	-1	-1	0.1850	0	100	0	0	
UHPGC4	-1	-1	+1	+1	+1	0.1850	0	100	50	50	
UHPGC5	-1	+1	-1	-1	-1	0.1850	40	0	0	0	
UHPGC6	-1	+1	-1	+1	+1	0.1850	40	0	50	50	
UHPGC7	-1	+1	+1	-1	+1	0.1850	40	100	0	50	
UHPGC8	-1	+1	+1	+1	-1	0.1850	40	100	50	0	
UHPGC9	+1	-1	-1	-1	-1	0.2500	0	0	0	0	
UHPGC10	+1	-1	-1	+1	+1	0.2500	0	0	50	50	
UHPGC11	+1	-1	+1	-1	+1	0.2500	0	100	0	50	
UHPGC12	+1	-1	+1	+1	-1	0.2500	0	100	50	0	
UHPGC13	+1	+1	-1	-1	+1	0.2500	40	0	0	50	
UHPGC14	+1	+1	-1	+1	-1	0.2500	40	0	50	0	
UHPGC15	+1	+1	+1	-1	-1	0.2500	40	100	0	0	
UHPGC16	+1	+1	+1	+1	+1	0.2500	40	100	50	50	
UHPGC17A	0	0	0	0	0	0.2175	20	50	25	25	Central points
UHPGC17B	0	0	0	0	0	0.2175	20	50	25	25	
UHPGC17C	0	0	0	0	0	0.2175	20	50	25	25	
UHPGC18	0.23	0.5	-1	-1	-1	0.2250	30	0	0	0	Verification points
UHPGC19	0.23	0.5	+1	-1	-1	0.2250	30	100	0	0	
UHPGC20	0.23	0.5	-1	-1	-1	0.2250	30	0	0	0	
UHPGC21	+1	-1	-1	+1	-1	0.2500	0	0	50	0	
UHPGC22	-1	-1	+1	+1	-1	0.1850	0	100	50	0	
UHPGC23	-0.88	0	+1	0.44	-1	0.2400	20	100	36	0	
UHPGC24	+1	0	+1	0.44	-1	0.2500	20	100	36	0	
UHPGC25	0.23	+1	+1	0.12	-1	0.2250	40	100	28	0	
UHPGC26	-0.54	+1	+1	0.12	-1	0.2000	40	100	28	0	
UHPGC27	0.23	0.5	+1	0.12	-1	0.2250	30	100	28	0	
UHPGC28	-0.88	-1	-1	-1	-1	0.1890	0	0	0	0	
UHPGC29	-0.88	0	+1	-1	-1	0.1890	20	100	0	0	
UHPGC30	-0.88	-1	+1	+1	-1	0.1890	0	100	50	0	
UHPGC31	-0.88	0	-1	+1	-1	0.1890	20	0	50	0	
UHPGC32	+1	0.25	+1	-1	-1	0.2500	25	100	0	0	
UHPGC33	+1	0.25	+1	-1	-1	0.2500	25	100	0	0	
UHPGC34	+1	0.25	+1	-1	-1	0.2500	25	100	0	0	
UHPGC35	+1	0.25	+1	-1	-1	0.2500	25	100	0	0	

Table 2 – Mixture proportioning of evaluated concretes

Materials	Type HS cement	Glass powder-1 (GP1)	Total cementitious materials (TCM)	GP1/TCM	Silica Fume (SF)	Fine glass powder (FGP)	Total fine powders (TFP)	FGP/TFP	Water	w/b	Quartz sand (QS)	Glass sand (GS)	Total sand (TS)	GS/TS	Quartz powder (QP)	Glass powder-2 (GP2)	Total powders (TP)	GP2/TP	Steel fiber	PCE-based HRWRA
Unit	kg/m³									ratio	kg/m³									
UHPGC1	786	0	786	0%	218	0	218	0%	155	0.1850	472	472	944	50%	236	0	236	0%	158	51.4
UHPGC2	801	0	801	0%	111	111	222	50%	163	0.1850	961	0	961	0%	240	0	240	0%	158	43.6
UHPGC3	788	0	788	0%	219	0	219	0%	155	0.1850	946	0	946	0%	0	236	236	100%	158	51.6
UHPGC4	788	0	788	0%	109	109	218	50%	155	0.1850	473	473	946	50%	0	236	236	100%	158	56.2
UHPGC5	464	309	773	40%	215	0	215	0%	158	0.1850	928	0	928	0%	232	0	232	0%	158	42.2
UHPGC6	464	310	774	40%	107	107	214	50%	158	0.1850	464	464	928	50%	232	0	232	0%	158	42.2
UHPGC7	458	306	764	40%	212	0	212	0%	156	0.1850	458	458	916	50%	0	229	229	100%	158	41.6
UHPGC8	465	310	775	40%	108	108	216	50%	158	0.1850	931	0	931	0%	0	233	233	100%	158	42.3
UHPGC9	748	0	748	0%	208	0	208	0%	224	0.2500	897	0	897	0%	224	0	224	0%	158	25.5
UHPGC10	752	0	752	0%	104	104	208	50%	235	0.2500	451	451	902	50%	226	0	226	0%	158	16.4
UHPGC11	740	0	740	0%	206	0	206	0%	224	0.2500	444	444	888	50%	0	222	222	100%	158	20.2
UHPGC12	754	0	754	0%	105	105	210	50%	236	0.2500	905	0	905	0%	0	226	226	100%	158	8.2
UHPGC13	436	291	727	40%	202	0	202	0%	223	0.2500	436	436	872	50%	218	0	218	0%	158	15.8
UHPGC14	442	294	736	40%	102	102	204	50%	223	0.2500	883	0	883	0%	221	0	221	0%	158	20.1
UHPGC15	437	291	728	40%	202	0	202	0%	223	0.2500	874	0	874	0%	0	218	218	100%	158	15.9
UHPGC16	439	293	732	40%	102	102	204	50%	229	0.2500	439	439	878	50%	110	110	220	100%	158	8.0
UHPGC17	608	152	760	20%	158	53	211	25%	194	0.2175	684	228	914	25%	114	114	228	50%	158	29.0
UHPGC18	524	224	748	30%	208	0	208	0%	191	0.225	898	0	898	0%	224	0	224	0%	158	40.8
UHPGC19	521	223	744	30%	208	0	208	0%	190	0.225	894	0	894	0%	0	223	223	100%	158	40.5
UHPGC20	524	224	748	30%	208	0	208	0%	191	0.225	898	0	898	0%	224	0	224	0%	158	40.8
UHPGC21	755	0	755	0%	105	105	210	50%	229	0.25	906	0	906	0%	226	0	226	0%	158	20.6
UHPGC22	796	0	796	0%	111	111	222	50%	162	0.185	956	0	956	0%	0	239	239	100%	158	43.4
UHPGC23	640	160	800	20%	142	80	222	36%	174	0.240	960	0	960	0%	0	240	240	100%	0	32.7
UHPGC24	604	151	755	20%	134	76	210	36%	229	0.250	906	0	906	0%	0	227	227	100%	0	15.6
UHPGC25	456	304	761	40%	152	59	211	28%	200	0.225	913	0	913	0%	0	228	228	100%	0	31.1
UHPGC26	466	311	777	40%	155	60	216	28%	173	0.200	932	0	932	0%	0	233	233	100%	0	42.3
UHPGC27	536	230	766	30%	153	60	213	28%	201	0.225	919	0	919	0%	0	230	230	100%	0	31.3
UHPGC28	810	0	810	0%	225	0	225	0%	176	0.189	972	0	972	0%	243	0	243	0%	0	43.1
UHPGC29	636	159	795	20%	221	0	221	0%	173	0.189	954	0	954	0%	0	239	239	100%	0	42.5
UHPGC30	812	0	812	0%	113	113	226	50%	176	0.189	975	0	975	0%	0	244	244	100%	0	37.6
UHPGC31	644	161	805	20%	112	112	224	50%	175	0.189	967	0	967	0%	242	0	242	0%	0	32.9
UHPGC32	562	187	749	25%	208	0	208	0%	227	0.250	899	0	899	0%	0	225	225	100%	0	20.4
UHPGC33	562	187	749	25%	208	0	208	0%	227	0.250	899	0	899	0%	0	225	225	100%	0	20.4
UHPGC34	562	187	749	25%	208	0	208	0%	227	0.250	899	0	899	0%	0	225	225	100%	0	20.4
UHPGC35	562	187	749	25%	208	0	208	0%	227	0.250	899	0	899	0%	0	225	225	100%	0	20.4

Table 3 – Chemical composition (%) of Type HS cement, quartz sand, quartz powder, glass powder, and silica fume

	Identification	Type HS cement, C	Quartz powder, QP	Quartz sand, QS	Silica fume, SF	Glass sand, GS	Glass powders, GP1 and GP2	Fine glass sand, FGP
Chemical composition (%)	Silicon Dioxide (SiO_2)	22.00	99.80	99.80	99.80	73.00		
	Iron Oxide (Fe_2O_3)	4.30	0.09	0.04	0.09	0.40		
	Aluminum Oxide (Al_2O_3)	3.50	0.11	0.14	0.11	1.50		
	Calcium Oxide (CaO)	65.6	0.38	0.17	0.40	11.30		
	Titanium Dioxide (TiO_2)	0.20	0.25	0.02	--	0.04		
	Sulfur trioxide (SO_3),	2.30	0.53	--	--	--		
	Magnesium Oxide (MgO)	1.90	0.20	0.01	0.20	1.20		
	Sodium oxide (Na_2O)	0.07	0.25	--	0.20	13.00		
	Potassium Oxide (K_2O)	0.80	3.50	0.05	0.50	0.50		
	Equivalent alkali (Na_2O_{eq})	0.90	--	--	--	--		
	Zinc oxide (ZnO)	0.09	--	--	0.25	--		
	Loss on ignition (LOI)	1.00	0.32	0.20	3.50	0.60		
Boge	C_3S	50.00	--	--	--	--		
	C_2S	25.00	--	--	--	--		
	C_3A	2.00	--	--	--	--		
	C_4AF	14.00	--	--	--	--		
Physical properties	Unit weight	3.21	2.73	2.70	2.20	2.60	2.60	2.60
	Blaine surface area (m^2/kg)	430	--	--	20,000	--	380	10.000
	Mean-particle size, d_{50}, (μm)	11	13	250	0.15	275	12	3.8
	Maximum-particle size, d_{max}, (μm)	--	--	600	--	630	100	10

Table 4 – Concrete properties

Mixture	Slump flow (mm)		Concrete temperature (°C)	SP dosage (kg/m^3)	Air content (%)	Unit weight (kg/m^3)	$f_{c1.2.3\text{-}d\text{-}NC}$ (MPa)	$f_{c7\text{-}d\text{-}NC}$ (MPa)	$f_{c28\text{-}d\text{-}NC}$ (MPa)	$f_{c56\text{-}d\text{-}NC}$ (MPa)	$f_{c91\text{-}d\text{-}NC}$ (MPa)	$f_{c2\text{-}d\text{-}HC}$ (MPa)
	Before damping	After damping										
UHPGC1	200	238	29	51.4	2.3	2490	36	102	159	169	178	208
UHPGC2	225	250	--	43.6	1.4	2552	50	109	173	190	200	213
UHPGC3	200	220	--	51.6	4.5	2438	23	110	159	172	193	225
UHPGC4	215	230	--	56.2	2.4	2492	9	76	150	166	182	197
UHPGC5	200	225	27	42.2	3.3	2423	15	69	134	155	171	187
UHPGC6	225	263	25	42.2	4.0	2408	20	75	139	145	160	188
UHPGC7	220	250	--	41.6	6.3	2322	12	67	132	142	172	195
UHPGC8	210	230	--	42.3	2.4	2451	11	50	132	148	162	179
UHPGC9	245	280	25	25.5	3.9	2387	28	96	141	155	161	174
UHPGC10	240	280	25	16.4	4.0	2393	31	80	133	142	150	168
UHPGC11	265	290	27	20.2	3.3	2376	23	97	149	171	183	192
UHPGC12	275	300	25	8.2	4.4	2388	35	89	142	160	172	187
UHPGC13	220	250	27	15.8	4.8	2299	17	72	123	137	151	165
UHPGC14	280	305	--	20.1	4.0	2347	17	65	116	131	149	163
UHPGC15	235	270	--	15.9	3.3	2339	18	66	131	153	162	185
UHPGC16	280	310	24	8.0	5.3	2300	17	62	110	125	140	158
UHPGC17A	245	270	28.5	31.6	3.4	2406	17	83	149	166	180	200
UHPGC17B	250	285	24	31.6	3.27	2410	17	83	149	166	178	198
UHPGC17C	250	275	24	31.6	3.6	2402	18	81	146	164	176	201
UHPGC18	250	285	24	31.6	3.3	2410	17	83	149	166	178	198
UHPGC19	250	275	24	31.6	3.6	2402	18	81	146	164	176	201
UHPGC20	265	285	31.9	40.8	2.94	2395	7	89	131	153	170	183
UHPGC21	235	275	29	40.5	3.08	2406	8	94	142	171	180	193
UHPGC22	235	270	--	40.8	3.42	2433	23	88	130	154	175	187
UHPGC23	320	350	25	20.6	--	--	28	90	136	151	169	181
UHPGC24	250	280	--	43.4	2.40	2488	51	104	160	185	196	211
UHPGC25	230	--	36	32.7	3.10	2353	--	94	156	178	188	208
UHPGC26	300	--	36	15.6	3.82	2258	49	87	138	154	167	182
UHPGC27	285	300	36	31.1	3.10	2272	22	78	141	166	170	190
UHPGC28	265	290	36	42.3	2.90	2258	32	92	153	164	171	192
UHPGC29	285	--	36	31.3	4.30	2258	42	--	148	169	173	194
UHPGC30	188	--	36	43.1	2.85	2364	55	105	162	171	182	199
UHPGC31	220	--	29	42.5	4.49	2306	48	94	171	183	184	222
UHPGC32	245	--	29	37.6	2.46	2356	48	--	177	176	191	200
UHPGC33	250	277	32	32.9	2.50	2335	30	--	152	161	181	193
UHPGC34	265	--	29	20.4	--	2306	48	88	136	163	173	190
UHPGC35	220	--	29	20.4	--	2306	--	85	138	157	168	193
UHPGC1	220	--	29	20.4	--	2306	48	84	136	159	169	193
UHPGC2	220	--	29	20.4	--	2306	48	86	139	161	172	190

Table 5 – Statistical models (in **coded** values) to SP dosage, air content, unit weight, and concrete strengths at different ages and curing conditions as a function of water-to-binder ratio (*w/b*), percentage of glass powder 1-to-cement by weight (*GP1/C*), percentage of glass powder 2-to-quartz powder by weight (*GP2/QP*), percentage of fine glass powder-to-silica fume by weight (*FGP/SF*), and percentage of glass sand-to-quartz sand by weight (*GS/QS*)

Models for:	Predicted statistical models expressed in **coded values** (*w/b*, *GP1/C*, *GP2/QP*, *FGP/SF*, and *GS/QS* from -1 to +1)	Eq.	R^2
SP dosage (kg/m^3) =	31.36-15.07*w/b-2.81*GP1/C-0.82*GP2/QP-1.71*FGP/SF+0.16*GS/QS+1.51*w/b*GP1/C-2.36*w/b*GP2/QP-1.40*w/b*FGP/SF-1.33*w/b*GS/QS-0.73*GP1/C*GP2/QP+1.33*GP1/C*FGP/SF-1.76*GP1/C*GS/QS-0.11*GP2/QP*FGP/SF+0.85*GP2/QP*GS/QS+0.92*FGP/SF*GS/QS	(1A)	1.00
Air content (%) =	3.77+0.51*w/b+0.32*GP1/C+0.39*GP2/QP-0.37*FGP/SF+0.43*GS/QS-0.35*w/b*GP1/C-0.21*w/b*GP2/QP+0.41*w/b*FGP/SF-0.24*GP1/C*GP2/QP+0.46*GP1/C*GS/QS-0.26*GP2/QP*FGP/SF	(2A)	0.96
Unit weight (kg/m^3) =	2397.21-51.44*w/b-34.44*GP1/C-16.81*GP2/QP+20.81*FGP/SF-20.06*GS/QS+11.56*w/b*GP1/C+4.44*w/b*GP2/QP-7.94*w/b*FGP/SF+8.69*GP1/C*GP2/QP-5.44*GP1/C*GS/QS+3.44*GP2/QP*FGP/SF-8.81*GP1/C*GS/QS+8.19*GP2/QP*FGP/SF-5.19*GP2/QP*GS/QS	(3A)	1.00
7d-*f*c-NC (MPa) =	80.56-1.91*w/b-14.58*GP1/C-3.04*GP2/QP-4.51*FGP/SF-1.38*GS/QS+2.53*w/b*GP1/C+3.34*w/b*GP2/QP+0.81*w/b*GS/QS-1.23*GP1/C*GP2/QP+1.78*GP1/C*FGP/SF+4.66*GP1/C*GS/QS-3.41*GP2/QP*FGP/SF-1.04*FGP/SF*GS/QS	(4A)	1.00
28d-*f*c-NC (MPa) =	140.43-8.34*w/b-11.67*GP1/C-0.92*GP2/QP-2.06*FGP/SF-2.11*GS/QS+1.23*w/b*GP1/C+3.23*w/b*GP2/QP-3.41*w/b*FGP/SF-0.83*GP1/C*FGP/SF+0.99*GP1/C*GS/QS-2.56*GP2/QP*FGP/SF-0.73*GP2/QP*GS/QS-1.82*FGP/SF*GS/QS	(5A)	0.95
56d-*f*c-NC (MPa) =	155.61-7.05*w/b-11.85*GP1/C+0.85*GP2/QP-2.96*FGP/SF-4.02*GS/QS+1.61*w/b*GP1/C+4.69*w/b*GP2/QP-4.20*w/b*FGP/SF+1.19*w/b*GS/QS-1.85*GP1/C*FGP/SF-1.90*GP2/QP*FGP/SF-2.18*FGP/SF*GS/QS	(6A)	0.92
91d-*f*c-NC (MPa) =	169.51-9.45*w/b-9.44*GP1/C+2.86*GP2/QP-3.39*FGP/SF-3.27*GS/QS+1.55*w/b*GP1/C+2.98*w/b*GP2/QP-2.20*w/b*FGP/SF-2.29*GP1/C*GP2/QP-2.26*GP1/C*FGP/SF-3.21*GP2/QP*FGP/SF+1.87*GP2/QP*GS/QS-2.98*FGP/SF*GS/QS	(7A)	0.94
2d-*f*c-HC (MPa) =	188.57-12.45*w/b-9.01*GP1/C-3.17*GP2/QP-4.94*FGP/SF-2.64*GS/QS+2.68*w/b*GP1/C+3.39*w/b*GP2/QP-1.42*GP1/C*GP2/QP+1.54*GP1/C*GS/QS-4.57*GP2/QP*FGP/SF-1.60*GP2/QP*GS/QS-1.21*FGP/SF*GS/QS	(8A)	0.92

Table 6 – Statistical models (in **absolute** values) to SP dosage, air content, unit weight, and concrete strengths at different ages and curing conditions as a function of water-to-binder ratio (*w/b*), percentage of glass powder 1-to-cement by weight (*GP1/C*), percentage of glass powder 2-to-quartz powder by weight (*GP2/QP*), percentage of fine glass powder-to-silica fume by weight (*FGP/SF*), and percentage of glass sand-to-quartz sand by weight (*GS/QS*)

Models for:	Predicted statistical models expressed in **absolute values** (*w/b* = 0.185-0.250, GP1/C = 0%-40% by wt., GP2/QP = 0%-40% by wt., FGP/SF = 0%-50% by wt., and GS1/QS = 0%-50% by wt.)	Eq.	R^2
SP dosage (kg/m^3) =	113.98719-353.74692*w/b-0.58681*GP1/C+0.29954*GP2/QP+0.21969*FGP/SF+0.36113*GS/QS+2.31835*w/b*GP1/C-1.45389*w/b*GP2/QP-1.71717*w/b*FGP/SF-1.63332*w/b*GS/QS-0.000727575*GP1/C*GP2/QP+0.0026596*GP1/C*FGP/SF-0.00352615*GP1/C*GS/QS-0.00009156*GP2/QP*FGP/SF+0.00068234*GP2/QP*GS/QS+0.00147368*FGP/SF*GS/QS	(1B)	1.00
Air content (%) =	-1.48324+20.42308*w/b+0.12277*GP1/C+0.04526*GP2/QP-0.11337*FGP/SF-0.0011*GS/QS-0.54135*w/b*GP1/C-0.12654*w/b*GP2/QP+0.50077*w/b*FGP/SF-0.000238125*GP1/C*GP2/QP+0.00092125*GP1/C*GS/QS-0.0002055*GP2/QP*FGP/SF	(2B)	0.96
Unit weight (kg/m^3) =	2843.34033-1830.76923*w/b-5.31274*GP1/C-1.16394*GP2/QP+2.84731*FGP/SF-0.24250*GS/QS+17.78846*w/b*GP1/C+2.73077*w/b*GP2/QP-9.76923*w/b*FGP/SF+0.0086875*GP1/C*GP2/QP-0.010875*GP1/C*FGP/SF-0.017625*GP1/C*GS/QS+0.00655*GP2/QP*FGP/SF-0.00415*GP2/QP*GS/QS	(3B)	1.00
7d-fc-NC (MPa) =	162.29684-264.23077*w/b-1.83637*GP1/C-0.41567*GP2/QP-0.0735*FGP/SF-0.41558*GS/QS+3.89423*w/b*GP1/C+2.05769*w/b*GP2/QP+0.99231*w/b*GS/QS-0.00123125*GP1/C*GP2/QP+0.0035625*GP1/C*FGP/SF+0.0093125*GP1/C*GS/QS-0.002725*GP2/QP*FGP/SF-0.00167*FGP/SF*GS/QS	(4B)	1.00
28d-fc-NC (MPa) =	215.14552-289.23077*w/b-1.00356*GP1/C-0.38512*GP2/QP+1.03783*FGP/SF-0.022000*GS/QS+1.89423*w/b*GP1/C+1.98846*w/b*GP2/QP-4.19231*w/b*FGP/SF-0.0016625*GP1/C*FGP/SF+0.0019875*GP1/C*GS/QS-0.002045*GP2/QP*FGP/SF-0.000585*GP2/QP*GS/QS-0.00291*FGP/SF*GS/QS	(5B)	0.95
56d-fc-NC (MPa) =	236.84949-318.07692*w/b-1.03957*GP1/C-0.57240*GP2/QP+1.24281*FGP/SF-0.39188*GS/QS+2.48077*w/b*GP1/C+2.88462*w/b*GP2/QP-5.16923*w/b*FGP/SF+1.46154*w/b*GS/QS-0.0037*GP1/C*FGP/SF-0.00152*GP2/QP*FGP/SF-0.00348*FGP/SF*GS/QS	(6B)	0.92
91d-fc-NC (MPa) =	252.68219-362.30769*w/b-0.76303*GP1/C-0.26844*GP2/QP+0.79142*FGP/SF-0.087*GS/QS+2.38462*w/b*GP1/C+1.83077*w/b*GP2/QP-2.70769*w/b*FGP/SF-0.0022875*GP1/C*GP2/QP-0.004525*GP1/C*FGP/SF-0.00257*GP2/QP*FGP/SF+0.0015*GP2/QP*GS/QS-0.00476*FGP/SF*GS/QS	(7B)	0.94
2d-fc-HC (MPa) =	318.60253-569.61538*w/b-1.35135*GP1/C-0.2379*GP2/QP+0.034*FGP/SF-0.0545*GS/QS+4.11538*w/b*GP1/C+2.08462*w/b*GP2/QP-0.001425*GP1/C*GP2/QP+0.003075*GP1/C*GS/QS-0.00366*GP2/QP*FGP/SF-0.00128*GP2/QP*GS/QS-0.00194*FGP/SF*GS/QS	(8B)	0.92

Table 7 – Statistical parameters measuring repeatability of test results (n = 3)

Predicted statistical models for:	$(\bar{x})$	σ	*SE* (%)	*RE* (%)
SP dosage	31.6 kg/m^3	0.0 kg/m^3	0.0	0.0
Air content	3.43%	0.17%	0.3	8.1
Unit weight	2406 kg/m^3	4.0 kg/m^3	6.7	0.3
$f_{c7\text{-d-NC}}$	82.3 MPa	1.15 MPa	1.9	2.4
$f_{c28\text{-d-NC}}$	148.0 MPa	1.42 MPa	2.4	1.6
$f_{c56\text{-d-NC}}$	165.3 MPa	1.11 MPa	1.9	1.1
$f_{c91\text{-d-NC}}$	178.0 MPa	2.03 MPa	3.4	1.9
$f_{c2\text{-d-HC}}$	199.3 MPa	1.44 MPa	2.4	1.2

Table 8 – UHPGC for various construction applications

Criteria	Class A	Class B	Class C
Flowability of UHPC	Semi flowable	flowable	highly flowable
Average flow diameter, mm (in.)	200	230	260
w/b	0.185- 0.2	0.19-0.21	0.23-0.25
Superplasticizer	High dosage	Moderate dosage	Low dosage
Steel fiber (%)	2	2	2
f'$_c$-2d-HC, MPa	> 200	175-200	160-175
f'$_c$-28d-NC, MPa	> 160	> 140	> 120
f'$_c$-91d-NC, MPa	> 180	> 160	> 140

Table 9 – Examples for UHPGC mixtures of various classes in Table 8

	Materials	UHPGC class A	UHPGC class B	UHPGC class C
Mix design (kg/m^3)	water	193	211	236
	Cement	640	608	739
	SF	142	158	205
	FGP	80	53	0
	GP1	138	140	0
	GP2	244	240	222
	QP	0	0	0
	QS	960	684	443
	GS	0	228	443
	Superplasticizer	45	25	8
	Steel fiber	158	158	158
Performance	Slump flow, mm	230	260	290
	f'_c-2d-HC, MPa	205	200	175
	f'_c-28d-NC, MPa	170	158	138
	f'_c-91d-NC, MPa	185	175	162

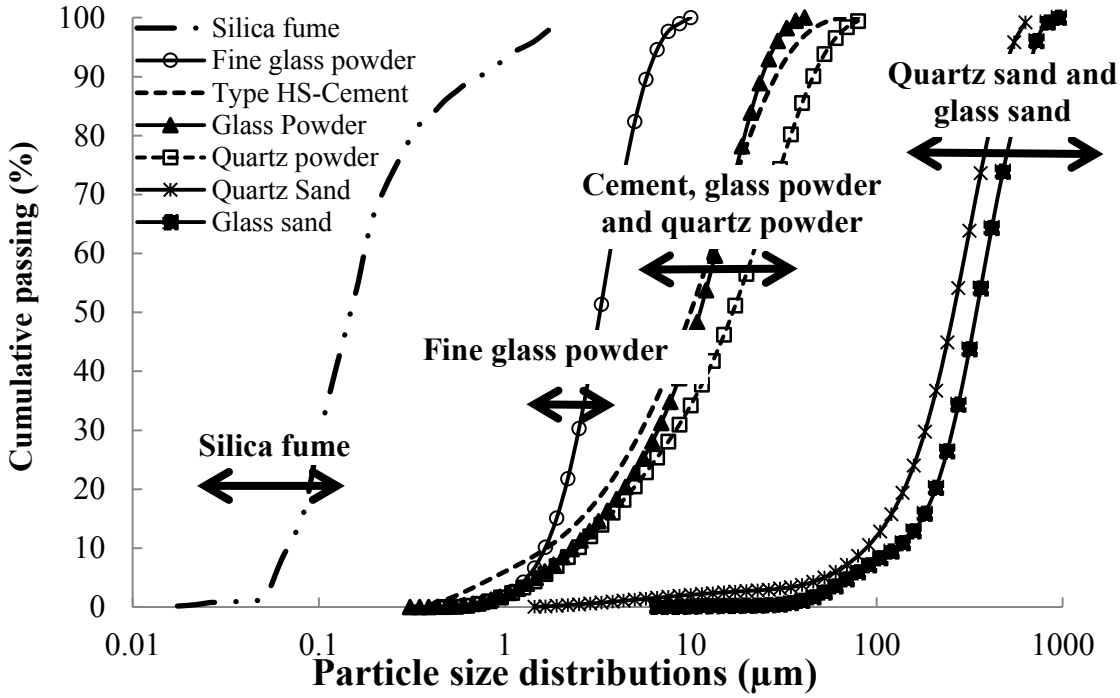

Fig. 1 – Particle-size distributions of individual materials used in the UHPC mix design

(A) Type HS cement

(B) quartz powder

(C) silica fume

(D) quartz sand

(E) glass powder

(F) fine glass powder

(G) glass sand

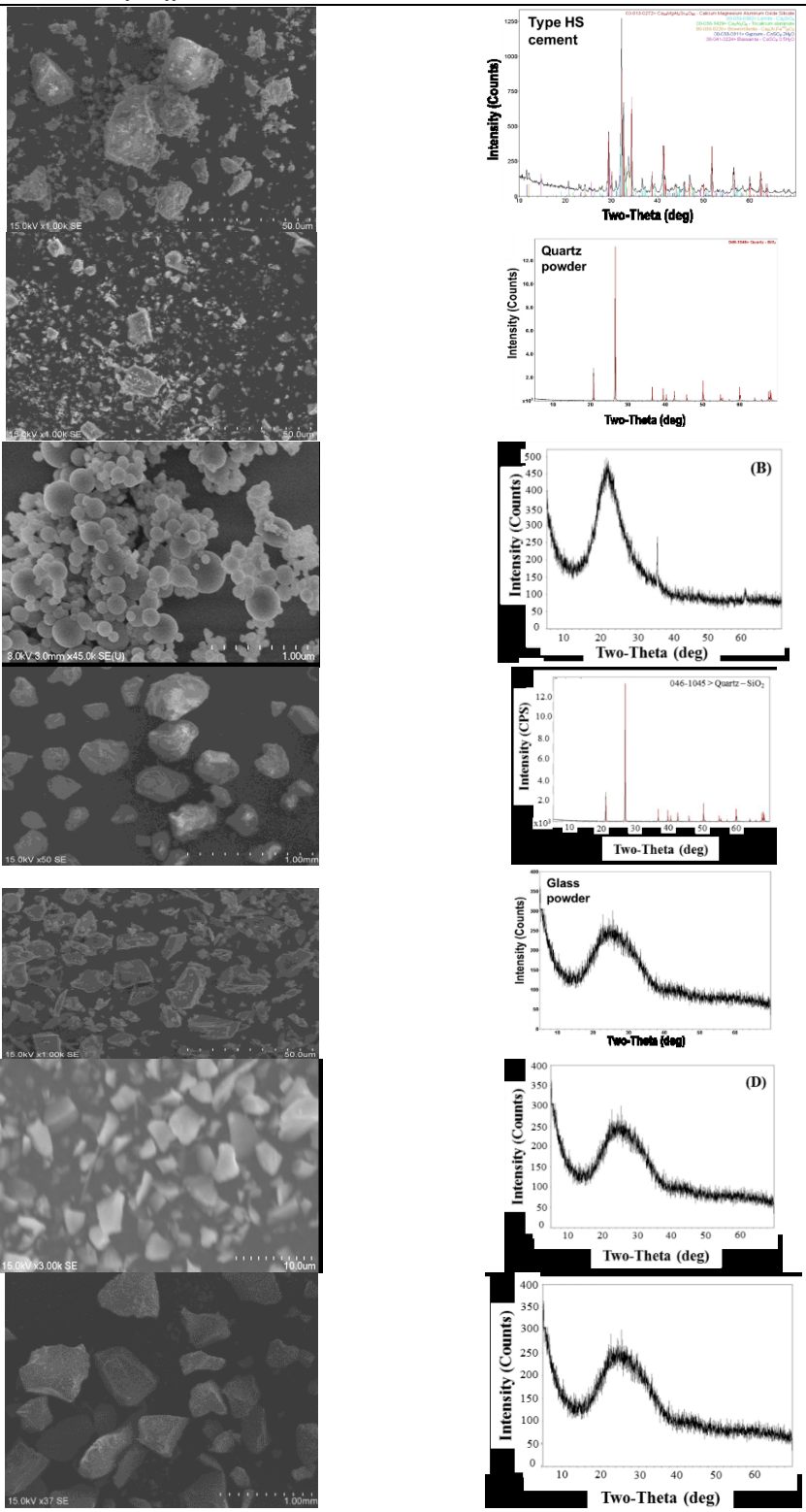

Fig. 2 – Photomicrograph (left) and X-ray diffraction patterns (right) for (A) Type HS cement, (B) quartz powder, (C) silica fume, (D) quartz sand, (E) glass powder, (F) fine glass powder, and (G) glass sand

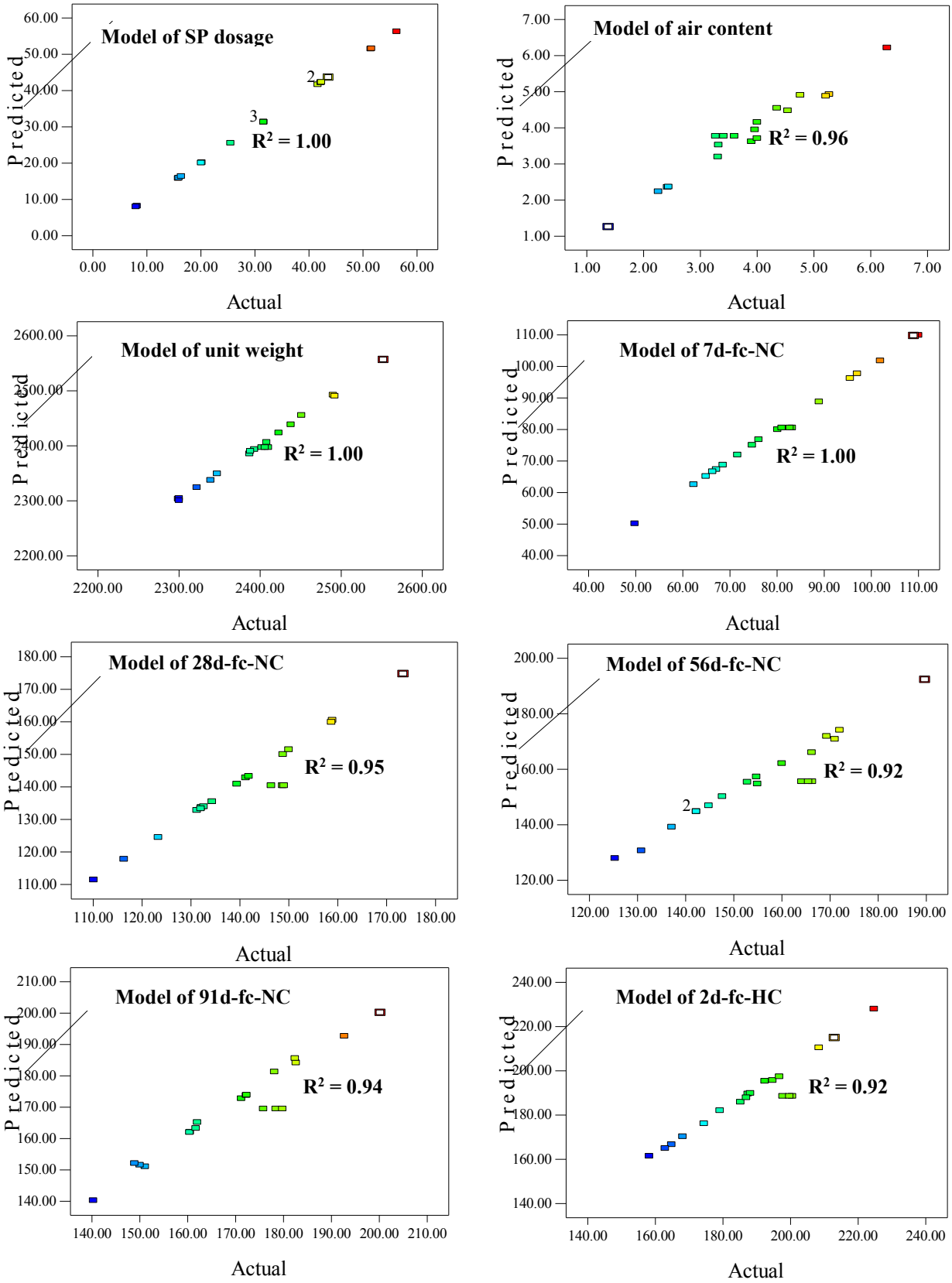

Fig. 3 – Measured versus predicted responses using derived statistical models

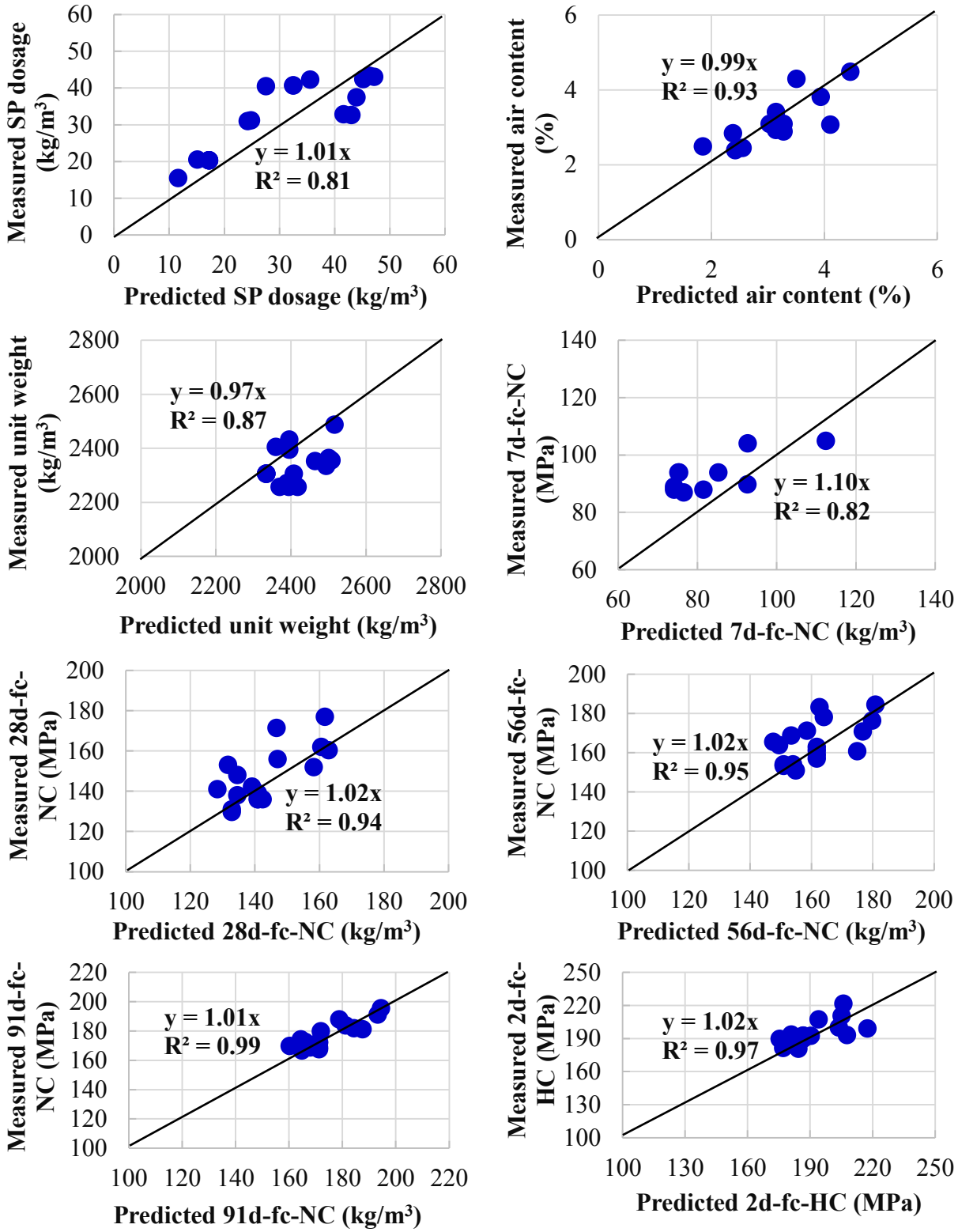

Fig. 4 – Predicted responses using equations in Tables 5 and 6 versus measured responses for UHPC18 to UHPC35 listed in Table 4

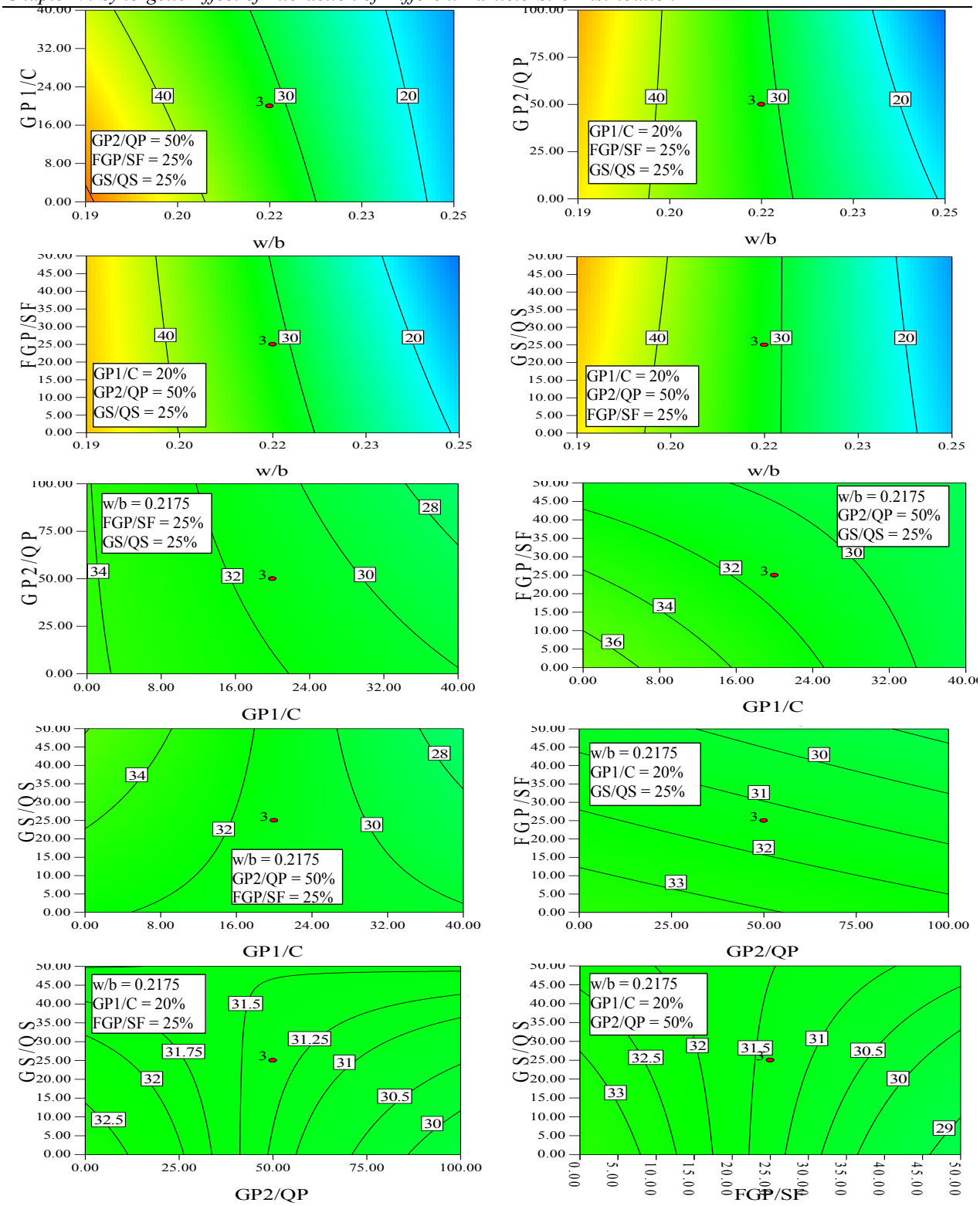

Fig. 5 – Contour diagram for the trade-off the effect of water-to-binder ratio (*w/b*), percentage of glass powder 1-to-cement by weight (*GP1/C*), percentage of glass powder 2-to-quartz powder by weight (*GP2/QP*), percentage of fine glass powder-to-silica fume by weight (*FGP/SF*), and percentage of glass sand-to-quartz sand by weight (*GS/QS*) on SP dosage

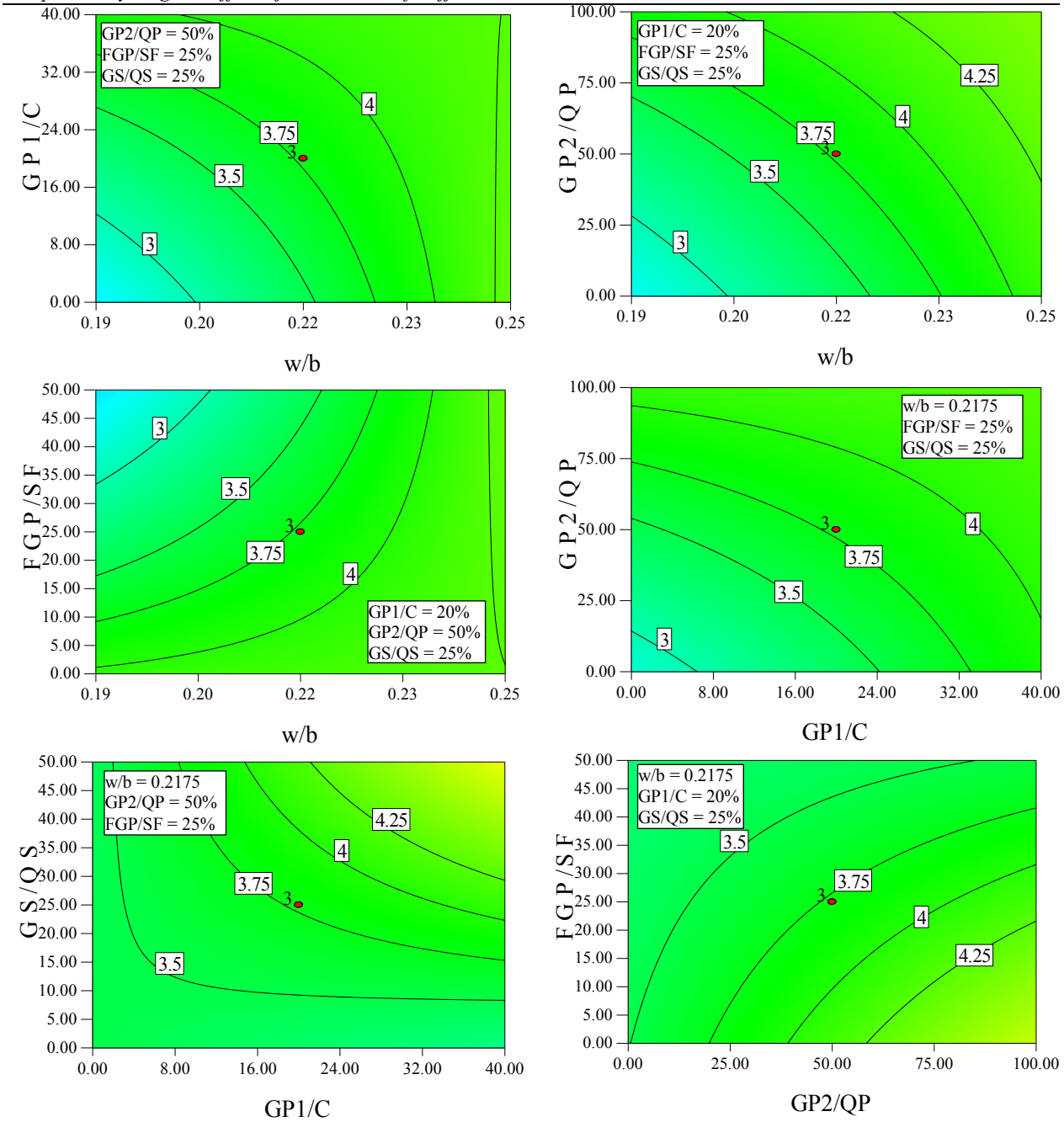

Fig. 6 – Contour diagram for the trade-off the effect of water-to-binder ratio (*w/b*), percentage of glass powder 1-to-cement by weight (*GP1/C*), percentage of glass powder 2-to-quartz powder by weight (*GP2/QP*), percentage of fine glass powder-to-silica fume by weight (*FGP/SF*), and percentage of glass sand-to-quartz sand by weight (*GS/QS*) on air content

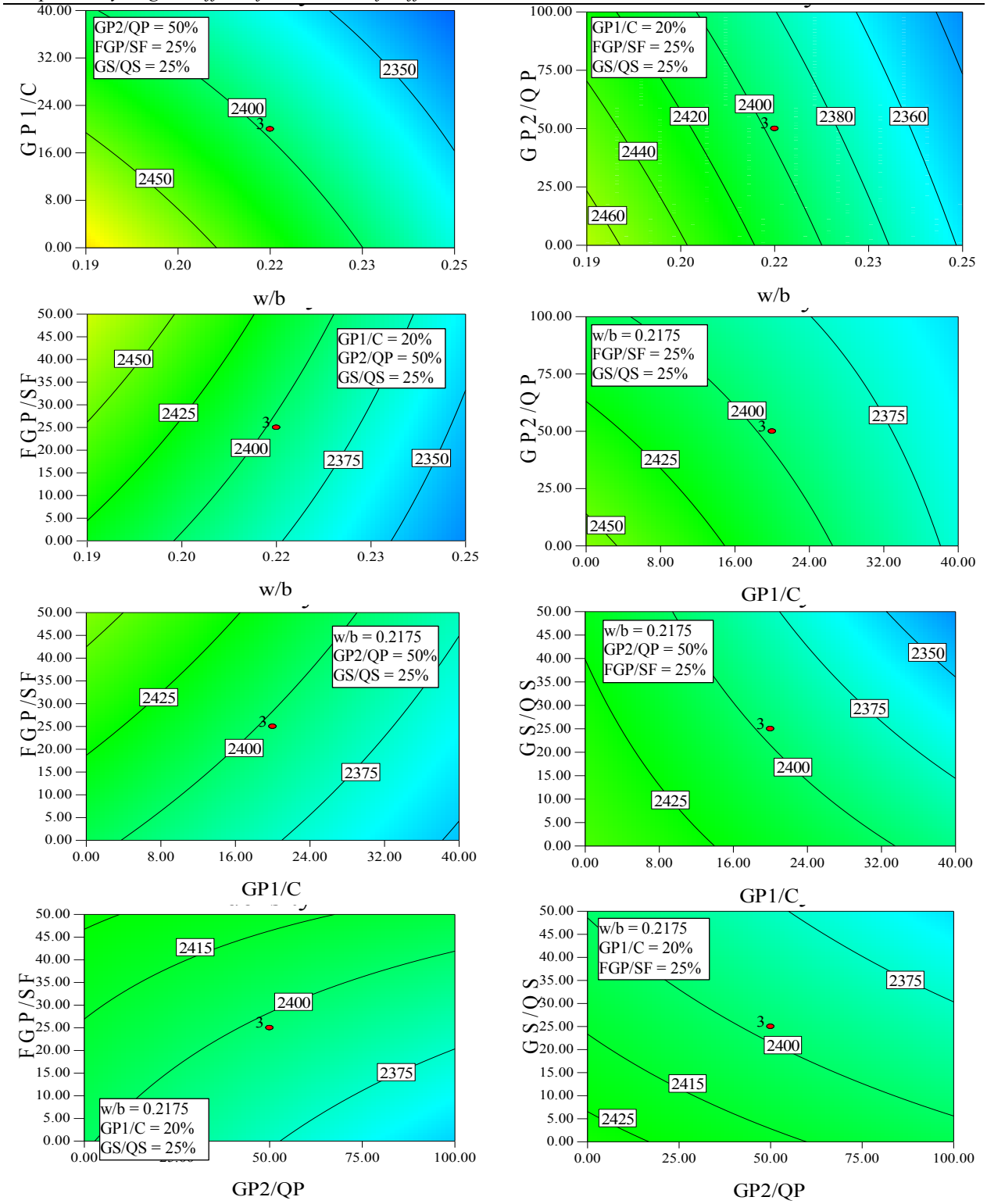

Fig. 7 – Contour diagram for the trade-off the effect of water-to-binder ratio (*w/b*), percentage of glass powder 1-to-cement by weight (*GP1/C*), percentage of glass powder 2-to-quartz powder by weight (*GP2/QP*), percentage of fine glass powder-to-silica fume by weight (*FGP/SF*), and percentage of glass sand-to-quartz sand by weight (*GS/QS*) on unit weight

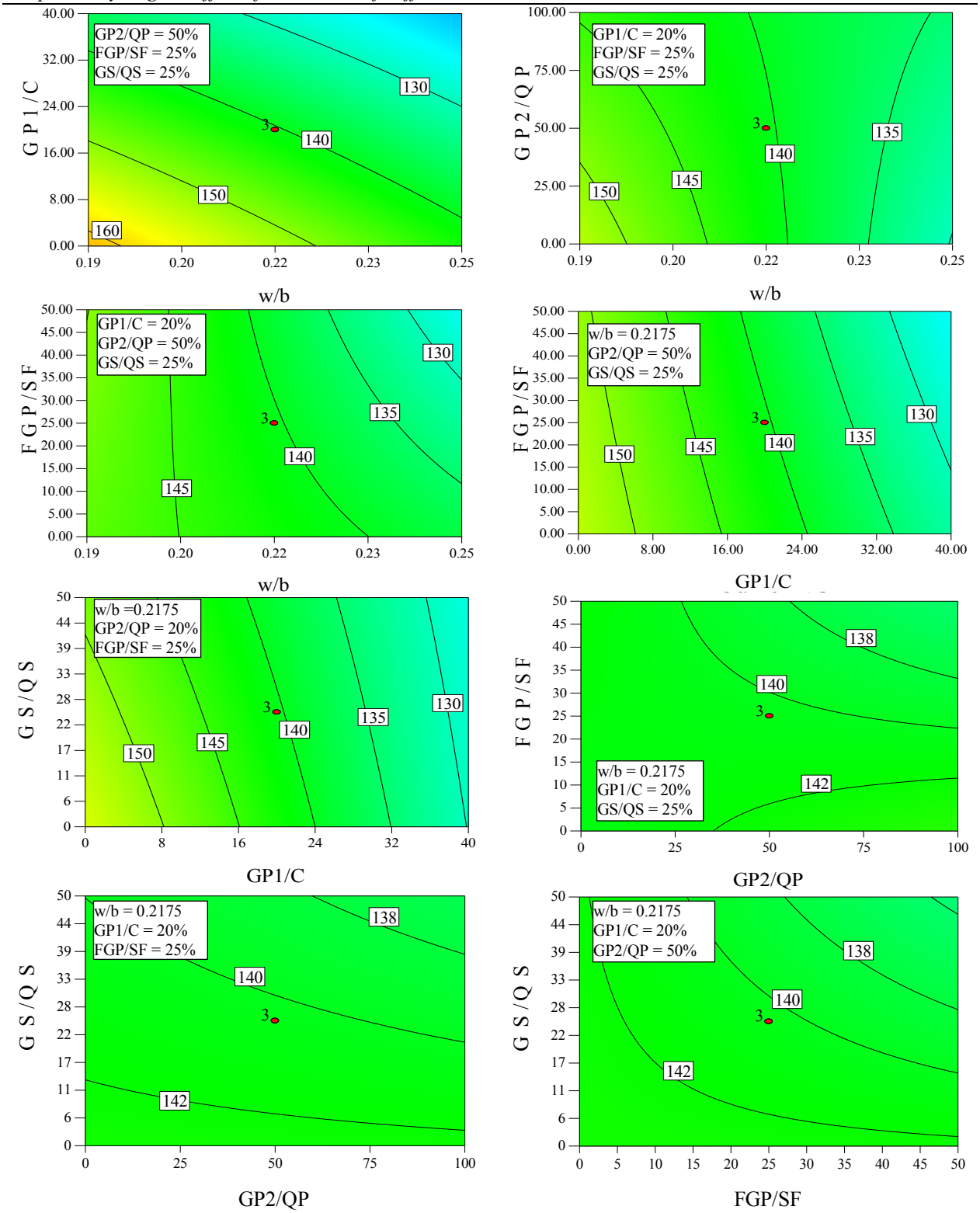

Fig. 8 – Contour diagram for the trade-off the effect of water-to-binder ratio (*w/b*), percentage of glass powder 1-to-cement by weight (*GP1/C*), percentage of glass powder 2-to-quartz powder by weight (*GP2/QP*), percentage of fine glass powder-to-silica fume by weight (*FGP/SF*), and percentage of glass sand-to-quartz sand by weight (*GS/QS*) on 7d-fc-NC

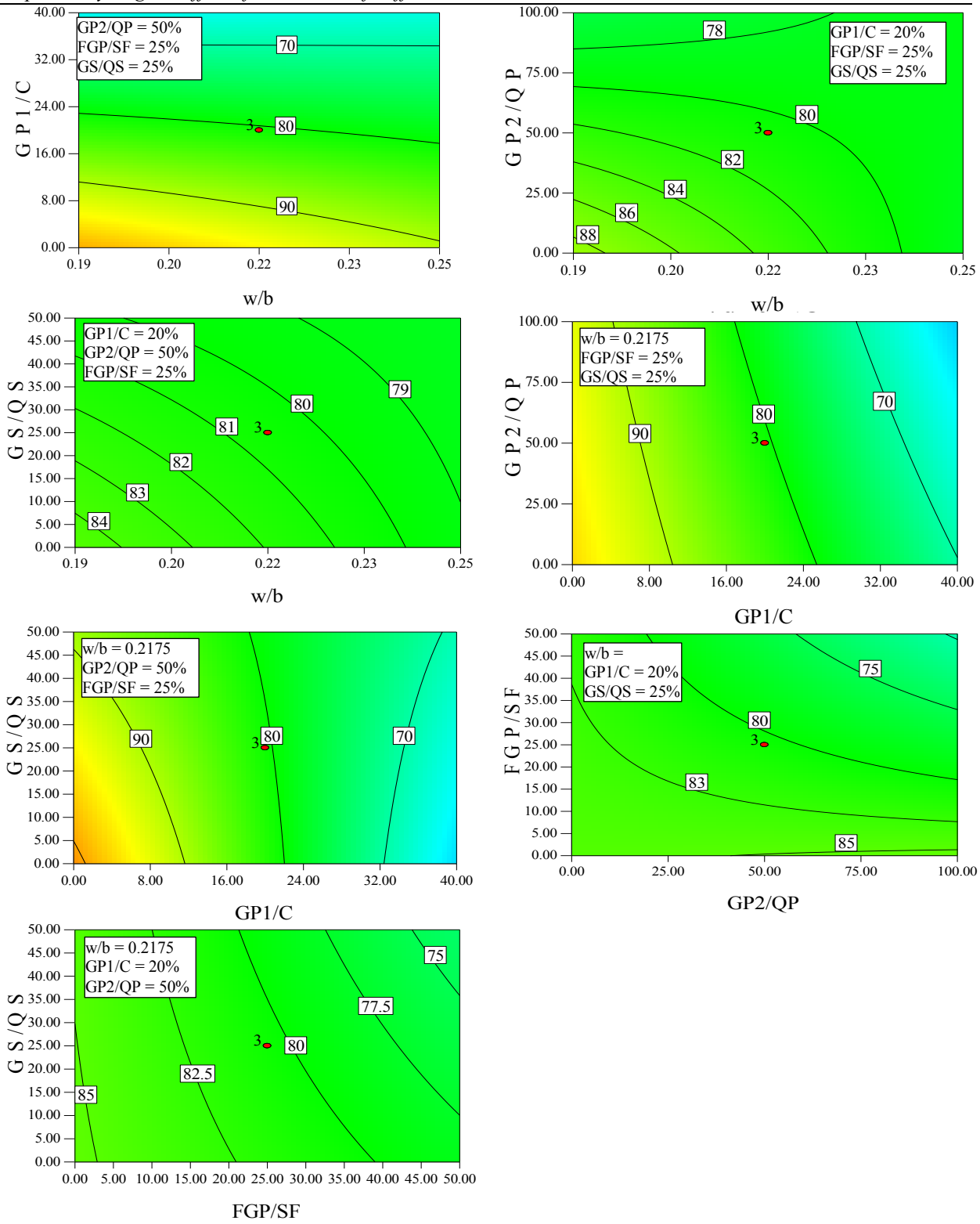

Fig. 9 – Contour diagram for the trade-off the effect of water-to-binder ratio (*w/b*), percentage of glass powder 1-to-cement by weight (*GP1/C*), percentage of glass powder 2-to-quartz powder by weight (*GP2/QP*), percentage of fine glass powder-to-silica fume by weight (*FGP/SF*), and percentage of glass sand-to-quartz sand by weight (*GS/QS*) on 28d-fc-NC

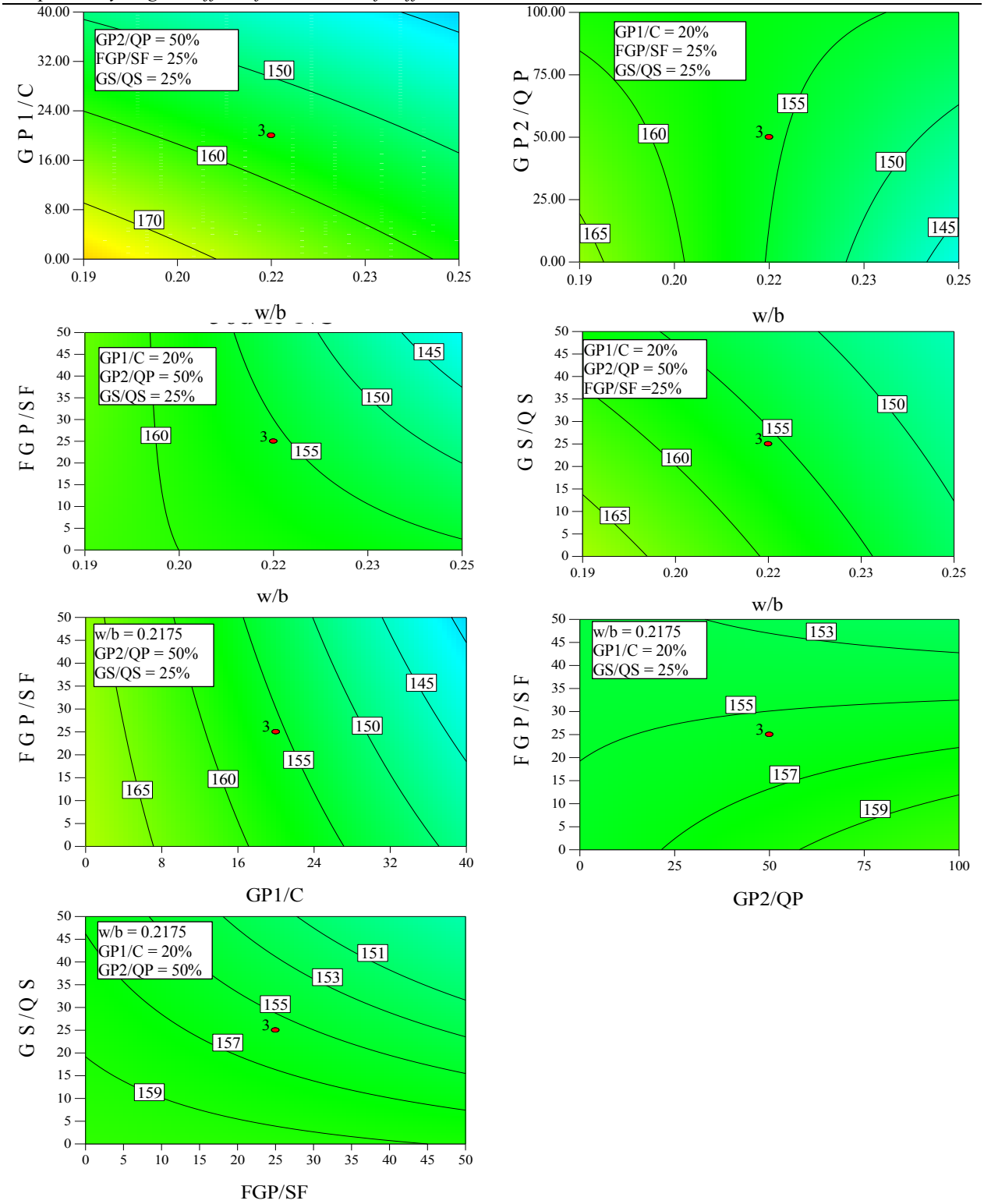

Fig. 10 – Contour diagram for the trade-off the effect of water-to-binder ratio (*w/b*), percentage of glass powder 1-to-cement by weight (*GP1/C*), percentage of glass powder 2-to-quartz powder by weight (*GP2/QP*), percentage of fine glass powder-to-silica fume by weight (*FGP/SF*), and percentage of glass sand-to-quartz sand by weight (*GS/QS*) on 56d-fc-NC

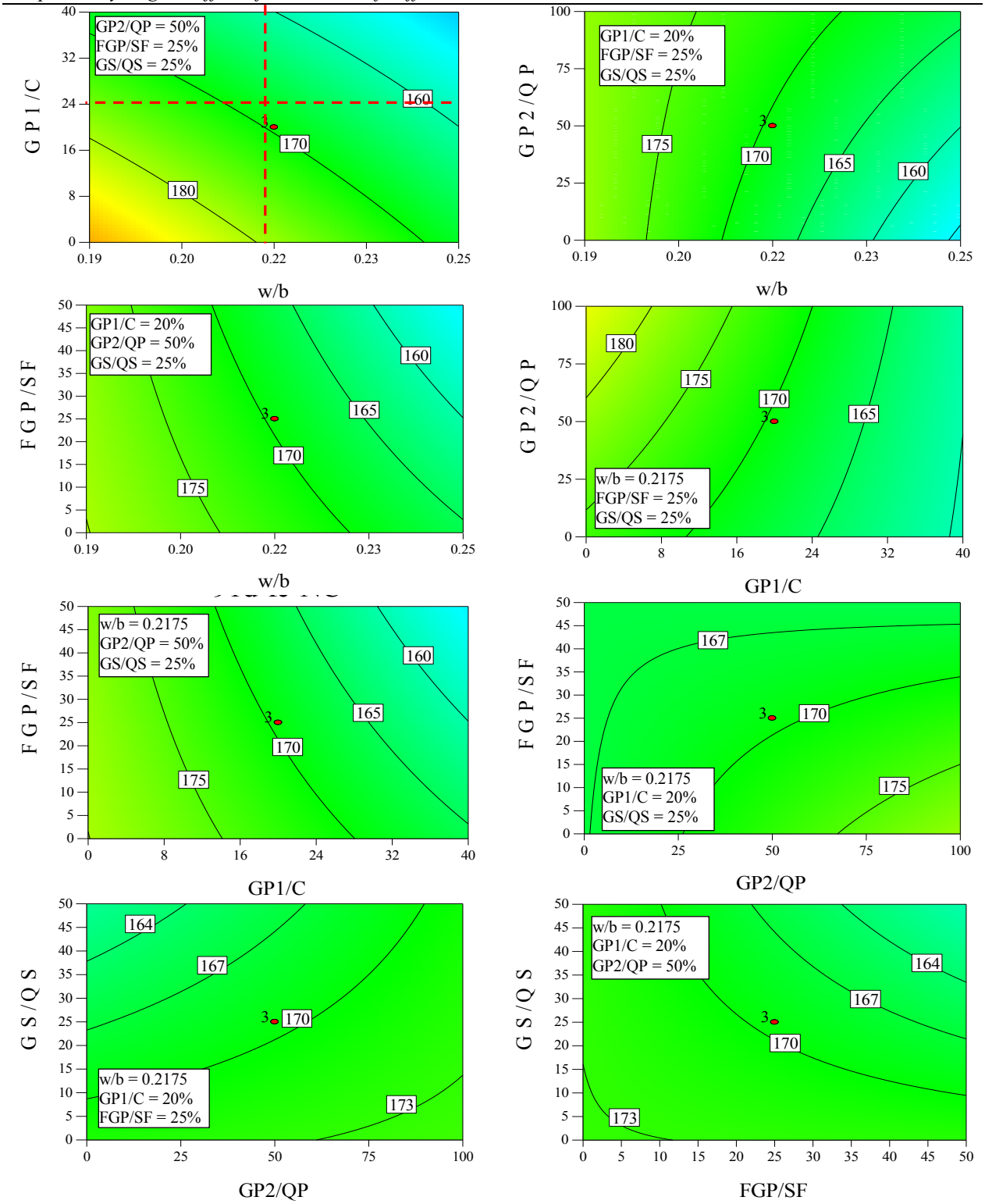

Fig. 11 – Contour diagram for the trade-off the effect of water-to-binder ratio (*w/b*), percentage of glass powder 1-to-cement by weight (*GP1/C*), percentage of glass powder 2-to-quartz powder by weight (*GP2/QP*), percentage of fine glass powder-to-silica fume by weight (*FGP/SF*), and percentage of glass sand-to-quartz sand by weight (*GS/QS*) on 91d-fc-NC

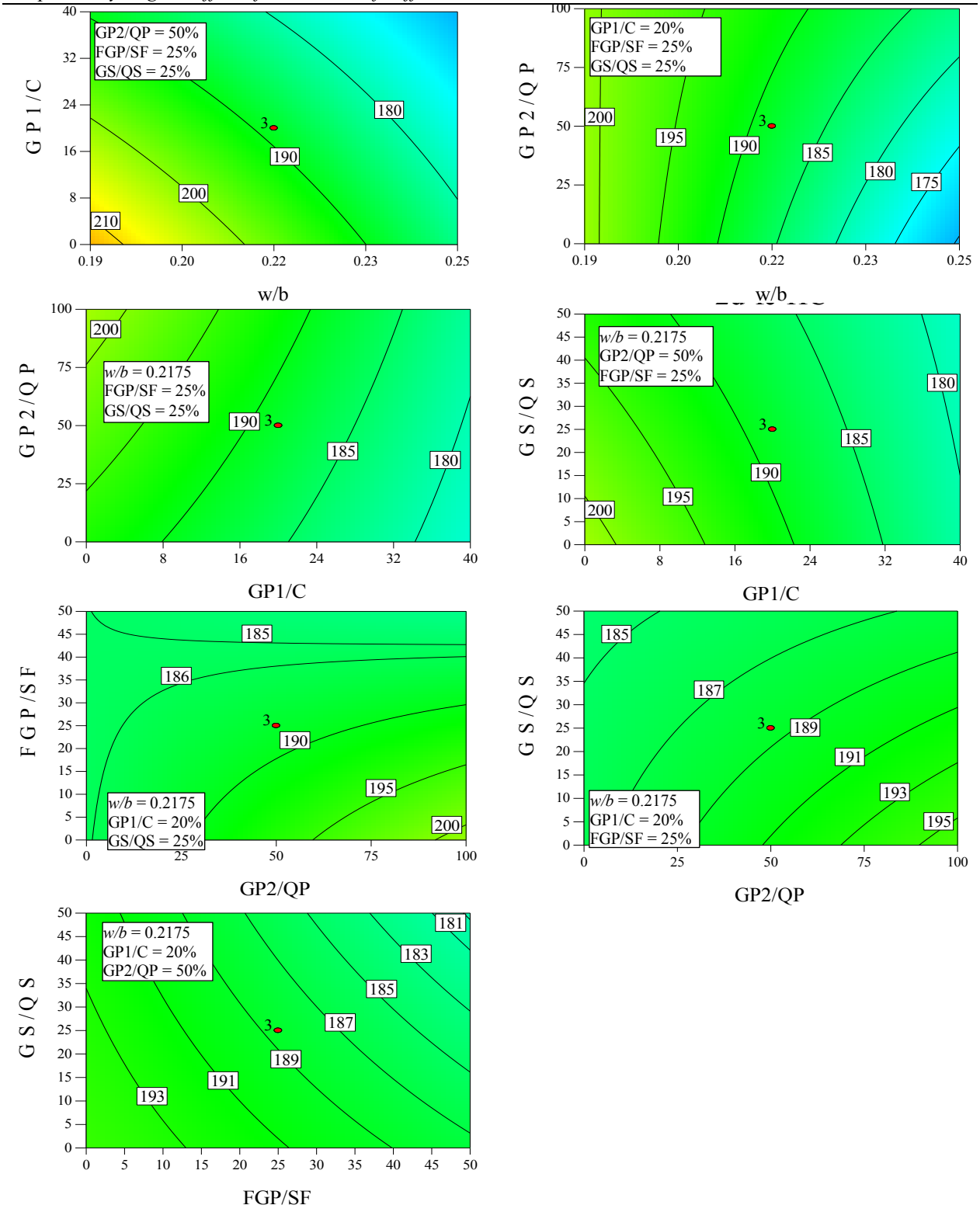

Fig. 12 – Contour diagram for the trade-off the effect of water-to-binder ratio (*w/b*), percentage of glass powder 1-to-cement by weight (*GP1/C*), percentage of glass powder 2-to-quartz powder by weight (*GP2/QP*), percentage of fine glass powder-to-silica fume by weight (*FGP/SF*), and percentage of glass sand-to-quartz sand by weight (*GS/QS*) on 2d-fc-HC

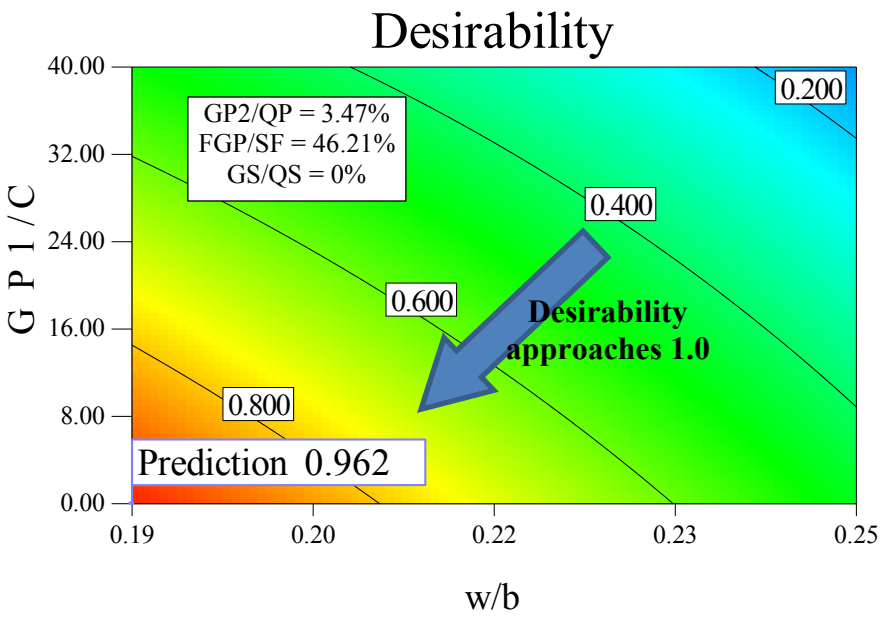

Fig. 13 – Contour diagram showing the tradeoff between the various mixture ingredients (parameters) for UHPC production with specific desirability

8 Scale-up and Field Validation of UHPGC

8.1 Introduction

This chapter presents the critical step with respect to scaling up production and conducting field validation of UHPGC. In the preceding chapter, UHPGC was produced in a 10 l laboratory-scale mixer. This scale-up project was conducted as two tasks: (1) The effect of mixing technique at a pilot scale on rheological (ConTec viscometer, V-funnel flow time test, JRing test, and L-box test), mechanical (f'_c, modulus of elasticity, tensile strength, stress–strain behavior, flexural characteristics), and durability (freezing and thawing, alkali–silica reaction, mechanical abrasion, scaling, permeability, and shrinkage) properties for selected UHPGCs was determined, (2) Field validation of UHPGC for large-scale structures.

In the first task, UHPGC without fibers and with 1% fiber were compared in this chapter. The possibility of producing the optimized UHPGC, which was developed in laboratory with a small-scale mixer, on an industrial scale with a pilot plant, and for casting two footbridges at the University of Sherbrooke campus, is presented. The full characterization results of the optimized UHPGC mixture used to cast the footbridges is highlighted in this chapter.

Descriptions of the materials, mix designs, and mixing sequence used in these experimental tests are given in this chapter.

8.2 Paper 6: Study of Rheological and Mechanical Performance of Ultra-High-Performance Glass Concrete

Reference:

Soliman N., Tagnit-Hamou A. (24-25 July 2014) Study of Rheological and Mechanical Performance of Ultra-High-Performance Glass Concrete. *2nd FRC Joint ACI-fib International Workshop, Fibre Reinforced Concrete: from Design to Structural Applications*.

Soliman N., Tagnit-Hamou A. (2015) Study of Rheological and Mechanical Performance of Ultra-High Performance Glass Concrete, *ACI Special Publication (ACI SP)*.

Study of Rheological and Mechanical Performance of Ultra-High-Performance Glass Concrete

Authors and Affiliation

Nancy A. Soliman, is a member of the ACI international and Sherbrooke local chapters, and CRIB. She is a PhD candidate in the Department of Civil Engineering, University of Sherbrooke, QC, Canada. Her research interest includes NDT, UHPC, microstructure, and sustainable development.

Arezki Tagnit-Hamou, FACI, is a professor in the Department of Civil Engineering at the University of Sherbrooke, QC, Canada. He is also the Head of the cement and concrete group as well as holding an industrial chair on valorization of glass in materials. He is a member of ACI Committees 130 (Sustainability of Concrete) and 555 (Concrete with Recycled Materials), and RILEM TC DTA. His research interests include alternative supplementary cementitious materials, cement and concrete physicochemistry and microstructure, and sustainable development.

ABSTRACT

A new type of green ultra-high-performance glass concrete (UHPGC) was developed at the Université de Sherbrooke using waste glass having of varying particle-size distributions (PSD). UHPGC provides several technological, economical, and environmental advantages. It reduces the production cost of ultra-high performance concrete (UHPC) and carbon footprint of traditional UHPC structures. This paper presents the rheological and mechanical properties of selected UHPGCs. The rheology of the UHPGCs was improved by using non-absorptive glass particles. The UHPGC greatly improves concrete microstructure, resulting in higher mechanical and durability properties, which are comparable to those of conventional UHPC. The strength and rigidity gains were due to the fact that the glass particles acted as inclusions with very high strength and elastic modulus. A special mix design of UHPGC was developed for innovative

pedestrian bridges at Sherbrooke university campus. Concrete performances of this UHPGC are also presented on this paper.

Keywords

Durability, packing density, sustainability, ultra-high-performance concrete (UHPC), waste glass.

1. INTRODUCTION

A typical UHPC mix contains Portland cement, silica fume (SF), quartz sand (QS) having a maximum size of 600 μm, quartz powder (QP), and, possibly, very fine steel fiber (Richard and Cheyrezy, 1995). Such a mix has very low water-to-binder ratio (*w/b*) and contains a high amount of superplasticizer (SP). Depending on its composition and curing temperature, the resultant material can exhibit compressive strength higher than 150 MPa, flexural strength greater than 15 MPa, and elastic modulus above 50 GPa (Richard and Cheyrezy, 1994; Lee et al., 2005; Schmidt et al., 2005). It can also resist freeze-thaw and scaling cycles without visible damage, and it is nearly impermeable to chloride ions penetration (Roux et al., 1996)

Typical UHPCs are designed with high cement contents ranging from 800 to 1000 kg/m^3 (Richard and Cheyrezy, 1995). This huge amount of cement not only affects production costs and consumes natural sources, but it negatively impacts the environment through CO_2 emissions and the greenhouse effect (Aïtcin, 2000). The use of (25% to 35%) of SF by the cement weight with limited available resource and high cost is considered as one of the impediments of UHPC use in the concrete market. Moreover, the use of quartz powder (QP) in UHPC with small-diameter crystalline quartz particles raises concerns about respiratory health concerns (World Health Organization, 2000).

Ultra-high-performance glass concrete (UHPGC) is a new UHPC technology that constitutes a breakthrough in green concrete mix design (Tagnit-Hamou and Soliman 2014). The development resulted from using waste glass of varying PSD. The UHPGC mixtures were optimized based on the packing-density theory to the granular matrix. UHPGC is a fiber-reinforced concrete characterized by a very dense microstructure, which enhances durability via a discontinuous pore structure. The UHPGC can be designed with decreased content of cement, SF, QP, and QS given

the incorporation of various waste-glass products of different PSDs such as glass sand (GS), glass powder (GP), and fine glass powder (FGP). Fiber, high-range water-reducing admixture (HRWRA), and very low water to binder ratio (w/b) are also used in the design of the UHPGC. The research program aimed to study the behavior of this type of concrete and determining the overall performance (rheological characteristics, mechanical performance, and durability). Two UHPGC mixtures with and without steel fibers subjected to two different curing conditions are selected. Another optimized UHPGC mixture was used to build innovative green pedestrian bridges at Sherbrooke University.

2. Experimental Program

2.1 Mix-Design Optimization

The mix design was developed in three steps. First, the packing density of granular composition was optimized by using de Larrard's compressible packing model (1999). The optimal packing density selected was 0.78, obtained when combining the QS, GP, cement, and SF. Second, the optimum superplasticizer dosage for each *w/b* yielding specific rheological characteristics for obtaining a self-consolidating matrix as well as high strength was determined using a full-factorial design approach. Lastly, fiber was added to improve UHPGC ductility without significantly altering the rheological properties of the fresh mix. Figure 1 presents the typical mix components of UHPC and UHPGC.

	0.1 µm	100 µm	600 µm
Typical UHPC	Silica fume	Portland cement and quartz powder	Quartz sand

	0.1 µm	100 µm	600 µm
Typical UHPGC	Silica fume	Portland cement and glass powder	Quartz sand

Figure 1: Comparison of UHPGC and UHPC composition

2.2 Materials

The rheology of UHPC is strongly influenced by cement fineness and the C_3A and C_3S contents. A high-sulphate-resistant cement (Type HS cement), which is formulated specifically with low C_3A content, was selected. The HS cement contains 50% C_3S, 25% C_2S, 2% C_3A, and 14% C_4AF. It has a specific gravity of 3.21, Blaine fineness of 370 m^2/kg, and mean particle diameter (d_{50}) of 11 μm. The silica fume (SF) used in this study has silica content of 99.8%, specific gravity of 2.20, specific surface area of 20,000 m^2/kg, and d_{50} of 0.15 μm. Quartz sand (QS) with a maximum particle-size diameter (d_{max}) of 600 μm was used as granular materials. It has a d_{50} of 250 μm, silica content of 99.8%, and specific gravity of 2.70. Glass powder (GP) with a d_{max} of 100 μm, silica content of 73%, Na_2O content of 13%, and specific gravity of 2.60 was used. A polycarboxylate-based (PCE) high-range water-reducing admixture (HRWRA) with a specific gravity of 1.09 and solids content of 40% (Sika Viscocrete 6200) was used as superplasticizer. To enhance ductility, steel fibers 13 mm in length and 0.2 mm in diameter were incorporated in fiber reinforced mixture.

2.3 Testing Procedures

This research was carried out with the automatic concrete pilot plant with a 500-l capacity at the Université de Sherbrooke. To achieve a homogeneous mixture, all powder materials were mixed for 10 minutes. Half of the SP diluted in some of the mixing water was added between 3 and 5 minutes. The remaining water and superplasticizer was added between 3 and 5 minutes. The mixing was continued for an additional 3 minutes after adding fiber, if any. Once mixing had been completed, the fresh properties were measured, including fresh concrete temperature, unit weight, and air content. The concrete's flow was measured with the flow-table test.

Then, the specimens were stored at 20 ºC, 100% RH for 24 h, then removed from the molds, and cured. Two curing regimes were implemented after demoulding. In the standard curing regime, the samples were stored in a fog room (20 ± 2ºC, RH > 100%) until testing. The second mode of curing was steam cured at 90ºC and RH = 100% for 48 hours. A UHPGC that did not contain any fibers was tested and compared with another that contained 1% fiber. They will be identified in the following as the Non-Fiber and the Fiber mix.

The concretes were tested to determine the fresh and rheological properties, mechanical performance (compressive, tensile, flexural strengths, and modulus of elasticity), and durability characteristics (resistance to mechanical abrasion, scaling, freeze-thaw cycling, chloride-ion penetration, and drying shrinkage). All these tests methods were done according to ASTM Slandard test methods.

3. Results and Discussion

3.1 Fresh Properties

Table 1 presents the fresh concrete's temperature, unit weight, air content, and slump-flow diameter (without shock). Clearly, incorporating the GP resulted in a self-consolidating UHPGC with a slump-flow diameter of 300 mm for the non-fiber mixture and 290 mm for the fiber mixture. This allows the UHGPC to be practically self-placing. The results indicate it was possible to maintain highly similar flows for both the fiber and non-fiber mixes.

Table 1: Fresh properties of UHPGC

Mixture	Slump Flow (mm)	Unit Weight (kg/m^3)	Air Voids (%)	Temperature (ºC)
Non-Fiber	300	2330	3.2	22
Fiber	290	2390	3.3	23

3.2 Mechanical Properties

3.2.1 Compressive Strength

Compressive strength tests for the UHPGCs were carried according to ASTM C39 on cylindrical specimens measuring 100 mm in diameter and 200 mm in length. The tests were conducted at ages 7, 28, and 91 days for the normally cured samples and at 48 hours for the steam-cured samples. Figure 2 illustrates the compressive strength results of the two UHPGC mixtures measured at different ages and under different curing regimes. For steam curing, the compressive strengths of the non-fiber and fiber mixtures were 191 and 187 MPa, respectively. As can be seen, the fiber addition did not significantly increase significantly the compressive strength, since

fibers accounted for only 1% of the total volume of the UHPGC. As shown in the figure, the steam curing accelerated the achievement of final strength in a short time. The 28 d compressive testing of the non-fiber and fiber mixtures under normal curing were approximately similar (146 and 141 MPa, respectively). The compressive strength for normal curing at 91 days was 170 and 171 MPa for non-fiber and fiber mixtures, respectively. This can be accounted by the pozzolanic reactivity of the glass powder and enhancement of the UHPGC's microstructure. The difference in compressive strength between the steam-cured specimens at 48 hours and normal-cured specimens at 91 days was only about 10%.

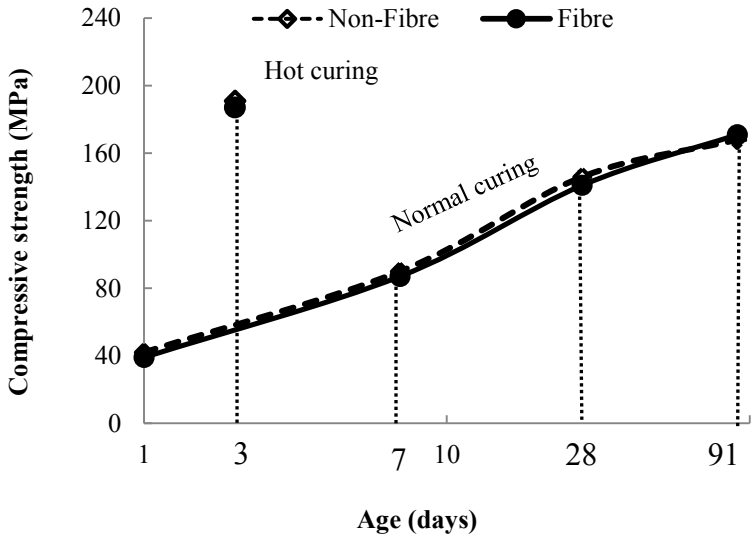

Figure 2: Compressive strength of the tested UHPGCs for different curing times

3.2.2 Toughness

The modulus of rupture (MOR) was calculated according to ASTM C 1018 as $MOR = PL/bd^2$ on the assumption of a linear-elastic stress state, where: P = applied force, L = span, b = specimen width, and d = specimen depth. The MOR versus mid-span deflection curves for the fiber concrete mixtures tested at 91 days of normal curing is shown in Figure 3. The initial crack, maximum, and failure loads and the corresponding mid-span deflections are shown in Figure 3. The fiber concrete show ductile failure mode, unlike the brittle failure mode of the concrete without fiber.

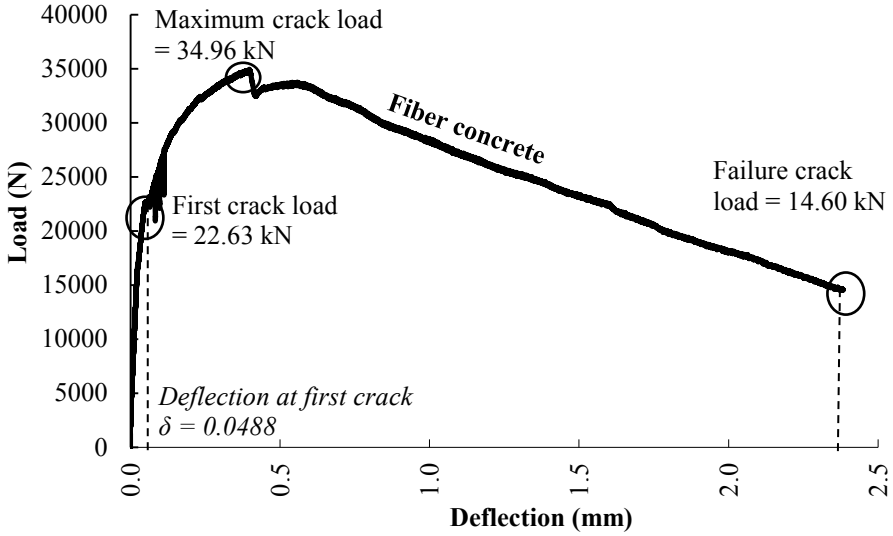

Figure 3: Flexural load-deflection curve of third-point bending test at 91 days

3.2.3 Flexural Strength

Flexural testing was conducted according to ASTM C 1018. Figure 4 provides the results. The inclusion of 1% fiber increased the flexural strength from 17 to 20 MPa after 91 days of normal curing and from 17 to 21 MPa after 48 hours of steam curing. The heat treatment did not show a significant increase in flexural strength, with only 1 MPa difference between the steam curing and 91 days of normal curing.

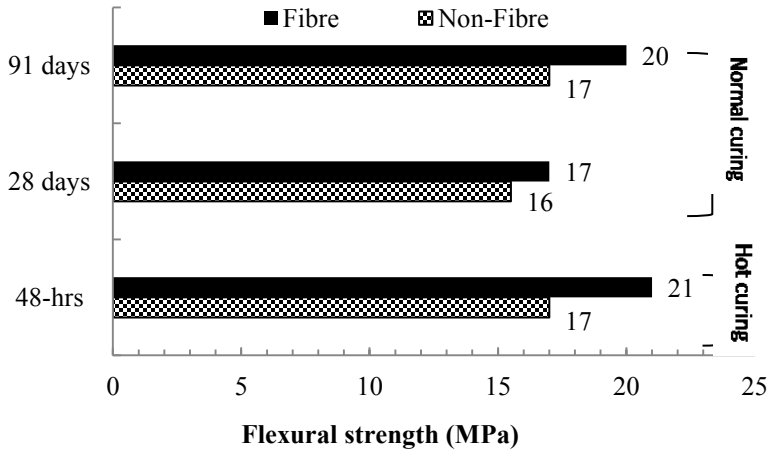

Figure 4: Effect of fiber, curing types, and age on UHPGC flexural strength

3.2.4 Modulus of Elasticity

Modulus of elasticity was measured on 100×200 mm cylinders according to ASTM C 469. The obtained results, indicating that normal or steam curing, different age, and fiber content did not significantly affect the elastic modulus value. The measured values for all concrete mixtures were about 50 ± 2 GPa.

3.3 Durability

3.3.1 Scaling Resistance

Scaling resistance was measured for the fiber and non-fiber UHPGC mixtures according to ASTM C 672. After 50 freeze–thaw cycles, the scaled-off mass ranged from 13 to 21 g/m^2. These values are low compared to the salt scaling of UHPC reported in the literature, which varied from (8 to 60 g/m^2) for studies conducted on 28 to 50 freeze–thaw cycles (Graybeal, 2006; Dugat et al., 1996).

3.3.2 Abrasion Resistance

Concrete abrasion resistance was measured according to ASTM C 944. The average value for the relative volume loss index of UHPGC ranged from approximately 1.10 to 1.23. For typical UHPCs, the relative volume loss index ranges 1.1 to 1.7 (Perry and Zakariasen, 2004; Bonneau et al., 1997).

3.3.3 Resistance to Freeze–Thaw Cycles

The UHPGC's resistance to freeze–thaw cycling was measured according to ASTM C666. The test was conducted 1000 freeze-thaw cycles. The results show that the normal- and steam-cured specimens with or without fiber maintained dynamic moduli of elasticity close to their original states before testing, with a magnitude equal to or greater than 102%. It is worth mentioning that no specimens showed any deterioration or cracking after the end of freeze-thaw cycles.

3.3.4 Resistance to Chloride-Ion Penetration

Rapid chloride-ion penetration testing was conducted on the UHPGC specimen according to ASTM C1202 (Table 2). The test was performed at 28 and 91 days for the normally cured specimens and after 48 hours (2 days) for the steam-cured ones. According to ASTM C1202, the obtained results indicate "negligible" chloride-ion permeability, regardless of curing regime.

Table 2: Charges passed during the rapid chloride-ion penetration test

Curing Method	Mixture	Age (days)	Charges Passed (Coulombs)
Normal curing	Non-fiber	28	30
	Fiber		28
Normal curing	Non-fiber	91	18
	Fiber		20
Steam curing	Non-fiber	2	8
	Fiber		7

3.3.5 Dry Shrinkage

The drying-shrinkage test was conducted according to ASTM C157 for both normal- and steam-curing conditions. Figure 5 illustrates the variations in drying-shrinkage deformation over time for the UHPGCs test under normal- and steam-curing conditions. The figure shows a sudden drying shrinkage deformation of about 400 to 460 μstrain in the case of both the fiber and non-fiber mixtures that were steam cured. These deformation values did not significantly increase afterwards, given that most of the hydration occurred during steam curing and that the rate of hydration was relatively slow thereafter. In case of normal curing, drying-shrinkage deformation increased over time (major part of drying shrinkage occurred during the first 20 days after casting) before achieving relative stability at 90 days, given the increasing rate of hydration. The fiber UHPGC exhibited lower shrinkage compared to the non-fiber mixture. For example, at 20 days, the drying-deformation values were 180 and 260 μstrain for the fiber and non-fiber mixtures, respectively. The corresponding values at 90 days were 540 and 620 μstrain.

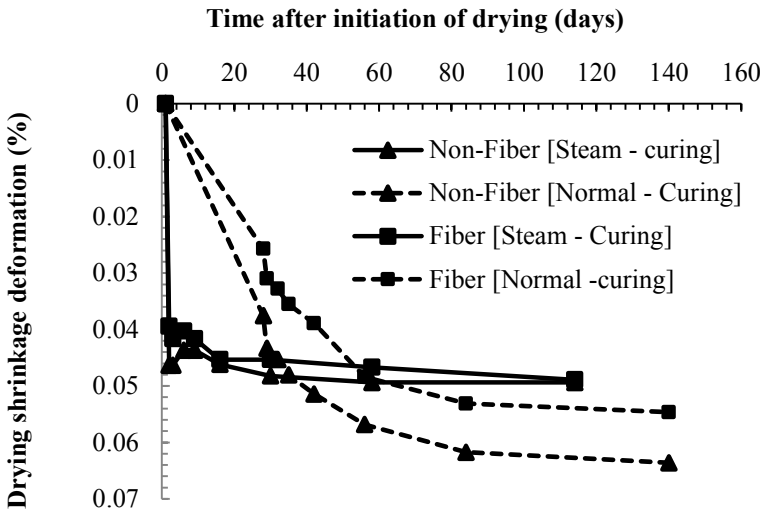

Figure 5: Variations of drying shrinkage deformation over time for the UHPGCs

4. Structural application

As mentioned above an optimized UHPGC mixture was used to produce two pedestrian footbridges (Figure 6) to replace deteriorated wooden footbridges at the University of Sherbrooke campus (Tagnit-Hamou et al., 2015). The footbridges were designed to meet the university's architectural and structural requirements for pedestrian use as well as to be in compliance with the university's regulation on sustainable development.

This UHPGC mixture has *w/b* 0.24 with 2.5% polyvinyl alcohol (PVA) fibers having 13 mm in length and 0.2 mm in diameter. The PVA fiber was incorporated in the mix to avoid the spot corrosion on the surface which is associated with the steel fiber; especially because the bridges are exposed to sever environmental conditions with the frequent use of deicing salts. However, the 2.5% of PVA fiber decrease the compressive strength but it improved greatly the ductility.

The use of UHPGC technology with high mechanical properties enabled the designer to create thin sections that are light, graceful, innovative in geometry, and produced with a relatively low cost and low environmental footprint. Each bridge had a total weight of around 4000 kg. The structural system has a length of 4910 mm in, a width of 2500 mm , and a thickness of 75 mm. The arch slab is supported by longitudinal ribs of variable heights and a constant width of 130 mm (Fig. 10-a, b). The arch slab was reinforced with welded wire reinforcement (M10 at 300 mm in both directions) placed at the mid height of the slab. Each rib was reinforced with a single M20 reinforcing bar located near the bottom of the rib.

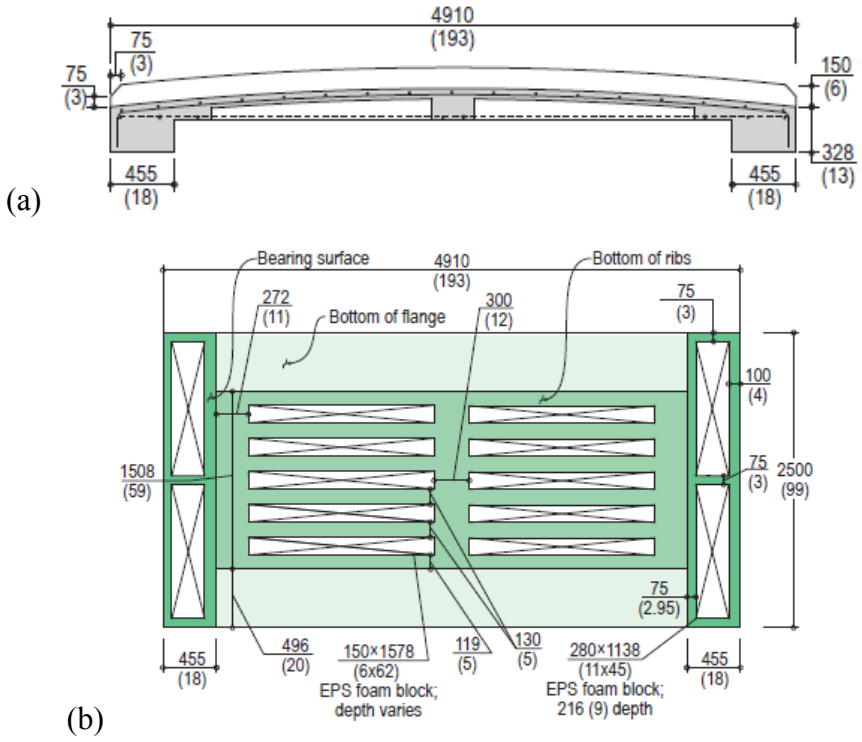

Fig. 6 – Bridge: (a) schematic longitudinal section at centerline, (b) bottom view showing concrete dimensions in mm (nearest in.)

Concrete Performance

Fresh properties - Tests were performed to obtain basic fresh concrete properties including slump flow, unit weight, air content, and temperature. Testing results are 280 mm without tamping, 2231 kg/m3, 3.5%, and, 22°C respectively.

Mechanical properties – Compressive strength tests were carried at 1, 7, 28, and 91 days after normal curing. The 28 and 91-day compressive strengths of this UHPGC were 96 and 127 MPa, respectively (Table 3). The increase in compressive strength of about 33% from 28 days to 91 days indicates the effect of the pozzolanic reactivity of glass powder. Other test like indirect splitting tensile strength, flexural strength, and modulus of elasticity were also performed.

Table 3: Mechanical properties of UHPGC

Properties	Concrete age, days			
	1	7	28	91
Compressive strength, MPa	12	52	96	127
Splitting tensile strength, MPa	--	--	10	11
Flexure strength, MPa	--	--	10	12
Modulus of elasticity, GPa	--	--	41	45

Durability properties - The abrasion test show an average value of the relative volume-loss index of 1.35 mm. The scaling resistance, after 50 freezing-and-thawing cycles, was very low (12 g/m^2). The 28 and 91-day specimens exhibited to chloride-ion penetration test presented negligible value of 10 coulombs in both cases. The relative dynamic modulus was 100% after 1000 freezing-and-thawing cycles.

5. Conclusions

A new type of ultra-high-performance glass concrete (UHPGC) was developed through the use of waste-glass powder with varying particle-size distribution. The typical UHPGC mixture was optimized using the packing-density method. In this study, 400 kg per meter cubic of glass powder was successfully used to replace various components in traditional ultra-high performance concrete (UHPC).

Two types of UHPGC were tested, with and without fiber, under two curing regimes (normal and steam curing). The concrete mixtures presented excellent workability with high slump. This is attributed to the use of non-absorptive glass particles and optimized packing density. Mechanical performance was excellent and comparable to conventional UHPC.

The construction of two footbridges at the University of Sherbrooke using the UHPGC shows the potential for the material to be used in future projects. The UHPGC will produce highly energy efficient, environmentally friendly, affordable, and resilient structures.

The use of UHPGC provides several advantages, such as using waste glass, reducing UHPC production costs, and decreasing the environmental footprint of conventional UHPC.

6. Acknowledgements

The authors are acknowledging the SAQ Industrial Research Chair for the financial support. The authors would like also to express their appreciation and thanks to Professor Pierre-Claude Aïtcin, and Dr. Ahmed Omran for their cooperation and advice during this research project.

7. References

Aïtcin, P-C. (Sept. 2000) Cements of Yesterday and Today – Concrete of Tomorrow. Cement and Concrete Research, Vol. 30, No. 9, pp. 1349-1359

Bonneau, O.; Lachemi, M.; Dallaire, E.; Dugat, J.; Aïtcin, P-C. (July-Aug. 1997) Mechanical Properties and Durability of Two Industrial Reactive Powder Concretes. ACI Materials Journal, Vol. 94, No. 4, pp. 286-290.

de Larrard F. (1999), Concrete Mixture Proportioning: A Scientific Approach, E&FN Spon, London

Dugat, J.; Roux, N.; Bernier, G. (May 1996) Mechanical Properties of Reactive Powder Concretes. Materials and Structures, Vol. 29, pp. 233-240.

Graybeal, B.A. (Aug. 2006) Material Property Characterization of Ultra-High Performance Concrete. FHWA-HRT-06-103

Perry, V.; Zakariasen, D. (Aug. 2004) First Use of Ultra-High Performance Concrete for an Innovative Train Station Canopy. Concrete Technology Today, Vol. 25, No. 2, pp. 1-2.

Richard, P.; Cheyrezy, M. (1994) Reactive Powder Concretes with High Ductility and 200-800 MPa Compressive Strength. ACI SP 144, pp. 507-518.

Richard, P.; Cheyrezy, M. (1995) Composition of Reactive Powder Concretes. Cement and Concrete Research. Vol. 25, No. 7, pp. 1501-1511.

Roux, N.; Andrade, C.; Sanjuan, M. (1996) Experimental Study of Durability of Reactive Powder Concretes. Journal of Materials in Civil Engineering, Vol. 8, Issue 1, pp. 1-6.

Schmidt, M.; Fehling, E. (2005) Ultra-High-Performance Concrete: Research, Development and Application in Europe. ACI SP, Vol. 225, pp. 51-77.

Tagnit-Hamou, A., and Soliman, N., "Ultra-High Performance Glass Concrete and Method for Producing same," U.S. Patent Application. No. 61/806,083, file March 28, 2013, Accepted March 2014.

Tagnit-Hamou, A.; Soliman, N.; Omran, A. F.; Mousa, M. T.; Gauvreau, N.; and Provencher, MF.; (March 2015) "Novel Ultra-High-Performance Glass Concrete," Journal of ACI Concrete International. V. 39, No. 3, pp. 53-59.

World Health Organization, (2000), "Crystalline Silica", Quartz Concise International Chemical Assessment, Document 24,

8.3 Paper 7: Laboratory Characterization and Field Application of Novel Ultra-High Performance Glass Concrete

Reference:

Soliman N., Omran A.F., Tagnit-Hamou A. (2015) Laboratory Characterization and Field Application of Novel Ultra-High Performance Glass Concrete. *ACI Materials Journal*. 41 (in press).

Laboratory Characterization and Field Application of Novel Ultra-High Performance Glass Concrete

Authors and Affiliation

Nancy A. Soliman, is a member of the ACI international and Sherbrooke local chapters, and CRIB. She is a PhD candidate in the Department of Civil Engineering, University of Sherbrooke, QC, Canada. Her research interest includes NDT, UHPC, microstructure, and sustainable development.

Ahmed F. Omran, is a postdoctoral fellow of Department of Civil Engineering, University of Sherbrooke and assistant professor of University of Minoufiya, Egypt. He holds BS and MS degrees in Civil Engineering from University of Minoufiya. He received Ph.D. degree from University of Sherbrooke. He is an active member of RILEM TC-233 FPC Committee. His research interests include durability of cement-based materials, development of new alternative supplementary cementitious materials (ASCM), sustainable development, concrete rheology, and formwork pressure.

Arezki Tagnit-Hamou, FACI, is a professor in the Department of Civil Engineering at the University of Sherbrooke, QC, Canada. He is also the Head of the cement and concrete group as well as holding an industrial chair on valorization of glass in materials. He is a member of ACI Committees 130 (Sustainability of Concrete) and 555 (Concrete with Recycled Materials), and RILEM TC DTA. His research interests include alternative supplementary cementitious materials, cement and concrete physicochemistry and microstructure, and sustainable development.

ABSTRACT

A new type of ecological ultra-high performance concrete (UHPC) was developed at University of Sherbrooke using waste glass of varying particle-size distributions, named ultra-high performance glass concrete (UHPGC).[1] The current research presents laboratory characterization

of various UHPGC mixtures in comparison to traditional UHPC mixtures. The research focuses on large-scale application through a scaling-up by using concrete pilot plant. The research presents also field validation of the optimized UHPGC mixture by erection of two footbridges as a case study. The UHPGC provides high workability and enhanced rheological properties, given the zero absorption of glass particles and optimized packing density of the entire material matrix. The UHPGC greatly improves the concrete microstructure, resulting in higher mechanical and durability properties, which are greater than the traditional UHPC. A compressive strength greater than 200 MPa (29,007 psi) can be obtained for the UHPGC. The higher mechanical properties allowed the footbridges design with about 60%-reduced sections compared to normal concrete. The UHPGC improves durability resulting in reduction of maintenance cost. Compared to traditional UHPC, the UHPGC reduces carbon footprint and production cost of UHPC by employing more than 400 kg/m^3 of glass materials, and also save money spent for the treatment and landfilling of glass cullets.

Keywords: Field validation, Footbridges, Glass powder, Large-scale production, Sustainability, Ultra-High Performance Concrete. UHPGC Characterization

INTRODUCTION

Ultra-high performance concrete (UHPC)

Conventional vibrated concrete (CVC) has numerous problems such as corrosion of steel reinforcement and fragility of concrete construction. As a result, most of structures made with conventional concrete require annual maintenance.[2] Currently, there is a critical need for advanced high-performance building materials for infrastructure and repair.[3]

The ultra-high performance concrete (UHPC) can be designed to eliminate some of the characteristic weaknesses of CVC.[4] The UHPC is defined worldwide as concrete with superior mechanical, ductility, and durability properties. Typical UHPC is composed of very high cement content (800 to 1000 kg/m^3), higher content of silica fume (SF) (25% to 35%, by weight of cement), quartz powder (QP) quartz sand (QS) and steel fiber.[4] The steel fiber in the UHPC improves the material's ductility and tensile capacity. With the UHPC, compressive strength (f_c)

greater than 150 MPa (22,000 psi), flexural strength (f_{fl}) of up to 15 MPa (2,200 psi), elastic modulus (E_c) of 45 GPa (6,500 ksi), and minimal long-term creep or shrinkage can be achieved.[5,6] The UHPC can also resist freeze–thaw cycles and de-icing salt scaling without any visible damage, and it is nearly impermeable to chloride-ion penetration.[7]

Currently, the UHPC is used in the construction of special prestressed and precast concrete elements, such as decks and abutments of lightweight bridges, marine platforms, precast walls, concrete repair, and urban furniture and other architectural applications.[3,8]

The UHPC confers some economic advantages to overcome this issue such as (1) reducing or eliminating the passive reinforcement in structural elements given its design with steel fiber, (2) reducing the dimensions of concrete elements due to its ultra-high mechanical properties, (3) reducing the self-weight of structural elements by more than 70%, (4) extending the service life of structure, and (5) lowering maintenance costs given its superior durability properties.[9-11]

The huge amount of cement (800 and 1000 kg/m^3) in the UHPC not only affects the production cost and consumes natural resources, it also has a negative impact on the environment through the CO_2 emissions and greenhouse effect.[11] The higher SF content, with high cost and limited resources, incorporated in the UHPC (25%–35%, by cement weight) is also another obstacle to the wide use of the UHPC in concrete market. Moreover, the use of fine crystalline QP in UHPC raises concerns about respiratory health.[12]

Glass material in concrete

Post consumption glass can be recycled several times without significant alternation of its physical and chemical properties.[13] In Europe, as indicated by the latest glass recycling industry report published by the European Container Glass Federation (FEVE), the average of glass recycling rate in 2011 has risen above the threshold by 70% (over 12 million tons).[14] Large quantities of glass cannot be recycled because of colour mixing, or expensive recycling cost.[13] For example, in Quebec, only 49% of the glass was recovered in 2008, the rest has been landfilled.[15] According to USEPA, Americans generated 11.5 million tons of glass in the municipal solid waste stream and only 28% of this glass was recovered for recycling.[16] The amount of waste glass is gradually increased over the recent years due to an ever-growing use of

glass products. Most of the waste glass has been dumped into landfill sites, which is undesirable as it is not biodegradable and less environmentally friendship.

Waste glass material when crushed and ground at different particle sizes is considered as an innovative, durable and sustainable material to be used in concrete. In recent years, attempts have been made to use waste glass as alternative supplementary cementitious materials (ASCM) or ultra-fine filler in concrete, depending on its chemical composition and particle size.[17-19] The ground glass of a particle size finer than 38 μm exhibits pozzolanic behaviour, which contributes to concrete's strength and durability.[20-22] The glass powder (GP) can be incorporated as partial cement replacement in different concrete types.[23-27] The GP was also successfully used in UHPC mixtures to replace totally the QP and partially the SF.[1,27,28] Besides, reuse of very fine ground waste GP (with a particle size of 30 μm or smaller) can be used as ASCM to partially replace cement in concrete and this significantly decrease the adverse effects caused by the alkali–silica reaction.[29-31]

Based on these researches, there is a high value and feasibility of incorporating waste GP in concrete considering its economic and technical advantages.

Novel ultra-high performance glass concrete (UHPGC)

A new type of UHPC that constitutes a breakthrough in sustainable concrete technology is the ultra-high performance glass concrete (UHPGC) that can be designed using "waste glass" materials of different particle-size distributions (PSD).[1] The UHPGC can be designed with a reduced amount of cement of up to 50%. In the UHPGC, glass sand (GS) with an average mean-particle diameter (d_{50}) of 400 μm can replace up to 100% of QS. The GP with d_{50} of 10 μm can also replace up to 100% of QP and up to 50% of cement. Fine glass powder (FGP) with d_{50} of 3 μm can replace up to 70% of SF. The UHPGC also includes fiber, high-range water-reducing admixture (HRWRA), and very low water-to-binder ratio (w/b).[1]

The workability and rheological properties of the UHPGC are improved due to the zero adsorption of glass particles. The UHGPC can be practically self-placed without the need to internal vibration. Depending on the composition and curing temperature, the f_c values ranged from 130 to 260 MPa (19,000 to 38,000 psi), f_{fl} greater than 12 MPa (1,740 psi), splitting-tensile strength (f_{sp}) of up to 10 MPa (1,500 psi), and E_c of 45 GPa (6,500 ksi) can be obtained for the

UHPGC.[1] The UHPGC is characterized by excellent durability due to its high packing density and lack of interconnected pores. The UHPGC can be considered as an innovative low-cost, sustainable, and green UHPC.

The current research presents mix-design optimization of a total of nine UHPGC and two traditional UHPC mixtures for recommending an optimum UHPGC mixture for field validation. A comparison between the two traditional UHPC and the corresponding UHPGC mixtures are highlighted. This research is mainly proposed to evaluate the possibility of producing the optimized UHPGC, which was developed in laboratory using small-scale mixer, on industrial large-scale using pilot plan and using it in the casting of two footbridges at University of Sherbrooke campus. The research presents also the full characterization results of the optimized UHPGC mixture used in the footbridges' casting.

RESEARCH SIGNIFICANCE

Currently, there is a critical need for advanced building materials for North America domestic infrastructures, not only for new high-performance construction, but also for repair and enhancing the performance of existing structures. The required materials should be highly energy efficient, environmentally friendly, sustainable, affordable, and resilient. These materials should also meet multi-hazard/performance design criteria and be easily produced and incorporated into construction methods and practice. Furthermore, these materials must be cost effective through the structure's life cycle. An innovative low-cost, durable, sustainable, and green ultra-high performance concrete designed with waste glass particles of varying particle-size distributions and named as UHPGC is presented in this study as one of these materials. The current research shows how to transfer the UHPGC technology from laboratory to a full-scale production as well as a case study of UHPGC application in field through casting of two footbridges.

MIX-DESIGN OPTIMIZATION

Methodology undertaken to develop UHPGC mixtures

The mix design of the UHPGC is developed according to three main steps; optimization of packing density of granular materials (QS, GP, cement, and SF), optimization of *w/b* and HRWRA dosage, and optimization of the fiber content.[1] The packing density of the granular materials is optimized using compressible packing model.[32] The PSD of each of the QS, GP, cement, and SF as well as the combination of the four ingredients are presented in Fig. 1. The figure shows continuous particle distribution of the combined ingredients obtained using the compressible packing model. The optimal packing density when combining the QS, GP, cement, and SF is 0.78%. This enables using approximately 400 kg/m^3 of GP in the UHPGC mixture. Both *w/b* and HRWRA dosage used in the UHPGC are optimized to produce concrete with certain rheological characteristics and strength requirements. The fiber content is optimized without significant alteration of the rheological properties of the fresh mixture. The fiber optimization depends mainly on the fiber type and content.

Mixture proportioning

In total, nine UHPGC mixtures in addition to two traditional UHPC mixtures (UHPC-1 and UHPC-2) were prepared and tested in this research (Table 1). The UHPGC mixtures 0.225-0% and 0.250-0% were selected to satisfy the requirements of the architect of having a very flowable concrete for fill efficiently the bridges during casting. To investigate the effect of type and content of fiber on the flowability and mechanical properties, steel and Polyvinyl alcohol (PVA) fibers were employed. The volume fraction for the steel fiber was 2.0%, while the PVA fiber was used with volume fractions of 2.5% and 4.0%. The two types and content of fiber were selected as per the architectural requirement. The coded name of the UHPGC mixtures is a combination of three parts; *w/b*, type of fiber (S: for steel fiber and P: for the PVA fiber), and the fiber content in percentage. For example, the 0.225-P4.0% mixture has *w/b* of 0.225, and with 4.0% PVA fiber.

The two traditional UHPC (UHPC-1 and UHPC-2 mixtures), with *w/b* of 0.225 and 0.250, respectively, were designed with the same mix design method applied in the UHPGC described earlier. The UHPC-1 can be considered as the reference for the UPHGC 0.225-0%; the GP was used to replace 25% of cement and the entire QP content in the UPHGC 0.225-0%. The UHPC-2 can also be considered as the reference for the UHPGC 0.250-0%, with GP replacement by 25% of cement and 100% of QP.

Materials

In general, the contents of C_3A and C_3S in cement as well as cement fineness are critical for controlling concrete rheology.[11] This is more pronounced in case of the UHPC that is designed with higher cement content. Therefore, high sulphate-resistance cement (Type HS cement) with low C_3A and C_3S contents was selected for making the UHPGC mixtures. The HS cement has specific gravity of 3.21, Blaine surface fineness of 370 m^2/kg (201 yd^2/lb), and d_{50} of 11 µm**.** The SF used in the mixture proportioning complies with CAN/CSA A3000 specifications, and has specific gravity of 2.20, Blaine surface area of 20,000 m^2/kg (11,000 yd^2/lb), and d_{50} of 0.15 µm. The QS used has specific gravity of 2.70, maximum-particle size (d_{max}) of 600 µm, and d_{50} of 250 µm. The QP with a specific gravity of 2.73 and d_{50} of 13 µm was used as filler. The GP has specific gravity of 2.60 and d_{max} of 100 µm. Table 2 shows the chemical composition of the materials used in this study. A polycarboxylate-based HRWRA with specific gravity of 1.09 and solid content of 40% (Sika Viscocrete 6200) was employed in the mixtures. PVA and steel fiber with the properties presented in Table 3 were used in the UHPGC mixtures proportioning.

Testing procedures

All the concrete mixtures were batched using high energy shear mixer with a capacity of 10 liters. To achieve a homogeneous mixture and avoid particles agglomeration, all powder materials were mixed for 10 min before water and HRWRA addition. Approximately half of the HRWRA diluted in half of the mixing water was gradually added over 3.0 min of mixing. The remaining water and HRWRA were then gradually added during other 2.0 min of mixing. The mixing continued for additional 3.0 min before fiber addition, if any, then resuming mixing for extra 2.0 min.

Upon the terminal of mixing, the fresh properties of the UHPGC mixtures were measured. The tests included concrete temperature, unit weight, and air content (ASTM C 185). Slump-flow diameter using flow table and mini-slump cone without tamping (ASTM C1437) was also measured.

Cubes measuring 50×50×50 mm (2×2×2″) were sampled for the f_c testing at different ages. The cubes were covered with plastic sheets and stored at 23°C (73°F) and 50% relative humidity (RH) for 24 hours before demoulding. After demoulding, the samples were subjected to two different curing regimes: normal curing (NC) and hot steam curing (HC). In the NC, the samples were stored in a fog room of a temperature of 23°C (73°F) and RH of 100% till the day of testing. The HC mode composed of curing the samples at 90ºC and 100% RH for 48 hours before testing.

The f_{sp} was measured using 100×200 mm (4×8″) cylinders that were cured for 48 hours in HC condition (90ºC and 100% RH) after demoulding.

Properties of mix-design optimization

Fresh properties

The fresh properties of the tested mixtures are shown in Table 4. The slump flow increased to 250 mm (9.8″) for the 0.225-0% mixture compared to 235 mm (9.25″) for the UHPC-1 and from 265 mm (10.4″) for the 0.25-0% mixture compared to 250 mm (9.8″) for the UHPC-2. The workability of fresh UHPGC is improved due to the partial replacement of cement (25%) by non-absorptive glass particles and by total replacement of QP by the GP in the UHPGC mixtures. The increased flowability associated with incorporation of GP may also be due to the non-formation of binding products between particles as the case when using cement.

The results indicate that the workability of concrete is affected by the increase in the PVA-fiber content. A loss in the slump flow spread from 245 mm (9.6″) to 180 mm (7.1″) was measured when the PVA fiber content increased from 2.5% to 4.0% in the 0.225-P2.5% and 0.225-P4.0% mixtures, respectively, given that these two mixtures are proportioned with similar HRWRA dosage (Fig. 2). The slump loss is also associated with an increase in the air content. For the aforementioned mixtures, the air content increased from 4.0% to 5.1% (too high), respectively. The inclusion of 2.0% of steel fiber in the 0.225-S2.0% and 0.250-S2.0% mixtures has not shown any significant effect on the concrete workability. Only 10 and 5 mm (0.39″ and 0.20″) loss in the spread diameter was measured for the 0.225-S2.0% and 0.250-S2.0% mixtures compared to the two corresponding reference mixtures without fiber, respectively.

The four UHPGC mixtures with PVA fiber additions of 2.5% and 4.0% (0.225-P2.5%, 0.225-P4.0%, 0.250-P2.5%, and 0.250-P4.0%) required higher dosages of HRWRA to secure acceptable range of concrete workability. The workability of UHPC mixtures clearly decreases with increasing the fiber content greater than 2.5%, by volume, due to the increase of the interference between granular materials and fibers.[33-35] The higher HRWRA dosages in these four mixtures led to a delay of concrete setting and ought to keep the concrete in the moulds for two days before demoulding.

Compressive strength

The f_c results under NC (at ages of 1 or 2 days based on concrete setting, 7, 28, and 91 days) and under HC (at age of 2 days) for the tested mixtures are presented in Fig. 2.

The f_c results for the 0.225-0% showed increases of 18 MPa (2,611 psi) after 91-days NC and 21 MPa (3,046 psi) after 2-days HC compared to the UHPC-1. The 0.25-0% showed also an increase of 26 MPa (3,771 psi) in the f_c after both 91-days of NC and 2-days of HC compared to UHPC-2 (Fig. 2). This increase in the f_c can be referred to the pozzolanic reactivity of GP, given that GP was used to replace 25% of cement weight and 100% of QS. The incorporation of GP leads to enhancement of the microstructure and increase the f_c. This strength and rigidity improvements are due to the fact that glass particles act as inclusions having a very high strength and elastic modulus that have a strengthening effect on the overall hardened matrix.

As expected, concrete mixtures with higher *w/b* of 0.250 showed about 10% lower f_c values than the mixtures designed with 0.225 *w/b*. The concrete samples subjected to HC for only 2 days showed slightly greater f_c results compared to those obtained after 91 days of NC. The UHPGC mixture designed with PVA fiber exhibited lower f_c values compared to the corresponding mixture without fiber. This decrease in the f_c becomes worst with incorporating higher content of the PVA fiber. For example, the 91-day f_c values of 147 and 136 MPa (21,320 and 19,725 psi) were measured for the 0.225-P2.5% and 0.225-4.0% mixtures, respectively, compared to 181 MPa (26,252 psi) for the corresponding 0.225-0% mixture. The UHPGC mixtures with 2% steel fiber yielded approximately similar f_c results compared to corresponding mixture without fiber. The results of the f_c for the UHPGC mixtures without fiber or with 2.0% steel fiber show an average increase in the f_c of about 40% compared to the concrete mixtures containing PVA fiber.

Based on these observations, it can be concluded that the type and content of fiber have a great influence on the f_c of UHPGC.

Splitting-tensile strength

The fiber addition is necessary in specific structural applications where tensile strength and ductility are required by concrete design. The increase in f_{sp} accomplished by addition of fiber to the UHPGC matrix is clearly shown in Fig. 2. The 0.225-S2.0% mixture with 2.0% of steel fiber resulted in an increase in the f_{sp} of about 57% compared to the reference mixture (0.225-0%). About 44% improvement of the f_{sp} was also determined for 0.250-S2.0% compared to corresponding reference 0.250-0% mixture. With the PVA fiber addition, no improvement in the tensile strength of concrete was noticed. However, the ductility is greatly enhanced with the addition of PVA fiber as it will be explained later. The PVA fiber is still recommended rather than the steel fiber in architectural exterior elements that are exposed to environmental conditions, which leads to corrosion of steel fiber and making un-wanted corrosion spots on the concrete surface. Only the steel fiber parts that appeared on the concrete surface after sand blasting are subject to corrosion, where the embedded steel fiber in the UHPGC does not have such problem, given the very high dense concrete matrix and almost negligible permeability. The 0.225-0% mixture showed about 10% increase in the f_{sp} compared to UHPC-1, where the 0.250-0% presented about 18% increase compared to the UHPGC-2.

Selection of UHPGC mixture for bridge casting

The UHPGC exhibited higher mechanical strength than the reference without GP. The inclusion of GP in UHPC enhances also the rheology of fresh UHPGC due to the replacement of cement by non-absorptive glass particles and the optimized packing density. By replacing 25% of cement and entire QP by GP, the amount of GP used was greater than 400 kg/m^3. This can allow reducing the production cost and carbon footprint of traditional UHPC.

Among the tested nine UHPGC mixtures, the 0.240-P2.5% mixture was recommended for the bridge casting for many reasons. The 0.240-P2.5% is designed with *w/b* of 0.240 leading to a f_c value of 146 MPa (21,000 psi) at 91-days of NC and 156 MPa (23,000 psi) at 2.0 days of HC.

This strength was the highest following the two mixtures without fiber (0.225- 0% and 0.250-0%) and the two mixtures with steel fiber (0.250-S2.0% and 0.250-S2.0%). The 0.240-P2.5% mixture is designed with PVA fiber (2.5%) which is demanded by the architects to avoid the corrosion problems associated with the steel fiber; especially the bridge is exposed to severe environmental conditions. However, the 2.5% of PVA fiber have not enhanced the tensile strength, but it improved greatly the ductility, as it will be explained later in the full characterization phase. The HRWRA dosage for the 0.240-P2.5% mixture (solid content of 16 kg/m^3) is lower than the dosages employed in the other four UHPGC mixtures with PVA fiber (solid content of 24 kg/m^3 in 0.225-P2.5% and 0.225-4.0%, and solid content of 22 kg/m^3 in 0.250-P2.5% and 0.250-4.0%). This enabled avoiding the delayed setting problem of concrete that undertaken after 2.0 days for these four mixtures. For the 0.240-P2.5% mixture, the concrete setting took place faster, allowing mould removal within 1.0 day. The excellent flowability described by 275 mm (11″) spread diameter was also one of the encouraging reasons for selecting such mixture for the bridge casting to ensure final good finishing without the need to excess vibration for concrete consolidation.

The NC regime was selected in the next phase (full characterization) for two reasons. There was no significant difference in the mechanical properties between the 2 days of HC and 91-days of NC. The NC is also considered more cost-effective than the HC.

PERFORMANCE OF SELECTED UHPGC MIXTURE

The selected UHPGC mixture from the mix-design optimization (0.240-P2.5% mixture) was re-produced using full-scale batching plant of the University of Sherbrooke. The sample preparation and test results carried out for this mixture are presented below.

Specimen preparation

The selected 0.240-P2.5% mixture was produced at University of Sherbrooke laboratory using a pilot-scale automatic concrete plant with a paddle-type stationary pan mixer and a 500-l (18 ft^3) capacity. To achieve a homogeneous mixture and avoid particle agglomeration, all powder materials were mixed for 10 min before water and HRWRA addition. About half of the HRWRA

was diluted in half of the mixing water, and gradually added over three to 5.0 min. The remaining water and HRWRA as well as the fibers were then added over an additional 3.0 to 5.0 min of mixing. The total mixing time was about 16 to 20 min, including powder homogenisation. After mixing, the fresh properties, including spread diameter using the flow-table test (ASTM C 1437), unit weight, air content (ASTM C 185), and concrete temperature were measured. ConTec 6 rheometer was employed to determine the rheological properties [yield stress (τ_o) and plastic viscosity (μ_{pl})]. The tests that are normally carried out for self-consolidating concrete to determine fresh properties, passing ability, and stability were also conducted to evaluate the UHPGC performance in fresh state. The tests included slump-flow diameter with Abraham cone (ASTM C143), time to reach 500 mm (20″) spread diameter (T_{500}), visual stability index (VSI), J-Ring spread diameter and blockage ratio, and the L-Box test.

The f_c tests (ASTM C39) were carried out on 100×200 mm (4×8″) cylindrical specimens at 1, 7, 28, and 91 days. Similar cylindrical specimens were also sampled for f_{sp} testing (ASTM C496) and E_c (ASTM C469) both at 28 and 91 days. The f_{fl} (ASTM C78) and toughness (ASTM C1018) were tested at 28 and 91 days using third-point loading on 400×100×100 mm (16×4×4″) prisms. The stress–strain relationship for concrete under compression loading was carried out on 150×300 mm (6×12″) cylinders according to ASTM C469 at age of 150 days. Two cylindrical specimens of 150 mm (6″) in diameter for the resistance to mechanical abrasion (ASTM C944), two small slabs measuring 260×280×75 mm (10.2×11×3″) for de-icing salt scaling (ASTM C672), three prisms of 75×75×350 mm (3×3×13.8″) for the resistance to freeze-thaw cycles (ASTM C666) were prepared. Cylindrical specimens of 100×200 mm (4×8″) for measuring the resistance to chloride-ion penetration using the rapid chloride penetration (RCP) test (ASTM C1202) were sampled. The electrical current was recorded at 1.0-minute intervals for a total time of 6.0 hours, resulting in the values of total "Coulombs" passed. The test was performed after curing time of 28 and 91 days. The resistivity of the UHPGC was carried out on cylindrical samples (100×200 mm or 4×8″) after 91 days of normal curing, according to the proposed (ASTM WK37880).

The samples were stored at a temperature of 23°C (73°F) for 24 hours before demoulding. After demoulding, the specimens were stored in a fog room at 23°C (73°F) and 100% RH until testing.

Fresh and rheological properties

The slump-flow diameter using flow table and mini-slump cone without tamping was initially measured immediately after mixing in the full-scale plant and found to be about 230 mm (9″). To secure similar slump flow as the optimized mixture, an additional HRWRA dosage of 2.0 l/m^3 (solid content of 0.8 kg/m^3) was added. The final slump-flow diameter was 280 mm (11″). The unit weight of 2230 kg/m^3 (140 lb/ft^3), air content of 3.5%, and concrete temperature of 22°C (72°F) were also measured for this concrete mixture.

The slump-flow diameter measured with Abraham cone was 780 mm (30.7″). The T_{500} was 6.8 s, which explains the relatively high viscosity. The VSI was 0, which means no evidence of segregation. In order to ensure the concrete flows adequately around the reinforcement bars, the difference between the slump-flow diameter and the J-Ring spread diameter should not exceed 50 mm (2″) according to the German SCC guideline[36] or 10 mm (0.38″) according to EFNARC.[37] This value was only 5 mm (0.2″) for the 0.240-P2.5% mixture, indicating excellent passing ability. The blockage ratio for the J-Ring test was 0.83. The self-levelling index for the L-Box test with two steel rods was 1.0 (the limit accepted under the EFNARC[37] guideline ranges between 0.8 and 1.0). The time for the leading edge of the concrete to reach the end of the 600 mm (24″) long horizontal section of the L-Box was 9.8 s. These enhanced fresh properties obtained with the UHPGC derive from the large incorporation of GP with zero absorption.

The shear stress (τ) and shear rate ($\dot{\gamma}$) follows the Bingham model ($\tau = \tau_0 + \mu_{pl} \cdot \dot{\gamma}$) with $R^2 = 1.0$, as illustrated in Fig. 3. The concrete had a very low τ_0 of 0.2 Pa, which explains the higher flowability and a relatively high μ_{pl} of 25.3 Pa.s as previously indicated by the T_{500} of 6.8 s.

Mechanical properties

The mechanical properties of concrete after different curing ages are listed in Table 5.

Compressive strength

The measured 28- and 91-day f_c values of the current UHPGC (0.240-P2.5% mixture) were 96 and 127 MPa (14,000 and 18,000 psi), respectively. These values were found to be about 12% lower than the measured values in the optimization part, given that the f_c here was measured

using cylindrical specimens vs. cube specimens in the optimization part. The increase in the f_c of about 32% between 28 days and 91 days was due to the GP's pozzolanic reactivity. This 91-day strength is lower than the one of UHPC containing steel fiber (160 MPa or 32,000 psi) reported in literature.[5,35,38,39] This difference in the compressive strength is due the fact that the mixtures tested in literature incorporated 2 to 4% steel fiber addition compared to PVA fiber in the current UHPGC. The PVA fiber was shown earlier in the optimization part to reduce the f_c. However, the use of PVA fiber was required for architectural purpose.

Splitting-tensile strength, flexural strength and Elastic Modulus

The results of the f_{sp}, f_{fl}, and E_c conducted at 28 and 91 days are included in Table 5. The current 91-day f_{sp} (11.0 MPa or 1,600 psi) was found approximately similar to that obtained after two days of HC in the optimization part (11.8 MPa or 1,700 psi). The E_c results were improved by about 15% at 91 days compared to the 28 days results (51 *vs*. 44 GPa, or 7,397 *vs.* 6,381 ksi, respectively) due to the pozzolanic activity of the GP at later age.

Toughness

The modulus of rupture (MOR) was calculated as $\mathrm{MOR} = \mathrm{PL}/\mathrm{bd}^2$ on the assumption of a linear-elastic stress state, where: P = applied force, L, b, and d = span, width, and depth of specimen.

The MOR versus mid-span deflection curves for specimens tested at 28 and 91 days are shown in Fig. 4. The UHPGC specimens showed linear elastic behavior up to the initial cracking, before reaching the maximum stress. That is followed by a strain-hardening phase and subsequent strain-softening phase till failure. The UHPGC specimens showed ductile failure mode, unlike the brittle failure mode of the conventional concrete.[40] The initial crack, maximum, and failure loads and the corresponding strengths and mid-span deflections are indicated in Table 6 for the tested UHPGC mixture at 28 and 91 days. The results show an improvement in the flexural capacity or the MOR of the tested prisms from the 28 to the 91 days (from 7.3 to 9.2 MPa, or 1,000 to 1,350 psi, respectively). These values for the MOR at 28 to the 91 were slightly lower than the corresponding f_{fl} values in Table 5 (10 and 12 MPa, or 1,450 to 1,750 psi, respectively).

This difference can be due to variation in loading rates between the two testing machines used in the two test methods. The toughness indices (I_5, I_{10}, and I_{20}) and the residual strength factors ($I_{5,10}$ and $I_{10,20}$) as per the ASTM C1018 have been calculated at age 28 and 91 days and the values are indicated in Table 6. The results of the toughness indices have not shown any significant changes between 91 and 28 days.

Stress–Strain curve under compression

The stress–strain curve obtained under compression loading for the tested UHPGC mixture is shown in Fig. 5. Typical stress-strain curve for ordinary concrete with a compressive strength of about 35 MPa (5,000 psi) is included in the figure for the comparison. The ultimate compressive strength measured for the UHPGC was about 122 MPa (17,700 psi) at a corresponding strain of 0.0027. The stress relaxation following the ultimate load indicated in the figure is due to the presence of PVA fiber in the UHPGC mixture. The UHPGC mixtures showed increase in both the f_c and the E_c (slope of the linear part of the curve) compared to the normal concrete. The E_c values of the UHPGC and normal concrete, calculated from the slope of the linear part of the curve, are 52.8 and 21.5 GPa (7,700 and 3,100 ksi), respectively.

Durability properties

Resistance to mechanical abrasion

Resistance to mechanical abrasion is an important parameter in designing the footbridges with UHPGC as the footbridges will be subjected to abrasion induced by snow removal tracker. According to ASTM C944, the mechanical abrasion resistance of concrete is defined by the relative volume-loss index. This index for the UHPGC was 1.35 mm (0.05″) after 28 days of NC. For a typical UHPC, this index ranges from 1.1 to 1.7 mm (0.04 to 0.07″).[7,33,41] The maximum limit specified in ASTM C944 is 3.0 mm (0.125″).

Resistance to de-icing salt scaling

To evaluate concrete durability, the mass loss from the concrete surface due to freezing and de-icing salt scaling was measured. De-icing salt scaling is an important parameter for concrete structures exposed to saltwater or where the de-icing salts are employed on the concrete surface such as the pavement and bridge deck made with concrete. After 56 freeze–thaw cycles, the scaled mass was about 12 g/m^2 (41 lb/in.^{2}), which is very low compared to the limit specified in the ASTM C672 (1000 g/m^2 or 3417 lb/in.^{2}). The measured value (12 g/m^2, or 41 lb/in.^{2}) lies within range reported in the literature for the traditional UHPC (8 - 60 g/m^2, or 27 - 205 lb/in.^{2} after 28 to 50 freeze–thaw cycles.[33,41]

Resistance to freeze–thaw cycles

The resistance to the freeze-thaw cycles according to ASTM C666 showed an average dynamic modulus of elasticity of 101% after 1000 cycles with no evidence to deterioration or cracking at the end of the test. The obtained results are due to the fact that the UHPGC has very dense matrix which can be attributed to the lack of interconnected pores. Minimal degradation of traditional UHPC was found after 600 to 800 cycles.[42,43] After subjecting UHPC samples to 1000 freeze-thaw cycles, the relative dynamic modulus reduces to 90%.[44] The obtained results (101%) of the UHPGC mixture are consistent with the extended freeze–thaw resistance reported in literature. The typical relative dynamic moduli after 1000 freeze-thaw cycles for HPC and CVC are 78% and 39% of their initial values, respectively, compared to 101% in the current UHPGC.[41,45]

Resistance to chloride-ion penetration

The dense matrix of the UHPPC is required to prevent the ingress of detrimental materials by acting as a sealing layer to enhance the durability of structures. The average values of the total coulombs passed using the RCP test were 5 and 3 Coulombs at 28 and 91 days, respectively. These results are within the “negligible” classification according to ASTM C1202. This ion-chloride penetration value is very low compared to CVC, HPC, and traditional UHPC. The value of total charge passed for the traditional UHPC with standard heat treatment was 18 Coulombs and 360 Coulombs for the untreated sample.[41] The total charge passed through heat-treated UHPC sample was 10 Coulombs.[33]

Resistivity

The low corrosion rate in concrete is partly due to the high resistance of the material to conduct an electric current. The resistivity of the UHPGC showed an extremely high value of 3500 kΩ.cm. It is worth noting that the typical resistivity values for the UHPC without fiber is about 1130 kΩ·cm, and with 2.0% addition of steel fiber the resistivity reduces to 137 kΩ.cm. The resistivity value of the HPC is 96 kΩ.cm, and 16 kΩ.cm for the CVC.[7]

FIELD VALIDATION

The optimized and full-characterized UHPGC mixture in the last sections was used to cast two footbridges (Fig. 6) to replace deteriorated wooden footbridges at the University of Sherbrooke main campus.[46] The footbridges were designed with the UHPGC to meet the university's architectural and structural requirements for pedestrian use as well as to be in compliance with the university's regulation on sustainable development. The use of UHPGC technology with high mechanical properties enabled the designer to create thin sections that are light, graceful, innovative in geometry, and produced with a relatively low cost. Each bridge had a total weight of around 4.0 tons (8800 lb). The structural system consisted of an arch slab 4910 mm (193″) in length, 2500 mm (98″) in width, and 75 mm (3″) in thickness supported by longitudinal ribs of variable heights and a constant width of 130 mm (5″) (Fig. 6-a, b). The concrete volume of about 2.0 m^3 (3 yd^3) was required for each bridge, which is equivalent to about 40% of the concrete volume is case of using the CVC in the bridge casting. The arch slab was reinforced with welded wire reinforcement (M10 at 300 mm or 12″) in both directions placed at the mid height of the slab. Each rib was reinforced with a single M20 reinforcing bar located near the bottom of the rib. One of the two footbridges was instrumented with two thermocouples (at center of bridge deck and center of supporting edge beam) and one vibrating wire strain gauge (at center of bridge deck) to monitor concrete temperature and deformation over time.

Casting of UHPGC footbridges

The pilot concrete plant with 500-l (18 ft^3) capacity at the University of Sherbrooke laboratory was employed to prepare four batches of UHPGC (with similar mixing sequences mentioned earlier) for a total of 2.0 m^3 (3 yd^3) for each footbridge. The four batches were loaded in one hopper that used in the bridge casting. Due to the excellent UHPGC fluidity and self-placing properties, the entire concrete was placed in the bridge formwork within 12 min. Unlike the traditional UHPC, the UHPGC required only 1.0 minute of internal vibration to ensure good consolidation and removal of entrapped air. After casting, the exposed concrete parts were covered with plastic sheet until formwork removal. The formwork was removed 24 hours after placement and the bridge was totally covered with a plastic sheet and stored at laboratory conditions for 28 days. Before the bridges were transported to their installation sites, wooden and steel handrails were fixed. A truck-mounted crane and straps were used to lift and install the bridges on conventional concrete abutments with neoprene bearing pads.

Bridge monitoring

The changes of the concrete temperature with time for the instrumented footbridge obtained using the two thermocouples for a period of four months are given in Fig. 7 (on right axis). The temperature reached approximately 53°C (127 °F) in the first days after casting, followed by gradual decrease to laboratory temperature of 23°C (73°F). After curing at laboratory temperature for 28 days, the two footbridges were transferred to the field sites, where the temperature dropped below zero, as shown by the sudden drop in the temperature curve. In some nights, the temperature fell to -30°C (-22°F).

Fig. 7 (left axis) shows the changes of deformation with time obtained from the vibrating-wire strain gauge. A deformation of about 430 µstrain was noted at the end of laboratory curing, followed by a sudden increase at the field site due to temperature changes and removal of the plastic sheet (thermal change and additional drying shrinkage). The total deformation was as much as 1200 µstrain in some days. The isothermal deformation was about 800 µstrain.

CONCLUSIONS

A new type of UHPC has been developed using waste glass materials, creating UHPGC. The new material exhibited excellent workability and rheological properties due to the zero absorption of the glass particles and optimized packing density for the entire material matrix. The UHPGC greatly improved the concrete microstructure, which not only yields higher mechanical properties, but also leads to superior durability properties. The mechanical and durability characteristics of the UHPGC are comparable or even much better than those obtained from the conventional UHPC. The higher mechanical properties of UHPGC allowed the footbridges design with reduced sections (a reduction in the concrete volume of about 60% compared to normal concrete). The improved durability performance evaluated for the UHPGC can contribute in reducing the maintenance cost and the cover concrete.

The construction of two footbridges at the University of Sherbrooke using the UHPGC shows the potential for the material to be produced on large scale and used in future projects. The UHPGC can assure highly energy efficient, environmentally friendly, affordable, and resilient structures. The UHGPC can significantly reduce the UHPC cost and also save money spent for the treatment and landfilling of glass cullets.

ACKNOWLEDGMENTS

This research was funded by the Société des Alcools du Québec (SAQ) Industrial Chair on "Valorization of Glass in Materials" and The INNOV Grants from NSERC. The authors gratefully acknowledge these supports.

REFERENCES

1. Tagnit-Hamou, A., and Soliman, N., "Ultra-High Performance Glass Concrete and Method for Producing same," *U.S. Patent Application*. No. 61/806,083, file March 28, 2013, Accepted March 2014.
2. Gupta, P.R., and Shiu, K.N., "Effective Repair and Maintenance Strategies for Parking Structures," *Concrete Repair Bulletin*, July/August 2014, pp. 30-34

3. U.S. Department of Homeland Security (DHS) Science and Technology (S&T) Directorate's Infrastructure Protection and Disaster Management Division (IDD) "UHPC Ultra-High Performance Concrete," Technical report, pp. 23, (http://www.dhs.gov).

4. Richard, P., and Cheyrezy, M., "Reactive Powder Concretes with High Ductility and 200-800 MPa Compressive Strength", *ACI SP 144*, 1994, pp. 507-518.

5. Richard, P., and Cheyrezy, M., "Composition of Reactive Powder Concretes," *Cement and Concrete Research*, V. 25, No. 7, 1995, pp. 1501-1511.

6. Dugat, J.; Roux, N.; and Bernier, G., "Mechanical Properties of Reactive Powder Concretes," *Materials and Structures*, V. 29, May 1996, pp. 233-240.

7. Roux, N.; Andrade, C.; and Sanjuan, M., "Experimental Study of Durability of Reactive Powder Concretes," *Journal of Materials in Civil Engineering*, V. 8, No. 1, 1996, pp. 1-6.

8. Schmidt, M., and Fehling, E., "Ultra-High-Performance Concrete: Research, Development and Application in Europe," *ACI SP 225*, 2005, pp. 51-77.

9. Klemens, T., "Flexible Concrete Offers New Solutions", *Concrete Construction*, V. 49, No.12, Dec. 2004, pp. 72.

10. Racky, P., "Cost-effectiveness and Sustainability of UHPC", *Proceedings of the International Symposium on Ultra-High Performance Concrete*, Kassel, Germany, V. 13, No.15, Sept 2004, pp. 797-805.

11. Aïtcin, P-C., "Cements of Yesterday and Today - Concrete of Tomorrow," *Cement and Concrete Research*, V. 30, No. 9, Sept. 2000, pp. 1349-1359.

12. World Health Organization (WHO), "Health Systems: Improving Performance," *World Health Organization Report*, 2000, pp. 215.

13. Shayan A.; Xu A., "Value-Added Utilisation of Waste Glass in Concrete," *Cement and Concrete Research*, V. 34. No. 1, 2004, pp. 81-89.

14. FEVE, Collection for Recycling Rate in Europe, The European Container Glass Federation, 2013 "http://www.feve.org/FEVE-STATIS-2013/Recycling-2011-Glass-coll.html" (Date accessed: 11 Sept. 2013).

15. Recyc-Québec, "Le Verre Fiches Informatives", In French, 2010.

16. USEPA, Wastes-Resource Conservation-Common Wastes & Materials, "Glass," (http://www.epa.gov/osw/conserve/materials/glass.htm), (Date accessed: 10 Sept. 2013).

17. Zidol, A.; Tohoue Tognonvi, M.; and Tagnit-Hamou, A., "Effect of Glass Powder on Concrete

Sustainability," *1st International Conference on Concrete Sustainability (ICCS13), Ref # 0229*. 2012.

18. Zidol, A.; Pavoine, A.; and Tagnit-Hamou, A., "Effect of Glass Powder on Concrete Durability," *International Congress on Durability of Concrete, Trondheim, Norvège, ICDC2012-D-11-00153*. 2012.
19. Terro, M.J., "Properties of Concrete Made with Recycled Crushed Glass at Elevated Temperatures," *Building and Environment*, V. 41, No. 5, 2006, pp. 633-639.
20. Idir, R.; Cyr, M.; and Tagnit-Hamou, A., "Use of Waste Glass as Powder and Aggregate in Cement-Based Materials," *In: SBEIDCO – 1st international conference on sustainable built environement infrastructures in developing countries ENSET Oran (Algeria)*, October 12–14, 2009, pp. 109–16.
21. Shi, C.; Wu, Y.; Riefler, C.; and Wang, H., "Characteristic and Pozzolanic Reactivity of Glass Powders," *Cement and Concrete Research*, V. 35, 2005, pp. 987–993.
22. Shayan, A.; and Xu, A., "Performance of Glass Powder as a Pozzolanic Material in Concrete: a Field Trial on Concrete Slabs," *Cement and Concrete Research*, V. 36, 2006, pp. 457–468.
23. Roz-Ud-Din, N.; and Parviz S., "Strength and Durability of Recycled Aggregate Concrete Containing Milled Glass as Partial Replacement for Cement," *Constr Build Mater*, V. 29, 2012, pp. 368–77.
24. Shao, Y.; Lefort, T.; Moras, S.; and Rodriguez, D., "Studies on Concrete Containing Ground Waste Glass," *Cement and Concrete Research*, V. 30, 2000, pp. 91–100.
25. Khmiri, A.; Samet, B.; and Chaabouni, M., "A Cross Mixture Design to Optimise the Formulation of a Ground Waste Glass Blended Cement," *Construction and Building Materials*, V. 28, 2012, pp. 680–686.
26. Cong, K.S.; and Feng, X., "The Effect of Recycled Glass Powder and Reject Fly Ash on the Mechanical Properties of Fiber-Reinforced Ultra-high Performance Concrete," *Advanced Material Science Engineering*, *Article ID 263243*, 2012, pp. 8.
27. Vaitkevicius, V.; Serelis, E.; and Hilbig, H., "The Effect of Glass Powder on the Microstructure of Ultra-High Performance Concrete," *Construction and Building Materials*, V. 68, 2014, pp. 102–109.
28. Soliman, N.; Aïtcin; P.- C.; and Tagnit-Hamou, A., "New Generation of Ultra-High Performance Glass Concrete," *Advanced Concrete and Technologies. Lightweight and Foam Concretes. Education and Training, Publisher: RILEM and CEB-fib, ISBN 978-5-7264-0809-5*, V. 5, Chapter 24, May 12-16, 2014, pp 218-227.
29. Zerbino, R.; Giaccio, G; Batic, O.R.; and Isaia, G.C., "Alkali–Silica Reaction in Mortars and

Concretes Incorporating Natural Rice Husk Ash," *Construction and Building Materials*, V. 36, 2012, pp. 796–806.

30. Juengera, M.C.G.; and Ostertag, C.P., "Alkali–Silica Reactivity of Large Silica Fume-Derived Particles," *Cement and Concrete Research*, V. 34, 2004, pp. 1389–402.
31. Andrea, S.; and Chiara, B.M.. "ASR Expansion Behavior of Recycled Glass Fine Aggregates in Concrete," *Cement and Concrete Research*, V. 40, 2010, pp. 531–536.
32. de Larrard F., "Concrete Mixture Proportioning: A Scientific Approach," *E&FN Spon, London*, pp. 1999.
33. Bonneau, O.; Lachemi, M.; Dallaire, E.; Dugat, J.; and Aïtcin, P-C., "Mechanical Properties and Durability of Two Industrial Reactive Powder Concretes," *ACI Materials Journal*, V. 94, No. 4, July-Aug. 1997, pp. 286-290.
34. Nielsen, C.V., "Triaxial Behavior of High-Strength Concrete and Mortar," *ACI Materials Journal*, V. 95, No. 2, 1998, pp. 144-151.
35. Rossi, P., "Development of New Cement Composite Materials for Construction," *Proceedings of the Institution of Mechanical Engineers, Part L: Journal of Materials: Design and Applications*, V. 219, No. L1, Feb. 2005, pp. 67-74.
36. Brameshuber, W.; and Uebachs, S., "Practical Experience with the Application of Self-Compacting Concrete in Germany," *Proceedings of the Second Int. Symp. on Self-Compacting Concrete*, Tokyo, Japan, 2001, pp. 687-696.
37. EFNARC, "Specification and Guidelines for Self-Compacting Concrete," (http://www.efnarc.org), February 2002, pp 32.
38. Wuest, J., "Etude exploratoire des propriétés mécaniques de bétons de fibres ultra performants de structures," *Diploma thesis, MCS, Swiss Federal Institute of Technology (EPFL). Lausanne, Switzerland*, 2004. [In French.]
39. Perry, V., and Zakariasen, D., "First Use of Ultra-High Performance Concrete for an Innovative Train Station Canopy," *Concrete Technology Today*, V. 25, No. 2, Aug. 2004, pp. 1-2.
40. Habel, K.; Viviani, M.; Denarié, E.; and Brühwiler, E, "Development of the Mechanical Properties of an Ultra-High Performance Fiber Reinforced Concrete (UHPFRC)," *Cement and Concrete Research*, V. 36, No. 7, July 2006, pp. 1362 - 1370.
41. Graybeal, B., "Characterization of the Behavior of Ultra-High Performance Concrete," PhD dissertation, University of Maryland.

42. Federal Highway Administration (FHWA), "Achieving the Promise of Ultra-High-Performance Concrete," *Focus*, Nov. 2004, (http://www.tfhrc.gove/focus/nov04/01.htm).

43. Gao, R.; Liu, Z.-M.; Zhang, L.-Q.; and Stroeven; P., "Static Properties of Reactive Powder Concrete Beams," *Key Engineering Materials*, V. 302-303, 2006, pp. 521-527.

44. Lee, M.-G.; Chiu, C.-T.; and Wang; Y.-C, "The Study of Bond Strength and Bond Durability of Reactive Powder Concrete," *Journal of ASTM International*, V. 2, No. 7, 2005, pp. 104-113.

45. Shaheen, E, and Shrive, N.G., "Optimization of mechanical properties and durability of reactive powder concrete," *ACI Materials Journal*, V. 103, No. 6, 2006, pp. 444-451.

46. Tagnit-Hamou, A.; Soliman, N.; Omran, A. F.; Mousa, M. T.; Gauvreau, N.; and Provencher, MF.; "Novel Ultra-High Performance Glass Concrete," *Journal of ACI Concrete International*. V. 39, No. 3, March 2015, pp. 53-59.

LIST OF TABLES

LIST OF FIGURES

Table 1 – Mixtures proportioning in kg/m^3 (lb/yd^3)

Materials	UHPC-1	0.225-0%	0.225-S2.0%	0.225-P2.5%	0.225-P4.0%	UHPC-2	0.250-0%	0.250-S2.0%	0.250-P2.5%	0.250-P4.0%	0.240-P2.5%
water	215 (362)	219 (369)	215 (362)	212 (357)	209 (352)	242 (408)	239 (403)	234 (394)	231 (389)	228 (384)	224 (378)
Cement	773 (1303)	572 (964)	561 (946)	553 (932)	545 (919)	759 (1279)	562 (947)	550 (927)	541 (912)	533 (898)	549 (925)
Silica fume	215 (362)	212 (357)	208 (351)	205 (346)	203 (342)	211 (356)	208 (351)	204 (344)	200 (337)	197 (332)	204 (344)
Glass powder	--	420 (708)	411 (693)	406 (684)	403 (679)	--	412 (694)	404 (681)	397 (669)	391 (659)	403 (679)
Quartz sand	927 (1563)	915 (1542)	896 (1510)	885 (1492)	872 (1470)	910 (1534)	899 (1515)	881 (1485)	866 (1460)	853 (1438)	888 (1497)
Quartz Powder	232 (391)	--	--	--	--	228 (384)	--	--	--	--	--
HRWRA*	16.8 (28)	16 (27)	16 (27)	24 (40)	24 (40)	8 (13)	8 (13)	8 (13)	22 (37)	22 (37)	16 (27)
PVA fiber	--	--	--	32.5 (55)	52 (88)	--	--	--	32.5 (55)	52 (88)	32.5 (55)
Steel fiber	--	--	158 (266)	--	--	--	--	158 (266)	--	--	--

*Solid content

Table 2 – Chemical composition of Type HS cement, quartz sand, glass powder, and silica fume (% of total)

Identification	Quartz sand	Quartz powder	Glass powder	HS cement	Silica fume
Silicon Dioxide (SiO_2)	99.8	99.8	73	22	99.8
Iron Oxide (Fe_2O_3)	0.04	0.09	0.4	4.3	0.09
Aluminum Oxide (Al_2O_3)	0.14	0.11	1.5	3.5	0.11
Calcium Oxide (CaO)	0.17	0.38	11.3	65.6	0.4
Titanium Dioxide (TiO_2)	0.02	0.25	0.04	0.2	--
Sulfur trioxide (SO_3),	--	0.53	--	2.3	--
Magnesium Oxide (MgO)	0.008	0.20	1.2	1.9	0.20
Sodium oxide (Na_2O)	--	0.25	13	0.07	0.20
Potassium Oxide (K_2O)	0.05	3.5	0.5	0.8	0.50
Equivalent alkali (Na_2O_{eq})	--	--	--	0.9	--
Zinc oxide (ZnO)	--	--	--	0.09	0.25
Loss on ignition (LOI)	0.2	0.32	0.6	1.0	3.50
C_3S		--		50	
C_2S		--		25	
C_3A		--		2.0	
C_4AF		--		14	

Table 3 – Properties of steel and PVA fibers

Fiber type	Steel fiber	Polyvinyl alcohol (PVA) fiber
Shape	Straight	Straight monofilament
Specific gravity	7.8	1.3
Length, mm (in.)	30 (1.2)	13 (0.5)
Equivalent diameter, mm (in.)	1.0 (0.04)	0.2 (0.008)
Tensile strength, MPa (psi)	850 (123, 282)	400 (58,015)

Table 4 – Fresh properties of laboratory optimized mixtures

Property	UHPC-1	0.225-0%	0.225-S2.0%	0.225-P2.5%	0.225-P4.0%	UHPC-1	0.250-0%	0.250-S2.0%	0.250-P2.5%	0.250-P4.0%	0.240-P2.5%
Slump-flow diameter, mm (in.)	235 (9.3)	250(9.6)	240(9.3)	245(9.6)	180(7.1)	250 (9.8)	265(9.1)	260(8.9)	285(11.2)	205(8.1)	275(10.8)
Air void (%)	3.1	2.2	2.1	4.0	5.1	2.3	2.5	1.5	4.6	6.2	3.3
Unit weight, kg/m^3 (lb/yd^3)	2336 (3938)	2310 (3894)	2405 (4054)	2226 (3752)	2220 (3742)	2295 (3868)	2305 (3885)	2377 (4007)	2184 (3681)	2181 (3676)	2231 (3761)
Concrete temperature °C (°F)	28 (82)	24 (75)	26 (79)	25 (77)	26 (79)	27 (81)	23 (73)	24 (75)	24 (75)	25(77)	24 (75)

Table 5 – Mechanical properties of pilot-plant produced UHPGC (0.240-P2.5% mixture)

Properties	Concrete age, days			
	1	7	28	91
Compressive strength (f_c), MPa (psi)	12 (1,740)	52 (7,542)	96 (13,924)	127 (18,420)
Splitting-tensile strength (f_{sp}), MPa (psi)	--	--	10 (1,450)	11 (1,595)
Flexural strength (f_{fl}), MPa(psi)	--	--	10 (1,450)	12 (1,740)
Modulus of Elasticity (E_c), GPa (ksi)	--	--	44 (6,382)	51 (7,397)

Table 6 – Flexural and toughness properties of pilot-plant produced UHPGC (0.240-P2.5%)

Concrete age (days)	28 days	91 days
First-crack load, kN (Ib)	20.8 (4,676)	27.1 (6,092)
Max-crack load, kN (Ib)	24.4 (5,485)	30.6 (6,879)
Failure-crack load, kN (Ib)	8.0 (1,798)	11.6 (2,608)
Strength at first-crack, MPa (psi)	6.3 (907)	8.1 (1,178)
Maximum strength (modulus of rupture, MOR), MPa (psi)	7.3 (1,059)	9.2 (1,334)
Failure strength, MPa (psi)	2.4 (350)	3.5 (505)
Deflection at first-crack, mm (in.)	0.037 (0.001)	0.038 (0.002)
Deflection at maximum crack load, mm (in.)	0.048 (0.002)	0.398 (0.016)
Maximum deflection at failure, mm (in.)	3.537 (0.139)	3.548 (0.140)
Toughness index I_5	4.7	4.8
Toughness index I_{10}	8.7	8.9
Toughness index I_{20}	17.0	17.0
Residual strength factor $I_{5,10} = 20(I_{10}-I_5)$	80.6	83.6
Residual strength factor $I_{10,20} = 10(I_{20}-I_{10})$	83.5	80.4

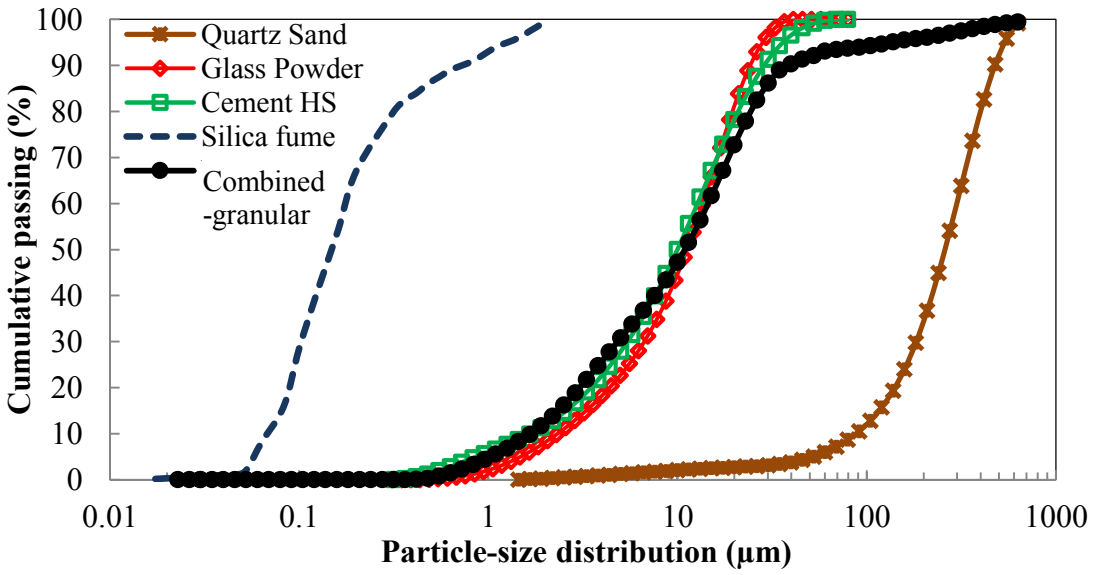

Fig. 1 – Particle-size distributions of individual materials and combined-granular materials used in the UHPGC mixture (1 in. = 25400 µm)

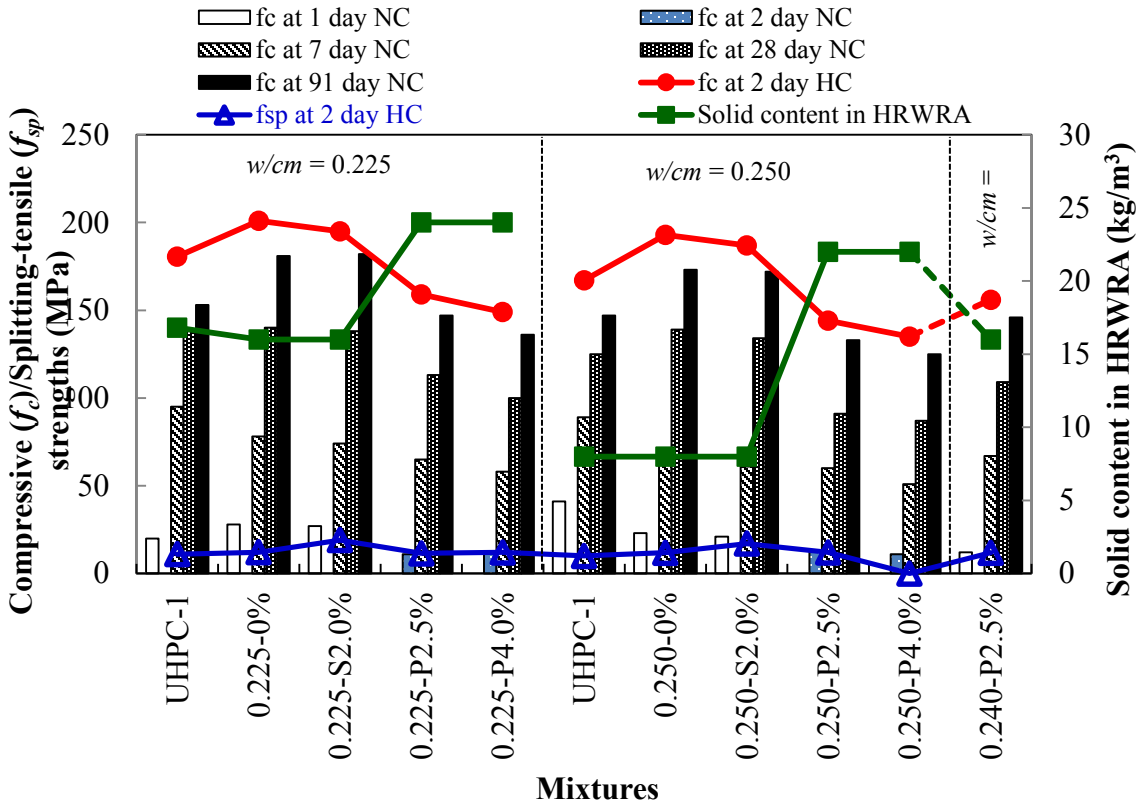

Fig. 2 – Compressive strength (f_c) at different ages under normal curing (NC) and hot curing (HC), splitting-tensile strength (f_{sp}) after 2-days of HC, and HRWRA dosages for the tested mixtures (1.0 MPa = 145 psi, 1.0 kg/m^3 = 1.6856 lb/yd^3)

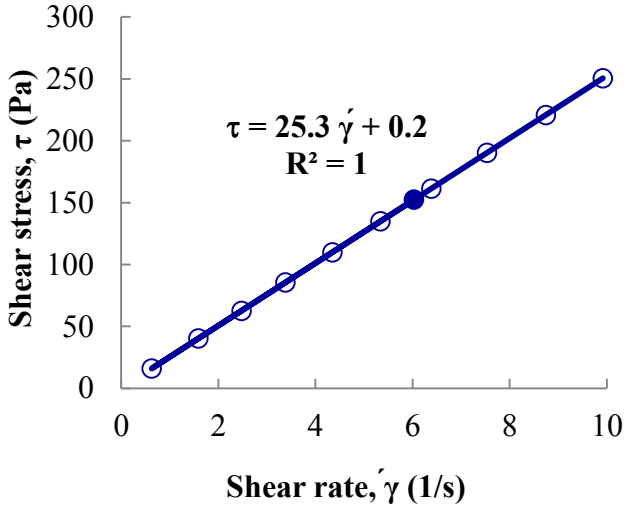

Fig. 3 – Relationship between shear stress and corresponding shear rate for the UHPGC (0.240-P2.5% mixture)

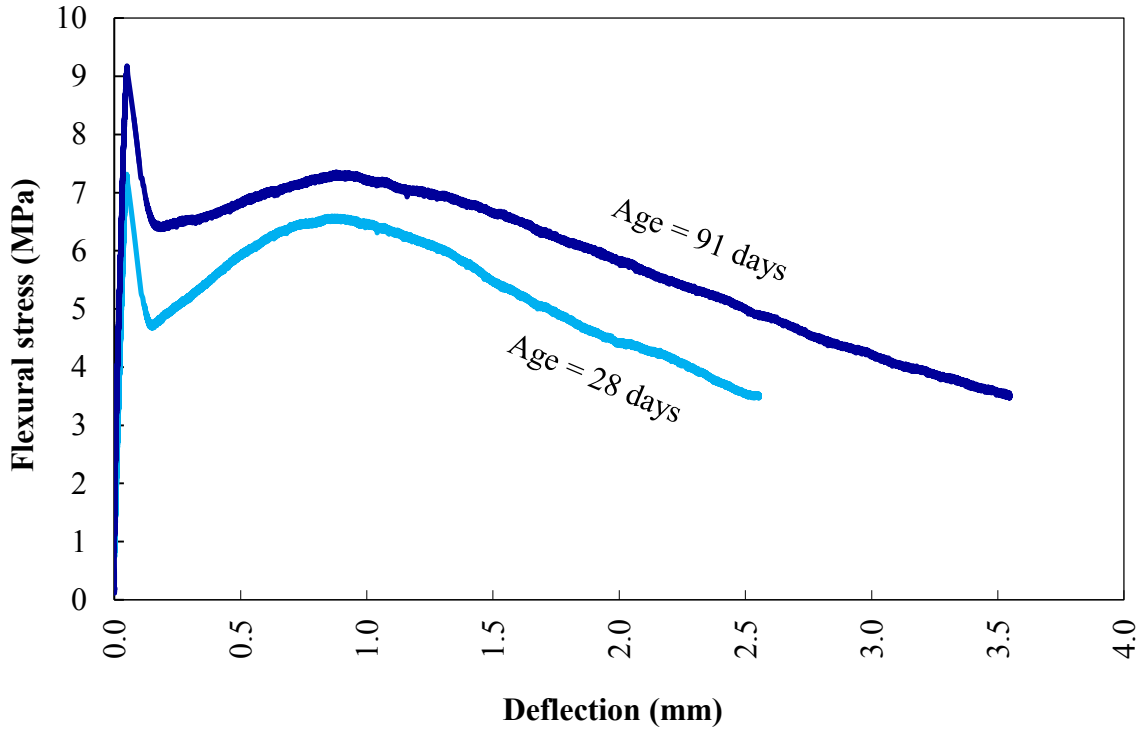

Fig. 4 – Flexural stress-deflection curve of third-point bending test at 28 and 91 days for UHPGC (0.240-P2.5% mixture)

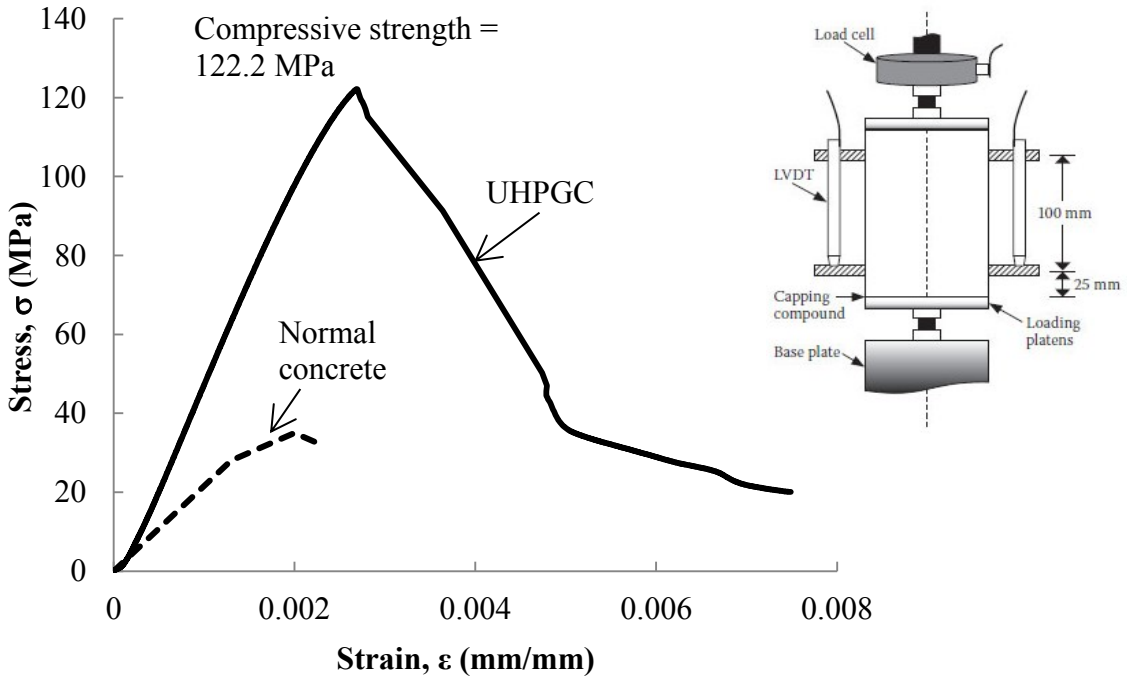

Fig. 5 – Stress–strain relationship of the of UHPGC (0.240-P2.5% mixture)

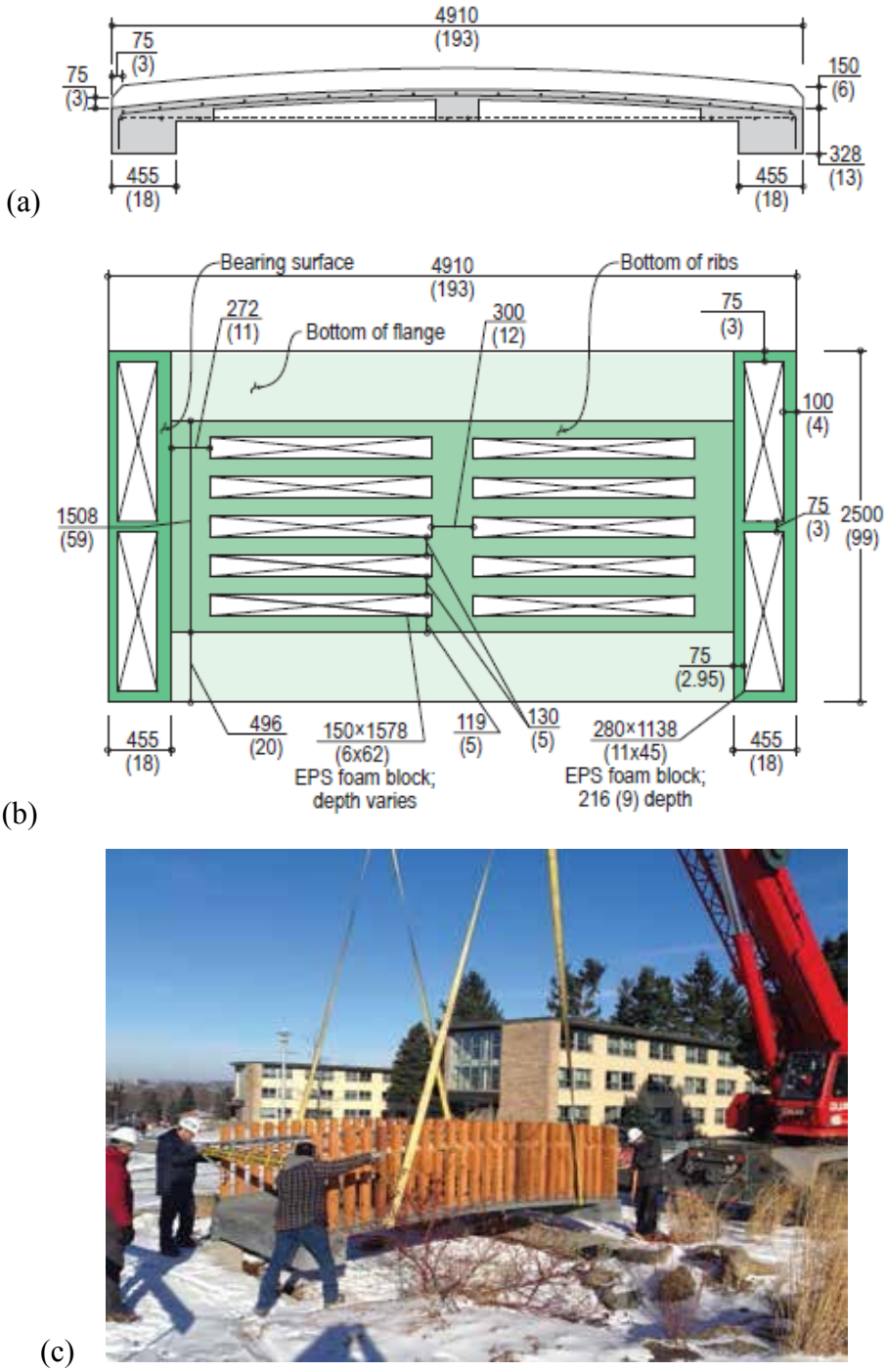

Fig. 6 – Bridge: (a) schematic longitudinal section at centerline, (b) bottom view showing concrete dimensions in mm (nearest in.), and (c) installation in the site

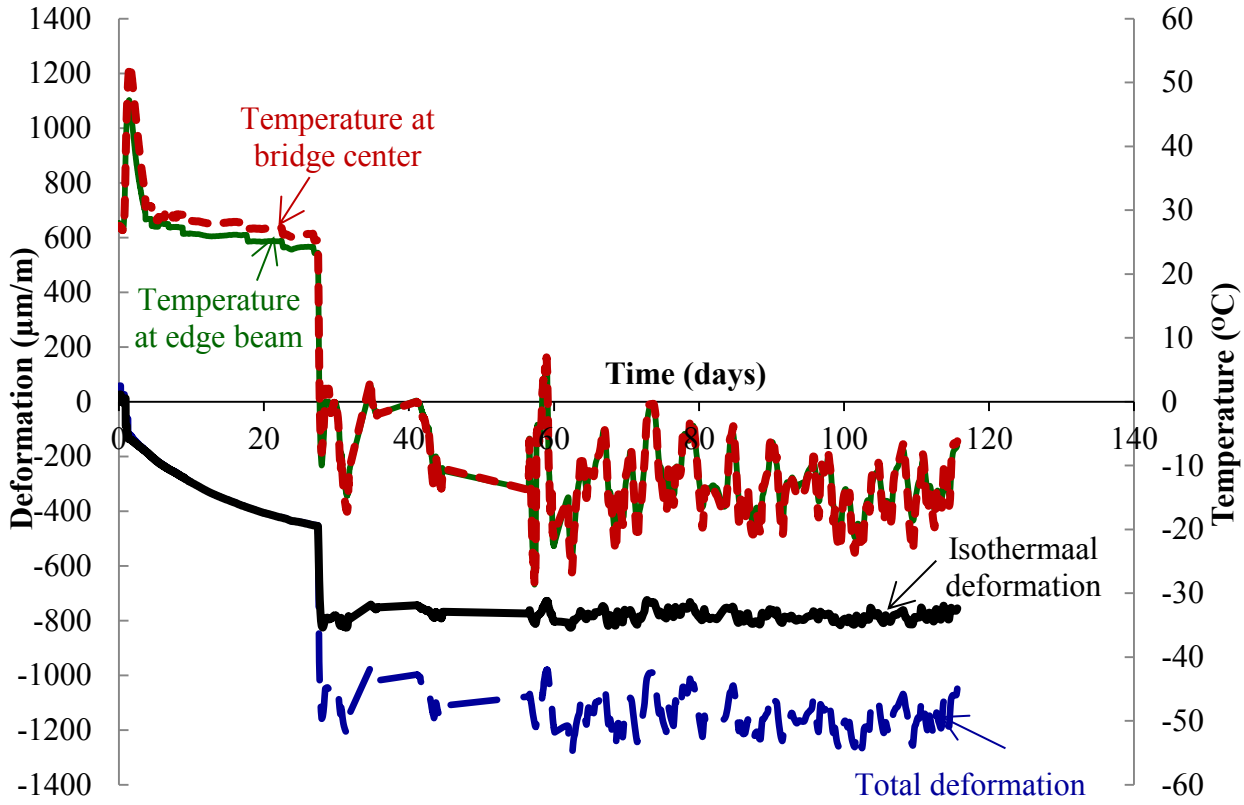

Fig. 7 – Variations in deformation and temperature with time obtained from the instrumented footbridge

9 Conclusions and Future work

9.1 Conclusions

The research reported on in this thesis investigated the possibility of using waste-glass materials with different particle-size distributions to make UHPC. The general conclusions of this research are as follows:

- UHPC mixtures can be designed and produced with locally available materials using the compressible packing model (CPM) (Sedran and de Larrard, 2000) and statistical-design approaches. Three different UHPC mixture types with slump flows between 130 and 300 mm and compressive strengths between 135 and 225 MPa were produced to respond to various construction demands.
- The packing density definitely affects rheological properties, and therefore fresh-concrete workability. UHPC's higher packing density yields a mixture with low viscosity due to the increased lubricant effect (with the addition of more fine materials) and increased yield stress (due to the increased compactness and friction between granular particles). Flowability, however, also depends on the fineness of the additions. The positive effect of an increase in maximum packing density competes with the negative effect of an increase in specific surface. Therefore, the optimal packing density, not the maximum packing density, should be considered for UHPC design to provide for proper workability and placement conditions.
- Water content has a much greater impact on UHPC flowability than the HRWRA dosage. Increasing the water content increases the solubility of HRWRA, thereby improving matrix flowability. Increasing the HRWRA dosage alone does not further improve workability.
- CPM (Sedran and de Larrard, 1999) can be applied to different glass sands with different particle-size distributions to obtain an optimal glass sand with an ideal particle-size

distribution curve and optimum packing density with unitary, binary, and ternary combinations.

- Glass sand with an ideal particle-size distribution curve [mean particle diameter (d_{50}) of 275 μm (GS-275)] was obtained during this research work, increased workability (10% higher), and 13% lower compressive strength than the reference UHPC.
- An optimum UHPC mixture can be designed using glass sand as 50% replacement of quartz sand. This mixture ensured increased flowability and slightly lower compressive-strength properties compared to the reference concrete.
- Incorporating 50% glass sand to replace quartz sand can give UHPC with a very dense microstructure and without any alkali–silica reaction.
- Sustainable ultra-high-performance glass concrete (UHPGC) with low greenhouses gases has been developed through the use of glass powder. The glass powder was used to replace cement and quartz powder in conventional UHPC. UHPGC can be designed with a ternary system of cement, glass powder, and silica fume. This UHGPC offers enhanced fresh behavior owing to its negligible water-absorption capability and smooth surface; the higher glass-powder content results in greater workability.
- Calorimetric analysis shows that replacing cement with GP reduces the maximum heat flow and total heat due to the dilution of cement in the concrete mixture. Replacing the quartz powder, however, didn't affect total heat. Up to 20% replacement of cement with glass powder accelerated the hydration kinetics. Beyond this level, hydration was delayed due to the dilution effect. Replacing the quartz powder accelerated hydration at every percentage of replacement.
- The BSC images of the reference mixture, 80C/20GP, and 0QP/100GP subjected to hot curing for 48 h produced a C–S–H hydration rim around cement and GP particles. Partial separation of QP particles from the surrounding C–S–H phase was also observed.
- In terms of concrete compressive-strength development, the optimum replacement rate of cement with glass powder was 20%, although 50% seems to be the optimum replacement with respect to flowability and sustainability. Compared to the reference, the mix with 50% glass powder exhibited 90% strength at 2 days under hot curing and 100% strength at 91 days under normal curing.

- Up to 100% of quartz powder can be replaced with glass powder and achieve compressive strengths up to 234 MPa after hot curing. Compared to the reference, the concrete with total quartz-powder replacement exhibited higher increases in compressive strength of about 12% and 17% at 56 and 91 days, respectively, under normal curing.
- UHPGC can be produced with glass powder replacing both cement and quartz powder, such as in 80C20GP/0QP100GP, which recorded compressive strength, flexural strength, and modulus of elasticity of 220 MPa, 29 MPa, and 55 GPa, respectively. The total amount of glass powder used was about 400 kg/m^3.
- Glass powder can be ground finer with an air classifier and jet mill to produce fine glass powder of various levels of fineness or particle-size distributions.
- Based on the energy consumption of the air classifier and jet mill, as well as the workability and compressive strength properties of concrete containing fine glass powder at various levels of fineness, a fine glass powder with a particle-size distribution having a mean particle size of 3.8 μm is recommended to replace silica fume when producing UHPC.
- The particle-size distribution (PSD) of cement exhibits a gap at the micro scale that needs to be filled with finer materials such as SF. Filling this gap solely with SF requires a high amount of SF (25% to 30% by cement weight). This significantly decreases UHPC workability and increases concrete cost. The optimum FGP herein had a PSD between that of the cement and SF to help reduce the SF content and enhance concrete performance. This is due to the fact that the SF used in this study had a specific surface area of 22,000 m^2/kg, which is approximately double that of the FGP (10,000 m^2/kg). Therefore, the net total surface area of the SF and FGP blend decreased when FGP was used as an SF replacement. Consequently, the water needed to lubricate particle surfaces decreased as a result of the decrease in the net particle surface area, increasing the slump flow at the same *w/b*. Moreover, the excess water enhanced cement hydration, thereby improving compressive strength up to a given level.
- Thirty percent can be recommended as the optimum ratio for replacing silica fume with fine glass powder with a view to compressive-strength development. Compared to the concrete mix with silica fume, the mix with 30% fine glass powder exhibited 15% higher strength after 2 days of hot curing. The 70% replacement ratio with fine glass powder

yielded approximately similar strength and enhanced the workability by 50% compared to the mixture with silica fume alone, but evidenced setting-time retardation. The 50% fine-glass-powder replacement can be considered as the optimum replacement ratio, as it enhanced the workability (20%) and strength (8%), while not retarding the setting time at all. Compared to silica fume, the fine glass powder had a positive effect on compressive strength under normal curing conditions.

- The maximum heat flow increased and the time to reach the peak hydration flow was delayed with increasing levels of silica-fume replacement with fine glass powder due to the fact that fine glass powder can accelerate cement hydration via the adsorption of calcium ions from the liquid phase and serve as nucleation and growth sites for C-S-H and other hydrates. GP's high alkali (Na_2O) content may act as catalyst in the formation of calcium silica hydrate at an early age.
- The negligible water-absorption capability and smooth surface of waste-glass materials compared to cement and silica-fume particles enhanced concrete workability.
- The mechanical performance of the UHPGC was enhanced by the reactivity of the amorphous waste glass and optimizing the packing density. The waste-glass products in the UHPGC have pozzolanic behavior and react with the portlandite generated by the cement hydration. This, however, is not the case with quartz sand and quartz powder in conventional UHPC. The waste-glass addition enhances clogging of the interface between particles. Waste-glass particles have high rigidity, which increases the concrete's elastic modulus.
- The UHPGC has extremely good durability. Its capillary porosity is very low, and the material is extremely resistant to chloride-ion permeability (≈ 8 coulombs). Its abrasion resistance (volume loss index) is less than 1.3. UHPGC experiences virtually no freeze–thaw deterioration, even after 1000 freeze–thaw cycles. UHPGC's improved durability can contribute to reducing maintenance costs and concrete cover.
- UHPGC's higher mechanical properties made it possible to design footbridges with reduced sections (concrete volume reduced by about 60% compared to normal concrete).
- The construction of two footbridges at the University of Sherbrooke with the UHPGC shows the potential for the material to be produced on large scale and used in future projects.

- In addition, high amounts of waste glass cause environmental problems if stockpiled or sent to landfills. Moreover, the use of waste glass in UHPGC could save millions of dollars that would otherwise be spent for treatment and placing waste glass in landfills. It provides an alternative solution to the construction companies in producing UHPC at low cost.
- In the case of a typical UHPC, reducing the amount of quartz sand, quartz powder, cement, silica fume, and HRWRA and using local materials can significantly reduce UHPC costs and reduce the carbon footprint and energy consumption involved in cement production and transportation of materials. Moreover, the environmental and health hazardous caused by using crystaline materials (quartz powder and quartz sand) can be avoided when waste-glass materials are used.

9.2 Future work

This study has revealed several aspects of the experiments and numerical simulation involved with using waste-glass materials to make UHPC that should be studied further.
Based on the study reported on herein, the following areas need investigation to completely assess the application of waste-glass materials in UHPC.

- Optimize the rheological and thixotropic properties of fresh UHPC incorporating waste-glass materials according to application.
- Extensive hydration and microstructural investigations are required to better explain the hydration mechanisms of glass materials in UHPC.
- Study the early-age cracking that can occur with UHPC made with waste-glass materials.
- Scale up production and field applications of UHPC in various full-scale structural elements. Study the impacts of waste-glass materials on structural efficiency, initial and life-cycle economy, and sustainability of concrete structures.
- Develop new design equations and test methods for current construction codes and guidelines to adjust for the higher strength and durability characteristics associated with UHPC.
- Carry out life-cycle assessment (LCA) for the use of waste-glass materials in producing UHPC and compare the results with conventional UHPC and other concrete classes.

10 APPENDIX

10.1 Introduction

The appendix contains four peer-reviewed conference papers and one non-peer-reviewed journal paper that have either been published or are forthcoming.

Paper 8 (Using Ultra-Fine-Glass-Powder Silica to Produce Ultra-High-Performance Concrete) presents the results of producing FGP with an air classifier and jet mill. The GP was ground at classifier speeds ranging from 0 to 22,000 rpm. The finely ground GP (FGP) was employed to replace the entire SF content in conventional UHPC. The effect of different levels of FGP fineness on UHPC workability and compressive-strength properties was investigated in this research. The method for mix-design optimization, mixture compositions, material properties, and test methods used for this research are detailed in the following sections.

Paper 9 (Green Ultra-High-Performance Glass Concrete) presents an overview of the use of glass with various degrees of fineness (GS, GP, and FGP) to produce UHPC. The paper presents different UHPGC mixtures to suit different concrete applications in terms of rheology and strength requirements.

Paper 10 (A New Generation of Ultra-High-Performance Glass Concrete) presents the rheological behavior and mechanical performance of the two selected UHPGCs. A UHPGC without fibers was tested and compared to another concrete with 1% fiber.

Paper 11 (Novel Ultra-High-Performance Glass Concrete) presents the materials, structural design, manufacturing, and installation of pedestrian bridges built entirely with UHPGC at Sherbrooke University campus.

10.2 Paper 8: Using Ultra Fine Glass Powder to Produce Ultra-High-Performance Concrete

Reference:

Soliman N.A., Tagnit-Hamou A. (March 12–16, 2016) The study of Using Fine Glass Powder to Produce Ultra High Performance Concrete. 8th International Conference on Nano-Technology in Construction (NTC 2016), Sharm El-Sheikh, Egypt. (Awarded best paper).

Using Ultra Fine Glass Powder Silica to Produce Ultra-High-Performance Concrete

N.A. Soliman, A. Tagnit-Hamou

[1] *Cement and Concrete Research Group, Dept. of Civil Eng., University of Sherbrooke*

ABSTRACT

High contents of silica fume (SF) (25% to 30% of cement content) are an essential constituent for the ultra-high-performance concrete (UHPC) fabrication due to its extreme fineness and high amorphous silica content. This high content of SF with limited resources and high cost is considered as one of the impedances of the UHPC use in the concrete market. This gives the motivation to search for other materials with similar functions to partially or fully substitute the SF in the UHPC. The possibility of using fine-glass powder (FGP) to produce UHPC was investigated in this study. The results show that the FGP enhances concrete workability with 50% greater slump flow than in case of SF mixtures. The compressive strength of UHPC incorporating 100% FGP, with a mean-particle size of 3.8 μm can achieve 150 MPa with normal curing and 180 MPa with steam curing conditions.

Keywords

Glass powder, Low cost, packing density, Sustainability, Ultra-high-performance concrete.

INTRODUCTION

A typical UHPC mix contains portland cement, silica fume (SF), quartz sand having a maximum size of 600 μm, quartz powder, and eventually steel fiber [1-7]. Such a typical mix has very low water-to-binder ratio (*w/b*) and contains high amount of superplasticizer (SP). Depending on its composition and its curing temperature, this material can exhibit compressive strength up to 150 MPa, flexural strength greater than 15 MPa, and elastic modulus above 50 GPa [4,8]. It can also resist freeze-thaw and scaling cycles without visible damage, and it is nearly impermeable to chloride-ion penetration [2]. These excellent characteristics of UHPC are achieved by the

enhancement of the homogeneity by eliminating coarse aggregate, enhancement of packing density by optimizing the granular mixture through a wide distribution of powder size classes, improvement of matrix properties by using pozzolanic materials, by reducing the *w/b*, the microstructure improvement through the post-set heat treatment; and by enhancement of ductility by including small steel fibers [8].

In UHPC, SF with extreme fineness and high amorphous silica content has three main functions: filling voids in next larger granular class (cement), enhancing lubrication of the mix due to the perfect sphericity of its particles, and producing secondary hydrates by pozzolanic reaction with the hydration products from primary cement hydration [1]. The amount of SF in UHPC is typically about 25%, by weight of the total binder materials. The amount of SF theoretically required for the reaction with products of cement hydration is 18%. The optimal SF content increases to about 25% to obtain a denser mixture. Tests revealed that greater compressive strength could be achieved with 30% SF [8]. However, the limited available resource and high cost restrain the application of SF in modern construction industry. This gives motivation to search for other materials to substitute SF, but yielding similar functions.

Post-consumption glass can be recycled in many countries several times without significant alternation of its physical and chemical properties [9]. In Europe, as indicated by the latest glass recycling industry report published by the European Container Glass Federation (FEVE), the average rate of glass recycling in 2011 has risen above the 70% threshold (over 12 million tons) [10]. In other countries, large quantities of glass cannot be recycled because of colour mixing, or expensive recycling cost [9]. For example, in Quebec/Canada, only 49% of glass was recovered in 2008 [11], the rest was landfilled. According to USEPA in 2011, Americans generated 11.5 million tons of glass in the municipal solid waste streams and only 28% of the glass was recovered for recycling [12]. Waste glass material when crushed and ground at different particle size (0-20 mm) is considered as an innovative, durable and sustainable material to be also used in concrete as supplementary materials [13,14] and aggregate [15].

The current research aimed at developing an innovative low-cost and sustainable UHPC by using finely ground glass powder (FGP) to various fineness to replace SF. The effect of different fineness of FGP on workability and compressive strength of UHPC was investigated. The optimization of UHPC mixtures were carried out based on packing density theory.

EXPERIMENTAL PROGRAM

The fineness is one of the most important properties of materials which relates to both the physical and chemical effects (i.e. porous structure, filler effect, pozzolanic reaction, grinding energy, and workability of mixture). In this research, glass powder was grinded using classifier to different fineness between 2.8 to 12.0 µm. The finely ground GP (FGP) was employed to replace the entire SF content in the traditional UHPC. The effect of different fineness of FGP on workability and compressive strength properties of UHPC was investigated in this research. The method for mix-design optimization, mixture compositions, material properties, and test methods undertaken in this research are detailed in the following sections.

Mix-Design Optimization

The mix design was developed in two steps (packing density of granular materials and compatibility between the cement and superplasticizer). The packing density for all granular materials was determined using compressible packing model of de Larrard [16]. The selected optimal packing density was 0.79%, it was a combination of QS, QP, cement, and SF. When replacing the total SF quantity by FGP, the optimal packing density became 0.75%. This results in using about 229 kg/m^3 of FGP to replace SF.

The optimum amount of superplasticizer for various *w/b* that gives specific rheological characteristics to obtain self-consolidating matrix as well as high strength was evaluated using a full-factorial design approach. Fig. 1 presents the typical mix components of UHPC compared to UHPGC. Fig. 2 presents the particle-size distributions for QS, GP of different fineness, cement, SF, and combined granular UHPGC materials. Continuous particle distribution of the entire mixture can be observed from the figure.

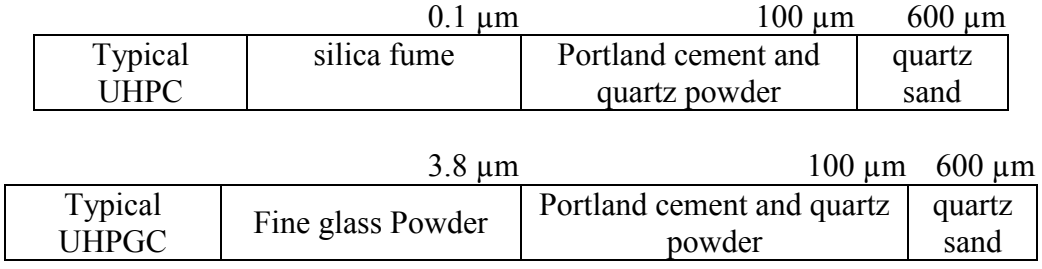

Fig. 1: Comparison between composition of UHPGC and UHPC

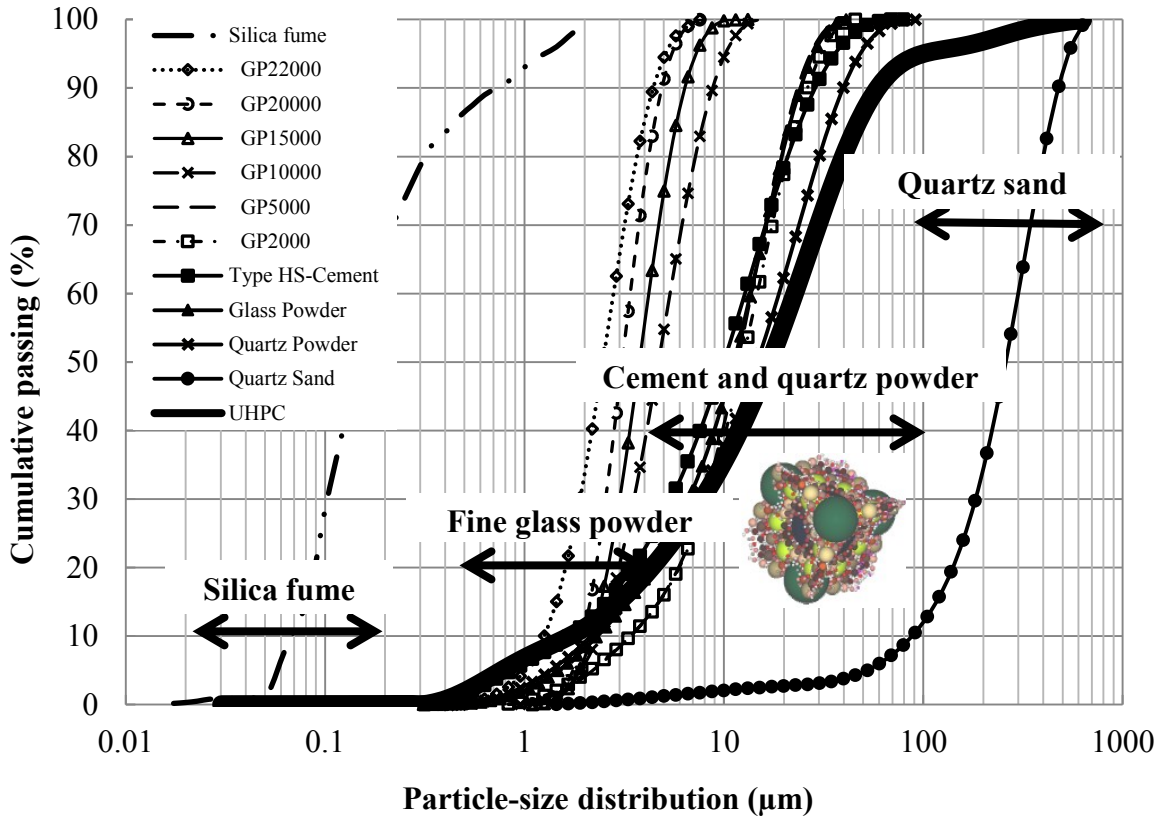

Fig. 2: Particle-size distributions of individual and combined-granular materials used in UHPC mix design

Mixture Compositions

A total of five UHPGC mixtures were designed to study the effect of fineness of GP on the fresh and mechanical properties of the UHPC (Table 1). One traditional mixture prepared with cement, SF, QP, and QS without GP. Four mixtures containing GP of different mean-particle size diameters (d_{50}) of 2.8, 3.8, 5.0, and 12.0 µm to replace totally the SF in the UHPC reference mixture. In all concrete mixtures, the cement, QS, QP, *w/b*, and HRWRA amounts were kept constants. All concrete mixtures were designed with fixed *w/b* of 0.189 and superplasticizer dosage of 1.5% (percentage of solid content in the superplasticizer to the binder content). The number in the mixture name represents the d_{50} of the GP used in the mixture. For example, the GP-5.0 mixture had d_{50} equals 5 µm.

Material properties

The selection of cement is critical when making UHPC in order to control its rheology. The rheology of concrete is strongly influenced by the fineness, and C_3A and C_3S contents of the cement. This is even more critical in the case of UHPGC as the cement particles are very close to each other, due to the very low *w/b* used. Therefore, it is important to select cement having the lowest content of C_3A and C_3S. Consequently, high-sulphate resistance cement, which is formulated specifically with low C_3A content, was selected. It had the Bogue composition of 50% C_3S, 25% C_2S, 14% C_3A, and 14% C_4AF. Its specific gravity is 3.21, Blaine fineness of 370 m^2/kg, and d_{50} of 11 μm. The SF complied with CAN/CSA A 3000 specifications, had silica content of 99.8%, specific gravity of 2.20, specific surface area of 20,000 m^2/kg, and d_{50} of 0.15 μm was used in the mixture. The QS was used as a granular material having a maximum particle-size diameter (d_{max}) equals 600 μm and d_{50} of 250 μm. It has silica content of 99.8% and specific gravity of 2.70. The GP used had d_{max} of 100 μm with silica content of 73%, Na_2O_{eq} content of 13%, and specific gravity of 2.60. Polycarboxylate-based high-range-water-reducing admixture (HRWRA) was used as superplasticizer (Sika Viscocrete 6200).

Table 1: UHPC mixtures proportioning (in kg/m^3)

	Reference	(100% replacement SF by GP of different fineness)			
Material		GP-12.0	GP-5.0	GP-3.8	GP-2.8
Type HS cement	810	823	823	823	823
Silica fume	225	--	--	--	--
Glass powder-12.0	--	229	--	--	--
Glass powder-5.0	--	--	229	--	--
Glass powder-3.8	--	--	--	229	--
Glass powder-2.8	--	--	--	--	229
Water	196	199	199	199	199
Quartz sand	972	987	987	987	987
Quartz powder	243	247	247	247	247
Solid content in HRWRA	13	13	13	13	13

Concrete Batching and Test methods

To achieve a homogeneous mixture and avoid agglomeration of very fine particles, all powders were mixed in dry state before water and superplasticizer additions. To improve flowability, superplasticizer was added gradually in two shots. About ½ of mixing water containing ½ of the superplasticizer dosage was added during 3 to 5 min of mixing. The remaining water and superplasticizer was added during additional 3 to 5 min of mixing at high speed.

As soon as the mixing was completed, the measurements of fresh properties of the UHPGC started. The tests included fresh concrete temperature, unit weight and air content (ASTM C 185). The rheology of the concrete was measured using the flow-table test according to (ASTM C 1437).

The concrete was sampled by taking cube specimens of 50 mm for the compressive strength test (ASTM C 39). The specimens were remained tightly covered with plastic sheets at laboratory temperature for 24 hours before demoulding.

Two curing regimes were implemented after demoulding. In the normal curing regime (NC), the samples were stored in a fog room (temperature of 20 ± 2oC and relative humidity (RH) of 100%) until testing. The second mode of curing was hot or steam curing (HC) at 90ºC and RH of 100% for 48 hours.

RESULTS AND DISCUSSIONS

Optimizing FGP Granulometry

A classifier was used to grind the GP to smaller particle sizes. The GP was ground at various classifier speeds between 0 and 22,000 rpm. At the lower speeds (up to 5,000 rpm), it was capable of grinding relatively large quantity of GP (about 750 g/hour), but the energy of the classifier was not enough to grind the GP to finer particles. The d_{50} remained constant at 12 µm with small increase in the Blaine surface between 382 to 420 m^2/kg (Table 2). Higher grinding speeds between 10,000 and 22,000 rpm were then applied, which were efficient to produce

powder with d_{50} of 2.8 µm at 22,000 rpm. The production rate at this high speed was only 20 g/hour.

Table 2: Optimizing granulometry of fine glass powder using classifier

Classifier speed (rpm)	0	2000	5000	10000	15000	22000
Blaine surface (m^2/kg)	382	382	420	950	10000	12000
Maximum particle-size diameter, d_{max} (µm)	50	40	38	15	10	8
Mean particle-size diameter, d_{50} (µm)	12.0	12.0	12.0	5.0	3.8	2.8
Production rate of glass powder (g/hour)	750	750	750	500	270	20

Effect of FGP on Fresh UHPGC Properties

The aimed slump flow diameter for all UHPGC mixtures made with GP of various fineness were regarded between 170 to 250 mm for the practical applications. Fig. 3 shows the required superplasticizer dosages and measured slump flow diameters for the tested UHPC mixtures. It can be seen that the fineness of GP strongly influences the workability of UHPC mixtures. When adding GP of finer particles to replace totally the SF, the superplasticizer dosage was found to decrease. The GP-12 mixture containing the coarser particles required a higher amount of superplasticizer (2.5%) compared to 1.5% for the reference mixture. The respective superplasticizer dosages for the GP with d_{50} of 5.0, 3.8, and 2.8 µm were 2.0%, 1.5%, and 1.5%, respectively. This may be due to the fact that the coarser GP lead to less packing density (0.65 for the GP-12 mixture) and needs higher amount of mixing water than the mixture made with fine GP. However, this amount dramatically reduces when the d_{50} of GP decreases from 12 to 5 µm, then to 3.8 µm. The mixture made with GP of a d_{50} less than 3.8 µm (GP-2.8) required a similar amount of superplasticizer as the GP-3.8 and the reference mixture.

It can be concluded from these findings that the FGP with d_{50} of 3.8 µm can be used successfully to replace SF leading to higher workability properties while maintaining the same superplasticizer dosage.

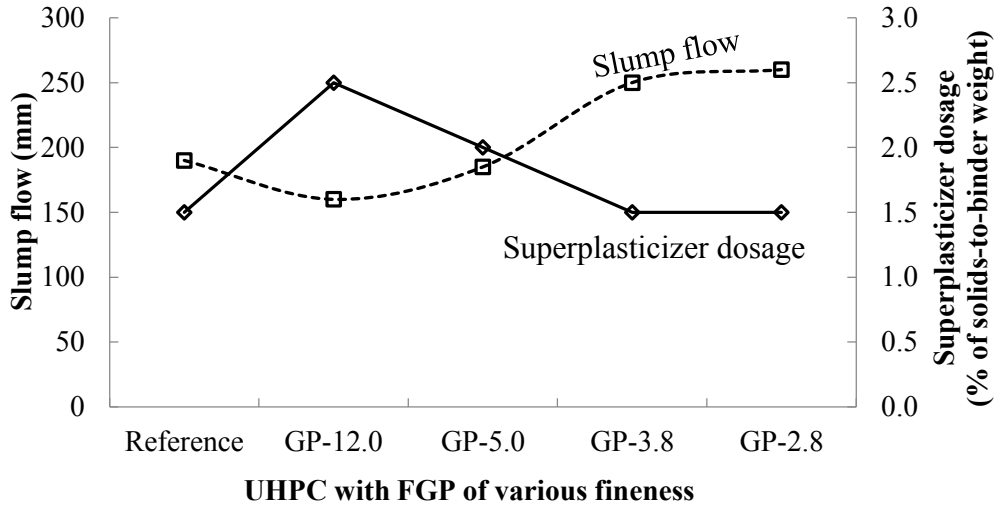

Fig. 3: Slump flow diameter and superplasticizer dosage for UHPGC mixtures with fine glass powder (FGP) of different mean-particle size diameters

Effect of FGP on Compressive Strength

Fig. 4 shows the effect of FGP of various fineness (d_{50} from 2.8 to 12 μm) as replacement to the total SF on compressive strength results of UHPC over time and under the NC and HC curing conditions. It can be seen also that the compressive strength of UHPC increases when using FGP of smaller d_{50}. The development of the compressive strength of the GP-3.8 mixture was found similar to that of the GP-2.8 mixture, with compressive strength values over 150 MPa after 2-day HC.

The compressive strength development for the mixtures containing FGP were lower than that of the reference mixture, due to the better filler effect of the SF. It has to be noted here that he FGP was used to replace 100% of SF. The performance could be optimized when mixing the FGP and SF at given replacement rate.

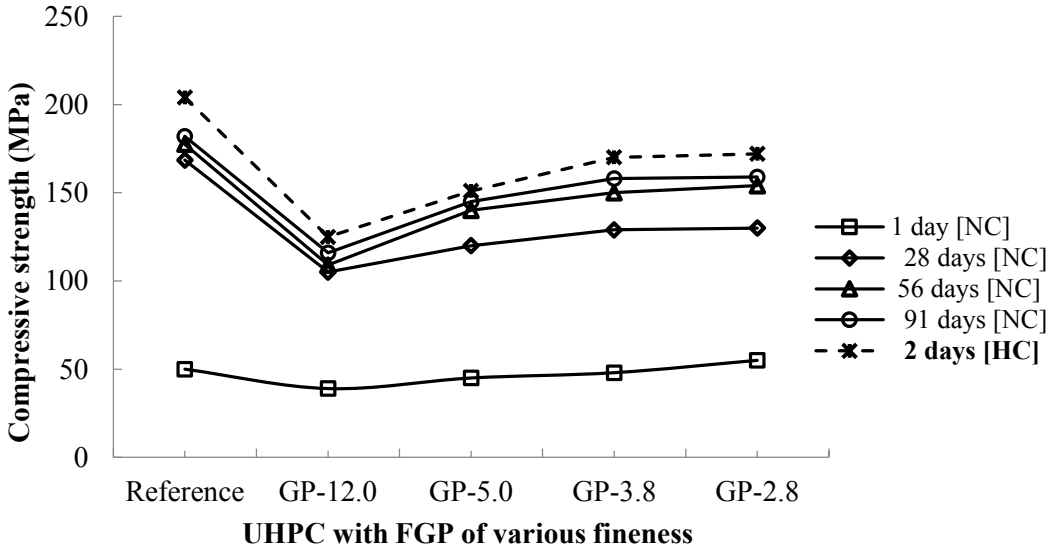

Fig. 4: Compressive strength subjected to different curing periods and conditions for the fine glass powder of different mean-particle size diameters

Based on the workability and compressive strength results of the tested UHPGC mixtures, the FGP with a d_{50} of 3.8 μm can be selected to replace SF in the UHPC production. On the other hand, the grinding energy consumptions were measured at 3.0 and 7.5 kWh/kg for producing the FGP-3.8 and FGP-2.8, respectively. This difference in energy increases dramatically the grinding cost. Therefore, the reasonable mean-particle size of FGP to make UHPC can be proposed to be in the range 3.8 μm in terms of energy consumption, and workability and compressive strength properties.

CONCLUSIONS

Based on the above results, the following conclusions can be drawn:

- A new type of ultra-high performance glass concrete (UHPGC) has been developed through the use of glass powder. This glass powder was obtained by grinding recycled glass culets.
- The UHPC mixes when optimized by packing density method, allows incorporating about 230 kg/m^3 of fine glass powder to replace 100 of silica fume. Concrete mixes with fine glass powder presents excellent workability with higher slump due to the non-absorptive glass particles and optimized packing density.

- The UHPGC with fine glass powder can provide mechanical performance comparable to the traditional UHPC.
- The optimal mean-particle size diameter of the glass powder is about 3.8 μm in terms of energy consumption, and workability and compressive strength properties.
- UHPGC provides several advantages through: usage of waste glass, reduce production cost of UHPC.

ACKNOWLEDGMENT

This research was funded by Société des Alcools du Québec (SAQ). The authors gratefully acknowledge this support. The writers would also like to acknowledge the support of the Université de Sherbrooke to support this work.

REFERENCES

1. P. Richard, and M. Cheyrezy "Composition of Reactive Powder Concretes" Cement and Concrete Research. Vol. 25, No. 7, p.p. 1501-1511 (1995).
2. P. Richard, and M. Cheyrezy "Reactive Powder Concretes with High Ductility and 200-800 MPa Compressive Strength" ACI SP 144, p.p. 507-518 (1994).
3. N. Roux, C. Andrade, and M. Sanjuan "Experimental Study of Durability of Reactive Powder Concretes" Journal of Materials in Civil Engineering, Vol. 8, Issue 1, p.p. 1-6 (1996).
4. M. Schmidt, and E. Fehling "Ultra-High-Performance Concrete: Research, Development and Application in Europe" ACI SP Vol. 225, p.p. 51-77 (2005).
5. M-G. Lee, C-T. Chiu, and Y-C. Wang "The Study of Bond Strength and Bond Durability of Reactive Powder Concrete" Journal of ASTM International, Vol. 2, No. 7, p.p. 104-113 (2005).
6. F. de Larrard, and T. Sedra "Optimization of Ultra-High-Performance Concrete by the Use of a Packing Model" Cement and Concrete Research, Vol. 24, No. 6, p.p. 997-1009 (1994).
7. V. Matte, M. Moranville, F. Adenot, C. Riche, and J.M. Torrenti "Simulated Microstructure and Transport Properties of Ultra-High Performance Cement-Based Materials" Cement and Concrete Research, Vol. 30, No. 12, p.p. 1947-1954 (2000).

8. P-C. Aïtcin "Cements of Yesterday and Today – Concrete of Tomorrow" Cement and Concrete Research, Vol. 30, No. 9, p.p. 1349-1359 (2000).
9. A. Shayan, and A. Xu "Value-Added Utilisation of Waste Glass in Concrete" Cement and Concrete Research, Vol. 34, No. 1, p.p. 81-89 (2004).
10. FEVE. "Collection for Recycling Rate in Europe" The European Container Glass Federation. http://www.feve.org/FEVE-STATIS-2013/Recycling-2011-Glass-coll.html (Cited 11 Sept. 2013).
11. Recyc-Québec "Le Verre Fiches Informatives" (2010).
12. USEPA. "Wastes-Resource Conservation-Common Wastes & Materials Glass". http://www.epa.gov/osw/conserve/materials/glass.html (Cited 10 Sept. 2013).
13. A. Zidol, M.T. Tognonvi, and A. Tagnit-Hamou "Effect of Glass Powder on Concrete Sustainability" 1st International Conference on Concrete Sustainability (ICCS13), Ref # 0229 (2012).
14. A. Zidol, A. Pavoine, and A. Tagnit-Hamou "Effect of Glass Powder on Concrete Durability" International Congress on Durability of Concrete, Trondheim, Norvège, ICDC2012-D-11-00153. (2012).
15. M.J. Terro "Properties of Concrete Made with Recycled Crushed Glass at Elevated Temperatures" Building and Environment, Vol. 41, No. 5, p.p. 633-639 (2006).
16. F. de Larrard "Concrete Mixture Proportioning: a Scientific Approach" London: Modern Concrete Technology Series, E&FN SPON, (1999).

10.3 Paper 9: Green Ultra-High-Performance Glass Concrete

Reference:

Soliman N, Tagnit-Hamou A., Omran A. (18-20 July 2016) Green Ultra-High-Performance Glass Concrete. *First International Interactive Symposium on UHPC, Des Moines, Iowa, USA*.

Green Ultra-High-Performance Glass Concrete

(1) Arezki Tagnit-Hamou, (corresponding author) Professor and head of cement and concrete group, University of Sherbrooke, Canada. Address: 2500 Blvd. Université, Sherbrooke, Quebec, Canada J1K 2R1, Phone: 819-821-7993, E-mail: A.Tagnit@USherbrooke.ca
(2) Nancy Soliman, PhD Candidate, University of Sherbrooke, Canada.
(3) Ahmed Omran, Research associate, University of Sherbrooke, Canada.

Abstract:

This paper presents research work on the development of a green type of ultra-high-performance concrete at the University of Sherbrooke using ground glass powders with different degrees of fineness (UHPGC). In UHPGC, glass is used to replace quartz sand, cement, quartz powder, and silica-fume particles. UHPGC design is based on particle packing density, mechanical properties, and specific rheology. Mixes are designed to suit the rheology and mechanical performances of different concrete applications. Depending on composition and curing conditions, UHPGC can provide improved rheology (mini-slump spread of 260 mm), higher mechanical properties (compressive strength greater than 200 MPa, flexural strength more than 25 MPa). A case study of using this UHPGC is presented through the design and construction of a footbridge.

Keywords: Ultra-high-performance concrete, Sustainability, Waste-glass materials, Glass powder, Footbridge.

1. Introduction

A typical UHPC mix contains Portland cement, silica fume (SF), quartz powder (QP), quartz sand (QS) with a maximum size of 600 μm, and possibly steel fiber [1-6]. Such typical mixes have a very low water-to-binder ratio (*w/b*) and high superplasticizer contents. Depending on composition and curing temperature, this material can exhibit compressive strength (f_c) of up to 150 MPa, flexural strength in excess of 15 MPa, and elastic modulus above 50 GPa [4,7]. It can also resist freeze–thaw and scaling cycles without any damage, and it is nearly impermeable to

chloride-ion penetration [2]. These outstanding characteristics of UHPC are achieved by enhancing homogeneity, eliminating coarse aggregate, enhancing the packing density by optimizing the granular mixture through a wide distribution of powder size classes, improving matrix properties, incorporating pozzolanic materials, reducing the *w/b*, improving the microstructure, applying post-set heat treatment, and enhancing ductility by including small steel fibers [7].

When producing cement-based materials, consideration must be given not only to good mechanical and durability characteristics, but also to the environmentally friendly, ecological, and socioeconomic benefits [8]. A typical UHPC design has a cement content of 800 to 1000 kg/m^3 [1,2]. This high cement content not only affects production costs and consumes natural sources; it also negatively affects the environment through CO_2 emissions and greenhouse effect [8]. The QP has an immediate and long-term harmful effect on the human health because it is human carcinogen. Because of the large difference in grain-size distributions between portland cement and ultrafine SF, high amount of ultrafine SF (25% to 30% by cement weight) have to be used to fill the pores between the cement particles. This significantly decreases the workability of UHPC and increases concrete cost. All these drawbacks are considered as impediments to the wide use of UHPC in the concrete market.

Despite that the post-consumption glass can be recycled in many countries several times without significantly altering of its physical and chemical properties, large quantities of glass cannot be recycled because of high breaking potential, color mixing, or expensive recycling cost [9]. Most waste glass is dumped into landfills, which is undesirable because it is not biodegradable and not very environmentally friendly [10]. Attempts in recent years have been made to use waste-glass powder (GP) as an alternative supplementary cementitious material (ASCM) or ultrafine filler in concrete, depending on its chemical composition and particle-size distribution (PSD) [11-12]. GP with a mean-particle size (d_{50}) finer than 75 μm exhibits pozzolanic behavior, which contributes to concrete strength and durability [13-15]. GP can be used to partially replace cement in different types of concrete [16-19], which significantly decreases the adverse effects caused by alkali–silica reaction [20]. Based on this research, incorporating waste GP in concrete provides high value and feasibility because of the economic and technical advantages.

This article presents the development of an innovative, low-cost, and sustainable UHPGC through the use of glass with various degrees of fineness to replace cement, QP, QS, and SF

particles. This research highlights the UHPGC design method used to produce various mixtures to suit different concrete applications in terms of rheology and strength requirements. Erection of footbridge at University of Sherbrooke Campus using UHPGC is also presented as a full-scale application.

2. UHPGC Description

UHPGC is a new type of UHPC that is a sustainable concrete incorporating granulated post-consumer waste glass ground to a specific fineness [21]. Glass sand (GS) can replace QS; GP can partially replace cement and completely replace QP; and fine glass powder (FGP) can partially replace SF.

UHPGC mix designs were developed by optimizing (1) the packing density of the granular materials using the compressible packing model [20], (2) *w/b* and HRWRA dosage using a full-factorial design approach, and (3) fiber content [21]. Figure 1 presents the continuous particle-size distributions (PSDs) of the combination of the all ingredients to produce UHPGC. The *w/b* and HRWRA dosage used in UHPGC are optimized to produce concrete with certain rheological characteristics and strength requirements. The fiber content is optimized without significant alteration of the rheological properties of the fresh mixture. The fiber optimization depends mainly on the fiber type and content.

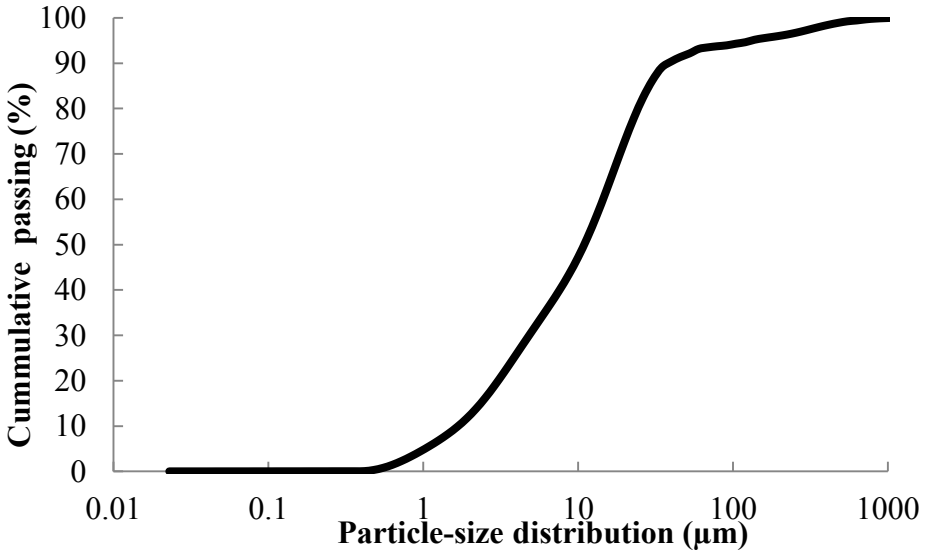

Figure 1. Particle-size distribution of materials used in this study and UHPGC

UHPGC can be produced with a lower water-to-binder ratio (*w/b*) due to the glass particles with zero absorption. UHPGC has enhanced rheological properties, so that it is practically self-placing without the need for internal vibration. UHPGC has enhanced rheological properties and workability due to the glass particles' zero adsorption. Depending on composition and curing temperature, UHPGC's f_c can range from 130 to 260 MPa, while it's flexural strength (f_{fl}) can exceed 15 MPa, tensile strength (f_{sp}) exceed 10 MPa, and elastic modulus (E_c) exceed 45 GPa. UHPGC is characterized by excellent durability due to high packing density and lack of interconnected pores. This concrete has negligible chloride-ion penetration, low mechanical abrasion, and very high resistance to freeze–thaw cycles and deicing chemicals [21]. UHPGC can be considered an innovative low-cost, sustainable, and green UHPC.

3. UHPGC Mix Designs for Various Construction Applications

3.1 UHPGC Classes

Based on the research conducted to develop UHPGC using waste-glass materials [21], four different UHPGC mixture types can be delimited in responding to various construction demands (Table 1). The UHPC mixtures in Class A are characterized by low flowability of less than 200 mm but with 2-day f'_c under hot curing conditions (HC) of more than 200 MPa. Concrete mixes in Class A have a *w/b* between 0.15 and 0.19. Highly flowable UHPC can be obtained, as in Class C, with higher *w/b* between 0.23 and 0.25. The UHPC mixtures in Class C are characterized by 2-day f'_c under HC between 160 and 175 MPa. The concrete mixes in Class B blend the characteristics of those in Classes A and C. All UHPGC mixtures in Classes A, B, and C are designed with steel fiber. The mixtures in Class D are designed for architectural applications, with the steel fiber being replaced with polyvinyl alcohol (PVA) fiber. The concretes in this Class are characterized by higher flowability (260 mm) and moderate strength [91-day f'_c of more than 120 MPa under normal curing conditions (NC)].

Table 1. UHPC with local materials for various construction applications

Characteristics	Class A	Class B	Class C	Class D (architecture)
Flowability	Semi-flowable	Flowable	Highly flowable	Highly flowable
Average mini-slump flow diameter, mm	200	230	260	260
w/b	0.15–0.19	0.19–0.23	0.23–0.25	0.23–0.25
% of solids in superplasticizer/cement weight	1–3	1–3	1–3	0.225–0.25
Steel fiber (%)	2	2	2	--
PVA fiber	--	--	--	2.5
2-day-HC *f'c*, MPa	>200	175–200	160–175	--
28-day-NC *f'c*, MPa	>160	>140	>130	>100
91-day-NC *f'c*, MPa	>180	>150	>140	>120
Flexural strength, MPa	>25	>20	>15	>10
Modulus of elasticity, GPa	>50	>45	>40	>40
Chloride-ion penetration	Negligible	Negligible	Negligible	Negligible
Relative dynamic modulus of elasticity after 1000 freeze–thaw cycles	100%	100%	100%	100%

3.2 Examples of Various UHPGC Classes

3.2.1 Material Properties and Mixture Proportioning

Type HS cement formulated with a low C_3A content was selected to provide high sulfate-resistance. SF compliant with CAN/CSA A3000-13 "Cementitious materials compendium" specifications, QS, and GP with Na_2O content of 13% were used in the UHPGC mixture. Table 2 provides the properties of these materials. This mixture had more than 400 kg/m^3 of GP as cement replacement. A polycarboxylate-based HRWRA with a specific gravity of 1.09 and solids content of 40% (Sika Viscocrete 6200) was used. The polyvinyl alcohol (PVA) fibers used were 13 mm in length and 0.2 mm in diameter, and had a specific gravity of 1.3 and tensile strength of 400 MPa.

Table 3 presents the mixture proportions for seven UHPGC mixtures covering the various concrete Classes described in Table 1. As shown in the table, the design allowed using GP in all mixes in contents varying between 222 and 403 kg/m^3. FGP contents ranging from 53 to 113 kg/m^3 were used to partially replace the ultrafine SF in UHPGC-1 to 4. GS was also used as a

25% replacement of QS in UHPGC-3 and 50% in both UHPGC-4 and 6. A 2% volume fraction of steel fiber was used for UHPGC-1 to 6, while 2.5% PVA fiber was used for UHPGC-7.

Table 2. Material properties

Property	HS Cement	Silica Fume	Glass Powder	Fine glass powder	Glass Sand	Quartz Sand
Silica, %	--	99.8	73	73	73	99.8
Specific gravity	3.21	2.20	2.60	2.60	2.60	2.70
d_{max}, μm	<100	<1	<100	<10	<800	<600

Table 3. UHPGC mixture compositions for various construction applications (Kg/m^3)

	Class A		Class B		Class C		Class D
Materials	UHPGC-1	UHPGC-2	UHPGC-3	UHPGC-4	UHPGC-5	UHPGC-6	UHPGC-7
Water	196	193	211	186	215	236	224
Cement	812	640	608	790	561	739	544
Silica fume	113	142	158	109	208	205	204
Fine glass powder	113	80	53	109	--	--	--
Glass powder	244	382	380	237	411	222	403
Quartz sand	974	960	684	474	896	443	888
Glass sand	--	--	228	474	--	443	--
Superplasticizer*	13	13	10	17	16	10	16
PVA fiber	--	--	--	--	--	--	32.5
Steel fiber	158	158	158	158	158	158	--

*Solids content

3.2.2 UHPGC Performance

Table 4 provides the workability and *f'c* after 2 days of HC (*f'c-2d-HC*), 28 days of NC (*f'c-28d-NC*), and 91 days of NC (*f'c-91d-NC*) of the seven UHPGC mixtures. A mini-slump spread of more than 230 mm indicates higher concrete workability. Strength results satisfy the requirements given in Table 1. As shown in the table, the mechanical strength for the samples subjected to 2 days of HC was greater than those obtained under the normal curing conditions, even after 91 days of curing. The concrete mixtures in Class A showed the highest strength results (*f'c-2d-HC* of 210 and 205 MPa for UHPGC-1 and 2, respectively), while those in Class C were the lowest (*f'c-2d-HC* of 169 and 175 MPa for UHPGC-5 and 6, respectively). The concrete in Class B exhibited moderate strength (*f'c-2d-HC* of 200 and 190 MPa for UHPGC-3

and 4, respectively). UHPGC-7 (Class D) tested at 135 MPa for the *f'c-2d-HC* due to the inclusion of the PVA fiber.

Table 4. Performance characteristics of UHPGC mixtures used for various construction applications

	Class A		Class B		Class C		Class C
Materials	UHPGC-1	UHPGC-2	UHPGC-3	UHPGC-4	UHPGC-5	UHPGC-6	UHPGC-7
Mini-slump flow, mm	240	230	260	250	270	290	270
f'c-2d-HC, MPa	210	205	200	190	169	175	135
f'c-28d-NC, MPa	177	170	158	150	130	138	100
f'c-91d-NC, MPa	191	185	175	165	155	162	127

4. Field Applications

4.1 Footbridge Design

Once successfully developed in the laboratory, the UHPGC was used to fabricate a footbridge to replace the deteriorated wooden structure on the University of Sherbrooke's campus (Figure 2). UHPGC-7 (Table 2) was used to cast the bridge. UHPGC-7 was produced at the University of Sherbrooke's laboratory in a 500 L capacity pilot-scale automatic concrete plant with a paddle-type stationary pan mixer. All powder materials were mixed for 10 minutes. About one half of the HRWRA diluted in half of the mixing water was added over 3 to 5 min of mixing. The PVA fibers and remaining water and HRWRA were added during 3 to 5 additional minutes of mixing. The footbridge was designed to meet the university's architectural and structural requirements for pedestrian use as well as to comply with the university's regulation on sustainable development. The UHPGC's mechanical properties made it possible to fabricate the spans with relatively small cross sections; the bridge's total weight was around 4000 kg. The structure is expected to be durable with high abrasion and impact resistance. The structural system consisted of an arch slab 4.91 m in length, 2.5 m in width, and 0.075 m in thickness supported by longitudinal ribs of variable height and a constant width of 0.13 m [22]. The arch slab was reinforced with welded-wire reinforcement (M10 at 300 mm in both directions) placed at slab

mid-height. Each rib was reinforced with a single M20 reinforcing bar located near the bottom of the rib.

The bridge mold was built by Beton Genial Company (specialist in UHPC production), and then transported to the university's laboratory for casting. The mold was made of urethane-rubber facing with specific Shore's hardness. The mold was designed so that the bridge was cast upside down, allowing the relatively complex shape to be formed with integral non-slip areas on the deck, very smooth surfaces elsewhere, and no joints. Handrails were attached to the bridge before it was transported to the installation site. The bridges were mounted on conventional concrete abutments with neoprene bearing pads.

Figure 2. UHPGC Footbridge built at the University of Sherbrooke

4.2 Concrete Performance

Fresh properties. The fresh concrete slump was about 280 mm without tamping, 2230 kg/m^3 unit weight, 3.5% air content, and 22°C for the fresh concrete temperature.

Mechanical properties. The f_c tests were carried at 1, 7, 28, and 91 days after NC. The 28 and 91-day f_c values of this UHPGC were 96 and 127 MPa, respectively (Table 5). The f_c gains of about 33% from 28 days to 91 days indicates the effect of the pozzolanic reactivity of glass powder. Other mechanical tests—including indirect splitting tensile strength, flexural strength, and modulus of elasticity—were also performed (see Table 5).

Durability properties. The mechanical abrasion test shows an average relative volume-loss index of 1.35 mm. The mass loss after 56 freeze–thaw cycles with deicing salts was very low (12 g/m^2). The 28- and 91-day specimens subjected to the chloride-ion penetration test yielded a negligible value of 10 Coulombs. The relative dynamic modulus of elasticity was 100% after 1000 freeze–thaw cycles.

Table 5. Mechanical properties of the UHPGC

Properties	Concrete Age, Days			
	1	7	28	91
Compressive strength, MPa	12	52	96	127
Splitting tensile strength, MPa	--	--	10	11
Flexure strength, MPa	--	--	10	12
Modulus of elasticity, GPa	--	--	41	45

5. Conclusions

A new type of UHPC has been developed using waste-glass materials, resulting in UHPGC. The new material exhibited excellent workability and rheological properties due to the zero absorption of the glass particles as well as the material's optimized packing density. The UHPGC evidenced an improved microstructure with higher mechanical properties and superior durability properties comparable to conventional UHPC. The UHPGC can be developed with different mix designs for various construction applications. The mechanical properties of the UHPGC made it possible to design a footbridge with reduced cross sections (about a 60% reduction in concrete volume compared to normal concrete). The UHPGC's improved durability performance can reduce maintenance costs. The construction of footbridge at the University of Sherbrooke with the UHPGC demonstrates the material's potential for large-scale production. The UHPGC can be used to build highly energy-efficient, environmentally friendly, affordable, and resilient structures. It can also significantly reduce UHPC costs and save the money spent for the treatment of glass cullets and their disposal in landfills.

6. References

1. Richard, P. and Cheyrezy, M., "Composition of Reactive Powder Concretes," *Journal of Cement and Concrete Research*. Vol. 25, No. 7, 1995, pp. 1501–1511.
2. Richard, P. and Cheyrezy, M., "Reactive Powder Concretes with High Ductility and 200-800 MPa Compressive Strength," *ACI SP 144*, 1994, pp. 507–518.
3. Roux, N. Andrade, C. and Sanjuan M., "Experimental Study of Durability of Reactive Powder Concretes," *Journal of Materials in Civil Engineering*, Vol. 8, Issue 1, 1996, pp. 1–6.
4. Schmidt, M. and Fehling, E., "Ultra-High-Performance Concrete: Research, Development and Application in Europe," *ACI SP*, Vol. 225, 2005, pp. 51–77.
5. Lee, M.-G. Chiu, C.-T. and Wang, Y.-C., "The Study of Bond Strength and Bond Durability of Reactive Powder Concrete," *Journal of ASTM International*, Vol. 2, No. 7, 2005, pp. 104–113.
6. de Larrard, F. and Sedra T., "Optimization of Ultra-High-Performance Concrete by the Use of a Packing Model," *Journal of Cement and Concrete Research*, Vol. 24, No. 6, 1994, pp. 997–1009.
7. Matte, V. Moranville, M. Adenot, F. Riche, C. and Torrenti, J.M., "Simulated Microstructure and Transport Properties of Ultra-High Performance Cement-Based Materials," *Journal of Cement and Concrete Research*, Vol. 30, No. 12, 2000, pp. 1947–1954.
8. Aïtcin, P-C. "Cements of Yesterday and Today – Concrete of Tomorrow," *Journal of Cement and Concrete Research*, Vol. 30, No. 9, 2000, pp. 1349–1359.
9. Shi, C. Wu, Y. Riefler, C. and Wang, H., "Characteristic and Pozzolanic Reactivity of Glass Powders," *Journal of Cement and Concrete Research*, Vol. 35, 2005, pp. 987–993.
10. Shayan, A. and Xu, A., "Performance of Glass Powder as a Pozzolanic Material in Concrete: a Field Trial on Concrete Slabs," *Journal of Cement and Concrete Research*, Vol. 36, 2006, pp. 457–468.
11. Roz-Ud-Din, N. and Parviz, S., "Strength and Durability of Recycled Aggregate Concrete Containing Milled Glass as Partial Replacement for Cement," *Journal of Construction and Build Materials*, Vol. 29, 2012, pp. 368–77.
12. Shao, Y. Lefort, T. Moras, S. and Rodriguez, D., "Studies on Concrete Containing Ground Waste Glass," Journal of Cement and Concrete Research, Vol. 30, 2000, pp. 91–100.
13. Idir, R. Cyr, M. Tagnit-Hamou A. Pozzolanic properties of fine and coarse color-mixed glass cullet [J]. Cem Concr Compos, 2011, 33(1): 19-29.

14. Cong, K.S. and Feng, X., "The Effect of Recycled Glass Powder and Reject Fly Ash on the Mechanical Properties of Fiber-Reinforced Ultra-high Performance Concrete," *Advanced Material Science Engineering*, Article ID 263243, 2012, pp. 8.
15. Vaitkevicius, V. Serelis, E. and Hilbig, H., "The Effect of Glass Powder on the Microstructure of Ultra-High Performance Concrete," *Journal of Construction and Building Materials*, Vol. 68, 2014, pp. 102–109.
16. Soliman, N. Aïtcin, P.-C. and Tagnit-Hamou, A., "New Generation of Ultra-High Performance Glass Concrete," *Advanced Concrete and Technologies*. Lightweight and Foam Concretes. Education and Training, Publisher: RILEM and CEB-fib, ISBN 978-5-7264-0809-5, V. 5, Chapter 24, May 12-16, 2014, pp 218-227.
17. Zerbino, R. Giaccio, G. Batic, O.R. and Isaia, G.C., "Alkali–Silica Reaction in Mortars and Concretes Incorporating Natural Rice Husk Ash," *Construction and Building Materials*, Vol. 36, 2012, pp. 796–806.
18. Juengera, M.C.G. and Ostertag, C.P., "Alkali–Silica Reactivity of Large Silica Fume-Derived Particles," *Journal of Cement and Concrete Research*, Vol. 34, 2004, pp. 1389–402.
19. Andrea, S. and Chiara, B.M., "ASR Expansion Behavior of Recycled Glass Fine Aggregates in Concrete," *Journal of Cement and Concrete Research*, Vol. 40, 2010, pp. 531–536.
20. de Larrard, F., "Concrete Mixture Proportioning: A Scientific Approach," CRC Presas1999, pp 448.
21. Tagnit-Hamou, A., and Soliman, N., "Ultra-High Performance Glass Concrete and Method for Producing same," *U.S. Patent Application*. No. 61/806,083, file March 28, 2013, Accepted March 2014.
22. Tagnit-Hamou, A. Soliman, N. Omran, A.F. Mousa, M.T. Gauvreau, N. and Provencher, M.F. "Novel Ultra-High-Performance Glass Concrete," *Journal of ACI Concrete International*. Vol. 39, No. 3, March 2015, pp. 53-59.

7. Acknowledgements

This research was funded by the SAQ Industrial Chair on Valorization of Glass in Materials, and the authors gratefully ack

10.4 Paper 10: A New Generation of Ultra-High Performance Glass Concrete

Reference:

Soliman N., Aïtcin P.- C., and Tagnit-Hamou A. (May 12-16, 2014) New Generation of Ultra-High-Performance-Glass-Concrete. *Advanced Concrete and Technologies. Lightweight and Foam Concretes. Education and Training*. Publisher: RILEM and CEB-fib, ISBN 978-5-7264-0809-5, Volume 5, Chapter 24, pp 218-227.

A New Generation of Ultra-High Performance Glass Concrete

Nancy Soliman, Ph.D. Candidate, Université de Sherbrooke, Québec, Canada
Arezki Tagnit-Hamou, Professor, Université de Sherbrooke, Québec, Canada
Pierre-Claude Aïtcin, Professor, Université de Sherbrooke, Québec, Canada

Annotation:

A new type of ecologic Ultra-High Performance Glass Concrete (UHPGC) has been developed at the Université de Sherbrooke through the use of waste glass materials having different particle size distribution obtained from glass culets. These powders were used to replace quartz sand, cement, quartz powder and silica fume particles. The UHPGC provides several advantages (technological, economical, and environmental). It reduces the production cost of Ultra-High Performance Concrete (UHPC) and decrease the carbon foot print of a traditional UHPC structure. The rheology of fresh UHPGC is improved due to the replacement of cement and silica fume particles by non-absorptive glass particles. Depending on its composition and the curing temperature, UHPGC compressive strength ranges between 150 and 250 MPa, flexural strength above 20 MPa, tensile strength greater than 10 MPa, elastic modulus in about 50 GPa. This strength and rigidity improvements are due to the fact that glass particles act as inclusions having a very high strength and elastic modulus that have a strengthening effect on the overall hardened matrix.

Keywords; Waste Glass, Sustainability, Ultra-High Performance Concrete (UHPC), Steel Fibers, Packing density, durability, mechanical performance, green concrete

1. Introduction

A typical UHPC mix contains Portland cement, silica fume, quartz sand having a maximum size of 600 μm, quartz powder and eventually very fine steel fibre [1, 3, 4, 5, 6, and, 7]. Such a typical mix has very low water to binder ratio (*w/b*) and contains high amount of superplasticizer

(SP). Depending on its composition and its curing temperature, this material can exhibit compressive strength up to 150 MPa, flexural strength greater than 15 MPa, and elastic modulus above 50 GPa [2, 5]. It can also resist freeze-thaw and scaling cycle without visible damage, and it is nearly impermeable to chloride ions penetration [3]. These excellent characteristics of UHPC are achieved by the enhancement of the homogeneity by the eliminating of coarse aggregate, the enhancement of the packing density by the optimization of the granular mixture through a wide distribution of powder size classes, the improvement of the matrix properties by addition of pozzolanic materials and by reducing (*w/b*), the improve of the microstructure through post-set heat treatment; and by the enhancement of ductility by including small steel fibers [2].

Not only good mechanical and durability characteristics, but also the environmental friendly, ecological, and socioeconomic benefits have to be considered now when producing cement-based materials [8]. Typical UHPC are designed with a high cement content ranging between 800 and 1000 kg/m^3 [1, 2]. This huge amount of cement not only affects the production cost and consumes natural sources, but also has a negative effect on the environmental conditions through CO_2 emission and greenhouse effect [7]. Moreover, because of the lack powder having a grain size distribution between that of Portland cement and SF, 25% to 35% of SF has to be used. This is high amount of the material which is now very limited resource and high costly is considered as one of the impedances of the UHPC use in the concrete market.

Post consumption glass can be recycled in many countries several times without significant alternation in its physical and chemical properties [9]. In Europe, as indicated by the latest glass recycling industry report published by the European Container Glass Federation (FEVE), the average of glass recycling rate in 2011 has risen above the 70% threshold (over 12 million tons) [10]. But in other country large quantities of glass cannot be recycled because of colour mixing, or expensive recycling cost [9]. For example, in Quebec, only 49% of the glass was recovered in 2008 [11], the rest having gone the way of landfills. According to USEPA, in 2011, Americans generated 11.5 million tons of glass in the municipal solid waste stream and only 28 percent of the glass was recovered for recycling [12]. Waste glass material when crushed and ground at different particle size (0-20 mm) is considered as an innovative, durable and sustainable material to be also used in concrete as supplementary materials [13,14] and aggregate [15].

2. Experimental program

The research program under taken at the Université de Sherbrooke aimed at developing an innovative low-cost, sustainable, and green UHPGC by using glass. The optimization of UHPGC mixes has been carried out based on the optimization of packing density theory. The experimental program was aimed to evaluate the rheological behaviour and mechanical performance of this new type of UHPGC.

2.1 Mix- design optimization

The mix design was developed in two steps. In the first step, the packing density of granular composition was optimized. In this study, the packing density for all granular mixtures was determined by using the compressible packing model of de Larrard [16]. The selected optimal packing density was 0.80%, which obtained when combination of, QS, GP, cement, and SF. It resulted in use of 500 kg of glass powder for 1 m^3 of UHPGC.

In a second step, the compatibility between the cement and superplasticizer was studied. The optimum amount of superplasticizer for each *w/b* that gives specific rheological characteristics to obtain self-consolidating matrix as well as high strength was evaluated using a full-factorial design approach. Finally, fibres were added to improve UHPGC ductility without altering too much the rheological properties of fresh mix. Fig. 1 presents the typical mix components of UHPC and UHPGC. Fig. 2 presents the particle size distribution for quartz sand, glass powder, cement, SF, and the UHPGC. Continuous particle distribution of reference mixture can be observed from the figure.

	0.1 µm	100 µm 600 µm	
Typical UHPC	silica fume	Portland cement and quartz powder	quartz sand

	0.1 µm	100 µm	600 µm
Typical UHPGC	silica fume	Portland cement and glass powder	quartz sand

Fig. 1. Comparison of composition of UHPGC and UHPC

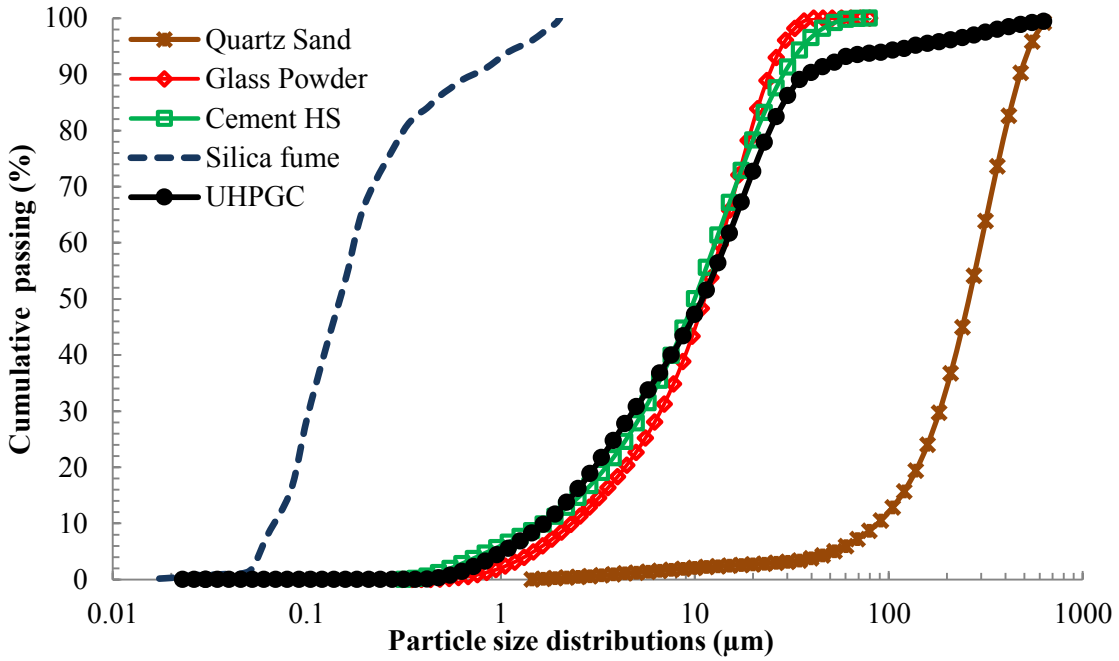

Fig. 2. Particle-size distribution of materials used in this study and UHPGC

2.2 Materials

Cement: the selection of the cement is critical when making UHPC in order to control its rheology. As in the case of any concrete or mortar the rheology of UHPC is strongly influenced by the fineness of the cement and its C_3A and C_3S contents, the two most reactive components of Portland cement. This is even more critical in the case of UHPGC as the cement particles are very close to each other, because the very low *(w/b)* used. Therefore, it is important to select cement having the lowest content of C_3A and C_3S. Consequently, high-sulphate resistance cement, which is formulated specifically with low C_3A content, has been selected. It had the following Bogue composition; 50% C_3S, 25% C_2S, 14% C_3A, and 14% C_4AF. Its specific gravity was 3.21, its Blaine fineness 370 (m^2/kg) and its d_{50} was equal 11µm.

Silica-fume: the silica fume used in this study complied with CAN/CSA A3 000 specifications. It had silica content of 99.8%. Its specific gravity was 2.20, its specific surface area was 20,000 (m^2/kg). Its d_{50} was equal to 0.15 µm.

***Quartz sand*:** the quartz sand was used as granular materials having a maximum particle size equal to 600 µm. Its d_{50} was equal to 250 µm. It has silica content of 99.8%. Its specific gravity was 2.70.

***Waste glass materials*:** the glass powder having a maximum particle size of 100 µm is referred as glass powder. The silica content of the powder was 73% and its Na_20 content 13%. Its specific gravity was 2.60.

***Superplasticizer*:** the superplasticizer used is polycarboxylate based-HRWRA.

2.3 Experimental procedure

It is important to start by mixing all the powders in a dry state to be able to achieve a homogeneous mixture then to add water and superplasticizer, because, otherwise the very fine particles tend to agglomerate and form chunk. The gradual addition of HRWR can improve flowability; it was not possible to do it in one case. The half volume of water containing half the amount of superplasticizer was added between 3 to 5 min. Finally, addition of the remaining water and superplasticizer was done while the mix was mixed for about 5 min at high speed. Fibers were added during the following 3 minutes.

As soon as the mixing was completed, the measurements of the fresh properties of the UHPGC started. The tests included fresh concrete temperature, as well as unit weight and air content was tested following to (ASTM C 185 – 02) standard. The rheology of the concrete was measured using the flow table test according to (ASTM C 1437-07) standard.

Then, the specimens were stored of 20 ºC, 100% RH for 24 h, then removed from the moulds, and cured according to different curing regimes until the testing.

Two curing regimes were implemented after demoulding. In the standard curing regime, the samples were stored in a fog room (20 ± 2ºC, RH > 100%) until testing. The second mode of curing was steam cured at 90ºC and RH = 100% for 48 hours.

A UHPGC that did not contain any fibers was tested and compare with another that contained 1% fiber. They will be identified in the following as the Non-Fiber and the Fiber mix.

3. Results and discussions

3.1 Fresh properties

Table 1 presents fresh concrete temperature, unit weight, air content, and slump-flow spread (without chock). It is seen that the incorporation of the glass powders resulted in producing a self-consolidating UHPGC with a slump flow 300 mm for the non- fibre concrete and 290 mm for the fibre concrete. UHGPC can be practically self-placing. The second mix had a content of 1% of fibres and it was possible to keep almost the same flow as the one that did not contain any fibres. It seen that the polycarboxylate used entrained a high amount of entrapped air over 3% in that case. In this mixture a defoaming agent was not used.

Tab. 1. Fresh properties of UHPGC

Mixture	Slump flow (mm)	Theoretical unit weight (kg/m^3)	Air voids (%)	Temperature (ºC)
Non-Fibre	300	2330	3.2	22
Fibre	290	2390	3.3	23

3.2 Mechanical properties

3.2.1 Compressive strength

The compressive strength of the various UHPGC was measured at different ages as seen in Fig. 3. The compressive strengths of the mixtures without fibre and with fibre were 191 and 187 MPa after steam curing, respectively. It can be seen that the compressive strength is practically not increased by the fibers, due to the low content of the fibres which occupied 1% of the volume of the UHPGC mix, as shown in Fig. 3. Also, Fig. 3 compares compressive strengths obtained for normal curing and the steam curing. It is seen globally that the heat treatment did not increase significantly the compressive strength. It is only accelerate the achievement of the final strength. The difference between the two different curing regimes after 91 days of normal curing is less than 10%.

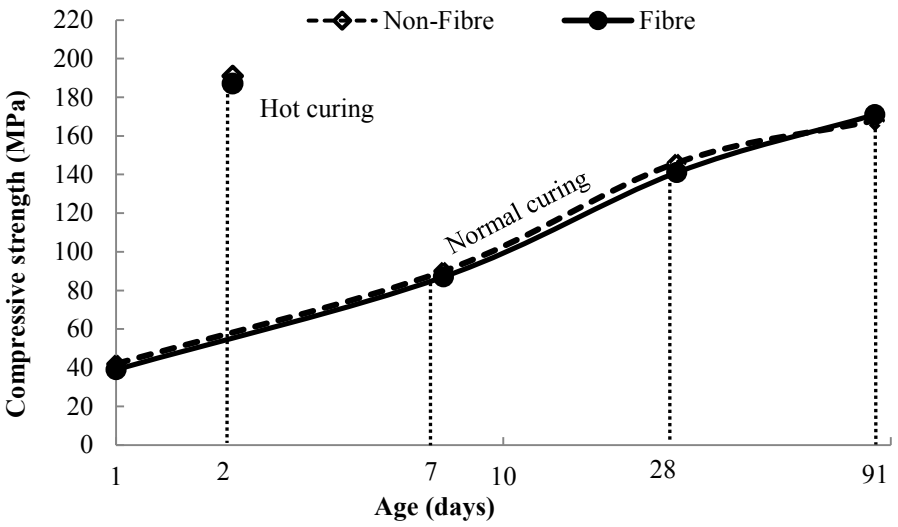

Fig. 3. Compressive strength of UHPGC

3.2.2 Flexural strength

The ASTM C 1018 standard test method was used to determine the flexure strength. The flexural strength results are shown in Fig. 4. As can be seen, the inclusion of the fibres increased the flexural strength of UHPGC. The UHPGC made with 1% fibres had flexural strength of 20 MPa under standard curing for 91 days and 21 MPa under steam curing regime. It is seen globally that the heat treatment did not increase significantly the flexural strength.

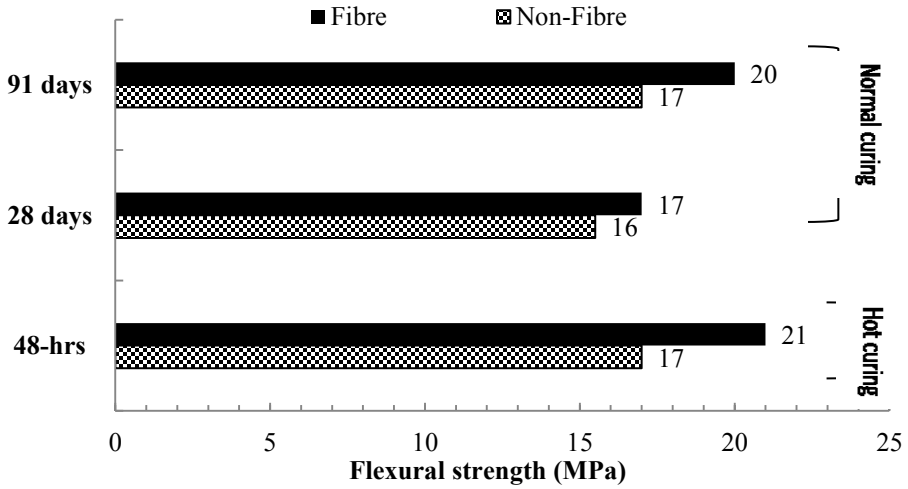

Fig. 4. Effect of fiber, curing types and age on flexural strength of UHPGC

The same type of results was obtained also when measuring the splitting strength according to ASTM C496 standard. The UHPGC made with 1% fibre had tensile strength of 15MPa under standard curing for 91 days and 16 MPa under steam curing regime.

3.2.3 Modulus of elasticity

Modulus of elasticity was measured on 100×200 mm cylinders from each of two curing regime following the ASTM C 469 standard. Table 2 presents the values of the modulus of elasticity. The elastic modulus is not significantly affected by the type of curing, age and fibres content.

Tab. 2. Modulus of Elasticity of UHPGC

Age and type of curing	Non-Fibre	Fibre
48-hours hot curing	50 GPa	51 GPa
28 days normal curing	48 GPa	49 GPa
91days normal curing	49 GPa	49 GPa

3.3 Durability of UHPGC

3.3.1 Abrasion resistance

Abrasion resistance can be an important parameter for design in certain circumstance. It was measured according to ASTM C944 standard. Abrasion resistance in concrete is usually measured as a relative volume loss index. Glass is used as a reference material, which has a relative volume loss index of 1.0. The abrasion test was performed on two specimens from each of the two curing regimes as well as with and without fibre. The value of a relative volume loss index of UHPGC ranges from approximately 1 to 1.2 as seen in Fig. 5. For typical UHPC, a relative volume loss index range from approximately 1.1 to 1.7 [17, 18]. By comparison, the relative volume loss index is 2.8 for a high performance concrete (HPC) and 4.0 for a normal concrete [19].

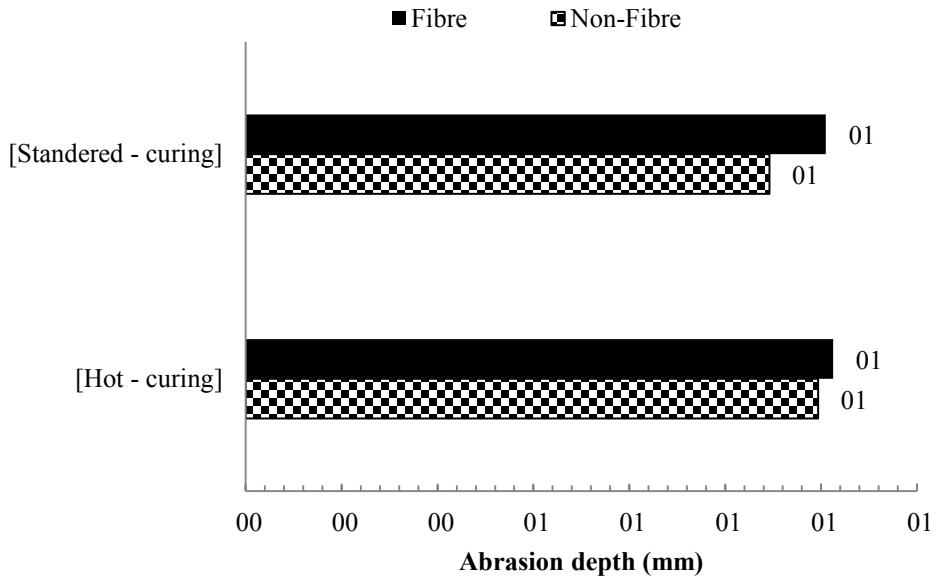

Fig. 5. Relative volume loss induced by abrasion test for UHPGC (ASTM C944)

3.3.2 Scaling resistance

Scaling resistance was measured according to ASTM C672 standard. The weight loss measured was between 13 to 21 g/m^2 after 50 freeze-thaw cycles as presented in Fig. 6, which is very low value. Estimate of salt scaling of UHPC reported in the literature vary from approximately 8 to 60 g/m^2 for studies conducted between 28 and 50 freeze-thaw cycles [19, 20]. The mass lost from salt scaling of HPC and NC are much higher than that of UHPC at (150 g/m^2) for HPC and (1500 g/m^2) for normal concrete [21].

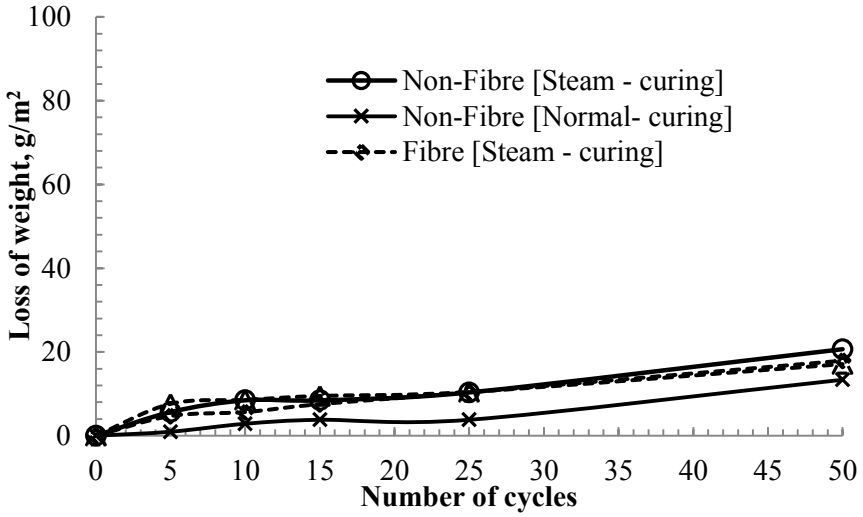

Fig. 6. Changes of salt scaling of UHPGC at different cycles of the test (ASTM C672)

3.3.3 Resistance to freeze-thaw cycles

The freeze-thaw resistance of UHPGC was tested according to ASTM C666 standard. Periodically, the cycling is stopped and the dynamic modulus of elasticity of the specimens was measured. Fig. 7 provides the results for 300 freeze-thaw cycles. The results show that the specimens with normal or heat curing and with or without fibre maintained their dynamic modulus characteristics close to their original UHPC.

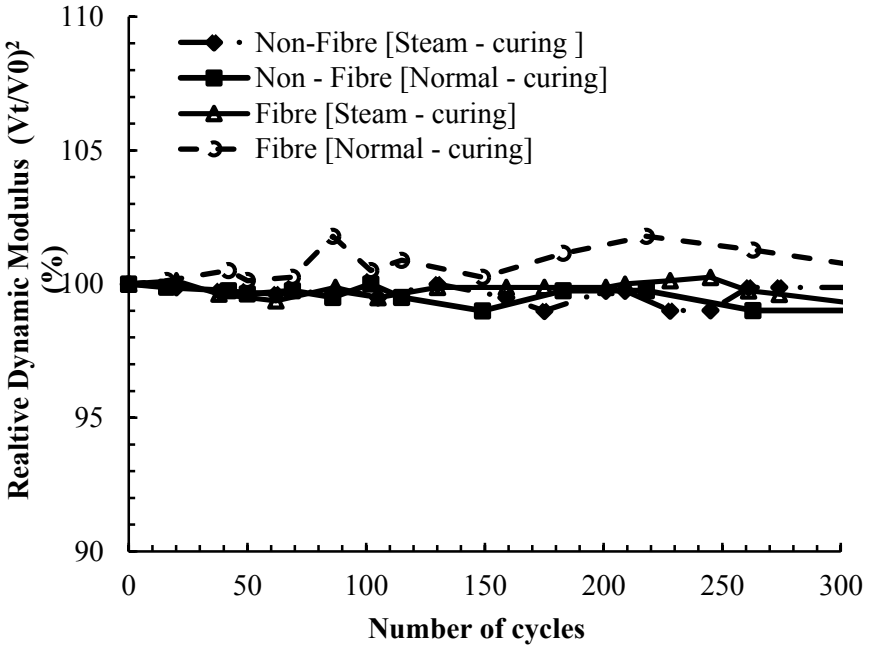

Fig. 7. Change in relative dynamic modulus with freeze-thaw cycles for UHPGC (ASTM C666)

3.3.4 Chloride-ion permeability

Rapid chloride ion penetrability tests were completed on UHPGC specimens according to ASTM C1202. The electrical current was recorded at 1 minute intervals over the 6 hour time frame, resulting in the total coulombs passed value shown in Table 3. Two or three specimens were tested for each condition. The specimens were tested at both 28 and 91 days for normal curing and 48 hours hot curing with and without fibre. The results show that the chloride ion permeability is very low, regardless of the curing regime applied.

Tab. 3. Charges passed during the rapid chloride ion penetrability test (ASTM C1202)

Curing Method	Mixture	Tests	Age (days)	Coulombs passed
Normal curing	Non	2	28	30
	Fibre			28
Normal curing	Non	2	91	18
	Fibre			20
Steam curing	Non	2	2	8
	Fibre			7

3.3.5 Resistance to alkali-silica reaction

Alkali-silica reaction testing was performed in accordance with ASTM C1260 standard. The only modification made to this standard was that the test duration was extended from 14 to 28 days to provide more time for the initiation of the alkali-silica reaction if any. Table 4 provides the results from these tests. In all the cases, the expansion was approximately an order of magnitude below the specification that define innocuous alkali-silica reaction behaviour which is 0.10%.

Tab. 4. Alkali-silica reactivity expansion (ASTM C1260)

Mixture	Tests	Expansion (%)
Non Fibre	2	0.004
Fibre	2	0.009

4. Conclusions

A new type of Ultra-High Performance Glass Concrete (UHPGC) has been developed through the use of waste glass powders having different particle size distribution. These glass powders were obtained from recycled glass culets. These powders were used to replace cement and quartz powder particles. Typical UHPGC mixes where optimized by the packing density method. In the present experiment the amount of glass powders used was 500 kg per meter cubic.

Two types of UHPGC where tested one with fibre the other without fibres under two curing regimes (normal and steam curing). Concrete mixes presented excellent workability with high slump; this is due to the non-absorptive glass particles and optimized packing density.

Mechanical performances were excellent and comparable to conventional ultra-High performance concrete (UHPC). UHPGC provides several advantages through: usage of waste glass, reduce the production cost of ultra-High performance concrete UHPC and decrease of the carbon footprint of typical UHPC.

5. Acknowledgment

This research was funded by Société des Alcools du Québec (SAQ). The authors gratefully acknowledge this support. The writers would also like to acknowledge the support of the Université de Sherbrooke to support this work.

6. References

1. Richard P., Cheyrezy M. Composition of Reactive Powder Concretes // Cement and Concrete Research. 1995. Vol. 25. No. 7. p.p. 1501-1511.
2. Richard P., Cheyrezy M. Reactive Powder Concretes with High Ductility and 200-800 MPa Compressive Strength // ACI SP 144. 1994. p.p. 507-518.
3. Roux N., Andrade C., Sanjuan M. Experimental Study of Durability of Reactive Powder Concretes // Journal of Materials in Civil Engineering. 1996. Vol. 8. Issue 1. p.p. 1-6.
4. Schmidt M., Fehling E. Ultra-High-Performance Concrete: Research, Development and Application in Europe // ACI SP Vol. 225. 2005. p.p. 51-77.
5. Lee M-G., Chiu C-T., Wang Y-C. The Study of Bond Strength and Bond Durability of Reactive Powder Concrete // Journal of ASTM International. July/Aug. 2005, Vol. 2, No. 7. p.p. 104-113.
6. de Larrard F., Sedra, T. Optimization of Ultra-High-Performance Concrete by the Use of a Packing Model // Cement and Concrete Research. 1994. Vol. 24. No. 6. p.p. 997-1009.
7. Matte V., Moranville M., Adenot F., Riche, C., Torrenti J.M. Simulated Microstructure and Transport Properties of Ultra-High Performance Cement-Based Materials // Cement and Concrete Research. 2000. Vol. 30. No. 12. p.p. 1947-1954.
8. Aïtcin P-C. Cements of Yesterday and Today – Concrete of Tomorrow // Cement and Concrete Research, Sept. 2000. Vol. 30. No. 9. p.p. 1349-1359

9. Shayan A., Xu A. Value-Added Utilisation of Waste Glass in Concrete // Cement and Concrete Research. 2004. Vol. 34. No. 1. p.p. 81-89.
10. FEVE. Collection for Recycling Rate in Europe // The European Container Glass Federation. 2013 http://www.feve.org/FEVE-STATIS-2013/Recycling-2011-Glass-coll.html (Date accessed: 11 Sept. 2013).
11. Recyc-Québec. Le Verre Fiches Informatives // 2010.
12. USEPA. Wastes-Resource Conservation-Common Wastes & Materials // Glass. Last updated on 17 June 2013. http://www.epa.gov/osw/conserve/materials/glass.htm. (Date accessed: 10 Sept. 2013.)
13. Zidol A., Tohoue Tognonvi M., Tagnit-Hamou A. Effect of Glass Powder on Concrete Sustainability // 1st International Conference on Concrete Sustainability (ICCS13), Ref # 0229. 2012.
14. Zidol A., Pavoine A., Tagnit-Hamou A. Effect of Glass Powder on Concrete Durability // International Congress on Durability of Concrete, Trondheim, Norvège, ICDC2012-D-11-00153. 2012.
15. Terro MJ. Properties of Concrete Made with Recycled Crushed Glass at Elevated Temperatures // Building and Environment. 2006. Vol. 41. No. 5. p.p. 633-639.
16. de Larrard, F., (1999) "Concrete Mixture Proportioning: a Scientific Approach," E&FN Spon, London.
17. Perry V., Zakariasen D. First Use of Ultra-High Performance Concrete for an Innovative Train Station Canopy // Concrete Technology Today, Aug. 2004. Vol. 25. No. 2. p.p. 1-2.
18. Bonneau O., Lachemi M., Dallaire E., Dugat J., Aïtcin P-C. Mechanical Properties and Durability of Two Industrial Reactive Powder Concretes // ACI Materials Journal, July-Aug. 1997. Vol. 94. No. 4. p.p. 286-290.
19. Roux N., Andrade C., and M.A. Sanjuan. Experimental Study of Durability of Reactive Powder Concretes. //Journal of Materials in Civil Engineering, Feb. 1996, Vol. 8, No. 1: 1-6.
20. Dugat J., Roux N., Bernier G. Mechanical Properties of Reactive Powder Concretes. // Materials and Structures. May 1996. Vol. 29. p.p. 233-240.
21. Schmidt M., and E. Fehling. Ultra-High-Performance Concrete: Research, Development and Application in Europe. //7th International Symposium on Utilization of High Strength High Performance Concrete, 2005. Vol.1: 51-77.

Authors

Nancy Soliman, Ph.D. Candidate at the Department of Civil Engineering of Université de Sherbrooke. Her research interests are valorization of new and by-product materials, ultra-high strength concrete, and packing density.

Arezki Tagnit-Hamou, is a full professor at the Department of Civil Engineering of Université de Sherbrooke and Fellow of the American Concrete Institute (FACI). He is the director of the Research Centre for Concrete Infrastructures at University of Sherbrooke (CRIB-US). His research areas are ecological concretes and the valorization of by-products.

Pierre-Claude Aïtcin, Emirate Professor at the Department of Civil Engineering of Universite de Sherbrooke. This research interests are High Performance Concrete, Ultra- High Performance concrete and sustainability of concrete structure.

10.5 Paper 11: Novel Ultra-High Performance Glass Concrete

Reference:

Tagnit-Hamou A., Soliman N., Omran A., Mousa M., Gauvreau N., and Provencher M. (2016) Novel Ultra-High Performance Glass Concrete. *Concrete International*, 37(3):41-47.

Novel Ultra-High Performance Glass Concrete

New material used to fabricate pedestrian bridges on Sherbrooke University campus

Arezki Tagnit-Hamou, Nancy Soliman, Ahmed Omran, Mohammed Mousa, Nicolas Gauvreau, and MFrancine Provencher

Authors and Affiliation

Arezki Tagnit-Hamou, FACI, is a professor in the Department of Civil Engineering at the University of Sherbrooke, QC, Canada. He is also the Head of the cement and concrete group as well as holding an industrial chair on valorization of glass in materials. He is a member of ACI Committees 130 (Sustainability of Concrete) and 555 (Concrete with Recycled Materials), and RILEM TC DTA. His research interests include alternative supplementary cementitious materials, cement and concrete physicochemistry and microstructure, and sustainable development.

Nancy A. Soliman, is a member of the ACI international and Sherbrooke local chapters, and CRIB. She is a PhD candidate in the Department of Civil Engineering, University of Sherbrooke, QC, Canada. Her research interest includes NDT, UHPC, microstructure, and sustainable development.

Ahmed F. Omran, is a postdoctoral fellow of Department of Civil Engineering, University of Sherbrooke and assistant professor of University of Minoufiya, Egypt. He holds BS and MS degrees in Civil Engineering from University of Minoufiya. He received Ph.D. degree from University of Sherbrooke. He is an active member of RILEM TC-233 FPC Committee. His research interests include durability of cement-based materials, development of new alternative supplementary cementitious materials (ASCM), sustainable development, concrete rheology, and formwork pressure.

Mohammed T. Mousa is a Ph.D. student at Department of Civil Engineering, Université de Sherbrooke, QC, Canada, and a civil engineer at Helwan University, Egypt. He got his BSc. in

civil engineering from Benha University, and MSc. and Ph.D. degrees in civil engineering from Helwan University. His research interests include cement-based materials, and structural behavior.

Nicolas Gauvreau, is the co-founder, Vice President, and Technical Director of Bétons Génial Inc., QC, Canada. He has more than 20 years of experience in prefabricated concrete and molds. His company specializes in unique and innovative manufacturing processes.

MFrancine Provencher is an architect member of L'Ordre des architectes du Québec (OAQ) since 1984 and has been credentialed as a LEED AP since 2004 with BD+C speciality. She is director of Planning and Sustainability Department at the Building Services of Université de Sherbrooke, QC, Canada, since 1993.

Ultra-high-performance concrete (UHPC) is defined worldwide as concrete with superior mechanical, ductility, and durability properties. A typical UHPC is composed of cement, quartz powder (QP), silica fume (SF), quartz sand (QS), and steel fibers.[1] UHPC achieves compressive strengths of at least 150 MPa (22,000 psi), flexural strengths up to 15 MPa (2200 psi), elastic moduli of up to 45 GPa (6500 ksi), and minimal long-term creep or shrinkage.[2] It can also resist freezing-and-thawing cycles and scaling conditions without visible damage, and it is nearly impermeable to chloride ions.[3] UHPC is thus a promising material for special pre-stressed and precast concrete elements (decks and abutments for lightweight bridges, decks, and marine platforms; urban furniture; and precast walls), concrete repair, and architectural facade elements.[4]

Although UHPC is relatively expensive to produce, it presents some economic advantages because its enhanced properties allow:

- Reduction or elimination of passive reinforcement in structural elements;
- Reductions in the thickness and self-weight of concrete elements; and
- Increases in service life accompanied with reductions in maintenance costs.[5]

UHPC is designed with a very high cement content ranging between 800 and 1000 kg/m^3 (1350 and 1690 lb/yd^3), which leads to high production costs, consumes natural sources, and increases

CO_2 emissions. These factors and others such as a relatively high SF content (25 to 35% by weight of cement) are considered impediments to UHPC use in the concrete market.

Ultra-high-performance glass concrete (UHPGC) is a new type of UHPC that constitutes a breakthrough in sustainable concrete technology,[6] as it comprises granulated post-consumer glass with a specific particle-size distribution (PSD) developed using glass sand, high amounts of glass powder, and moderate contents of fine glass powder. UHPGC is a fiber-reinforced concrete characterized by a very dense microstructure, which enhances durability via a discontinuous pore structure. While UHPGC can be designed with less cement, silica fume, quartz powder, and quartz sand than typical UHPC, it still contains fibers and a high-range water-reducing admixture (HRWRA).

UHPGC can be produced with low water-to-binder ratio (*w*/*b*), yet because the glass particles have zero absorption, its rheological properties allow it to be practically self-placing

Depending on UHPGC composition and curing temperature, the concrete's compressive strength can range from 130 to 260 MPa (20,000 to 40,000 psi), while flexural strength can exceed 15 MPa (2200 psi), tensile strength can exceed 10 MPa (1500 psi), and elastic modulus can exceed 45 GPa (6500 ksi).

UHPGC is characterized by excellent durability. Due to its high packing density and lack of interconnected pores, UHPGC has negligible chloride-ion penetration, low mechanical abrasion, and very high freezing-and-thawing resistance.

Pedestrian Bridges

Developing UHPGC was one of the main goals of the University of Sherbrooke's industrial chair on the valorization of waste glass in materials. After a major research program, this newly developed concrete was used to fabricate new footbridges to replace deteriorated wooden structures on the University of Sherbrooke campus, Sherbrooke, QC, Canada. The technology enabled the designer to create thin sections that are light, graceful, and innovative in geometry and form at a relatively low cost. In addition, the structure is expected to be durable with high abrasion and impact resistance.

Materials

As with any concrete or mortar, UHPC rheology is strongly affected by cement fineness as well as the two most reactive components in portland cement C_3A and C_3S. The cement characteristics are even more critical in the case of UHPGC, as the very low *w*/*b* results in close packing of the cement particles. It's particularly important to select cement with the lowest contents of C_3A and C_3S. The cement selected for the UHPGC footbridges was formulated with a low C_3A content in order to provide high sulphate-resistance. The cement properties included: Bogue composition of 50% C_3S, 25% C_2S, 2% C_3A, and 14% C_4AF; specific gravity of 3.21; Blaine fineness of 370 m^2/kg; and D_{50} of 11 μm.

Other materials used in the UHPGC mixture included:

- SF compliant with CAN/CSA-A3000-13 "Cementitious materials compendium" specifications with silica content of 99.8%, specific gravity of 2.20, specific surface area of 20,000 m^2/kg, and D_{50} of 0.15 μm;
- QS with maximum particle size of 600 μm, D_{50} of 250 μm, silica content of 99.8%, and specific gravity of 2.70;
- Glass powder (GP) with maximum particle size of 100 μm, silica content of 73%, Na_20 content of 13%, and specific gravity of 2.60;
- Polycarboxylate-based HRWRA, marketed as Sika Viscocrete 6200; and
- Polyvinyl alcohol (PVA) fibers with13 mm (0.5 in.) length and 0.2 mm (0.008 in.) diameter.

Concrete mixture

The mixture design was developed in three steps. In the first step, the packing density of the granular composition (QS, GP, cement, and SF) was optimized to 0.78% using the compressible packing model.[7] The resulting mixture comprised 410 kg/m^3 (690 lb/yd^3) of GP. In the second step, the optimum HRWRA dosage was determined for a range of *w*/*b* values, yielding the rheological characteristics needed to obtain a self-consolidating matrix as well as adequate strength. In the third step, the fiber content was optimized as needed to improve the UHPGC ductility without significantly altering the rheological properties of the fresh mixture.

Table 1 provides the compositions for the UHPGC mixtures with *w*/*b* of 0.24 used in this project.

Design

The footbridges were designed to meet the university's architectural and structural requirements for pedestrian use as well as to be in compliance with the university's regulation on sustainable development. Because the mechanical properties of the UHPGC allowed the spans to be constructed with relatively small cross sections, each bridge had a total weight of about 4000 kg (8800 lb).

The structural system consisted of an arch slab 4910 mm (193 in.) in length, 2500 mm (98 in.) in width, and 75 mm (3 in.) in thickness supported by longitudinal ribs of variable height and a constant width of 130 mm (5 in.). Using the mechanical-properties determined during our testing program, the section was designed to meet strength and serviceability limits as per the University's requirements. The arch slab was reinforced with welded wire reinforcement (M10 at 300 mm [12 in.] in both directions) placed at the mid-height of the slab. Each rib was reinforced with a single M20 reinforcing bar located near the bottom of the rib. Fig. 1 (a) shows the footbridge reinforcement arrangement and Fig. 1 (b) provides the concrete dimensions. One footbridge was instrumented with thermocouples and vibrating-wire strain gauges so that temperature and deformation could be monitored over time.

Formwork

The mold for the bridges was built at the Bétons Génial Inc. plant and then transported to the university's integrated laboratory for innovative and sustainable materials and structural valorization research. Bétons Génial Inc. designed and built a reusable wooden mold integrating a urethane-rubber facing with specific Shore's hardness. The facing was designed to produce a textured, non-slip walking surface on the decks and very smooth, joint free surfaces on other surfaces of the bridges (Fig. 2). Although UHPGC shrinkage is very low, the liner material was selected to accommodate concrete shrinkage and minimize the risk of creating microcracks during concrete curing. The mold was designed so that the bridge could be cast upside down, allowing the relatively complex shape to be formed with integral non-slip areas on the deck, very smooth surfaces elsewhere, and no joints.

Production

The UHPGC was produced at Sherbrooke University laboratory using a pilot-scale automatic concrete plant with a paddle-type stationary pan mixer with a 500 L (18 ft^3) capacity. To achieve a homogeneous mixture and avoid particle agglomeration, all powder materials were dry mixed for 10 minutes before the water and HRWRA additions. About half of the HRWRA was diluted in half of the mixing water, and this was gradually added over the next 3 to 5 minutes of mixing time. The remaining water and HRWRA as well as the fibers were then added over the following 3 to 5 minutes of mixing time. The total mixing time was 20 minutes.

Four batches of concrete were produced for a total of 2.0 m^3 (3 yd^3) for each footbridge. Concrete production and placement took 2 hours. Once the four batches had been loaded into the hopper, the UHPGC's fluidity and self-placing properties allowed the placing of the concrete into the mold in fewer than 12 minutes without external vibration. While the UHPGC couldn't be described as self-compacting, it flowed extremely well. Only 1 minute of internal vibration was required to ensure good compaction. After casting, exposed concrete was covered with plastic sheeting until the mold was removed. For each bridge, the mold was removed 24 hours after placement. First, an overhead crane was used to open the mold by separating its two parts with straps and anchors (Fig. 3 (a)). The bridge was then lifted and rotated (Fig. 3 (b)). After form removal, plastic sheeting was placed over each footbridge to allow continued curing.

The UHPGC's fresh and rheological properties were measured after mixing. Specimens needed for compressive, tensile, and flexural strength tests as well as modulus of elasticity, resistance to mechanical abrasion, scaling, freezing-and-thawing resistance, chloride-ion penetration, and resistivity tests were then fabricated. Tests were performed according to ASTM International standards. The samples were stored at 23°C (73°F) and 100% relative humidity (RH) for 24 hours before mold removal, after which they were stored in a fog room at 23°C (73°F) and 100% RH until testing.

Installation

Before the bridges were transported to their installation sites, wooden and steel railings were attached (Fig. 4). A simple flatbed truck was used for transportation to the site (Fig. 5), and a truck-mounted crane and straps were used to lift and install the bridges on conventional concrete abutments with neoprene bearing pads. Lifting and placing took a little less than an hour.

Concrete Performance

Fresh properties

Tests were performed to obtain basic fresh concrete properties including slump flow (ASTM C1437, "Standard Test Method for Flow of Hydraulic Cement Mortar"), unit weight, air content, and temperature (ASTM C 185 – 02, "Standard Test Method for Air Content of Hydraulic Cement Mortar") ; values were 280 mm (11 in.) without tamping, 2231 kg/m^3 (140 lb/ft^3), 3.5% , and 22°C (°F), 22°C (72°F) respectively.

To examine the concrete's ability for self-placement without consolidation or segregation issues, various tests normally carried out for self-consolidating concrete were performed. The slump-flow diameter with the Abrams cone (ASTM C143/C143M, "Standard Test Method for Slump of Hydraulic-Cement Concrete") was 780 mm (31 in.). The time to reach a 500 mm (20 in.) spread diameter (T_{500}) was 6.8 s, which explains the relatively high viscosity. The visual stability index (VSI) was 0, which means no evidence of segregation.

In order to ensure the concrete flows adequately around the reinforcement bars, the difference between the slump-flow diameter and the J-Ring spread diameter should not exceed 50 mm (2 in.) according to the German SCC guideline[8] or 10 mm (0.4 in.) according to EFNARC.[9] This value was only 5 mm (0.2 in.) for the UHPGC, indicating excellent passing ability. The blockage ratio for the J-Ring test was 0.83. The self-leveling index for the L-Box test with two steel rods was 1.0 (the limit accepted under the EFNARC 2002 guideline is between 0.80 and 1.0). The time for the leading edge of the concrete to reach the end of the 600 mm (24 in.) long horizontal section was 9.8 s. This UHPGC's enhanced fresh properties derive from the large incorporation of glass powder with zero absorption.

Mechanical properties

Compressive-strength tests were carried out according to ASTM C39/C39M, "Standard Test Method for Compressive Strength of Cylindrical Concrete Specimens," on 100×200 mm (4x8 in.) cylindrical specimens at 1, 7, 28, and 91 days after normal curing. The 28- and 91-day compressive strengths of this UHPGC were 96 and 127 MPa (14,000 and 18,500 psi), respectively. The increase in compressive strength of about 33% from 28 days to 91 days indicates the glass powder's pozzolanic reactivity.

Other test conducted at 28 and 91 days included: indirect splitting tensile strength according to ASTM C496/C496M, "Standard Test Method for Splitting Tensile Strength of Cylindrical Concrete Specimens," on 100×200 mm (4x8 in.) cylindrical specimens; flexural strength according to ASTM C78/C78M, "Standard Test Method for Flexural Strength of Concrete (Using Simple Beam with Third-Point Loading)," on 100×100x400×mm (4x4x16 in.) prisms; and modulus of elasticity was measured according to ASTM C469/C469M, "Standard Test Method for Static Modulus of Elasticity and Poisson's Ratio of Concrete in Compression," on 100×200 mm (4x8 in.) cylinders. Table 2 lists the concrete's mechanical properties.

Durability properties

Concrete abrasion was measured according to ASTM C944/C944M, "Standard Test Method for Abrasion Resistance of Concrete or Mortar Surfaces by the Rotating-Cutter Method." The average value of the relative volume-loss index was 1.35 mm (0.05 in.). For a typical UHPC, the relative volume-loss index ranges from 1.1 to 1.7 mm (0.04 to 0.07 in.),[10] which itself is small relative to that for HPC (2.8 mm [0.11 in.]) and normal concrete (4.0 mm [0.16 in.]) [3].

Scaling resistance was measured according to ASTM C672/C672M, "Standard Test Method for Scaling Resistance of Concrete Surfaces Exposed to Deicing Chemicals." After 50 freezing-and-thawing cycles, the scaled mass was 12 g/m^2 (0.04 oz/ft^2). The scaled mass reported for UHPC in the literature, varies from about 8 to 60 g/m^2 (0.20 oz/ft^2) for samples subjected to 28 to 50 freezing-and-thawing cycles[11]

Resistance to chloride-ion penetration was evaluated per ASTM C1202, "Standard Test Method for Electrical Indication of Concretes Ability to Resist Chloride Ion Penetration." The 28- and

91-day specimens exhibited values below 10 Coulombs, respectively, indicating "negligible" chloride-ion permeability.

Resistance to freezing-and-thawing was measured according to ASTM C666/C666M, "Standard Test Method for Resistance of Concrete to Rapid Freezing and Thawing." Relative dynamic modulus was 100% after 700 freezing-and-thawing cycles

The resistivity test was carried out on 100×200 mm (4x8 in.) cylindrical sample (after 91 days of curing). An extremely high value of 3470 kΩ·cm was obtained. For comparison, the resistivity is 1130 kΩ·cm for traditional UHPC without fibers, 96 kΩ·cm for HPC, and 16 kΩ·cm for normal concrete [3].

Bridge instrumentation

The temperature changes in one footbridge were monitored with two thermocouples: one inserted in the center of the deck and another in the center of the supporting (edge) beam. Fig. 6 provides the results from the two thermocouples. The temperature reached approximately 53°C (127°F) in the first days after casting, followed by gradual drop to laboratory temperature. After curing at laboratory temperature (around 23°C [73°F]) for 28 days, the footbridges were transferred to the field sites, where the temperature dropped below zero, as shown by the sudden drop in the temperature curve. Some nights, the temperature fell to -30°C (-22°F).

A vibrating wire gauge was inserted at the center of the instrumented bridge deck to measure deformation due to shrinkage (Fig. 6). A strain of about 430 μm/m was measured at the end of laboratory curing, followed by a sudden increase in the deformation at the field site due to the temperature changes and removal of the plastic sheeting (the strains resulted from temperature change and additional drying shrinkage). The total strain was as much as 1200 μm/m on some days. After deducting thermal expansion, the isothermal strain was about 800 μm/m.

Summary

A new type of UHPC has been developed using recycled glass, creating UHPGC. The new material exhibited excellent workability and rheological properties due to the zero absorption of

the glass particles and optimized packing density for the entire material matrix. The mechanical properties were found to be excellent and comparable to conventional UHPC.

The construction of two UHPGC footbridges at the University of Sherbrooke shows the potential for the material to be used in future projects. UHPGC will produce highly energy efficient, environmentally friendly, affordable, and resilient structures.

Acknowledgment

This research was funded by the SAQ Industrial Chair on Valorization of Glass in Materials and the authors gratefully acknowledge this support. The authors would also like to acknowledge the support of the University of Sherbrooke in conducting this project.

Reference

1. Richard, P., and Cheyrezy, M., "Reactive Powder Concretes with High Ductility and 200-800 MPa Compressive Strength," *SP 144*, American Concrete Institute, Farmington Hills, MI, 1994, pp. 507-518.
2. Richard, P., and Cheyrezy, M., "Composition of reactive powder concretes," *Cement and Concrete Research*, V. 25, No. 7, Oct. 1995, pp. 1501-1511.
3. Roux, N.; Andrade, C.; and Sanjuan, M., "Experimental Study of Durability of Reactive Powder Concretes," *Journal of Materials in Civil Engineering*, V. 8, No. 1, Feb. 1996, pp. 1-6.
4. Schmidt, M.; and Fehling, E., "Ultra-high-performance concrete: research, development and application in Europe," *SP 225*, American Concrete Institute, Farmington Hills, MI, 2005, pp. 51-77.
5. Aïtcin, P-C., "Cements of Yesterday and Today - Concrete of Tomorrow," *Cement and Concrete Research*, V. 30, No. 9, Sept. 2000, pp. 1349-1359.
6. Tagnit-Hamou, A., and Soliman, N.,"Ultra-High Performance Glass Concrete and Method for Producing same," U.S. Patent Application No. 61/806,083, Accepted March 2014.
7. de Larrard, F., *Concrete Mixture Proportioning: A Scientific Approach*, CRC Presas1999, 448 pp.

8. Brameshuber, W., and Uebachs, S., "Practical Experience with the Application of Self-Compacting Concrete in Germany," *Proceedings of the Second International Symposium on Self-Compacting Concrete*, Tokyo, Japan, 2001, pp. 687-696.
9. EFNARC, "Specification and Guidelines for Self-Compacting Concrete," (http://www.efnarc.org), Feb. 2002, pp. 32.
10. VSL Proprietary Limited. 2003. Introduction to Ductal® – Frequently Asked Questions. VSL Proprietary Limited. http://www.ductal.com/Introduction%20to%20 Ductal.pdf.
11. Bonneau, O., Lachemi, M., Dallaire, E., Dugat, J., and P.-C. Aïtcin. 1997. Mechanical Properties and Durability of Two Industrial Reactive Powder Concretes. ACI Materials Journal, July-Aug., Vol. 94, No. 4: 286-290.

Table 1: UHPGC mixture design

Materials	kg/m^3
Type HS cement (C)	555
Silica fume (SF)	205
Glass powder (GP)	410
Water	226
Syntactic fiber	32.5
Quartz sand (QS)	888
HRWRA (solid content)	17

Note: 1 kg/m^3 = 1.69 lb/yd^3

Table 2: Mechanical properties of UHPGC

Properties	Concrete age, days			
	1	7	28	91
Compressive strength, MPa	12	52	96	127
Splitting tensile strength, MPa	--	--	10	11
Flexure strength, MPa	--	--	10	12
Modulus of elasticity, GPa	--	--	41	45

Note: 1 MPa = 145 psi; 1 GPa = 145 ksi

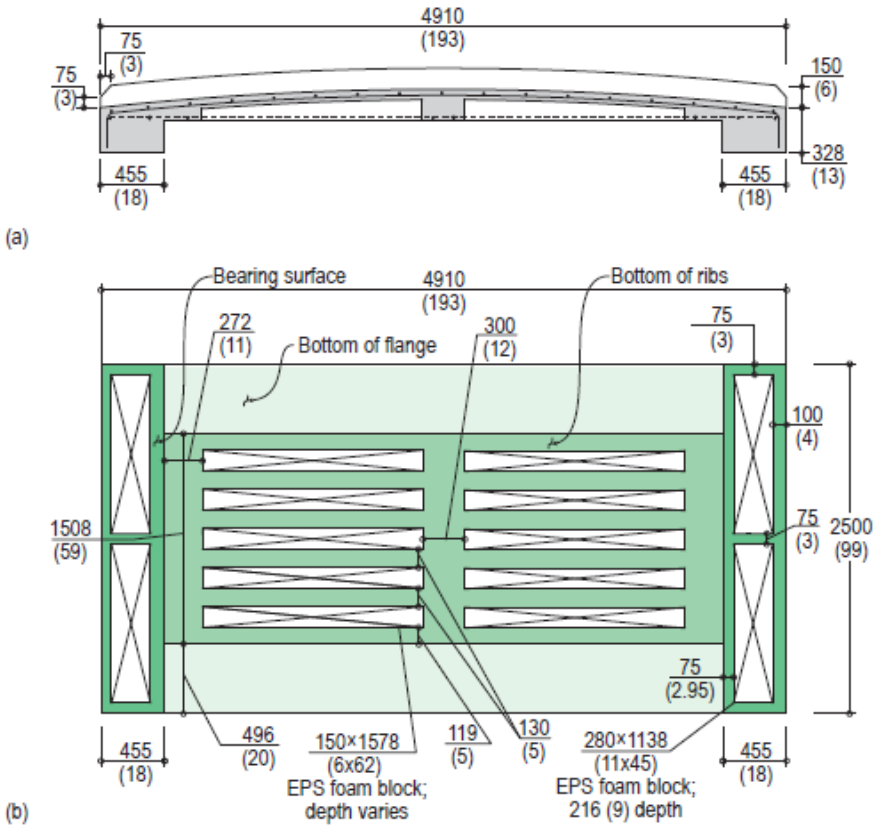

Fig. 1: Bridge schematic: (a) longitudinal section at centerline and (b) bottom view showing concrete dimensions. Dimensions are in mm (nearest in.)

(a)  (b) 

Fig. 2: The footbridge mold was designed to provide formed surfaces on all exposed face: (a) a wooden insert was fabricated in the shape of the deck wearing surface and curbs; and (b) the insert was used as the master to cast the urethane rubber liner used for production of the footbridges

(a)  (b) 

Fig. 3: The footbridge was cast upside down. The mold base held the urethane rubber liner shown in Fig. 2, and the mold was closed with a separate wooden insert that formed the curved and ribbed bottom surfaces of the footbridge: (a) the insert is removed from the mold base, exposing the bottom concrete surfaces and the expanded polystyrene blocks indicated in Fig. 1; and (b) the footbridge was pulled from the mold using straps and anchors, and a steel frame was attached in preparation for flipping the completed structure

Fig. 4: As final preparation before shipping to the jobsite, wooden and steel railings were attached to the UHPGC curbs

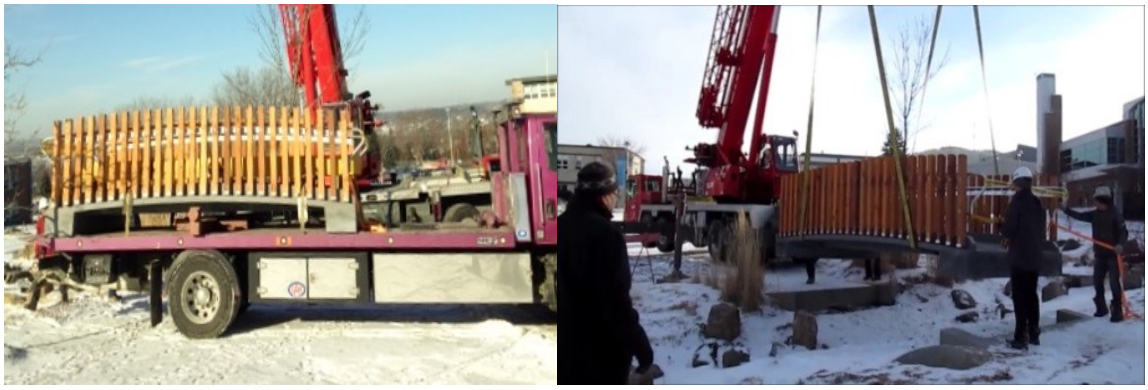

Fig. 5: The completed footbridges were transported on a flatbed truck and installed with a truck-mounted crane

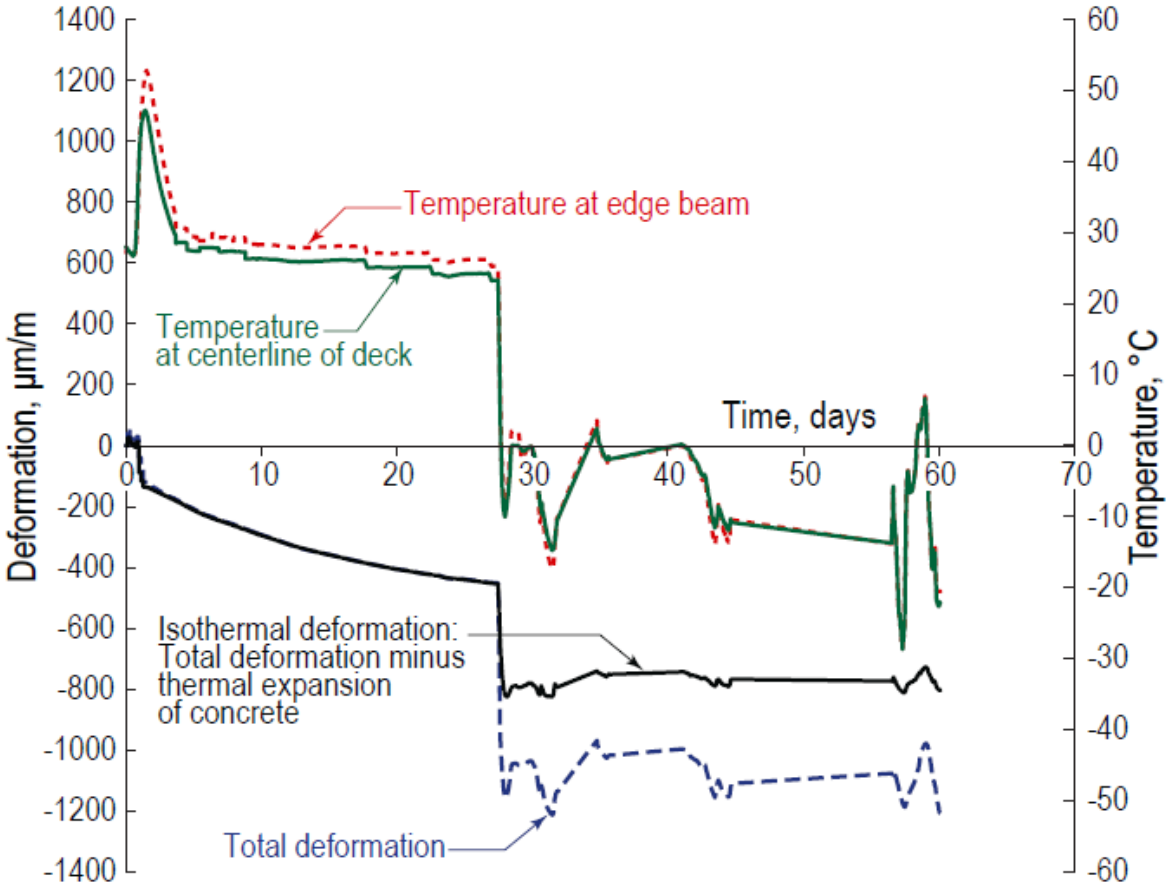

Fig. 6: Variations of deformation and temperature with time obtained from the instrumented bridge (Note: °F = 1.8 x °C + 32°)